# Cyclic amino acids as building blocks for organocatalysts, peptides and total synthesis

**Dissertation**

**Zur Erlangung des Doktorgrades der Naturwissenschaften**

**Dr. rer. nat.**

**der Fakultät für Chemie und Pharmazie**

**der Universität Regensburg**


vorgelegt von

**Thomas Johannes Ertl**

aus Ergoldsbach

**Regensburg 2017**

| | |
|---|---|
| Die Arbeit wurde angeleitet von: | Prof. Dr. O. Reiser |
| Promotionsgesuch eingereicht am: | 31.07.2017 |
| Promotionskolloquium am: | 22.09.2017 |
| Prüfungsausschuss: | Vorsitz: Prof. Dr. Jörg Heilmann |
| | 1. Gutachter: Prof. Dr. Oliver Reiser |
| | 2. Gutachter: PD Dr. Sabine Amslinger |
| | 3. Prüfer: Prof. Dr. Frank-Michael Matysik |

Der experimentelle Teil der vorliegenden Arbeit wurde im Zeitraum von November 2013 bis Januar 2017 am Lehrstuhl von Prof. Dr. Oliver Reiser, Institut für Organische Chemie, Universität Regensburg und im Dezember 2013 an der Universität Salzburg (Österreich) bei Prof. Dr. Chiara Cabrele angefertigt.

Herrn Prof. Dr. Oliver Reiser möchte ich herzlich für die Überlassung des äußerst interessanten Themas, die anregenden Diskussionen und seine stete Unterstützung während der Durchführung dieser Arbeit danken.

*Meiner Familie*

*Im Besonderen meinem Großvater*

*Auch aus Steinen, die einem in den Weg gelegt werden,*

*kann man etwas Schönes bauen.*

*(Johann Wolfgang von Goethe)*

# Abbreviations

| | |
|---|---|
| Å | angstrom |
| Ac | acetyl |
| AcOH | acetic acid |
| Ala | alanine |
| Alloc | allyloxycarbonyl |
| ACC | aminocyclopropane carboxylic acid |
| ACPC | aminocyclopentane carboxyliacid |
| APC | aminopyrrolidine carboxylic acid |
| aq | aqueous |
| azabox | aza-bis(oxazoline) |
| Bn | benzyl |
| Boc | *tert*-butyloxycarbonyl |
| BHT | 2,6-Di-*tert*-butyl-4-methylphenol |
| bp | boiling point |
| brsm | based on recovered starting material |
| brine | saturated NaCl solution |
| Bz | benzoyl (PhCO) |
| °C | degrees Celsius |
| calcd. | Calculated |
| Cbz | carboxybenzyl |
| CD | circular dichroism |
| CDI | 1,1'-carbonyldiimidazol |
| conc. | concentrated |
| COSY | correlation spectroscopy |
| $cm^{-1}$ | wavenumbers |
| d | days |
| DBU | Diazabicycloundecene |
| DABCO | 1,4-Diazabicyclo[2.2.2]octane |
| DCC | *N*,*N*`-dicyclohexylcarbodiimide |
| DCM | dichloromethane |
| *de* | diastereomeric excess |
| DEPT | distortionless enhancement by polarization transfer |
| DIAD | diisopropyl azodicarboxylate |
| DIPEA | *N*,*N*-diisopropylethylamine |
| DMA | *N*,*N*-Dimethylaniline |
| DMF | *N*,*N*-dimethylformamide |
| DMAP | *N*,*N*-dimethyl-4-aminopyridine |
| DMSO | dimethyl sulfoxide |
| *dr* | diastereomeric ratio |
| EA | ethyl acetate |
| EDC | 1-Ethyl-3-(3-dimethylaminopropyl) carbodiimid |
| *ee* | enantiomeric excess |
| equiv | equivalent(s) |
| ESI | electrospray ionization |
| Et | ethyl |
| *et al.* | and others |
| Fmoc | fluorenylmethyloxycarbonyl |

| | |
|---|---|
| FT | Fourier transform |
| GABA | $\gamma$-amino butyric acid |
| h | hour |
| HRMS | high resolution mass spectroscopy |
| HP | high pressure |
| HPLC | high performance liquid chromatography |
| Hz | Hertz |
| *i*Pr | iso-propyl |
| IR | infrared |
| LAH | lithium aluminium hydride |
| Me | methyl |
| MeCN | acetonitrile |
| MHz | mega Hertz |
| min | minute |
| mp | melting point |
| Ms | mesyl |
| MS | mass spectrometry |
| *n*BuLi | *n*-buthyllithium |
| NMR | nuclear magnetic resonance |
| NOE | nuclear Overhauser effect |
| NOESY | nuclear Overhauser effect spectroscopy |
| *p* | *para* |
| Ph | phenyl |
| ppm | parts per million |
| PG | protecting group |
| Pro | proline |
| ref. | reference |
| $R_f$ | retention factor |
| rt | room temperature |
| SPPS | solid phase peptide synthesis |
| Su | succinimid |
| *t*Bu | *tert*-butyl |
| T3P | Propylphosphonic anhydride |
| *T* | temperature |
| TBAB | tetrabutylammonium bromide |
| Tf | trifluoromethanesulfonyl |
| TFA | trifluoroacetic acid |
| THF | tetrahydrofuran |
| TLC | thin layer chromatography |
| TMS | trimethylsilyl |
| Ts | *p*-toluenesulfonyl |
| vs | versus |
| VT | variable temperature |
| v/v | volume to volume ratio |
| wt% | weight % |
| w/w | weight to weight ratio |

# Table of contents

# A. Introduction

Living cells are producing $10^{11}$ different proteins in which the amino acid sequence from only a quarter is known. Proteins are large macromolecules with a molecular weight around 5-500 kDa, which are involved in the coordination of almost all physiological processes. In the human body, proteins appear as structural proteins as a part of the connective tissue or in cell membranes as receptors or ion channels. They can also be considered as molecular machines since they are catalyzing chemical reactions as enzymes or providing protection as antibodies in the human immune system. Moreover, proteins can be used as small transporters or to regulate metabolic processes.[1] Proteins are consisting out of polypeptides, which are stabilized by disulfide bonds, salt bridges or hydrogen bonds. These interactions are determining the three-dimensional structure of a protein and consequently its function. The smallest unit of polypeptides is represented by the amino acids.[2] Advisably, amino acids are designated as the building blocks of life. The proteins essential for life as we know are build up of twenty α-amino acids, designated as proteinogenic amino acids. However, there are more than 400 non-proteinogenic amino acids known with different functions such as hormones or metabolites. In nature, mainly microorganisms produce ammonia out of molecular nitrogen, which is used for the construction of amino acids or proteins by plants or microorganisms itself. In mammals, amino acids are produced from intermediates of the metabolic cycles, mainly of the citric acid cycle.[3,4] In industry, amino acids are synthesized via fermentation, chemical synthesis or extraction methods in thousand ton scales per year and are mainly used as food additives, medical products, cosmetics, detergents or synthetic polymers.[5]

The *Strecker*-reaction represents the first one-pot multicomponent synthesis of α-amino acids even before its isolation from natural sources. Simple condensation of acetaldehyde **1** with ammonia in the presence of hydrogen cyanide gave rise to α-amino nitrile **2**. Subsequent hydrolysis yielded the α-amino acid alanine **3** (Scheme 1).[6]

**Scheme 1:** Presentation of the *Strecker* synthesis.

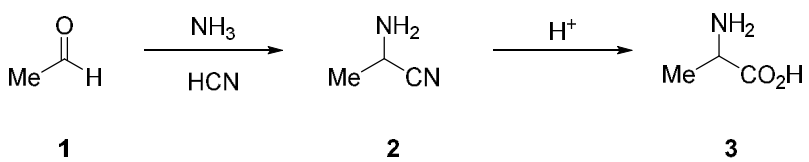


**1** **2** **3**

Though this reaction was developed more than 150 years ago, it remained very popular since it provides a robust, direct and economically viable access towards naturally as well as non-naturally α-amino acids. It is not surprising that based on the high demand of enantioenriched α-amino acids, in particular, asymmetric *Strecker* reactions attracted much attention in organic chemistry in the last fifty years.[7]

Besides α-amino acids, also β- and γ-amino acids represent key structural elements in various agrochemical or pharmaceutical target molecules and reveal interesting properties, for instance as anticancer agents (**4**),[8] antibiotics (**5**),[9] enzyme–inhibitors (**6**)[10] or as an influenza neuramidase inhibitor (**7**)[11] (Figure 1). The probably most prominent example for a naturally occurring γ-amino acid displays γ-amino butyric acid **8** (GABA), the major inhibitory neurotransmitter in the mammalian central nervous system, which also plays an essential role in several brain malfunctions like epilepsy or Alzheimer´s disease. Due to its low lipophilicity and the poor availability to cross the blood-brain barrier, the synthesis of more lipophilic GABA derivatives like Baclofen **9**, a muscle relaxant and antispastic agent, was the objective of a great number of studies.[12]

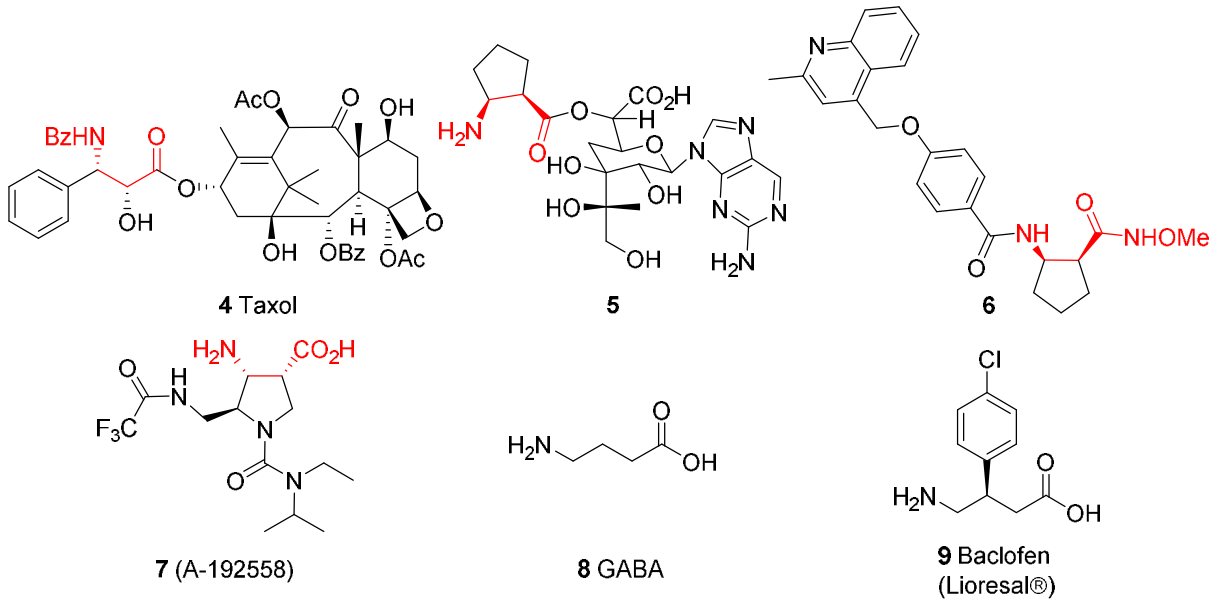


**Figure 1:** Presentation of selected of β- and γ-amino acids.

In particular, conformationally constrained cyclic β- and γ-amino acids have generated great interest in synthetic and medicinal chemistry as they are found in natural products and antibiotics such as amipurimycin (**5**).[13] In comparison to α-amino acids, the additional bonds and dihedral angles in the corresponding β- and γ-analogues result in a higher degree of

conformational freedom.[14] In cyclic residues, the torsion angles are dependent on the geometry of the ring system and are more restricted (Figure 2).[15]

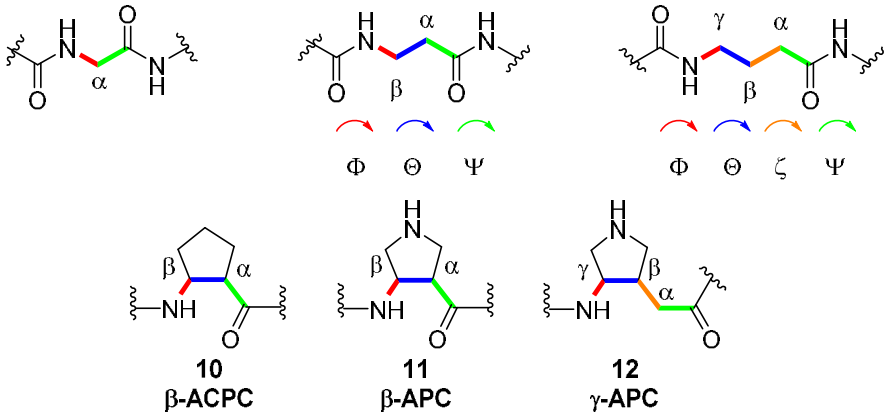


**Figure 2:** Torsion angles in α-amino acid, acyclic β- and γ-amino acid (top) and cyclic β- and γ-amino acid (bottom).

Due to their conformational restrictions and their well-defined geometry, cyclic amino acids are of particular interest in the synthesis of peptidomimetics or foldamers. Foldamers are defined as artificial peptides with strong tendency to adopt a specific conformation.[16] Cyclic amino acids are known to stabilize various secondary structure motifs in synthetic oligomers because of their well-defined geometry and to increase the stability of α-peptides against proteolytic degradation.[17] Aminocyclopentane carboxylic acid **10** (ACPC) represents together with aminopyrrolidine carboxylic acid **11** (APC) a frequently used building block for foldamers synthesis. For instance, *Gellman et al*. used *trans*-ACPC among others for the design of homo-β-peptide **13** and demonstrated that the secondary structure could be controlled by alternation as well as the nature of the used β-amino acids. NMR and X-ray studies of **13** proved that the predicted 12-helical conformation was adopted caused by a 12-membererd ring hydrogen bond system (Figure 3).[16b] *Berlicki et al*. published α,β-alternating foldamer **14** using *cis*-ACPC, which revealed a stable 16/18-helical structure in methanol.[18] Very recently, *Burgess et al*. investigated the cyclization of linear precursors containing APC building blocks towards cyclic peptides such as **15**. They could show, that the efficiency of cyclization was strongly depended on the absolute stereochemistry of APC building block and the (*S*,*S*)-*cis*-APC turned out to be the best.[19]

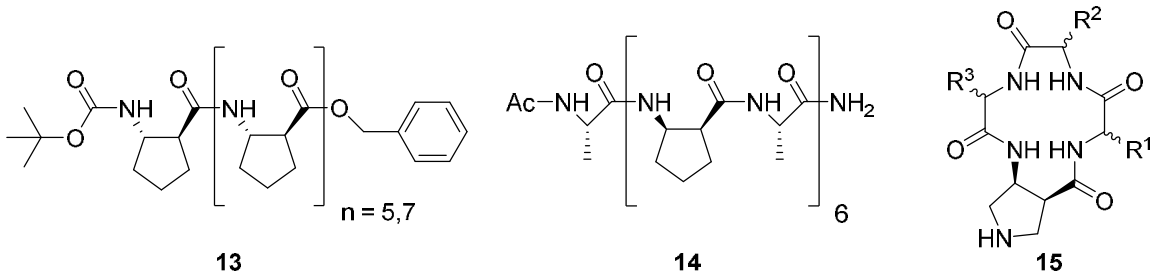


**13** **14** **15**

**Figure 3:** Selection of some ACPC and APC containing peptides.

Since for various applications enantiopure β- and γ-amino acids are required, the development of enantioselective syntheses of β- and γ-amino acids was of great interest in the last twenty years. The probably most prominent and simplest method to get access to β-amino acids displays the synthesis from α-amino acids by an *Arndt-Eistert* homologation (Scheme 2).[20] Activation of the carboxylic acid **16** followed by conversion to the corresponding diazo compound **17** employing diazomethane is the first step toward β-amino acids. Subsequent *Wolff*-rearrangement in the presence of Ag-salts provides the desired β-amino acid **18**.

**Scheme 2:** *Arndt-Eistert* homologation of α-amino acids toward β-amino acids.

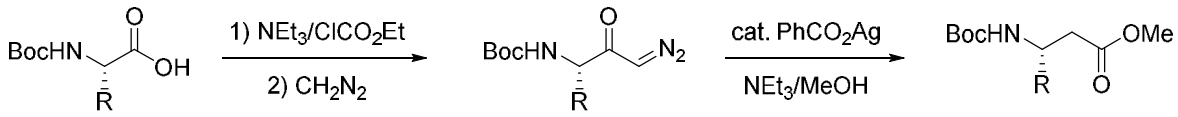


**16** **17** **18**

Continuous improvements and optimization demonstrate the importance of this method till today.[21] The focus of the present thesis is on the enantioselective synthesis and application of *cis*-β- and γ-amino acids based on aminocyclopentane carboxylic acid ACPC (**10**) and aminopyrrolidine carboxylic acid APC (**11** and **12**). Therefore, the following chapters will give an overview of asymmetric synthetic strategies exclusively toward these types of building blocks.[22]

## 1. Synthetic strategies towards aminocyclopentane carboxylic acid

In 1996, one of the first examples of an enantioselective synthesis of ACPC, the so-called cispentacin synthesis, was developed by *Davies et al*. (Scheme 3).[23] This method is based on the conjugate addition of homochiral lithium amide **19** to the unsaturated cyclic ester **20** and gives access to *cis*-β-amino ester **21** in high yields and diastereopurity. Its big advantage is the

facile accessibility of both enantiomers of **21** by employing either the (*R*)- or (*S*)-enantiomer of the lithium amide **19**. Removal of the chiral auxiliary by hydrogenolysis and the *tert*-butyl ester provided *cis*-ACPC **22** in 62% yield over 3 steps in enantiomerically pure form. By diastereoselective epimerization of compound **21** using KO*t*Bu, the corresponding *N*-protected *trans*-ACPC **24** can be easily prepared in 47% yield over 5 steps.[24]

**Scheme 3:** Synthesis of *cis*- and *trans*-ACPC by conjugate addition from α,β-unsaturated ester reported by *Davies at al*.

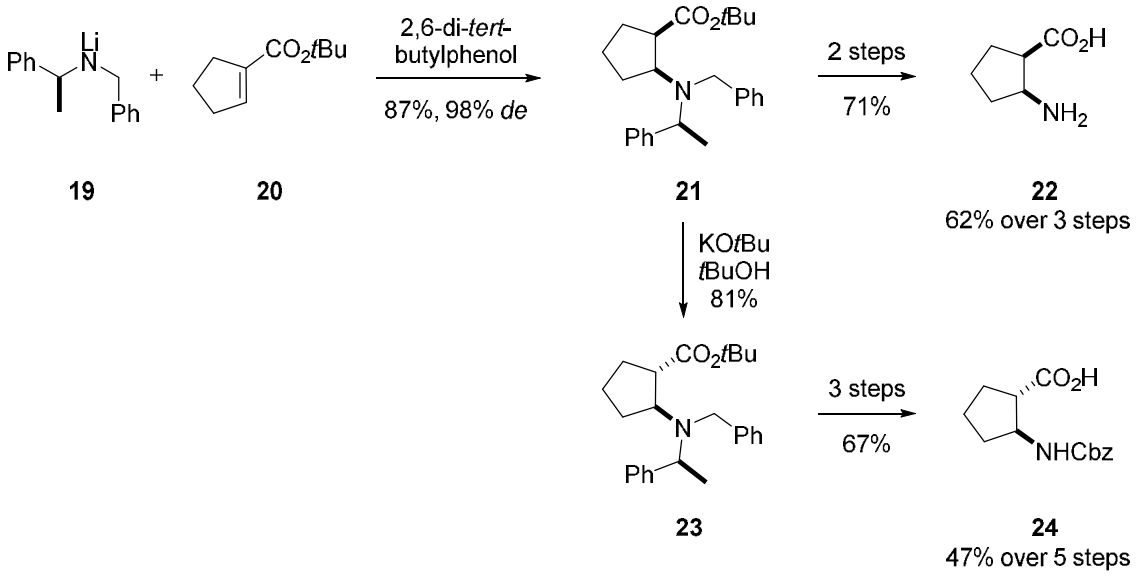


This method is also applicable to a broad variety of acyclic α,β-unsaturated acceptors[25] such as formyl carboxylate **25**, leading to hydroxy-functionalized β-amino ester **26** in a moderate yield of 66% but in excellent diastereoselectivities (Scheme 4).[26] Subsequent transformations of the functional groups provided the free hydroxy β-amino acid **27** in 57% yield over 3 steps in enantiomerically pure form.

**Scheme 4:** Synthesis of hydroxy-functionalized cyclic β-amino acids.

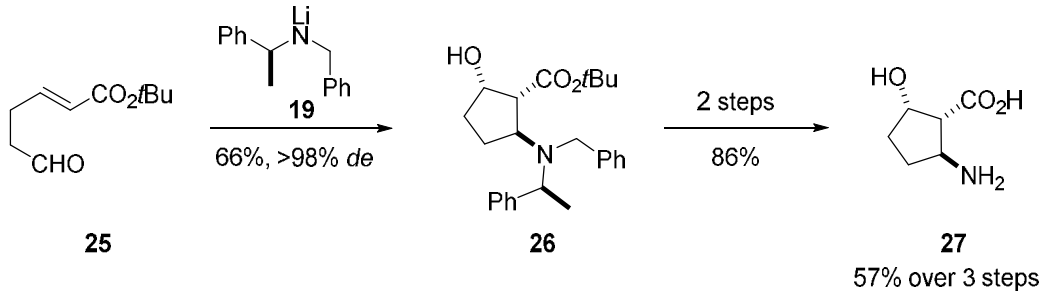


Another rapid and facile procedure for the synthesis of *cis*-ACPC represents the ring-opening transformation of bicyclic β-lactam **30** by *Fülöp et al*. (Scheme 5).[27] Derived from the cycloaddition of chlorosulfonyl isocyanate and cyclopentane **28**, racemic β-lactam **30** can be

converted enzymatically to the enantiopure *cis*-ACPC **22** and the unreacted lactam in high yields each (pathway A). Moreover, the enantiomer (*ent*)-**22** can be also prepared in 96% *ee* out of racemic **32** by acidic lactam ring-opening of **30** followed by enzymatic ethyl ester hydrolysis (pathway B).

**Scheme 5:** Enzymatically β-lactam ring-opening towards *cis*-ACPC by *Fülöp et al.*

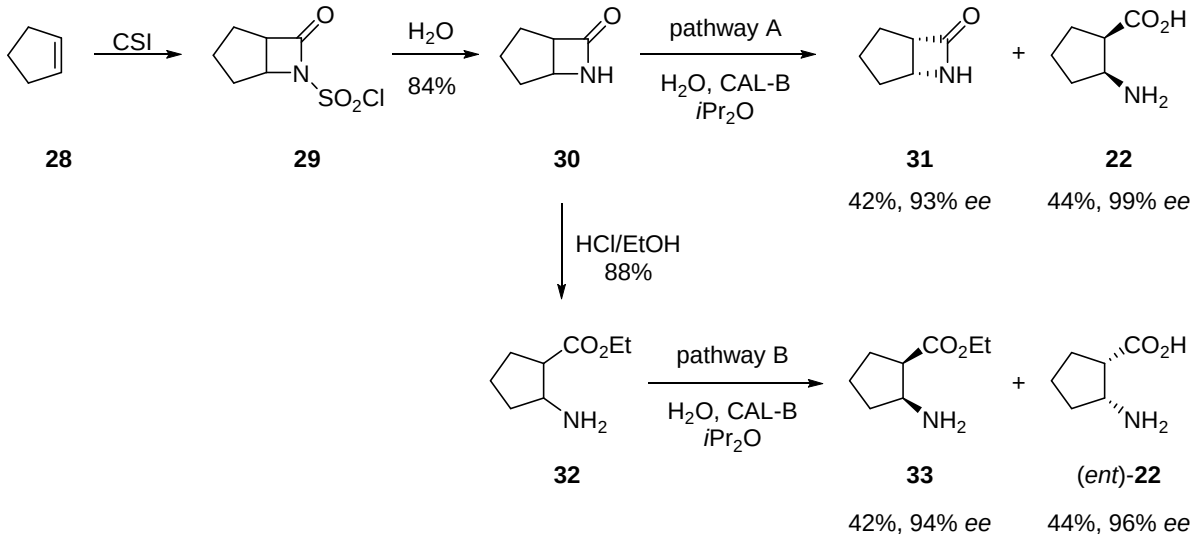


In 2003, *Bolm et al.* developed a three-step cinchona alkaloid mediated asymmetric opening of cyclic *meso*-anhydride **34** in the presence of benzyl alcohol yielding the optically active hemiester **35** with excellent enantioselectivities (Scheme 6). A nice feature of this procedure represents the facile accessibility of both enantiomers of **35** by using either quinine or quinidine. *Curtius degradation* led to the *N*-protected β-amino ester **36** and subsequent recrystallization increased the enantiomeric excess to higher than 99.7%. Hydrogenolysis of the protecting groups furnished cispentacin **22** in 67% yield over 3 steps.[28]

**Scheme 6:** Three-step quinine mediated desymmetrization by *Bolm et al.*

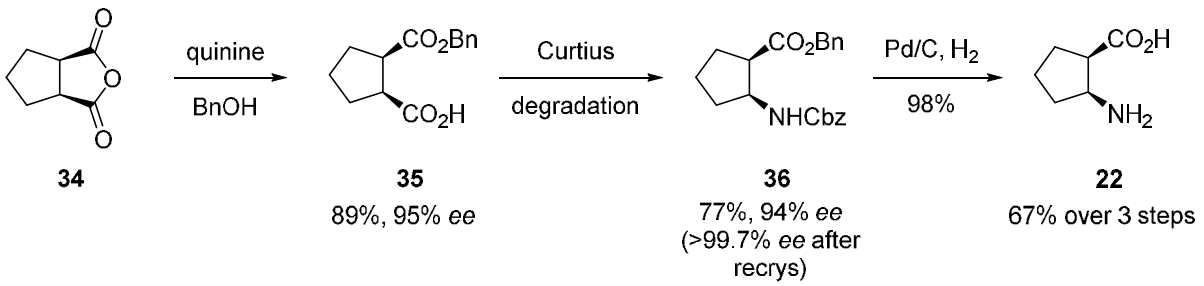


A further interesting approach towards to enantiopure *cis*-ACPC was reported by *Aggerwal et al.* in 2003.[29] Herein, the first key step was the conversion of dithiane **37** toward phosphonate dioxide **38** via asymmetric sodium periodate with in >98% *ee*. Subsequent *Horner-*

*Wadsworth-Emmons* olefination gave dithioacetal **39**, which was used in the following for an intramolecular nitrone cycloaddition (**40**) to obtain **41**. By reductive cleavage of N-O bond in isoxazolidine **41** and removal of the dithioacetal unit *cis*-ACPC **22** was prepared in 10% over 6 steps.

**Scheme 7:** Synthesis of *cis*-ACPC from enantiomerically pure ketene dithioacetal reported by *Aggerwal et al*.

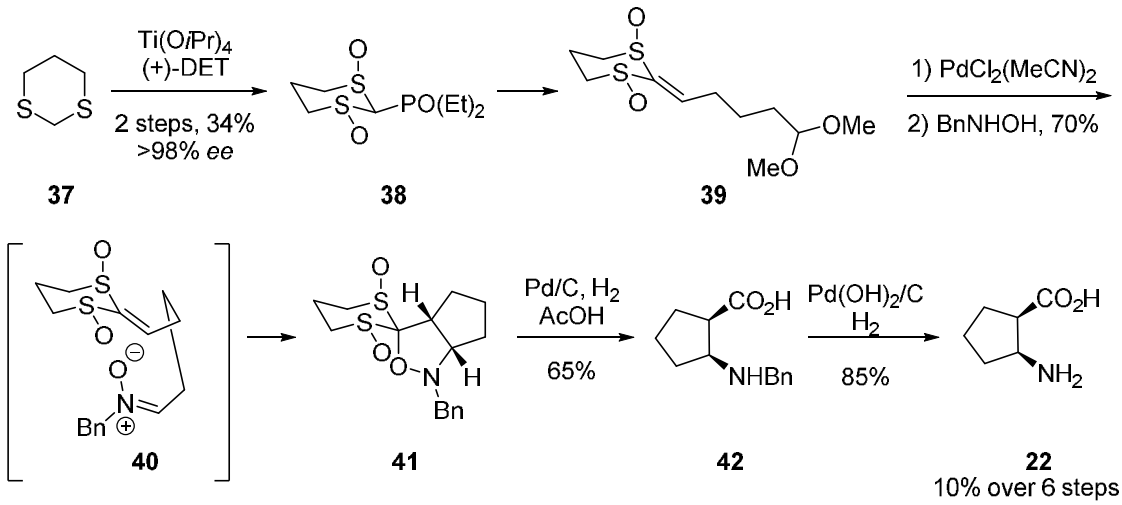


In 2013, *Pou et al*. developed an organocatalytic tandem Michael addition/cyclization with cyclopentene-2-carbaldehyde **43** and *N*-(benzyloxycarbonyl)hydroxylamine **44** using diphenylprolinol trimethylsilyl ether **45** as chiral amine catalyst. Isoxazolidinone **46** was obtained in 98% yield with an enantiomeric excess of 96%, which was further transformed to the desired cispentacin via oxidation with pyridinium dichromate and reductive ring-opening of the corresponding ketone over 2 steps and 95% yield.[30]

**Scheme 8:** Organocatalytic tandem Michael addition/cyclization reaction reported by *Pou et al*.

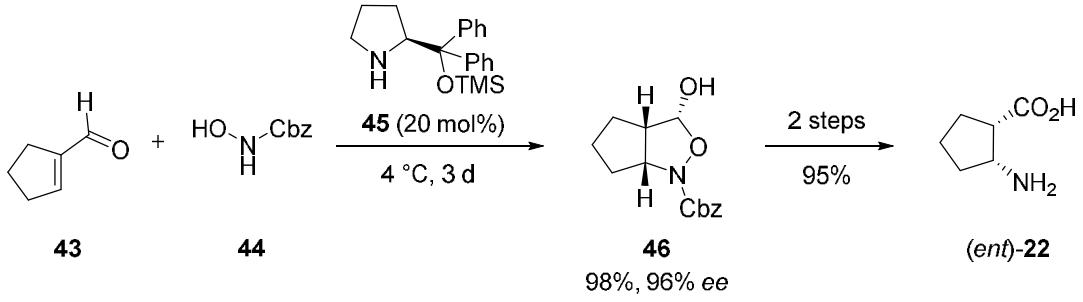


*Gardiner et al*. reported a versatile ring-closing metathesis approach by applying the chiral amino acid pool towards *trans*-ACPC starting from readily available (*S*)-methionine **47** (Scheme 9).[31] The α-amino acid was converted to optically pure β-amino ester **48** involving allylation and *Arndt-Eistert* homologation in 3 steps. By ring-closing metathesis employing

Grubbs´ II catalyst the *N*-protected *trans*-ACPC **49** was finally synthesized in 34% over 4 steps.

**Scheme 9:** Construction of *trans*-ACPC from (*S*)-methionine reported by *Gardiner et al*.

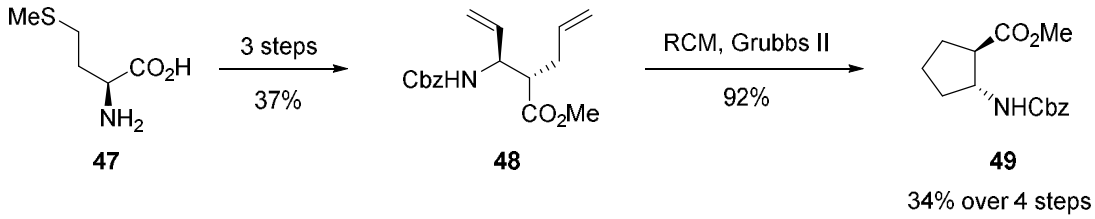


**47** **48** **49**

34% over 4 steps

## 2. Synthetic strategies towards aminopyrrolidine carboxylic acid

Pyrrolidine derived β-amino acids attracting growing interest since they have been utilized together with ACPC as building blocks for the construction of artificial peptides with antimicrobial activities.[32] The conjugate addition method of *Davies* described above (Scheme 3) also displays an efficient method for the construction of pyrrolidine derived β-amino acids (Scheme 10).[33] For this purpose, benzyl protected *N*-heterocyclic α,β-unsaturated acceptor **50** was a suitable starting material and *cis*-β-amino ester **51** was obtained in 79% yield and an excellent diastereomeric excess. The corresponding *trans*-isomer **53** can be synthesized in analogy to its carbocyclic derivative **23** by epimerization at C-1 in the presence of KO*t*Bu in refluxing *t*BuOH. Reductive cleavage of the benzyl groups and *tert*-butyl ester hydrolysis yielded the enantiopure *cis*-APC **52** in 77% over 3 steps and the *trans*-APC **54** in 56% over 4 steps, respectively.

**Scheme 10:** Synthesis of *cis*- and *trans*-ACPC by conjugate addition from α,β-unsaturated ester reported by *Bunnage at al.*

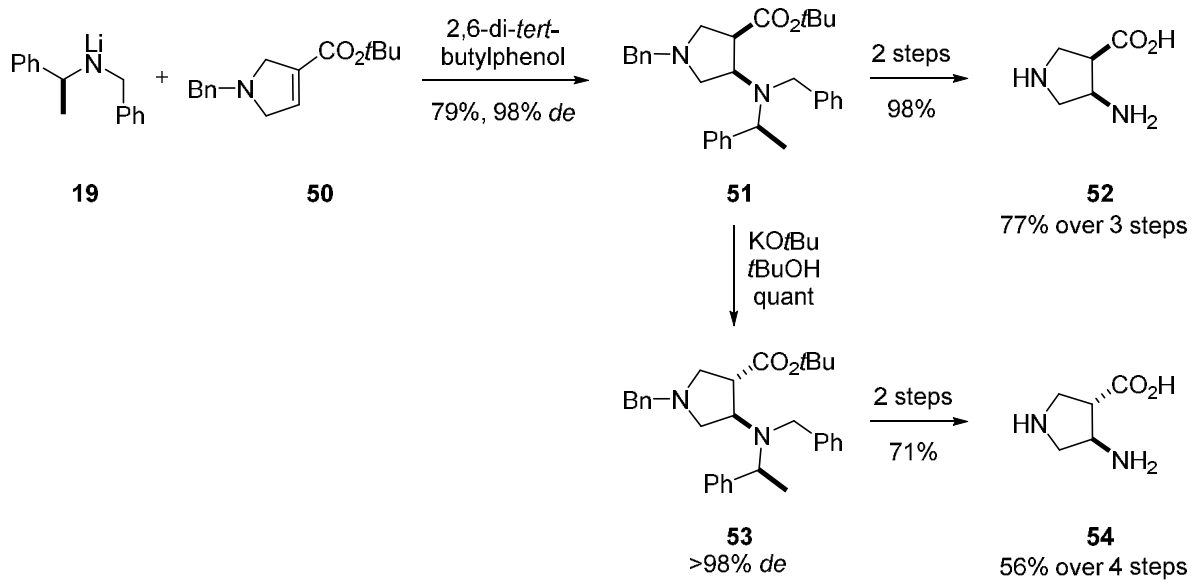


With their cispentacin synthesis in 2003, *Aggerwal et al*. demonstrated that chiral dithio ketenes are also applicable to get access to *cis*-APC **52** (Scheme 11, compare Scheme 7). This method displayed the first asymmetric synthesis of desired *cis*-APC **52**.[29] Dithio ketene **57**, derived from chiral phosphonate **38** and amino acetal **56**, was cyclized to fused isoxazoline **58** by a 1,3-intramolecular cycloaddition using *p*TsOH and BnNHOH. Isoxazoline ring-opening and removal of the *N*-protecting groups furnished *cis*-APC **52** in 20% yield over 9 steps.

**Scheme 11:** Synthesis of *cis*-APC from enantiomerically pure ketene dithioacetal reported by *Aggerwal et al*.

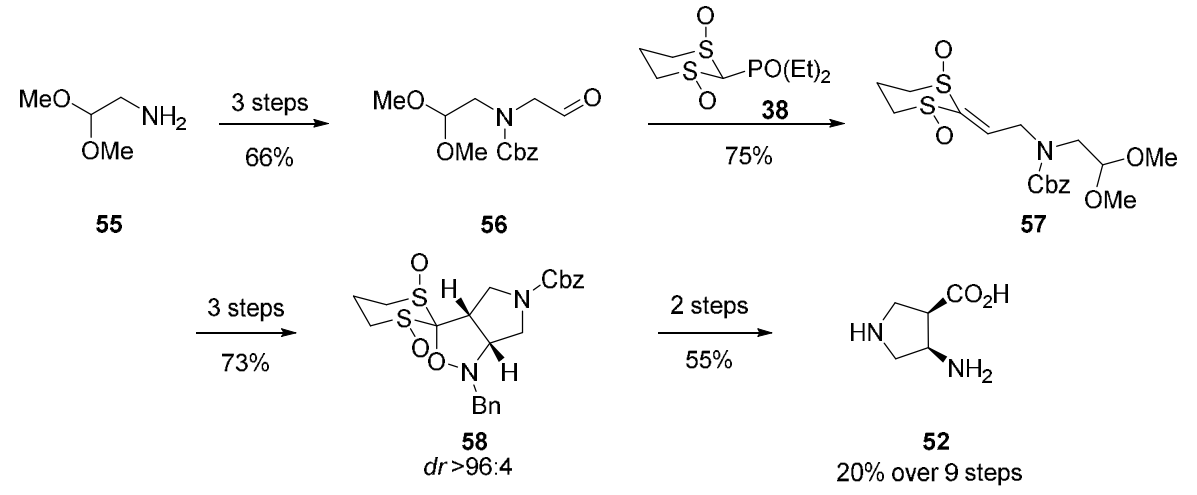


In the same year, *Hanselmann et al.* reported a methodically similar synthetic route towards *cis*-APC.[34] For the construction of isoxazolines **62** and **63**, a metal induced chelation-controlled 1,3-dipolar cycloaddition was the key step. For this, aldehyde **59** was condensed with chiral hydroxylamine **60** toward nitrone **61** resulting in a highly diastereoselective

isoxazoline formation. After separation of the diastereomers, reductive ring-opening and oxidation reaction orthogonally protected *cis*-APC **64** was obtained in 49% over 4 steps.

**Scheme 12:** Isoxazoline based synthetic approach towards *cis*-APC by *Hanselmann et al*.

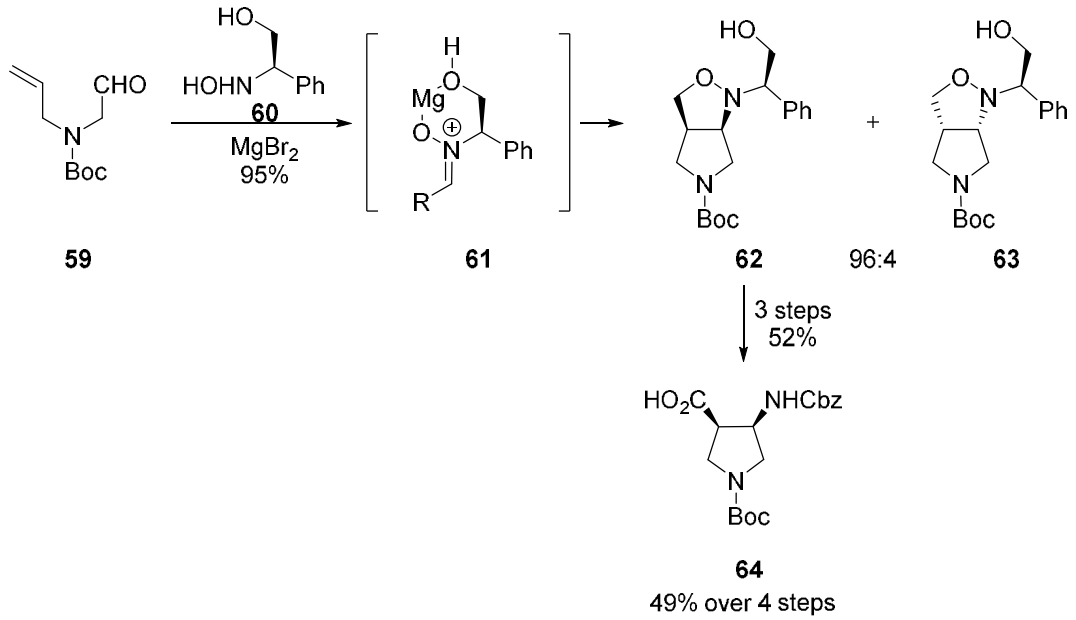


## 3. Synthetic strategies towards carbocyclic and pyrrolidine derived γ-amino acids

The great potential of acyclic as well as cyclic γ-amino acids for the synthesis of γ-peptides[15b,35] or heterogeneous backbone foldamers[36] was already demonstrated in various literature reports. In particular, a great variety of contributions were given by *Fleet et al*.,[37] *Kessler et al*.,[38] *Sharma et al*.[39] *Gellman et al*.[40] or *Aitken et al*.[41] However, a closer look to the literature reveals, that five-membered ring γ-amino acids display an minority and the majority of utilized γ-amino acids are acyclic, four- or six-membered rings or carbohydrate derived sugar amino acids. Some selected syntheses for five-membered ring γ-amino acids are presented hereinafter.

Recently, *Gellman et al*. reported an enantioselective synthesis for *trans*-γ-aminomethyl cyclopentane carboxylic acid (γ-AMCP) in multigram quantities and its utilization as building blocks for α,γ-peptides (Scheme 13).[42] The stereoselective Michael addition of nitromethane to aldehyde **43** catalyzed by **45** and benzoic acid furnished the nitro alcohol **66** in 95% yield and >99% enantiomeric excess. Subsequent reduction of the nitro group and oxidation of the alcohol to the corresponding carboxylic acid provided the enantiopure γ-AMCP **66** within

24% over 5 steps. However, to the best of our knowledge, synthetic approach toward the *cis*-isomer of **66** was not reported yet in the literature.

**Scheme 13:** Organocatalytic Michael addition as key step towards γ-AMCP by *Gellman et al.*

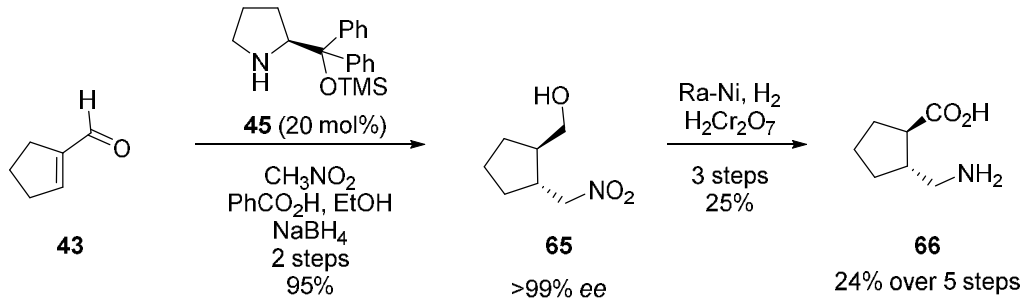


In their studies about self-assembling cyclic peptides, *Granja et al.* employed conformationally restricted γ-aminocyclopentanecarboxylic acid (γ-Acp) **70** which was derived form commercially available γ-lactam (±)-**67** (Scheme 14).[43] The resolution with (*R*)-α-methylbenzylamine (MBA) after the hydrolysis of compound **67** led to the Boc protected cyclopentene **68**. Finally, hydrogenation of the double bond produced the desired γ-amino acid in 69% yield over 4 steps and 97% *ee*. Otherwise, **70** can also be obtained by resolution of the fully saturated racemic γ-amino acid **69**. However, for the crucial resolution step, no yield was reported in the literature.

**Scheme 14:** Asymmetric resolution of racemic lactam towards γ-Acp reported by *Granja et al.*

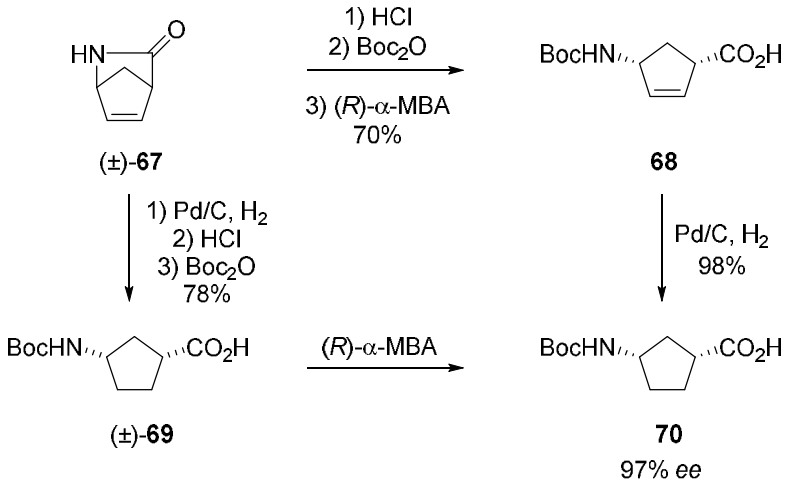


In 2012, *Kanger et al.* developed a thiourea-catalyzed cascade reaction to get access to trisubstituted pyrrolidine derivatives (Scheme 15).[44] The selectivity of this reaction was highly depended on the *N*-protecting group of the crotonate **71**. While benzyl protected derivatives of **71** were obtained in high diastereomeric ratios but with poor enantiopurity, tosyl protected pyrrolidines could be isolated in a moderate diastereomeric ratio but with high

enantiomeric excess in the case of the major isomer **74** and modest enantiopurity for the minor isomer **75**. By this method, pyrrolidine derived γ-amino acid ester **76** was yielded in 58% over 2 steps.

**Scheme 15:** Thiourea-catalyzed synthesis of trisubstitued pyrrolidines reported by *Kanger et al.*

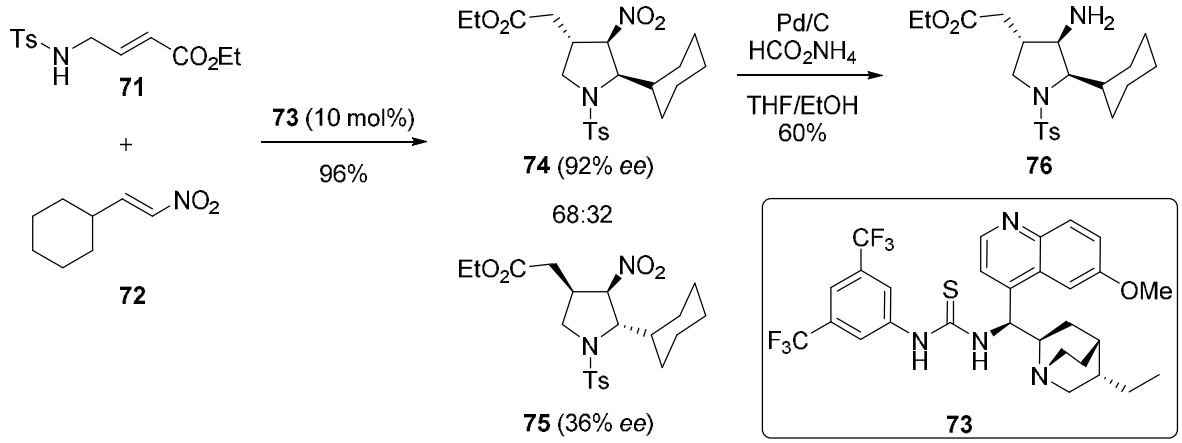


As mentioned above, this review will only give an overview of the most relevant syntheses for building blocks employed in this work. In particular, the related derivatives of these building blocks have aroused enormous interest in chemistry and drug research, resulting in a huge amount of publications in the last twenty years. All in all, carbocyclic and heterocyclic five-membered ring β- and γ-amino acids display important and interesting building blocks for a great variety of applications. In the present thesis, the five-membered ring β-amino acids ACPC and APC will be utilized as a central building block in short- to longer chain peptides. Moreover, due to the very small amount of literature known procedures for the synthesis of *N*-heterocyclic γ-amino acids such as **12**, a new enantioselective method should be developed to get access to this type of γ-amino acids.

# B. Main Part

## 1. Synthesis of APC and ACPC building blocks

The first part of the present thesis deals with the application of literature-known cyclic β-amino acids aminopyrrolidine carboxylic acid **79** (APC) and aminocyclopentane carboxylic acid **80** (ACPC) in organocatalysis and peptides. For this application, enantiomerically pure building blocks are essential. The core structure of the *cis*-APC-**78**[33] and *cis*-ACPC-**21**[24] building blocks was built up by employing the method of *Davies et al*.[23] (Scheme 16). Herein, the conjugate addition of a homochiral lithium amide **19** to a α,β-unsaturated acceptor **77**/**20** plays the key role. This approach guarantees a highly enantioselective and diastereoselective outcome of the reaction, which is crucial for the intended applications of the building blocks. Moreover, depending on the applied enantiomer of **19**, access to both enantiomers of the desired building blocks is possible. To get access to orthogonally protected building blocks **79** and **80**, well-established procedures in our group were employed.[45,46]

**Scheme 16:** Key step in the synthesis of APC and ACPC building blocks according to *Davies et al*. towards orthogonally protected building blocks **14** and **15**.

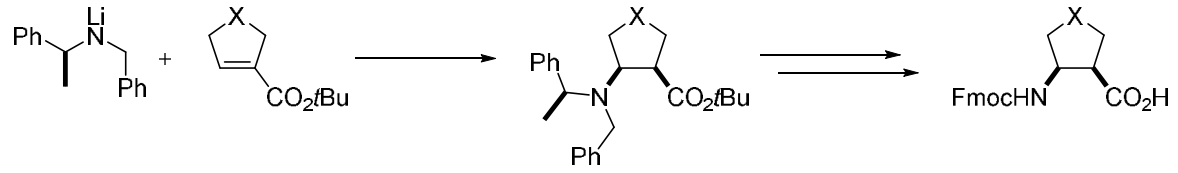


**19** **77** X = *N*-Boc, **20** X = $CH_2$ **78** X = *N*-Boc, **21** X = $CH_2$ **79** X = *N*-Boc, **80** X = $CH_2$

The synthesis of APC-**79** starts from glycine methyl ester **81** (Scheme 17). After Boc-protection, the cyclization with KO*t*Bu and *tert*-butyl acrylate provided the potassium salt **83**, which was subsequently reduced with $NaBH_4$ to the corresponding alcohol **84**. For the dehydration step, a *Mitsunobu* type reaction by the treatment of **84** with $PPh_3$ and DIAD was initially carried out. Due to the scale of 375 mmol, the toxicity and the cost of DIAD, a one pot tosyl protection of the alcohol 84, followed by elimination of the tosylate with pyridine as base and solvent was performed. Unfortunately, this alternative method revealed preparative limitations of the scale and delivered the desired product **77** only in 17% yield, although first test reactions provided yields up to 70%.[45] In summary, the α,β-unsaturated acceptor **77** was obtained in 11% yield over four 4 steps starting from glycine **81** (lit.[46] 39%).

**Scheme 17:** Synthesis of **77** towards APC building blocks.

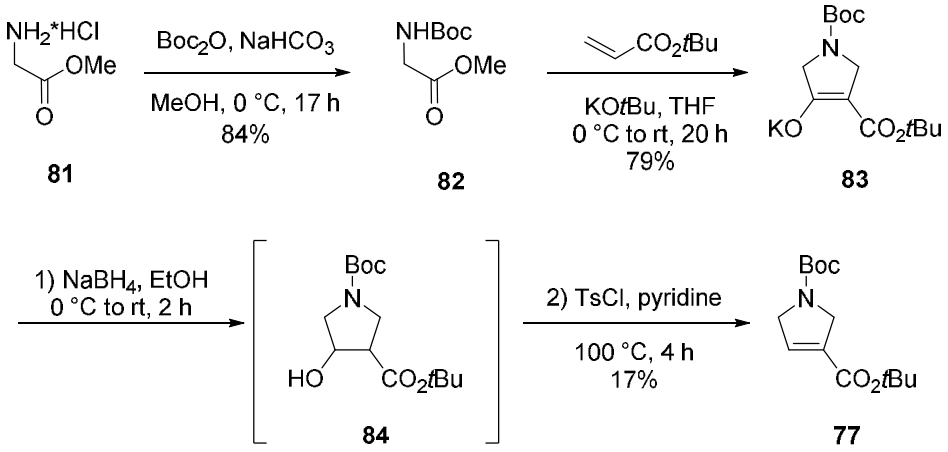


The addition of homochiral lithium amide **19** to the α,β-unsaturated acceptor **77** is the key step in synthetic route towards APC building blocks (Scheme 18). Depending on the applied chiral amine **19**, the absolute stereochemistry of the building blocks will be set in this step. The formation of enantio- and diastereopure addition-products was achieved by performing the reaction under low-temperature conditions at -95 °C and the use of the weak and bulky proton source 2,6-di-*tert*-butyl-4-methylphenol (BHT). The synthesis of the APC **78** was performed on a 12 times bigger scale than in literature reported[33] (3.72 mmol *vs.* 43 mmol) and the desired product was obtained in 25% yield (lit. 46%). The occurrence of elimination products caused by γ-deprotonation competes with the lithium amide addition, reduced the yield. This fact is also discussed in the literature and may be attributable to the activating and directing effect of the *N*-Boc protection.[47] However, suggestions how to prevent this elimination were not reported.[33]

**Scheme 18:** Synthesis of APC **79**.

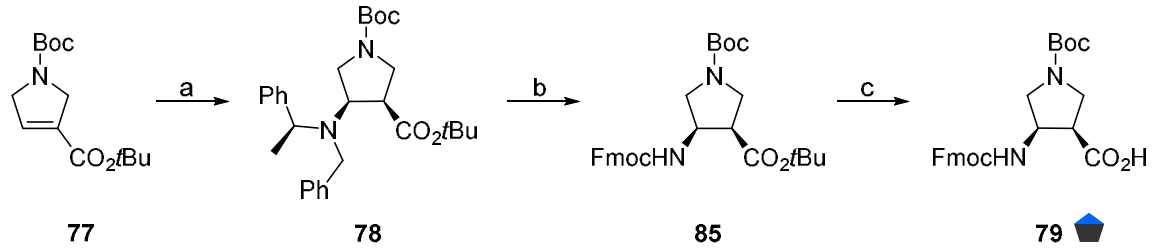


**Reagents and conditions**: (a) i) (*S*)-**19**, THF, -95 °C to -78 °C, 3h; ii) BHT, THF, -95 °C, 25%, *de* >99%; (b) i) $H_2$ (20 bar), $Pd(OH)_2/C$, AcOH, MeOH, rt, 24 h; ii) FmocOSu, $NaHCO_3$, dioxane/water, 0 °C to rt , 24 h, 86% over two steps; (c) i) TFA, DCM, rt, 24 h, quant.; ii) $Boc_2O$, $NaHCO_3$, dioxane/water, 0 °C to rt, 48 h, 88% over 2 steps.

Going forward with the desired APC **79**, further transformations of **78** were necessary. The benzyl groups on the amine were removed by catalytic hydrogenolysis in the autoclave,

followed by Fmoc protection to obtain **85** in 86% over 2 steps (lit.[46] 92%). The required free carboxylic acid in APC **79** was generated by hydrolysis of the *tert*-butyl ester with trifluoroacetic acid, which also caused cleavage of the Boc group. After Boc reprotection, the desired APC **79** was obtained in 88% over 2 steps (lit.[46] 51%) and 19% over 5 steps starting from **77** (lit.[46] 15%).

The addition product (*ent*)-**78** was prepared from **77** in analogy to its enantiomer by using (*R*)-**19** as the chiral amine in 31% yield (Scheme 19). Following the same transformations of the functional groups, (*ent*)-APC **79** was obtained in 16% yield over 5 steps.

**Scheme 19:** Synthesis of (*ent*)-APC **79**.

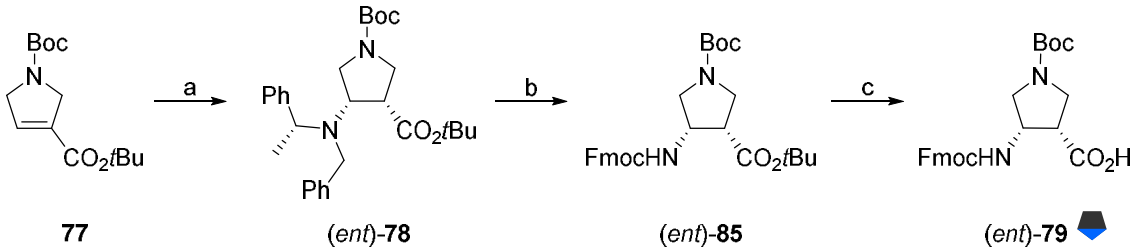


**Reagents and conditions**: (a) i) (*R*)-**19**, THF, -95 °C to -78 °C, 3h; ii) BHT, THF, -95 °C, 31%, *de* >99%; (b) i) $H_2$ (20 bar), $Pd(OH)_2/C$, AcOH, MeOH, rt, 24 h; ii) FmocOSu, $NaHCO_3$, dioxane/water, 0 °C to rt , 24 h, 59% over two steps; (c) i) TFA, DCM, rt, 24 h, quant.; ii) $Boc_2O$, $NaHCO_3$, dioxane/water, 0 °C to rt, 48 h, 85% over 2 steps.

To avoid the undesired deprotection of the Boc group during hydrolysis of **85** to **79**, alternative methods have been explored.[a)] A closer look at the literature revealed that this could be quite challenging. Nevertheless, two promising methods were found and tested. Aplying *Montmorillonite KSF* as an acidic ion exchange resin[48] was not successful: no conversion of the starting material was observed. The second attempt was the use of $I_2/H_2O$ in refluxing acetonitrile by *in situ* generation of HI, advertised as a mild deprotection method.[49] Indeed, under these conditions, a selective *tert*-butyl ester cleavage under preservation of the Boc group was possible but only in poor yields (Scheme 20). Also, much longer reaction times were necessary compared to those reported in the literature. Taking these poor results into account, the selective *tert*-butyl ester cleavage was not explored further, and the Boc deprotection and subsequent reprotection sequence was accepted given the satisfying yields obtained this way.

[a)] Results partially taken from Bachelor thesis of A. Röther (supervised by T. Ertl).

**Scheme 20:** Attempt for selective *tert*-butyl hydrolysis to preserve of the Boc group.

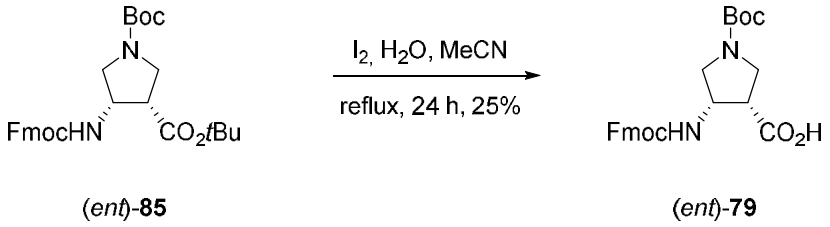


(*ent*)-**85** (*ent*)-**79**

For the synthesis of the ACPC building blocks, the same method was applied like for the APC building blocks. For the construction of the cyclopentane **20** and the subsequent addition of the chiral amines already literature-known procedures were available, allowing to get access to the desired compounds in multi-gram quantities. First, the cyclopentane core structure **88** was built up by the cyclization of di-*tert*-butyl-ester **87** (Scheme 21). After reduction of the keto group by $NaHB_4$, the dehydration was carried out by mesylation of the alcohol followed by elimination with DBU. This way, **20** was obtained in 39% yield over 5 steps from **86** (lit.[24] 39%).

**Scheme 21:** Synthesis of **20** towards ACPC building blocks.

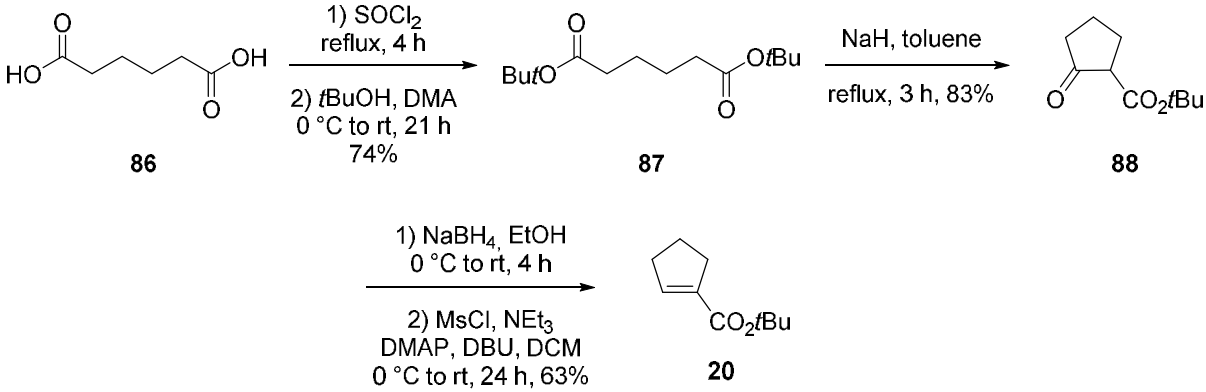


**86** **87** **88** **20**

In case of the ACPC building blocks, the addition of the chiral amine to **20** was performed in analogy to the APC building blocks (Scheme 22). This time, no byproducts during the addition of the chiral amine were observed and **21** was obtained in 88% yield (lit.[24] 87%). Furthermore, the same transformations of the functional groups as for the APC building blocks were required. Removal of the benzyl groups of **21** by hydrogenolysis was followed the *tert*-butyl ester hydrolysis. The corresponding free amino acid was subsequently submitted to Fmoc-protection to obtain the desired building block **80** in 19% yield over 4 steps (lit.[24] 11%).

**Scheme 22:** Synthesis of ACPC **80**.

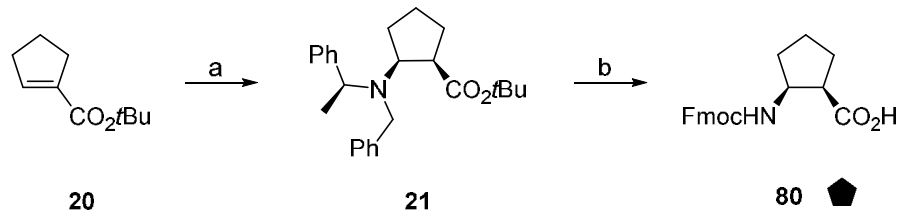


**Reagents and conditions**: (a) i) (*S*)-**19**, THF, -95 °C to -78 °C, 3h; ii) BHT, THF, -95 °C, 88%, *de* >99%; (b) i) $H_2$ (15 bar), Pd/C, AcOH, MeOH, rt, 22 h; ii) TFA, DCM, rt, 24 h; iii) FmocOSu, $NaHCO_3$, dioxane/water, 0 °C to rt, 48 h, 21% over 3 steps.

(*ent*)-**80** was synthesized in the same way as its enantiomer and the addition product (*ent*)-**21** was obtained in 80% yield with excellent diastereomeric excess. After transformation of the functional groups, (*ent*)-**80** was obtained in 14% yield over four steps (Scheme 23).

**Scheme 23:** Synthesis of (*ent*)-**80**.

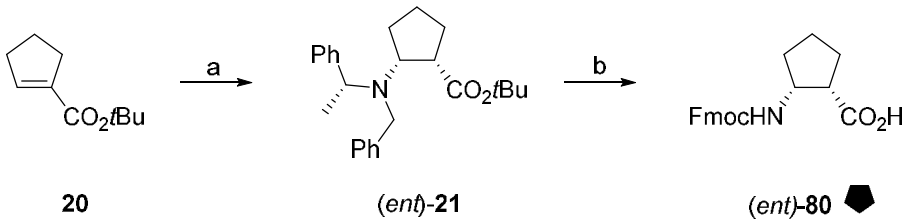


**Reagents and conditions**: (a) i) (*R*)-**19**, THF, -95 °C to -78 °C, 3h; ii) BHT, THF, -95 °C, 80%, *de* >99%; (b) i) $H_2$ (15 bar), Pd/C, AcOH, MeOH, rt, 22 h; ii) TFA, DCM, rt, 24 h; iii) FmocOSu, $NaHCO_3$, dioxane/water, 0 °C to rt, 48 h, 18% over 3 steps.

Having APC and ACPC in hand in multi-gram quantity, their utilization in (peptide-related) organocatalysis and peptides was investigated and will be discussed in the following chapters.

# 2. APC building block in organocatalysis

## 2.1 β-Proline in asymmetric *anti*-Mannich-Type Reactions

The publication of two pioneering articles in 2000, discussing the utilization of cyclic chiral secondary amines as efficient catalysts for the functionalization of carbonyl compounds, inspired an explosion of research in the field of organocatalysis. *List et al.* reported the (*L*)-proline catalyzed asymmetric Aldol reaction between acetone and various aldehydes.[50] Almost simultaneously, *MacMillan et al.*[51] published the first amino-catalyzed Diels-Alder-reaction and demonstrated the activation of α,β-unsaturated aldehydes by an imidazolidinone-based catalyst.[52] Since this year a colossal amount of organocatalysts has been developed and applied in various organocatalytic reactions.[53]

The asymmetric Mannich and Mannich-type reaction represent an important method for the C-C bond formation, providing access to enantiomerically enriched aminocarbonyl derivatives. The abundant occurrence of nitrogen in drugs or natural products increased the popularity of the Mannich reaction.[54] The first proline-catalyzed three component Mannich reaction was discovered by *List* in 2000 and since then there have been intensive studies towards the development of more efficient catalysts.[55] In the last 15 years, various metal catalysts such as Pd, Zn, Cu and Y as well as metal free proline-[56] or cinchona alkaloid based organocatalysts[57,58] were applied in Mannich and Mannich-type reactions. Since α-amino acid derivatives can be built up by α-imino esters, the *anti*-Mannich reaction and applicable catalysts are gaining more focus.[59,60]

In the case of pyrrolidine-related catalysts, the position of the acidic group on the ring is essential for the diastereoselectivity of the Mannich reaction (Scheme 24). Typically, the *syn*-isomer is obtained, if α-proline **91** was applied. The superior *trans*-enamine is forming the transition state **92** and the *re* face of the enamine reacts with the *si* face of the imine. However, the *anti*-isomer can be synthesized by the use of the isomeric β-proline **94**. Therefore, the *syn*-enamine is forming properly positioned transition state **95** and the proton transfer occurs from the acid at the 3-position.[59,60]

**Scheme 24:** *Syn* and *anti*-dependency on the chosen catalyst in Mannich reactions reported by *Barbas et al.*[59]

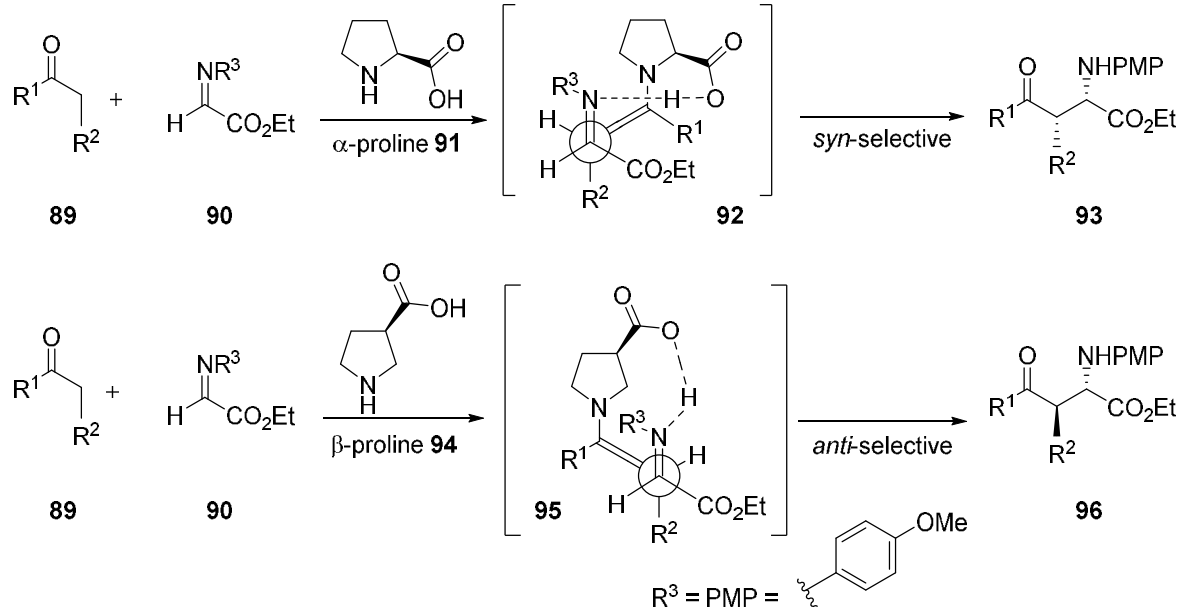


*Barbas et al.*[59,60] already employed β-proline catalyst **94** successfully in *anti*-Mannich reactions for ketones and aldehydes with excellent yields and diastereo- and enantioselectivities (Figure 4). In contrast, catalyst **97** was ineffective for the conversion of ketones contrary to aldehydes because of the unfavorable steric interaction of the enamine with the methyl group in position 5. In the previous chapter, the synthesis of APC building blocks was described. An intermediate of the synthetic sequence, the addition product (*ent*)-**78** already contains the core structure of β-proline **94**. (*ent*)-**78** also contain two benzyl groups at position 4 of the pyrrolidine ring. This was thought to be beneficent for catalysis in two ways: on the one hand, the increased steric bulk could lead to higher selectivities (Figure 4) while on the other hand, being in 4-position should not have a significant detrimental effect as in the aforementioned 5-position.

**Figure 4:** Comparison of addition product (*ent*)-**78** with literature catalysts **94** and **97** and proposed preferred transition state of (*ent*)-**78**.

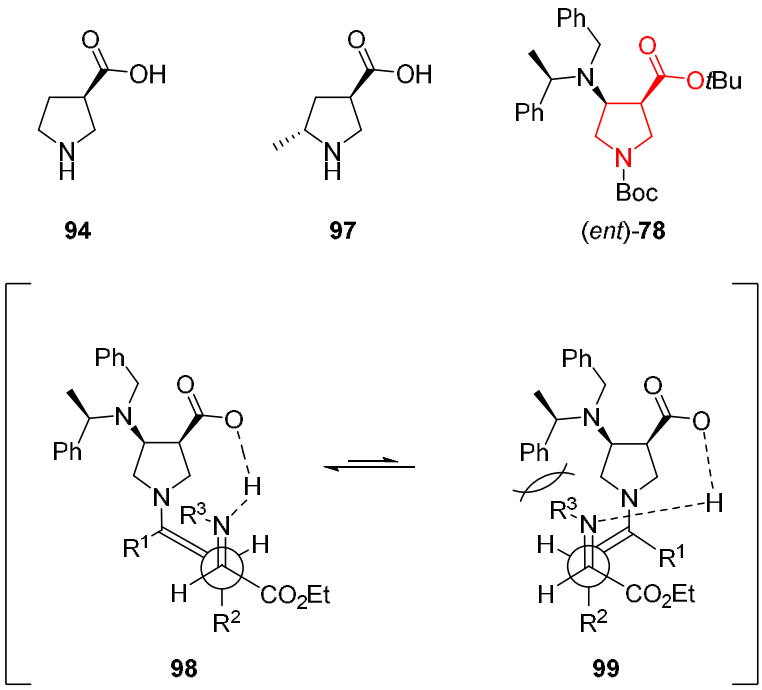


Also, the phenyl groups would increase the lipophilicity of the catalyst, improving its solubility in a broader variety of organic solvents.[61] Due to these considerations, it was envisioned to submit this new β-proline derivative to *anti*-Mannich type reactions to evaluate its catalytic activity.

## 2.2 Synthesis of the β-proline derivative and its catalytic activity in the *anti*-Mannich reaction

With the addition product (*ent*)-**78** in hand, only the *tert*-butyl ester and the Boc group needed to be removed to obtain the free β-proline derivative (*ent*)-**100** as its TFA salt. The counter ion was removed by ion exchange chromatography which unfortunately decreased the yield of the desired catalyst dramatically. It was found, that the benzyl groups of the catalyst are not stable against aqueous ammonia which was initially used for eluation of the catalyst from the ion exchange resin. Nevertheless, the desired β-proline derivative (*ent*)-**100** was isolated in 17% yield (Scheme 25).

**Scheme 25:** Synthesis of β-proline derivative (*ent*)-**100**.

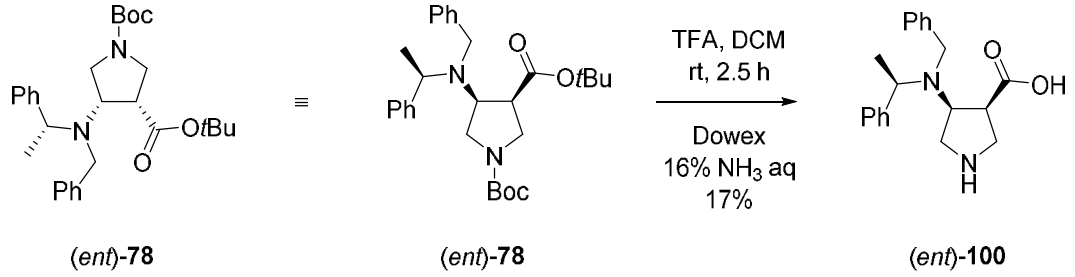


(*ent*)-**78** (*ent*)-**78** (*ent*)-**100**

As benchmark reaction, the indirect *anti*-Mannich reaction between diethyl ketone **104** and imine **103** was chosen as it is well studied in the literature.[59,60] The required imine **103** was synthesized out of ethyl 2-oxoacetate **101** and 4-methoxyaniline **102** in 45% yield (Scheme 26).

**Scheme 26:** Synthesis of imine **103** for the indirect *anti*-Mannich test reaction.[59]

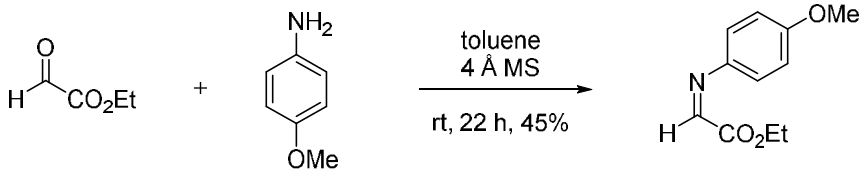


**101** **102** **103**

With imine **103** in hand, different solvents were examined (Table 1). First results proved that the new β-proline derivative (*ent*)-**100** is indeed capable of catalyzing *anti*-Mannich reactions. In contrary, literature catalyst **97** (entry 1) was almost unreactive in the conversion of ketones. But yields in DMSO were low and could not be increased by longer reaction times (Table 1, entry 3 *vs.* 4). Nevertheless, the best diastereoselectivities were achieved in DMSO and were quite comparable to the literature results (entry 2). However, changing the solvent to protic solvents like *i*PrOH or MeOH improved the yields up to 21%. The best yield of *anti*-Mannich product was achieved by using the TFA salt of the catalyst but accompanied with the dramatic decrease of diastereoselectivity (entry 7). It seems that the catalytic amount of acid supports the conversion of the imine but with poor selectivity. Even the increased lipophilicity of the catalyst did not lead to an improvement of the yield or the selectivity in DCM (entry 10). A plausible explanation for the slow conversion of (*ent*)-1**00** could be the sterical interaction of the benzyl groups similar to the methyl group in catalyst **97**. Another reason for the decreased catalytic activity could be the additional backbone nitrogen, which might be involved in hydrogen bonding of the intermediate and may interrupt the proton transfer in catalytic step (Figure 5).

**Table 1:** Solvent screening and evaluation of catalyst (*ent*)-**100** in *anti*-Mannich reaction.[b]

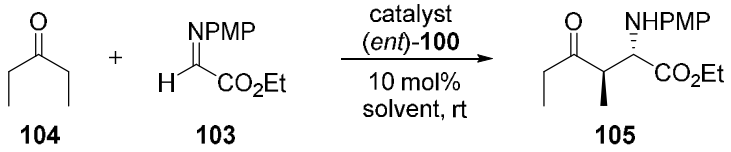


104 103 105

| entry | catalyst | solvent | time (h) | yield [a] (%) | *dr* [b] (*anti*/*syn*) | *ee* [c] (%) |
|---|---|---|---|---|---|---|
| 1[d] | **97** (20 mol%) | DMSO | 72 | <10 | n.d. | n.d. |
| 2[e] | **91** (10 mol%) | *i*PrOH | 20 | 91 | 97:3 | 97 |
| 3 | (*ent*)-**100** | DMSO | 23 | 13 | 88:12 | 67 |
| 4 | (*ent*)-**100** | DMSO | 65 | 10 | 93:7 | 70 |
| 5 | (*ent*)-**100** | DMSO/*i*PrOH (1:1) | 65 | 9 | 78:22 | 53 |
| 6 | (*ent*)-**100** | *i*PrOH | 23 | 20 | 82:18 | 54 |
| 7[f] | (*ent*)-**100** | *i*PrOH | 72 | 44 | 51:49 | n.d. |
| 8 | (*ent*)-**100** | MeOH | 23 | 21 | 74:26 | n.d. |
| 9 | (*ent*)-**100** | THF | 23 | 22 | 56:44 | n.d. |
| 10 | (*ent*)-**100** | DCM | 23 | 21 | 65:35 | n.d. |

a) isolated yield (containing *anti*- and *syn*-diastereomers); b) determined by $^1$H NMR and/or chiral HPLC; c) determined by chiral HPLC; d) taken from ref[59]; e) taken from ref[59]; f) TFA-salt of the catalyst.

In summary, the new β-proline derivative (*ent*)-**100** did not produce results as well as β-proline catalyst **94** in *anti*-Mannich reactions. Moreover, with β-proline **94** a much simpler catalyst was already available and therefore no further attempts were tried to apply β-proline derivative (*ent*)-**100** as an organocatalyst.

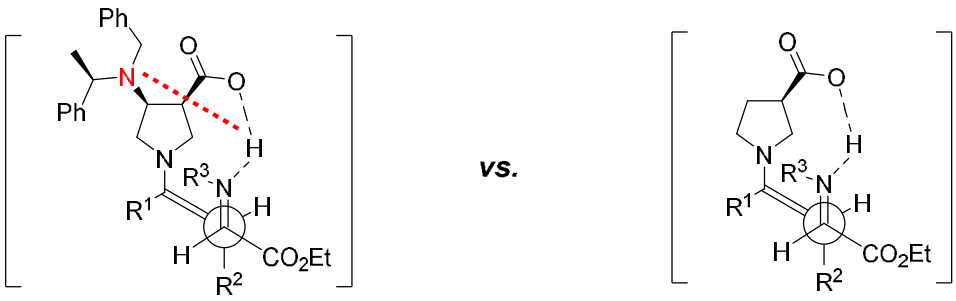


**Figure 5:** Presentation of the transition states of (*ent*)-**100** (left) and **91** (right) in *anti*-Mannich reaction and a possible explanation for the poor catalytic activity of (*ent*)-**100** caused by intramolecular hydrogen bonding.

[b] Results are partially taken from the Bachelor thesis of M. Schmalzbauer (supervised by T. Ertl).

# 3. APC and ACPC building blocks in tripeptide organocatalysis

## 3.1 High pressure as an alternative activation mode in organocatalysis

While the advantages of organocatalysis such as low costs, utilization of non-toxic, metal-free catalysts and new activation modes are often praised, one of the main disadvantages cited are the low reaction rates, often causing the use of high catalysts loadings compared in metal catalysis.[62,63,64] To overcome this problem, various activation modes such as microwave irradiation, heating and ultrasonic sounds are practicable. However, these activation modes often result in a decrease of selectivity or decomposition of reactants.[65,66]

An alternative to thermal activation is the use of high pressures, as it is milder and a non-destructive activation mode, which can accelerate a chemical reaction by compression. Compression of a reaction medium initiates a higher concentration of the reactants, changes the rate of intermolecular diffusion and therefore the rate of effective collisions increases.[67] In principle, every reaction can be accelerated by pressure if its volume of activation $\Delta V^{\ddagger}$ is negative. The volume of activation is defined as the difference between the volume of the transition state and the volume of reactants.[68] That also means that the generation of side products or decomposition can be suppressed upon pressurization.[65,67] Especially reaction types like *Mannich*, *Aldol*, *Michael*, *Baylis-Hillman*, cycloadditions and cross-coupling reactions are susceptible for pressure activation.[69,70,71]

For example, a dramatic increase of turnover numbers in palladium-catalyzed arylation of 2,3-dihydrofuran by high-pressure activation was published by *Reiser et al.* in 1996.[72] Recently, *Kwiatkowski et al*. demonstrated the construction of quaternary stereocenters such as **107** via 1,4-conjugate addition under high-pressure activation, obtaining products which were not accessible under ambient pressure conditions (Scheme 27).[73]

**Scheme 27:** Construction of quaternary stereocenters via 1,4-addition reported by *Kwiatkowski et al.*[73c]

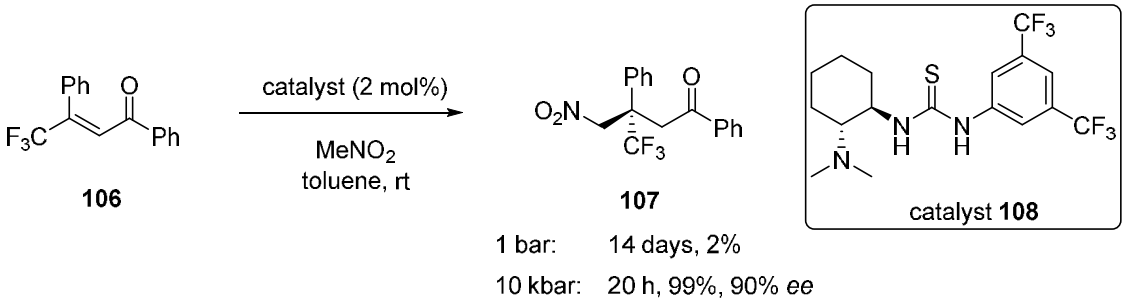

Meanwhile, *Hayashi and co-workers* demonstrated that the generation of high pressure does not require complicated device. They were able to generate pressures up to 2 kbar by simply freezing water inside a sealed autoclave vessel at -20 °C.[74,75,76]

### 3.2 Organocatalysts containing short-chain peptides

With the pioneering work of *Miller et al.*[77,78] two decades ago, the value of short-chain peptides for asymmetric catalysis was recognized. Since then, the field of peptide-based organocatalysis has constantly been expanded by a variety of contributions, especially of the *Wennemers*[79,80]group. Nowadays, peptidomimetic organocatalysts are applied in different reaction types like *Michael*,[81,82,83] *Friedel-Crafts*-type,[84] aldol-type,[85,86,87,88] conjugate additions,[89] epoxidations,[90,91,92] 1,4- or 1,6-additons[93] and cyclopropanation reactions[94] (Scheme 28). Especially their ability for immobilization on resins[95] makes peptidic catalysts interesting for continuous flow catalysis[96] and facilitating the overall recyclability.[97]

**Scheme 28:** Two examples of short-chain peptides applied in the asymmetric aldol reaction[98] (A) and cyclopropanation[94] (B).

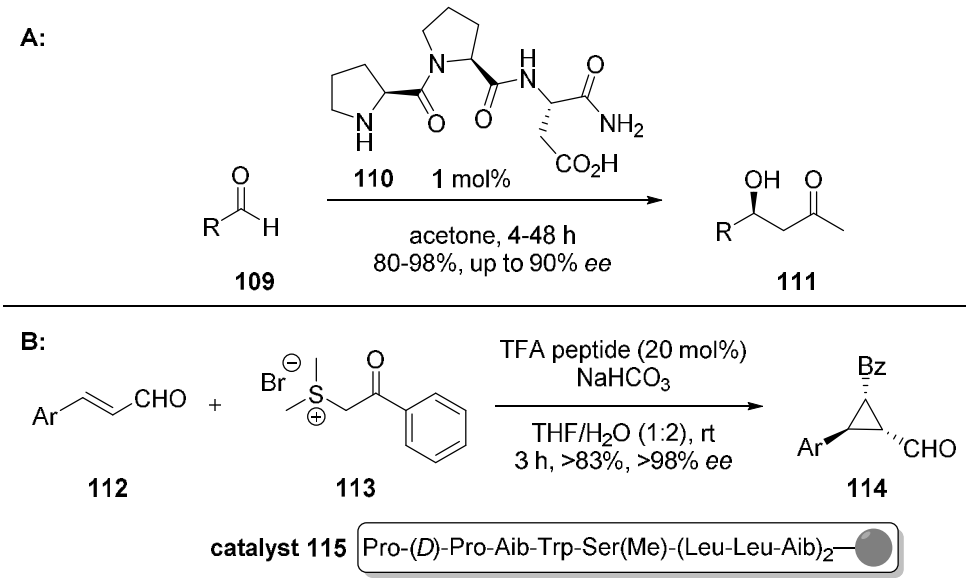


In short-chain peptide catalysts, the right balance between flexibility and rigidity is crucial for their efficiency. It is known, that constrained backbone building blocks like cyclic β-amino acids can stabilize secondary structure motifs in oligomers.[99,100,45]

In the *Reiser* group, there is particular interest in the synthesis and investigation of tripeptide organocatalysts of the sequence H-Pro-**Xxx**-Pro-OH, wherein **Xxx** is a rigid cyclic β-amino

acid. The rigidity of this central building block should bring the two functional groups of the proline units in close proximity for efficient catalysis. In previous studies, tripeptides **116** and **117**, containing rigid β-ACC[101] building block (Figure 6), proved to be an effective catalyst in aldol reaction and were investigated under ambient- and high-pressure conditions.[102,103,75] It was found out, that tripeptide **116** acts as a superior catalyst compared to its isomer **117**, due to internal hydrogen bonding leading to a fixed conformation of **117**, in contrast to a more flexible conformation of **116**. This flexibility is necessary to take position of the functional groups for an optimal conformation for catalysis.

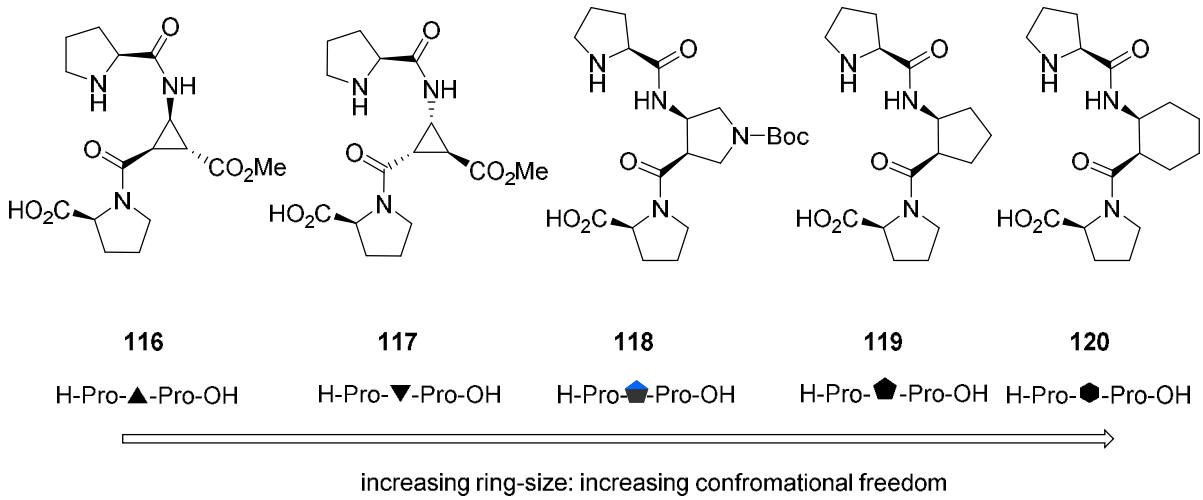


**Figure 6:** Series of tripeptides organocatalysts of the sequence H-Pro-**Xxx**-Pro-OH.

The increasing ring size of the different building blocks is accompanied with a higher degree of conformational freedom. This should result in a change of conformation upon pressurization and hopefully in a more effective catalytic system compared to that under ambient pressure. In the row of small and rigid building blocks towards bigger ring systems the cyclopropane derivative **116** was already examined in detail in our group,[102,103,75] the synthesis and evaluation of cyclobutyl[104] and cyclohexyl[105] **120** derivatives is part of ongoing investigations in the *Reiser* group.

Following this concept, the synthesis of APC and ACPC derived tripeptides will be described in the following chapters. Also, the catalytic activity of these new derivatives will be evaluated in the aldol reaction under ambient- and high-pressure conditions.

### 3.3 Synthesis of APC based tripeptides

The initial idea was the use of previously synthesized APC and ACPC building blocks (chapter 1) without any further modification of the protecting groups.[c)] In the beginning, the first step was the coupling of **79** with (*L*)-proline benzyl ester to arrive dipeptide **121** (Scheme 29). For this coupling step, a protocol[106] using *n*-propane phosphonic acid anhydride (T3P) as coupling reagent was followed. This protocol was known to give promising features such as high yields, low epimerization, simple reaction setup and product isolation. Indeed, the desired dipeptide **121** was isolated in a good yield of 77% and no epimerization was detected by NMR analysis or mass spectrometry. The Fmoc group in **121** was removed under basic conditions followed by coupling of the corresponding amine with *N*-Cbz protected (*L*)-proline to obtain the protected tripeptide in 56% yield. As both protecting groups are susceptible to hydrogenolysis, the free tripeptide could be easily synthesized by hydrogenation. However, cleavage of both groups at atmospheric pressure was not successful and required hydrogen pressure up to 40 bar. This provided the desired free catalyst **118** in 43% yield over 4 steps from **79**.

**Scheme 29:** Synthesis of APC-tripeptide organocatalyst **118** from **79**.

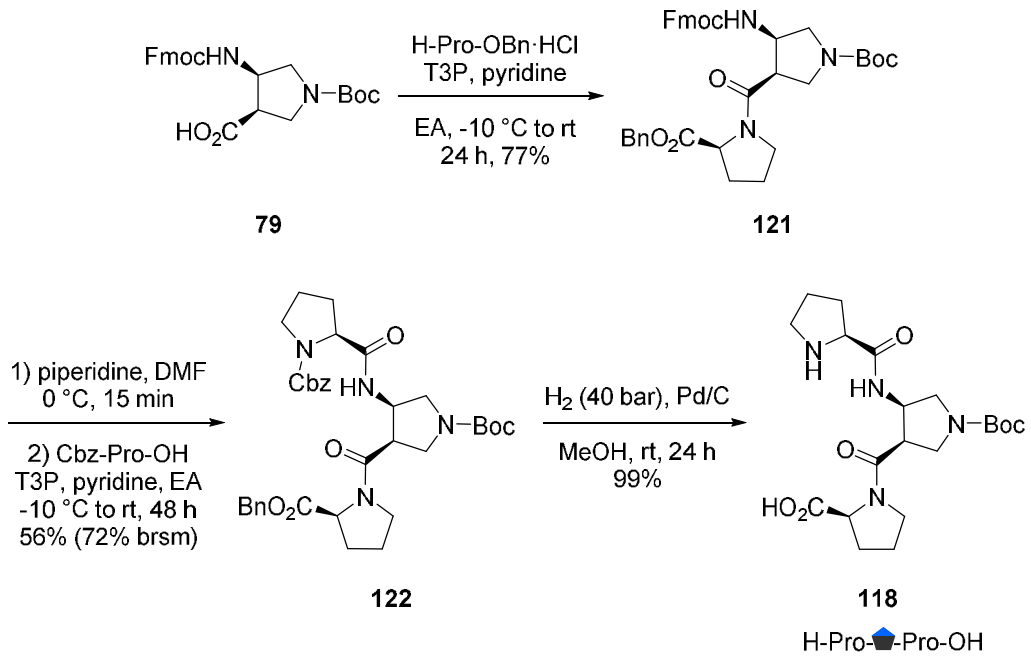


The low yield of 56% during the Fmoc deprotection and subsequent coupling step can be explained by the formation of a diketo-diazepane derivative **124** (Scheme 30). Initially, the

[c)] Partially taken from the Bachelor thesis of T. Götz (supervised by T. Ertl).

Fmoc deprotection/coupling sequence was performed at ambient temperature which led to complete conversion of **121** to **123**. During the base-induced deprotection of the Fmoc group, the corresponding free amine **123** cleaved off the benzyl ester to form the diazepane derivative **124**.

**Scheme 30:** Side product formation during Fmoc deprotection/coupling sequence.

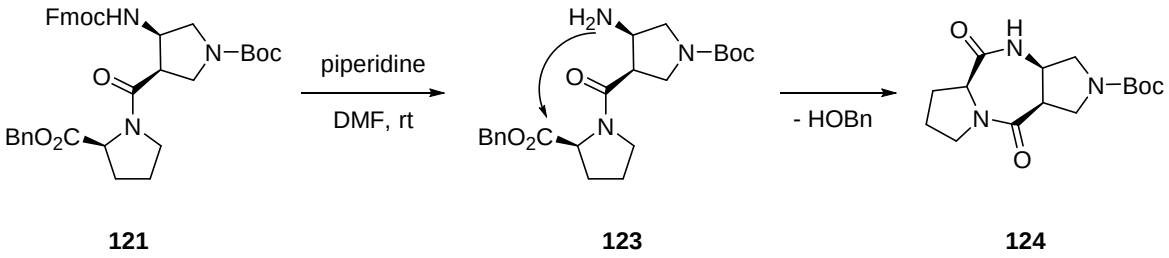


This kind of side reaction is also known from Fmoc SPPS, which is depending on the structure of the C-terminus and can cause complete cleavage of the peptide of the resin.[107] To avoid this side reaction, the literature suggests the application of a bulky resin linker. Regarding the intended use of the catalyst and the required quantity, a resin supported synthesis was not deemed the method of choice. Decreasing the temperature during the deprotection to 0 °C by cooling in an ice bath partially suppressed the conversion to the diazepane derivative **124** and the desired tripeptide could be isolated in 56% yield.

**Scheme 31:** Synthesis of tripeptide organocatalyst **127** from (*ent*)-**79**.

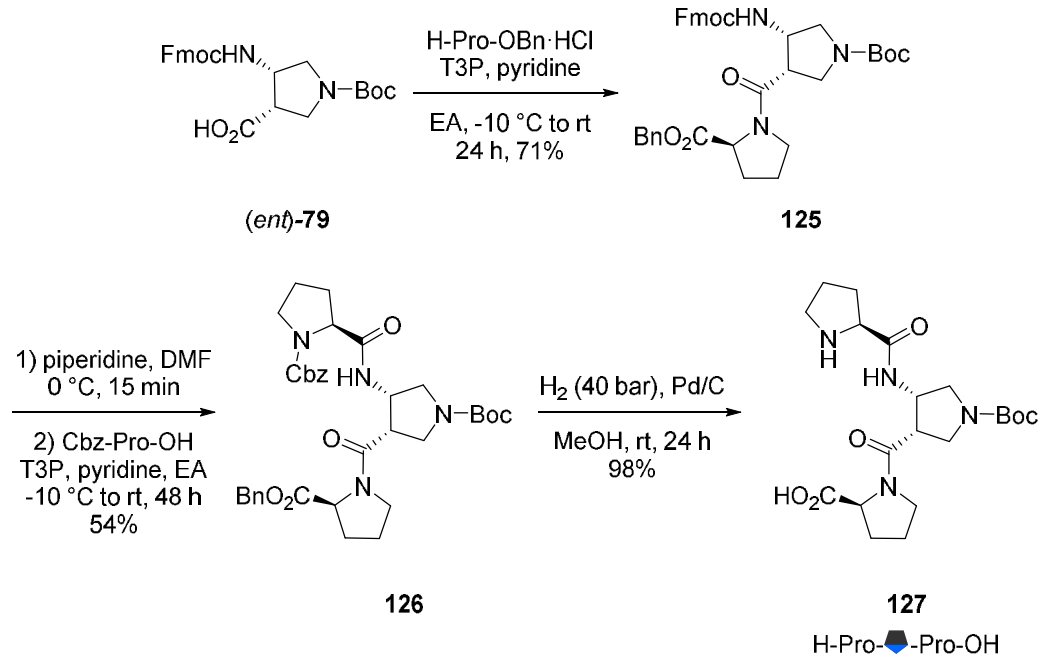

The corresponding diastereomer **127** was synthesized in analogy to **118** with similar yields of 38% over 4 steps (Scheme 31). Although the Fmoc deprotection/coupling sequence was challenging, it still delivered the desired tripeptide **126** in 54% yield.

After all coupling steps, the isolated products were investigated towards the occurrence of epimerization. This was accomplished by $^{1}$H NMR analysis or HPLC/mass spectrometry. Especially on the stage of the (protected/unprotected) tripeptide, NMR analysis was quite tricky up to impossible, as the flexibility of the compounds caused significant signal doubling and broadening. This signal broadening was induced by the free rotatable C-N bonds in the Fmoc and Boc protecting groups, as well as partially hindered rotation around the amidic peptide bonds placed at the N-terminus of the proline units. This occurrence can lead to the formation of *cis*- and *trans*-conformers.[108]

It is important to note that in both isomers of the APC organocatalysts, the Boc group of the APC building block should remain, as it should negate any influence of the additional nitrogen on catalysis. Moreover, this additional amine also gives the opportunity to immobilize the APC catalysts onto a solid phase resin for a possible recovery of the catalysts.

### 3.4 Synthesis of ACPC based tripeptides

For the synthesis of the ACPC based tripeptides, the same synthetic route as for the APC isomers was followed. The first coupling of the ACPC building blocks with (*L*)-proline benzyl ester gave rise to the dipeptides **128** and **130** in 73% and 61% yield respectively, similar to the APC derivatives. However, applying the same conditions for the Fmoc deprotection/coupling sequence did not provide any of the desired tripeptides, leading only to the formation of the corresponding diketo-diazepane (Scheme 32).

**Scheme 32:** First attempts at the synthesis of the ACPC based tripeptides.

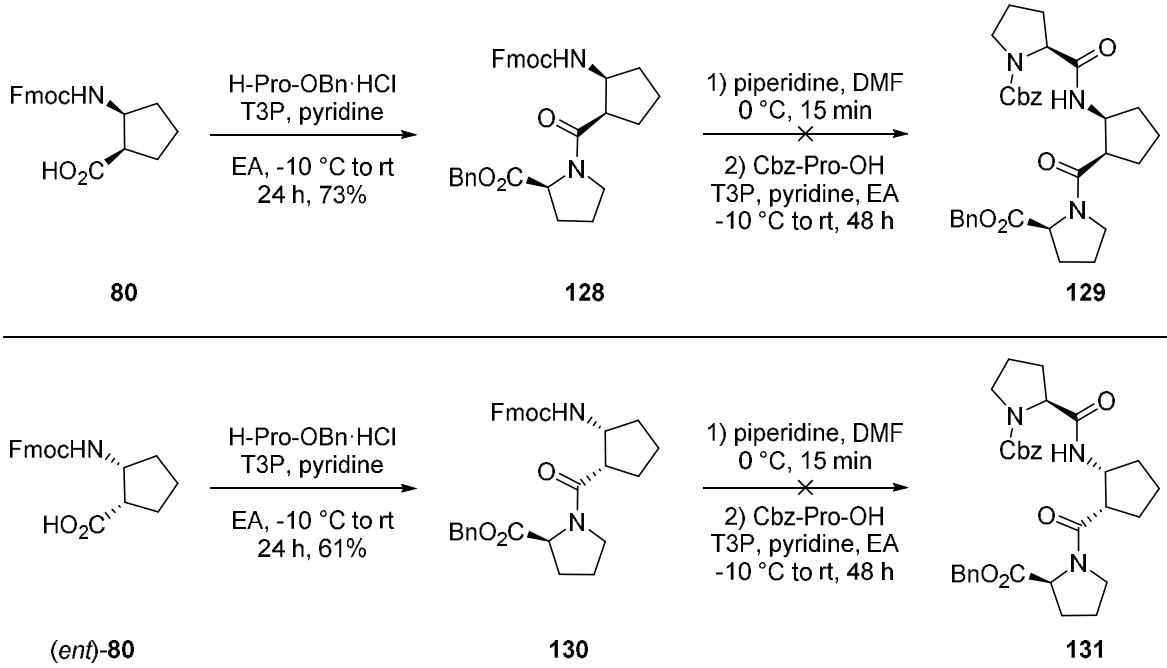


As side product formation could not be circumvented through the usage of lower temperatures, a new coupling strategy needed to be investigated to get access to the ACPC based tripeptides. A first alternative method was a change in the coupling sequence (Scheme 33). Therefore, it was decided to start from the addition product (*ent*)-**21** first. The hydrogenolysis of the benzyl groups in (*ent*)-**21** yielded the free amine (*ent*)-**132** which would not undergo undesired cyclization. The free amine (*ent*)-**132** should be submitted to coupling with preactivated Cbz-protected (*L*)-proline to provide the dipeptide **133**. After hydrolysis of the *tert*-butyl ester, the corresponding free carboxylic acid could then be coupled with (*L*)-proline benzyl ester to get **131**, followed by removal of all protecting groups by hydrogenolysis.

**Scheme 33:** New intended route towards ACPC based tripeptides

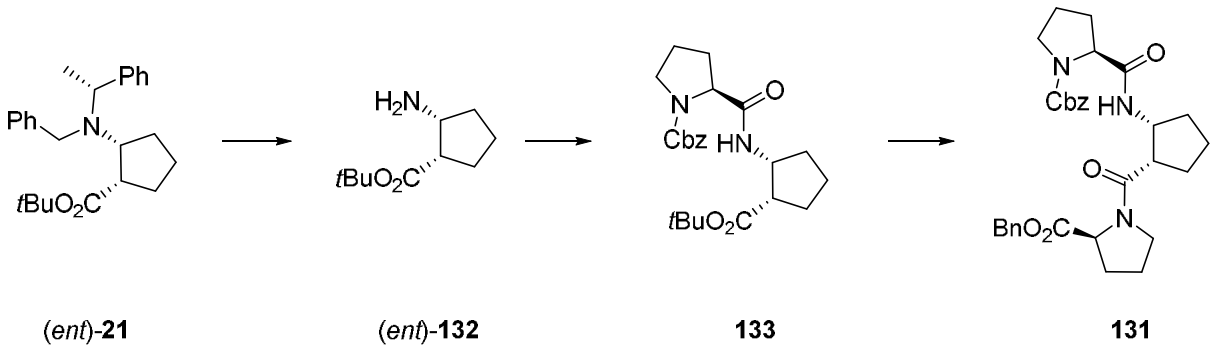


(*ent*)-**21** (*ent*)-**132** **133** **131**

After hydrogenolysis of (*ent*)-**21**, the free amine (*ent*)-**132** was directly submitted to the first coupling reaction under the same conditions as employed for the synthesis of **128**. Surprisingly, this method did not show any conversion of the starting material, in contrast to the good results of the previous couplings. Even the application of EDC or HATU as coupling reagents did not provide the desired dipeptide **133** (Scheme 34).

**Scheme 34:** Attempts to get access to dipeptide **133**.

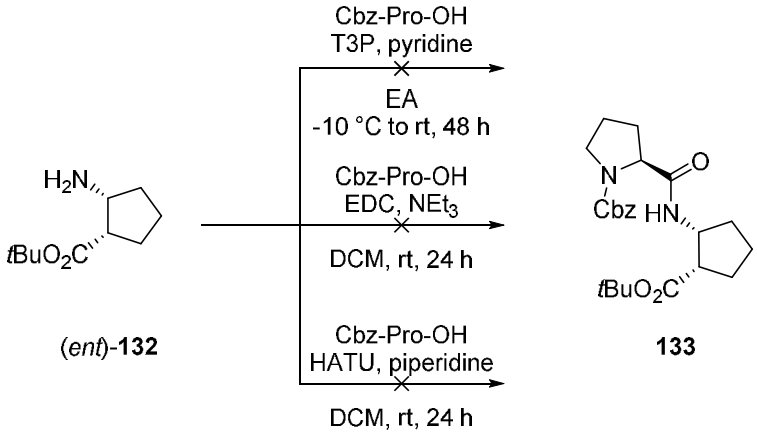


A possible explanation could be the sterical hindrance of the *tert*-butyl ester impeding the coupling of the amine and the activated Cbz-proline. To prove this concept, the *tert*-butyl ester in (*ent*)-**132** was converted to the corresponding methyl ester **134** (Scheme 35).

**Scheme 35:** Conversion of *tert*-butyl ester in (*ent*)-**21** to methyl ester (*ent*)-**134** and attempted coupling towards dipeptide **136**.

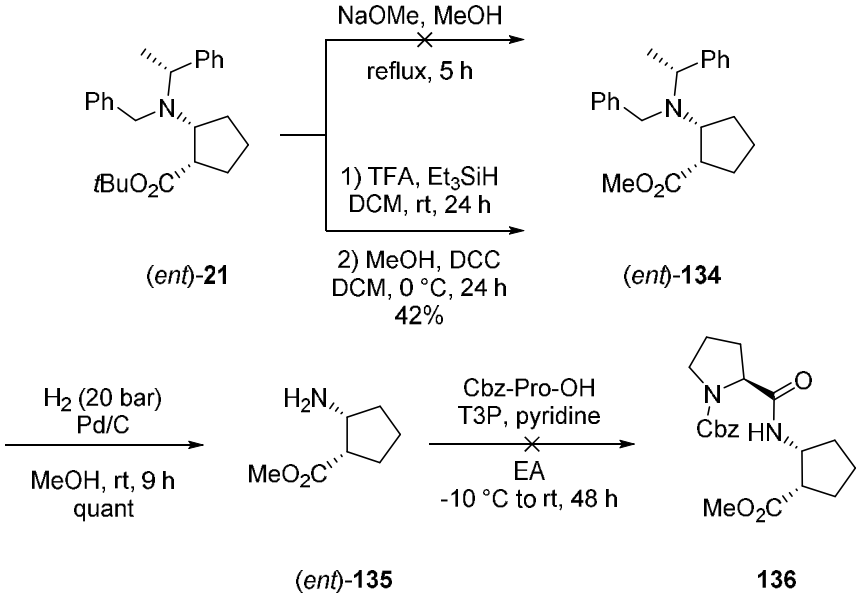


For the synthesis of methyl ester (*ent*)-**134**, two different procedures were employed. In a first attempt, a transesterification procedure by *Fox et al.*[109] using NaOMe in refluxing MeOH was applied. However, no conversion of the starting material was observed. Another attempt provided the desired methyl ester (*ent*)-**134** in moderate yield of 42% after *tert*-butyl ester hydrolysis with TFA and subsequent esterification with DCC and methanol. After hydrogenolysis of the benzyl groups in (*ent*)-**134**, the corresponding amine (*ent*)-**135** was again submitted to coupling with Cbz-proline. However, this modified strategy did not provide the desired dipeptide, suggesting that the sterical hindrance of *tert*-butyl ester was not decisive.

Another reason could be the less reactivity of the free amine undergoing coupling reaction with the activated carboxylic acid. Regarding this, *Suppo et al.*[110] reported an alternative method with inverted reactive components, using activated α-aminoesters which then react with the free carboxylic acid. Transferred to the here discussed challenge, the required activated β-aminoester **138** can be readily prepared by coupling the free amine (*ent*)-**132** with 1,1-dicarbodiimidazole **137** (CDI) yielding **138** in a moderate yield of 51% (Scheme 36).

**Scheme 36:** Preparation of the activated β-aminoester **138**.

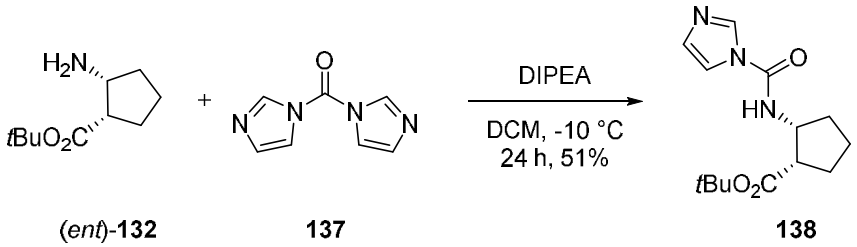


(*ent*)-**132** **137** **138**

This reaction was strongly dependent on the concentration of the solution and the rate of addition of the amine. In all attempts, the formation of the β-aminoester was accompanied by the occurrence of a side-product. If amine addition to the CDI solution was too rapid, the activated β-aminoester coupled with the free amine to the corresponding urea **139** (Scheme 37). Even decreasing the temperature did not circumvent this problem and just resulted in a slower conversion to the dimer.

**Scheme 37:** Formation of the urea **139** during the preparation of desired β-aminoester **138**.

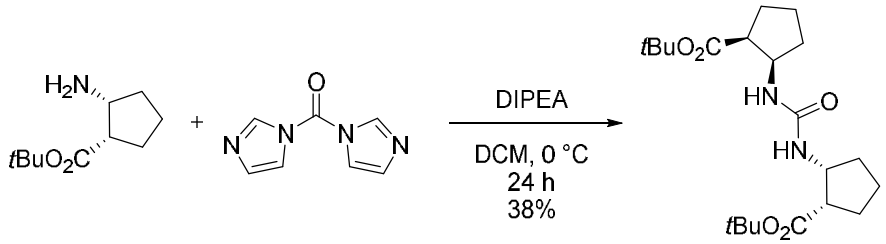


(*ent*)-**132** **137** **139**

In principle, the occurrence of this class of substance is interesting since it can normally be obtained by *Curtius* rearrangement,[111] presents a chiral urea core structure and may be utilized in urea organocatalysis.[112] Due to the excessive reactivity of the generated β-amino ester, the method was rendered to be inapplicable. A method needed to be found in which the reactivity of the coupling partners is high enough, while a trapping reagent could be used to prevent the formation of side products.

Fortunately, a similar problem was already investigated in the *Reiser* group during the synthesis of β-ACC dipeptides **141**, which required special coupling techniques to prevent ring-opening during Fmoc-deprotection of **140b**.[113] In a batch reaction, the Boc protecting group in **140a** was removed by HCl in EA to isolate to corresponding hydrochloride salt, followed by coupling with an activated amino acid (Scheme 38 top). Since these acidic conditions could not be applied in peptide synthesis following Fmoc strategy, another *N*-protecting group which can be removed under neutral or weakly basic conditions needed to be

found. Considering these facts, the Alloc group seemed to be the protecting group of choice.[114] It can be cleaved off by a catalytically amount of Pd(0)-source under non-acidic conditions in the presence of an allyl scavenger to avoid allylation of the corresponding free amine.[115] Therefore, coupling of Alloc-protected **142** can be performed easily by *in situ* deprotection in the presence of an activated amino acid **143** (Scheme 38 bottom). Moreover, its applicability in a tandem deprotection/coupling reaction and the suppression of forming diketopiperazines was already proven.[116]

**Scheme 38:** Utilization of the Alloc group in peptide synthesis reported to *Zorn et al*.[113]

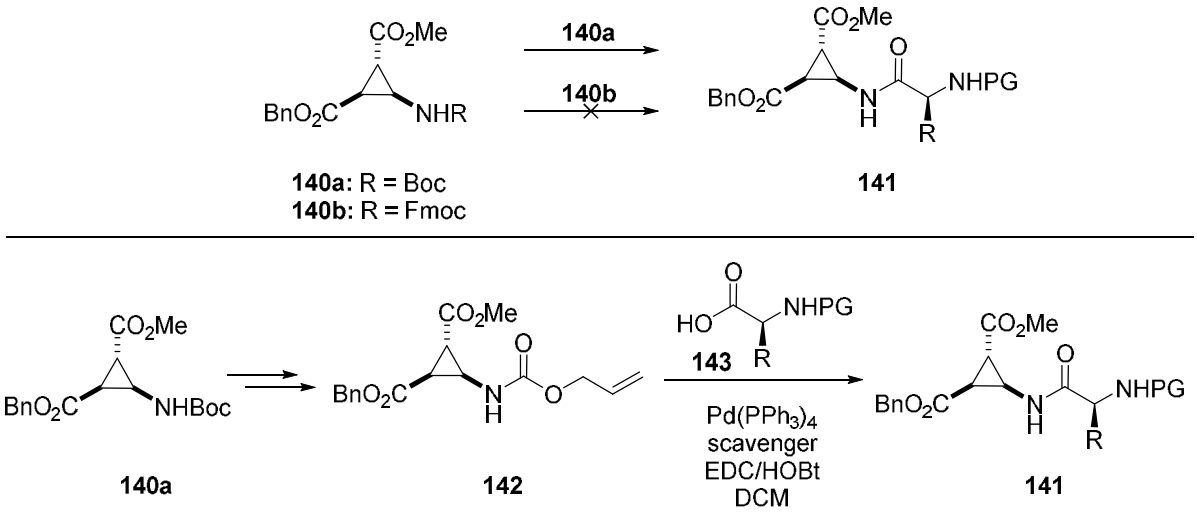


Regarding the task of coupling the ACPC based dipeptide **128** with Cbz protected (*L*)-proline, this method was thought to inhibit the diketodiazepane formation. An additional advantage would also be the toleration of the benzyl ester group under the applied conditions, hence chosen Cbz or benzyl protected (*L*)-proline units could still be used. Only the Fmoc protecting group in the ACPC building blocks needed to be replaced by the Alloc group (Scheme 39). This was accomplished in a similar fashion to the introduction of the Fmoc group (compare chapter 1, Scheme 22) by removal of the benzyl groups by hydrogenolysis in **21** and *tert*-butyl ester hydrolysis with TFA. The corresponding amino acids were isolated as their hydrochloride salts and were subsequently submitted to Alloc protection to obtain the desired building blocks **144** and (*ent*)-**144** in 30% and 65% yield respectively over 3 steps.

**Scheme 39:** Preparation of Alloc-protected ACPC building blocks **144** and (*ent*)-**144**.

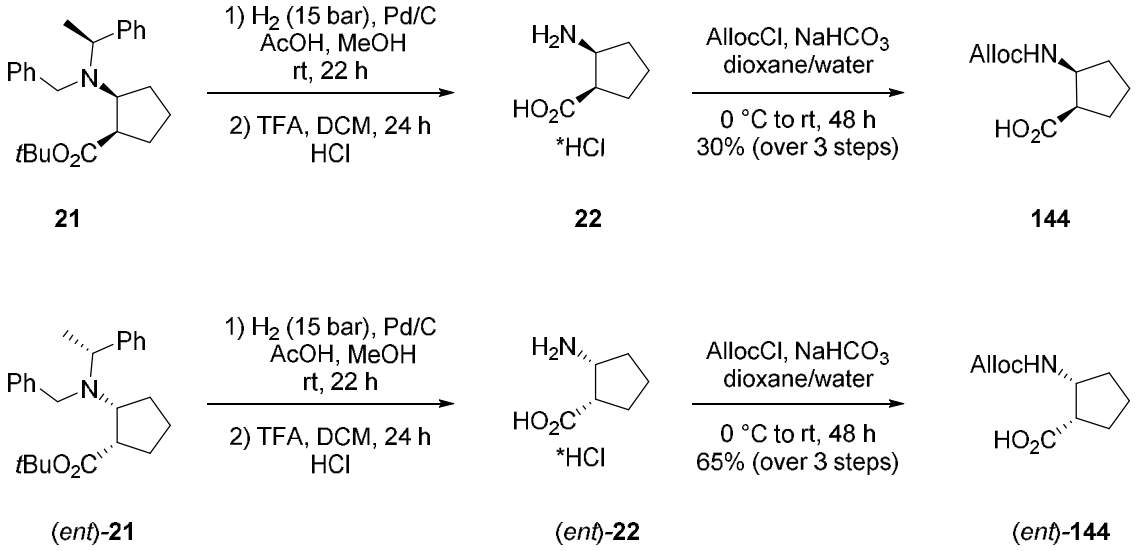


The new Alloc-protected ACPC building blocks **144** and (*ent*)-**144** were submitted to dipeptide coupling under the same conditions as for the APC based dipeptides, achieving comparable yields (Scheme 40 and Scheme 41). The subsequent key step was the tandem Alloc deprotection/coupling reaction of *Zorn et al.*[113] Using preactivated Cbz protected (*L*)-proline with EDC/HOBt, the desired tripeptides **129** and **131** were obtained in 61% and 87% yield respectively after 20 minutes by using DABCO as a scavenger and 10 mol% of $Pd(PPh_3)_4$.[117] Unfortunately, remaining triphenylphosphineoxide from the Alloc-coupling could not be separated completely from the product, although different solvent mixtures for column chromatography or various attempts for recrystallizations were tried. Nevertheless, after the final deprotection step triphenylphosphineoxide residues could be easily removed by simple washing with hexanes.

**Scheme 40:** Synthesis of tripeptide organocatalyst **119**.

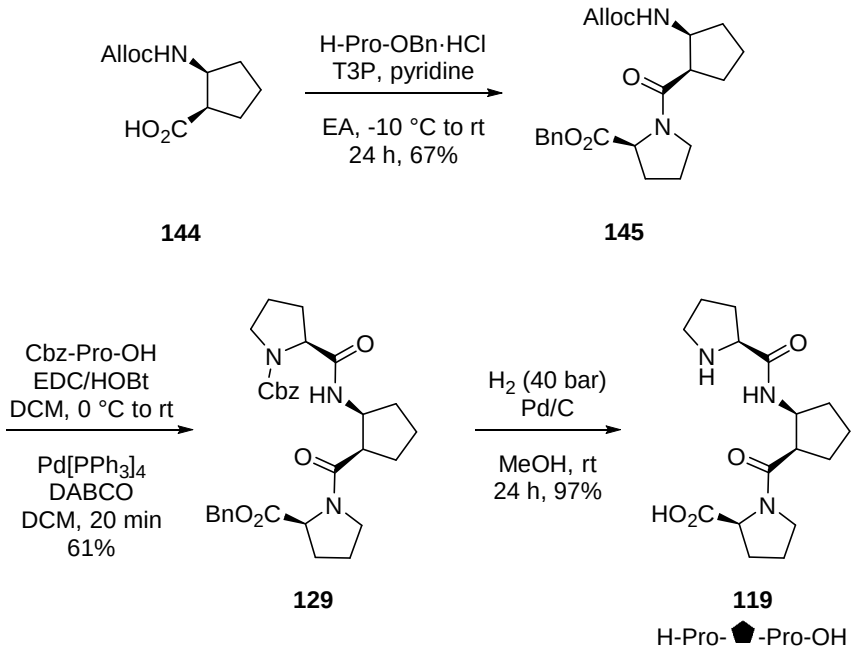


In this way, tripeptide organocatalyst **119** was prepared in 12% yield over 6 steps (from addition product **21**) (Scheme 40) and its isomer **147** in 38% yield (Scheme 41).

**Scheme 41:** Synthesis of tripeptide organocatalyst **147**.

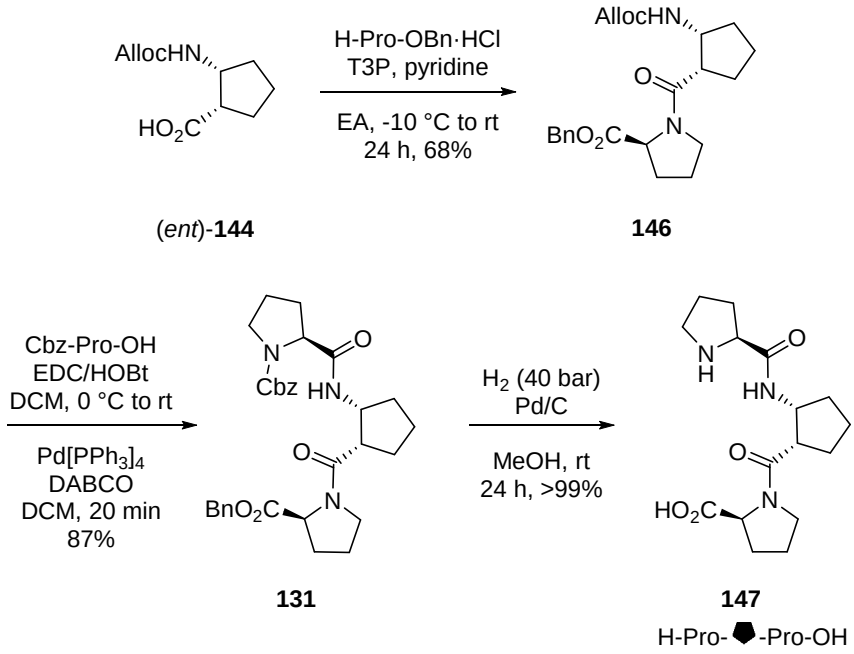


No epimerization was observed after the coupling steps, determined by $^{1}$H NMR or HPLC/mass spectrometry.

### 3.5 Evaluation of catalytic activity of APC and ACPC based tripeptides in organocatalysis

The obtained APC and ACPC based tripeptide organocatalysts were tested in a benchmark reaction between acetone **148** and *p*-nitrobenzaldehyde **149** under ambient- and high-pressure conditions. Special focus was whether high pressure was influencing the reactivity of the different catalysts as well as the conformational equilibrium, which could affect the selectivity. The obtained results of the five-membered ring derivatives were compared to those of three-membered ring derivate **116**[75] to investigate if the different ring size can be a decisive factor regarding reactivity and selectivity (Table 2).

Interestingly, entry 1 and 2 show that an uncatalyzed background reaction occurred at ambient pressure, but to a much lower degree than under high-pressure conditions. Nevertheless, no product was formed. A further conclusion can be drawn, that high pressure increased the reactivity of all organocatalysts. In the case of the APC derivatives, (entries 3 *vs*. 4 and 5 *vs*. 6) elevated pressures led to a more than eightfold increase of reactivity (reaction time reduced from 24 to 6 h), similar to the β-ACC derivative (entries 11 vs. 12). The ACPC derivatives (compare entries 7 *vs*. 8 and 9 *vs*. 10) showed lower (factor of three for **119**, a factor of two for **147**), although still significant increase in reactivity. Interestingly, the ACPC tripeptides revealed an increase of selectivity upon pressurization contrary to the ACC or APC derivatives.

**Table 2:** Organocatalyzed aldol reaction under ambient- and high-pressure conditions.

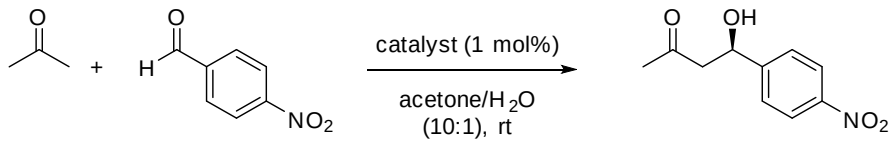


**148** **149** **150**

| entry[a] | | catalyst | time (h) | pressure (bar) | conversion (%)[b] | yield (%)[c] | *ee* (%)[d] |
|---|---|---|---|---|---|---|---|
| 1 | | - | 24 | 1 | 37 | - | - |
| 2[e] | | - | 24 | 4600 | 14 | n.d. | - |
| 3 | **118** | H-Pro-◆-Pro-OH | 24 | 1 | 23 | 10 | 49 (*R*) |
| 4 | **118** | H-Pro-◆-Pro-OH | **6** | **4600** | **43** | **21** | **43 (*R*)** |
| 5 | **127** | H-Pro-⬟-Pro-OH | 24 | 1 | 49 | 37 | 33 (*R*) |
| 6 | **127** | H-Pro-⬟-Pro-OH | **6** | **4600** | **91** | **75** | **20 (*R*)** |
| 7 | **119** | H-Pro-À-Pro-OH | 24 | 1 | 97 | 82 | 31 (*R*) |
| 8 | **119** | H-Pro-À-Pro-OH | **6** | **4600** | **80** | **57** | **41 (*R*)** |
| 9 | **147** | H-Pro-Á-Pro-OH | 24 | 1 | 48 | 28 | 15 (*R*) |
| 10 | **147** | H-Pro-Á-Pro-OH | **6** | **4600** | **36** | **14** | **22 (*R*)** |
| 11[e] | **116** | H-Pro-p-Pro-OH | 24 | 1 | 84 | 68 | 69 (*R*) |
| 12[e] | **116** | H-Pro-p-Pro-OH | **4** | **4800** | **97** | **73** | **67 (*R*)** |

a) 1.0 mmol aldehyde; b) determined by isolated starting material after column chromatography; c) isolated yield after column chromatography; d) determined by chiral HPLC; e) taken from ref[75], 10 mol% catalyst.

Based on this observation it can be assumed that a rigid ring system (β-ACC) with a low degree of conformational freedom appears to be necessary for efficient catalytic performance. Moreover, a more flexible system (ACPC) with a higher degree of conformational freedom shows less selectivity in catalytic performance at ambient pressure, but the latter could be increased by pressure.

In the case of APC- and ACPC derivatives, one diastereomer of the catalysts always showed higher catalytic activity compared to the other. This observation may be explained by intramolecular hydrogen bonding resulting in a fixed conformation. It can be assumed from $^{1}$H NMR of the free catalysts, that more active catalysts **127** and **119** reveal very broad signals. This indicates that a high flexible system allows functional groups to be positioned into a desired conformation, similar to the β-ACC catalyst **116**.[75] In contrast, the signals of

**118** and **147** are much sharper and this might be induced by intramolecular hydrogen bonding leading to a fixed conformation and resulting in a lower catalytic activity.

It could also be observed, that the APC-derived catalysts showed a lower catalytic activity as their ACPC-derived isomers. This effect may be explained by the lower solubility of the APC-derived catalysts caused by the additional Boc group. Another reason for the decreased catalytic activity could be that the additional nitrogen of the pyrrolidine ring system is involved in internal hydrogen bonding and might interrupt the proton transfer in the catalytic step. To get an insight into the possible conformations of the APC- and ACPC-derived tripeptide organocatalysts, further NMR studies, especially under high-pressure conditions and molecular modeling calculations need to be carried out, which will be the objective in future studies in the *Reiser* group.

## 4. APC building block in peptide foldamers

The previous chapter described the introduction of the APC into short tripeptides. Before the APC building block would be introduced into longer chain naturally occurring neuropeptide Y (NPY) ligands (chapter 5), it was intended to introduce the APC building block into an artificial peptide to investigate its influence on secondary structure formation. Artificial peptides, with a strong tendency to adopt a specific conformation, are defined as foldamers.[16] *Gellman*[118] and *Seebach*[119] pioneered this chapter in chemistry in the late 1990´s and ever since the developments in this field have thrived enormously.[120] Since many biological processes are mediated by protein-protein interactions, the main motivation of foldamer design is the development of scaffolds adopting specific structures, to mimic parts of these poly-peptides and their functions. However, the interruption of protein-protein interactions is associated with a major amount of diseases. Therefore, peptidic foldamers can be a crucial instrument for the investigation and manipulation of these interactions.[16b,120b]

To compare the APC building block with its structurally related cyclopentane derivative ACPC, which was already employed in foldamers, the APC building block was introduced into α,β-peptide **151**. This peptide was previously designed in our group[46] according to the stereochemical patterning approach of *Martinek* and *Fülöp et al.*[121] Following this approach, every adjacent amino acid revealed the opposite stereochemistry of the one used before. The α,β-alternating foldamer **14**[18] was already shown to form a stable right-handed helix in organic solvents contrary to its behaviour in aqueous media and served as an idol peptide. Since **151** should serve as a model peptide to investigate the properties of the APC building block, only three ACPC building blocks in **14** were exchanged by APC building blocks for facile determination of the possible influence on the adopted secondary structure.

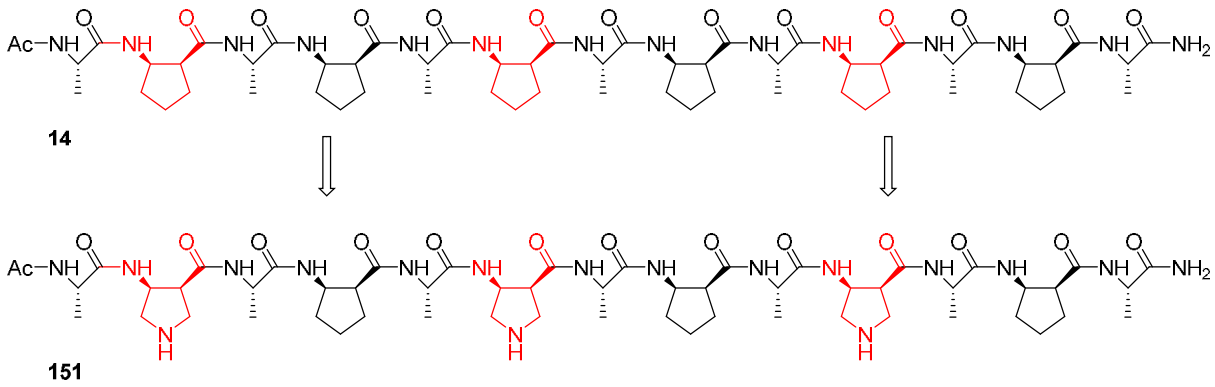


**Figure 7:** Synthesized 13-mer foldamer **151** based on model peptide **14**.

**151** was synthesized in cooperation with Prof. Dr. C. Cabrele (University of Salzburg) on an automated peptide synthesizer, applying Fmoc-chemistry and double-coupling strategy with HBTU/HOBt/DIPEA. The synthesis was performed on a Rink-amide MBHA polystyrene resin for C-terminal amidation followed by acidic cleavage and purification by preparative HPLC.

In order to get an insight into the solution structure of **151**, circular dichroism (CD) spectra in four different solvent systems were recorded. CD spectroscopy displays a valuable and commonly applied tool for the conformational analysis of peptides and proteins. Circular dichroism is defined by the different absorption of left- and right-handed circular polarized light by treatment of a chiral sample, resulting in the generation of elliptically polarized light. This method affords insight into the secondary structure motifs of peptides and proteins from amide chromophores and the tertiary structure from aromatic amino acid residues such as Phe, Tyr or Trp. The peptide bonds display the main chromophore in peptides which are encircled by a chiral environment caused by the three-dimensional orientation of the peptide backbone. The peptide bond absorption can be observed between 180 and 300 nm. The peptide chromophore displays the lowest energy transition, which occurs between 210 and 220 nm and reflects the n→π* transition of non-bonding electrons of the carbonyl group. The π→π* transition of π-electrons of the carbonyl group can be observed around 190 nm. The energy and intensity of these transitions is dependent of the dihedral angles of the amino acid units and is related to the secondary structure. Consequently, CD spectroscopy is a highly sensitive method to determine changes in the secondary structure and allows identification of different secondary structures like α-helices, β-sheets or random coils due to characteristic shapes of the graphs.[114,122] However, contrary to α-peptides, where an correlation between CD spectra and the secondary structure exists, for unnatural peptides these correlations can be only accumulated by experience and need to be proved by alternative methods as NMR spectroscopy or X-ray diffraction. Nevertheless, CD spectra can give a first hint of the adopted conformation of unnatural peptides.[123]

CD spectra were recorded in water, methanol and phosphate buffer (100 mM, pH 7.0) to determine the conformation under physiological conditions (Figure 8). To mimic the membrane environment, **151** was investigated in phosphate buffer mixed with trifluoroethanol (TFE, 30%) which is known as a structure-inducing co-solvent.[124] All spectra were normalized to the peptide concentration and the number of amide bonds.

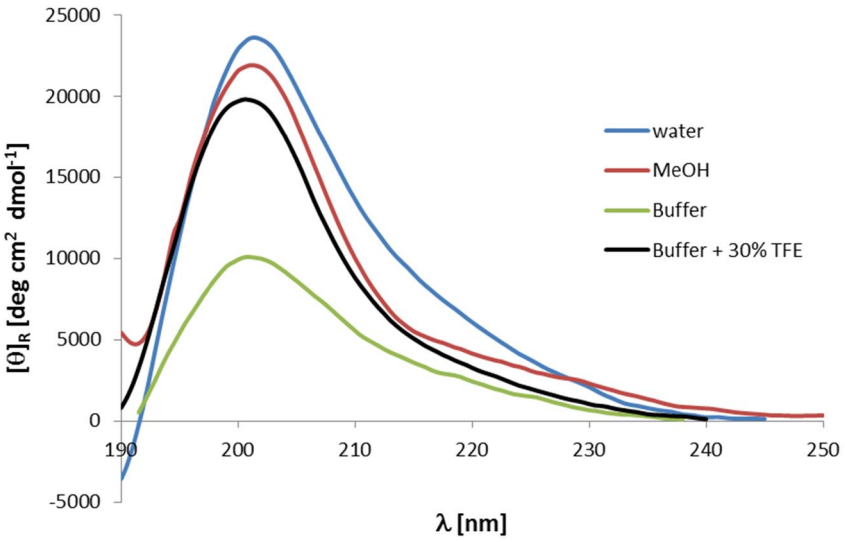


**Figure 8:** CD spectra of **151** in water, methanol, buffer (100 mM, pH 7.0) and buffer + TFE. Peptide concentration was 125 µM.

In general, the shapes of the graphs of **151** are comparable to the spectra of **14**. In particular, in methanol and buffer mixed with TFE the graphs are in accordance with idol peptide **14**, which was shown by 2D-NMR investigations and molecular dynamics calculations to adopt a right-handed helix.[18] The CD spectra in all solvents have a strong maximum near 200 nm, indicating a helical structure of **151**. However, the CD signal of **151** in water was considerably more intense than of **14**, indicating that **151** is more structured in water contrary to **14**. This can be explained by the presence of the polar APC building block in the peptide sequence stabilizing secondary structure motifs in aqueous media. Though the intensity of **151** in buffer is weaker than in water, it showed considerably higher intensity in buffer mixed with TFE. Regarding this, APC containing peptides should adopt stable structures under physiological conditions in a membrane environment, a crucial aspect regarding further application of the APC building blocks in NPY ligands. It can be concluded, that the influence of the APC building blocks on the secondary structure of peptides is similar to that of the ACPC building block. This finding allows and facilitates a comparison of the APC containing NPY analogues with its ACPC analogues, which will be discussed in the following chapter.

# 5. Neuropeptide Y Analogues

## 5.1 Neuropeptide Y

Neuropeptide Y (NPY) is one of the most abundant neuropeptides in our central and peripheral nerve system.[125] It contains 36 amino acids and has considerable sequence similarities with its closely related pancreatic polypeptide (PP) and peptide YY (PYY) analogues.[126,127,128] NPY was first isolated from the porcine brain,[129] along with PP from the pancreas and PYY from the intestine which constitutes the NPY family.[130,131,132] It was assumed that this peptide family reveals a similar secondary structure due to the high sequence homology. The first three-dimensional structure was determined by X-ray from avian pancreatic polypeptide where a turn (amino acids 9-13) connects a polyproline-like helix (1-8) with an *anti*-parallel α-helix (14-31). The amidated C-terminus (32-36) exists in a flexible loop conformation (Figure 9).[133,134]

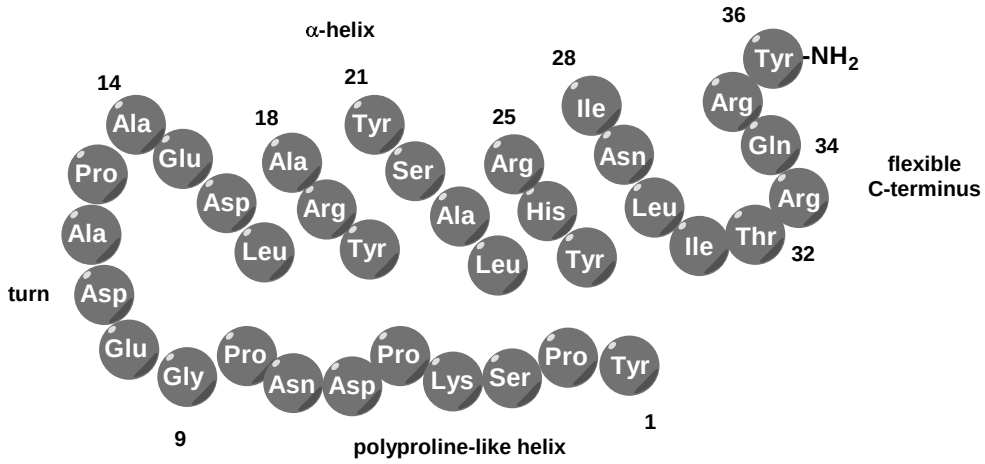


**Figure 9:** Structure of porcine NPY according to *Allen*.[135]

The highly conserved C-terminus of NPY was shown to be crucial for its biological activity by single amino acid substitutions (point mutation studies). In particular, by performing (*L*)-alanine scan, a significant decrease or loss of affinity was observed due to replacing the arginine residues in position 33/35 as well as C-terminal tyrosineamide.[136] The significance of C-terminal area was also emphasized in other reports by different amino acid substitution of several NPY analogues.[127,137]

In humans, NPY activates four to the G-protein coupled receptors (GPCR), the so-called NPY-receptors ($Y_1R$, $Y_2R$, $Y_4R$, $Y_5R$) which are involved in the regulation of various central

and peripheral biological processes (Table 3).[138] So far, five NPY receptor have been cloned from mammals ($y_6$ was found to be functional in mice), and several additional receptors like $Y_3$ have been postulated based on pharmacological investigations.[139]

**Table 3:** Overview of receptor subtypes in human and mediated biological effects by NPY.[140]

| receptor subtype | mediated biological effect |
|---|---|
| $Y_1$ | blood pressure, food intake (+), ethanol consumption, depression, anxiolysis sedation, hormone release, pain sensitivity, angiogenesis. |
| $Y_2$ | food intake (-), blood pressure, seizures (-), bone formation, pain sensitivity, angiogenesis, depression, gastrointestinal motility, circadian rhythms. |
| $Y_4$ | gastrointestinal motility, food intake. |
| $Y_5$ | food intake (+), circadian rhythms, seizure, anxiety, luteinizing hormone secretion (-). |

The $Y_4R$ differs from the other subtypes since it shares only low sequence identity. NPY binds strongly to $Y_1R$, $Y_2R$, $Y_5R$ contrary to $Y_4R$ which prefers PP over NPY and PYY.[141] Nevertheless, the $Y_4R$ was considered to play a key role in the regulation of energy metabolism or feeding behavior since $Y_4R$ agonists were proposed as potent agents against obesity. Moreover, expression of $Y_1$ and $Y_2$ receptor was found in different tumors like breast cancer or prostate cancer[142,143] and have been proposed as potential tumor markers.[144]

Due to the various functions of the different receptor subtypes, synthetic analogues of NPY ligands with high receptor selectivity and affinity would be desirable as a pharmacological tool for elucidation of biological roles and as a potential therapeutic device.[145] Referring to this and the fact the number of known selective $Y_4R$ ligands is very low[127] this project deals with the search for new selective $Y_4R$ NPY analogues and this will be described in the following chapters.

## 5.2 Dimeric pentapeptide derived from hNPY C-terminus as high-affinity $Y_4R$ radioligand[146]

[d] As already mentioned above, there is particular interest in the investigation of new selective $Y_4R$ ligands. In the literature, the diastereomeric mixture of dimeric peptide **152** was described as a high-affinity $Y_4$ receptor agonist. Generally, the arginine residues in the C-terminal area of NPY are important for receptor binding[147] and D/L-2,7-Diaminooctanedioyl-bis-(YRLRY-$NH_2$) **152** comprises the same pentapeptide sequence of the C-terminus (Figure 10). But the data reported for **152** refer only to the diastereomeric mixture.[148]

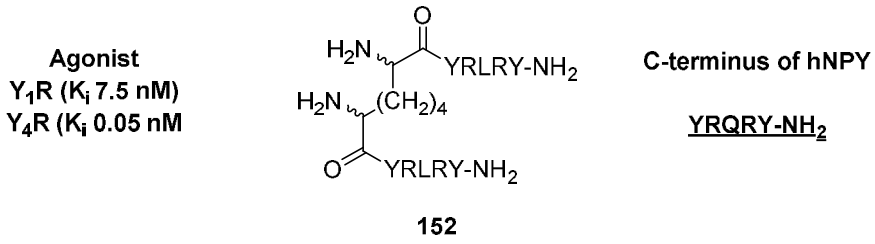


**Figure 10:** Diastereomeric mixture of D/L-2,7-Diaminooctanedioyl-bis-(YRLRY-$NH_2$) **152** as high-affinity $Y_4R$ agonist according to *Balasubramaniam et al.*

It was intended to synthesize diastereomerically pure isomers of **152** for the following pharmacological investigation of each diastereomer. The retrosynthetic approach is displayed in Scheme 42. It was envisioned to build up **152** out of two C-terminus derived pentapeptides and enantiopure 2,7-diaminosuberic acid **153** as a linker.

**Scheme 42:** Retrosynthetic analysis of **152**.

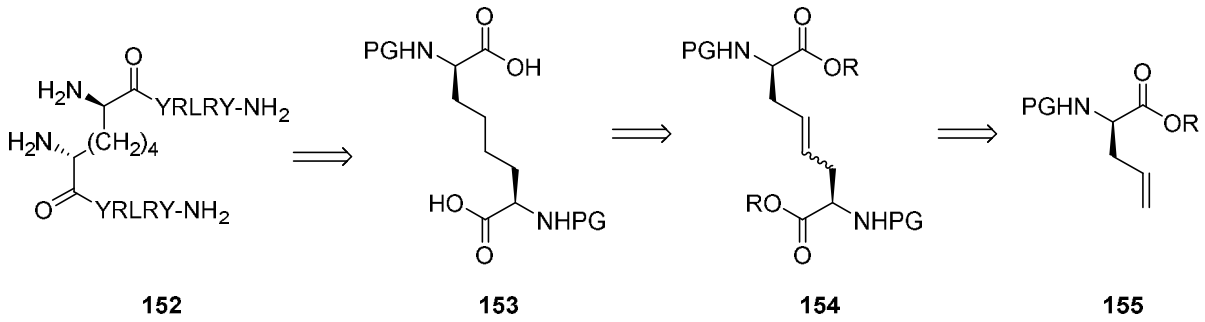


[d] Reprinted (adapted) with permission from Kuhn, K. K.; **Ertl, T**.; Dukorn, S.; Keller, M.; Bernhardt, G.; Reiser, O.; Buschauer, A. *J. Med. Chem.* **2016**, *59*, 6045–6058. Copyright 2017 American Chemical Society. The synthesis of compounds **164**, **166** and **167** was performed by T. Ertl. Synthesis of allylglycine esters **165** and (2*R*,7*R*)-**152** and (2*S*,7*S*)-**152** and related radioligand [$^3$H](2*R*,7*R*)-**169** was performed by K. Kuhn. Pharmacological investigations and characterizations were performed by K. Kuhn and S. Dukorn (AK Buschauer, Institute of Pharmacy, University of Regensburg) and are added for completion and better understanding of the current and following chapter.

Linker **153** and its pre-structure **154** could be synthesized from enantiopure allylglycine ester **155** in cross-metathesis reaction.

Construction of differently protected 2,7-diaminosuberic acid structures was already attempted by methods such as *Kolbe* electrolysis of appropriate glutamic acid derivatives,[149] Pd-catalyzed coupling of dihalides and iminobenzophenones derived from the chiral pool α-amino acids,[150] Pd-catalyzed Suzuki coupling of organoborane reagents,[151] or dimerization of bislactim ethers also derived from the chiral amino acid pool.[152]

Similar to the intended route, *Aguilera et al.* used enantiopure alkynes **156** which were coupled to cyclic acetylenes **158** to get access to 2,7-diaminosuberic acid structures (Scheme 43). Utilization of tungsten catalyst in the key cross-coupling step provided **158** with a moderate yield of 60% and yielded (*R*,*R*)-2,7-diaminosuberic acid **159** in 21% over 4 steps.[153]

**Scheme 43:** Cross-coupling reaction applying tungsten catalyst by *Aguilera et al.*

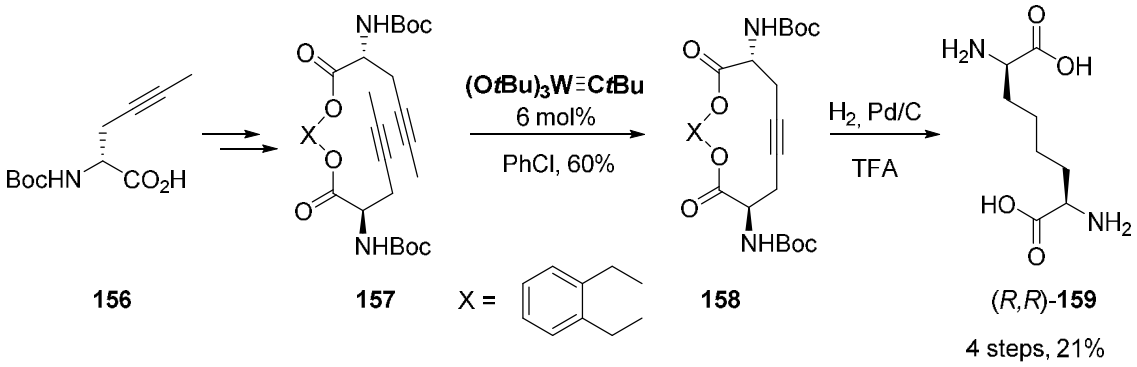


*Grubbs* and co-workers used more familiar Ruthenium catalyst (Grubbs´ I)[154] for cross-metathesis of acyclic alkene **160**, since direct coupling of allylglycine was not possible (Scheme 44). The cyclic alkene **161** was obtained in a very good yield of 85% in the key step and (*S*,*S*)-2,7-diaminosuberic acid **159** was yielded in 77% over 4 steps.[155]

**Scheme 44:** Construction of (*S*,*S*)-**159** applying Grubbs´ I catalyst reported by *Grubbs et al.*

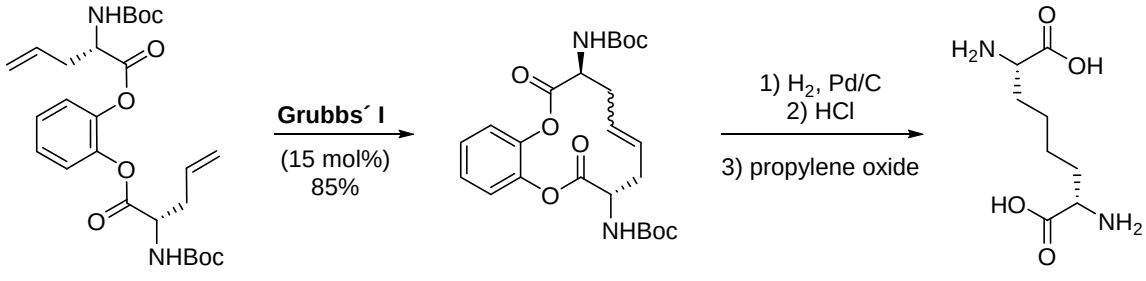

The utilization of anchored amino acids like in **160** also reveals the advantage of getting access to unsymmetrical dimers with different protecting groups. Previous methods of connecting different units of amino acids required the separation of undesired self-metathesis products.[156] Therefore, employing this anchored templates provides an unambiguous and flexible technique towards unsymmetrical 2,7-diaminosuberic acid structures or related compounds.[157,158]

In their studies about the spacer dependency to the biological activity of novel thiocolochicine-podophyllotoxin conjugates, *Passarella et al*. applied Grubbs´ II catalyst[159] for the construction of (*S*,*S*)-2,7-diaminosuberic acid structure **164** from *N*-Boc-allylglycine benzyl ester **162** (Scheme 45). Next, core structure **163** was obtained in a moderate yield of 64% and subsequent hydrogenolysis of the benzyl ester could be combined with the reduction of the double bond in a one-pot step providing **164** in 63% yield over 2 steps.[160]

**Scheme 45:** Two steps synthesis of (*S*,*S*)-**165** applying Grubbs´ II catalyst according to *Passarella et al.*

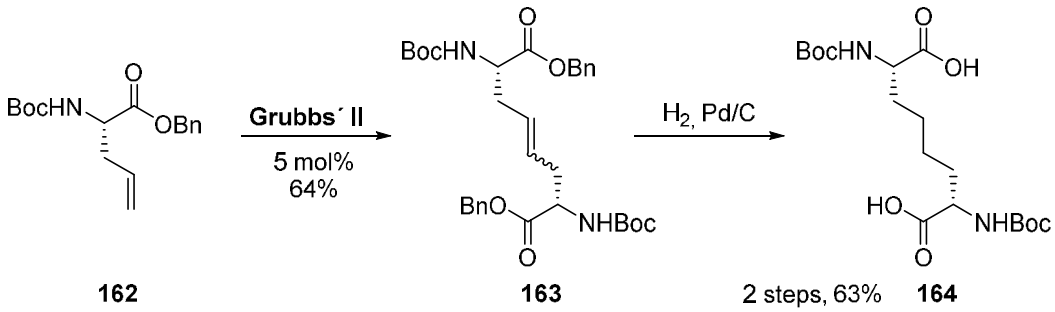


In respect to the literature syntheses, commercially available enantiopure (*R*)- and (*S*)-allylglycine was used for cross-metathesis after esterification and *N*-Boc protection (**165**) by analogy with procedures reported from literature.[161,162] Employing Grubbs´ I catalyst provided the desired cross-metathesis product in an unsatisfactory yield of 18% with 49% conversion of starting material (Table 4, entry 1). However, utilization of Grubbs´ II catalyst increased the yield of **166** up to 89%, whereas changing the solvent to reach higher temperatures didn´t succeed and led to the occurrence of various side-products. Reduction of the double bond was accomplished by catalytic hydrogenation using Pd/C and EtOH as solvent to obtain **167** in 70% yield.

**Table 4:** Construction of 2,7-diaminosuberic acid core structure **166** by cross-metathesis reaction.

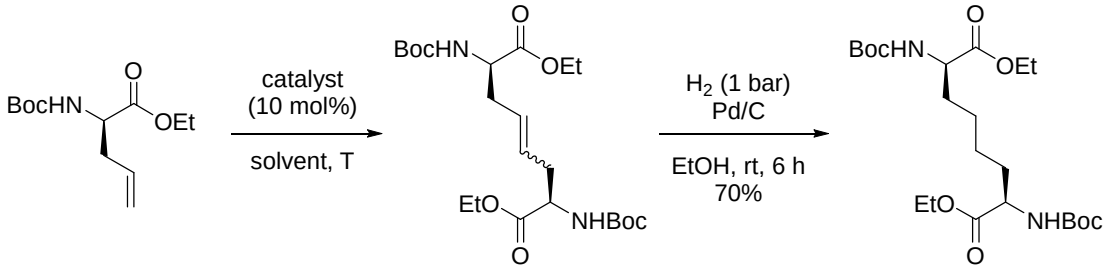


**165** **166** **167**

| entry | catalyst | solvent | *T* (°C) | time (h) | yield **166** (%) |
|---|---|---|---|---|---|
| 1 | Grubbs I | DCM | 70 | 28 | 18[a)] |
| 2 | Grubbs II | DCM | 70 | 11 | 89 |
| 3 | Grubbs II | toluene | 110 | 3 | 67 |

a) 49% conversion.

Although hydrogenation with Pd/C worked quite well, it was envisioned using Grubbs´ II catalyst would make a nicer feature since it was shown to be also an effective catalyst mediating hydrogenation reactions.[163] Employing this strategy, allylglycine ester **165** was submitted to cross-metathesis reaction to build up **166** without isolation, followed by hydrogenation using the same Grubbs´ catalyst (Table 5). The first approach, by simply adding hydrogen balloon after performed metathesis reaction did not lead to any conversion towards **167**.

**Table 5:** Tandem cross-metathesis/hydrogenation sequence applying with Grubbs´ II catalyst.

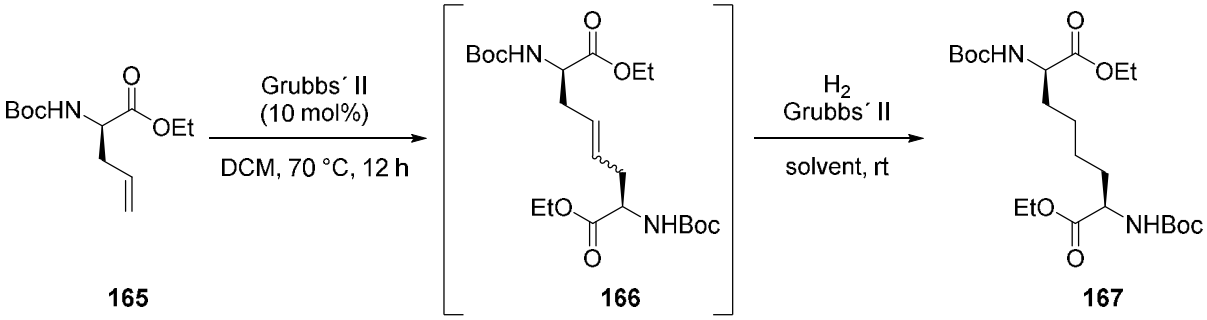


**165** **166** **167**

| entry | solvent | $H_2$ (p) | time (h) | yield **167** (%) |
|---|---|---|---|---|
| 1 | DCM | 1 bar | 16 | - |
| 2[a)] | EtOH | 1 bar | 151 | 83 |
| 3 | EtOH | 20 bar | 20 | 95 |

a) In total 25 mol% of Grubbs´ II was used.

After exchanging the solvent from DCM to EtOH, the hydrogenation was performed at ambient pressure of hydrogen gas. Under these conditions, full conversion of metathesis product **166** was achieved after almost one week and required the further addition of the catalyst. Finally, hydrogenation at 20 bar in the autoclave afforded the desired product in 95% yield. Improved yields and no need of isolation and workup after metathesis display the convenience of this protocol contrary to other reported procedures applying Pd/C as a catalyst.[160] Then, hydrolysis of the ethyl ester quantitatively provided the diacids (*R*,*R*)-**164** and (*S*,*S*)-**164** in 95% and 74% yield, respectively over 2 steps from *N*-Boc-protected allylglycine ethyl ester (*R*)-**165** and (*S*)-**165** (Scheme 46).[146]

**Scheme 46:** Two-step enantioselective synthesis of (*R*,*R*)-**164** and (*S*,*S*)-**164**.

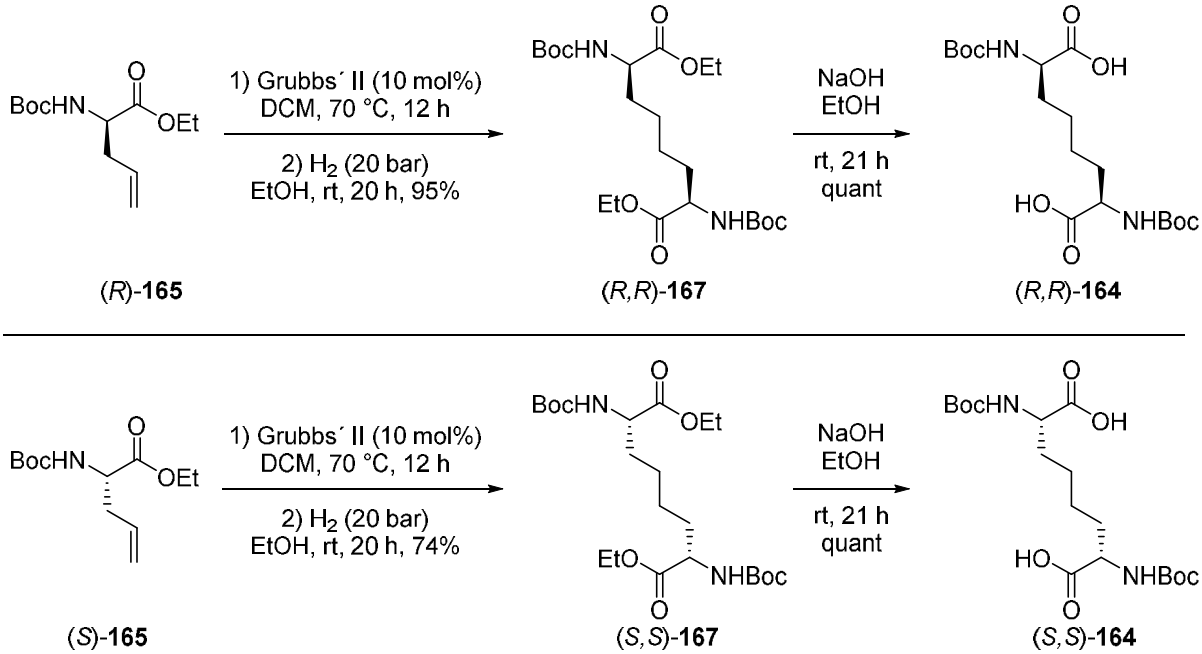


The pentapeptide synthesis was carried out manually on a Siber amide resin applying double coupling and following Fmoc-strategy (Scheme 47). After cleavage from the resin, the pentapeptides were coupled with *in situ* activated (*R*,*R*)-**164** and (*S*,*S*)-**164** providing the dimeric peptides (2*R*,7*R*)-1**52** and (2*S*,7*S*)-**152** after deprotection.[146]

**Scheme 47:** Synthesis of dimeric peptides (2*R*,7*R*)-**152** and (2*S*,7*S*)-**152**.[146]

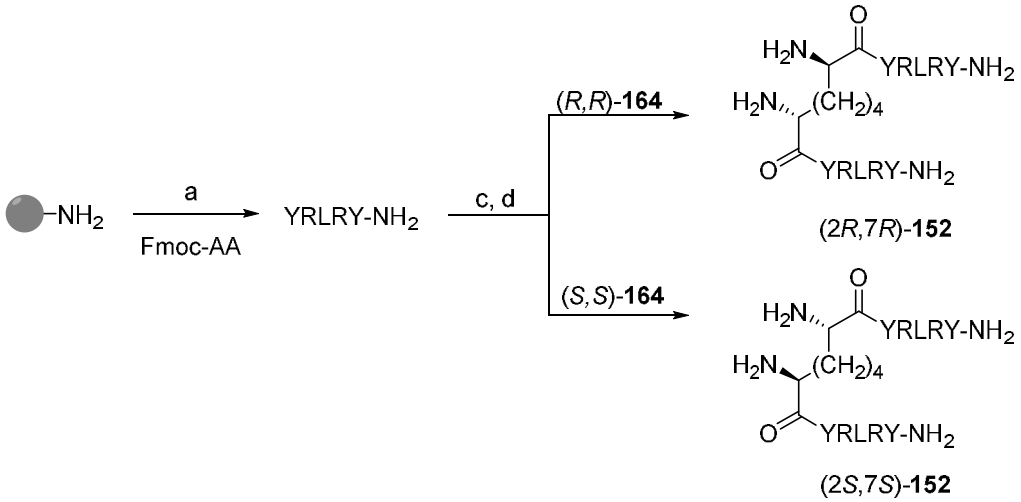


**Reagents and conditions:** a) Pentapeptide synthesis, SPPS, Fmoc-strategy: Fmoc-AA/HBTU/HOBt/DIPEA, DMF/NMP (8:2), double coupling at rt, 60 min, Fmoc deprotection was carried out with 20% piperidine in DMP/NMP (8:2), rt, 2x10 min; b) DCM/TFA (97:3), 10x6 min; c) HBTU/HOBt/DIPEA, DMF, 35 °C, 16 h; d) TFA/$H_2O$ (95:5), rt, 2.5 h, 29% for (2*R*,7*R*)-**152** and 34% for (2*S*,7*S*)-**152**.

With respect to the decelerated $Y_4R$ agonistic activity of the diastereomeric mixture **152**, dimeric peptides (2*R*,7*R*)-**152** and (2*S*,7*S*)-**152** were investigated for $Y_4R$ agonism in an aequorin $Ca^{2+}$ assay and a luciferase gene reporter assay on genetically engineered CHO and HEK293 cells, respectively. Indeed, the $Y_4R$ potency was affected by the configuration of the stereocenters in the 2,7-diaminosuberic acids. In the luciferase assay, (2*R*,7*R*)-**152** ($EC_{50}$ = 1.6 nM) was twelve times more potent than (2*S*,7*S*)-**152** ($EC_{50}$ = 19 nM). In the aequorin assay, the difference was less noticeable ((2*R*,7*R*)-**152** ($EC_{50}$ = 6.9 nM), (2*S*,7*S*)-**152** ($EC_{50}$ = 18 nM)).[146]

Based on the results obtained from the functional assays, (2*R*,7*R*)-**152** was selected for the synthesis of the corresponding tritiated analogue **169** by treating (2*R*,7*R*)-**152** with commercially available succinimidyl [$^3$H]propionate **168** (Scheme 48).[146]

**Scheme 48:** Preparation of radioligand [$^3$H](2*R*,7*R*)-**169**.

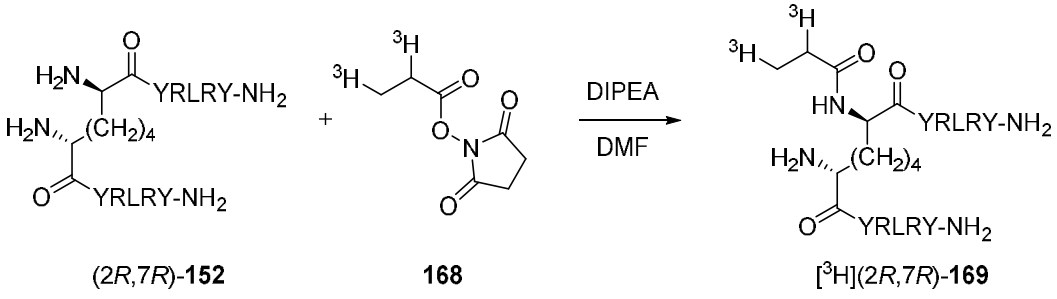

The newly obtained radioligand [$^3$H](2*R*,7*R*)-**169** was characterized by saturation binding experiments, performed on intact CHO-h$Y_4$-$G_{qi5}$-tAEQ cells in a HEPES (sodium free) buffer according to *Balasubramaniam et al.*[148] ($K_d$ = 0.67 ± 0.1 nM).[146] Subsequently, [$^3$H](2*R*,7*R*)-**170** was used for the determination of binding data of (2*R*,7*R*)-**152** and (2*S*,7*S*)-**152** at the $Y_4$ receptor in competition binding experiments. Also herein, (2*R*,7*R*)-**152** ($K_i$ = 0.45 ± 0.14 nM) revealed a higher affinity compared to (2*S*,7*S*)-**152** ($K_i$ = 2.3 ± 0.16 nM).[146]

In parallel to this project, *Thompson et al.*[164] independently synthesized peptide analogues of **152**, including the pure diastereomers (2*R*,7*R*)-**152** and (2*S*,7*S*)-**152**. Pharmacological data are in good agreement with those to here reported,[146] but affinities and potencies were obtained from different assays.

In summary, the synthesis of enantiopure diaminosuberic acids (*R*,*R*)-**164** and (*S*,*S*)-**164** was accomplished by cross-metathesis reaction promoted by Grubbs´ II catalyst giving access to single diastereomers of (2*R*,7*R*)-**152** and (2*S*,7*S*)-**152** individually. In competition binding experiments, (2*R*,7*R*)-**152** revealed to be superior to (2*S*,7*S*)-**152**. Moreover, [$^3$H](2*R*,7*R*)-**169** was established as a useful new pharmacological tool for the $Y_4$R which will be applied in the following chapter as high-affinity radioligand in competition binding studies.[146]

### 5.3 APC and ACPC building blocks in truncated NPY analogues

On the way to selective $Y_4$ receptor ligands, also a different approach was pursued. As mentioned above, $Y_4$ receptor prefers PP over PYY or NPY in contrast to $Y_1$, $Y_2$ or $Y_5$. A comparison of the amino acid sequence of hNPY (human neuropeptide Y) and hPP (human pancreatic polypeptide) reveals an accordance of 47%, especially the C-terminus (32-36) shows an identical sequence with the exception that proline (P, hPP) is replaced by glutamine (Q, hNPY) (Figure 11). As already mentioned in the previous chapter, the important residues for $Y_4$ receptor binding were located in the C-terminal region (Tyr[20,27,36]; Arg[25,33,35] and Thr[32]), based on Ala-scan studies on pNPY (porcine neuropeptide Y), which differs only at position 17 (Leu instead of Met) from hNPY.[127]

| | 1 | 11 | 21 | 32 |
|---|---|---|---|---|
| hNPY: | *H*-YPSKPDNPGE | DAPAEDMARY | YSALRHYINLI | TRQRY-$NH_2$ |
| hPP: | *H*-APLEPVYPGD | NATPEQMAQY | AADLRRYINML | TRPRY-$NH_2$ |

**Figure 11:** Amino acid sequence of hNPY and hPP.

It was also shown by previous studies, that the length of the NPY molecule is essential for receptor subtype recognition. Full length of NPY (1-36) was required for binding to $Y_1$R, whereas truncated analogues as NPY (13-36), NPY (18-36) and NPY (25-36) were only tolerated at the $Y_2$R.[165,166] Moreover, manipulation of the C-terminus of truncated NPY analogues (25-36 or 28-36) by single amino acid substitution revealed a shift of the selectivity profile of these analogues.[127,167,168]

Cyclic β- or γ-amino acids are known to induce or stabilize secondary structure motifs and can increase the stability of α-peptides due to proteolytic degradation.[17,169] β-ACC,[167,170] β-ACBC[171] (amino cyclobutyl carboxylic acid) and β-ACPC[18,120b,172] have already been used in our group together with collaborators for the investigation of peptidomimetics or peptide foldamers. Recently, constrained β-ACC **140** was introduced to position 32 and/or 34 in the C-terminal region of truncated NPY (25-36), directly next to crucial arginine units in position 33 and 35. The introduction of β-ACC building blocks induced a shift of the selectivity profile from the $Y_2$R of unsubstituted NPY (25-36) to the $Y_1$R and its affinity was strongly depended on the position of substitution and the applied stereochemistry of the β-ACC (Figure 12). It was assumed that the introduction of β-ACC rigidifies the flexible C-terminus to induce or stabilize a distinct secondary structure motif which is responsible for the selectivity shift. One

β-ACC in position 34 was enough to achieve nanomolar affinity ($K_i$ 37 nM) whereas the introduction of a second β-ACC did not improve the affinity. Analogues containing β-ACC with opposite stereochemistry (q, compare Figure 6, **117**) were inactive at all investigated receptors.[167]

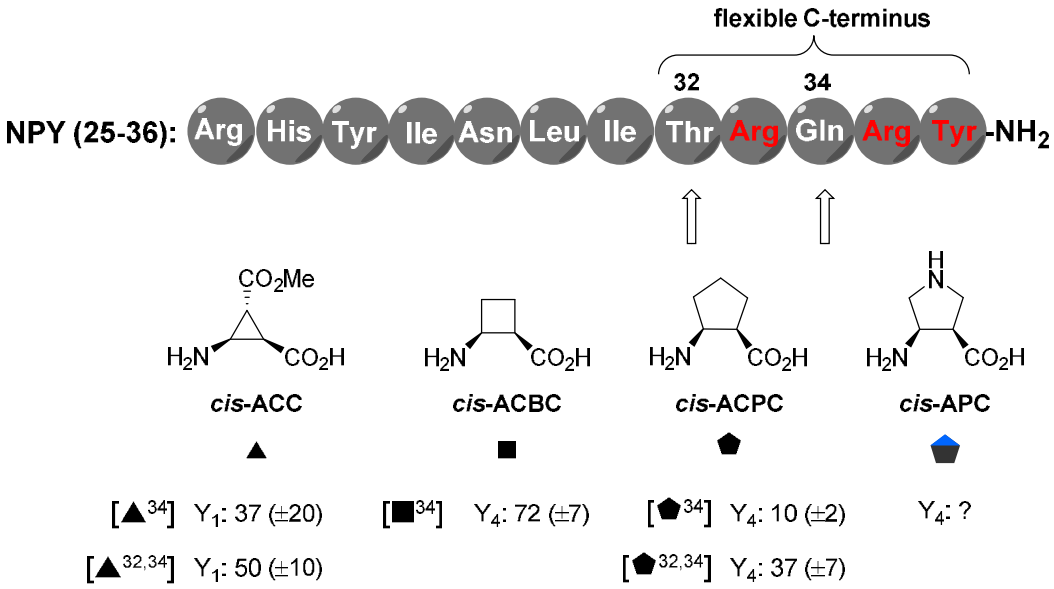


**Figure 12:** Overview of $K_i$ values (nM) of selected literature reported compounds.

Analogues substituted with β-ACBC and β-ACPC building blocks gained affinity at the $Y_4$ receptor, wherein the β-ACPC analogues were superior to the β-ACBC, achieving the best results by the introduction of one β-ACPC in position 34 ($K_i$ 10 nM). Similar to β-ACC containing analogues, the introduction of a second β-ACPC lead to a four-fold decrease in affinity ($K_i$ 37 nM).[173]

Due to the geometric similarity to β-ACPC, we envisioned the introduction of β-APC building blocks into truncated NPY (25-36) analogues. Under physiological conditions, the cyclic amine of β-APC will be protonated and could improve the affinity of corresponding NPY analogues, since β-APC would be placed next to positively charged arginine residues, which were discussed to be crucial for the selectivity and affinity of NPY ligands.

The APC containing NPY analogues were synthesized in cooperation with Prof. C. Cabrele in her laboratory at the University of Salzburg on an automated peptide synthesizer, applying Fmoc-chemistry and double-coupling procedure with HBTU/HOBt/DIPEA. The synthesis was performed on a Rink-amide MBHA polystyrene resin for C-terminally amidation. In accordance to the previous analogues, β-APC building blocks were introduced in position 32

and/or 34 (**170**, **171**, **172**, **173**) as well together with β-ACPC building blocks (**174**, **175**) (Figure 13).

The binding profile of all synthesized NPY analogues was determined by radioligand competition binding assay in the group of Prof. Dr. A. Buschauer under the supervision of *K. Kuhn* and *S. Dukorn*. The tests were carried out according to previously described procedure[146] on MCF-7 cells expressing $Y_1R$, CHO cells expressing $Y_2R$ and $Y_4R$, and HEC-1B cells expressing $Y_5R$ by displacement of radioligands [$^3$H]propionyl-pNPY ($Y_1R$, $Y_2R$, $Y_5R$) and [$^3$H](2*R*,7*R*)-**169** ([$^3$H]UR-KK193, $Y_4R$) (Table 6 and Figure 14).

For comparison of the binding data of the APC analogues with the ACPC analogues, literature compound **180** ([$Y^{32}$,À$^{34}$]-NPY(PP)-(32-36))[173] was also tested in here applied radioligand competition binding assay, since the ACPC analogues were investigated in a flow cytometry binding assay (Table 6, entry 5). Indeed, the $K_i$ value obtained from radioligand binding assay is in good agreement as reported in the literature reported[173] (124 nM *vs.* 105 nM) and permits comparison of the new APC analogues with the ACPC analogues.

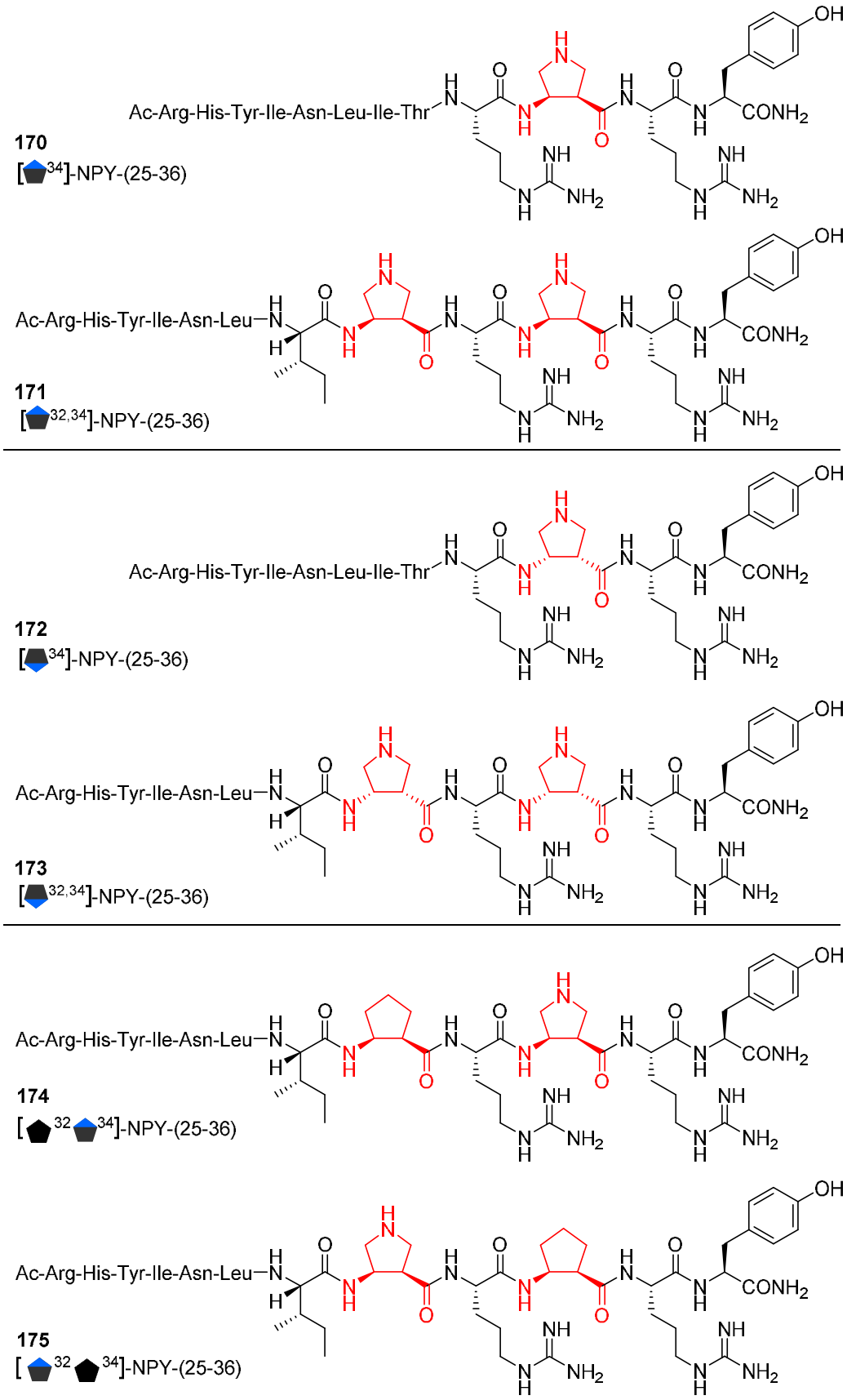


**Figure 13:** Amino acid sequences of synthesized NPY (25-36) analogues.

**Table 6:** Binding data of synthesized NPY analogues at human $Y_1R$, $Y_2R$, $Y_4R$, $Y_5R$ subtypes.

| entry | | compound | $Y_1$ [a] | $Y_2$ [b] | $Y_4$ [c] | $Y_5$ [d] |
|---|---|---|---|---|---|---|
| 1[e] | **176** | [ p $^{32,34}$]-NPY-(25-36) | **50** | >1000 | - | 617 |
| 2[f] | **177** | [ ¢ $^{34}$]-NPY-(25-36) | >1000 | >1000 | **72** ± 7 | >1000 |
| 3[f] | **178** | [ À $^{34}$]-NPY-(25-36) | >1000 | >1000 | **10** ± 2 | >500 |
| 4[f] | **179** | [ À $^{32,34}$]-NPY-(25-36) | >1000 | >1000 | **37** ± 7 | >500 |
| 5 | **180** | [Y$^{32}$, À $^{34}$]-NPY(PP)-(32-36) | – | – | 124 ± 14 [105 ± 42][f] | – |
| 6 | **170** | [ ◆ $^{34}$]-NPY-(25-36) | >5000 | >5000 | 413 ± 76 | 4102 ±1220 |
| 7 | **171** | [ ◆ $^{32,34}$]-NPY-(25-36) | >5000 | >5000 | **40** ±2 | >5000 |
| 8 | **172** | [ ◆ $^{34}$]-NPY-(25-36) | >5000 | >5000 | 4252 ± 1396 | >5000 |
| 9 | **173** | [ ◆ $^{32,34}$]-NPY-(25-36) | >5000 | >5000 | 446 ± 69 | >5000 |
| 10 | **174** | [ À $^{32}$ ◆ $^{34}$]-NPY-(25-36) | >5000 | >5000 | **42** ± 9 | 4546 ± 1367 |
| 11 | **175** | [ ◆ $^{32}$ À $^{34}$]-NPY-(25-36) | >5000 | >5000 | **20** ± 4 | 4753 ± 1091 |

Sequences and affinities (as $K_i$-values (nM)) of truncated NPY analogues on hY receptors ($K_i$-values were provided by *K. Kuhn* and *S. Dukorn*); a) – d) Data represent mean values ± SEM of at least two independent experiments performed in triplicate. Assays were performed as previously described: ref[146,174] a) Radioligand competition binding assay with [$^3$H]propionyl-pNPY ($K_d$ = 3.4 nM, c = 5 nM) using MCF-7-h$Y_1$ cells; b) Radioligand competition binding assay with [$^3$H]propionyl-pNPY ($K_d$ = 1.4 nM, c = 1 nM) using CHO-h$Y_2$-$G_{qi5}$-mtAEQ cells; c) Radioligand competition binding assay with [$^3$H](2*R*,7*R*)-**169** ([$^3$H]UR-KK193) ($K_d$ = 0.67 nM, c = 0.6 nM) using CHO-h$Y_4$R-$G_{qi5}$-mtAEQ cells; d) Radioligand competition binding assay with [$^3$H]propionyl-pNPY ($K_d$ = 4.83 nM, c = 4 nM) using HEC-1B h$Y_5$R cell; e) Taken from ref [167]; f) Taken from ref [173].

All APC containing NPY analogues revealed $Y_4R$ selectivity (Table 6, entry 6-11) except compounds **170**, **174** and **175,** which also showed very less affinity at the $Y_5R$ . In accordance with the ACPC and ACBC containing ligands (entry 2-4), all new analogues were biologically inactive at the $Y_1R$ and $Y_2R$. Moreover, the affinities of APC analogues were strongly depended on the stereochemical configuration of the APC building blocks, similar to β-ACC derivatives.[167]

The disubstituted APC analogues **171** and **173** [APC$^{32,34}$]-NPY-(25-36) showed about ten times higher affinities than its monosubstituted analogues **170** and **172** (entry 7 *vs.* 6, $K_i$ 40 *vs.* 413 nM and entry 9 *vs.* 8, $K_i$ 446 *vs.* 4252 nM). This is in contrast to the corresponding ACPC containing analogues (entry 3 and 4) and may indicate that APC$^{32}$ substitution is more tolerated than in position 34. This is supported by the about 40-fold less affinity of **170** [APC$^{34}$]-NPY-(25-36) compared to corresponding analogue **178** [ACPC$^{34}$]-NPY-(25-36)

(entry 6 *vs.* 3, $K_i$ 413 *vs.* 10 nM). The best affinity of compounds containing APC only was achieved with **171** [APC$^{32,34}$]-NPY-(25-36) (entry 7, $K_i$ 40 nM) in similar range to the corresponding ACPC analogue **179** [ACPC$^{32,34}$]-NPY-(25-36) (entry 4, $K_i$ 37 nM), designating that double APC substitution is better tolerated than single substitution.

For direct comparison of ACPC and APC substitution, both building blocks were introduced together in position 32 and 34 alternately to obtain a kind of hybrid NPY analogues. In these analogues, the order of substitution was essential for their affinities. Analogue **175** [APC$^{32}$ ACPC$^{34}$]-NPY-(25-36) was superior by a factor of two in $Y_4$ affinity in comparison to its corresponding analogue **174** [ACPC$^{32}$ APC$^{34}$]-NPY-(25-36) (entry 11 *vs* 10, $K_i$ 20 *vs.* 42 nM) indicating that an aliphatic residue as ACPC is more preferred in position 34 than a charged building block as APC.

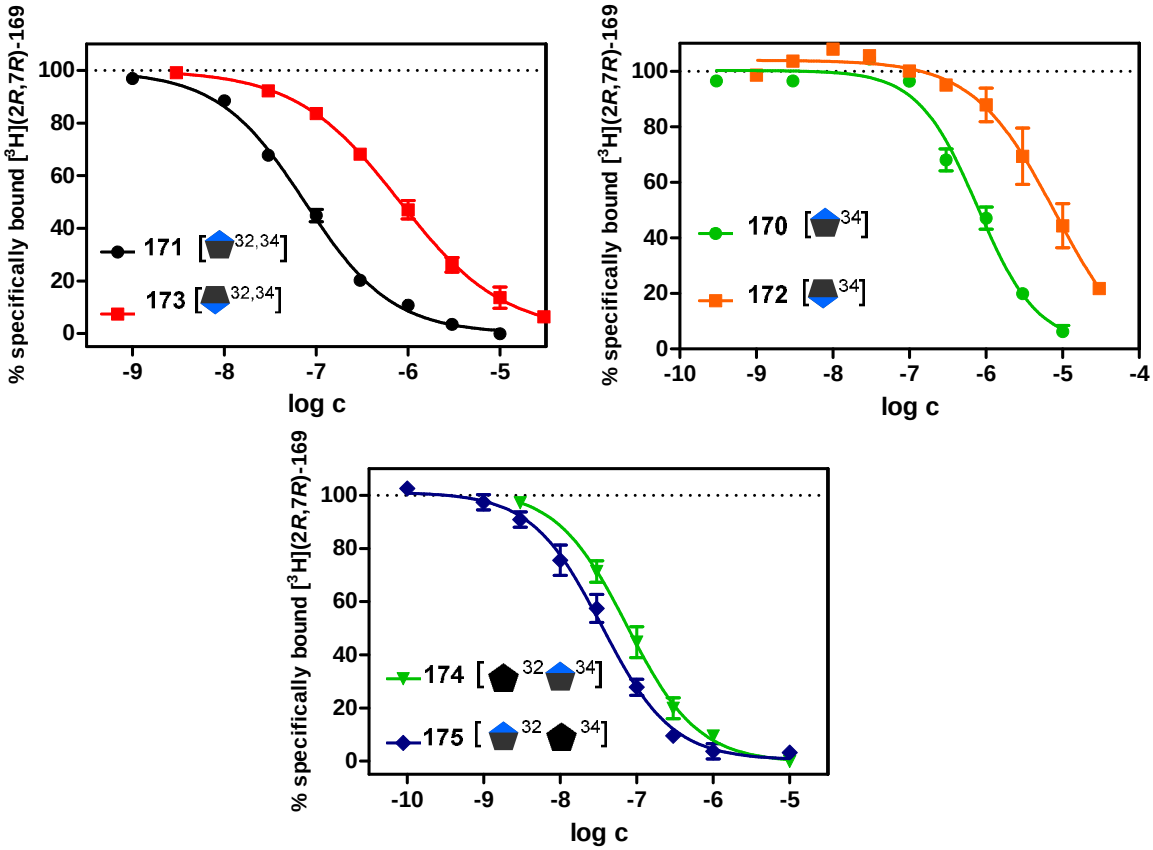


**Figure 14:** Binding curves of new APC containing NPY analogues **170**, **171**, **172**, **173**, **174** and **175** on human $Y_4$R obtained by radioligand competition binding assay on CHO-h$Y_4$R-G$q_{i5}$-mtAEQ cells using [$^3$H](2*R*,7*R*)-**169** as radioligand (c = 0.6 nM); log *c* on the *x*-axis refers to the decadic logarithm of the molar ligand concentration. The binding curves were provided by *K. Kuhn*. At least two independent experiments were performed in triplicate.

In summary, by the introduction of APC building blocks to truncated NPY (25-36) new $Y_4$R selective analogues were obtained. In particular, the best results were achieved with **171**

[APC$^{32,34}$]-NPY-(25-36) and **175** [APC$^{32}$ ACPC$^{34}$]-NPY-(25-36) analogues and the affinities are quite comparable to its analogue **179** [ACPC$^{32,34}$]-NPY-(25-36).

### 5.4 Conformational studies of truncated APC containing NPY analogues

The new APC containing NPY analogues were investigated by CD spectroscopy to get insight into their solution conformation. CD spectra of each peptide were recorded in phosphate buffer (100 mM, pH 7.0) to determine the conformation under physiological conditions. For mimicking membrane environment, the peptides were investigated in phosphate buffer mixed with trifluoroethanol (TFE, 30%), which is known as a structure-inducing co-solvent.

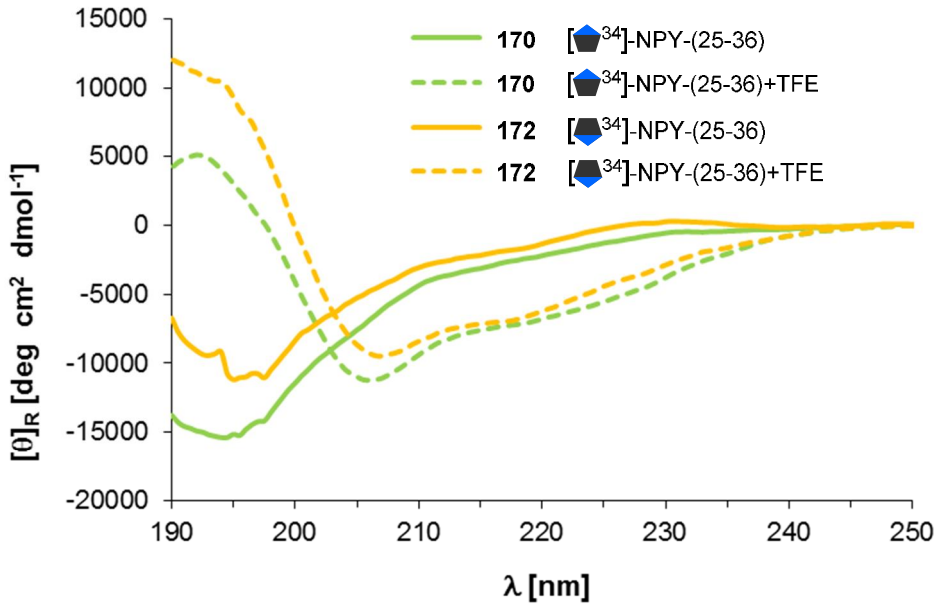


**Figure 15:** CD spectra of **170** and **172** in buffer and buffer + TFE. Peptide concentration was 125 µM in buffer (100 mM, pH 7.0) and 96 µM in buffer + TFE.

The monosubstituted peptides **170** and **172** were flexible in buffer, as indicated by the negative CD band below 200 nm and the weak CD contribution between 200 and 230 nm (Figure 15). Upon addition of TFE, the peptides adopted a short helical structure, shown by the CD maximum around 195 nm and two local minima around 208 and 220 nm. But **170** and **172** showed around 40-fold and 400-fold respectively less affinity at $Y_4R$ than their ACPC containing analogue **178** (Table 6, entry 3). **178** was reported to adopt helically structure[173] which is indicating, that the charge of APC$^{34}$ has a negative influence on the $Y_4R$ binding of

the APC containing NPY-ligands, but is not disturbing the formation of a short helix. The negative influence of the charged building block is supported by comparison with the native sequence of hPP, which contains an uncharged amino acid at position 34 ($Pro^{34}$) and is more preferred of $Y_4R$. Moreover, **170** was a bit less helical than **172** demonstrated by less intense CD band and by a slight blue shift of the band around 208 nm. This is in correlation with the binding profile of both ligands, wherein **170** was 10-fold more affine to $Y_4R$ than **172** and supports the finding, that high helically structures are not required alone for $Y_4R$ binding.

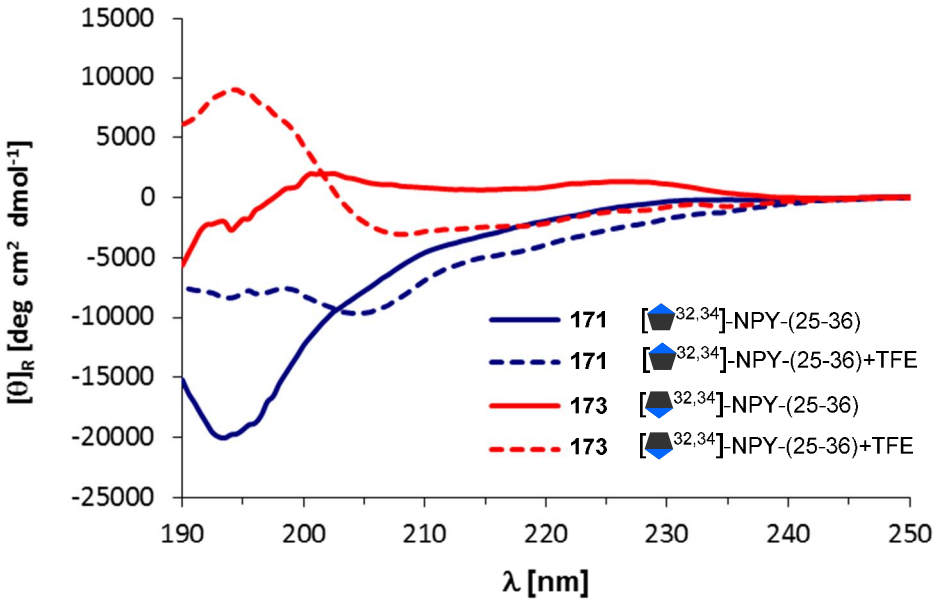


**Figure 16:** CD spectra of **171** and **173** in buffer and buffer + TFE. Peptide concentration was 125 µM in buffer (100 mM, pH 7.0) and 96 µM in buffer + TFE.

Similar to the monosubstituted peptides, **171** and **173** were flexible in buffer (Figure 16). But there is already a significant difference in the intensity observable, implying that **173** is already more structured in buffer and **171** is arranged as a random coil. However, upon addition of TFE, **173** adopted a turn-like structure motif, as shown by weak CD intensities around 195 nm, 208 and 220 nm, which seems not to be tolerated for binding at the $Y_4R$. This weak intensity of **173** may also occur from building aggregates. However, **171** seems to be very less helical upon the addition of TFE but shows good binding on $Y_4R$. Obviously, the less helically character in **171** permits the formation of a preferred C-terminally conformation, which compensates the negative influence of the charged APC building blocks and allows

binding on $Y_4R$, contrary to **170**. However, due to the weaker intensities of the CD-bands, it can be concluded, that both APC building blocks act as a α-helix breaker.

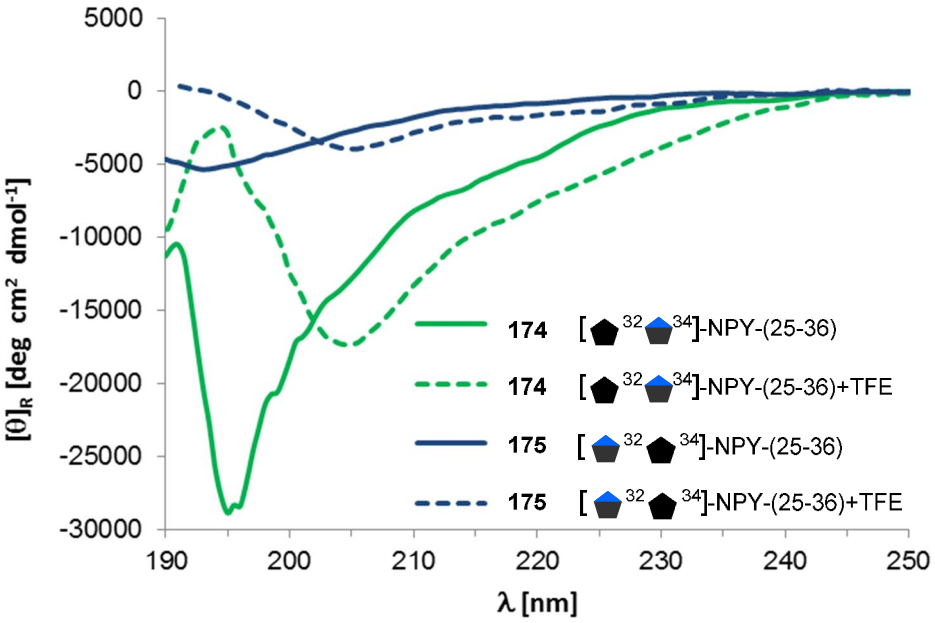


**Figure 17:** CD spectra of **174** and **175** in buffer and buffer + TFE. Peptide concentration was 100 µM in buffer (100 mM, pH 7.0) with or without 30% TFE.

The hybrid peptide **174** showed similar behavior as its analogue **171** (Figure 17). It was flexible in buffer and adopted less helically structure motifs by the addition of TFE resulting in similar affinity (Table 6, **171**: $K_i$ 40 nM; **174**: $K_i$ 42 nM). **175** was also flexible in buffer and adopted helically structure motifs by the addition of TFE, but less intensive than **174** or **171**. As mentioned above, a charged building block in position 34 is less tolerated than in position 32 and supports the 2-fold higher affinity of **175** compared to **174**.

### 5.5 Conclusion and Outlook

In this chapter, it was described that the introduction of charged APC building blocks into truncated NPY (25-36) delivered selective $Y_4R$ ligands with comparable affinities like its ACPC containing analogues. The best results were obtained with hybrid analogue **175** [$APC^{32}$ $ACPC^{34}$]-NPY-(25-36) suggesting that introduction of a charged amino acid at position 32 is more tolerated than in position 34, whereas aliphatic residue is more preferred in position 34. This is supported by comparison of literature compound **178** [$ACPC^{34}$]-NPY-(25-36) ($K_i$ 10 nM)[173] with **170** [$APC^{34}$]-NPY-(25-36) ($K_i$ 413 nM) and **174** [$ACPC^{32}$ $APC^{34}$]-NPY-(25-36) ($K_i$ 42 nM) with **175** [$APC^{32}$ $ACPC^{34}$]-NPY-(25-36) ($K_i$ 20 nM). All ligands containing an aliphatic residue in position 34 revealed a better affinity than its analogue with a charged building block in position 34. This result is in accordance with the native hPP sequence, containing an aliphatic residue such as Pro in position 34 which was discussed to be more preferred for $Y_4R$ binding than the native hNPY sequence.

The method of introducing cyclic amino acids shows high potential as it offers a great variety of possible substituents. Considering the already applied *cis*-building blocks, the next logical step would be the incorporation *trans*-building blocks and their corresponding γ-amino acids too (Figure 18).

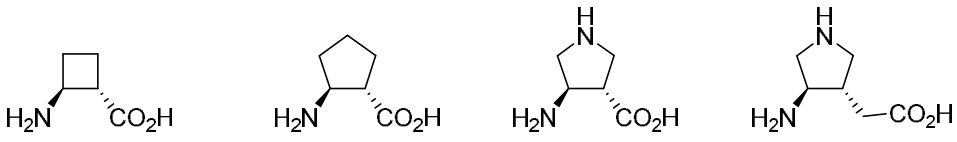


**Figure 18:** Possible *trans*-β-amino acid building blocks for application in truncated NPY analogues.

For this purpose, *trans*-ACPC **185** was synthesized from addition product **21** by epimerization with KO*t*Bu in refluxing *t*BuOH (Scheme 49).[24] This method delivered the desired building block (*S,S*)-**23** in diastereomerically pure form in 70% yield. Contrary to the previously described route towards *cis*-ACPC building blocks (chapter B1, Scheme 22) the order of the following modification steps was slightly changed. After hydrogenolysis of the benzyl groups, the free amine was subsequently functionalized with the Fmoc group for later intended solid phase peptide synthesis. Finally, hydrolysis of the *tert*-butyl ester provided **185** in 46% over 4 steps from **21**, ready for SPPS. However, utilization of **185** in NPY analogues was not possible anymore in this project.

**Scheme 49:** Synthesis of *trans*-ACPC building block **185** ready for SPPS.

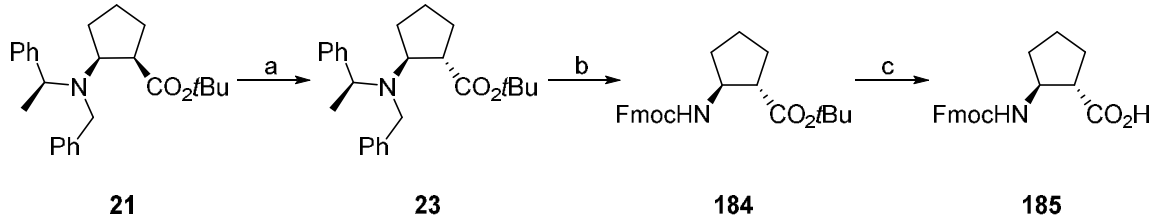


**21** **23** **184** **185**

**Reagents and conditions:** (a) KO*t*Bu, *t*BuOH, reflux, 8 h, 70%; (b) i) $H_2$ (20 bar), Pd/C, MeOH, rt, 14 h; ii) FmocOSu, $NaHCO_3$, dioxane/water, 0 °C to rt, 48 h, 65%; c) TFA, $Et_3SiH$, DCM, 0 °C to rt, 24 h, quant.

Corresponding *trans*-APC building block **54** is also reasonable for NPY substitution and would be accessible by the same route as *trans*-ACPC building block **185**.

A logical continuation of the *cis*-APC building block is the installation of various functional groups on the secondary ring amine and its evaluation in truncated NPY analogues (Scheme 50).

**Scheme 50:** Possible functionalized APC building blocks for NPY substitution.

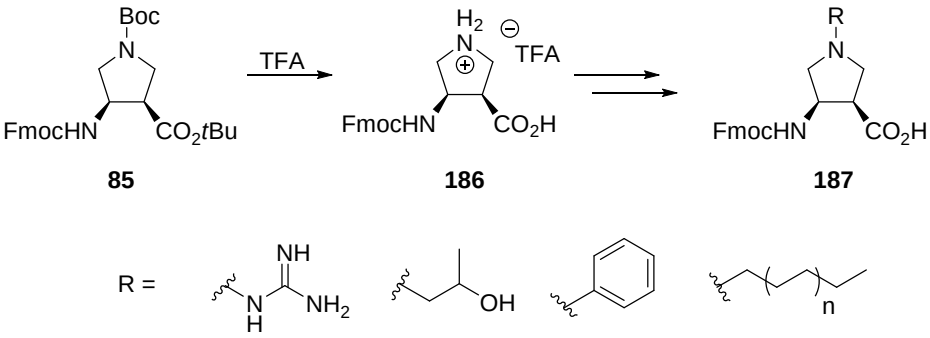


**85** **186** **187**

Getting access to functionalized APC building blocks should be simple by making use of the undesired Boc deprotection during APC building block synthesis (Chapter 1, Scheme 18) which provides **186**. This enables the installation of the desirable functional groups. Following this route, it would be possible to add the guanidine group, which is part of the amino acid arginine and designated to be crucial for NPY receptor recognition and activity. Furthermore, it is also possible to investigate the influence of hydrophobic groups such as phenyl or long-chained alkyl groups. The development and investigation of new building blocks for NPY substitution is still worthwhile and is the objective of current projects in the *Reiser* group.

# 6. Transformation of monocyclopropanated *N*-Boc-pyrrole

## 6.1 Ring-opening of monocyclopropanated *N*-Boc-pyrrole

### 6.1.1 Synthesis of homo-β-proline

[e] Homo-β-proline (3-pyrrolidineacetic acid, **188**) is a structural analogue of the nonproteinogenic *γ*-amino acid and neurotransmitter γ-aminobutyric acid (GABA) and was first mentioned in the late 1950s in a series of Japanese patents.[175] Studies on its biological potential appeared around twenty years later when a group of Danish scientists discovered that **188** is an inhibitor of GABA uptake.[176] Further studies on *N*-substituted derivatives of **188** emphasized its potential as a modulator of neuronal and glial GABA'ergic function.[177] Besides its biological activity, the core structure of **188** is a common structural element in many classes of natural products[178] and is also used as a central building block and/or pharmacophore in drug development, as proved by the large body of literature making use of this particular scaffold.[179]

Racemic homo-β-proline (±-**188**) is commercially available from a handful of suppliers ranging at approx. 20-200 USD/mmol. Commercial sources for the enantiopure material are scarce with higher costs. This may be due to the limited number of reported syntheses for either racemic or enantiopure **188**. Until now there are a total of ten synthetic protocols reported in the literature that aim for the synthesis of **188**,[180] and only two of these are of enantioselective nature.[181]

Given the highly interesting properties combined with the restricted accessibility, it was envisioned to synthesize enantiomerically pure **188** from monocyclopropanated pyrrole **190** (Scheme 51) utilizing the unique properties of donor-acceptor cyclopropanes that allow the ring-opening of the weakest bond in the three-membered ring.[182]

**Scheme 51:** Retrosynthesis of homo-β-proline **189** from *N*-Boc-pyrrole **192**.

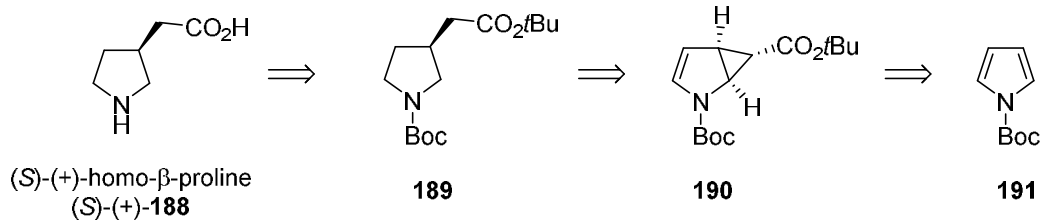


[e] Reprinted (adapted) with permission from Pilsl, L.; **Ertl, T.**; Reiser, O. *Org. Lett.* **2017**, *19*, 2754–2757. Copyright 2017 American Chemical Society.

While furans can be cyclopropanated with ethyldiazoacetate in high enantioselectivities (>90% *ee*) using Cu-(I)-bis(oxazoline) complexes,[183,184] the corresponding transformation of *N*-Boc pyrrole **191** has proven to be challenging in the past (<50% *ee*).[185] Sterically more demanding aryldiazoacetates derived from arylglycines in combination with chiral Rh(II)-catalysts were reported to achieve the cyclopropanation of **191** in 79% *ee*,[186] however, with the parent diazoacetates derived from glycine attempts to utilize Rh(II)-catalysts only led to alkylation products rather than cyclopropanation of **191**.[187]

Nevertheless, the asymmetric cyclopropanation of *N*-Boc-pyrrole was recently achieved in the *Reiser* group by *Pilsl* with enantioselectivity up to 93% *ee* by a combination of *tert*-butyl substituted diazoacetate **192** with the *tert*-butyl substituted aza-bis(oxazoline) ligand **193** (azabox). Getting access to the enantiopure product was achieved based on the fact that suitable conditions for an enantioenrichment by recrystallization from hexanes could be found. Furthermore, pioneering experiments of cyclopropane ring-opening towards homo-β-proline **188** were already carried out but accompanied with dramatic erosion of enantiopurity (Scheme 52).[75]

**Scheme 52:** Successful cyclopropanation of *N*-Boc-pyrrole **191** and original experiments towards homo-β-proline **188** by *Pilsl*.[75]

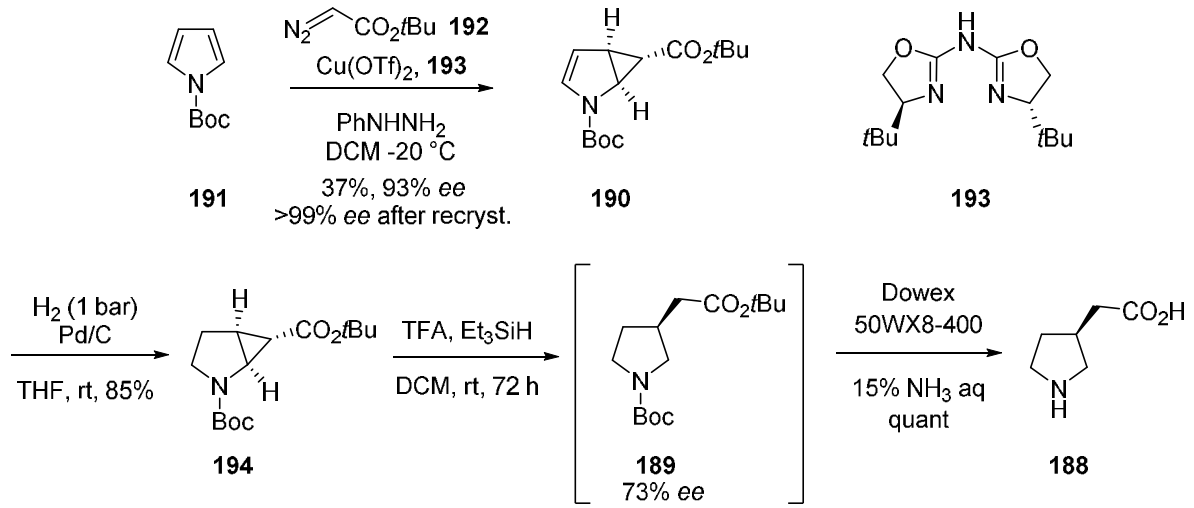


Therefore, it became obvious that the cyclopropane ring-opening under complete conservation of enantiopurity would be the major challenge in this route towards **188**. The following chapter describes the attempts in optimization for the synthesis of homo-β-proline **188** and represents a continuation of the work of *Pilsl*.[75]

For the asymmetric cyclopropanation of *N*-Boc-pyrrole **191**, azabox ligand **193** needed to be synthesized first. The azabox ligands were developed in the *Reiser* group[188,189] and are sterically demanding, similar to bis(oxazoline) ligands.[190] Azabox ligands were already successfully applied in various applications,[191] allow the possibility of electronic variation through alkylation on the central nitrogen and can be readily immobilized on various supports, which facilitates catalyst recovery.[192]

The synthesis of azabox ligand **193** started with the reduction of commercially available amino acid L-*tert*-Leucine **195** to the corresponding amino alcohol **196** (Scheme 53).[193] Oxazolidinone **197** was obtained by cyclization of aminoalcohol **196** with diethyl carbonate, which was subsequently alkylated by using *Meerwein´s reagent* to afford ethoxyoxazoline **198** in 86% yield over two steps. As second coupling partner towards azabox ligand **193**, aminooxazoline **199** was generated by the reaction of amino alcohol **196** with cyanogen bromide. Finally, desired azabox ligand **193** was obtained by acid catalyzed coupling of ethoxyoxazoline **198** and aminooxazoline **199** in 60% yield.

**Scheme 53:** Synthesis of aza-bis(oxazoline) ligand **193** according to *Werner et al*.[189]

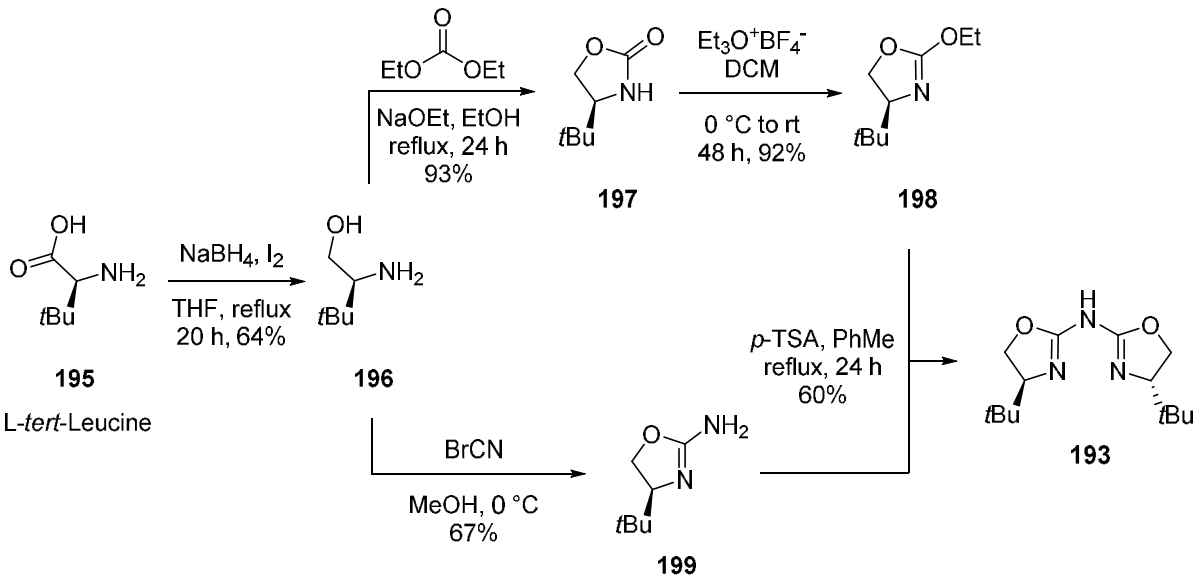


Subsequently, *N*-Boc-pyrrole **191** was cyclopropanated with *tert*-butyldiazoacetate **192** under the previously reported conditions[75] and cyclopropane **190** was obtained in 37% yield (lit.: 39% average) (Scheme 54) and with enantioselectivities up to 75%. However, recrystallization from hexanes gave access to enantiopure cyclopropanated pyrrole **190**.

**Scheme 54:** Asymmetric cyclopropanation of *N*-Boc-pyrrole **191** using azabox ligand **193** according to *Pilsl*.

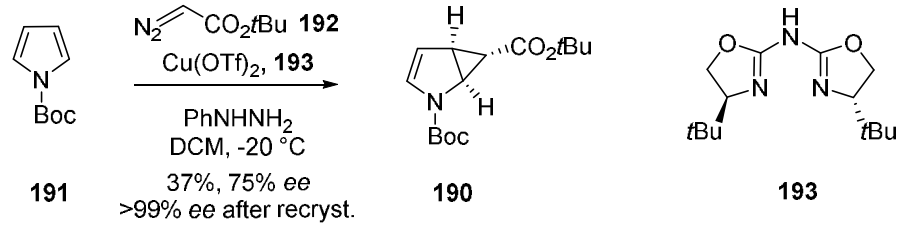


Focused on the steps forward to homo-β-proline **188**, reduction of the double bond in cyclopropane **190** was accomplished by hydrogenation using Pd/C at ambient pressure. However, application of this condition required chromatographic purification since the hydrogenation was accompanied by the occurrence of a byproduct which could be isolated in 6% yield (Table 7, entry 1). This byproduct could be identified as the 6-membered ring derivative **200** of desired fully-saturated cyclopropane **194** and will be discussed in detail in chapter 6.3.

**Table 7:** Optimization attempts for the hydrogenation of cyclopropanated *N*-Boc-pyrrole **190**.

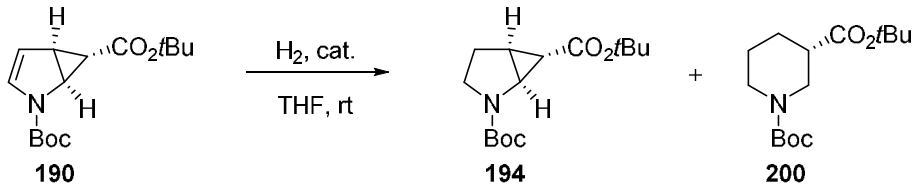


| entry | catalyst | mol% | $H_2$ (bar) | time (h) | **194** (%) | **200** (%) |
|---|---|---|---|---|---|---|
| 1 | Pd/C (10%) | 2.4 | 1 | 1.5-6 | 85 | 6 |
| 2 | Pd/C (10%) | 2.4 | 20 | 4 | 99 | - |
| 3 | Rh/C (5%) | 1.3 | 1 | 1 | >99 | - |
| 3 | Rh/C (5%) | 0.14 | 1 | 8 | >99 | - |

Optimization of the hydrogenation step was carried out by changing the pressure of hydrogen gas or the catalyst, resulting in a complete suppression of the formation of **200**. Quantitative yields of **194** without the necessity for a chromatographic purification were achieved using either Pd/C (Table 7, entry 2) or Rh/C (Table 7, entry 3). Moreover, the amount of applied Rh/C was reduced to 0.14 mol% (Table 7, entry 4) based on starting material **190** which elongated the reaction time up to 8 h. However, desired **194** could be obtained in quantitative yield under optimized conditions.

Next, suitable conditions for cyclopropane ring-opening with the full conservation of enantiopurity needed to be found. We envisioned the use of $Sc(OTf)_3$ for cyclopropane ring-opening, which was already applied in our group by *Roy* for Lewis acid-catalyzed multicomponent *Povarov* reactions getting access to compounds like **205** (Scheme 55). In this type of reaction, intermediary iminium ion **204** originating from cyclopropane ring-opening was trapped by furan migration.[194]

**Scheme 55:** $Sc(OTf)_3$ catalyzed multicomponent reaction towards **205** by *Roy et al.*

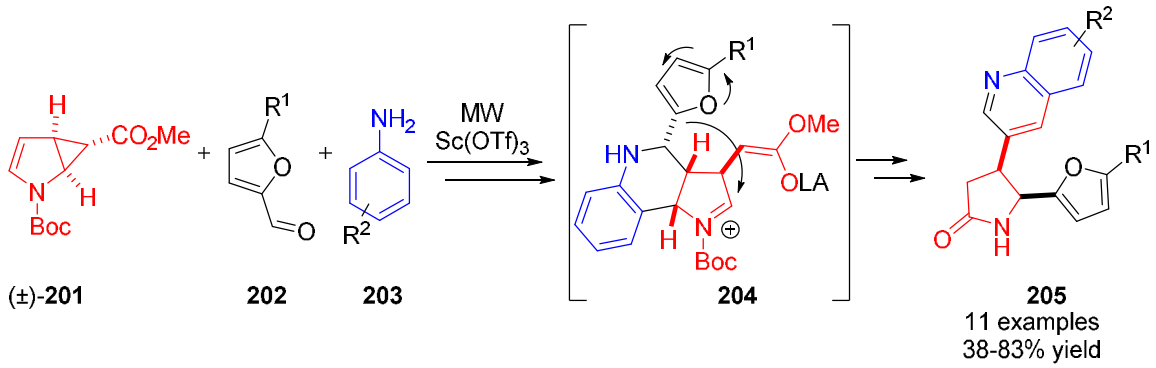


Based on these studies, first attempts using a combination of $Sc(OTf)_3$ and $Et_3SiH$ for ring-opening of **194** were tried under microwave irradiation (Table 8, entry 1), but the desired ring-opening product **189** was not detected and only starting material **194** was recovered. However, conversion was detected by the occurrence of highly polar spots on TLC, which might suggest the formation of the partially or already fully deprotected product **188**. Indeed, applying higher temperatures under microwave irradiation provided the fully deprotected ring-opening product **188**. Making use of this feature of simultaneous ring-opening/deprotection of the Boc group and *tert*-butyl ester provided **188** after simple isolation by centrifugation (entry 2). Removal of the triflate counter-ion by ion-exchange chromatography yielded the free amino **188** acid in 83%. However, comparison of the optical rotation value with the literature reports revealed a dramatic loss of enantiopurity (+ 3.0 *vs.* +9.6, *c* 1, $H_2O$, ref[176c]).

**Table 8:** First attempts of cyclopropane ring-opening using $Sc(OTf)_3$.

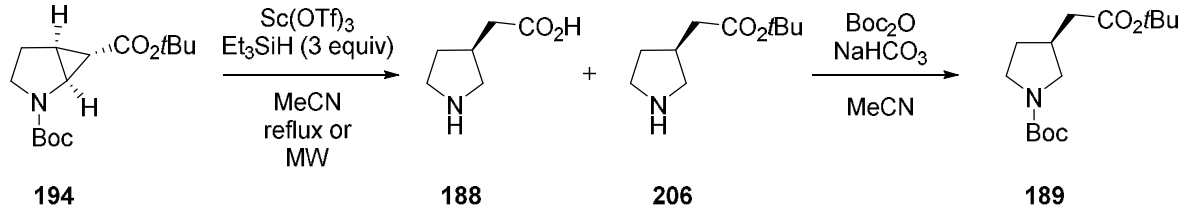


**194** **188** **206** **189**

| entry | acid (equiv) | *T* (°C) | time | conversion (%) | yield (%) | *ee* [a] (%) | $[\alpha]_D^{20}$ |
|---|---|---|---|---|---|---|---|
| 1 | $Sc(OTf)_3$ (0.3) | 30-80 (MW) | 60 min (6x10) | 46 | **194** (54) | - | - |
| 2 | $Sc(OTf)_3$ (0.3) | 150 (MW) | 15 min | 100 | **188** (83) | - | +3.0 |
| 3 | $Sc(OTf)_3$ (0.3) | 115 (MW) | 15 min | 100 | **189** (22)[b] | 4 | - |
| 4 | $Sc(OTf)_3$ (0.3) | 82 | 24 h | 100 | **189** (25)[b] | 11 | - |
| 5 | $Sc(OTf)_3$ (0.1) | 25 | 3 d | 9 | **194** (91) | - | - |

a) Determined by chiral HPLC; b) isolated yield of **189** after reprotection/derivatization for chiral HPLC analysis.

Optical rotation alone is not always ideal to judge the enantiopurity of a compound. Hence, it was tried to get access to the ring-opened pyrrolidine **189** in order to determine the enantiomeric ratio by chiral HPLC. Indeed, after microwave irradiation at lower temperatures or under reflux conditions, the crude contained a mixture of completely and partially deprotected ring-opening product (**188** and **206**) (entry 3 and 4). Therefore, it was decided to submit **206** to Boc-reprotection for the determination of enantiopurity by chiral HPLC, since HPLC conventional analysis for **206** was not possible due to the lack of a suitable chromophore. On the contrary, analysis of **189** was possible and conditions for chiral HPLC separation were already available from previous studies.[75] It became obvious from HPLC analysis that **189** could be only obtained in racemic form and the temperature for the cyclopropane ring-opening step is crucial for keeping the enantiopurity of the product. Since the conversion of starting material at ambient temperature was very slow, further investigations applying $Sc(OTf)_3$ were refrained (entry 5).

Regarding the temperature dependence of the ring-opening/deprotection sequence, it was decided to apply TFA/$Et_3SiH$ under milder conditions as previously employed. The decreased temperature required longer reaction times, but due to the relatively slow conversion during

the ring-opening/deprotection cascade, it was possible to obtain fully protected cyclopropane-opening product **189**, which was isolated, purified and investigated by chiral HPLC (Table 9, entry 2). By this way, it could be confirmed that the temperature is crucial for the cyclopropane ring-opening step and **189** could be isolated with >99% *ee*. However, achieving full conversion of **194** into **189** required longer reaction time up to 17 days and sequential addition of TFA and $Et_3SiH$ (entry 3), but finally desired homo-β-proline **188** was obtained in 89% yield. The results from the chiral HPLC analysis of intermediate **189** nicely support the optical rotation data of the obtained products and are fitting quite well to the literature reports.[195] The scalability of the newly developed synthetic route was demonstrated by starting from 1.00 g (3.6 mmol) of cyclopropanated pyrrole **190**, followed by hydrogenation towards **194**, resulting in 457 mg of **188** in an overall yield of >99% without the necessity to isolate either **194** or **189** (entry 4 and Scheme 58).

**Table 9:** Optimization of cyclopropane ring-opening.

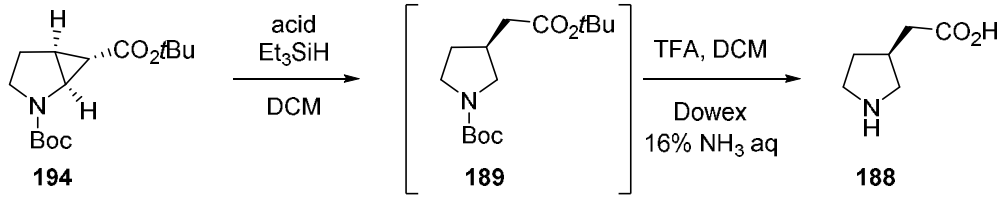


| entry | acid (equiv) | $Et_3SiH$ (equiv) | *T* (°C) | time (d) | conversion of **194** [a] (%) | yield (%) | *ee* [b] (%) | $[\alpha]_D^{20}$ |
|---|---|---|---|---|---|---|---|---|
| 1[c] | TFA (2) | 3 | 25 | 3 | 100 | **189** (50) | 72 | 7.7 |
| 2 | TFA (2) | 3 | 0 | 5 | 47 | **189** (33) | >99 | - |
| 3 | TFA (8) | 12 | 0 | 17 | 100 | **188** (89) | - | 9.1 |
| 4[d] | TFA (8) | 12 | 0 | 17 | 100 | **188** (>99) | - | 9.5 |
| 5[e] | $BF_3{\cdot}OEt_2$ (1.2) | 10 | 0 | 2 | 95 | **189** (53) | 97 | - |
| 6 | $BF_3{\cdot}OEt_2$ (1.2) | 10 | 0 | 2 | 100 | **188** (99) | - | 8.6 |

a) Based on reisolated starting material **194**; b) determined by chiral HPLC; c) taken from ref[75] d) 1.00 g (3.6 mmol) of **190** used as starting material; e) reaction was stopped after 2 days to for HPLC analysis of **189**.

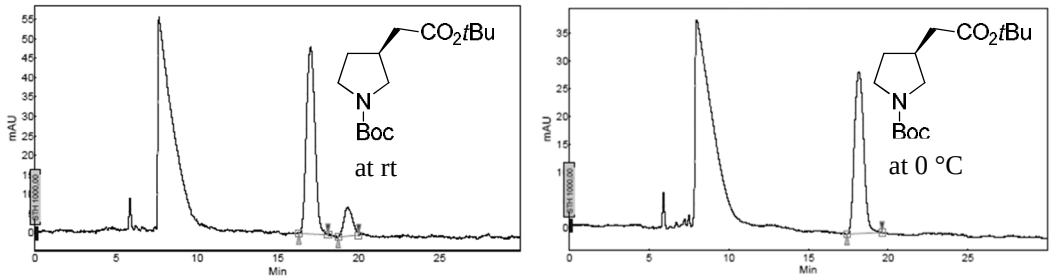


**Figure 19:** Analytical HPLC chromatograms of **189** after ring-opening at ambient temperature (left, 73% *ee*) and at 0 °C (right, >99% *ee*). Phenomenex Lux Cellulose-1, *n*-heptane/*i*PrOH 99:1, 0.5 mL/min, 200 nm ($t_r$ = 18.16 min; 19.31 min).

When $BF_3 \cdot OEt_2$ was applied under the same conditions, the reaction time could be decreased dramatically to 2 days along with only a slight erosion of enantiopurity. For analytical purposes, **189** was isolated and characterized (entries 5 and 6, Scheme 56); however, the crude could also be directly converted to **188** in overall quantitative yield starting from **194**.

**Scheme 56:** Optimized ring-opening/deprotection cascade towards homo-β-proline **188**.

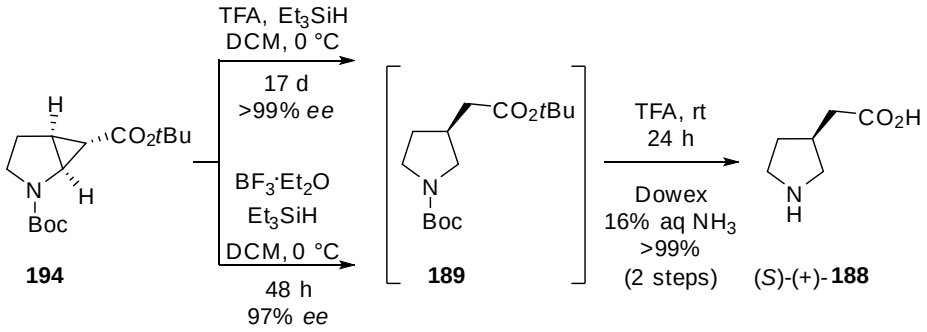


Epimerization during the ring-opening sequence can occur due to the abstraction of the proton in position 3 by the conjugate base of TFA, the trifluoroacetate anion (Scheme 57). Obviously, this abstraction occurs faster at higher temperature (Scheme 57, Pathway B) than the competitive trapping of the corresponding iminium ion **207** with a hydride ion as provided by $Et_3SiH$ (Scheme 57, Pathway A). This may be explained by the high acidity of the proton in position 3 caused by the electron-withdrawing iminium ion moiety and the stability of **208** in a conjugated system. As a matter of fact, this proton must be acidic enough to be abstracted by a weak base such as the trifluoroacetate anion.

**Scheme 57:** Proposed mechanism for cyclopropane ring-opening and possible epimerization.

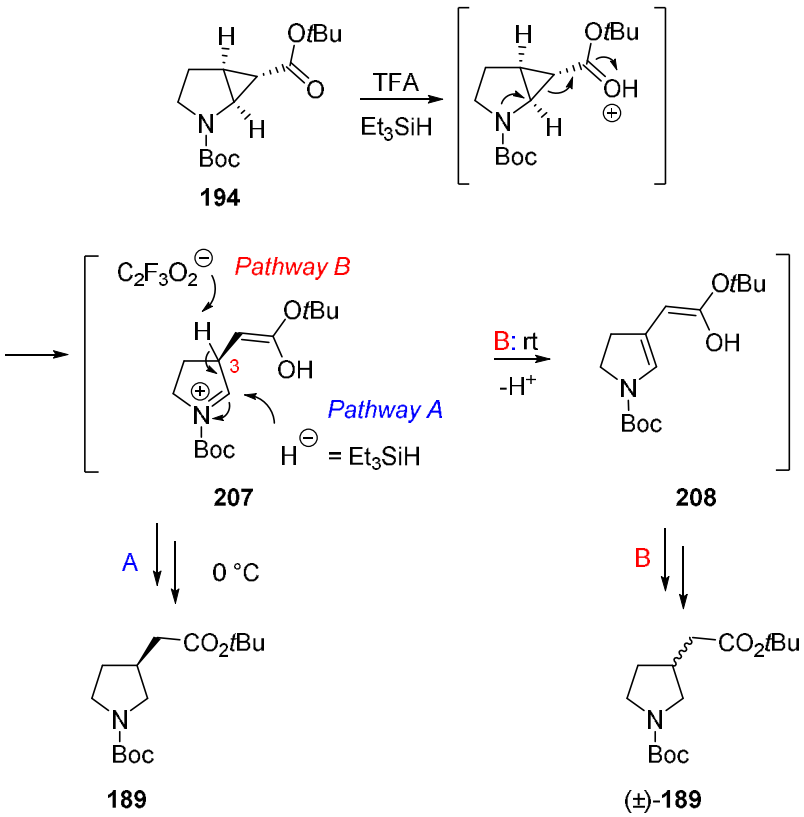


In summary, based on enantiopure cyclopropanated *N*-Boc-pyrrole **190**, a two-step route towards enantiomerically pure homo-β-proline **188** was developed, which can be obtained in quantitative yields and without the need for chromatographic purification of the intermediates (Scheme 58).[196]

**Scheme 58:** Optimized two-step synthesis of homo-β-proline **188** from cyclopropanated pyrrole **190**.

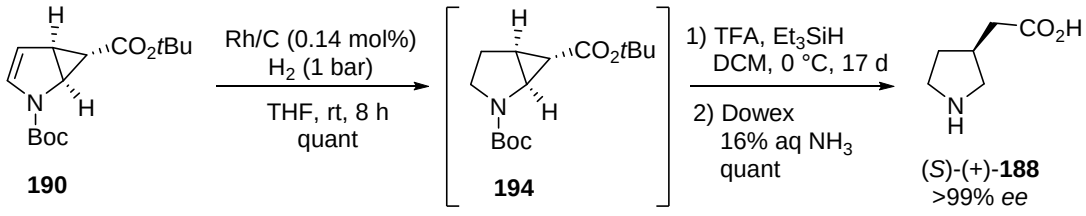

### 6.1.2 Synthesis of orthogonally protected 4-aminopyrrolidin-3-yl acetic acid

As already mentioned in chapter 5.5, besides the incorporation of cyclic β-amino acids in the C-terminal area of NPY ligands it would also be interesting to introduce cyclic γ-amino acids. After the successful ring-opening of **194**, it was envisioned to make use of this well-established method to get access to the γ-amino acid 4-aminopyrrolidin-3-yl acetic acid **210** (Scheme 59). Therefore, it was intended to open the cyclopropane ring in amine **209**, which can be accessible by functionalization of the enecarbamate double bond of **190**.

**Scheme 59:** Retrosynthesis of 4-aminopyrrolidin-3-yl acetic acid **210**.

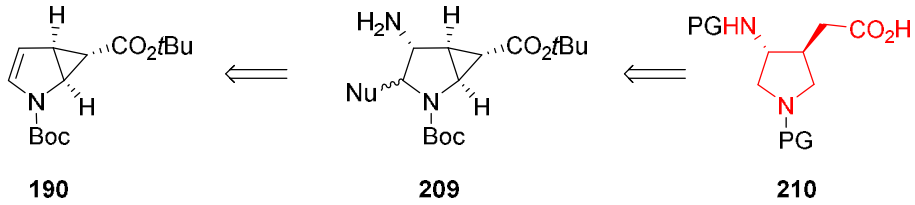


**190** **209** **210**

The introduction of the amine function can be accomplished by azidomethoxylation of the enacarbamate double bond in **211**, based on the studies of *Norton Matos et al.*[197] Herein, they utilized ceric ammonium nitrate (CAN) as an oxidizing reagent in the presence of $NaN_3$ and methanol for the preparation of *N*-heterocycles like **212**.

**Scheme 60:** Azidomethoxylation of an enecarbamate by *Norton Matos et al.*

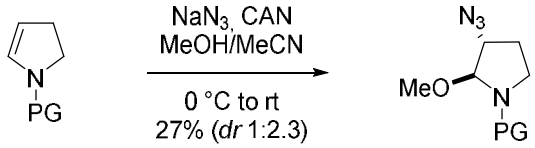


**211** **212**

According to this method, enantiopure cyclopropane **190** was submitted to azidomethoxylation providing the corresponding azide **213** in a moderate yield of 43% (Scheme 61).

**Scheme 61:** Azidomethoxylation of *tert*-butyl cyclopropane **190**.

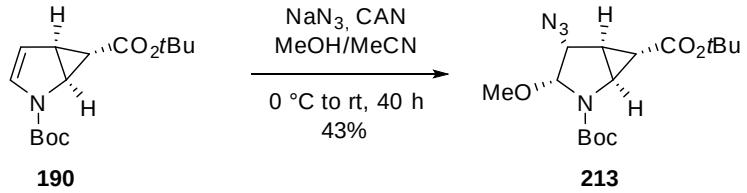


**190** **213**

However, in the $^{1}$H NMR of **213**, a partial splitting of the signals was observed, indicating the presence of inseparable diastereomers or rotational isomers, so called rotamers (restricted rotation around the C-N bond due to steric hindrance). The presence of rotamers can be proven and distinguished from the existence of diastereomers by the dynamic behavior of $^{1}$H NMR signals in variable temperature NMR measurements.

Therefore, three $^{1}$H NMR spectra at different temperatures were measured. It is clearly visible that the signals start melting together from lower to higher temperatures, which proves the rotameric behavior and excludes the presence of diastereomers.

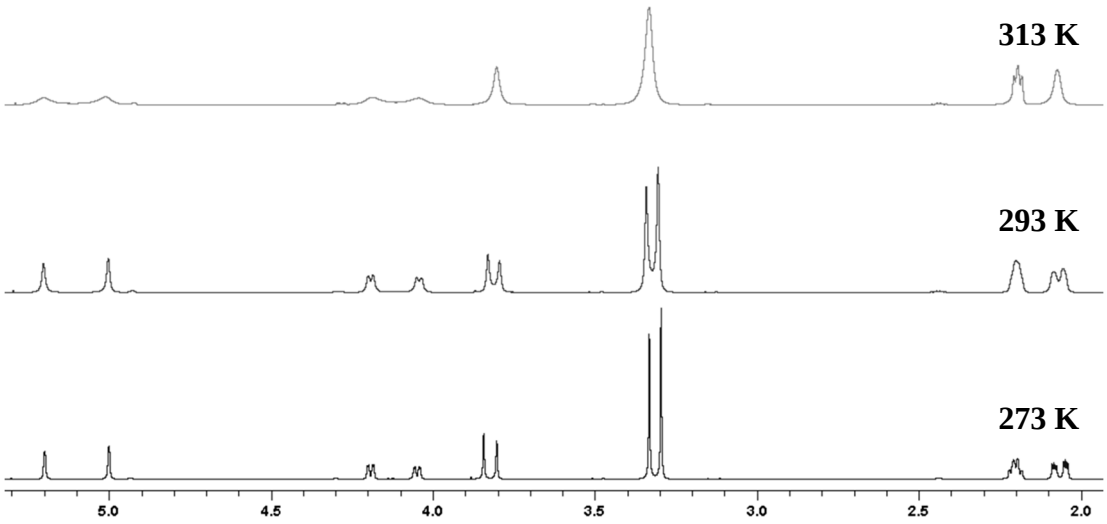


**Figure 20:** Excerpts from $^{1}$H NMR spectra of **213** at 273, 293 and 313 K in $CDCl_3$ (400 MHz kryo). Upon heating, the signals melt together, proving the existence of rotamers.

The absolute configuration of **213** was determined by performing NOESY experiments. Regarding that the absolute configuration of the cyclopropane ring hydrogens was already known, the configuration of the azide and methoxy group could be determined by NOE cross peaks revealing that the azide and methoxy group are *syn*-orientated to each other (Figure 21). Moreover, it was determined that the azide and the methoxy group orientate on the convex face of the bicycle. As a result, the *trans*-configured γ-amino acid will be obtained after cyclopropane ring-opening.

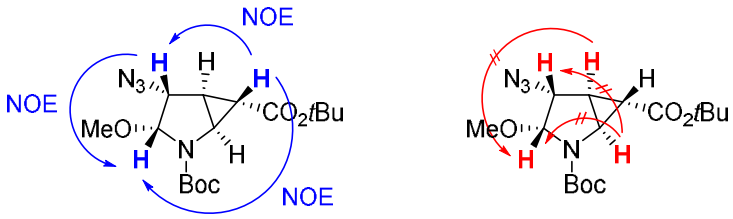


**Figure 21:** Determination of absolute configuration of **213** by the presence (left) or absence (right) of NOE cross peaks.

Concerning the synthesis of the desired γ-amino acid, the azide function was reduced to the corresponding amine **214** by hydrogenation under atmospheric pressure using Pd/C, whereas the application of *Staudinger* conditions[198] did not result in any conversion of azide **213** (Scheme 62). Since the γ-amino acid should be prepared ready for use in later intended SPPS, the free amine was Fmoc-protected providing compound **215** in 88% yield over 2 steps from azide **213**.

**Scheme 62:** Synthesis of Fmoc-protected cyclopropane **215** from azide **213**.

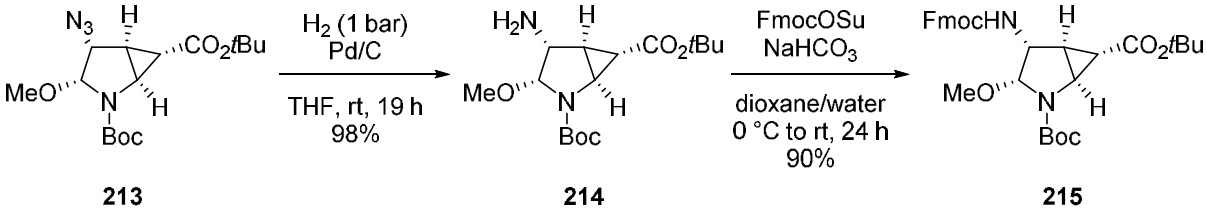


The next goal was to establish suitable conditions for the removal of the methoxy group. In their studies about diastereoselective functionalization of enecarbamates, *Dhimane et al.* applied $BF_3 \cdot OEt_2$ and $Et_3SiH$ under low-temperature conditions for reduction of α-aminoether moieties.[199] As demonstrated in chapter 6.1, cyclopropane ring-opening was also accomplished by using $BF_3 \cdot OEt_2$ and $Et_3SiH$, revealing the opportunity to perform the demethoxylation and ring-opening in a one-pot reaction.

Indeed, even under low-temperature conditions, demethoxylation occurred quite fast under full conversion of the starting material. The subsequent ring-opening reaction was performed at 0 °C and accelerated by the addition of accessory $BF_3 \cdot OEt_2$ and $Et_3SiH$ (Scheme 63). Moreover, the simultaneous deprotection of the Boc group took also place. Consequently, complete deprotection of the Boc group and *tert*-butyl ester was accomplished by addition of an excess of TFA. However, for later intended utilization in peptide synthesis the free carboxylic acid function as well as Boc-protected side chain amine were required. Complying with this, the free ring amine was submitted to Boc protection again providing the

orthogonally protected γ-amino acid **217** in 51% yield over 4 steps from Fmoc protected fused ring **215**.

**Scheme 63:** Demethoxylation/ring-opening/deprotection sequence towards γ-amino acid **217**.

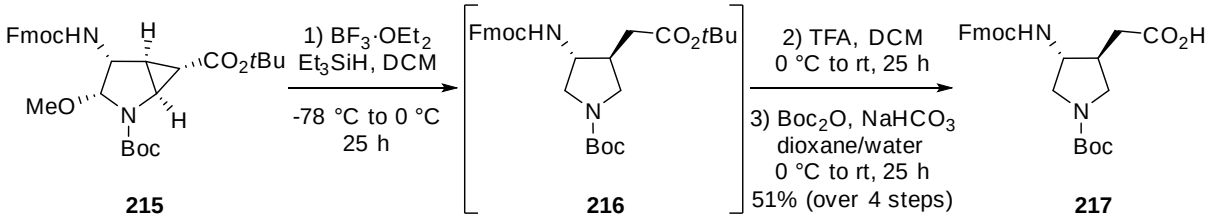


The demethoxylation/ring-opening/deprotection sequence was performed without the necessity to isolate the intermediates. For analytical purposes demethoxylated and ring-opened pyrrolidine **213** was isolated, purified, characterized and analyzed by chiral HPLC to determine the enantiopurity. Indeed, no epimerization during reaction cascade could be observed and the orthogonally protected *trans*-γ-amino acid was obtained in 19% yield over 7 steps from cyclopropanated *N*-Boc pyrrole **190**.

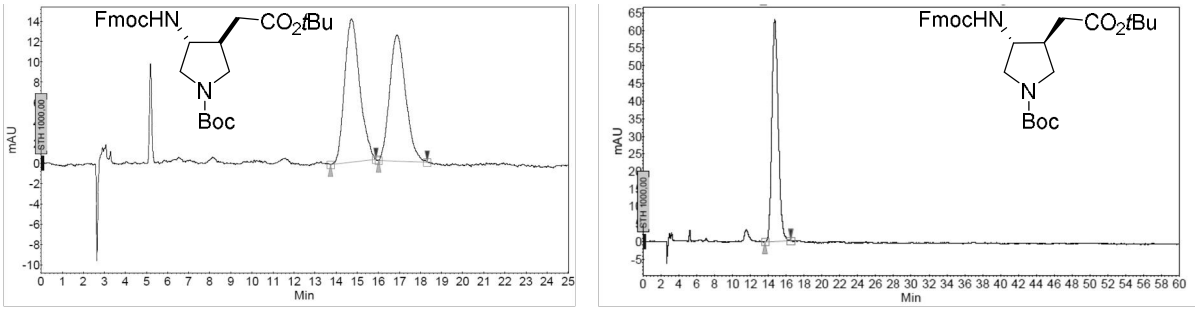


**Figure 22:** Analytical HPLC chromatogram of **216** after demethoxylation/ring-opening (left, *rac*; right, >99% *ee*). Phenomenex Lux Cellulose-1, *n*-heptane/*i*PrOH 80:20, 1.0 mL/min, 215 nm ($t_r$ = 14.72 min; 16.89 min).

Getting access to the corresponding *cis*-γ-amino acid **220** should be possible by adapting an iodocarbamation protocol of *Norton Matos*[197] providing iodo-carbamate bicycle **218** (Scheme 64). Treatment of compound **218** with a strong base in methanol would result in a migration/methanolysis and introduce the amine function in the desired position. Applying the above established demethoxylation/ring-opening/deprotection method would provide the desired *cis*-γ-amino acid **220**.

**Scheme 64:** Reasonable synthetic route towards *cis*-γ-amino acid **220** according to *Norton Matos et al.*[197]

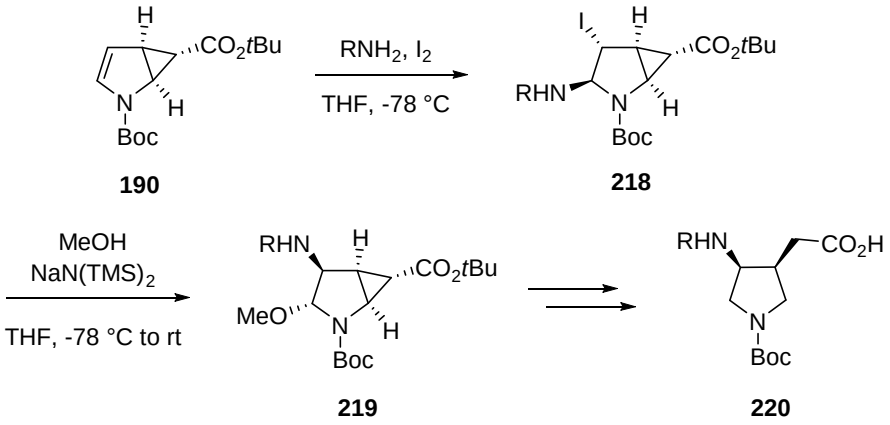


In summary, an enantiopure synthesis for orthogonally protected *trans*-4-aminopyrrolidin-3-yl acetic acid **217** from enantiopure monocyclopropanated *N*-Boc pyrrole **190** was developed. As the key step, a demethoxylation/ring-opening/deprotection cascade was performed under full conservation of enantiopurity and without the need for chromatographic purification of the intermediates.

### 6.1.3 Further functionalization attempts on monocyclopropanated *N*-Boc-pyrrole

Based on the ring-opening procedure developed in the previous chapters, further investigations on nucleophiles to trap the proposed iminium species **207** were carried out. Therefore, different nucleophiles with different (Lewis)-acids were applied in the ring-opening reaction of **194** to generate **221** (Table 10). At first, weak heteroatom nucleophiles were tried, but the desired product **221** was not formed (Table 10, entries 1-4). Instead, another product was isolated which could be identified as the ring-opening/lactonization product **222**.[200] Obviously, the employed nucleophiles were not strong enough to trap the iminium ion and lactonization occurs.

**Table 10:** Investigation of different trapping reagents for ring-opening reaction.

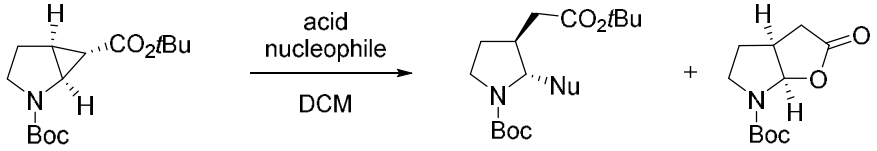


**194** **221** **222**

| entry | acid (equiv) | nucleophile (equiv) | T (°C) | time (d) | conv. [a] (%) | product (%) |
|---|---|---|---|---|---|---|
| 1 | TFA (2) | BnOH (3) | 25 | 6 | 72 | **222** (40) |
| 2 | TFA (2) | AllylOH (5) | 25 | 7 | 58 | not identified |
| 3 | TFA (2) | $BocNH_2$ (5) | 25 | 7 | n.d. | not identified |
| 4[b] | TFA (2) | $H_2O$ (5) | 25 | 7 | 90 | **222** (52) |
| 5 | TFA (2) | TMS-allyl (5) | 25 | 2 | 45 | **221** (4) |
| 6 | TFA (8) | TMS-allyl (12) | 0 | 17 | 85 | **222** (55) |
| 7 | TFA (8) | TMS-vinyl (12) | 0 | 14 | n.d. | **222** (15) |
| 8 | TFA (2) | TMS-CN (5) | 25 | 2 | 20 | complex mixture |
| 9 | $BF_3{\cdot}OEt_2$ (1) | TMS-allyl (10) | 0 | 3 h | n.d. | **221** (22) |
| 10 | $BF_3{\cdot}OEt_2$ (1) | TMS-vinyl (10) | 0 | 3 | 90 | **222** (n.d.) |
| 11 | $BF_3{\cdot}OEt_2$ (1) | TMS-vinyl (20) | 0 | 5 | 99 | **222** (n.d.) |
| 12 | $BF_3{\cdot}OEt_2$ (1) | TMS-CN (10) | 0 | 2.5 h | 100 | complex mixture |

a) Determined by recovered starting material **194**; b) MeCN was used as solvent instead of DCM.

When carbon nucleophiles were applied, only with TMS-allyl, the desired product could be generated but in poor yield (entry 5). Even multiple additions of acid and nucleophile over 17

days only led to the formation of lactonization product **222**, indicating that even at lower temperature ring-opening and deprotection occur faster than nucleophilic addition (entry 6). Nevertheless, the yield of allyl-**221** could be improved up to 22% by using $BF_3 \cdot OEt_2$ and excess of the nucleophile. Another nucleophile, TMS-vinyl was unreactive and only lactonization product was obtained (entries 7, 10 and 11) contrary to TMS-CN, which resulted in the generation of a complex mixture due to the high reactivity (entries 8 and 12).

Since the addition of the allyl-group was the only successful, a one-pot reaction towards **224** was performed (Scheme 65). TMS-allyl was used in combination with $BF_3 \cdot OEt_2$ as Lewis acid, followed by the complete deprotection of **223** by using TFA since partial deprotection during ring-opening was expected. The unprotected amino acid of **224** was then obtained as a diastereomeric mixture, which was submitted to Boc-protection to enable separation of diastereomers. However, separation of diastereomers of **224** was not possible (*dr* 1:1.2).

**Scheme 65:** Ring-opening/allyl addition/reprotection cascade towards **224**.

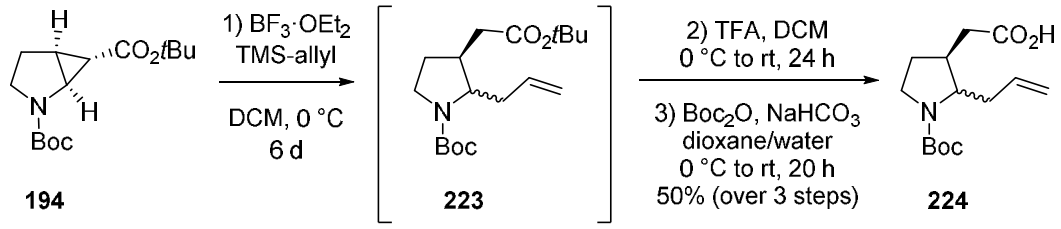


In particular, the addition of vinyl- or cyanide-functionality would be a worthwhile objective, since it would give access to the synthesis of kainoids (**227**),[201] a group in which kainic acid (**228**)[202] is a prominent representative (Scheme 66). Kainoids are an important class of natural non-proteinogenic amino acids, revealing a pyrrolidine moiety with two carboxylic acid groups as their characteristic structure.

**Scheme 66:** Reasonable synthetic routes towards kainoid core structure **228.**

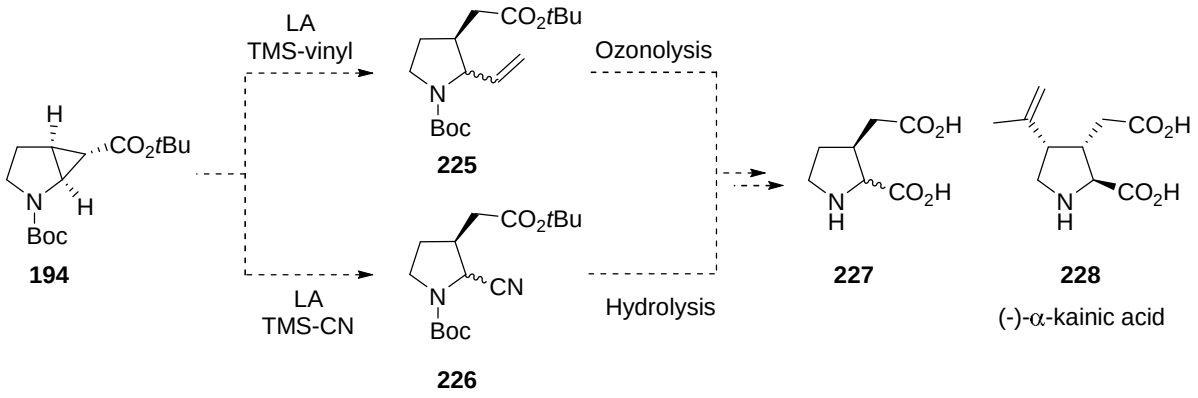

However, the attempts applying different nucleophiles in the ring-opening reaction were not successful, so it was tried to improve the yield of the lactonization product **222**. Therefore, cyclopropane **194** was treated only with TFA at ambient temperature to obtain the desired **222** in 53% yield (Scheme 67). The reason why the yield could not be increased may be due to the simultaneous deprotection of the Boc-group. In order to determine the enantiopurity, the reaction was performed at 0 °C with an elongated reaction time of seven days. However, **222** was obtained in 16% yield and though enantiopure starting material was used, isolated product revealed the enantiomeric excess of 39%. This indicates that epimerization takes place even at lower temperature when there is no suitable trapping reagent available.

**Scheme 67:** Synthesis of racemic and optical active **222**.

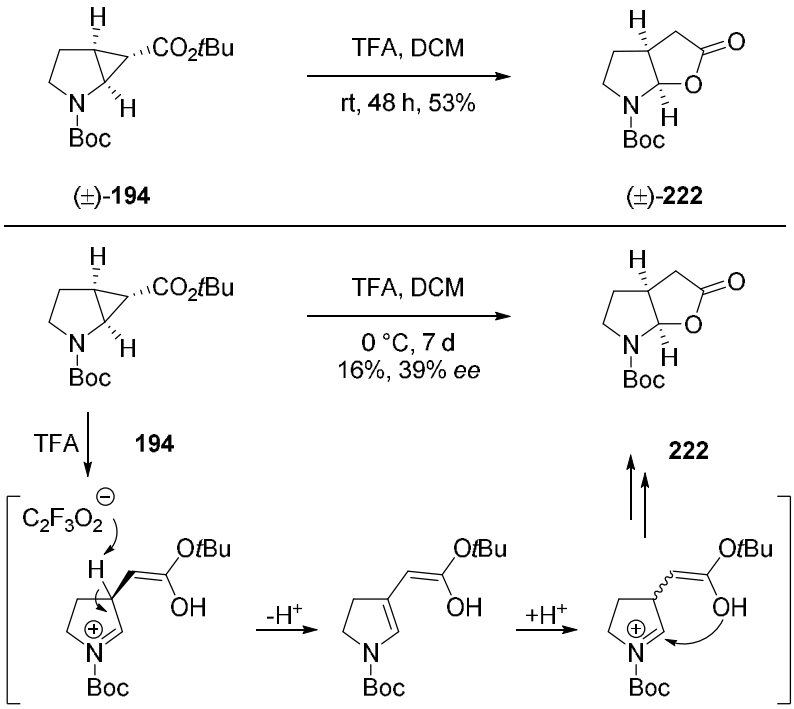


In summary, application of different nucleophiles as trapping reagents in the ring-opening emphasized to be challenging due to the less nucleophilicity of applied nucleophiles. However, a variety of nucleophiles can be still investigated accompanied by different reaction conditions since nucleophilicity can differ according to the applied solvents. Moreover, it turned out that a suitable nucleophile is necessary for trapping the iminium ion to prevent epimerization during the ring-opening reaction. Further investigations would be worthwhile since such reactions give access to core structures of interesting natural products.

### 6.2 Transesterification of monocyclopropanated *N*-Boc-pyrrole

[f] As in chapter 6.1.1 mentioned, the cyclopropanation of *N*-Boc-pyrrole was a challenging objective, and thus, the corresponding monocyclopropanated *N*-Boc-pyrrole methyl ester has not been accessible via an enantioselective route. It was only obtained via enzymatic resolution[101c] or by chiral separation[203] of racemic **201**. Since methyl ester **201** was proven to be a valuable building block for the construction of pyrrolidinones such as **205**[194] and **229**[203] or β-ACC **140** (Figure 23),[204] it would be desirable to get access to methyl ester **201** in enantiopure form.

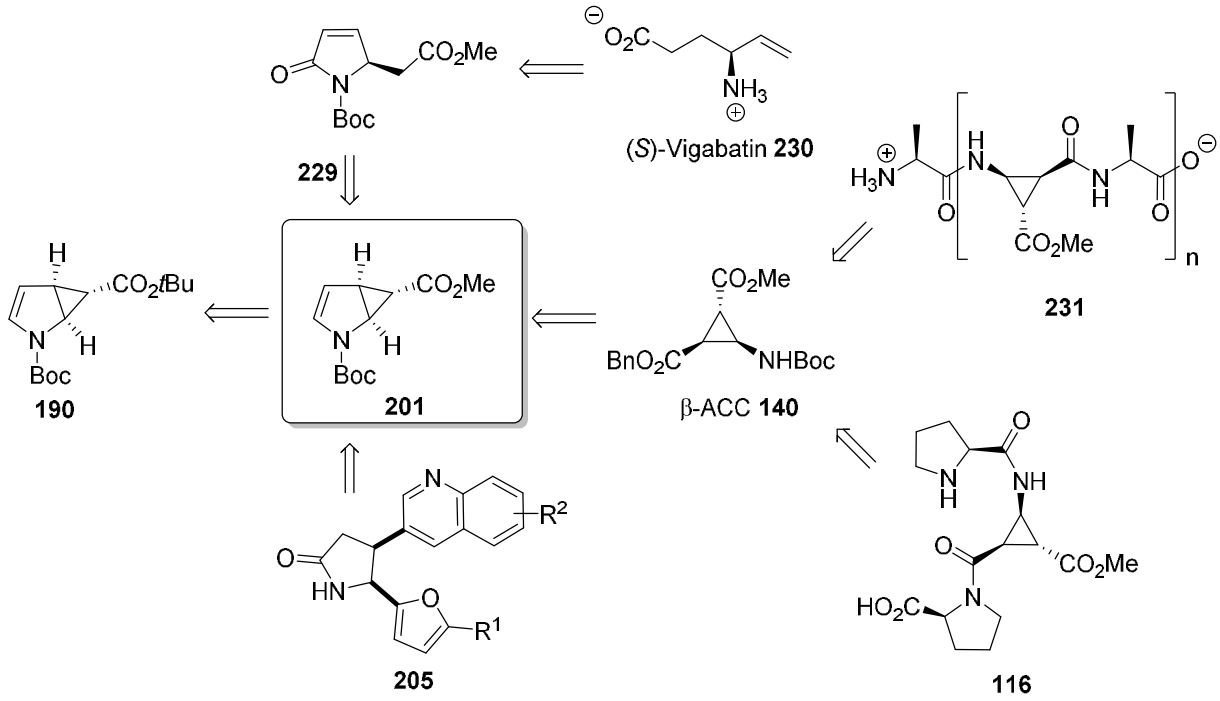


**Figure 23:** Excerpt of chosen applications based on methyl-cyclopropane **201**.

Since the cyclopropanation of *N*-Boc-pyrrole can be performed in an enantioselective way by using *tert*-butyl acetoacetate, it would be logical to utilize **190** for transesterification from *tert*-butyl ester to methyl ester to get access to **201**. First attempts were already performed in our group[75] following a procedure of *Fox et al.*[109] by using sodium methoxide in refluxing methanol for the transesterification. Indeed, the transesterification was proven to transform **190** into **201** without erosion of enantiopurity. However, it was carried out only with enantioenriched starting material (80% *ee*). Nevertheless, it was intended to perform the

[f] Reprinted (adapted) with permission from Pilsl, L.; **Ertl, T.**; Reiser, O. *Org. Lett.* **2017**, *19*, 2754–2757. Copyright 2017 American Chemical Society.

transesterification under the same conditions but with enantiopure starting material (Scheme 68). Compared to previous results[75] the yield could be improved from 46% to 67% by a modified work-up procedure. Furthermore, the desired methyl-cyclopropane **201** was delivered in enantiopure form (Figure 24).

**Scheme 68:** Conversion of *tert*-butyl-cyclopropane **190** into methyl-cyclopropane **201** according to the procedure of *Fox et al.*

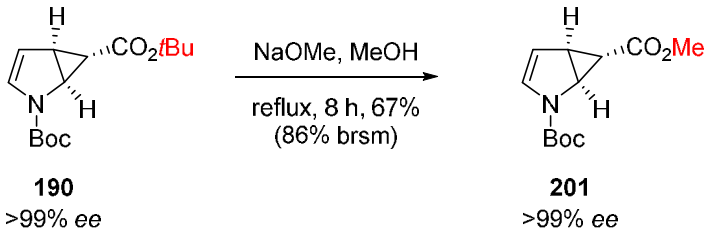


**190**
>99% *ee*

**201**
>99% *ee*

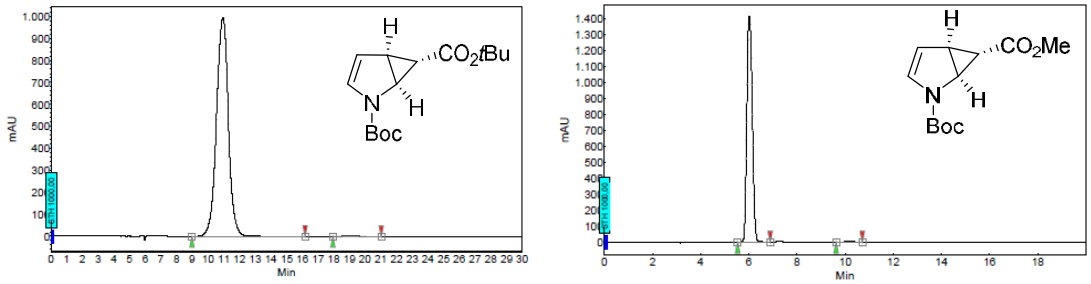


**Figure 24:** Analytical HPLC chromatogram for *tert*-butyl-cyclopropane **190** (left, >99% *ee* (Phenomenex Lux Cellulose-2, *n*-heptane/*i*PrOH 98:2, 0.5 mL/min, 254 nm; $t_r$ = 10.95 min, 19.02 min)) and methyl-cyclopropane **201** (right, >99% *ee* (Phenomenex Lux Cellulose-1, *n*-heptane/*i*PrOH 99:1, 1 mL/min, 240 nm; $t_r$ = 6.02 min, 10.12 min)).

Moreover, *Otera's*[205] tin oxide catalysts **232** and **233** were also utilized in the above-described transesterification. These catalysts can be simply synthesized out of dibutyltinoxide, dibutyltinchloride and NaSCN (Scheme 69) and were used in transesterifications or acetalizations and were frequently applied in our group in the synthesis towards γ-butyrolactones such as **236** (Scheme 70).[204]

**Scheme 69:** Synthesis of tin oxide catalysts according to *Otera et al.*

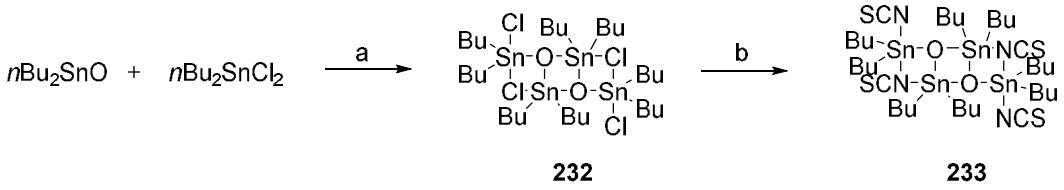


**232**

**233**

**Reagents and conditions:** (a) Toluene, reflux, 5.5 h, 98%; (b) NaSCN, EtOH, reflux, 5.5 h, 99%.

**Scheme 70:** Example for applied *Otera* catalysts in the *Reiser* group by *Kreuzer*.[206]

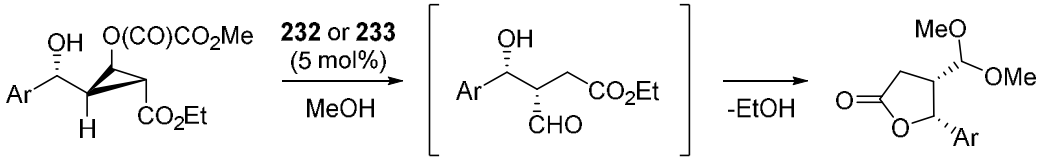


**234** **235** **236**

However, the applied catalysts turned out to be inactive in the conversion of *tert*-butyl ester **190** (Table 11).

**Table 11:** Attempts to apply *Otera* catalysts for the transesterification step.

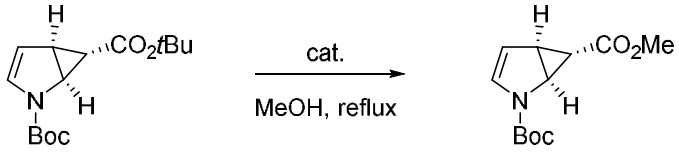


**190** **201**

| entry | cat. | mol% | time (h) | yield (%) [a] |
|---|---|---|---|---|
| 1 | **232** | 5 | 24 | <5 |
| 2 | **233** | 10 | 45 | ~7 |

a) Estimated from $^{1}$H NMR of the crude of reaction mixture without an internal standard.

Nevertheless, from now on methyl ester cyclopropane **201** is accessible again by transesterification of enantiopure *tert*-butyl cyclopropane **190** by using NaOMe in refluxing methanol. This compound was established to be a key building block for a great amount of applications in the *Reiser* group in the last 20 years.

### 6.3 Ring-expansion of monocyclopropanated *N*-Boc-pyrrole

As described in chapter 6.1.1 (Table 7), a byproduct was formed during the hydrogenation of monocyclopropanated *N*-Boc-pyrrole **190**, which was identified as the 6-membered ring **200** (Figure 25).

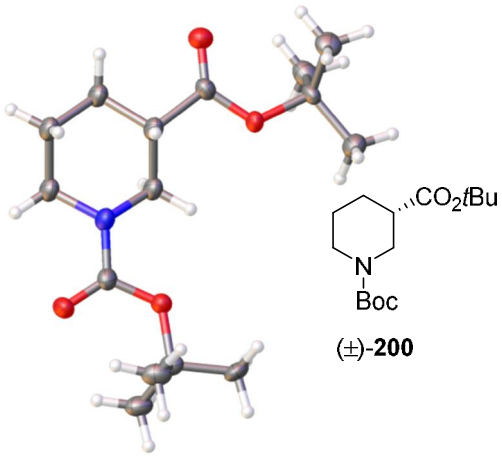


**Figure 25:** Single crystal X-ray structure of (±)-**200** (*C* = grey, *H* = white, *O* = red, *N* = blue).

The formation of **200** stands for an interesting result since it would be expected that the bond between the donor (D) and acceptor (A) (dashed) moiety of the cyclopropane should be cleaved. It's a known fact that the bond between D and A on the cyclopropane is typically the longest and thus the weakest. Nonetheless, the inner bond of the cyclopropane ring was cleaved (Scheme 71).[182]

**Scheme 71:** Expected and isolated byproducts of hydrogenolysis of **190**.

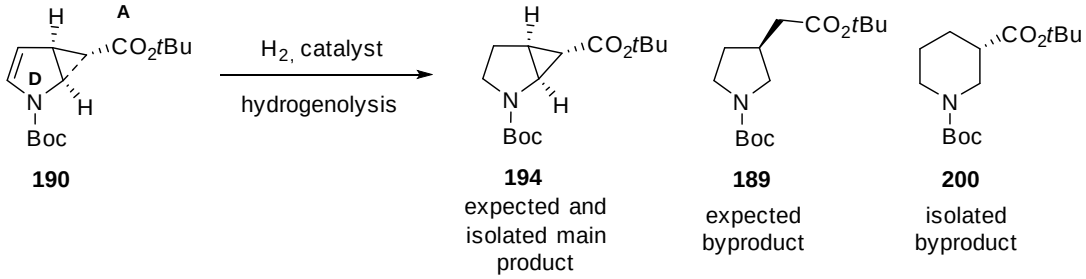


The 6-membered ring **200** represents the *N*-Boc protected *tert*-butyl ester derivative of Nipecotic acid **237**. To access **237**, hydrogenation of enantiopure **190** was performed and the desired 6-membred ring **200** was obtained in improved yield of 19%. It should be mentioned, that in previous experiments (compare chapter 6.1.1) **200** was isolated in only 5-6% yield. Finally the hydrolysis of the Boc group and *tert*-butyl ester was followed to afford the free amino acid **237** (Scheme 72).

**Scheme 72:** Hydrogenation of cyclopropanated pyrrole **190** towards Nipecotic acid **237**.

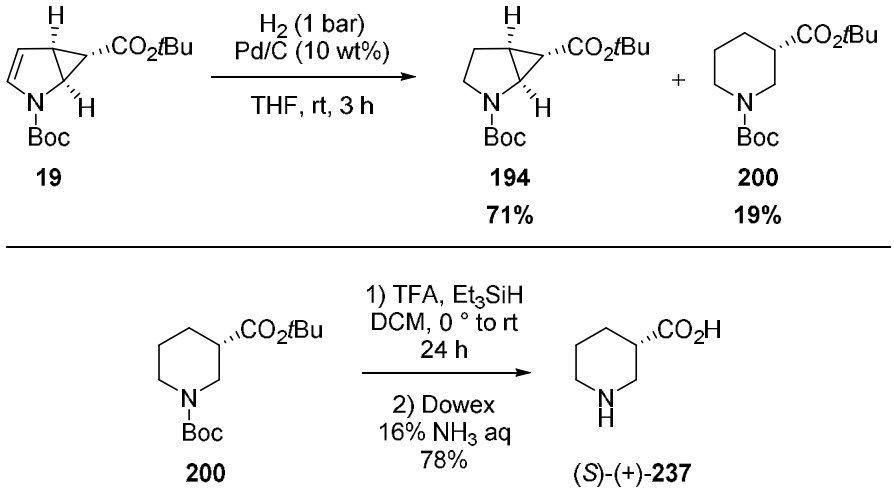


The absolute configuration of **200** could be determined by optical rotation measurement since optical rotation value for the free amino acid **237** was already reported in the literature.[207] Spectroscopic data of **237** were in agreement with those in the literature and in particular, the optical rotation value (+4.7, (*c* 1, $H_2O$) smoothly fitted to the reported data (+4.7, (*c* 1, $H_2O$, (*S*)-enantiomer)).[207] The result from optical rotation measurement nicely supports the chiral HPLC analysis of **200** which proves, that no epimerization during the hydrogenation occurred and **200** was isolated as the (*S*)-enantiomer.

Nipecotic acid **237** can be considered as a conformationally restricted GABA analogue and it builds the core structure of various GABA uptake inhibitors such as Tiagabine **238**, which is used in the treatment of epilepsy.[208,209] It is accessible via *classical* hydrogenation[210] or by electrolytic hydrogenation[211] of its aromatic analogue, Nicotinic acid (**239**). The (*R*)-enantiomer of Nipecotic acid was found to be more potent than the (*S*)-enantiomer and each enantiomer can be obtained by resolution of the racemate via enzymatic *N*-acetylation,[212] fractional crystallization[207,213] or by asymmetric hydrogenation[214] of Nicotinic acid.[215]

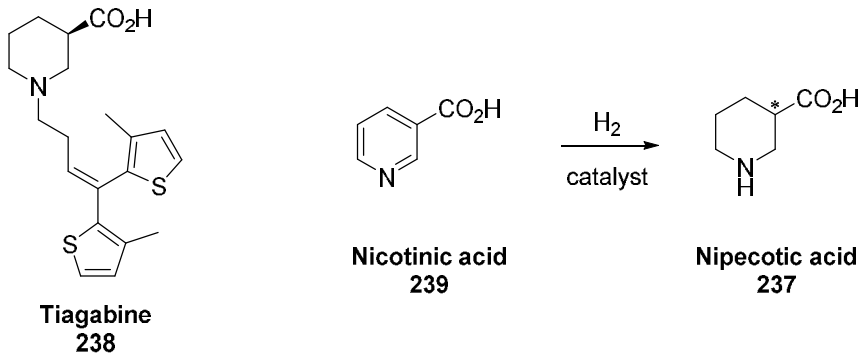


**Figure 26:** Chemical structures of Tiagabine and Nicotinic acid.

Due to its various medicinal applications and the fact that *N*-Boc-protected Nipecotic acid *tert*-butyl ester **200** can be obtained as a byproduct in enantiopure form hydrogenation of **190**, it was envisioned to find the best conditions for a selective cyclopropane ring-opening towards **200**.

### 6.3.1 Hydrogenolysis of cyclopropanated *N*-Boc-pyrrole towards Nipecotic acid

Nipecotic acid ester **200** was obtained during hydrogenation of **190**, so it was obvious to investigate the hydrogenation step more in detail. Hydrogenolysis of small rings with a high degree of ring strain is well-known in the literature as it is a valuable tool for synthetic chemistry. First examples were reported in 1907 by *Willstätter* and *Bruce*, obtaining alkane **241** from hydrogenolysis of cyclopropane **240** by using Nickel catalysts (Scheme 73).[216] *Danishefsky et al*.[217] or *de Meijere et al*.[218] demonstrated that highly strained *spiro*-annelated cyclopropanes such as **242** or **244** even react under milder conditions to the corresponding compounds **243** and **245**. Very recently, *Nishii et al*. reported a highly regioselective reductive Pd-catalyzed ring-opening of 2-arylcyclopropane-1,1-dicarboxylic diesters such as **246** under mild conditions.[219]

**Scheme 73:** Literature precedents for the catalytic hydrogenolysis of cyclopropane moieties.

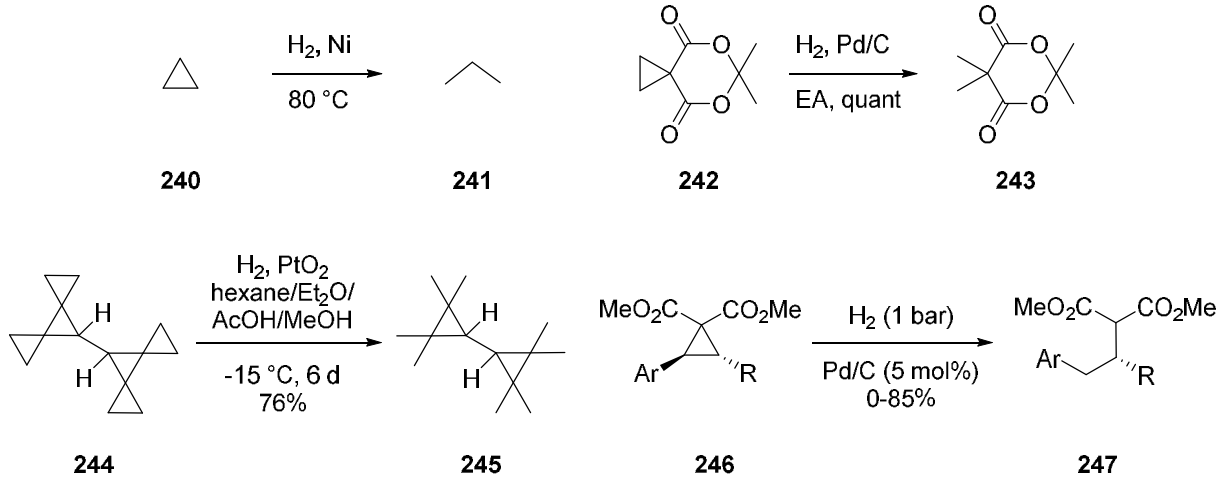


Therefore, in this study different catalysts were tested if the yield of desired 6-membered ring could be improved (Table 12). Compared to the original conditions providing **200** (entry 1), only Platinum catalysts led to the formation of the desired 6-membered (entries 2,3 and 6,7). Application of Rhodium catalyst delivered the fully saturated product **194** exclusively and

without the need of further purification (entries 4,5 and see chapter 6.1.1, Table 7). Due to the fast conversion of the starting material, it was decided to extend the reaction time to determine possible conversion of the fully saturated fused ring towards the 6-membered ring. However, no further conversion towards the 6-membered ring was observed. Furthermore, a Nickel- and the *Lindlar* catalyst were employed (entries 10 and 11). Particularly, the *Lindlar* catalyst was believed to show promising results because it is known to prevent the formation of alkanes during the hydrogenations of alkynes to alkenes. As expected, the rate of conversion was very slow but also the fully saturated fused ring was formed exclusively. The Nickel catalyst proved to be ineffective in the hydrogenation of **190**.

**Table 12:** Catalyst screening for hydrogenation of **190**.

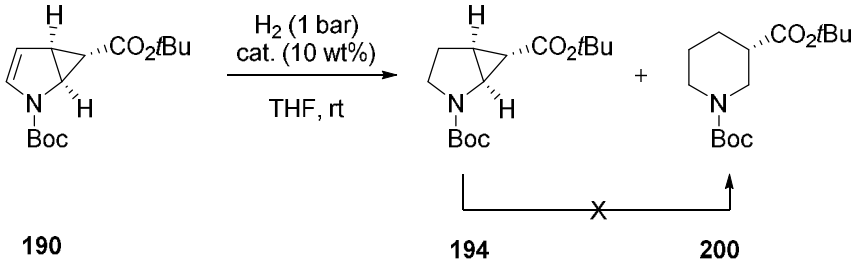


| entry [a] | catalyst | time | yield (%) [b] |
|---|---|---|---|
| 1 | Pd/C (10%) | 1.5 h | **194** (85), **200** (6) |
| 2 | Pt/C (10%) | 2 h | **194** (97), **200** (3) |
| 3 | Pt/C (10%) | 24 h | see entry 2 |
| 4 | Rh/C (5%) | 1 h | **194** (>99) |
| 5 | Rh/C (5%) | 24 h | see entry 4 |
| 6 | $Pt_2O \cdot H_2O$ | 2 h | **194** (87), **200** (1) |
| 7 | $Pt_2O \cdot H_2O$ | 5 d | see entry 6 |
| 8 | $Rh/Al_2O_3$ (5%) | 2 h | **194** (97) |
| 9 | $Rh/Al_2O_3$ (5%) | 24 h | see entry 8 |
| 10 | $Ni(PPh_3)_4(CO)_2$ | 24 h | no conversion |
| 11 [c] | *Lindlar* | 17 h | **194** (n.d.) |

a) In all entries, the total amount of used Pd/C was 10 wt% based on the starting material **190**; b) isolated yield; c) *Lindlar* catalyst: 5% Pd deposited on $CaCO_3$ poisoned with Pb.

In order to prove, if the double bond in **190** is essential for the formation of the 6-membered ring, the fully saturated fused ring **194** was submitted to hydrogenation under increased pressure and temperature (Table 13). Platinum on charcoal was chosen as the catalyst since it

is a more active catalyst than Pd/C. However, no conversion of the starting material was observed. Even forcing conditions only led to decomposition of starting material due to exothermic reaction in the autoclave vessel (entry 3) (caution: if the solvent is not degassed, Pt/C catalyzes the oxyhydrogen reaction and results in an ignition).

**Table 13:** Hydrogenolysis of **194** towards **200**.

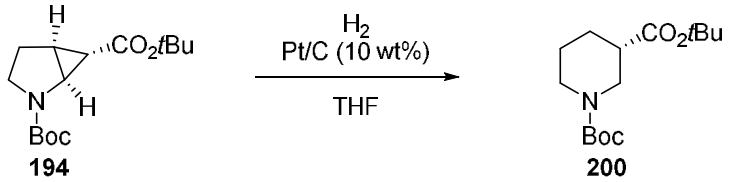


| entry [a)] | $H_2$ (bar) | *T* (°C) | time (h) | observation |
|---|---|---|---|---|
| 1 | 10 | 25 | 1 | no conversion |
| 2 | 20 | 40 | 1 | no conversion |
| 3 | 60 | 40 | 0.25 | decomposition exothermic reaction |

a) In all entries, the total amount (wt%) of applied Pt/C was based on the starting material **190**.

It became clear that the double bond in **190** seems to be crucial for the formation of the 6-membered ring. Moreover, different solvents like EA, acetone, EtOH or trifluoroethanol (TFE) were tested, partially resulting in a more sluggish reaction due to the formation of various side-products. Nevertheless, the fully saturated fused ring **194** was formed as the main product and no preference for the desired 6-membered ring was observed.

Considering the recent results, it can be concluded that the double bond is essential for the 6-membered ring formation. But in the previous attempts, by using balloon or autoclave vessel, an excess of hydrogen gas was available, resulting in a faster reduction of the double bond compared to the formation of the 6-membered ring. In order to prevent prolonged contact time of the substrate with the catalyst and hydrogen gas, hydrogenation was performed in a continuous flow system by using ThalesNano H-Cube Pro$^{TM}$. For this purpose, the substrate was dissolved in THF and passed through the reactor, containing a cartridge loaded with the catalyst (Figure 27).

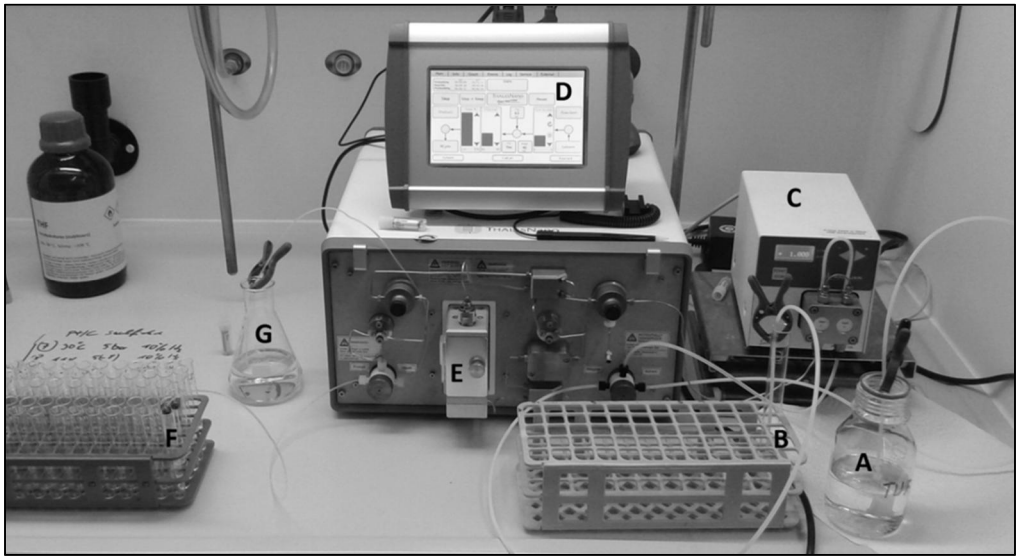


**Figure 27:** Display of the reaction setup for condition screening using the ThalesNano H-Cube Pro™. **A**: solvent THF; **B**: sample in THF; **C**: HPLC pump; **D**: control panel, display and adjustment of reaction parameters; **E**: reaction chamber containing catalyst cartridge and heating block; **F**: collected product mixture in solvent; **G**: waste drain.

Different conditions were screened but the desired 6-membered ring was only detected in traces amounts (Table 14). Interestingly, starting material was converted under increased temperature and missing hydrogen gas resulting in a complex mixture (entry 3). Similar to previous experiments, poisoned Pt-catalyst was employed to reduce the rate of hydrogenation, but even under forcing conditions only the fully saturated fused ring **194** was obtained as the main product (entries 4-7).

**Table 14:** Screening of reaction conditions for the catalytic hydrogenolysis of **190** under flow conditions.

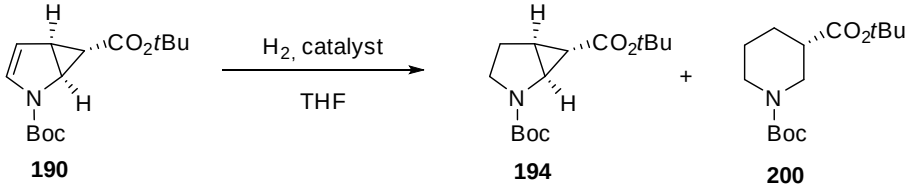


| entry [a] | catalyst | *T* (°C) | $H_2$ (bar) | conv. (%) [b] | observation |
|---|---|---|---|---|---|
| 1 | Pd/C (10%) | 25 | 5 | 100 | **194** |
| 2 | Pd/C (10%) | 90 | 5 | 100 | **194**, **200** traces |
| 3 | Pd/C (10%) | 90 | - | 10 | complex mixture |
| 4 | Pt/C (5%) sulfided | 90 | 5 | 90 | **194**, **200** traces |
| 5 | Pt/C (5%) sulfided | 110 | 5 | 90 | **194**, **200** traces |
| 6 | Pt/C (5%) sulfided | 130 | 20 | 90 | **194**, **200** traces |
| 7 | Pt/C (5%) sulfided | 150 | 40 | 90 | **194**, **200** traces |

a) 0.35 mmol (100 mg) **190**, 15 mL THF, 1 run, 1 mL/min; b) Estimated from TLC.

In a next step, it was studied, if the rate of hydrogenation and consequently the formation of **200** could be increased, by raising the amount of Pd/C (Table 15). Indeed, by using 100 wt% of Pd/C based on **190** the yield of desired 6-membered ring **200** could be improved up to 20% yield. However, this positive result was accompanied by the occurrence of various side-products, which hampered the purification and isolation of the desired products. Moreover, the fully saturated fused ring **194** was still the main product. Nevertheless, this observation indicated, that a complexation of the palladium to double bound could take place, which resulted activating the double bond and facilitating the formation of the 6-membered ring and further products.

**Table 15:** Hydrogenolysis of **190** with increased amount of Pd/C.

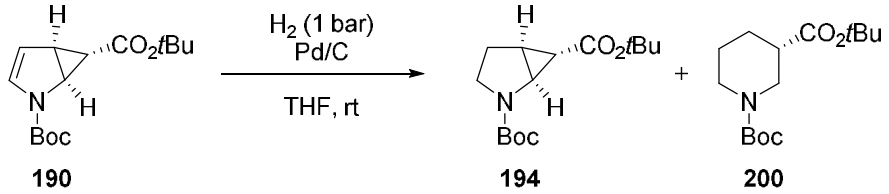


**190** **194** **200**

| entry [a)] | Pd/C (wt%) | time (h) | yield (%) |
|---|---|---|---|
| 1 | 10 | 1.5 | **194** (85), **200** (5) |
| 2 | 100 | 2 | **194** (n.d.), **200** (20) |

a) In all entries, the total amount of applied Pd/C (wt%) was based on the starting material **190**.

This is why an additional Pd-source was added to achieve complexation to the double bond (Table 16). It can be seen, that the additional Pd-source caused a decreased rate of hydrogenation displayed by elongated reaction time. It was assumed that the complexed Pd-source blocks the double bond to the Pd/C and delays the reduction of the double bond. However, in both cases, no increased formation of the 6-membered ring was observed. In particular, when Pd-(II)-acetate was used, the yield of **194** dropped dramatically caused by the formation of various side-products (entry 1). In the case of Pd-(0)-tetrakis exclusively the fully saturated fused ring **194** was formed again.

**Table 16:** Hydrogenolysis of **190** with an additional Pd-source.

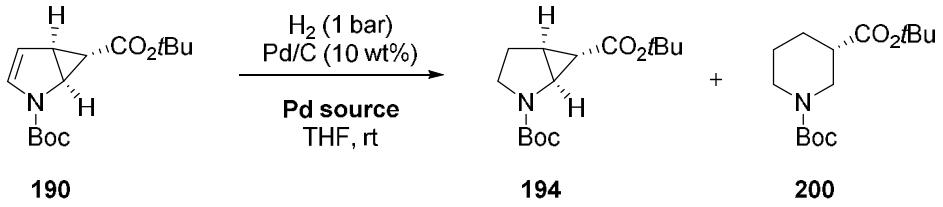


**190** **194** **200**

| entry [a)] | Pd source (equiv) | time (h) | yield (%) |
|---|---|---|---|
| 1 | $Pd(OAc)_2$ (0.5) | 24 | **194** (67), **200** (2) |
| 2 | $Pd(PPh_3)_4$ (0.5) | 24 | **194** (99), **200** (-) |

a) In all entries, the total amount of Pd/C (wt%) was based on the starting material **190**.

It became obvious that the selective hydrogenolysis of cyclopropanated *N*-Boc-pyrrole **190** to the desired 6-membered ring **200** will be a challenging objective. It was assumed, if proper conditions for the hydrogenolysis of **190** can not be found, maybe **190** can be manipulated in a way undergoing the desired transformation. Since hydrogenolysis of substituted cyclopropanes using Pd or Ni catalysts was already studied, selective scission of cyclopropane in **190** should be possible.[220] However, the background information of the literature on hydrogenolysis of cyclopropanes is not sufficient to establish common rules for the regioselective bond cleavage.[221] Nevertheless, there have been studies on influences of substituents on cyclopropanes. For example, *Gröger et al.*[222] investigated hydrogenolysis of 1,1-disubstituted cyclopropanes based on the studies of *Hoffmann et al.*[223] and *Günther*.[224] In their studies they observed, that electron donating substituents are weakening the where the very substituent is not connected, whereas electron-withdrawing groups are weakening the adjacent bonds.[222]

As a manipulation, the electron-withdrawing *tert*-butyl ester in **190** was reduced to the corresponding less electron withdrawing alcohol. The desired alcohol **248**[225] was obtained in 51% yield by using LAH (Scheme 74). Subsequently, hydrogenation was performed under the same conditions as in the previous experiments, however, showed no conversion of **248**. After changing the solvent from THF to MeOH, the desired 6-membered ring was obtained in 31% yield, although the fully saturated fused ring **249** was still the main product. Nevertheless, the isolated yield of the 6-membered ring could be increased from initially 5% to 31%. In order to prove the formation of the 6-membered ring **250**, the Boc group was removed to yield the free amino alcohol **251** which is a literature known comound. The spectroscopic data of **251** were in agreement with the literature data.[226]

**Scheme 74:** Hydrogenolysis of **248** towards desired 6-membered ring **250**.

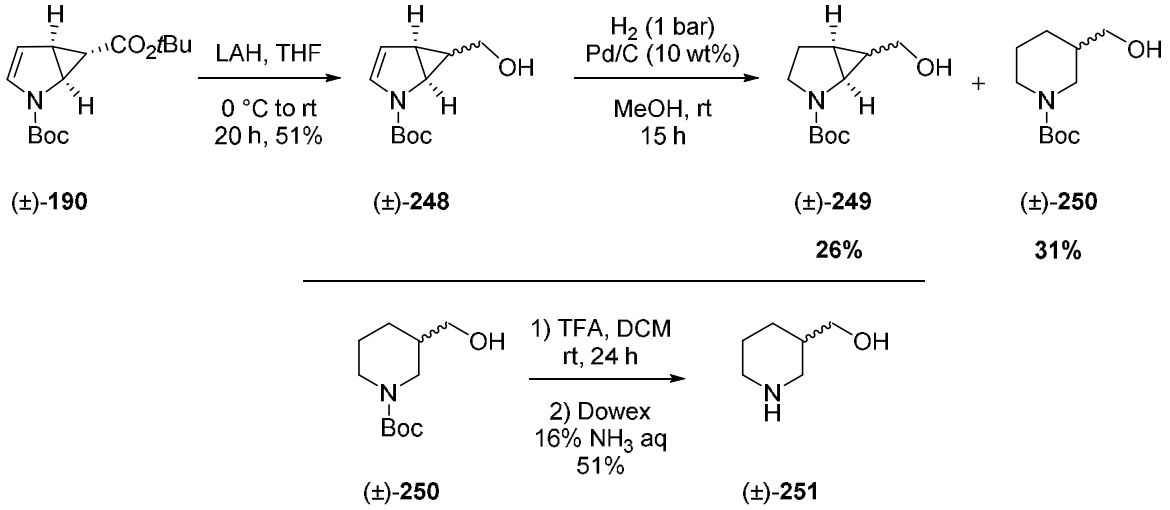


Also the influence of the *N*-protecting group in the hydrogenolysis reaction was investigated. For this, the Boc group was exchanged to the tosyl protecting group which would have less conjugation of enamine moiety with the *N*-protecting group. **252** was provided by *S. R. Park* and submitted to hydrogenolysis reaction. Interestingly, **252** was converted exclusively to the fully saturated fused ring **253** without any trace for the formation of the desired 6-membered ring. A possible explanation would be that the Ts-substituted **252** is more reactive to the hydrogenation since the double bond is more exposed to the other reaction components due to less conjugation with the *N*-protecting group. On contrary due to its involvement in a conjugated system with the $sp^2$ hybridized nitrogen, the double bond in **190** is less reactive to hydrogenation.

**Scheme 75:** Hydrogenation of **252** towards **253**.

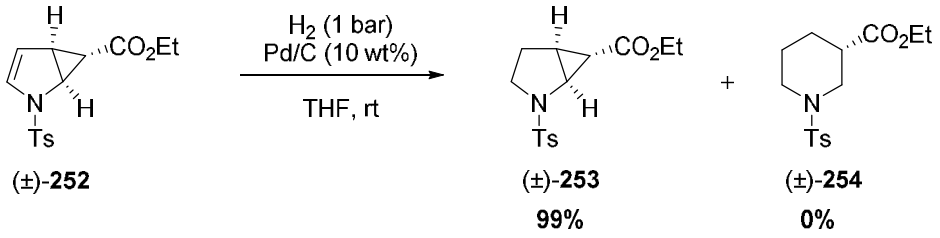


In summary, the yield of desired 6-membered ring in hydrogenolysis of **190** could be improved up to 31% by manipulation of the cyclopropane substituent. However, the literature studies are limited to the simple cyclopropanes with few numbers of substituents and when it comes to complex cyclopropanes, precedents are not fitting to the here employed system and

contradict themselves. Therefore, further attempts for selective ring-opening via hydrogenolysis were not performed anymore.

### 6.3.2 Further attempts at ring-expansion

From previous experiments, it was concluded that coordination of the palladium source to the double bond could facilitate the formation of the 6-membered ring. Therefore, it was envisioned to apply π-allylpalladium chemistry for ring expansion.[227] The palladium-catalyzed substitution has been developed in the early 1970s and there has been an enormous achievement in this field.[228,229,230,231] In principle, the π-allylpalladium complex **257** can be generated by binding of a Pd(0)-species to allylic compound **255**. Subsequent ionization by expelling of the allylic leaving group X, leads to the intermediate π-allylpalladium complex **257**. This complex is electrophilic and accommodates the nucleophilic attack onto it. After nucleophilic attack, the Pd-species is released and takes part in the catalytic cycle again (Scheme 76). The probably most prominent representative displays the *Tsuji-Trost* reaction.

**Scheme 76:** General reaction scheme of a palladium catalyzed allylic substitution.[231]

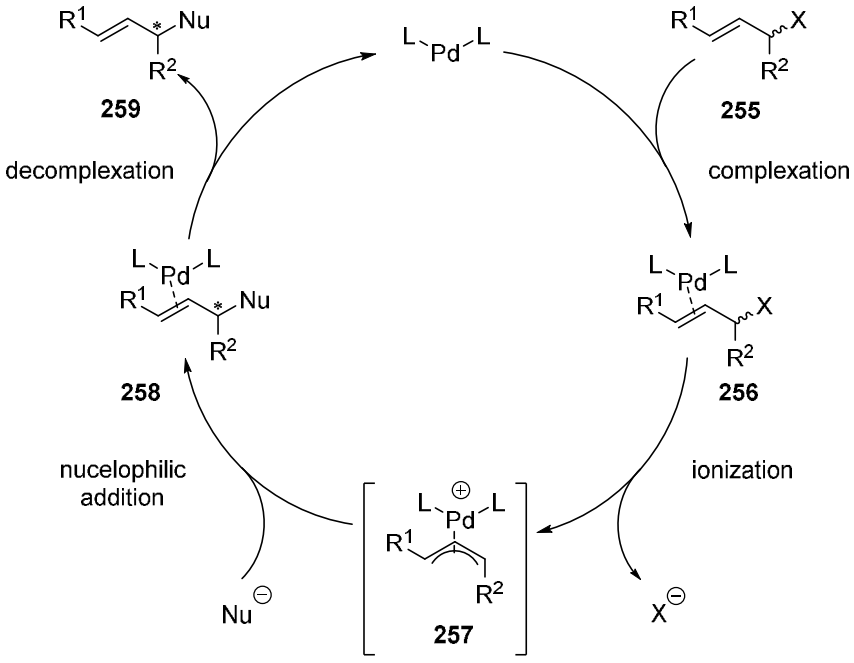


It was assumed, that **190** would undergo the typical Pd-catalyzed reaction initiated by the ring-opening of the cyclopropane so that $\eta^3$- π-allyl complex **260** can be made on the enamide moiety. Then applied nucleophile attacks and finally the substituted 6-membered ring **261** can be formed. Therefore, **190** was submitted to allylic substitution reaction catalyzed by

$Pd_2(dba)_3 \cdot CHCl_3$ in which various nucleophiles were applied (Table 17). But even under reflux conditions, no conversion of the starting material was observed. A plausible explanation would be that the cyclopropane ring-opening doesn´t occur to initiate the reaction, which hampers further nucleophilic attack.

**Table 17:** Attempts for the allylic substitution on **190**.

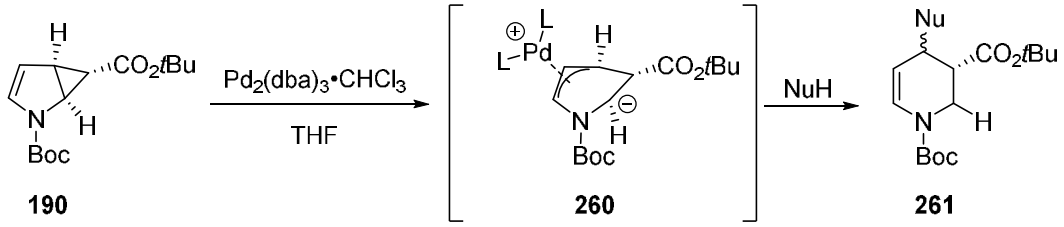


| entry | nucleophile | (equiv) | *T* (°C) | time (h) | result |
|---|---|---|---|---|---|
| 1 | 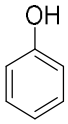 | 2 | 25 | 1 | no conversion |
| 2 | | | 70 | 24 | no conversion |
| 3 | 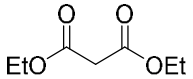 | 2 | 25 | 1 | no conversion |
| 4 | (Pyridine 0.2 equiv) | | 70 | 24 | no conversion |
| 5 | 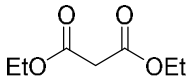 | 2 | 25 | 1 | no conversion |
| 6 | (NaH 1 equiv) | | 70 | 24 | no conversion |
| 7 | 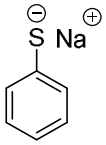 | 2 | 25 | 1 | no conversion |
| 8 | | | 70 | 24 | no conversion |

As the substrate was inactive to Pd-(0)-species and showed no conversion, no further attempts at π-allylpalladium formation were made in this work. Another possibility could be employing Pd-(II)-species in vinylcyclopropane activation.[232] For instance, *Wilhelm et al.* reported a chloropalladation of (+)-2-carene **262** by using $PdCl_2(MeCN)_2$ to generate the dimeric π-olefin complex **263**, on the convex face of **262**.[233] In chloroform (pathway A), palladium induced 1-7 bond cleavage which resulted in electrophilic activation of the cyclopropane ring and the formation of the preferred 6-membered ring complex **264**, followed by final trapping of the positive charge with a nucleophile. On the other hand, in benzene, cleavage of the 1-6 bond led to the preferred 7-membered ring complex **266**, which is similar to a $\eta^4$-1,3-diene complex. Then, nucleophilic attack of the chloride led to 7-membered ring

**267**. This drastic change in product selectivity was explained, that the increased polarity of the solvent increases the electrophilicity at the tertiary carbon of **262**. This means that the nucleophilic attack at the tertiary carbon may change to an $S_N1$-type reaction on going to a more polar solvent.

**Scheme 77:** Solvent dependent chloropalladation reported by *Wilhelm et al.*

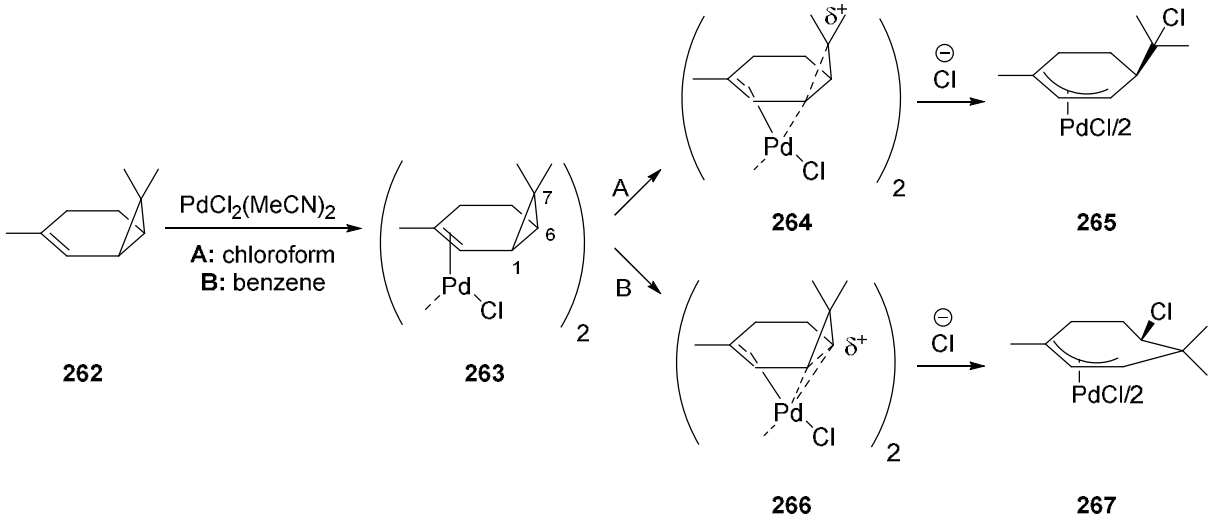


In the following scheme, the corresponding transformation of **190** according to the chloropalladation method of *Wilhelm et al.* is proposed.

**Scheme 78:** Proposed mechanism for chloropalladation of **190** towards 6-membered ring **271**.

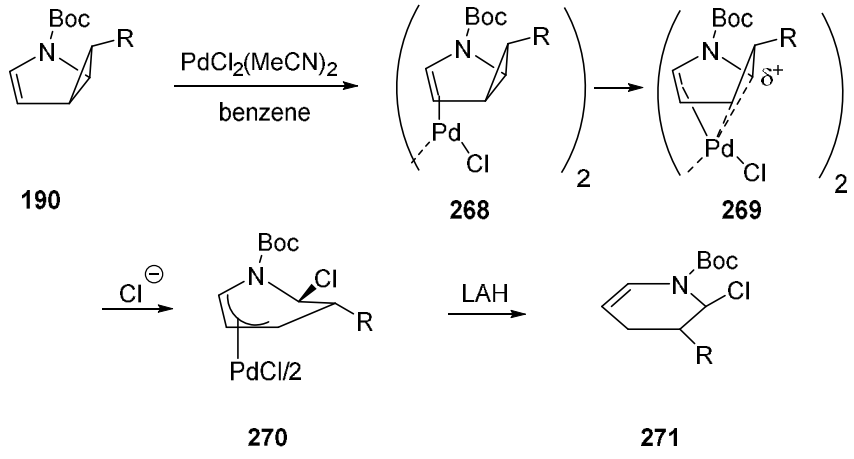


It looks promising to apply Pd-(II)-species in non-polar solvents to the transformation of *N*-Boc cyclopropanated pyrrole **190** towards the corresponding 6-membered ring as in the literature precedents. Further attempts at palladium-induced ring-opening of cyclopropane compounds are currently ongoing in the *Reiser* group.

### 6.3.3 Metal-free dipolar cycloaddition of cyclopropanated *N*-Boc-pyrrole

The following chapter describes an alternative method of cyclopropane ring-opening without any metal based Lewis acid or hydrogen gas. Inspired by the pioneering work of *Fowler et al.*, we envisioned thermal activation of cyclopropane ring to get access to 6-membered ring systems (Scheme 79). With the closely related compounds **272** and **276**, *Fowler et al.* already demonstrated in the 1970´s, that cyclopropanated pyrrole derivatives undergo cycloaddition reaction with suitable dipolarophiles. However, in this reaction, the scope of dipolarophiles is limited to highly activated alkenes and alkynes such as maleic anhydride, *N*-Phenylmaleimide and acetylene dicarboxylates. Moreover, discussion on the mechanism and many yields remain unreported.[234,235]

**Scheme 79:** Cycloaddition examples reported by *Tanny and Fowler*.

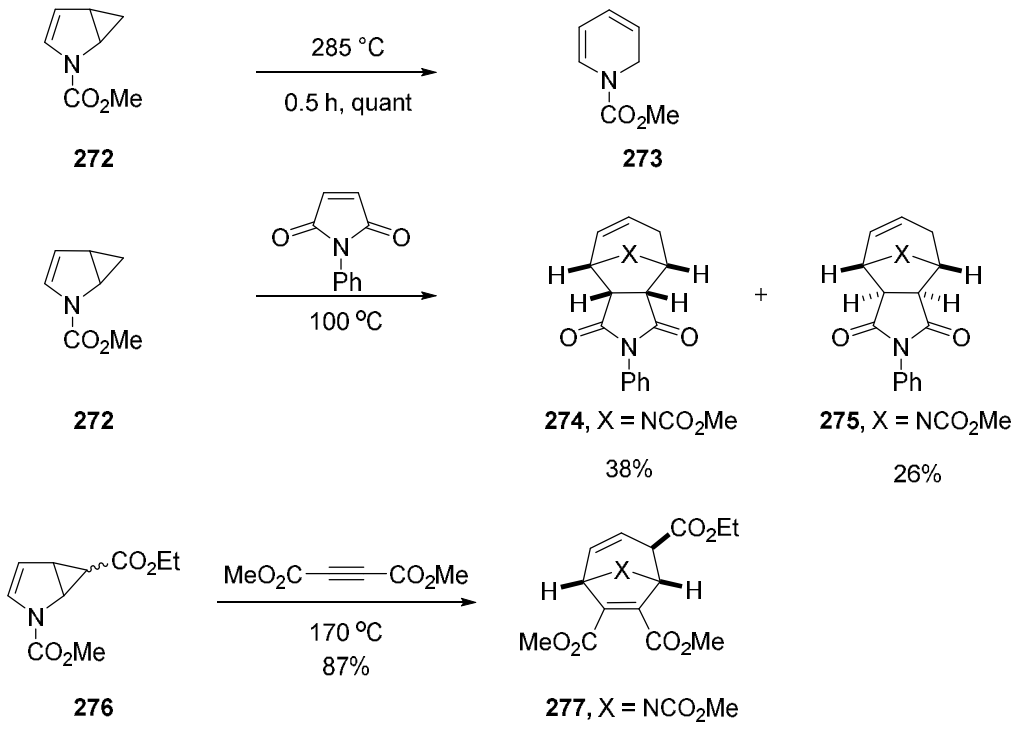


In 2013, the first mechanistic investigation of this cycloaddition was published by *Yu et al.* with homopyrrole **272** as the model substrate.[236] They showed by density functional theory calculations (DFT), that the low distortion energy from **272** to **278** is the main reason why such cyclopropanated pyrrole undergoes dipolar cycloaddition reactions. Under thermal activation, **272** can rearrange to **278**, a 1,3-dipole being a highly reactive species that can undergo dipolar cycloaddition reactions with suitable dipolarophiles. According to their

calculations, a diradical (pathway A) and a concerted (pathway B) mechanism were proposed (Scheme 80). The activation energy to the diradical intermediate **280** was calculated to be lower than that of the intermediate **281** by about 3.0 kcal/mol.

According to the IUPAC guidelines, the formed product **282** can be defined as a (5+2) or [4+2] cycloaddition product. There are two different notation systems to determine the type of cycloadditions.[237] In the first one, *a (i + j +...) cycloaddition is a reaction in which two or more molecules (or parts of the same molecule), respectively, provide units of i, j, ... linearly connected atoms: these units become joined at their respective termini by new σ-bonds so as to form a cycle containing (i + j + ...) atoms. In this notation, (a) a Diels–Alder reaction is a (4+2) cycloaddition, (b) the initial reaction of ozone with an alkene is a (3+2) cycloaddition […] (N.B.: parentheses (...) are used in the description based on numbers of atoms).*[237] On the other hand, in the second one, *the symbolism [i + j+ ...] for a cycloaddition identifies the numbers i, j, ... of electrons in the interacting units that participate in the transformation of reactants to products. In this notation the reaction (a) and (b) of the preceding paragraph would both be described as [2+4] cycloadditions* […].[237]

**Scheme 80:** Proposed diradical and concerted reaction pathways for the 1,3-dipolar cycloaddition reported by *Yu et al.*

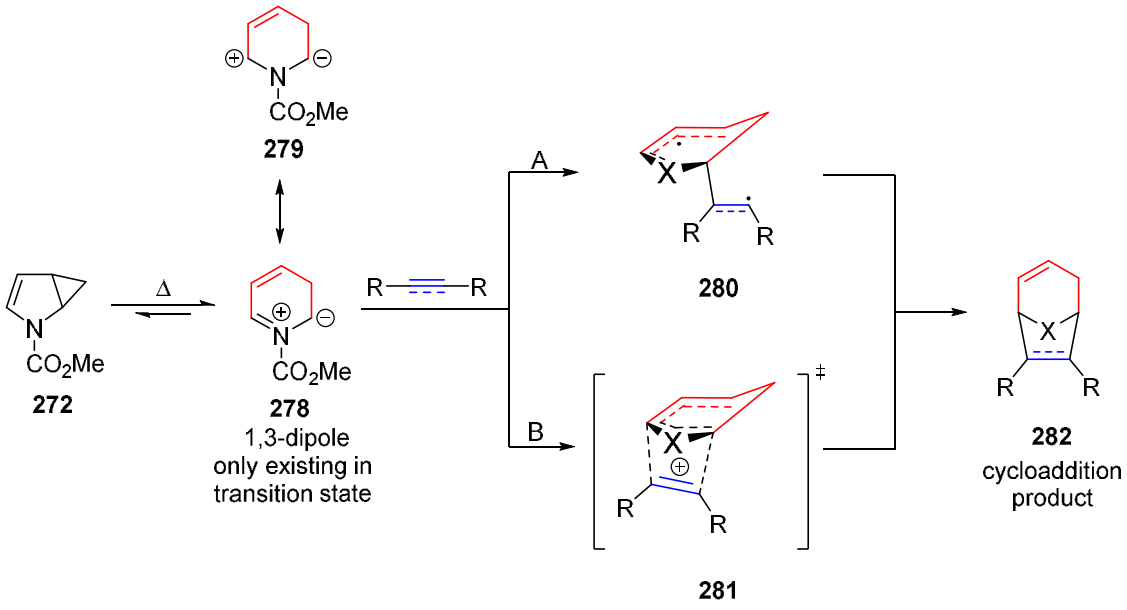


Based on the precedent studies, **190** was submitted to cycloaddition reactions employing *N*-Phenylmaleimide, maleic anhydride and acetylene dicarboxylate (Table 18). In contrary to the results of *Fowler et al.*, the reaction of *tert*-butyl ester-substituted cyclopropane **190** showed only poor results. In the reaction with *N*-Phenylmaleimide (entry 1) and dimethyl acetylenedicarboxylate (entry 3), almost no conversion of starting material was observed. In

the case of the reaction with maleic anhydride (entry 2), it occurred with full conversion of **190**. However, the low yield was thought to explain by decomposition of the maleic anhydride moiety during the reaction. To overcome the poor reactivity of **190**, the corresponding alcohol **248** was employed. As already implied in chapter 6.3.2, manipulation of the electronic and steric properties of substituents on the cyclopropane to less electron withdrawing could change the reactivity of the cyclopropane ring. Indeed, the reactivity of **248** was improved resulting in full conversion and products **286** and **288** (entries 4 and 6) could be isolated in satisfying yields. Besides to prevent the decomposition of the anhydride moiety in the product, the reaction temperature was reduced to 40 °C, but the yield of product **285** (entry 5) was dropped again. It was found that the purification by column chromatography triggered the anhydride ring-opening and dropped the yield dramatically.

**Table 18:** Cycloaddition reactions of cyclopropanated *N*-Boc-pyrroles **190** and **248**.

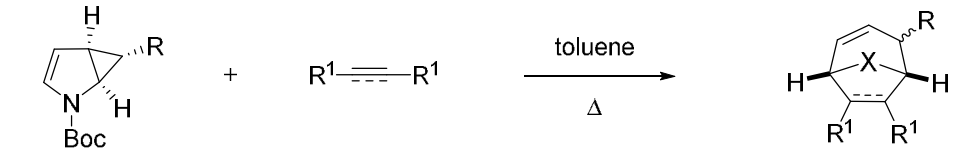


**190**, R = $CO_2tBu$
**248**, R = $CH_2OH$

| entry | R | $R^1$ | *T* (°C) | time (h) | result |
|---|---|---|---|---|---|
| 1 | $CO_2tBu$ | 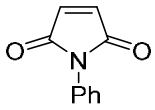 | 100 | 24 | 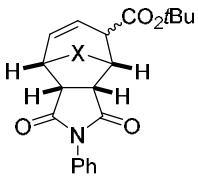 **283**, X = NBoc, traces |
| 2 | $CO_2tBu$ | 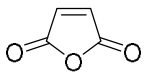 | 100 | 24 | 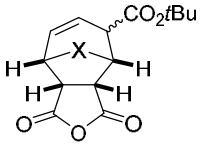 **284**, X = NBoc, 20% *dr* 1:1.7 |
| 3 | $CO_2tBu$ | 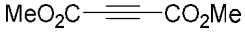 | 100 | 24 | 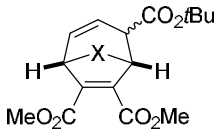 **285**, X = NBoc no conversion |

| | | | | | |
|---|---|---|---|---|---|
| 4 | $CH_2OH$ | 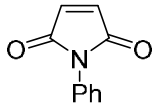 | 100 | 17 | 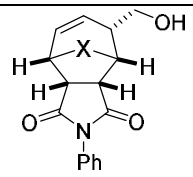 **286**, X = NBoc, 42% single diastereomer |
| 5 | $CH_2OH$ | 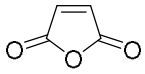 | 40 | 3 | 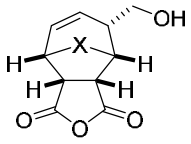 **287**, X = NBoc, 13% single diastereomer |
| 6 | $CH_2OH$ |  | 100 | 14 | 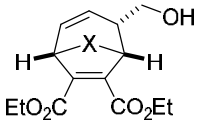 **288**, X = NBoc, 59% single diastereomer |

In summary, it was demonstrated in this chapter, that cyclopropanated pyrrole derivatives could be utilized in metal-free or thermal cycloaddition reactions. This method gives access to complex fused ring systems and has potential to be utilized in the synthesis of Cocaine derivatives since the obtained cycloaddition product contains already the its core structure (Scheme 81). Further investigations on the cycloaddition and its applications to the Cocaine synthesis are already in progress in the *Reiser* group.

**Scheme 81:** Possible application of the cycloaddition product as precursor for the Cocaine synthesis.

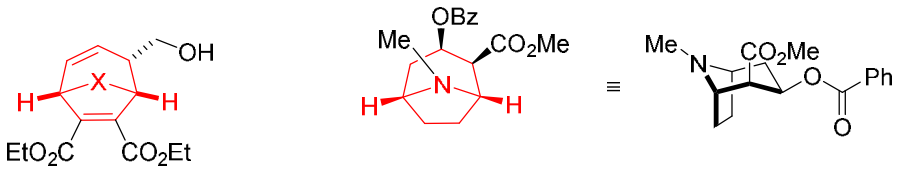

**288**, X = NBoc

(*S*)-(+)-Cocaine (**289**)

# C. Summary

The present thesis deals with the synthesis and application of β- and γ-amino acids based on aminopyrrolidine carboxylic acid (APC) and aminocyclopentane carboxylic acid (ACPC) as organocatalysts, as structural elementes in peptides and as building blocks for total syntheses. In the first part, APC and ACPC were investigated regarding their catalytic activity in organocatalysis. The use of the *cis*-APC based organocatalyst (*ent*)-**100** in *anti*-Mannich reactions gave only poor results, whereas tripeptides containing *cis*-APC or *cis*-ACPC as central building block proved successful. In these tripeptides, both enantiomers of each five-membered ring amino acid were used (Scheme 82). The tripeptides were tested in terms of their catalytic performance related to the application of pressure, which could cause a change in the conformation of the catalysts, possibly resulting in an increased catalytic activity. For the APC-tripeptides as well as for the ACPC-tripeptides a three- to eightfold increase in the reaction rate upon pressurization from 1 bar to approximately 5 kbar was observed, but this was rather assigned to the general effect of pressure than to a change in the conformation of the catalysts. Only for the ACPC-tripeptides, a slight increase of enantioselectivity was observed upon pressurization, which could imply a change of the active catalytic conformation. As well, one isomer was found to be catalytically more active than the other, which might be explained by internal hydrogen bonding resulting in a conformationally less flexible catalyst.

**Scheme 82:** Chemical structures of tripeptide organocatalysts **127** and **119** for the intermolecular aldol reaction of acetone **148** and *p*-nitrobenzaldehyde **149**.

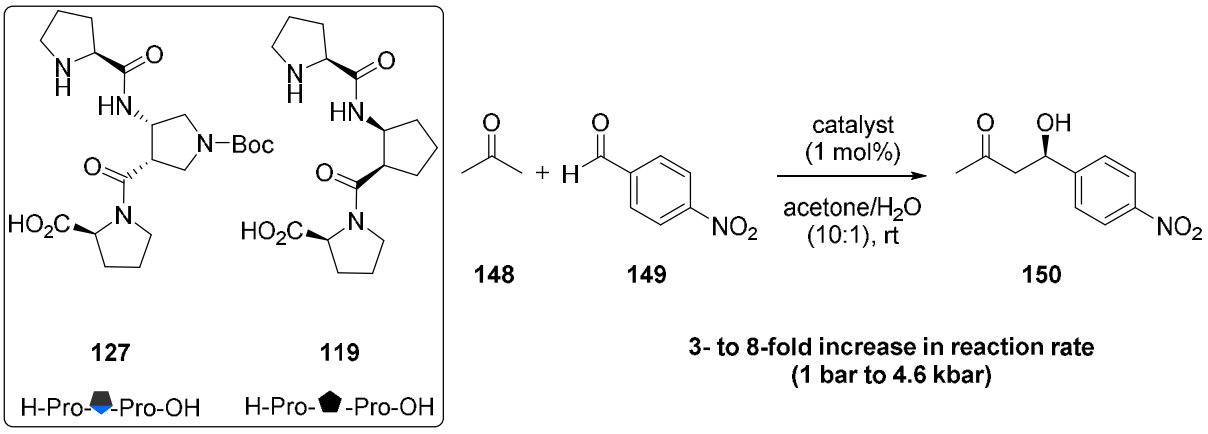


The second part of this thesis describes the introduction of APC and ACPC into longer-chained peptides. It could be implied by the exchange of unpolar ACPC to polar APC building blocks in an α,β-alternating model peptide that these more polar APC units can

stabilize helical structure motifs in aqueous media. By the introduction of APC into the highly conserved C-terminal area of truncated neuropeptide Y (NPY) analogues in position 32 and/or 34, new $Y_4$ receptor ($Y_4R$) selective ligands were obtained (Figure 28). Herein, ligands containing APC as well as ACPC building blocks could be identified as the most potent ones. It could be shown by the results of competition binding assays in combination with CD spectroscopy, that a helical structure of the ligand is not required alone for $Y_4R$ binding. Moreover, it could be shown that ligands containing nonpolar residues (ACPC) at position 34 are preferred for $Y_4R$ binding over ligands containing a polar residue (APC) at this position.

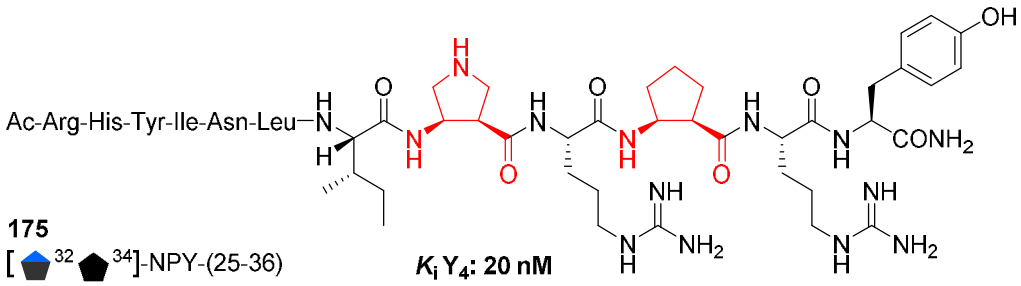


**Figure 28:** Chemical structure of an NPY analogue containing an APC as well as an ACPC building block.

The diastereomeric mixture of **152** was described in the literature as a high affinity $Y_4R$ agonist. Therefore, in cooperation with K. Kuhn (Institute of Pharmacy), the (*R*,*R*)- und (*S*,*S*)-diastereomeres each of **152** were synthesized via Grubbs´ metathesis cross coupling reaction starting from enantiopure allylglycine esters **165** (Scheme 83). As (*R*,*R*)-**152** was superior to (*S*,*S*)-**152** in binding assays, [$^3$H]-propionylation of (*R*,*R*)-**152** gave access to high affinity $Y_4R$ radioligand [$^3$H](*2R*,*7R*)-**169**, which was used as radioligand in the above mentioned competition binding assays.

**Scheme 83:** Two-step synthesis of diaminooctane diacid building block **165** for the synthesis of the new radioligand **169**.

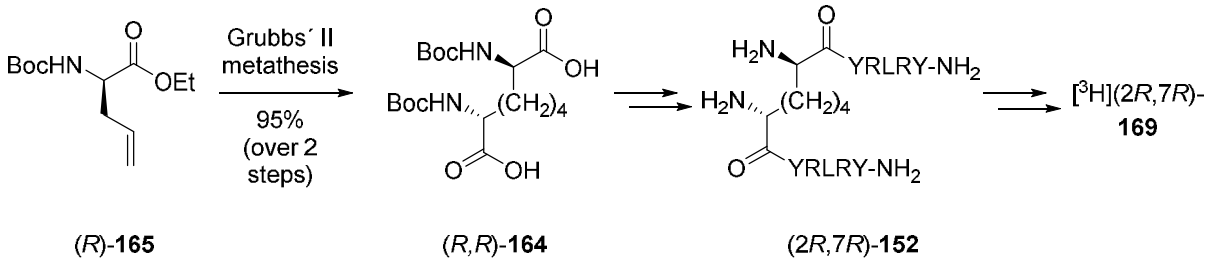


In the third part, cyclopropananted *N*-Boc-pyrrole **190** served as a platform for the synthesis of cyclic γ-amino acids. The biologically active GABA analogue (*S*)-(+)-homo-β-proline **188** could be obtained in a two-step synthesis starting from enantiopure **190** in quantitative yields (Scheme 84). The (Lewis)-acid catalyzed cyclopropane ring-opening under full conservation

of the enantiopurity represented the key step in this synthesis, in which the temperature of the reaction turned out to be the crucial parameter.

**Scheme 84:** Two-step synthesis of (*S*)-(+)-homo-β-proline **188** starting from **190**.

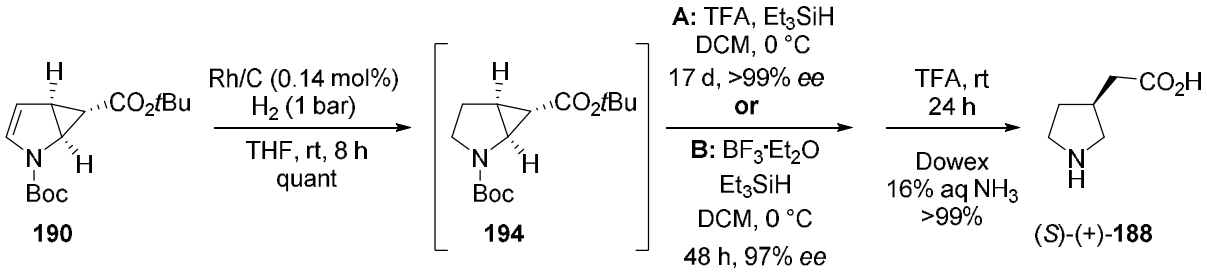


Moreover, the optimized reaction conditions for the cyclopropane ring-opening were applied to get access to the orthogonally protected *trans*-γ-aminopyrrolidine carboxylic acid **217** in enantiomerically pure form (Scheme 85). Since synthetic protocols towards this kind of γ-APC amino acids were not reported in the literature yet, this procedure represents the first enantioselective synthesis towards such compounds.

**Scheme 85:** Enantioselective synthesis of orthogonally protected γ-APC **217**.

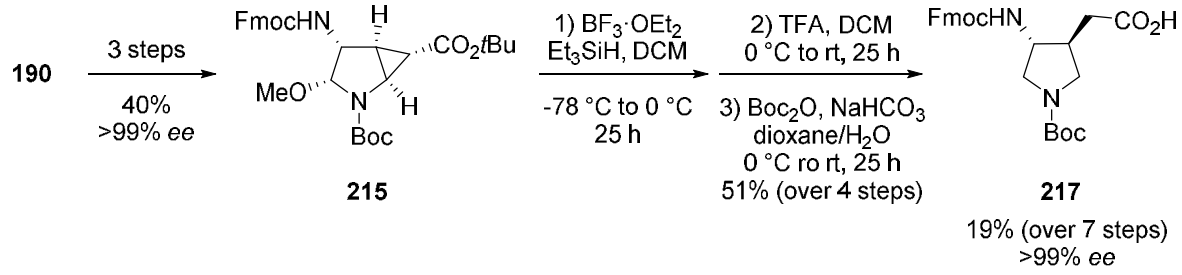


Moreover, cyclopropanated *N*-Boc-pyrrole **248** served as platform for the cycloaddition with various dipolarophiles to get access to fused cycles such as **288**, which contain already the core structure of cocaine (**289**). Current ongoing projects in the *Reiser* group were initiated by these findings.

**Scheme 86:** Cycloaddition reaction of cyclopropanated *N*-Boc-Pyrrole **248** towards the cocaine core structure **288**.

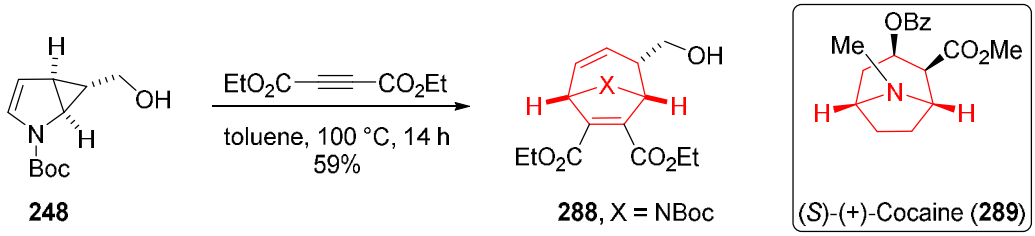

# D. Zusammenfassung

Die vorliegende Dissertation beschreibt die Synthese und Anwendung von β- und γ-Aminosäuren, basierend auf Aminopyrrolidin Carbonsäure (APC) und Aminocyclopentan Carbonsäure (ACPC) als Organokatalysatoren, als strukturgebende Elemente in Peptiden und als Bausteine für die Totalsynthese. Im ersten Abschnitt wurden APC und ACPC hinsichtlich ihrer Fähigkeit als Organokatalysator untersucht. Während der auf *cis*-APC basierende Organokatalysator (*ent*)-**100** in *anti*-Mannich Reaktionen nur unzureichende Ergebnisse lieferte, erzielten Tripeptide, welche als zentralen Baustein *cis*-APC oder *cis*-ACPC enthielten, positivere Resultate (Schema 1). Hierbei wurden beide Enantiomere der Fünfring Aminosäuren verwendet. Diese Tripeptide wurden bezüglich ihrer katalytischen Aktivität unter dem Einfluss von Druck untersucht, welcher eine konformative Änderung der Katalysatoren und somit eine Steigerung der katalytischen Aktivität bewirken sollte. Sowohl für die APC- als auch für die ACPC-basierenden Tripeptide konnte ein bis zu achtfacher Anstieg der Reaktionsgeschwindigkeit bei einem Druckanstieg von 1 Bar auf ca. 5 kBar beobachtet werden. Dieser Anstieg scheint jedoch eher auf den generellen Einfluss des Druckes zurückzuführen zu sein, als auf eine konformative Änderung des Katalysators. Lediglich die auf ACPC basierenden Tripeptide zeigten bei Druckanlegung einen leichten Anstieg der Enantioselektivität, was auf eine Änderung der katalytisch aktiven Konformation schließen lässt. Ebenso erwies sich je ein Isomer als katalytisch aktiver als das andere, was sich durch interne Wasserstoffbrückenbindungen und eine damit eingeschränkte Flexibilität der Katalysatoren erklären lässt.

**Schema 1:** Chemische Strukturformeln der katalytisch aktiveren Tripeptide **127** und **119** für die intermolekulare Aldolreaktion von Aceton und *p*-Nitrobenzaldehyd.

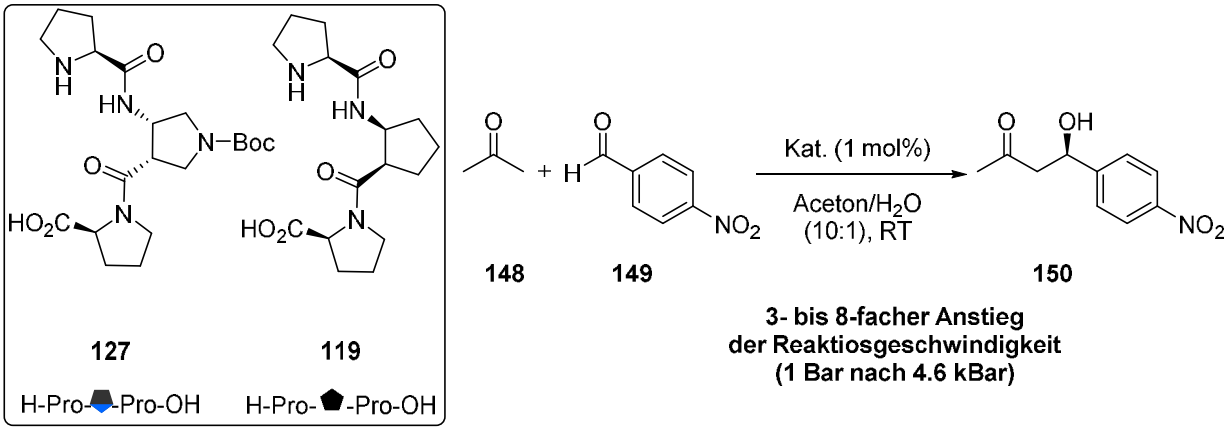

Der zweite Abschnitt behandelt den Einbau von APC- und ACPC-Bausteinen in längerkettige Peptide. Durch den Austausch von unpolaren ACPC- durch polare APC-Bausteine in einem α,β-alternierenden Modellpeptid konnte mittels CD-Spektroskopie gezeigt werden, dass positiv geladene APC Einheiten helikale Sekundärstrukturen in wässrigen Medien stabilisieren können. Durch den Einbau von APC-Bausteinen in den hochkonservierten C-Terminus von verkürzten Neuropeptid Y (NPY) Analoga in Position 32 und/oder 34 konnten neue Liganden gefunden werden, welche selektiv an den $Y_4$ Rezeptor ($Y_4R$) binden (Abbildung 1). Hierbei konnten Liganden, welche sowohl den APC- als auch den ACPC-Baustein enthielten, als potenteste Analoga identifiziert werden. Ebenso konnte anhand der Ergebnisse von Kompetitionsbindungtests in Kombination mit CD-Spektroskopie gezeigt werden, dass nicht zwingend eine helikale Struktur der NPY Liganden benötigt wird, um eine Bindung am $Y_4R$ zu erreichen. Außerdem konnte gezeigt werden, dass Liganden mit ungeladenen, aliphatischen Resten (ACPC) in Position 34 gegenüber geladenen, polaren Resten (APC) deutlich bevorzugt an den $Y_4R$ binden.

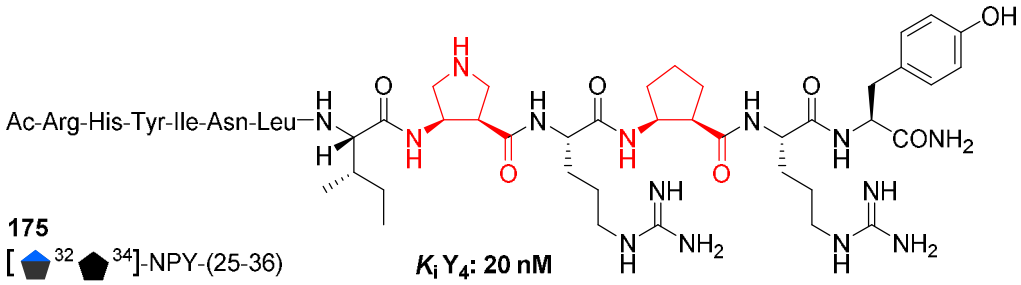


**Abbildung 1:** Chemische Strukturformel eines NPY Analogon, welches sowohl einen APC- als auch einen ACPC-Baustein enthält.

In der Literatur wird die Diastereomerenmischung von **152** als hoch affiner $Y_4R$ Agonist beschrieben. Deshalb wurden in Kooperation mit K. Kuhn (Institut für Pharmazie) die jeweiligen (*R*,*R*)- und (*S*,*S*)-Diastereomere von **152** mittels Grubbs´ Metathese ausgehend von enantiomerenreinen Allylglycin Estern **165** dargestellt (Schema 2). In pharmakologischen Untersuchungen zeigte sich (*R*,*R*)-**152** gegenüber (*S*,*S*)-**152** als überlegen und wurde mittels [$^3$H]-Propionylierung weiter zum Radioliganden **169** umgesetzt. [$^3$H](*2R*,*7S*)-**169** erwies sich als hoch affiner $Y_4R$ Radioligand und wurde in den zuvor erwähnten Kompetitionsbindungstests als Radioligand verwendet.

**Schema 2:** Zweistufensynthese von Diaminooctan Dicarbonsäure Bausteinen **165** für die Darstellung eines neuen dimerartigen Radioliganden **169**.

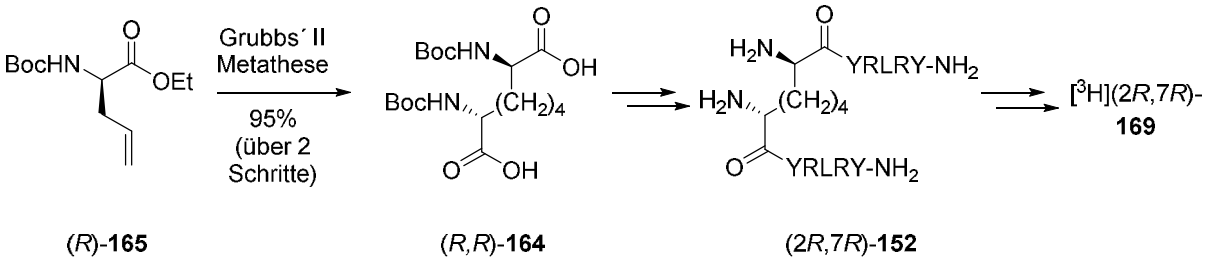


Im dritten Abschnitt diente cyclopropaniertes *N*-Boc-Pyrrol **190** als Basis für die Synthese von cyclischen γ-Aminosäuren. Ausgehend von enantiomerenreinen **190** konnte das biologisch aktive GABA Analogon (*S*)-(+)-homo-β-Prolin **188** in einer Zweistufensynthese in quantitativen Ausbeuten dargestellt werden (Schema 3). Schlüsselschritt war hierbei die (Lewis)-säurekatalysierte Cyclopropanöffnung unter vollem Erhalt des Stereozentrums, wobei die Reaktionstemperatur entscheidend war.

**Schema 3:** Zweistufensynthese von (*S*)-(+)-homo-β-Prolin **188** ausgehend von **190**.

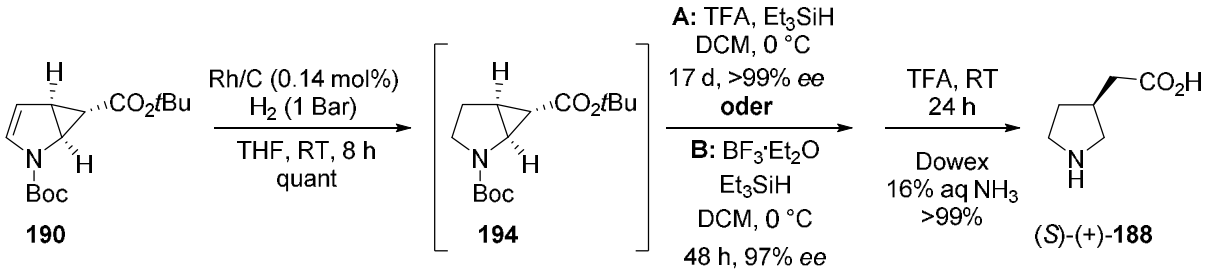


Ebenso konnte unter Verwendung der optimierten Bedingungen der Cyclopropanöffnung die orthogonal geschützte *trans*-γ-Aminopyrrolidin Carbonsäure **217** enantiomerenrein dargestellt werden (Schema 4). Ein Zugang zu solchen γ-APC Aminosäuren wurde in der Literatur bisher noch nicht beschrieben und somit stellt diese Route die erste enantioselektive Methode für diese Art von Aminosäuren dar.

**Schema 4:** Enantiomerenreine Darstellung von orthogonal geschützter γ-APC **217**.

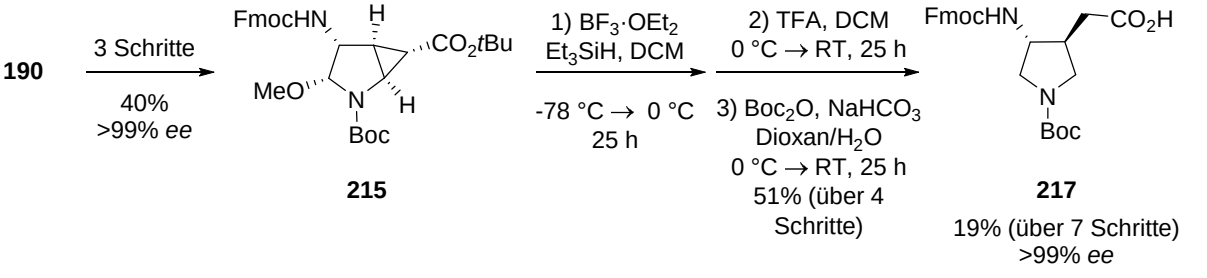

Außerdem konnte ausgehend von **248** durch Cycloaddition mit unterschiedlichen Dipolarophilen der Zugang zu Bicyclen wie **288** erreicht werden, welche bereits die Grundstruktur von Kokain **289** enthalten (Schema 5). Damit konnte die Grundlage für weitere Projekte gelegt werden, welche Gegenstand aktueller Forschungen am *AK Reiser* sind.

**Schema 5:** Cycloaddition von cyclopropaniertem *N*-Boc-Pyrrol **248** hin zur Kokaingrundstruktur **289**.

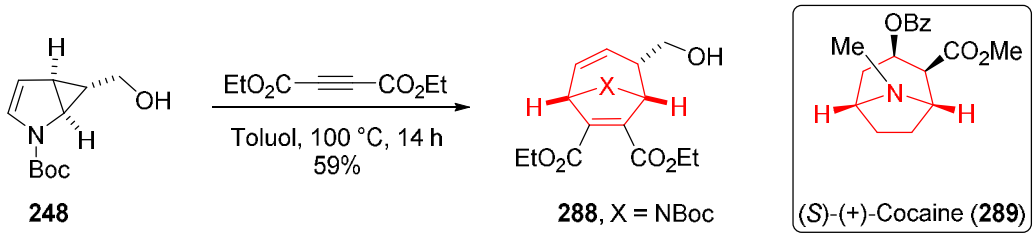


**248** **288**, X = NBoc (*S*)-(+)-Cocaine (**289**)

# E. Experimental Part

### 1. General Information

All moisture sensitive reactions were performed in prior flame-dried septum-sealed flasks under nitrogen atmosphere.

**Solvents and chemicals:** DCM, ethyl acetate and hexanes (60/40) were distilled prior to use for column chromatography. Anhydrous solvents were prepared according to standard procedures. Commercially available chemicals were used as received, without further purification.

**$^{1}$H NMR** spectra were recorded on Bruker Avance 300 (300 MHz), Bruker Avance 400 (400 MHz) and Bruker Avance III 600 TCI Cryo (600 MHz). The chemical shifts are reported in δ (ppm) relative to chloroform-d ($CDCl_3$ 7.26 ppm), methanol-$d_3$ or methanol-$d_4$ ($CD_3OH$/$CD_3OD$ 3.34 ppm), acetone-$d_6$ ($(CD_3)_2CO$ 2.05 ppm), deuterium oxide ($D_2O$, 4.79 ppm) or diemthylsulfoxide-$d_6$ ($(CD_3)_2SO$ 2.50 ppm). The spectra were analyzed by first order, the coupling constants (*J*) are reported in Hertz (Hz). Characterization of the signals: s, singulet; d, dublet; t, triplet; q, quartet; quin, quintet; m, multiplet; dd, double dublet; dt, double triplet; sept, septet. Integration is determined as a relative number of atoms.

**$^{13}$C NMR** spectra were recorded on Bruker Avance 300 (75.5 MHz) and Bruker Avance 400 (100.6 MHz). The chemical shifts are reported in δ (ppm) relative to chloroform ($CDCl_3$, 77.0 ppm, or methanol-$d_4$ ($CD_3OD$ 49.0 ppm), acetone-$d_6$ ($(CD_3)_2CO$ 29.84 ppm) or diemthylsulfoxide-$d_6$ ($(CD_3)_2SO$ 39.52 ppm). $^{13}$C NMR resonance assignment was aided by the use of DEPT 135 techniques (DEPT = Distortionless Enhancement by Polarization Transfer) to determine the number of hydrogens attached to each carbon atom and is declared as: + = primary or tertiary (positive DEPT signal), - = secondary (negative DEPT signal), Cq = quaternary (no DEPT signal) carbon atoms.

**High-performance liquid chromatography (HPLC)** was performed on a Varian 920-LC with DAD. Phenomenex Lux Cellulose-1 and 2, Chiracel OD-H and AS served as chiral stationary phase and mixtures of *n*-heptane and *i*PrOH were used for elution.

**RP-High performance liquid chromatography (RP-HPLC)** was performed on a Shimadzu LC20A series, Agilent 1100 series (AK König), Agilent UHPLC-MSD-system (AK König) or

on a system from Knauer (AK Buschauer). Machery-Nagel EC 250/4 Nucleodur 100-5 C18ec, Machery-Nagel VP 250/10 Nucleodur 100-5 C18ec, Phenomenex Luna 10 C18(2) 100A 250/21.2, Phenomenex Luna C18(2) 100A 150/2.0 or Machery-Nagel Nucleodur 250/21 100 C18 served as stationary phase and mixtures of MeCN + 0.05% TFA and Millipore water + 0.05% TFA were used for elution. Acetonitrile was removed before lyophilization. Lyophilization was carried out with a Christ Alpha 2-4 LD equipped with a vacuubrand RZ 6 rotary vane vacuum pump.

**Infra-red spectroscopy (IR)** in form of ATR-IR spectroscopy was carried out on a Biorad Excalibur FTS 3000 Spectrometer, equipped with a Specac Gate Diamond Single Reflection ATR-System or on an Agilent Cary 630 FT-IR.

**Mass spectrometry (MS)** was performed in the Central Analytic Department of the University of Regensburg on a Finnigan MAT 95, a Agilent Q-TOF 6540 UHD, a Finnigan MAT SSQ 710 A and a ThermoQuest Finnigan TSQ 7000.

**Melting points (mp)** were measured on a Büchi SMP-20 apparatus in a silicon oil bath. Values thus obtained were not corrected.

**Optical rotations** were determined in a Perkin Elmer 241 polarimeter or an Anton Paar MCP 500 at 589 nm wavelength (sodium-*d*-line) in a 1.0 dm measuring cell of ca. 2 mL volume and the specified solvent.

**Circular dichroism spectroscopy (CD)** was performed on a JASCO model J-710/720 at indicated temperatures and wavelengths between 260 and 190 nm in water, phosphate buffer pH = 7 (30% TFE added respectively) or MeOH by using the following parameters: 0.25 s response, 100 nm/min speed, 5 scans. The length of the cuvette was 1.0 mm. The CD Spectrum of the sole was recorded and subtracted from the raw data. The CD intensity is given as mean residue molar ellipticity /deg $cm^2$ $dmol^{-1}$).

**Thin layer chromatography (TLC)** was performed on alumina plates coated with silica gel (Merck silica gel 60 F 254, d = 0.2 mm, Machery-Nagel ALUGRAM® Xtra SIL G/UV254, d = 0.2 mm). Visualization was accomplished by UV light (λ = 254 nm), ninhydrin/acetic acid solution, potassium permanganate solution, vanillin/sulfuric acid solution or *Seebach´s Magic Stain*.

**High-pressure reactions** up to 5 kbar were performed using a self-custom-built hydraulic high-pressure apparatus from Unipress (Warsaw) using screw capped PTFE vials (1.9 mL) as reaction vessels. A 1:1 (v/v) mixture of decahydronaphthalene (a mixture of *cis* & *trans*) and 2,2,4-trimethylpentane was used as pressurizing medium.

**Radioligand competition binding assay** was performed in the group of Prof. Dr. A. Buschauer (Institute of Pharmacy at the University of Regensburg) under the supervision of S. Dukorn and K. Kuhn according to previously reported procedures.[146,174] Purity of tested compounds was >95% as determined by HPLC. Buffer I was used. IC50 values were converted to $K_i$ values according to the Cheng-Prussoff[238] equation and were provided by S. Dukorn and K. Kuhn.

## 2. Synthesis of compounds

*Following compounds were already available on stock in our laboratories:*

Grubbs catalyst I , 1,3-dimesityl-4,5-dihydro-1H-imidazol-3-ium tetrafluoroborate, *N*-Boc-pyrrole **191**.

*Following compounds were synthesized according to literature procedures and spectroscopic data matched well with those reported:*

chiral amine **19** und *ent*-**19**,[46] Grubbs catalyst II, [159b] $Pd(PPh_3)_4$,[117] *tert*-Leucinol **196**,[193] **232** and **233**.[205]

**Methyl-(*tert*-butoxycarbonyl)glycinate (82)**[46]

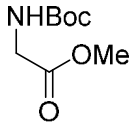


Glycine methyl ester hydrochloride salt **81** (90.15 g, 718 mmol, 1 equiv) was dissolved in MeOH (1.5 L) and cooled down to 0 °C. $NaHCO_3$ (180.9 g, 2.15 mol, 3 equiv) and $Boc_2O$ (156.7 g, 718 mmol, 1 equiv) were added and stirred in the defrosting ice bath for 17 h. The solvent was removed under reduced pressure and the resulting white residue was treated with DCM (400 mL) and water (400 mL). Phases were separated and the aqueous phase was extracted with DCM (2x). The combined organic layers were dried over $MgSO_4$, filtered and concentrated under reduced pressure to obtain the product as a colorless oil (114 g, 604 mmol, 84%).

**$^1$H NMR** (400 MHz, $CDCl_3$) δ = 5.04 – 4.97 (m, 1H), 3.91 (m, 2H), 3.75 (s, 3H), 1.45 (s, 9H).

**Potassium 1,4-bis(*tert*-butoxycarbonyl)-2,5-dihydro-1H-pyrrol-3-olate (83)**[33]

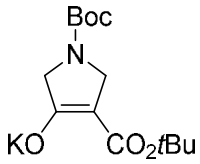


*N*-Boc-glycine methyl ester **82** (114.4 g, 604 mmol, 1 equiv) and *tert*-butyl acrylate (87.7 mL, 604 mmol, 1 equiv) were dissolved in THF (500 mL anhydrous) and cooled down to 0 °C. KO*t*Bu (81.4 g, 725 mmol, 1.2 equiv) was added portionwise and the reaction mixture was stirred for 20 h at ambient temperature. To the resulting thick mixture hexanes (100 mL) was added and the solid was collected by filtration. The yellow solid was washed with cold $Et_2O$ (2x) and dried under high vacuum to obtain the product as a pale yellow powder (155 g, 479 mmol, 79%).

**$^1$H NMR** (400 MHz, $CD_3OD$) δ = 4.12 – 4.05 (m, 2H), 3.79 – 3.72 (m, 2H), 1.49 – 1.42 (m, 18H).

**di-*tert*-Butyl 2,5-dihydro-1H-pyrrole-1,3-dicarboxylate (77)**[33]

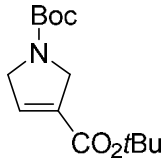


**83** (155 g, 479 mmol, 1 equiv) was dissolved in EtOH (800 mL) and cooled down to 0 °C. $NaBH_4$ (18.1 g, 479 mmol, 1 equiv) was added portionwise and the mixture was stirred for 15 min at this temperature, then at ambient temperature for 2 h. The mixture was again cooled to 0 °C, followed by the addition of water (150 mL), $NH_4Cl$ sat. solution (150 mL) and 2M HCl (300 mL) till no evolution of hydrogen gas was observed. Phases were separated and the aqueous phase was extracted with DCM (2x). The combined organic layers were dried over $MgSO_4$, filtered and concentrated under reduced pressure to obtain the corresponding alcohol (117 g, 407 mmol, 85%) which was used in the following step without further purification.
The alcohol (107.6 g, 374.5 mmol, 1 equiv) was dissolved in pyridine (500 mL), tosyl chloride (356.9 g, 1.8 mol, 5 equiv) was added and the reaction mixture was stirred for 4 h at 100 °C. Then the solvent was removed under reduced pressure and the resulting solid was treated with water (250 mL) and DCM (250 mL). The phases were separated, the organic layer was washed with 0.1M HCl (1x) and brine (1x), dried over $MgSO_4$, filtered and concentrated. The crude mixture was purified by column chromatography (PE/EA 19:1) and recrystallization (PE 2 mL/g) to obtain the product as a white solid (21.9 g, 81.5 mmol, 17% over two steps)

**$R_f$** = 0.56 (PE/EA 5:1). – **$^1$H NMR** (300 MHz, $CDCl_3$) δ = 6.65 – 6.58 (m, 1H), 4.33 – 4.18 (m, 4H), 1.51 – 1.43 (m, 18H).

**di-*tert*-Butyl-(3*R*,4*R*)-4-(benzyl((*S*)-1-phenylethyl)amino)pyrrolidine-1,3-dicarboxylate (78)**[33]

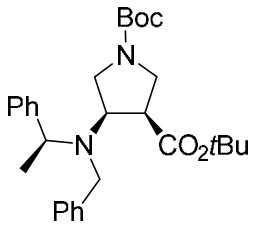


In a flame dried flask under $N_2$-atmosphere chiral amine (*S*)-**19** (14.56 g, 68.9 mmol, 1.6 equiv) was dissolved in THF (70 mL anhydrous) and cooled down to -78 °C in an acetone/$CO_{2(s)}$ bath. *n*-Butyllithium (40.0 mL, 64.5 mmol, 1.5 equiv) was added dropwise and the resulting pink solution was stirred for 15 min at this temperature. Then the mixture was cooled down to -95 °C in an acetone/$N_{2(l)}$ bath and **77** (11.60 g, 43 mmol, 1 equiv) in THF (20 mL anhydrous) was added dropwise. The mixture was stirred for 3 h at -78 °C before cooling down -95 °C again, followed by the dropwise addition of BHT (28.40 g, 129 mmol, 3 equiv) in THF (15 mL anhydrous). The yellow mixture was stirred in the defrosting ice bath for 1.5 h, followed by the addition of $Et_2O$ (50 mL) and sat. $NH_4Cl$ solution (50 mL). The phases were separated and the aqueous phase was extracted with $Et_2O$ (3x). The combined organic layers were washed with 10% citric acid solution (1x), sat. $NaHCO_3$ solution (1x) and brine (1x), dried over $MgSO_4$, filtered and concentrated under reduced pressure. The crude was purified by column chromatography (PE/EA 19:1) to obtain the product as a white solid (5.24 g, 10.9 mmol, 25%).

**$R_f$** = 0.32 (PE/EA 5:1). – **$^1$H NMR** (300 MHz, $CDCl_3$) δ = 7.41 – 7.11 (m, 10H), 4.33 – 4.14 (m, 1H), 4.04 – 3.89 (m, 1H), 3.66 – 3.17 (m, 6H), 3.12 – 3.02 (m, 1H), 1.45 (s, 9H), 1.43 – 1.33 (m, 11H) (signal doubling due to rotamers). – **$^{13}$C NMR** (101 MHz, $CDCl_3$) δ = 171.9, 171.7, 154.4, 154.1, 141.9, 141.6, 141.2, 141.1, 128.23, 128.19, 128.1, 127.2, 127.1, 126.81, 126.76, 81.02, 80.96, 79.2, 79.1, 62.6, 61.1, 57.7, 57.5, 51.9, 51.6, 48.4, 48.3, 47.7, 47.6, 47.3, 28.52, 28.45, 28.2, 28.1, 17.4, 16.4 (signal doubling due to rotamers).

**di-*tert*-Butyl-(3*R*,4*R*)-4-((((9H-fluoren-9-yl)methoxy)carbonyl)amino)pyrrolidine-1,3-dicarboxylate (85)**[46]

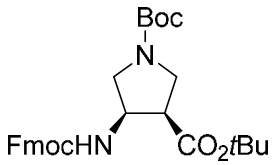


Due to the maximal capacity of the applied autoclave vessel the amount of the used compound **78** (3.55 g, 7.38 mmol) was divided into three portions and the subsequent hydrogenation/Fmoc-protection sequence was performed for each.

A solution of **78** (901 mg, 1.87 mmol) in MeOH (20 mL) and a catalytically amount of acetic acid was transferred into an autoclave, charged with $Pd(OH)_2$ (180 mg, 20wt% based on starting material, 20% Pd on charcoal, 13.7 mol% Pd) and stirred rapidly at ambient temperature under 20 bar of hydrogen gas for 24 h. The mixture was filtered over a plug of celite, washed with MeOH and the solvent was removed under reduced pressure to obtain the crude product as a white solid (731 mg, 2.55 mmol, >100%).

The crude was dissolved in water/dioxane (1:1, 10 mL each) and cooled down to 0 °C. $NaHCO_3$ (439 mg, 5.23 mmol, 2.05 equiv) and FmocOSu (861 mg, 2.55 mmol, 1 equiv) was added and the mixture was stirred in the defrosting ice bath for 24 h. The solvent was removed under reduced pressure and the resulting white residue was treated with sat. $NH_4Cl$ solution (20 mL) and extracted with DCM (3x). The combined organic layers were dried over $MgSO_4$, filtered and concentrated under reduced pressure. The crude was purified by column chromatography (PE/EA 5:1) to yield the product as a white fluffy solid (801 mg, 1.57 mmol, 84% over two steps). In total 3.23 g (6.35 mmol, 86%) of **85** were obtained.

**$R_f$** = 0.15 (PE/EA 5:1). – **$^1$H NMR** (300 MHz, $CDCl_3$) δ = 7.76 (m, 2H), 7.64 – 7.54 (m, 2H), 7.44 – 7.36 (m, 2H), 7.36 – 7.27 (m, 2H), 5.56 – 5.25 (m, 1H), 4.59 – 4.44 (m, 1H), 4.44 – 4.32 (m, 2H), 4.26 – 4.16 (m, 1H), 3.76 – 3.51 (m, 3H), 3.49 – 3.27 (m, 1H), 3.22 – 3.06 (m, 1H), 1.46 (s, 9H), 1.44 (s, 9H) (signal broadening due to rotamers). – **$^{13}$C NMR** (75 MHz, $CDCl_3$) δ = 170.6, 170.1, 155.8, 154.3, 143.8, 141.3, 127.8, 127.6, 127.1, 125.0, 124.8, 120.0, 82.3, 79.9, 67.1, 51.9, 51.5, 51.1, 50.4, 47.2, 47.1, 46.7, 46.1, 28.5, 28.0 (signal doubling due to rotamers). – **HPLC analysis** (Phenomenex Lux Cellulose-1, *n*-heptane/*i*PrOH 90:10, 1.0 mL/min, 215 nm): $t_r$ = **23.57** min, 27.34 min, >99% *ee*.

**(3*R*,4*R*)-3-((((9H-fluoren-9-yl)methoxy)carbonyl)amino)-4-carboxypyrrolidin-1-ium 2,2,2-trifluoroacetate (187)**[46]

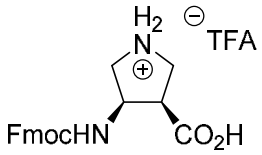


**85** (1.65 g, 3.24 mmol) was dissolved in DCM, TFA (10 mL) was added and the mixture was stirred at ambient temperature for 24 h. The volatiles were removed under reduced pressure und the resulting brown solid was dried under high vacuum for 24 h. Then the solid was dissolved in $CHCl_3$ and *n*-pentane alternately and the solvent was removed under reduced pressure. This step was repeated 5 times each to obtain a pale fluffy solid (1.47 g, 3.15 mmol, 97%). The product was used in the following step without further purification.

**(3*R*,4*R*)-4-((((9H-fluoren-9-yl)methoxy)carbonyl)amino)-1-(*tert*-butoxycarbonyl)pyrrolidine-3-carboxylic acid (79)**[46]

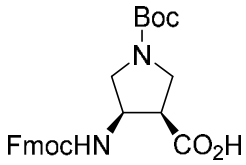


TFA salt **187** (2.14 g, 4.59 mmol, 1 equiv) was dissolved in water/dioxane (1:1, 20 mL each), $NaHCO_3$ (1.93 g, 22.93 mmol, 5 equiv) was added and the mixture was cooled down to 0 °C. Subsequently $Boc_2O$ (1.50 g, 6.55 mmol, 1.5 equiv) in dioxane (20 mL) was added dropwise and the mixture was stirred at ambient temperature for 48 h. Afterwards, EA (10 mL) was added, the phases separated and the aqueous phase was extracted with EA (2x). The combined organic layers were back extracted with sat. $NaHCO_3$ solution (1x) and the combined aqueous phases were acidified with 2M HCl to a pH of 2-3. The aqueous phase was extracted with EA (3x) and the combined organic layers were dried over $MgSO_4$, filtered and the solvent was removed under reduced pressure. The crude was purified by column chromatography (PE/EA 1:1 + 1 vol% AcOH) to obtain the product as a white fluffy solid (1.86 g, 4.07 mmol, 88%).

**$R_f$** = 0.46 (PE/EA 1:1 + AcOH). – **$^1$H NMR** (400 MHz, $CDCl_3$) δ = 7.79 – 7.68 (m, 2H), 7.62 – 7.47 (m, 2H), 7.44 – 7.27 (m, 2H), 6.99 – 6.89 (m, 0.5H) + 5.83 – 5.61 (m, 0.5H), 4.65 – 4.44 (m, 2H), 4.43 – 4.29 (m, 1H), 4.29 – 4.13 (m, 1H), 4.12 – 3.96 (m, 0.5H), 3.85 – 3.51 (m, 2H), 3.50 – 3.31 (m, 1H), 3.29 – 3.14 (m, 1H), 3.04 – 2.76 (m, 0.5H), 1.46 (s, 9H) (signal broadening and doubling due to rotamers). – **$^{13}$C NMR** (101 MHz, $CDCl_3$) δ = 175.0, 174.4, 157.7, 156.2, 154.8, 154.3, 143.9, 143.7, 143.5, 141.3, 129.0, 128.9, 127.8, 127.2, 127.1, 125.1, 124.9, 120.0, 80.5, 80.3, 68.0, 67.9, 67.2, 52.3, 51.9, 51.8, 51.4, 50.6, 50.0, 49.8, 47.21, 47.1, 46.6, 46.2, 45.4, 45.1, 28.5 (signal doubling due to rotamers). – **LRMS** (ESI): *m/z* = 397.1399 $[M+H-C_4H_8]^+$, 475.1837 $[M+Na]^+$, 805.3443 $[2M+H-C_4H_8]^+$, 905.3964 $[2M+Na]^+$.

**di-*tert*-butyl-(3*S*,4*S*)-4-(benzyl((*R*)-1-phenylethyl)amino)pyrrolidine-1,3-dicarboxylate ((*ent*)-78)**[33]

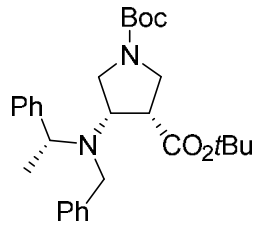


(*ent*)-**78** was prepared in analogy to its enantiomer **78** by using chiral amine (*R*)-**19** (8.79 g, 41.58 mmol, 1.6 equiv), *n*-butyllithium (24.37 mL, 38.98 mmol, 1.5 equiv), **77** (7.00 g, 25.99 mol, 1 equiv) and BHT (17.18 g, 77.97 mmol, 3 equiv). (*ent*)-**78** (3.85 g, 8.01 mmol, 31%) was obtained as colorless sticky solid. Spectroscopic data were identical to those for its enantiomer **78**.

**di-*tert*-Butyl-(3*S*,4*S*)-4-((((9H-fluoren-9-yl)methoxy)carbonyl)amino)pyrrolidine-1,3-dicarboxylate ((*ent*)-85)**[46]

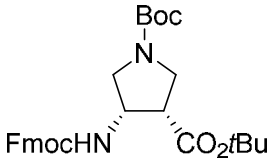


(*ent*)-**85** was prepared in analogy to its enantiomer **85** by using (*ent)*-**78** (1.86 g, 3.88 mmol) and $Pd(OH)_2$ (300 mg, 20wt% based on starting material, 20% Pd on charcoal, 11.0 mol% Pd). For the Fmoc protection $NaHCO_3$ (668 mg, 7.95 mmol, 2.05 equiv) and FmocOSu (1.31 g, 3.88 mmol, 1 equiv) were used. The product was obtained as a white fluffy solid (1.17 g,

2.3 mmol, 59% over two steps). Spectroscopic data were identical to those for its enantiomer **85**. – **HPLC analysis** (Phenomenex Lux Cellulose-1, *n*-heptane/*i*PrOH 90:10, 1.0 mL/min, 215 nm): $t_r$ = 23.57 min, **27.34** min, >99% *ee*.

**(3*S*,4*S*)-3-((((9H-fluoren-9-yl)methoxy)carbonyl)amino)-4-carboxypyrrolidin-1-ium 2,2,2-trifluoroacetate ((*ent*)-187)**[46]

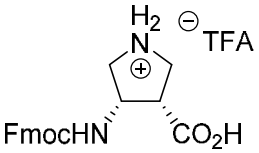


(*ent*)-**187** was prepared in analogy to its enantiomer **187** by using (*ent*)-**85** (2.65 g, 5.21 mmol) and 10 mL TFA to obtain the product as a pale fluffy solid (2.30 g, 4.94 mmol, 94%). The spectroscopic data were identical to those for its enantiomer **187**.

**(3*S*,4*S*)-4-((((9H-fluoren-9-yl)methoxy)carbonyl)amino)-1-(*tert*-butoxycarbonyl)pyrrolidine-3-carboxylic acid ((*ent*)-79)**[46]

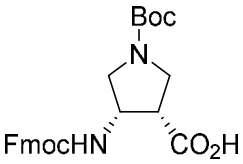


(*ent*)-**79** was prepared in analogy to its enantiomer **79** by using (*ent*)-**85** (2.05 g, 4.39 mmol), $NaHCO_3$ (1.85 g, 21.97 mmol, 5 equiv) and $Boc_2O$ (1.44 g, 6.59 mmol, 1.5 equiv). The product was obtained as a white fluffy solid (1.69 g, 3.72 mmol, 85% over two steps). The spectroscopic data were identical to those for its enantiomer **79**. – **LRMS** (ESI): *m/z* = 397.1400 $[M+H-C_4H_8]^+$, 475.1837 $[M+Na]^+$, 805.3454 $[2M+H-C_4H_8]^+$, 905.3977 $[2M+Na]^+$.

**di-*tert*-Butyl adipate (87)**[24,239]

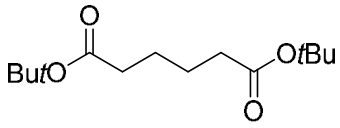


Adipic acid (40.0 g, 273 mmol, 1 equiv) was treated carefully with $SOCl_2$ (60 mL, 821 mmol, 3 equiv) and stirred at 60 °C for 4 h. The solvent was removed under reduced pressure to yield the adipoyl chloride as a yellow residue (bp of product: 105 °C at 3 mbar).

Adipoyl chloride was dissolved in $Et_2O$ (100 mL) and was added dropwise to an ice cold solution of *t*BuOH (78 mL, 841 mmol, 3 equiv) and *N*,*N*-dimethylaniline (104 mL, 821 mmol, 3 equiv) in $Et_2O$ (200 mL). During the addition the color changed from yellow to purple. The mixture was stirred in the defrosting ice bath for 24 h, diluted with water and the phases were separated. The organic layer was washed with 1M HCl (2x), sat. $NaHCO_3$ solution (2x), brine (1x), dried over $MgSO_4$ and filtered. The solvent was removed under reduced pressure and remaining *t*BuOH was removed by distillation under ambient pressure. The product was obtained after distillation under reduced pressure (bp 130 °C at 1 mbar) as a colorless oil which crystallized after standing in the fridge (51.94 g, 201 mmol, 74% over two steps).

**$^1$H NMR** (300 MHz, $CDCl_3$) δ = 2.28 – 2.18 (m, 4H), 1.69 – 1.57 (m, 4H), 1.44 (s, 18H).

***tert*-Butyl 2-oxocyclopentane-1-carboxylate (88)**[24]

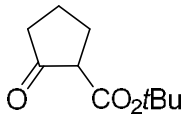


NaH (12.7 g, 317 mmol, 2 equiv, 60% dispersion in mineral oil) was suspended in toluene (270 mL anhydrous) and heated up to 60 °C. A solution of **87** (41.0 g, 158 mmol, 1 equiv) in toluene (50 mL anhydrous) was added dropwise via additional funnel and the mixture was stirred for 3 h at 100 °C. The mixture was allowed to cool down to ambient temperature before being cooled down to 0 °C, followed by the dropwise addition of MeOH and water (5 mL each). Sat. $NH_4Cl$ solution (50 mL) was added, the phases were separated and the organic layer was dried over $MgSO_4$, filtered and concentrated. The product was purified by distillation under reduced pressure (bp. 55 °C at 0.1 mbar) to yield a colorless oil (24.3 g, 131 mmol, 83%).

**$^1$H NMR** (300 MHz, $CDCl_3$) δ = 3.09 – 3.00 (m, 1H), 2.32 – 2.06 (m, 5H), 1.93 – 1.77 (m, 1H), 1.47 (s, 9H).

***tert*-Butyl cyclopent-1-ene-1-carboxylate (20)**[24]

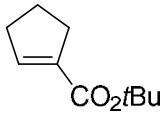


**88** (20.80 g, 113 mmol, 1 equiv) was dissolved in EtOH (280 mL) and cooled down to 0 °C. $NaBH_4$ (4.27 g, 113 mmol, 1 equiv) was added portionwise and the mixture was stirred at ambient temperature for 16 h. After cooling down to 0 °C, water was added till no precipitation of a white solid was observed. Sat. $NH_4Cl$ solution was added (350 mL, vigorous gas evolution) and the suspension was diluted with $Et_2O$ (300 mL). Phases were separated and the aqueous phase was extracted with $Et_2O$ (3x). The combined organic layers were dried over $MgSO_4$, filtered and concentrated.

The residue was dissolved in DCM (280 mL), cooled down to 0 °C and $NEt_3$ (94 mL, 677 mmol, 6 equiv) and DMAP (1.38 g, 11.3 mmol, 0.1 equiv) was added. A solution of MsCl (33.2 mL, 429 mmol, 3.8 equiv) in DCM (140 mL) was added dropwise and the mixture was stirred for 1 h at 0 °C, then at ambient temperature for 8 h. The mixture was diluted with water (400 mL), the phases were separated and the organic layer was washed with 1M HCl (1x), water (1x), sat. $NaHCO_3$ (1x) and brine (1x). The organic phase was dried over $MgSO_4$, filtered and the solvent was removed under reduced pressure.

The residue was dissolved in DCM (280 mL) and cooled down to 0 °C, followed by the addition of a solution of DBU (22 mL, 147 mmol, 1.3 equiv) in DCM (22 mL). The mixture was stirred for 1 h at 0 °C, then for 3 h at ambient temperature. The mixture was washed with 1 M HCl (1x) and brine (1x), dried over $MgSO_4$, filtered and concentrated under reduced pressure. The product was obtained after distillation under reduced pressure (bp 100 °C at 10 mbar) as a colorless oil (11.9 g, 70.6 mmol, 63% over three steps).

**$^1$H NMR** (300 MHz, $CDCl_3$) δ = 6.68 – 6.62 (m, 1H), 2.56 – 2.40 (m, 4H), 1.99 – 1.83 (m, 2H), 1.52 – 1.40 (m, 9H).

***tert*-Butyl-(1*R*,2*S*)-2-(benzyl((*S*)-1-phenylethyl)amino)cyclopentane-1-carboxylate (21)**[24]

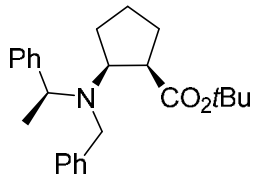


In a flame dried flask under $N_2$-atmosphere chiral amine (*S*)-**19** (13.8 g, 65.3 mmol, 1.6 equiv) was dissolved in THF (40 mL anhydrous) and cooled down to -78 °C by an acetone/$CO_{2(s)}$ bath. *n*-Butyllithium (22.7 mL, 61.3 mmol, 1.5 equiv) was added dropwise and the resulting red solution was stirred for 15 min at this temperature. Then the mixture was cooled down to -95 °C by an acetone/$N_{2(l)}$ bath and **20** (6.9 g, 40.8 mmol, 1 equiv) in THF (15 mL anhydrous) was added dropwise. The mixture was stirred for 3 h at -78 °C before cooling down -95 °C again, followed by the dropwise addition of BHT (27.0 g, 122.5 mmol, 3 equiv) in THF (15 mL anhydrous). The yellow mixture was stirred in the defrosting ice bath for 1.5 h, followed by the addition of $Et_2O$ (50 mL) and sat. $NH_4Cl$ solution (50 mL). The phases were separated and the aqueous phase was extracted with $Et_2O$ (3x). The combined organic layers were washed with 10% citric acid solution (1x), sat. $NaHCO_3$ solution (1x) and brine (1x), dried over $MgSO_4$, filtered and concentrated under reduced pressure. The crude was purified by column chromatography (PE/EA 30:1 → 19:1) to obtain the product as a pale yellow solid (13.6 g, 35.7 mmol, 88%).

**$R_f$** = 0.47 (PE/EA 19:1). – **$^1$H NMR** (300 MHz, $CDCl_3$) δ = 7.46 – 7.14 (m, 10H), 4.31 (q, *J* = 6.8 Hz, 1H), 4.02 (d, *J* = 15.5 Hz, 1H), 3.52 (d, *J* = 15.5 Hz, 1H), 3.16 – 3.04 (m, 1H), 2.95 – 2.86 (m, 1H), 1.90 – 1.60 (m, 6H), 1.51 (s, 9H), 1.38 (d, *J* = 6.9 Hz, 3H). – **$^{13}$C NMR** (75 MHz, $CDCl_3$) δ = 175.2, 143.0, 142.6, 128.13, 128.06, 128.0, 127.9, 126.8, 126.3, 80.0, 66.1, 58.0, 51.8, 48.5, 29.1, 28.3, 27.5, 22.2, 17.5.

**(1*R*,2*S*)-2-((((9H-fluoren-9-yl)methoxy)carbonyl)amino)cyclopentane-1-carboxylic acid (80)**[45]

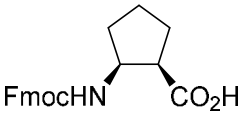


A solution of **21** (7.88 g, 20.76 mmol) in MeOH (30 mL) and acetic acid (10 mL) was transferred into an autoclave, charged with Pd/C (288 mg, 4wt% based on starting material, 10% Pd on charcoal, 1.3 mol% Pd) and stirred rapidly at ambient temperature under 15 bar of hydrogen gas for 22 h. The mixture was filtered over a plug of celite, washed with MeOH and the solvent was removed under reduced pressure.

The crude was dissolved in DCM (10 mL), TFA (10 mL) was added and the mixture was stirred at ambient temperature for 24 h. The volatiles were removed under reduced pressure and 2 M HCl (2 mL) was added. The precipitated solid was washed with cold $Et_2O$ (2x) and dried under high vacuum.

The white solid was dissolved in water/dioxane (1:1, 70 mL each), $NaHCO_3$ (3.58 g, 42.56 mmol, 2.05 equiv) was added and the mixture was cooled down to 0 °C. FmocOSu (7.00 g, 20.76 mmol, 1 equiv) was added portionwise and the mixture was stirred in the defrosting ice bath for 48 h. The solvent was removed under reduced pressure, and the resulting white residue was treated with sat. $NH_4Cl$ solution (20 mL) and extracted with DCM (2x). The combined organic layers were dried over $MgSO_4$, filtered and concentrated under reduced pressure. The crude was purified by column chromatography (DCM/MeOH 95:5) to obtain the product as a white fluffy solid (1.55 g, 4.41 mmol, 21% over three steps).

$\mathbf{R_f}$ = 0.54 (PE/EA 19:1). – **$^1$H NMR** (300 MHz, $CDCl_3$) δ = 7.75 (d, *J* = 7.5 Hz, 2H), 7.57 (d, *J* = 7.5 Hz, 2H), 7.47 – 7.26 (m, 4H), 7.07 – 6.94 (m, 0.5H) + 5.48 – 5.34 (m, 0.5H), 4.51 – 4.40 (m, 1H), 4.39 – 4.14 (m, 2H), 4.14 – 4.00 (m, 1H), 3.13 – 2.83 (m, 1H), 2.13 – 1.43 (m, 6H) (signal doubling due to rotamers). – **$^{13}$C NMR** (101 MHz, $CDCl_3$) δ = 179.1, 178.3, 158.2, 156.2, 143.9, 141.4, 127.8, 127.2, 125.1, 120.0, 67.8, 67.0, 55.6, 54.3, 47.1, 46.5, 32.1, 31.8, 27.9, 27.4, 22.6, 22.0 (signal doubling due to rotamers). – $\mathbf{[\alpha]_D^{20}}$ = -27.2 (*c* 0.5, $CHCl_3$, lit[240].: -29.0 *c* 0.5, $CHCl_3$).

***tert*-Butyl (1*S*,2*R*)-2-(benzyl((*R*)-1-phenylethyl)amino)cyclopentane-1-carboxylate ((*ent*)-21)**[24]

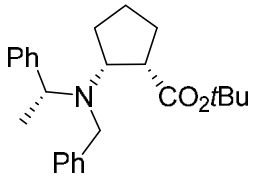


(*ent*)-**21** was prepared in analogy to its enantiomer **21** by using chiral amine (*R*)-**19** (10.1 g, 47.6 mmol, 1.6 equiv), *n*-butyllithium (16.5 mL, 44.6 mmol, 1.5 equiv), **20** (5.0 g, 29.7 mol, 1 equiv) and BHT (19.7 g, 89.2 mmol, 3 equiv). (*ent*)-**21** (9.0 g, 23.7 mmol, 80%) was obtained as colorless solid. Spectroscopic data were identical to those for its enantiomer **21**.

**(1*S*,2*R*)-2-((((9H-fluoren-9-yl)methoxy)carbonyl)amino)cyclopentane-1-carboxylic acid ((*ent*)-80)**[45]

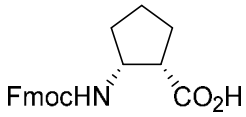


(*ent*)-**80** was prepared in analogy to its enantiomer **80** by using (*ent*)-**21** (6.95 g, 18.3 mmol), Pd/C (288 mg, 4wt% based on starting, 10% Pd on charcoal, 1.3 mol% Pd) and AcOH (10 mL). For the *t*Bu ester hydrolysis TFA (10 mL) was used. For the Fmoc protection $NaHCO_3$ (3.15 g, 37.5 mmol, 2.05 equiv) and FmocOSu (6.18 g, 18.3 mmol, 1 equiv) was used to obtain the product as a white fluffy solid (1.14 g, 3.3 mmol, 18% over three steps). Spectroscopic data were identical to those for its enantiomer **80**. – $\boldsymbol{[\alpha]_D^{20}}$ = +27.9 (*c* 0.5, $CHCl_3$, lit[240].: +28.5, *c* 0.5, $CHCl_3$).

**(3*S*,4*S*)-4-(Benzyl((*R*)-1-phenylethyl)amino)pyrrolidine-3-carboxylic acid ((*ent*)-100)**

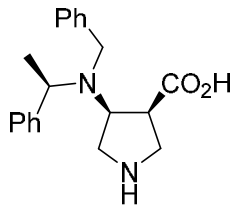


(*ent*)-**78** (875 mg, 1.8 mmol, 1 equiv) was dissolved in DCM (6 mL), TFA (2 mL) was added and the mixture was stirred at ambient temperature for 2.5 h. The solvent was removed under reduced pressure and the crude TFA salt was dissolved in 0.1 M HCl (4 mL). For removal of the counter ion the salt was loaded onto a column with DOWEX 50WX8-200 (2x4 cm, 2x activated with 0.1 M HCl). The column was washed with distilled water (200 mL) and the product was eluted with 16% $NH_3$ (aq.) to obtain the free amino acid after lyophilization as a white fluffy solid (98 mg, 0.3 mmol, 17%).

**$^1$H NMR** (400 MHz, $CDCl_3$ + TFA) δ = 10.41 – 8.81 (m, 1H), 7.47 – 7.15 (m, 10H), 4.31 – 4.13 (m, 1H), 4.01 – 3.86 (m, 2H), 3.86 – 3.72 (m, 1H), 3.61 – 3.28 (m, 3H), 3.20 – 3.05 (m, 1H), 2.66 – 2.50 (m, 1H), 1.56 – 1.35 (m, 3H). – **$^{13}$C NMR** (101 MHz, $CDCl_3$ + TFA) δ = 175.1, 138.2, 136.01, 130.1, 129.5, 128.9, 128.8, 128.6, 128.3, 128.2, 127.6, 60.6, 58.9, 52.3, 46.3, 44.5, 43.6, 13.4. – **IR** (neat): $\tilde{\nu}$ ($cm^{-1}$) = 3026, 2974, 2363, 1617, 1572, 1494, 1449, 1408, 1319, 1190, 1140, 1069, 969, 849, 786, 734, 700. – **mp** = 207 °C (decomposition). – $\boldsymbol{[\alpha]_D^{20}}$ = +3.1 (*c* 0.5, MeOH). – **LRMS** (ESI): *m/z* = 105.0700 $[C_8H_8]^+$, 221.1291 $[MH^+ - C_8H_8]$, 325.1914 $[M+H]^+$. – **HRMS** (ESI): *m/z* = 325.1914 $[M+H]^+$; calc. for $[C_{20}H_{25}N_2O_2]^+$ = 325.1911.

*General procedure for organocatalytic Mannich-type reaction under ambient- and high pressure conditions applying* (*ent*)-**100**

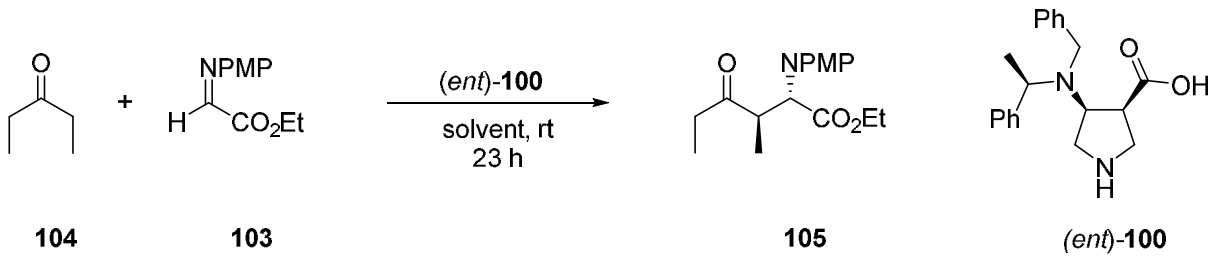


**104** **103** **105** *(ent)*-**100**

Catalyst (*ent*)-**100** (5 mg, 0.015 mmol, 0.1 equiv) was added to a solution of pentan-3-one **104** (160 µL, 1.5 mmol, 10 equiv) and imine **103** (31 mg, 0.15 mmol, 1 equiv) in the indicated solvent (1 mL) and stirred at ambient temperature for 23 h. The reaction was stopped by the addition of sat. $NH_4Cl$ solution (2 mL), the phases were separated and the aqueous was extracted with EA (2x). The combined organic layers were dried over $MgSO_4$, filtered and the solvent was removed under reduced pressure. The crude was purified by column chromatography (PE/EA 9:1) and the product was analyzed by NMR and chiral HPLC.

For reactions under high pressure conditions apparatus II was used and the reaction mixture was transferred into a PTFE vial. Pressure was generated manually and maintained for the indicated time period. The reaction was performed without stirring.

**Ethyl (2*S*,3*R*)-2-((4-methoxyphenyl)amino)-3-methyl-4-oxohexanoate (105)**[60]

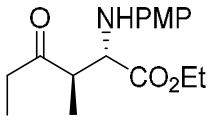


**$R_f$** = 0.32 (PE/EA = 5:1). – **$^1$H NMR** (400 MHz, $CDCl_3$) δ = 6.76 (d, *J* = 9.0 Hz, 2H), 6.70 – 6.61 (m, 2H), 4.22 – 4.09 (m, 3H), 3.77 – 3.70 (m, 3H), 3.08 – 2.98 (m, 1H), 2.58 – 2.50 (m, 2H), 1.24 – 1.19 (m, 3H), 1.19 – 1.16 (m, 3H), 1.08 – 1.02 (m, 3H). – **HPLC analysis** (Chiracel AS-H, *n*-heptane/*i*PrOH 99:1, 1 mL/min, 254 nm) $t_r$ = **22.62 min** (2*S*,3*R, trans*), 29.52 min (2*S*, 3*S cis*), 31.76 min (3*S*,3*R cis*), 37.20 min (2*R*,3*S trans*).

***tert*-Butyl (3*R*,4*R*)-3-((((9H-fluoren-9-yl)methoxy)carbonyl)amino)-4-((*S*)-2-((benzyloxy)carbonyl)pyrrolidine-1-carbonyl)pyrrolidine-1-carboxylate (121)**

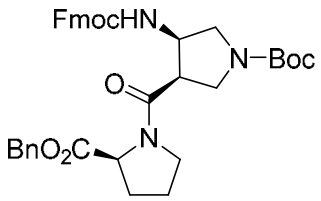


According to literature procedure[106] pyridine (107 µL, 1.33 mmol, 3 equiv) was added to a suspension of **79** (200 mg, 0.442 mmol, 1 equiv) and (*L*)-proline benzyl ester hydrochloride (118 mg, 0.486 mmol, 1.1 equiv) in EA (10 mL) at -10 °C. After stirring for 15 min, T3P (563 mg, 50 wt% in EA, 0.884 mmol, 2 equiv) was added dropwise and the mixture was stirred for 24 h in the defrosting ice bath. Water (10 mL) was added, the phases were separated and the aqueous phase was extracted with EA (3x). The combined organic layers were washed with brine (1x), dried over $MgSO_4$, filtered and concentrated under reduced pressure. The crude was purified by column chromatography (PE/EA 1:2) to afford the product as a white fluffy solid (219 mg, 0.342 mmol, 77%).

$\mathbf{R_f}$ = 0.51 (PE/EA 1:2). – **$^1$H NMR** (300 MHz, $CDCl_3$) δ = 7.76 (d, *J* = 7.5 Hz, 2H), 7.57 (d, *J* = 7.3 Hz, 2H), 7.44 – 7.26 (m, 4H), 6.01 – 5.61 (m, 1H), 5.29 – 5.03 (m, 2H), 4.60 – 4.45 (m, 2H), 4.39 – 4.10 (m, 3H), 3.84 – 3.25 (m, 7H), 2.32 – 1.81 (m, 5H), 1.54 – 1.39 (m, 9H) (signal doubling due to rotamers). – **$^{13}$C NMR** (101 MHz, $CDCl_3$) δ = 171.8, 171.5, 170.0, 169.1, 156.1, 154.2, 143.8, 141.3, 135.6, 128.8, 128.6, 128.5, 128.4, 128.2, 127.8, 127.7, 127.1, 125.5, 125.3, 125.2, 125.1, 120.05, 119.95, 79.9, 67.2, 67.0, 59.0, 47.3, 47.1, 29.0, 28.5, 24.8 (signal doubling due to rotamers). – **IR** (neat): $\tilde{\nu}$ ($cm^{-1}$) = 3302, 2974, 2885, 1692, 1640, 1505, 1446, 1401, 1241, 1162, 1107, 1032, 916, 738, 697. – **mp** = 67 °C. – $\mathbf{[\alpha]_D^{20}}$ = -37.7 (*c* 1, DCM). – **LRMS** (ESI): *m/z* = 584.2394 $[M+H-C_4H_8]^+$, 640.3019 $[M+H]^+$, 662.2837 $[M+Na]^+$, 1301.5787 $[2M+Na]^+$. – **HRMS** (ESI): *m/z* = 640.3019 $[M+H]^+$; calc. for $[C_{37}H_{41}N_3O_7]^+$ = 640.3017.

***tert*-Butyl (3*R*,4*R*)-3-((*S*)-2-((benzyloxy)carbonyl)pyrrolidine-1-carbonyl)-4-((*S*)-1-((benzyloxy)carbonyl)pyrrolidine-2-carboxamido)pyrrolidine-1-carboxylate (122)**

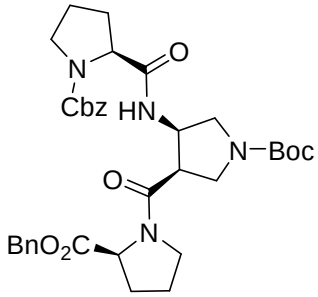


**121** (317 mg, 0.495 mmol, 1 equiv) was dissolved in DMF (6 mL) at 0 °C, a solution of piperidine in DMF (750 µL, 20 vol%) was added dropwise and the mixture was stirred for 15 min. The solvent was removed under reduced pressure and the resulting residue was dissolved in EA (10 mL) again. At -10 °C ((benzyloxy)carbonyl)-*L*-proline (148 mg, 0.594 mmol, 1.2 equiv), pyridine (120 µL, 1.49 mmol, 3 equiv) and T3P (630 mg, 50 wt% in EA, 0.991 mmol, 2 equiv) were added and the mixture was stirred for 24 h in the defrosting ice bath. Water (10 mL) was added, the phases were separated and the aqueous phase was extracted with EA (3x). The combined organic layers were washed with brine (1x), dried over $MgSO_4$, filtered and concentrated under reduced pressure. The crude was purified by column chromatography (DCM/MeOH 95:5) to yield the product as a white fluffy solid (180 mg, 0.277 mmol, 56%) along with starting material (50 mg, 0.078 mmol, 16%, 72% brsm).

**$R_f$** = 0.29 (DCM/MeOH 95:5). – **$^1$H NMR** (300 MHz, $CDCl_3$) δ = 7.41 – 7.24 (m, 10H), 5.24 – 4.95 (m, 4H), 4.70 – 4.55 (m, 1.5H), 4.44 – 4.12 (m, 1.5H), 3.81 – 3.26 (m, 9H), 2.33 – 1.74 (m, 8H), 1.49 – 1.38 (m, 9H) (signal doubling and broadening due to rotamers). – **$^{13}$C NMR** (101 MHz, $CDCl_3$) δ = 172.5, 172.3, 172.0, 171.8, 171.4, 169.4, 168.6, 167.0, 156.4, 155.6, 154.6, 154.2, 136.5, 135.7, 128.8, 128.6, 128.5, 128.3, 128.1, 79.8, 67.4, 66.8, 61.0, 59.1, 53.7, 52.2, 51.7, 47.2, 47.0, 45.1, 43.6, 31.3, 29.8, 29.1, 28.5, 28.4, 27.3, 24.7, 24.4, 23.6, 22.3 (signal doubling due to rotamers). – **IR** (neat): $\tilde{\nu}$ ($cm^{-1}$) = 3298, 2974, 2881, 2355, 1744, 1673, 1643, 1543, 1446, 1408, 1356, 1237, 1166, 1133, 1028, 984, 872, 738, 697. – **mp** = 62 °C. – $[\alpha]_D^{20}$ = -81.0 (*c* 1, DCM). – **LRMS** (ESI): *m/z* = 593.2610 $[M+H-C_4H_8]^+$, 649.3241 $[M+H]^+$, 671.3054 $[M+Na]^+$, 1319.6221 $[2M+Na]^+$. – **HRMS** (ESI): *m/z* = 649.3241 $[M+H]^+$; calc. for $[C_{35}H_{45}N_4O_8]^+$ = 649.3232.

**((3*R*,4*R*)-1-(*tert*-Butoxycarbonyl)-4-((*S*)-pyrrolidine-2-carboxamido)pyrrolidine-3-carbonyl)-*L*-proline (118)**

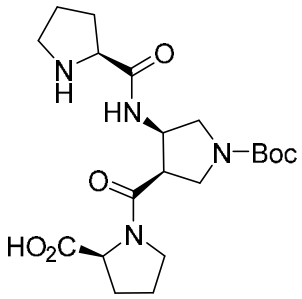


A solution of **122** (101 mg, 0.156 mmol) in MeOH (10 mL) was transferred into an autoclave, charged with Pd/C (10 mg, 10 wt% based on starting material, 10% Pd on charcoal, 6.3 mol% Pd) and stirred rapidly at ambient temperature under 40 bar of hydrogen gas for 24 h. After completion the mixture was filtered over a plug of celite, washed with MeOH and the solvent was removed under reduced pressure to obtain the pure product as a pale beige solid (66 mg, 0.156 mmol, 99%).

**$^{1}$H NMR** (300 MHz, $CD_3OD$) δ = 4.31 – 4.13 (m, 1H), 4.13 – 4.01 (m, H), 3.93 – 3.81 (m, 1H), 3.81 – 3.65 (m, 4H), 3.64 – 3.52 (m, 2H), 3.52 – 3.40 (m, 1H), 2.94 – 2.87 (m, 2H), 2.56 – 2.43 (m, 1H), 2.41 – 1.82 (m, 8H), 1.47 (s, 9H) (signal doubling due to rotamers). – **$^{13}$C NMR** (75 MHz, $CD_3OD$) δ = 169.58, 168.6, 156.2, 156.1, 81.5, 81.4, 69.8, 60.8, 57.6, 52.9, 52.7, 52.4, 41.1, 31.5, 31.0, 30.5, 28.8, 25.7, 25.0, 24.0, 23.9 (signal doubling due to rotamers). – **IR** (neat): $\tilde{\nu}$ ($cm^{-1}$) = 3217, 2974, 2885, 1673, 1628, 1561, 1449, 1401, 1362, 1252, 1162, 1047, 875, 767. – **mp** = 101-104 °C. – $\boldsymbol{[\alpha]_D^{20}}$ = -51.1 (*c* 1, MeOH). – **LRMS** (ESI): *m/z* = 425.2399 $[M+H]^+$. – **HRMS** (ESI): *m/z* = 425.2399 $[M+H]^+$; calc. for $[C_{20}H_{32}N_4O_6]^+$ = 425.2395.

***tert*-Butyl (3*S*,4*S*)-3-((((9H-fluoren-9-yl)methoxy)carbonyl)amino)-4-((*S*)-2-((benzyloxy)carbonyl)pyrrolidine-1-carbonyl)pyrrolidine-1-carboxylate (125)**

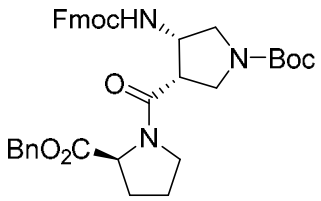


Pyridine (214 µL, 2.65 mmol, 3 equiv) was added to a suspension of (*ent*)-**79** (400 mg, 0.883 mmol, 1 equiv) and (*L*)-proline benzyl ester hydrochloride (235 mg, 0.972 mmol, 1.1 equiv) in EA (10 mL) at -10 °C. After stirring for 15 min, T3P (1.13 g, 50 wt% in EA, 1.77 mmol, 2 equiv) was added dropwise and the mixture was stirred for 24 h in the defrosting ice bath. Water (10 mL) was added, the phases were separated and the aqueous phase was extracted with EA (3x). The combined organic layers were washed with brine (1x), dried over $MgSO_4$, filtered and concentrated under reduced pressure. The crude was purified by column chromatography (PE/EA 1:2) to afford the product as a white fluffy solid (399 mg, 0.623 mmol, 71%).

**$R_f$** = 0.59 (PE/EA 1:2). – **$^1$H NMR** (300 MHz, $CDCl_3$) δ = 7.75 (d, *J* = 7.5 Hz, 2H), 7.65 (d, *J* = 7.4 Hz, 2H), 7.43 – 7.27 (m, 9H), 6.51 – 6.22 (m, 1H), 5.31 – 5.20 (m, 1H), 5.11 – 5.02 (m, 1H), 4.77 – 4.52 (m, 2H), 4.46 – 4.29 (m, 2H), 4.25 – 4.14 (m, 1H), 3.82 – 3.60 (m, 3H), 3.58 – 3.43 (m, 2H), 3.41 – 3.33 (m, 1H), 3.27 – 3.12 (m, 1H), 2.31 – 2.12 (m, 1H), 2.07 – 1.86 (m, 3H), 1.52 – 1.39 (m, 9H). – **$^{13}$C NMR** (101 MHz, $CDCl_3$) δ = 172.5, 170.2, 156.4, 154.3, 144.0, 143.9, 143.8, 141.3, 135.3, 128.8, 128.7, 128.5, 128.2, 127.74, 127.71, 127.1, 126.9, 125.4, 125.3, 120.04, 119.95, 79.6, 67.3, 67.1, 59.2, 51.8, 49.0, 47.5, 47.2, 46.9, 43.9, 42.9, 40.9, 29.0, 28.5, 24.9 (signal doubling due to rotamers). – **IR** (neat): $\tilde{\nu}$ ($cm^{-1}$) = 3313, 2974, 2881, 1692, 1640, 1539, 1446, 1401, 1326, 1230, 1166, 1118, 1131, 875, 738, 697. – **mp** = 87 °C. – **$[\alpha]_D^{20}$** = -22.8 (*c* 1, DCM). – **LRMS** (ESI): *m/z* = 584.2405 $[M+H-C_4H_8]^+$, 640.3032 $[M+H]^+$, 662.2849 $[M+Na]^+$, 1301.5817 $[2M+Na]^+$. – **HRMS** (ESI): *m/z* = 640.3032 $[M+H]^+$; calc. for $[C_{37}H_{41}N_3O_7]^+$ = 640.3017.

***tert*-Butyl (3*S*,4*S*)-3-((*S*)-2-((benzyloxy)carbonyl)pyrrolidine-1-carbonyl)-4-((*S*)-1-((benzyloxy)carbonyl)pyrrolidine-2-carboxamido)pyrrolidine-1-carboxylate (126)**

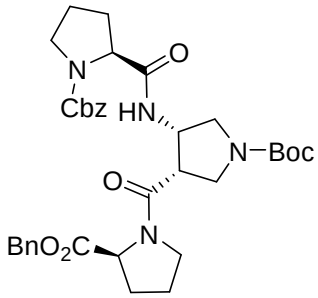


**125** (468 mg, 0.731 mmol, 1 equiv) was dissolved in DMF (4 mL) at 0 °C, a solution of piperidine in DMF (750µL, 20 vol%) was added dropwise and the mixture was stirred for 20 min. The solvent was removed under reduced pressure and the resulting residue was dissolved in EA (10 mL) again. At -10 °C ((benzyloxy)carbonyl)-*L*-proline (218 mg, 0.877 mmol, 1.2 equiv), pyridine (177 µL, 2.19 mmol, 3 equiv) and T3P (931 mg, 50 wt% in EA, 1.46 mmol, 2 equiv) were added and the mixture was stirred for 24 h in the defrosting ice bath. Water (10 mL) was added, the phases were separated and the aqueous phase was extracted with EA (3x). The combined organic layers were washed with brine (1x), dried over $MgSO_4$, filtered and the solvent was removed under reduced pressure. The crude was purified by column chromatography (DCM/MeOH 98:2) to yield the product as a white fluffy solid (254 mg, 0.391 mmol, 54%).

**$R_f$** = 0.11 (DCM/MeOH 98:2). – **$^1$H NMR** (400 MHz, $CDCl_3$) δ = 7.43 – 7.26 (m, 10H), 5.27 – 5.02 (m, 4H), 5.01 – 4.85 (m, 1H), 4.81 – 4.67 (m, 0.5H), 4.65 – 4.48 (m, 1H), 4.32 – 4.18 (m, 1H), 3.97 – 3.83 (m, 0.5H), 3.76 – 3.25 (m, 7H), 3.25 – 3.06 (m, 1.5H), 2.28 – 1.74 (m, 8H), 1.49 – 1.38 (m, 9H) (signal broadening and doubling due to rotamers). – **$^{13}$C NMR** (101 MHz, $CDCl_3$) δ = 173.1, 172.8, 172.7, 170.4, 155.1, 154.8, 154.2, 153.9, 136.9, 135.3, 128.8, 128.6, 128.5, 128.4, 128.1, 127.91, 127.85, 127.8, 79.7, 79.6, 67.3, 67.0, 66.9, 60.67, 59.2, 58.9, 49.5, 49.3, 49.1, 48.9, 48.5, 47.7, 47.5, 47.1, 47.0, 46.9, 42.8, 42.5, 31.5, 31.2, 30.6, 29.1, 28.9, 28.5, 25.0, 24.8, 24.4, 23.6 (signal doubling due to rotamers). – **IR** (neat): ṽ ($cm^{-1}$) = 3317, 2974, 2881, 1692, 1640, 1520, 1446, 1401, 1356, 1252, 1162, 1110, 984, 916, 875, 738, 697. – **mp** = 50 °C. – **$[\alpha]_D^{20}$** = -33.3 (*c* 1, DCM). – **LRMS** (ESI): *m/z* = 593.2614 $[M+H-C_4H_8]^+$, 649.3243 $[M+H]^+$, 671.3057 $[M+Na]^+$, 1319.6226 $[2M+Na]^+$. – **HRMS** (ESI): *m/z* = 649.3243 $[M+H]^+$; calc. for $[C_{35}H_{45}N_4O_8]^+$ = 649.3232.

**((3*S*,4*S*)-1-(tert-butoxycarbonyl)-4-((*S*)-pyrrolidine-2-carboxamido)pyrrolidine-3-carbonyl)-*L*-proline (127)**

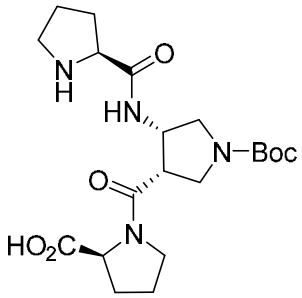


A solution of **126** (100 mg, 0.154 mmol) in MeOH (10 mL) was transferred into an autoclave, charged with Pd/C (10 mg, 10 wt% based on starting material, 10% Pd on charcoal, 6.1 mol% Pd) and stirred rapidly at ambient temperature under 40 bar of hydrogen gas for 24 h. After completion the mixture was filtered over a plug of celite, washed with MeOH and concentrated under reduced pressure to obtain the pure product as a pale white solid (64 mg, 0.150 mmol, 98%).

**$^{1}$H NMR** (400 MHz, $(CD_3)_2SO$) δ = 4.87 – 4.71 (m, 1H), 4.35 – 4.26 (m, 1H), 4.24 – 4.13 (m, 1H), 3.57 – 3.25 (m, 7H), 3.24 – 3.05 (m, 2H), 2.87 – 2.73 (m, 1H), 2.30 – 2.15 (m, 1H), 2.05 – 1.59 (m, 8H), 1.38 (s, 9H) (signal doubling due to rotamers). – **$^{13}$C NMR** (101 MHz, $(CD_3)_2SO$) δ = 177.3, 170.5, 169.2, 169.1, 153.8, 153.7, 78.9, 78.8, 61.2, 58.1, 49.6, 49.0, 48.8, 47.5, 47.3, 47.1, 46.1, 43.0, 42.0, 31.5, 29.9, 28.6, 24.7, 24.6 (signal doubling due to rotamers). – **IR** (neat): $\tilde{\nu}$ ($cm^{-1}$) = 3400, 3200, 2974, 2881, 1677, 1625, 1576, 1449, 1394, 1289, 1244, 1162, 1114, 1043, 879, 767. – **mp** = 149-150 °C. – $[\alpha]_D^{20}$ = -49.2 (*c* 1, MeOH). – **LRMS** (ESI): *m/z* = 425.2401 $[M+H]^+$, 849.4711 $[2M+Na]^+$. – **HRMS** (ESI): *m/z* = 425.2401 $[M+H]^+$; calc. for $[C_{20}H_{32}N_4O_6]^+$ = 425.2395.

**Benzyl ((1*R*,2*S*)-2-((((9H-fluoren-9-yl)methoxy)carbonyl)amino)cyclopentane-1-carbonyl)-*L*-prolinate (128)**

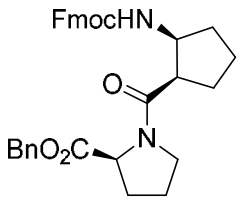


Pyridine (277 µL, 3.43 mmol, 3 equiv) was added to a suspension of **80** (402 mg, 1.14 mmol, 1 equiv) and (*L*)-proline benzyl ester hydrochloride (304 mg, 1.26 mmol, 1.1 equiv) in EA (20 mL) at -10 °C. After stirring for 15 min, T3P (1.46 g, 50 wt% in EA, 2.29 mmol, 2 equiv) was added dropwise and the mixture was stirred for 24 h in the defrosting ice bath. Water (10 mL) was added, the phases were separated and the aqueous phase was extracted with EA (3x). The combined organic layers were washed with brine (1x), dried over $MgSO_4$, filtered and concentrated under reduced pressure. The crude was purified by column chromatography (PE/EA 1:2) to yield the product as a white fluffy solid (450 mg, 0.83 mmol, 73%).

$\mathbf{R_f}$ = 0.59 (PE/EA 1:2). – **$^1$H NMR** (300 MHz, $CDCl_3$) δ = 7.76 (d, *J* = 7.4 Hz, 2H), 7.62 – 7.55 (m, 2H), 7.44 – 7.28 (m, 9H), 5.76 (d, *J* = 9.2 Hz, 1H), 5.27 (d, *J* = 12.3 Hz, 1H), 5.10 (d, *J* = 12.3 Hz, 1H), 4.51 (dd, *J* = 8.2, 4.1 Hz, 1H), 4.40 – 4.14 (m, 4H), 3.66 – 3.55 (m, 2H), 3.20 – 3.07 (m, 1H), 2.21 – 1.71 (m, 11H), 1.65 – 1.47 (m, 1H) (signal doubling due to rotamers). – **$^{13}$C NMR** (75 MHz, $CDCl_3$) δ = 173.0, 172.2, 156.2, 144.1, 144.0, 141.3, 135.8, 128.8, 128.6, 128.4, 128.2, 127.8, 127.1, 125.3, 125.2, 120.0, 67.0, 66.9, 58.9, 53.9, 47.24, 47.19, 44.9, 33.1, 29.2, 28.5, 24.9, 22.9. – **IR** (neat): ṽ ($cm^{-1}$) = 3313, 3063, 3034, 2952, 2873, 1714, 1632, 1505, 1438, 1382, 1326, 1237, 1166, 1088, 1028, 913, 738. – **mp** = 42 °C. – $\mathbf{[\alpha]_D^{20}}$ = -69.8 (*c* 1, DCM). – **LRMS** (ESI): *m/z* = 539.2549 $[M+H]^+$, 561.2358 $[M+Na]^+$, 1099.4831 $[2M+Na]^+$. – **HRMS** (ESI): *m/z* = 539.2548 $[M+H]^+$; calc. for $[C_{33}H_{35}N_2O_5]^+$ = 539.2540.

**Benzyl ((1*S*,2*R*)-2-((((9H-fluoren-9-yl)methoxy)carbonyl)amino)cyclopentane-1-carbonyl)-*L*-prolinate (130)**

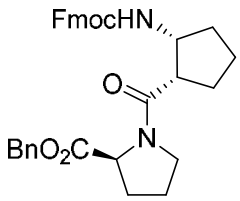


Pyridine (275 µL, 3.41 mmol, 3 equiv) was added to a suspension of (*ent*)-**80** (40 mg, 1.14 mmol, 1 equiv) and (*L*)-proline benzyl ester hydrochloride (303 mg, 1.25 mmol, 1.1 equiv) in EA (20 mL) at -10 °C. After stirring for 15 min, T3P (1.45 g, 50 wt% in EA, 2.28 mmol, 2 equiv) was added dropwise and the mixture was stirred for 24 h in the defrosting ice bath. Water (10 mL) was added, the phases were separated and the aqueous phase was extracted with EA (3x). The combined organic layers were washed with brine (1x), dried over $MgSO_4$, filtered and concentrated under reduced pressure. The crude was purified by column chromatography (PE/EA 2:1) to yield the product as a white fluffy solid (374 mg, 0.69 mmol, 61%).

**$R_f$** = 0.19 (PE/EA 2:1). – **$^1$H NMR** (400 MHz, $CDCl_3$) δ = 7.75 (d, *J* = 7.5 Hz, 2H), 7.69 – 7.60 (m, 2H), 7.45 – 7.19 (m, 9H), 6.13 (d, *J* = 9.0 Hz, 1H), 5.24 (d, *J* = 12.3 Hz, 1H), 5.07 (d, *J* = 12.3 Hz, 1H), 4.59 – 4.52 (m, 1H), 4.43 – 4.29 (m, 3H), 4.27 – 4.14 (m, 1H), 3.72 – 3.64 (m, 1H), 3.54 – 3.41 (m, 1H), 3.22 – 3.11 (m, 1H), 2.25 – 2.14 (m, 1H), 2.12 – 2.03 (m, 1H), 1.99 – 1.49 (m, 11H) (signal doubling due to rotamers). – **$^{13}$C NMR** (101 MHz, $CDCl_3$) δ = 172.93, 172.88, 172.7, 172.5, 158.0, 156.5, 144.3, 144.2, 141.8, 141.7, 141.3, 140.8, 135.6, 135.5, 130.1, 130.1, 130.01, 129.98, 128.7, 128.6, 128.42, 128.39, 128.3, 128.2, 127.8, 127.64, 127.61, 127.6, 127.09, 127.06, 127.04, 126.96, 126.91, 126.88, 126.85, 126.82, 125.5, 125.4, 120.02, 119.99, 119.9, 67.23, 67.15, 67.1, 66.8, 64.6, 59.6, 59.1, 59.0, 55.2, 55.0, 47.54, 47.47, 47.3, 47.1, 44.12, 44.07, 32.0, 31.9, 29.1, 27.6, 27.1, 25.0, 22.3, 22.1 (signal doubling due to rotamers). – **IR** (neat): $\tilde{\nu}$ ($cm^{-1}$) = 3324, 3063, 3034, 2952, 2873, 1714, 1632, 1520, 1435, 1349, 1323, 1237, 1170, 1080, 1028, 909, 738. – **mp** = 44 °C. – $\boldsymbol{[\alpha]_D^{20}}$ = -8.8 (*c* 1, DCM). – **LRMS** (ESI): *m/z* = 539.2549 $[M+H]^+$, 561.2360 $[M+Na]^+$, 1099.4829 $[2M+Na]^+$. – **HRMS** (ESI): *m/z* = 539.2549 $[M+H]^+$; calc. for $[C_{33}H_{35}N_2O_5]^+$ = 539.2540.

**Methyl (1*S*,2*R*)-2-(benzyl((*R*)-1-phenylethyl)amino)cyclopentane-1-carboxylate ((*ent*)-134)**

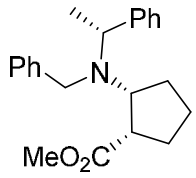


(*ent*)-**21** (515 mg, 1.36 mmol, 1 equiv) and $Et_3SiH$ (433 µL, 2.71 mmol, 2 equiv) were dissolved in DCM (4 mL) at 0 °C, TFA (2 mL) was added and the mixture was stirred in the defrosting ice bath for 24 h. The volatiles were removed under reduced pressure and the resulting residue was dried under high vacuum for 12 h. The crude was dissolved in DCM (6 mL anhydrous) and DMAP (33.2 mg, 0.27 mmol, 0.2 equiv) and MeOH (165 µL anhydrous, 4.07 mmol, 3 equiv) were added. A solution of DCC (294 mg, 1.43 mmol, 1.05 equiv) in DCM (2 mL anhydrous) was added dropwise at 0 °C and the mixture was stirred for 48 h at ambient temperature. The precipitate was filtered off, washed with DCM and the solvent was removed under reduced pressure. The crude was purified by column chromatography (PE/EA 50:1) to yield the product as a colorless oil (194 mg, 0.57 mmol, 42% over two steps).

**$R_f$** = 0.6 (PE/EA 9:1). – **$^1$H NMR** (300 MHz, $CDCl_3$) δ = 7.44 – 7.15 (m, 10H), 4.10 (q, *J* = 6.9 Hz, 1H), 3.86 (d, *J* = 14.9 Hz, 1H), 3.67 (s, 1H), 3.31 – 3.19 (m, 1H), 2.90 (td, *J* = 8.0, 4.5 Hz, 1H), 1.96 – 1.47 (m, 6H), 1.34 (d, *J* = 6.9, 3H). – **$^{13}$C NMR** (75 MHz, $CDCl_3$) δ = 178.0, 143.2, 142.1, 128.1, 128.11, 128.08, 127.99, 126.7, 126.5, 64.3, 57.2, 51.7, 51.4, 47.5, 28.5, 27.4, 22.9, 15.19. – **IR** (neat): ṽ ($cm^{-1}$) = 3060, 3026, 2952, 2870, 1725, 1494, 1449, 1367, 1293, 1241, 1196, 1162, 1073, 1028, 965, 909, 842, 812, 734. – $[\alpha]_D^{20}$ = +73.3 (*c* 1, DCM). – **LRMS** (ESI): *m/z* = 338.2139 $[M+H]^+$. – **HRMS** (ESI): *m/z* = 338.2116 $[M+H]^+$; calc. for $[C_{22}H_{28}NO_2]^+$ = 338.2115.

***tert*-Butyl (1*S*,2*R*)-2-(1H-imidazole-1-carboxamido)cyclopentane-1-carboxylate (138)**

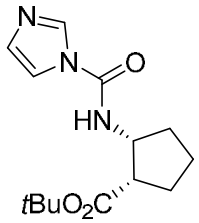


According to literature procedure[110] 1,1'-carbonyldiimidazole (325 mg, 2.00 mmol, 1.5 equiv) was dissolved in DCM (15 mL) and cooled down to -10 °C by the use of a cryostat. A solution of (*ent*)-**132** (247 mg, 1.34 mmol, 1 equiv) and DIPEA (233 µL, 1.34 mmol, 1 equiv) in DCM (3 mL) was added dropwise by an additional funnel over a period of 30 min and the mixture was stirred for 20 h at -10 °C. Water was added, the phases were separated and the aqueous phase was extracted with DCM (1x). The combined organic layers were dried over $MgSO_4$, filtered and the solvent was removed under reduced pressure (cooling trap/high vacuum) at ambient temperature. The product was obtained as a white solid (189 mg, 0.67 mmol, 51%).

**$R_f$** = 0.14 (PE/EA 1:1). – **$^1$H NMR** (300 MHz, $CDCl_3$) δ = 8.12 (s, 1H), 7.52 (d, *J* = 7.6 Hz, 1H), 7.37 – 7.31 (m, 1H), 6.99 (s, 1H), 4.46 – 4.32 (m, 1H), 2.98 – 2.83 (m, 1H), 2.05 – 1.85 (m, 3H), 1.83 – 1.67 (m, 2H), 1.63 – 1.46 (m, 1H), 1.36 – 1.28 (m, 9H). – **$^{13}$C NMR** (75 MHz, $CDCl_3$) δ = 174.3, 148.5, 136.1, 130.2, 115.9, 81.5, 53.6, 46.9, 31.9, 28.5, 27.9, 22.3. – **IR** (neat): $\tilde{\nu}$ ($cm^{-1}$) = 3544, 3198, 3123, 2974, 2873, 1718, 1666, 1513, 1476, 1364, 1319, 1285, 1244, 1218, 1144, 1099, 1066, 1010, 842, 745. – **mp** = 73-75 °C. – **$[\alpha]_D^{20}$** = +10.9 (*c* 1, DCM). – **LRMS** (ESI): *m/z* = 280.1659 $[M+H]^+$.

**di-*tert*-Butyl 2,2'-(carbonylbis(azanediyl))(1*S*,1'*S*,2*R*,2'*R*)-bis(cyclopentane-1-carboxylate) (139)**

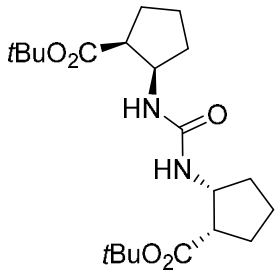

1,1'-Carbonyldiimidazole (533 mg, 3.29 mmol, 1.0 equiv) was dissolved in DCM (6 mL) and cooled down to 0 °C. A solution of (*ent*)-**132** (609 mg, 3.29 mmol, 1 equiv) and DIPEA (573 µL, 3.29 mmol, 1 equiv) in DCM (12 mL) was added dropwise via additional funnel over a period of 30 min and the mixture was stirred for 20 h in the defrosting ice bath. Water was added, the phases were separated and the aqueous phase was extracted with DCM (1x). The combined organic layers were dried over $MgSO_4$, filtered and the solvent was removed under reduced pressure. The product was obtained as a white solid (350 mg, 1.25 mmol, 38%).

$\mathbf{R_f}$ = 0.64 (PE/EA 1:1). – **$^1$H NMR** (300 MHz, $CDCl_3$) δ = 4.96 (d, *J* = 8.4 Hz, 2H), 4.33 – 4.22 (m, 2H), 2.88 – 2.74 (m, 2H), 1.91 – 1.45 (m, 12H), 1.42 – 1.32 (m, 18H). – **$^{13}$C NMR** (75 MHz, $CDCl_3$) δ = 174.2, 156.7, 80.5, 53.2, 47.5, 32.7, 28.1, 27.8, 22.2. – **IR** (neat): $\tilde{\nu}$ ($cm^{-1}$) = 3302, 2974, 2870, 2363, 1722, 1632, 1558, 1364, 1215, 1148, 943, 898, 846. – **mp** = 160-162 °C. – $\mathbf{[\alpha]_D^{20}}$ = +55.4 (*c* 1, DCM). – **LRMS** (ESI): *m/z* = 397.2702 $[M+H]^+$, 419.2514 $[M+Na]^+$, 815.5130 $[2M+Na]^+$. – **HRMS** (ESI): *m/z* = 397.2702 $[M+H]^+$; calc. for $[C_{21}H_{37}N_2O_5]^+$ = 397.2697.

**(1*R*,2*S*)-2-(((Allyloxy)carbonyl)amino)cyclopentane-1-carboxylic acid (144)**

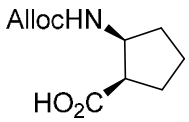

Hydrochloride salt **22** (1.18, 7.14 mmol, 1 equiv) was dissolved in water/dioxane (1:1, 20 mL each), $NaHCO_3$ (2.40 g, 28.56 mmol, 4 equiv) was added and the mixture was cooled down to 0 °C. Subsequently, AllocCl (1.14 mL, 10.71 mmol, 1.5 equiv) in dioxane (20 mL) was added dropwise and the mixture was stirred at ambient temperature for 48 h. Afterwards, EA (10

mL) was added, the phases were separated and the aqueous phase was extracted with EA (2x). The combined organic layers were back extracted with sat. $NaHCO_3$ solution (1x) and the combined aqueous phases were acidified to a pH of 2-3 by the addition of 2M HCl. The aqueous phase was extracted with EA (3x) and the combined organic layers were dried over $MgSO_4$, filtered and the solvent was removed under reduced pressure. The crude was purified by column chromatography (DCM/MeOH 19:1) to obtain the product as a colorless oil (458 mg, 2.15 mmol, 30%).

**$R_f$** = 0.51 (DCM/MeOH 9:1). – **$^1$H NMR** (400 MHz, $CDCl_3$) δ = 10.67 – 10.07 (m, 1H), 7.00 – 6.81 (m, 0.5H) + 5.58 – 5.41 (m, 0.5H), 5.98 – 5.80 (m, 1H), 5.37 – 5.13 (m, 2H), 4.57 (d, *J* = 25.1 Hz, 1H), 4.29 – 4.10 (m, 1H), 3.11 – 2.92 (m, 1H), 2.12 – 1.34 (m, 6H). – **$^{13}$C NMR** (101 MHz, $CDCl_3$) δ = 179.3, 178.4, 177.8, 163.6, 158.0, 155.9, 153.8, 132.8, 132.4, 130.9, 119.9, 117.8, 67.8, 66.4, 65.7, 55.2, 54.2, 52.0, 46.4, 45.6, 32.0, 31.7, 29.4, 28.3, 27.9, 27.4, 24.0, 22.6, 21.9 (signal doubling due to rotamers). – **IR** (neat): ṽ ($cm^{-1}$) = 3309, 3086, 2955, 2877, 1699, 1513, 1449, 1400, 1334, 1222, 1162, 1058, 991, 924, 775. – $[\alpha]_D^{20}$ = -45.0 (*c* 1, $CHCl_3$). – **LRMS** (ESI): *m/z* = 196.0971 $[M+H-H_2O]^+$, 214.1077 $[M+H]^+$, 236.0897 $[M+Na]^+$, 449.1885 $[2M+Na]^+$. – **HRMS** (ESI): *m/z* = 214.1077 $[M+H]^+$; calc. for $[C_{10}H_{16}NO_4]^+$ = 214.1074.

**(1*S*,2*R*)-2-(((Allyloxy)carbonyl)amino)cyclopentane-1-carboxylic acid ((*ent*)-144)**

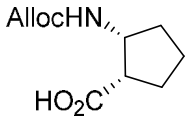


(*ent*)-**144** was synthesized in analogy to its enantiomer **144** by using (*ent*)-**22** (483 mg, 2.92 mmol, 1 equiv), $NaHCO_3$ (981 mg, 11.68 mmol, 4 equiv) and AllocCl (467 µL, 4.38 mmol, 1.5 equiv) to yield the product as a colorless oil (378 mg, 0.17 mmol, 65%). Spectroscopic data were identical to those for its enantiomer **144**. – $[\alpha]_D^{20}$ = +40.0 (*c* 1, $CHCl_3$).

**Benzyl ((1*R*,2*S*)-2-(((allyloxy)carbonyl)amino)cyclopentane-1-carbonyl)-*L*-prolinate (145)**

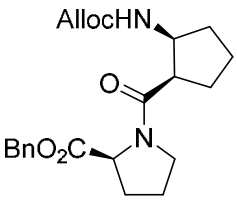


Pyridine (572 µL, 6.44 mmol, 3 equiv) was added to a suspension of **144** (458 mg, 2.15 mmol, 1 equiv) and (*L*)-proline benzyl ester hydrochloride (571 mg, 2.36 mmol, 1.1 equiv) in EA (20 mL) at -10 °C. After stirring for 15 min, T3P (2.73 g, 50 wt% in EA, 2.36 mmol, 2 equiv) was added dropwise and the mixture was stirred for 24 h in the defrosting ice bath. Water (10 mL) was added, the phases were separated and the aqueous phase was extracted with EA (3x). The combined organic layers were washed with brine (1x), dried over $MgSO_4$, filtered and concentrated under reduced pressure. The crude was purified by column chromatography (DCM/MeOH 9:1) to yield the product as a colorless oil (576 mg, 1.44 mmol, 67%).

**$R_f$** = 0.73 (DCM/MeOH 9:1). – **$^1$H NMR** (300 MHz, $CDCl_3$) δ = 7.40 – 7.27 (m, 5H), 5.97 – 5.78 (m, 1H), 5.68 – 5.54 (m, 1H), 5.32 – 5.01 (m, 4H), 4.50 (d, *J* = 5.9 Hz, 3H), 4.29 – 4.15 (m, 1H), 3.67 – 3.54 (m, 2H), 3.08 (dd, *J* = 14.8, 7.8 Hz, 1H), 2.23 – 1.45 (m, 12H) (signal doubling due to rotamers). – **$^{13}$C NMR** (75 MHz, $CDCl_3$) δ = 172.8, 172.1, 155.9, 135.7, 133.0, 128.7, 128.5, 128.3, 128.2, 117.4, 77.5, 77.3, 77.1, 76.7, 66.8, 65.3, 58.8, 53.7, 47.1, 44.9, 33.0, 29.10, 28.3, 24.8, 22.7. – **IR** (neat): ṽ ($cm^{-1}$) = 3309, 2955, 2877, 1714, 1632, 1502, 1435, 1326, 1237, 1162, 1092, 1043, 995, 920, 738, 700. – $[\alpha]_D^{20}$ = +94.6 (*c* 1, DCM). – **LRMS** (ESI): *m/z* = 401.2073 $[M+H]^+$, 423.1894 $[M+Na]^+$, 823.3891 $[2M+Na]^+$. – **HRMS** (ESI): *m/z* = 401.2073 $[M+H]^+$; calc. for $[C_{22}H_{29}N_2O_5]^+$ = 401.2071.

**Benzyl (*S*)-2-(((1*S*,2*R*)-2-((*S*)-2-((benzyloxy)carbonyl)pyrrolidine-1-carbonyl)cyclopentyl)carbamoyl)pyrrolidine-1-carboxylate (129)**

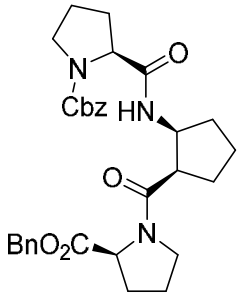


According to literature procedure[113] in a flame dried Schlenk flask under $N_2$-atmosphere ((benzyloxy)carbonyl)-*L*-proline (500 mg, 2.01 mmol, 3 equiv) was activated by stirring in DCM (10 mL anhydrous, degassed) with EDC·HCl (385 mg, 2.01 mmol, 3 equiv) and HOBt·$H_2O$ (307 mg, 2.01 mmol, 3 equiv) for 1 h at 0 °C and for 1 h at ambient temperature. This solution was added to a Schlenk-flask charged with $Pd(PPh_3)_4$ (77 mg, 0.067 mmol, 0.1 equiv), followed by the addition of **145** (268 mg, 0.699 mmol, 1 equiv) in DCM (6 mL anhydrous, degassed). Finally, DABCO (375 mg, 3.55 mmol, 5 equiv) was added and the mixture was stirred at ambient temperature for 20 min. After dilution with DCM, the organic phase was washed with sat. $NaHCO_3$ (1x), sat. $KHSO_4$ (1x) and sat. $NaHCO_3$ (1x), dried over $MgSO_4$, filtered and concentrated under reduced pressure. The crude was purified by column chromatography (DCM/MeOH 50:1) to yield the product as a white fluffy solid (224 mg, 0.409 mmol, 61%).

**$R_f$** = 0.23 (EA). – **$^1$H NMR** (400 MHz, $CDCl_3$) δ = 7.35 – 6.97 (m, 12H), 5.23 – 4.90 (m, 4H), 4.61 – 4.26 (m, 2H), 4.24 – 4.07 (m, 1H), 3.64 – 3.22 (m, 4H), 3.14 – 2.87 (m, 1H), 2.27 – 1.37 (m, 16H) (signal doubling due to rotamers). – **$^{13}$C NMR** (101 MHz, $CDCl_3$) δ = 172.7, 172.5, 172.2, 171.8, 171.5, 155.4, 154.5, 136.6, 135.8, 132.1, 132.01, 131.96, 128.7, 128.6, 128.5, 128.4, 128.2, 128.02, 127.95, 127.7, 127.1, 67.2, 66.7, 66.6, 61.1, 60.8, 58.8, 58.6, 51.4, 47.3, 47.2, 47.0, 44.9, 44.8, 33.4, 32.9, 31.2, 30.0, 29.2, 28.9, 28.7, 24.8, 24.6, 24.3, 23.6, 23.1, 22.9, 22.4 (signal doubling due to rotamers). – **IR** (neat): $\tilde{\nu}$ ($cm^{-1}$) = 3324, 2955, 2877, 1744, 1703, 1669, 1632, 1513, 1412, 1353, 1267, 1241, 1162, 1118, 1028, 984, 916, 745, 697. – **mp** = 90-91 °C. – **$[\alpha]_D^{20}$** = -111.0 (*c* 1, DCM). – **LRMS** (ESI): *m/z* = 548.2761 $[M+H]^+$, 570.2577 $[M+Na]^+$, 1117.5252 $[2M+Na]^+$. – **HRMS** (ESI): *m/z* = 548.2761 $[M+H]^+$; calc. for $[C_{31}H_{38}N_3O_6]^+$ = 548.2755.

**((1*R*,2*S*)-2-((*S*)-Pyrrolidine-2-carboxamido)cyclopentane-1-carbonyl)-*L*-proline (119)**

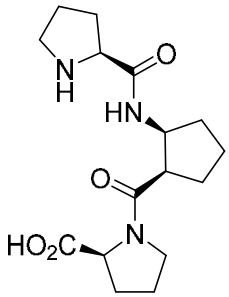

A solution of **129** (181 mg, 0.331 mmol) in MeOH (20 mL) was transferred into an autoclave, charged with Pd/C (36 mg, 20 wt% based on starting material, 10% Pd on charcoal, 10.2 mol% Pd) and stirred rapidly at ambient temperature under 40 bar of hydrogen gas for 24 h. After completion the mixture was filtered over a plug of celite, washed with MeOH and concentrated under reduced pressure to obtain the pure product as a pale golden solid (104 mg, 0.321 mmol, 97%).

**$^1$H NMR** (300 MHz, $CDCl_3$) δ = 4.59 – 4.42 (m, 1H), 4.40 – 4.16 (m, 2H), 3.68 – 3.55 (m, 1H), 3.55 – 3.33 (m, 2H), 3.32 – 3.20 (m, 1H), 3.15 – 2.98 (m, 1H), 2.49 – 1.38 (m, 14H). – **$^{13}$C NMR** (75 MHz, $CDCl_3$) δ = 178.0, 176.3, 173.4, 172.2, 170.1, 168.2, 62.3, 60.9, 59.8, 59.4, 52.3, 51.8, 47.6, 46.7, 45.7, 45.4, 44.6, 33.7, 32.8, 31.7, 30.9, 29.8, 29.7, 29.5, 28.6, 25.0, 24.8, 24.5, 23.6, 23.3, 23.0 (signal doubling due to rotamers). – **IR** (neat): ṽ ($cm^{-1}$) = 3257, 3056, 2952, 2873, 1669, 1606, 1442, 1386, 1334, 1293, 1192, 1047, 976, 920, 875, 745, 663. – **mp** = 95-110 °C. – $\boldsymbol{[\alpha]_D^{20}}$ = -92.7 (*c* 1, DCM). – **LRMS** (ESI): *m/z* = 324.1923 $[M+H]^+$, 647.3760 $[2M+H]^+$. – **HRMS** (ESI): *m/z* = 324.1923 $[M+H]^+$; calc. for $[C_{16}H_{26}N_3O_4]^+$ = 324.1918.

**Benzyl ((1*S*,2*R*)-2-(((allyloxy)carbonyl)amino)cyclopentane-1-carbonyl)-*L*-prolinate (146)**

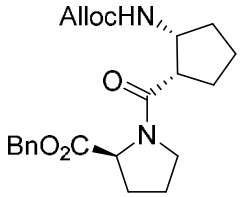

Pyridine (303 µL, 3.45 mmol, 3 equiv) was added to a suspension of (*ent*)-**144** (245 mg, 1.15 mmol, 1 equiv) and (*L*)-proline benzyl ester hydrochloride (306 mg, 1.26 mmol, 1.1 equiv) in

EA (20 mL) at -10 °C. After stirring for 15 min, T3P (1.46 g, 50 wt% in EA, 2.3 mmol, 2 equiv) was added dropwise and the mixture was stirred for 24 h in the defrosting ice bath. Water (10 mL) was added, the phases were separated and the aqueous phase was extracted with EA (3x). The combined organic layers were washed with brine (1x), dried over $MgSO_4$, filtered and concentrated under reduced pressure. The crude was purified by column chromatography (DCM/MeOH 9:1) to yield the product as a colorless oil (313 mg, 0.781 mmol, 68%).

**$R_f$** = 0.86 (DCM/MeOH 9:1). – **$^1$H NMR** (300 MHz, $CDCl_3$) δ = 7.42 – 7.28 (m, 5H), 6.00 – 5.78 (m, 2H), 5.35 – 5.09 (m, 5H), 4.65 – 4.43 (m, 3H), 4.36 – 4.23 (m, 1H), 3.75 – 3.60 (m, 1H), 3.57 – 3.41 (m, 1H), 3.21 – 3.06 (m, 1H), 2.30 – 1.46 (m, 14H) (signal doubling due to rotamers). – **$^{13}$C NMR** (75 MHz, $CDCl_3$) δ = 172.8, 172.7, 172.3, 172.2, 171.8, 169.6, 164.3, 156.2, 136.0 135.7, 135.3, 133.2, 131.7, 128.6, 128.51, 128.47, 128.3, 128.2, 128.11, 128.05, 127.9, 118.9, 117.3, 117.0, 67.5, 67.1, 66.8, 66.3, 65.2, 61.3, 59.5, 59.0, 58.6, 54.7, 53.7, 51.6, 48.0, 47.3, 46.8, 46.3, 45.7, 44.1, 33.4, 31.9, 29.6, 29.3, 29.0, 28.8, 27.2, 24.9, 23.2, 22.5, 22.0 (signal doubling due to rotamers). – **IR** (neat): $\tilde{\nu}$ ($cm^{-1}$) = 3824, 2952, 2877, 1714, 1632, 1509, 1431, 1382, 1323, 1233, 1162, 1092, 1028, 991, 816, 749, 700. – $[\alpha]_D^{20}$ = -9.5 (*c* 1, DCM). – **LRMS** (ESI): *m/z* = 401.2076 $[M+H]^+$, 823.3886 $[2M+Na]^+$. – **HRMS** (ESI): *m/z* = 401.2076 $[M+H]^+$; calc. for $[C_{22}H_{29}N_2O_5]^+$ = 401.2071.

**Benzyl (*S*)-2-(((1*R*,2*S*)-2-((S)-2-((benzyloxy)carbonyl)pyrrolidine-1-carbonyl)cyclopentyl)carbamoyl)pyrrolidine-1-carboxylate (131)**

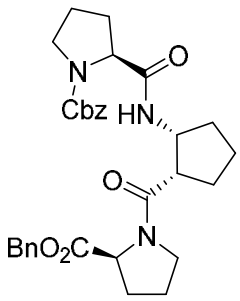


According to literature procedure[113] in a flame dried Schlenk flask under $N_2$-atmosphere ((benzyloxy)carbonyl)-*L*-proline (295 mg, 1.18 mmol, 3 equiv) was activated by stirring in DCM (10 mL anhydrous, degassed) with EDC·HCl (227 mg, 1.18 mmol, 3 equiv) and HOBt·$H_2O$ (181 mg, 1.18 mmol, 3 equiv) for 1 h at 0 °C and for 1 h at ambient temperature. This solution was added to a Schlenk-flask charged with $Pd(PPh_3)_4$ (46 mg, 0.039 mmol, 0.1 equiv), followed by the addition of **146** (158 mg, 0.394 mmol, 1 equiv) in DCM (6 mL

anhydrous, degassed). Finally, DABCO (221 mg, 1.97 mmol, 5 equiv) was added and the mixture was stirred at ambient temperature for 20 min. After dilution with DCM, the organic phase was washed with sat. $NaHCO_3$ (1x), sat. $KHSO_4$ (1x) and sat. $NaHCO_3$ (1x), dried over $MgSO_4$, filtered and concentrated under reduced pressure. The crude was purified by column chromatography (DCM/MeOH 50:1) to yield the product as a colorless oil (188 mg, 0.343 mmol, 87%).

**$R_f$** = 0.32 (DCM/MeOH 19:1). – **$^1$H NMR** (300 MHz, $CDCl_3$) δ = 7.39 – 7.24 (m, 12H), 5.26 – 4.94 (m, 5H), 4.68 – 4.36 (m, 2H), 4.35 – 4.18 (m, 1.5H), 3.89 – 3.75 (m, 0.5H), 3.65 – 3.30 (m, 4H), 3.29 – 3.17 (m, 0.5H), 3.17 – 2.88 (m, 1H), 2.81 – 2.63 (m, 0.5H), 2.28 – 1.40 (m, 17H) (signal doubling due to rotamers). – **$^{13}$C NMR** (75 MHz, $CDCl_3$) δ = 173.0, 172.6, 172.2, 155.01, 154.96, 137.0, 136.9, 135.5, 135.4, 132.1, 132.00, 131.98, 131.9, 128.66, 128.59, 128.5, 128.4, 128.3, 128.0, 127.8, 127.7, 67.1, 67.0, 66.9, 66.8, 60.8, 59.5, 59.1, 58.8, 52.6, 51.7, 47.6, 47.5, 47.1, 46.8, 46.4, 46.0, 43.7, 33.4, 32.0, 31.5, 31.2, 30.5, 29.1, 29.0, 27.8, 27.2, 25.0, 24.8, 24.3, 23.6, 23.3, 22.5, 22.2. – **IR** (neat): ṽ ($cm^{-1}$) = 3332, 2955, 2877, 1736, 1703, 1632, 1513, 1408, 1353, 1170, 1114, 1028, 984, 916, 745, 697. – $\boldsymbol{[\alpha]_D^{20}}$ = -32.9 (*c* 1, DCM). – **LRMS** (ESI): *m/z* = 548.2765 $[M+H]^+$, 570.2586$[M+Na]^+$. – **HRMS** (ESI): *m/z* = 548.2765 $[M+H]^+$; calc. for $[C_{31}H_{38}N_3O_6]^+$ = 548.2755.

**((1*S*,2*R*)-2-((*S*)-Pyrrolidine-2-carboxamido)cyclopentane-1-carbonyl)-*L*-proline (147)**

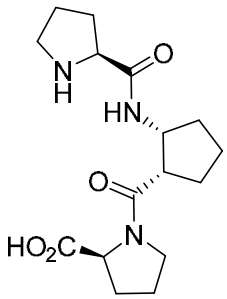


A solution of **131** (166 mg, 0.303 mmol) in MeOH (20 mL) was transferred into an autoclave, charged with Pd/C (32 mg, 20 wt% based on starting material, 10% Pd on charcoal, 9.9 mol% Pd) and stirred rapidly at ambient temperature under 40 bar of hydrogen gas for 24 h. After completion the mixture was filtered over a plug of celite, washed with MeOH and concentrated under reduced pressure to obtain the pure product as a pale white solid (98 mg, 0.303 mmol, >99%).

**$^{1}$H NMR** (300 MHz, $CDCl_3$) δ = 9.37 (d, *J* = 8.8 Hz, 1H), 9.27 – 9.01 (m, 1H), 8.94 – 8.49 (m, 1H), 5.07 – 4.92 (m, 1H), 4.85 – 4.65 (m, 1H), 4.14 – 4.01 (m, 1H), 3.97 – 3.79 (m, 1H), 3.63 – 3.47 (m, 1H), 3.46 – 3.30 (m, 2H), 2.98 – 2.77 (m, 1H), 2.33 – 1.58 (m, 14H), 1.55 – 1.36 (m, 1H) (signal doubling due to rotamers). – **$^{13}$C NMR** (75 MHz, $CDCl_3$) δ = 178.0, 171.1, 167.6, 60.9, 59.5, 50.6, 48.9, 47.3, 33.3, 29.0, 28.9, 27.3, 25.1, 24.6, 22.7. – **IR** (neat): $\tilde{\nu}$ ($cm^{-1}$) = 3049, 2952, 2873, 1673, 1617, 1561, 1438, 1326, 1382, 1244, 1192, 1039, 979, 916, 723, 697, 667. – **mp** = 150 °C (decomposition). – $\boldsymbol{[\alpha]_D^{20}}$ = -49.2 (*c* 1, DCM). – **LRMS** (ESI): *m/z* = 324.1933 $[M+H]^+$, 647.3763 $[2M+H]^+$. – **HRMS** (ESI): *m/z* = 324.1923 $[M+H]^+$; calc. for $[C_{16}H_{26}N_3O_4]^+$ = 324.1918.

*General procedure for organocatalytic aldol reactions under ambient and high pressure conditions applying tripeptide catalysts* **118, 119, 127, 147**.

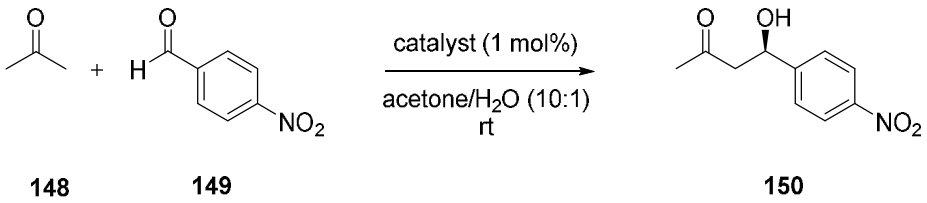


**148** **149** **150**

Tripeptide catalyst (0.01 mmol, 0.01 equiv) was added to a solution of *p*-nitrobenzaldehyde **149** (151 mg, 1 mmol, 1 equiv) in acetone/water (2 mL, 10:1, (v/v)) and the mixture stirred for 24 h at ambient temperature. Acetone was removed under reduced pressure and the resulting residue was treated with EA (10 mL) and water (5 mL). The phases were separated and the organic layer was washed with water (1x), dried over $MgSO_4$, filtered and concentrated under reduced pressure. The crude was purified by column chromatography (PE/EA 2:1) to obtain the product as a pale yellow solid.
For recycling of the catalyst, the aqueous phase was washed with $Et_2O$ (1x) and lyophilized.

For reactions under high pressure conditions apparatus II was used and the reaction mixture was transferred into a PTFE vial. Pressure was generated manually and maintained for 6 h. The reaction was performed without stirring.

**(*R*)-4-Hydroxy-4-(4-nitrophenyl)butan-2-one (150)**

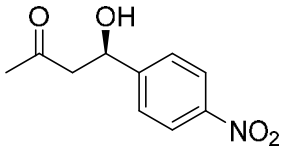


**$^1$H NMR** (300 MHz, $CDCl_3$) δ = 8.24 – 8.17 (m, 2H), 7.57 – 7.49 (m, 2H), 5.26 (dd, *J* = 7.7, 4.6 Hz, 2H), 3.74 – 3.41 (m, 1H), 2.88 – 2.82 (m, 2H), 2.22 (s, 3H). – **HPLC analysis** (Chiracel AS-H, *n*-heptane/*i*PrOH 70:30, 0.5 mL/min, 254 nm) $t_r$ = 24.24 min (*R*), 29.50 min (*S*).

*General procedure (1) for peptide synthesis*

The peptides were obtained by using automated solid phase synthesis on a Syro I synthesizer (Prof. Cabrele laboratory, University of Salzburg, Austria). Rink amide MBHA resin (30 mg, loading 0.59 mmol/g) was used. Double couplings (2 x 40 min) with Fmoc-amino acid/HOBt/HBTU (4 equiv) and DIPEA (8 equiv) were applied. Fmoc cleavage was performed with piperidine/DMF (40% (v/v) for 3 min and 20% (v/v) for 10 min. For *N*-terminal acetylation acetic anhydride and DIPEA in DMF (10 equiv each for 30 min) was used if desired. Simultaneously side-chain deprotection and cleavage from the resin was performed by treating with a mixture of TFA/TIS/water (90/5/5 v/v) for 3 h. The crude peptides were obtained after precipitation in ice-cold $Et_2O$ and centrifugation at 4 °C for 5 min followed by purification by preparative reversed phase HPLC.

**Ac-[(*L*)-Ala-(3*S*,4*S*)-APC-(L)-Ala-(1*S*,2*R*)-ACPC]$_3$-(*L*)-Ala-CONH$_2$ (151)**

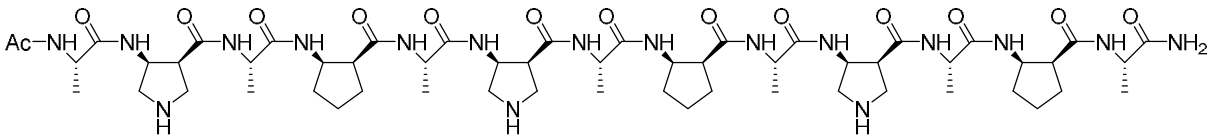

The title compound was synthesized according general procedure 1. Purification by preparative RP-HPLC (Phenomenex Luna C18, MeCN + 0.06% TFA 3 – 98% over 20 min, 21 mL/min, 220 nm, $t_r$ = 7.9 min) yielded **151** as a white fluffy solid (6.1 mg). – **HPLC analysis** (Machery-Nagel EC 250/4 Nucleodur 100-5 C18ec, MeCN + 0.05% TFA 3 – 98% in 40 min, 0.8 mL/min, 220 nm, $t_r$ = 15.3 min) – **LRMS** (ESI): *m/z* = 409.5734 $[M+3H]^{3+}$, 613.8545 $[M+2H]^{2+}$. – **HRMS** (ESI): *m/z* = 409.5734 $[M+3H]^{2+}$; calc. for $[C_{56}H_{94}N_{17}O_{14}]^{5+}$ = 409.5717.

**(2*R*,7*R*)-Diethyl 2,7-bis((*tert*-butoxycarbonyl)amino)oct-4-enedioate (166)**[146]

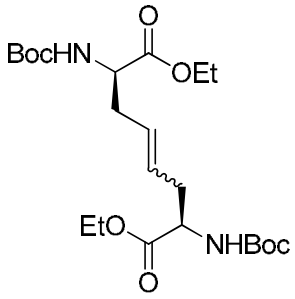


According to literature procedure in a flame-dried Schlenk flask **(*R*)-165** (106 mg, 0.43 mmol, 2 equiv) was dissolved in DCM (8 mL anhydrous) under $N_2$-atmosphere. Grubbs´ II catalyst (18.5 mg, 0.022 mmol, 0.1 equiv) was added and the reaction mixture was stirred under reflux for 11 h until all starting material was consumed. The solvent was removed under reduced pressure and the crude was purified by column chromatography (PE/EA 5:1) to obtain **166** (89 mg, 0.19 mmol, 89%) as a colorless oil.

**$R_f$** = 0.23 (PE/EA 5:1). – **$^1$H NMR** (300 MHz, $CDCl_3$) δ = 5.44 – 5.31 (m, 2H), 5.11 – 5.00 (m, 2H), 4.32 – 4.20 (m, 2H), 4.13 (qd, *J* = 7.1, 1.8 Hz, 4H), 2.51 – 2.31 (m, 4H), 1.42 – 1.32 (m, *18*H), 1.21 (t, *J* = 7.1 Hz, 6H). – **$^{13}$C NMR** (75 MHz, $CDCl_3$) δ = 171.9, 155.2, 128.5, 79.9 + 79.8, 61.44, 61.3, 53.1 + 53.0, 35.5, 28.3, 14.2 (signal doubling due to rotamers). – **IR** (neat): ṽ ($cm^{-1}$) = 3369, 2978, 2937, 1703, 1498, 1367, 1330, 1248, 1159, 1095, 1051, 1021, 969, 857, 779. – **$[\alpha]_D^{20}$** = -27.0 (*c* 1, $CHCl_3$). – **LRMS** (ESI): *m/z* = 459.2711 $[M+H]^+$, 481.2533 $[M+Na]^+$, 939.5163 $[2M+Na]^+$. – **HRMS** (ESI) *m/z* = 459.2711 $[M+H]^+$; calc. for $[C_{22}H_{39}N_2O_8]^+$ = 459.2701.

**(2*R*,7*R*)-Diethyl 2,7-bis((*tert*-butoxycarbonyl)amino)octanedioate (167)**[146]

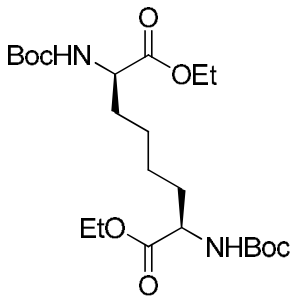


*Method applying Grubbs´II catalyst*: According to literature procedure[241] in a flame dried Schlenk flask under $N_2$-atmosphere (*R*)-**165** (300 mg, 1.23 mmol, 2 equiv) was dissolved in DCM (18 mL anhydrous). Grubbs´ II catalyst (52 mg, 0.06 mmol, 0.1 equiv) was added and the reaction mixture was stirred under reflux for 12 h. After all starting material was consumed the solvent was removed under reduced pressure and EtOH (10 mL) was added. Then the mixture was transferred into an autoclave and stirred under 20 atm of hydrogen gas at ambient temperature for 15 h. The reaction mixture was filtered and the solvent was removed under reduced pressure. The crude was purified by column chromatography (PE/EA 3:1) to yield **167** (268 mg, 0.58 mmol, 95% over two steps) as colorless oil.

*Method applying Pd/C*: Compound **166** (67 mg, 0.148 mmol) was dissolved in EtOH (6 mL, 0.02 M) and Pd/C (6 mg, 10 wt% based on starting material, 10% Pd on charcoal, 3.8 mol% Pd) was added. The flask was flushed ten times with hydrogen gas and the mixture was stirred for 6 h at ambient temperature. When all starting material was consumed the mixture was filtered over a plug of celite, washed with EA and concentrated in vacuo. The crude product was purified by column chromatography (PE/EA 9:1 → 5:1) to obtain the product as a colorless oil (48 mg, 0.104 mmol, 70%).

$\mathbf{R_f}$ = 0.3 (PE/EA 3:1). – **$^1$H NMR** (300 MHz, $CDCl_3$) δ = 5.04 – 4.94 (m, 2H), 4.24 – 4.06 (m, 4H + 2H), 1.79 – 1.46 (m, 4H), 1.42 – 1.34 (m, 18H), 1.33 – 1.17 (m, 4H + 6H). – **$^{13}$C NMR** (75 MHz, $CDCl_3$) δ = 172.8, 155.4, 79.8, 61.3, 53.3, 32.6, 28.3, 24.9, 14.2. – **IR** (neat): $\tilde{\nu}$ ($cm^{-1}$) = 3354, 2978, 2937, 2870, 1699, 1505, 1457, 1367, 1248, 1159, 1021, 861, 779. – $\mathbf{[\alpha]_D^{20}}$ = -14.8 (*c* 1, $CHCl_3$). – **LRMS** (ESI): *m/z* = 461.2866 $[M+H]^+$, 483.2684 $[M+Na]^+$, 943.5473 $[2M+Na]^+$. – **HRMS** (ESI) *m/z* = 461.2865 $[M+H]^+$; calc. for $[C_{22}H_{41}N_2O_8]^+$ = 461.2857.

**(2*R*,7*R*)-2,7-Bis((*tert*-Butoxycarbonyl)amino)octanedioic acid (164)**[146]

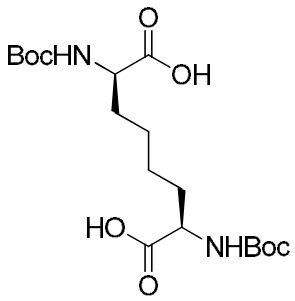


According to literature procedure[242] (*R*,*R*)-**167** (268 mg, 0.58 mmol, 1 equiv) was dissolved in EtOH (8 mL) and a 1M NaOH solution (1.2 mL, 1.16 mmol, 2 equiv) was added dropwise. The reaction was stirred at ambient temperature for 21 h till all starting material was consumed. Afterwards the pH of the solution was adjusted to pH 2 by the addition of 1M HCl solution, $H_2O$ and EA were added and the phases were separated. The aqueous layer was extracted with EA (3x) and the combined organic phases were dried over $MgSO_4$, filtered and concentrated under reduced pressure to yield the product as a white solid (238 mg, 0.58 mmol, quant)

$\mathbf{R_f}$ = 0.1 (PE/EA + AcOH 1:1). – **$^1$H NMR** (300 MHz, $CD_3OD$) δ = 4.13 – 3.91 (m, 2H), 1.97 – 1.72 (m, 2H), 1.71 – 1.57 (m, 2H), 1.51 – 1.36 (m, 22H). – **$^{13}$C NMR** (75 MHz, $CD_3OD$) δ = 176.4, 158.2, 80.5, 54.9, 32.7, 28.8, 26.6. – **IR** (neat): $\tilde{\nu}$ ($cm^{-1}$) = 3295, 2978, 2933, 2363, 1789, 1707, 1680, 1509, 1449, 1394, 1370, 1312, 1244, 1159, 1077, 1047, 1017, 946, 846, 790, 758, 697. – $\mathbf{[\alpha]_D^{20}}$ = +11.2 (*c* 1, DMF). – **LRMS** (ESI): *m/z* = 403.2096 $[M-H]^-$, 807.4236 $[2M-H]^-$. – **HRMS** (ESI) *m/z* = 403.2096 $[M-H]^-$; calc. for $[C_{18}H_{31}N_2O_8]^+$ = 403.2086.

**(2*S*,7*S*)-Diethyl 2,7-bis((*tert*-butoxycarbonyl)amino)oct-4-enedioate (166)**[146]

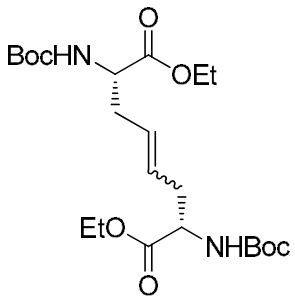


Compound (*S*,*S*)-(+)-**166** was prepared according to (*R*,*R*)-(-)-**166** by using (*S*)-**165** (105 mg, 0.43 mmol. 2 equiv) as starting material to obtain the product as colorless oil (47.3 mg, 0.1 mmol, 49%). Spectroscopic data were identical to those for its enantiomer (*R*,*R*)-(-)-**166**. – $[\alpha]_D^{20}$ = +27.9 (*c* 1, $CHCl_3$).

**(2*S*,7*S*)-Diethyl 2,7-bis((*tert*-butoxycarbonyl)amino)octanedioate (167)**[146]

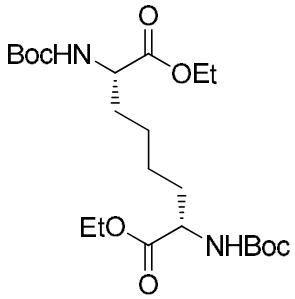


Compound (*S*,*S*)-(+)-**167** was prepared according to (*R*,*R*)-(-)-**167** by using (*S*)-**165** (303 mg, 1.2 mmol, 2 equiv) as starting material to obtain the product as a colorless oil (212 mg, 0.46 mmol, 74%). The spectroscopic data were identical to those for its enantiomer (*R*,*R*)-(-)-**167**. – $[\alpha]_D^{20}$ = +16.9 (*c* 1, $CHCl_3$).

**(2*S*,7*S*)-2,7-bis((*tert*-Butoxycarbonyl)amino)octanedioic acid (164)**[146]

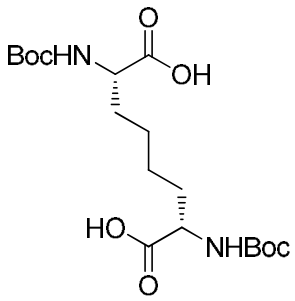


Compound (*S*,*S*)-(+)-**164** was prepared according to (*R*,*R*)-**164** by using (*S*,*S*)-**167** (212 mg, 0.46 mmol, 2 equiv) as starting material to obtain the product as a white solid (190 mg, 0.46 mmol, quant). The spectroscopic data were identical to those for its enantiomer (*R*,*R*)-**164**. – $[\alpha]_D^{20}$ = -9.8 (*c* 1, DMF, ref[243].: -15.2, 5% in DMF).

**Ac-Arg-His-Tyr-Ile-Asn-Leu-Ile-Thr-Arg-((3*R*,4*R*)APC)-Arg-Tyr-NH$_2$ (170)**

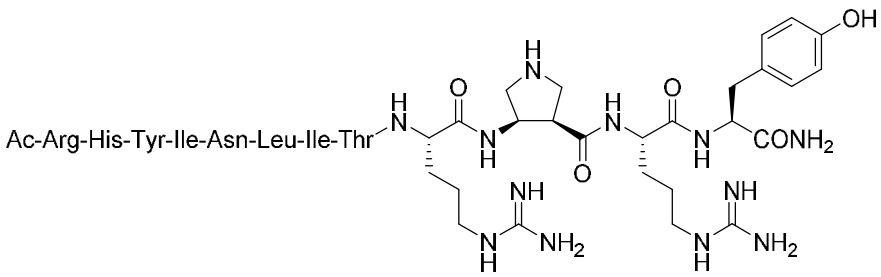


The title compound was synthesized according general procedure 1. Purification by preparative RP-HPLC (Machery-Nagel Nucleodur 250/21 100 C18, MeCN 15 – 50% over 30 min, 15 mL/min, 220 nm, $t_r$ = 16.1 min) yielded **170** as a white fluffy solid (8.3 mg). – **HPLC analysis** (Machery-Nagel EC 250/4 Nucleodur 100-5 C18ec, MeCN + 0.05% TFA 10 – 60% over 13 min, 0.8 mL/min, 220 nm, $t_r$ = 12.3 min) – **LRMS** (ESI): *m/z* = 332.3958 $[M+5H]^{5+}$, 415.2422 $[M+4H]^{4+}$, 553.3190 $[M+3H]^{3+}$, 829.4739 $[M+3H]^{2+}$. – **HRMS** (ESI): *m/z* = 553.3190 $[M+5H]^{3+}$; calc. for $[C_{75}H_{123}N_2O_{17}]^{3+}$ = 553.3181.

**Ac-Arg-His-Tyr-Ile-Asn-Leu-Ile-((3*R*,4*R*)APC)-Arg-((3*R*,4*R*)APC)-Arg-Tyr-NH$_2$ (171)**

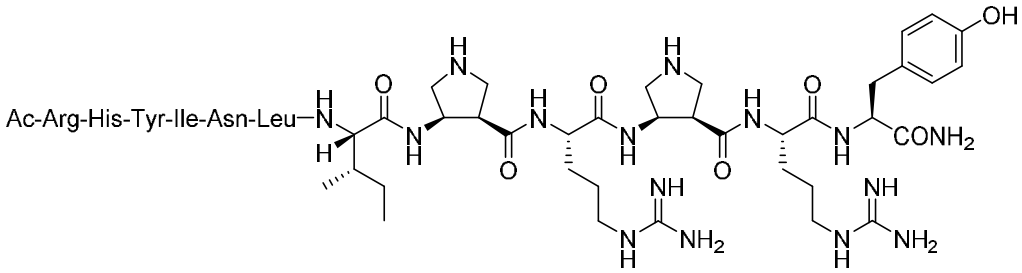


The title compound was synthesized according general procedure 1. Purification by preparative RP-HPLC (Machery-Nagel VP 250/10 Nucleodur 100-5 C18ec, MeCN + 0.05% TFA 10 – 32% over 25 min, 5 mL/min, 220 nm, $t_r$ = 12.7 min) yielded **171** as a white fluffy solid (5 mg). – **HPLC analysis** (Machery-Nagel EC 250/4 Nucleodur 100-5 C18ec, MeCN + 0.05% TFA 10 – 60% over 13 min, 0.8 mL/min, 220 nm, $t_r$ = 11.7 min) – **LRMS** (ESI): *m/z* = 334.5990 $[M+5H]^{5+}$, 417.9959 $[M+4H]^{4+}$, 556.9909 $[M+3H]^{3+}$. – **HRMS** (ESI): *m/z* = 334.5990 $[M+5H]^{5+}$; calc. for $[C_{76}H_{126}N_{27}O_{16}]^{5+}$ = 334.5970.

**Ac-Arg-His-Tyr-Ile-Asn-Leu-Ile-Thr-Arg-((3*S*,4*S*)APC)-Arg-Tyr-NH$_2$ (172)**

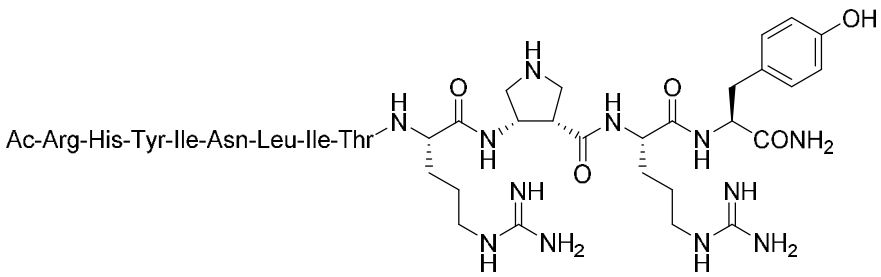


The title compound was synthesized according general procedure 1. Purification by preparative RP-HPLC (Machery-Nagel Nucleodur 250/21 100 C18, MeCN 15 – 50% over 30 min, 15 mL/min, 220 nm, $t_r$ = 15.5 min) yielded **172** as a white fluffy solid (8.6 mg). – **HPLC analysis** (Machery-Nagel EC 250/4 Nucleodur 100-5 C18ec, MeCN + 0.05% TFA 10 – 60% over 13 min, 0.8 mL/min, 220 nm, $t_r$ = 12.2 min) – **LRMS** (ESI): *m/z* = 332.3959 $[M+5H]^{5+}$, 415.2416 $[M+4H]^{4+}$, 553.391 $[M+3H]^{3+}$, 829.9747 $[M+2H]^{2+}$. – **HRMS** (ESI): *m/z* = 415.2416 $[M+4H]^{4+}$; calc. for $[C_{75}H_{124}N_{26}O_{17}]^{5+}$ = 415.2404.

**Ac-Arg-His-Tyr-Ile-Asn-Leu-Ile-((3*S*,4*S*)APC)-Arg-((3*S*,4*S*)APC)-Arg-Tyr-NH$_2$ (173)**

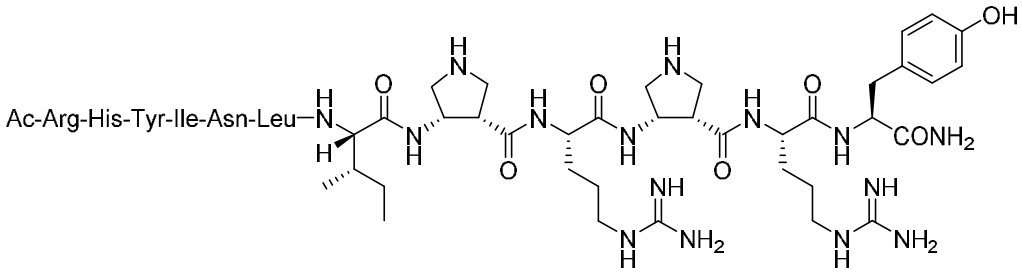


The title compound was synthesized according general procedure 1. Purification by preparative RP-HPLC (Machery-Nagel VP 250/10 Nucleodur 100-5 C18ec, MeCN + 0.05% TFA 10 – 32% over 25 min, 5 mL/min, 220 nm, $t_r$ = 12.8 min) yielded **173** as a white fluffy solid (1.3 mg). – **HPLC analysis** (Machery-Nagel EC 250/4 Nucleodur 100-5 C18ec, MeCN + 0.05% TFA 10 – 60% over 13 min, 0.8 mL/min, 220 nm, $t_r$ = 11.6 min) – **LRMS** (ESI): *m/z* = 334.5987 $[M+5H]^{5+}$, 417.9956 $[M+4H]^{4+}$, 556.9907 $[M+3H]^{3+}$. – **HRMS** (ESI): *m/z* = 334.5988 $[M+5H]^{5+}$; calc. for $[C_{76}H_{126}N_{27}O_{16}]^{5+}$ = 334.5970.

**Ac-Arg-His-Tyr-Ile-Asn-Leu-Ile-((1*R*,2*S*)ACPC)-Arg-((3*R*,4*R*)APC)-Arg-Tyr-NH$_2$ (174)**

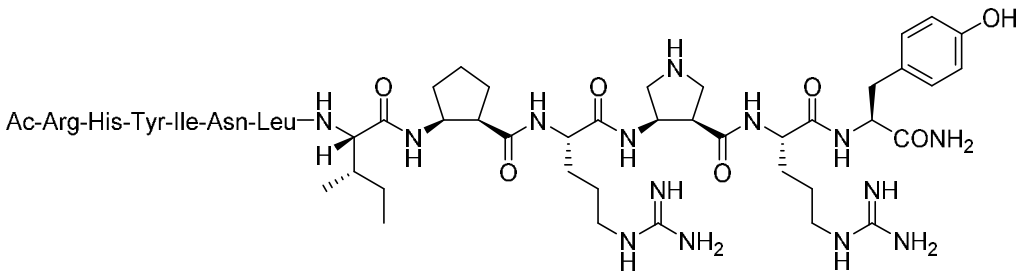


The title compound was synthesized according general procedure 1. Purification by preparative RP-HPLC (Machery-Nagel VP 250/10 Nucleodur 100-5 C18ec, MeCN + 0.05% TFA 10 – 32% over 25 min, 5 mL/min, 220 nm, $t_r$ = 15.8 min) yielded **174** as a white fluffy solid (2.4 mg). – **HPLC analysis** (Machery-Nagel EC 250/4 Nucleodur 100-5 C18ec, MeCN + 0.05% TFA 10 – 60% over 13 min, 0.8 mL/min, 220 nm, $t_r$ = 12.2 min) – **LRMS** (ESI): *m/z* = 334.4005 $[M+5H]^{5+}$, 417.7469 $[M+4H]^{4+}$, 556.6601 $[M+3H]^{3+}$, 834.4849 $[M+2H]^{2+}$. – **HRMS** (ESI): *m/z* = 834.4840 $[M+2H]^{2+}$; calc. for $[C_{77}H_{124}N_{26}O_{16}]^{5+}$ = 834.4839.

**Ac-Arg-His-Tyr-Ile-Asn-Leu-Ile-((1*R*,2*S*)ACPC)-Arg-((3*R*,4*R*)APC)-Arg-Tyr-NH$_2$ (175)**

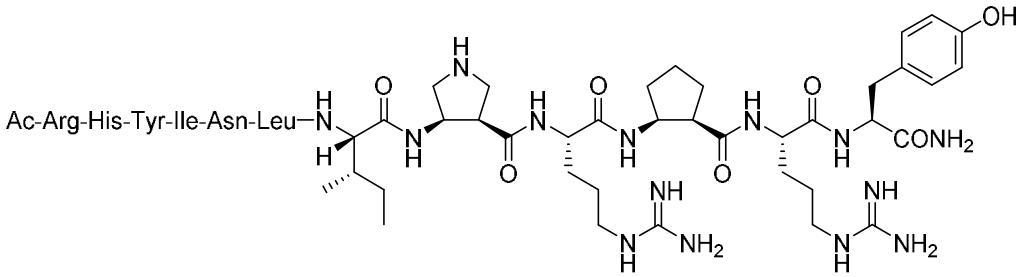


The title compound was synthesized according general procedure 1. Purification by preparative RP-HPLC (Machery-Nagel VP 250/10 Nucleodur 100-5 C18ec, MeCN + 0.05% TFA 10 – 32% over 25 min, 5 mL/min, 220 nm, $t_r$ = 15.5 min) yielded **175** as a white fluffy solid (4 mg). – **HPLC analysis** (Machery-Nagel EC 250/4 Nucleodur 100-5 C18ec, MeCN + 0.05% TFA 10 – 60% over 13 min, 0.8 mL/min, 220 nm, $t_r$ = 12.1 min) – **LRMS** (ESI): *m/z* = 334.3997 $[M+5H]^{5+}$, 417.7468 $[M+4H]^{4+}$, 556.6603 $[M+3H]^{3+}$, 834.4845 $[M+2H]^{2+}$. – **HRMS** (ESI): *m/z* = 834.4840 $[M+2H]^{2+}$; calc. for $[C_{77}H_{124}N_{26}O_{16}]^{5+}$ = 834.4839.

***tert*-Butyl (1*S*,2*S*)-2-(benzyl((*S*)-1-phenylethyl)amino)cyclopentane-1-carboxylate (23)**[24]

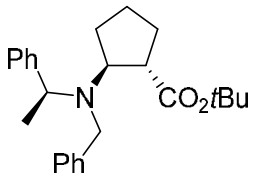


According to literature procedure[24] **21** (1.0 g, 2.63 mmol, 1 equiv) was dissolved in *t*BuOH (30 mL), KO*t*Bu (400 mg, 3.56 mmol, 1.35 equiv) was added and the mixture was stirred under reflux for 8.5 h. The mixture was allowed to cool down to ambient temperature, acidified with sat. $NH_4Cl$ solution (20 mL), diluted with $Et_2O$ (20 mL) and the phases were separated. The aqueous layer was extracted with $Et_2O$ (1x) and the combined organic layers were washed with brine (1x), dried over $MgSO_4$, filtered and the solvent was removed under reduced pressure. The crude was purified by column chromatography (PE/$Et_2O$ 20:1 → 2:1) to obtain the product as a colorless oil (696 mg, 1.83 mmol, 70%).

**$R_f$** = 0.37 (PE/$Et_2O$ 20:1). – **$^1$H NMR** (300 MHz, $CDCl_3$) δ = 7.48 – 7.12 (m, 10H), 3.89 (q, *J* = 6.8 Hz, 1H), 3.78 (d, *J* = 14.9 Hz, 1H), 3.68 (d, *J* = 14.9 Hz, 1H), 3.62 – 3.50 (m, 1H), 2.69 – 2.56 (m, 1H), 1.83 – 1.54 (m, 6H), 1.38 (s, 9H), 1.32 (d, *J* = 6.9, 3H). – **$^{13}$C NMR** (75 MHz, $CDCl_3$) δ = 175.6, 144.6, 142.1, 128.5, 128.2, 128.0, 127.9, 126.7, 126.6, 79.7, 64.0, 58.1, 50.2, 49.2, 29.7, 28.7, 28.2, 24.6, 16.2.

***tert*-Butyl (1*S*,2*S*)-2-((((9H-fluoren-9-yl)methoxy)carbonyl)amino)cyclopentane-1-carboxylate (184)**

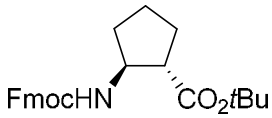


A solution of **23** (672 mg, 1.77 mmol, 1 equiv) in MeOH (15 mL) was transferred into an autoclave, charged with $Pd(OH)_2$/C (168 mg, 25wt%, 20% on charcoal, 14.0 mol%) and was stirred rapidly at ambient temperature under 20 bar of hydrogen gas for 14 h. After completion the mixture was filtered over a plug of celite, washed with MeOH and concentrated under reduced pressure (min. applied pressure 200 mbar).

The residue was dissolved in water/dioxane (1:1, 10 mL each), $NaHCO_3$ (305 mg, 3.63 mmol, 2.05 equiv) was added and the mixture was cooled down to 0 °C. FmocOSu (597 mg, 1.77 mmol, 1 equiv) was added portionwise and the mixture was stirred for 48 h in the defrosting ice bath. Water (5 mL) and EA were added (10 mL), the phases were separated and the

aqueous phase was extracted with EA (2x). The combined organic layers were dried over $MgSO_4$, filtered and the solvent was removed under reduced pressure. The crude was purified by column chromatography (PE/EA 5:1) to yield the product as a white fluffy solid (471 mg, 1.16 mmol, 65%).

**$R_f$** = 0.34 (PE/EA 5:1). – **$^1$H NMR** (300 MHz, $CDCl_3$) δ = 7.75 (d, *J* = 7.4 Hz, 2H), 7.60 (d, *J* = 7.3 Hz, 2H), 7.44 – 7.23 (m, 4H), 5.16 (d, *J* = 7.4 Hz, 1H), 4.53 – 4.33 (m, 2H), 4.29 – 4.09 (m, 2H), 2.61 – 2.44 (m, 1H), 2.21 – 2.05 (m, 1H), 2.02 – 1.78 (m, 2H), 1.76 – 1.61 (m, 2H), 1.57 – 1.47 (m, 1H), 1.45 (s, 9H). – **$^{13}$C NMR** (75 MHz, $CDCl_3$) δ = 173.8, 160.6 + 155.8, 144.0, 141.3, 127.7, 127.1, 125.1, 120.0, 80.6, 66.5 +61.3, 56.3, 51.5, 47.3, 33.2, 28.1, (28.0 hidden) 22.8. – **IR** (neat): ṽ ($cm^{-1}$) = 3350, 2955, 2873, 1722, 1688, 1535, 1446, 1367, 1392, 1244, 1148, 1036, 929, 849, 734. – **mp** = 114 °C. – **$[\alpha]_D^{20}$** = +32.3 (*c* 1, DCM). – **LRMS** (ESI): *m/z* = 352.1548 $[M+H-C_4H_8]^+$, 408.2168 $[M+H]^+$, 430.1994 $[M+Na]^+$, 837.4085 $[2M+Na]^+$. – **HRMS** (ESI): *m/z* = 408.2168 $[M+H]^+$; calc. for $[C_{25}H_{30}NO_4]^+$ = 408.2169.

**(1*S*,2*S*)-2-((((9H-fluoren-9-yl)methoxy)carbonyl)amino)cyclopentane-1-carboxylic acid (185)**[244]

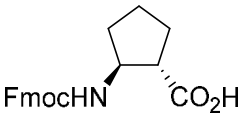


A solution of **185** (538 mg, 1.32 mmol, 1 equiv) and $Et_3SiH$ (422 µL, 2.64 mmol, 2 equiv) was treated with TFA (2 mL) at 0 °C and stirred for 24 h at ambient temperature. The volatiles were removed under reduced pressure, the resulting residue was dissolved in $CHCl_3$ and *n*-pentane alternately and the solvent was removed again. This co-evaporation step was repeated 5 times. The crude was purified by column chromatography (DCM/MeOH 98:2) to afford the product as a white fluffy solid (429 mg, 1.22 mmol, 92%).

**$R_f$** = 0.5 (DCM/MeOH 95:5). – **$^1$H NMR** (300 MHz, $CD_3OD$) δ = 7.78 (d, *J* = 7.4 Hz, 2H), 7.64 (d, *J* = 7.4 Hz, 2H), 7.42 – 7.26 (m, 4H), 4.39 – 4.29 (m, 2H), 4.23 – 4.06 (m, 2H), 2.62 (q, *J* = 7.8, 1H), 2.10 – 1.93 (m, 2H), 1.89 – 1.62 (m, 3H), 1.60 – 1.44 (m, 1H). – **$^{13}$C NMR** (75 MHz, $CD_3OD$) δ = 179.7, 158.5, 145.4, 145.3, 142.6, 128.8, 128.2, 126.2, 121.0, 67.8, 57.3, 52.1, 48.5 (hidden by solvent peak), 33.7, 30.0, 24.2. – **$[\alpha]_D^{20}$** = +32.3 (*c* 1.21, MeOH, lit[244].: +36.3, *c* 1.21, MeOH). – **LRMS** (ESI): *m/z* = 352.1554 $[M+H]^+$, 374.1367 $[M+Na]^+$, 725.2833 $[2M+Na]^+$.

**4-Methylbenzenesulfonyl azide (290)**[245]

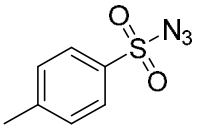

According to literature procedure[245] tosylchloride (35.2 g, 184.7 mmol, 1 equiv) was dissolved in acetone/water (250 mL/200 mL) and cooled down to 0 °C. $NaN_3$ (12.6 g, 193.9 mmol, 1.05 equiv) was added portionwise and the mixture was stirred for 2.5 h at 0 °C. Subsequently, the volume was reduced to its half under reduced pressure (water bath 38 °C, min. applied pressure 170 mbar) and the residue was extracted with $Et_2O$ (3x). The combined organic layers were dried over $MgSO_4$ and concentrated under reduced pressure (water bath 38 °C, min. applied pressure 600 mbar). Further residues of solvent can be removed by drying under high vacuum. The product was obtained as a colorless oil (32.8 g, 166 mmol, 90%) which crystalizes during storage in the freezer.

**$^1$H NMR** (300 MHz, $CDCl_3$) δ = 7.84 (d, *J* = 8.4 Hz, 2H), 7.41 (d, *J* = 8.0 Hz, 2H), 2.48 (s, 3H).

***tert*-Butyl-2-diazoacetate (192)**[246]

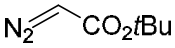

According to literature procedure[246] to an ice-cold solution of *n*-pentane (900 mL), *tert*-butyl acetoacetate (62.2 mL, 380 mmol, 1.0 equiv), tosyl azide (75.0 g, 380 mmol, 1.0 equiv) and TBAB (2.45 g, 7.61 mmol, 0.02 equiv) a precooled solution of NaOH (42.6 g in 354 mL water, 1.06 mol, 2.8 equiv) was added over 45 min. After complete addition, the mixture was allowed to warm up to ambient temperature and stirred for 15 h. Then the mixture was filtered through a plug of celite and the filtrate was transferred into a separating funnel. The phases were separated and the aqueous layer was extracted with *n*-pentane (3x). The combined organic layers were washed with water (2x) and brine (1x), dried over $MgSO_4$ and finally concentrated under reduced pressure (15 °C water bath, min applied pressure 110 mbar) to yield *tert*-butyl-2-diazoacetate (53.3 g, 375 mmol, 99%) as a yellow oil. The product was diluted with anhydrous DCM to the required concentration.

**$^1$H NMR** (300 MHz, $CDCl_3$) δ = 4.61 (bs, 1H), 1.48 (s, 9H).

**(*S*)-4-(*tert*-Butyl)oxazolidin-2-one (197)**[189]

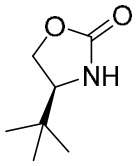

Sodium (902 mg, 39.25 mmol, 1.0 equiv) was dissolved in EtOH (70 mL, 99%) and (*S*)-*tert*-leucinol (4.60 g, 39.25 mmol, 1.0 equiv) and diethylcarbonate (5.22 mL, 43.18 mmol, 1.1 equiv) were added. Then the mixture was refluxed for 24 h. The solvent was removed under reduced pressure and the residue was treated with DCM and sat. $NH_4Cl$. The phases were separated and the aqueous phase was extracted with DCM (2x). The combined organic layers were dried over $MgSO_4$, filtered and concentrated under reduced pressure to give a white solid that was recrystallized from $Et_2O$ to yield **197** (4.56 g, 31.85 mmol, 81%) as a white solid.

**$^1$H NMR** (300 MHz, $CDCl_3$) δ = 6.34 (bs, 1H), 4.42 – 4.31 (m, 1H), 4.19 (dd, *J* = 9.0, 5.8 Hz, 1H), 3.59 (ddd, *J* = 9.0, 5.8, 1.0 Hz, 1H), 0.90 (s, 9H).

**(*S*)-4-(*tert*-Butyl)-2-ethoxy-4,5-dihydrooxazole (198)**[189]

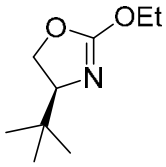

Oxazolidinone **197** (6.41 g, 44.7 mmol, 1.0 equiv) was dissolved in DCM (80 mL anhydrous) and cooled to 0 °C. At this temperature a solution of triethyloxonium tetrafluoroborate (10.21 g, 53.72 mmol, 1.2 equiv) in DCM (50 mL anhydrous) was added dropwise. The mixture was allowed to warm to ambient temperature and stirred for 48 h. Aferwards, the reaction mixture was poured into an ice-cold solution of $Na_2CO_3$ (50 mL) and extracted with DCM (3x). After drying over $MgSO_4$ and filtration, the solvent was removed under reduced pressure to give **198** (7.03 g, 41.05 mmol, 92%) as a yellow oil that was used without further purification.

**$^1$H NMR** (300 MHz, $CDCl_3$) δ = 4.31 – 4.27 (m, 1H), 4.22 – 4.15 (m, 1H), 3.76 (dd, *J* = 9.4, 6.6 Hz, 1H), 1.34 (t, *J* = 7.1 Hz, 6H), 0.88 (s, 9H).

**(*S*)-4-(*tert*-Butyl)-4,5-dihydrooxazol-2-amine (199)**[189]

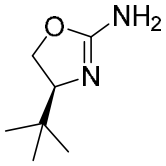

BrCN (5.80 g, 54.8 mmol, 1.08 equiv) was dissolved in MeOH (40 mL anhydrous) and cooled down to 0 °C. A solution of (*S*)-*tert*-leucinol **196** (5.93, 50.6 mmol, 1 equiv) in MeOH (80 mL anhydrous) was added dropwise and the mixture was stirred for 1 h at 0 °C. Subsequently, aqueous ammonia (25% (w/w), 30 mL) was added and the mixture was concentrated under reduced pressure. The residue was treated with NaOH (20% (w/w), 50 mL) and extracted with EA (4x). The combined organic phases were dried over $MgSO_4$, filtrated and concentrated under reduced pressure. Remaining starting material can be removed by drying under high vacuum in a water bath (50 °C) and the desired product **199** was obtained (4.82 g, 33.86 mmol, 67%) as a white solid.

**$^1$H NMR** (300 MHz, $CDCl_3$) δ = 4.22 (dd, *J* = 9.2, 8.3 Hz, 1H), 4.07 (dd, *J* = 8.3, 7.1 Hz, 1H), 3.74 (dd, *J* = 9.2, 7.1 Hz, 1H), 0.87 (s, 9H).

**(*S*)-Bis((*S*)-4-(*tert*-butyl)-4,5-dihydrooxazol-2-yl)amine (193)**[189]

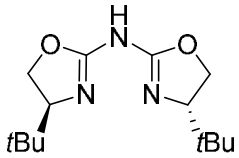

Aminooxazoline **199** (1.34 g, 9.44 mmol, 1.0 equiv) and ethoxyoxazoline **198** (1.94 g, 11.33 mmol, 1.2 equiv) were dissolved in toluene (20 mL anhydrous) and *p*-TSA (163 mg, 0.94 mmol, 0.1 equiv) was added. Then the reaction mixture was refluxed under $N_2$- atmosphere for 19 h. The solvent was removed under reduced pressure and the crude was purified by column chromatography (PE/EA = 1:9) to obtain **193** (1.2 g, 4.48 mmol, 40%) as a colorless crystalline solid that can be recrystallized from acetone.

**$^1$H NMR** (300 MHz, $CDCl_3$) δ = 4.35 – 4.27 (m, 2H), 4.15 (dd, *J* = 8.8, 6.7 Hz, 2H), 3.81 (dd, *J* = 9.4, 6.7 Hz, 2H), 0.90 (s, 18H).

**di-*tert*-Butyl (1*S*,5*S*,6*S*)-2-azabicyclo[3.1.0]hex-3-ene-2,6-dicarboxylate (190)**[196]

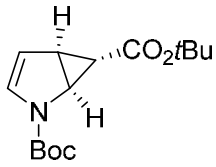


According to literature procedure[196] in a flame dried Schlenk flask under $N_2$-atmosphere $Cu(OTf)_2$ (324 mg, 0.89 mmol, 0.01 equiv) and *tert*-butyl aza-box ligand **193** (479 mg, 1.79 mmol, 0.02 equiv) were dissolved in DCM (25 mL anhydrous) and stirred for 2 h. A solution of *N*-Boc-pyrrole **191** (15.0 g, 89.7 mmol, 1 equiv) in DCM (45 mL anhydrous) was also prepared under $N_2$-atmosphere and cooled down to -20 °C by the use of a cryostat. The Cu/ligand mixture was added via syringe to this flask and phenylhydrazine (88.2 µL, 0.89 mmol, 0.01 equiv) was added dropwise. *tert*-Butyldiazoacetate (168.1 g, 134.6 mmol, 1.5 equiv, 11.38 wt% solution in DCM anhydrous) was added via an electronically controlled dropping system (wait: 10 s, pulse 0.5 s) over 36 h. The reaction mixture was stirred for additionally 6 h, filtered through basic alumina and washed with DCM (600 mL). The solvent was evaporated and the crude product was purified by column chromatography (PE/EA 50:1) to obtain **190** (9.32 g, 33.13 mmol, 37%, 55% *ee*) as a white solid. To obtain enantiopure material the product was recrystallized five times in refluxing hexanes (2 mL/g) to yield **190** (3.61 g, 12.8 mmol, 14%, >99% *ee*).

**$R_f$** = 0.45 (PE/EA = 9:1) – **$^1$H NMR** (300 MHz, $CDCl_3$) δ = 6.54 – 6.29 (m, 1H), 5.34 – 5.21 (m, 1H), 4.34 – 4.06 (m, 1H), 2.71 – 2.57 (m, 1H), 1.42 (s, 9H), 1.37 (s, 9H), 0.85 – 0.74 (m, 1H). – **$^{13}$C NMR** (75 MHz, $CDCl_3$) δ = 172.3, 172.0, 151.2, 151.0, 129.6, 129.4, 110.0, 81.4, 80.6, 44.0, 43.7, 31.6, 30.6, 28.2, 28.1, 24.0 (signal doubling due to rotamers). – **HPLC analysis** (Phenomenex Lux Cellulose-2, *n*-heptane/*i*PrOH 98:2, 0.5 mL/min, 254 nm): $t_r$ = **10.95 min**, 19.02 min, >99% *ee*.

**(1*S*,5*S*,6*S*)-di-*tert*-butyl 2-azabicyclo[3.1.0]hexane-2,6-dicarboxylate (194)**[196]

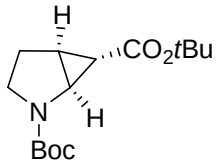


***Method applying autoclave and Pd/C:*** A solution of **190** (269 mg, 0.96 mmol) in THF (6 mL anhydrous) was transferred into an autoclave, charged with Pd/C (25 mg, 10 wt% based on starting material, 10% Pd on carbon, 2.4 mol%) and was stirred rapidly at ambient temperature under 20 bar of hydrogen gas for 4 h. After completion the mixture was filtered over a plug of celite and washed with DCM. The solvent was removed under reduced pressure to obtain the pure product as a white solid (268 mg, 0.95 mmol, 99%).

***Method applying Rh/C:*** In a flame dried flask **190** (1.07 g, 3.8 mmol) was dissolved in THF (20 mL anhydrous) and Rh/C (100 mg, 10wt% based on starting material, 5% Rh on charcoal, 1.3 mol%) was added. Subsequently, a balloon with hydrogen gas was attached and the atmosphere in the flask was flushed ten times with hydrogen gas. The mixture was stirred at room temperature for 1 h under hydrogen atmosphere (1 bar) and after full consumption of starting material the reaction mixture was filtered through a plug of celite. The solvent was removed under reduced pressure to obtain pure **194** (1.07 g, 3.79 mmol, >99%) as a white solid.

$\mathbf{R_f}$ = 0.54 (PE/EA = 5:1) – **$^1$H NMR** (300 MHz, $CDCl_3$) δ = 3.89 – 3.52 (m, 2H), 2.98 – 2.84 (m, 1H), 2.24 – 1.95 (m, 3H), 1.62 (dd, *J* = 3.7, 1.6 Hz, 1H), 1.45 (s, 9H), 1.42 (s, 9H). – **$^{13}$C NMR** (75 MHz, $CDCl_3$) δ = 170.4, 154.8, 80.7, 80.0, 44.2, 44.0, 28.5, 28.2, 27.0 25.5, 24.8. – **HPLC analysis** (Phenomenex Lux Cellulose-2, *n*-heptane/*i*PrOH 70:30, 0.5 mL/min, 215 nm): $t_r$ = **6.87 min**, 10.54 min, >99% *ee*.

**(*S*)-*tert*-Butyl 3-(2-(*tert*-butoxy)-2-oxoethyl)pyrrolidine-1-carboxylate (189)**[196]

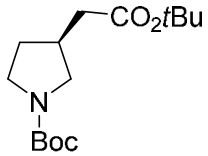


***Method applying TFA:*** **194** (107 mg, 0.37 mmol, 1 equiv) was dissolved in DCM (2 mL anhydrous) and cooled down to 0 °C by the use of a cryostat. $Et_3SiH$ (181 µL, 1.13 mmol,

3 equiv) and TFA (58 µL, 0.75 mmol, 2 equiv) were added dropwise and the solution was stirred for 7 days at 0 °C. The solvent was removed under reduced pressure and the crude was purified by column chromatography (PE/EA 9:1) to afford **189** (35 mg, 0.12 mmol, 33%) as a white solid. Starting material **194** (57 mg, 0.2 mmol, 53%) was reisolated as a white solid.

***Method applying $BF_3{\cdot}OEt_2$:*** **194** (208 mg, 0.73 mmol, 1 equiv) and $Et_3SiH$ (1.17 mL, 7.27 mmol, 10 equiv) were dissolved in DCM (6 mL) and cooled down to 0 °C by the use of a cryostat. Then $BF_3{\cdot}OEt_2$ (93 µL, 0.72 mmol, 1 equiv) was added dropwise and the mixture was stirred for 40 h at 0 °C. Subsequently, sat. $NaHCO_3$ (2 mL) and water (2 mL) were added and the phases were separated. The aqueous phase was extracted with DCM (1x), dried over $MgSO_4$ and filtered. The solvent was removed under reduced pressure and the crude product was purified by column chromatography (PE/EA 9:1) to obtain **189** (112 mg, 0.39 mmol, 53%) as a white solid.

**$R_f$** = 0.47 (PE/EA = 5:1) – **$^1$H NMR** (300 MHz, $CDCl_3$) δ = 3.61 – 3.49 (m, 1H), 3.48 – 3.34 (m, 7.4, 1H), 3.32 – 3.17 (m, 1H), 2.99 – 2.82 (m, 1H), 2.48 (sept, *J* = 7.7 Hz, 1H), 2.31 – 2.23 (m, 2H), 2.09 – 1.95 (m, 1H), 1.59 – 1.47 (m, 1H), 1.46 – 1.37 (m, 18H). **– $^{13}$C NMR** (75 MHz, $CDCl_3$) δ = 171.5, 154.6, 80.6, 79.2, 51.2, 50.8, 45.4, 45.0, 39.0, 35.5, 34.7, 31.5, 30.8, 28.5, 28.1 (signal doubling due to rotamers). – **$[\alpha]_D^{20}$ =** +18.9 (*c* 1, DCM, > 99% *ee*). – **HPLC analysis** (Phenomenex Lux Cellulose-1, *n*-heptane/*i*PrOH 99:1, 0.5 mL/min, 200 nm): $t_r$ = **18.16 min**, 22.52 min, > 99% *ee*.

**(*S*)-2-(Pyrrolidin-3-yl)acetic acid (188)**[196]

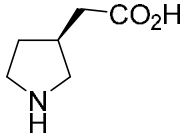


***Method deprotection of* 189: 189** (66 mg, 0.23 mmol, 1 equiv) was dissolved in DCM (4 mL) and cooled down to 0 °C. TFA (178 µL, 2.31 mmol, 10 equiv) was added and the mixture was stirred at ambient temperature for 24 h. The volatiles were removed in vacuo and the crude TFA salt of **188** was dissolved in 0.1 M HCl (8 mL). For removal of the counter ion the salt was loaded onto a column with DOWEX 50WX8-400 (2x4 cm, 2x activated with 0.1 M HCl). The column was washed with distilled water (250 mL) and finally eluted with 16% $NH_3$ (aq.)

to obtain the product after lyophilization as a slight beige colored solid (29.5 mg, 0.23 mmol, 99%).

***Method applying TFA:*** In a flame dried Schlenk flask **190** (1.0 g, 3.55 mmol, 1 equiv) was dissolved in THF (20 mL anhydrous) and Rh/C (10 mg, 1wt% based on starting material, 5% Rh on charcoal, 0.14 mol%) was added. A balloon with hydrogen gas (1 bar) was attached to the flask, the atmosphere was flushed 10 times with hydrogen gas and the mixture was stirred at ambient temperature for 8 h. After complete consumption of the starting material, the mixture was filtered over a plug of celite and the solvent was removed in vacuo.

The resulting white solid (1.0 g, 3.53 mmol) was dissolved in DCM (40 mL) and cooled down to 0 °C by the use of a cryostat. $Et_3SiH$ (1.69 mL, 10.6 mmol, 3 equiv) and TFA (545 µL, 7.1 mmol, 2 equiv) was added dropwise and the mixture was stirred for 17 d at 0 °C. After 6, 14 and 16 d the same amount of $Et_3SiH$ and TFA was added again. When all starting material was consumed, the mixture was allowed to warm up to ambient temperature, an excess of TFA (10 mL) was added and the mixture was stirred for 24 h at ambient temperature.

The volatiles were removed in vacuo and the crude was dissolved in 0.1 M HCl. The solution was loaded onto a column of DOWEX 50WX8-400 (4x2 cm, 2 times activated with 0.1 M HCl) and the resin was washed with distilled water (500 mL). The product was eluted with 16% $NH_3$ (aq.) and fractions were concentrated and lyophilized. The product **188** (457 mg, 3.54 mmol, >99%) was obtained as a slight beige-colored amorphous solid.

***Method applying $BF_3{\cdot}OEt_2$:*** **194** (206 mg, 0.727 mmol, 1 equiv) and $Et_3SiH$ (1.16 mL, 7.27 mmol, 10 equiv) were dissolved in DCM (6 mL anhydrous) and cooled down to 0 °C by the use of a cryostat. Then $BF_3{\cdot}OEt_2$ (92 µL, 0.72 mmol, 1 equiv) was added dropwise and the mixture was stirred for 48 h at 0 °C. When all starting material was consumed, an excess of TFA (4 mL) was added and the mixture was stirred for 24 h at ambient temperature.

The volatiles were removed in vacuo and the crude was dissolved in 0.1 M HCl. The solution was loaded onto a column of DOWEX 50WX8-400 (2x2 cm, 2 times activated with 0.1 M HCl) and the resin was washed with distilled water (500 mL). The product was eluted with 16% $NH_3$ (aq.) and the fractions were concentrated and lyophilized. The product **188** (93 mg, 0.72 mmol, 99%) was obtained as a slight beige-colored amorphous solid.

**$^1$H NMR** (400 MHz, $D_2O$) $\delta$ = 3.51 (dd, *J* = 11.7, 7.7 Hz, 1H), 3.46 – 3.39 (m, 1H), 3.33 – 3.24 (m, 1H), 2.92 (dd, *J* = 11.7, 8.9 Hz, 1H), 2.65 (sept, *J* = 7.4 Hz, 1H), 2.36 (d, *J* = 1.4 Hz,

1H), 2.34 (d, *J* = 2.1 Hz, 1H), 2.28 – 2.17 (m, 1H), 1.74 – 1.62 (m, 1H). – **$^{13}$C NMR** (101 MHz, $D_2O$) δ = 180.6, 49.9, 45.2, 40.1, 35.2, 29.7. – **$[\alpha]_D^{20}$ =** +9.5 (*c* 1, $H_2O$; Lit[176c].: +9.6, *c* 1, $H_2O$). – **LRMS** (ESI): *m/z* = 130.1 $[M+H]^+$. – **HRMS** (ESI): *m/z* = 130.0866 $[M+H]^+$; calc. for $[C_6H_{12}NO_2]^+$ = 130.0863.

**di-*tert*-Butyl-(1*S*,3*S*,4*R*,5*S*,6*S*)-4-azido-3-methoxy-2-azabicyclo[3.1.0]hexane-2,6-dicarboxylate (213)**

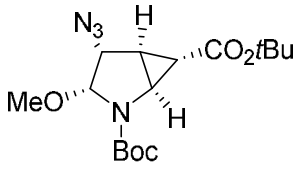


According to literature procedure[197] in a flame dried Schlenk-flask **190** (800 mg, 2.84 mmol, 1 equiv) and $NaN_3$ (277 mg, 4.27 mmol, 1.5 equiv) were dissolved in MeCN/MeOH (35 mL, 4:1, 0.08 M, anhydrous) and cooled down to 0 °C. A solution of cerium ammonium nitrate (4.68 g, 8.53 mmol, 3 equiv) in MeCN (85 mL, 0.1 M, anhydrous) was added dropwise and the solution was stirred at ambient temperature for 40 h. The mixture was diluted with water and extracted with $Et_2O$ (2x). The organic phases were washed with water (1x) and brine (1x), dried over $Mg_2SO_4$, filtered and concentrated under reduced pressure. The crude was purified by column chromatography (PE/EA 50:1 → 9:1) to obtain the product as a white solid (436 mg, 1.23 mmol, 43%).

**$R_f$** = 0.44 (PE/EA 9:1). – **$^1$H NMR** (400 MHz, $CDCl_3$) δ = 5.17 – 4.90 (m, 1H), 4.16 – 3.93 (m, 1H), 3.80 – 3.68 (m, 1H), 3.31 – 3.20 (m, 3H), 2.16 – 2.09 (m, 1H), 2.04 – 1.94 (m, 1H), 1.46 – 1.41 (m, 9H), 1.41 – 1.34 (m, 9H). – **$^{13}$C NMR** (101 MHz, $CDCl_3$) δ = 169.4, 169.0, 153.7, 153.2, 93.6, 93.4, 81.5, 81.3, 65.5, 64.6, 56.5, 56.3, 42.9, 42.8, 28.3, 28.11, 28.05, 26.4, 25.7, 25.6 (signal doubling due to rotamers). – **IR** (neat): $\tilde{\nu}$ ($cm^{-1}$) = 2978, 2937, 2098, 1714, 1698, 1690, 1476, 1460, 1408, 1367, 1315, 1252, 1159, 1118, 1084, 1028, 939, 875, 842, 764, 723. – **mp =** 66 °C. – **$[\alpha]_D^{20}$** = -53.8 (*c* 1, DCM). – **LRMS** (ESI): *m/z* = 377.1805 $[M+Na]^+$. – **HRMS** (ESI): *m/z* = 377.1805 $[M+Na]^+$; calc. for $[C_{16}H_{26}N_4NaO_5]^+$ = 377.1795.

**di-*tert*-Butyl (1*S*,3*S*,4*R*,5*R*,6*S*)-4-amino-3-methoxy-2-azabicyclo[3.1.0]hexane-2,6-dicarboxylate (214)**

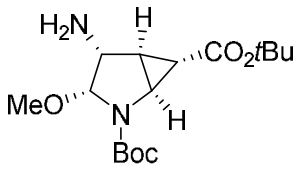


**213** (230 mg, 0.648 mmol) was dissolved in THF (6 mL anhydrous) and Pd/C (23 mg, 10 wt% based on starting material, 10% Pd on charcoal, 3.3 mol% Pd) was added. The flask was flushed ten times with hydrogen gas and the mixture was stirred at ambient temperature for 19 h. The mixture was filtered over a plug of celite and washed with MeOH. The solvent was removed under reduced pressure to obtain the pure product as colorless oil (209 mg, 0.636 mmol, 98%).

**$R_f$** = 0.05 (PE/EA 9:1). – **$^1$H NMR** (300 MHz, $CDCl_3$) δ = 4.94 – 4.71 (m, 1H), 4.06 – 3.82 (m, 1H), 3.40 – 3.31 (m, 1H), 3.29 – 3.17 (m, 3H), 1.98 – 1.90 (m, 1H), 1.89 – 1.80 (m, 1H), 1.42 (s, 9H), 1.36 (s, 9H), 1.31 – 1.21 (m, 1H). – **$^{13}$C NMR** (75 MHz, $CDCl_3$) δ = 168.9, 153.4, 153.0, 95.8, 79.9, 79.7, 57.2, 56.4, 55.2, 41.6, 29.2, 28.7, 27.3, 27.1, 25.0. – **IR** (neat): $\tilde{\nu}$ ($cm^{-1}$) = 2978, 2937, 1699, 1499, 1475, 1394, 1364, 1300, 1252, 1148, 1114, 1077, 1021, 939, 872, 842, 764, 723. – **$[\alpha]_D^{20}$** = -10.5 (*c* 1, DCM). – **LRMS** (ESI): *m/z* = 241.1185 [M+H-$C_4H_8$-MeOH]$^+$, 297.1809 [M+H-MeOH]$^+$, 351.1891 [M+Na]$^+$. – **HRMS** (ESI): *m/z* = 351.1891 [M+Na]$^+$; calc. for $[C_{16}H_{28}N_2NaO_5]^+$ = 351.1899.

**di-*tert*-Butyl (1*S*,3*S*,4*R*,5*R*,6*S*)-4-((((9H-fluoren-9-yl)methoxy)carbonyl)amino)-3-methoxy-2-azabicyclo[3.1.0]hexane-2,6-dicarboxylate (215)**

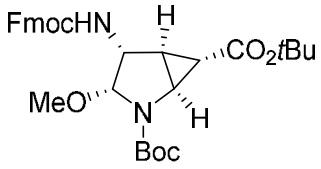


Amine **214** (188 mg, 0.572 mmol, 1 equiv) was dissolved in dioxane/water (1:1, 5 mL each), $NaHCO_3$ (96 mg, 1.14 mmol, 2 equiv) was added and the mixture was cooled down to 0 °C. FmocOSu (289 mg, 0.858 mmol, 1.5 equiv) in dioxane (10 mL) was added dropwise via additional funnel and the mixture was stirred at ambient temperature for 24 h. Water and EA (5 mL each) were added, the phases separated and the aqueous phase was extracted with EA

(2x). The combined organic phases were dried over $MgSO_4$, filtered and concentrated under reduced pressure. The crude was purified by column chromatography (PE/EA 9:1) and the product was obtained as a white fluffy solid (285 mg, 0.517 mmol, 90%).

**$R_f$** = 0.51 (PE/EA 9:1). – **$^1$H NMR** (300 MHz, $CDCl_3$) δ = 7.76 (d, *J* = 7.4 Hz, 2H), 7.67 – 7.54 (m, *2*H), 7.47 – 7.26 (m, 4H), 5.27 – 4.76 (m, 2H), 4.56 – 4.34 (m, 2H), 4.28 – 3.88 (m, 3H), 3.42 – 3.16 (m, 3H), 2.20 – 2.10 (m, 1H), 2.01 – 1.92 (m, 1H), 1.50 (s, 9H), 1.44 (s, 9H). – **$^{13}$C NMR** (75 MHz, $CDCl_3$) δ = 169.5, 155.3, 153.8, 144.5, 143.8, 143.7, 141.5, 141.4, 127.8, 127.6, 127.11, 127.06, 125.01, 124.98, 124.8, 120.1, 94.8, 81.3, 81.2, 66.8, 65.2, 56.5, 50.4, 47.2, 42.8, 28.4, 28.1, 26.2 (signal doubling due to rotamers). – **IR** (neat): $\tilde{\nu}$ ($cm^{-1}$) = 3313, 2978, 2937, 1703, 1524, 1449, 1394, 1367, 1297, 1244, 1151, 1080, 1032, 939, 838, 738. – **mp** = 90-91 °C. – $\boldsymbol{[\alpha]_D^{20}}$ = +5.0 (*c* 1, DCM). – **HPLC analysis** (Phenomenex Lux Cellulose-2, *n*-heptane/*i*PrOH 90:10, 1.0 mL/min, 215 nm): $t_r$ = **11.88 min**, 15.52 min, >99% *ee*. – **LRMS** (ESI): *m/z* = 519.2497 $[M+H\text{-}MeOH]^+$, 573.2581 $[M+Na]^+$, 1123.5270 $[2M+Na]^+$. – **HRMS** (ESI): *m/z* = 573.2581 $[M+Na]^+$; calc. for $[C_{31}H_{38}N_2NaO_7]^+$ = 573.2571.

**_tert_-Butyl-(3*R*,4*S*)-3-((((9H-fluoren-9-yl)methoxy)carbonyl)amino)-4-(2-(_tert_-butoxy)-2-oxoethyl)pyrrolidine-1-carboxylate (216)**

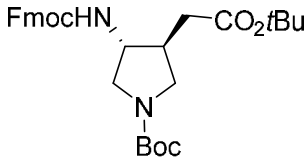


**215** (96 mg, 0.174 mmol, 1 equiv) was dissolved in DCM (4 mL anhydrous), $Et_3SiH$ (278 µL, 1.74 mmol, 10 equiv) was added and the flask was cooled down to -78 °C in an acetone/$CO_{2(s)}$ bath and stirred for 15 min. Then $BF_3{\cdot}OEt_2$ (44 µL, 0.348 mmol, 2 equiv) was added dropwise and the solution was stirred for 1 h at -78 °C and then for 23 h at 0 °C by the use of a cryostat. When all starting material was consumed the reaction was stopped by the addition of water (6 mL) and stirred for 10 min at ambient temperature. The phases were separated and the organic layer was dried over $MgSO_4$, filtered and concentrated under reduced pressure. After purification by column chromatography (PE/EA 5:1) the product was obtained as a colorless oil (28 mg, 0.053 mmol, 31%).

**$R_f$** = 0.55 (PE/EA 2:1). – **$^1$H NMR** (300 MHz, $CDCl_3$) δ = 7.81 – 7.73 (m, 2H), 7.63 – 7.52 (m, 2H), 7.45 – 7.37 (m, 2H), 7.35 – 7.27 (m, 2H), 5.31 – 5.21 + 5.00 – 4.89 (m, 1H), 4.48 – 4.35 (m, 2H), 4.26 – 4.15 (m, 1H), 3.95 – 3.77 (m, 2H), 3.74 – 3.61 (m, 1H), 3.11 – 2.89 (m, 2H), 2.52 – 2.20 (m, 3H), 1.45 (m, 18H). – **$^{13}$C NMR** (75 MHz, $CDCl_3$) δ = 171.5, 156.2, 154.3, 143.8, 143.7, 141.3, 127.8, 127.1, 125.0, 120.0, 81.4, 79.7, 66.8, 55.5, 53.5, 51.3, 49.0, 47.2, 39.2, 37.1 (signal doubling due to rotamers). – **IR** (neat): $\tilde{\nu}$ ($cm^{-1}$) = 3309, 2970, 2140, 1722, 1673, 1531, 1476, 1449, 1408, 1380, 1256, 1148, 1080, 1025, 943, 878, 842, 797, 738. – $[\alpha]_D^{20}$ = +20.4 (*c* 0.5, DCM). – **HPLC analysis** (Phenomenex Lux Cellulose-1, *n*-heptane/*i*PrOH 80:20, 1.0 mL/min, 215 nm): $t_r$ = **14.72 min**, 16.89 min, >99% *ee*. – **LRMS** (ESI): *m/z* = 424.2315 $[M+H-CO_2-C_4H_8]^+$, 467.2179 $[M+H-C_4H_8]^+$, 523.2803 $[M+H]^+$, 545.2620 $[M+Na]^+$, 1067.5364 $[2M+Na]^+$. – **HRMS** (ESI): *m/z* = 523.2803 $[M+H]^+$; calc. for $[C_{30}H_{39}N_2O_6]^+$ = 523.2803.

**2-((3*S*,4*R*)-4-((((9H-fluoren-9-yl)methoxy)carbonyl)amino)-1-(*tert*-butoxycarbonyl)pyrrolidin-3-yl)acetic acid (217)**

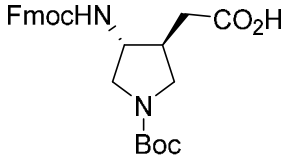


**215** (108 mg, 0.196 mmol, 1 equiv) was dissolved in DCM (4 mL anhydrous), $Et_3SiH$ (313 µL, 1.96 mmol, 10 equiv) was added and the solution was cooled down to -78 °C in an acetone/$CO_{2(s)}$ and stirred for 15 min. Then $BF_3{\cdot}OEt_2$ (49 µL, 0.392 mmol, 2 equiv) was added dropwise and the solution was stirred for 1 h at -78 °C and then for 21 h at 0 °C by the use of a cryostat. Then $Et_3SiH$ (157 µL, 0.981 mmol, 5 equiv) and $BF_3{\cdot}OEt_2$ (26 µL, 0.196 mmol, 1 equiv) was added again and stirred for additional 4 h. When all starting material was consumed, TFA (4 mL, excess) was added dropwise and stirred for 1 h at 0 °C. The mixture was allowed to warm up to ambient temperature and stirred for 24 h. The solvent was removed under reduced pressure and the resulting brown solid was dissolved in $CHCl_3$ and *n*-pentane alternately and concentrated under reduced pressure. This step was repeated five times and the resulting yellowish fluffy solid was dried under high vacuum for 24 h.

For Boc-protection the crude was dissolved in dioxane/water (1:1, 5 mL each), $NaHCO_3$ (82 mg, 0.980 mmol, 5 equiv) was added and the mixture was cooled down to 0 °C. $Boc_2O$ (128 mg, 0.588 mmol, 3 equiv) was added as a solution in dioxane (6 mL) via an additional

funnel. The mixture was stirred for 1 h at 0 °C and then for 24 h at ambient temperature. EA (5 mL) was added, the phases separated and the aqueous phase was extracted with EA (2x). The combined organic layers were washed with sat. $NaHCO_3$ solution (1x) and the combined aqueous phases were treated with 2M HCl to adjust pH 2-3. The aqueous phase was extracted with EA (3x) and the combined organic phases were dried over $MgSO_4$, filtered and concentrated under reduced pressure. The product was obtained after column chromatography (DCM/MeOH 19:1) as a white fluffy solid (47 mg, 0.099 mmol, 51% over 4 steps).

**$R_f$** = 0.41 (DCM/MeOH 9:1). – **$^1$H NMR** (400 MHz, $CD_3OD$) δ = 7.78 (d, *J* = 7.5 Hz, 2H), 7.64 (d, *J* = 7.4 Hz, 2H), 7.42 – 7.24 (m, 4H), 4.44 – 4.34 (m, 2H), 4.26 – 4.14 (m, 1H), 3.92 – 3.79 (m, 1H), 3.74 – 3.61 (m, 2H), 3.10 – 2.96 (m, 2H), 2.53 – 2.35 (m, 2H), 2.28 – 2.15 (m, 1H), 1.45 (s, 9H). – **$^{13}$C NMR** (75 MHz, $CD_3OD$) δ = 158.7, 156.3, 145.3, 142.7, 128.9, 128.2, 126.2, 121.0, 81.1, 67.8, 56.0, 55.3, 51.3, 50.8, 50.6, 42.2, 41.4, 39.3, 37.9, 28.8 (signal doubling due to rotamers). – **IR** (neat): ṽ ($cm^{-1}$) = 3280, 3067, 2974, 2359, 1669, 1558, 1476, 1420, 1367, 1240, 1189, 1140, 842, 801, 738. – **mp** = 159-162 °C. – $\mathbf{[\alpha]_D^{20}}$ = +8.7 (*c* 1, DCM). – **LRMS** (ESI): *m/z* = 367.1663 $[M+H-CO_2-C_4H_8]^+$, 411.1562 $[M+H-C_4H_8]^+$, 467.2186 $[M+H]^+$, 489.2007 $[M+Na]^+$, 955.4119 $[2M+Na]^+$. – **HRMS** (ESI): *m/z* = 467.2186 $[M+H]^+$; calc. for $[C_{26}H_{31}N_2O_6]^+$ = 467.2177.

**(±)-*tert*-Butyl-2-oxohexahydro-6H-furo[2,3-b]pyrrole-6-carboxylate (222)**

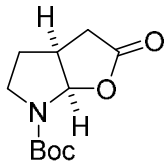


To a solution of (±)-**194** (99 mg, 0.349 mmol, 1 equiv) in DCM (2 mL) TFA (54 µL, 0.698 mmol, 2 equiv) was added dropwise and the mixture was stirred at ambient temperature for 48 h. The volatiles were evaporated and the crude was purified by column chromatography (PE/EA 1:1) to yield the product as a white solid (42 mg, 0.184 mmol, 53%).

**$R_f$** = 0.42 (PE/EA = 1:1). – **$^1$H NMR** (300 MHz, $CDCl_3$) δ = 6.10 – 5.90 (m, 1H), 3.56 – 3.39 (m, 2H), 3.10 – 2.94 (m, 1H), 2.74 (dd, *J* = 18.0, 8.9 Hz, 1H), 2.37 (d, *J* = 18.0 Hz, 1H), 2.27 – 2.09 (m, 1H), 1.76 – 1.60 (m, 1H), 1.39 (s, 9H). – **$^{13}$C NMR** (101 MHz, $CDCl_3$) δ = 175.3, 175.0, 153.6, 153.1, 92.4, 92.2, 81.3, 81.2, 45.9, 45.3, 38.7, 37.7, 35.1, 30.0, 29.2, 28.2 (signal doubling due to roatmers). – **IR** (neat): ṽ ($cm^{-1}$) = 2989, 2940, 2873, 1770, 1692, 1461, 1386,

1237, 1148, 1080, 1032, 931, 879, 779, 700, 674. – **mp** = 101-102 °C. – **LRMS** (ESI): *m/z* = 172.0605 $[M+H-C_4H_8]^+$, 228.1230 $[M+H]^+$, 250.1049 $[M+Na]^+$, 477.2209 $[2M+Na]^+$. – **HRMS** (ESI): *m/z* = 228.1230 $[M+H]^+$; calc. for $[C_{11}H_{18}NO_4]^+$ = 228.1230.

***tert*-Butyl (3a*S*,6a*R*)-2-oxohexahydro-6H-furo[2,3-b]pyrrole-6-carboxylate (222)**

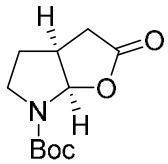

To a solution of **194** (113 mg, 0.398 mmol, 1 equiv) in DCM (2 mL) TFA (61 µL, 0.797 mmol, 2 equiv) was added dropwise and the solution was stirred at 0 °C for 7 d. After 2 and 6 d the same amount of TFA was added again. The volatiles were removed under reduced pressure and the crude was purified by column chromatography (PE/EA 1:1) to yield the product as a white solid (14 mg, 0.063 mmol, 16%).

Spectroscopic data were identical to those of its racemate (±)-**222**. – $[\alpha]_D^{20}$ = -75.9 (*c* 1, DCM). – **HPLC analysis** (Chiracel ASH, *n*-heptane/*i*PrOH 70:30, 0.5 mL/min, 215 nm): $t_r$ = 16.77 min, **20.60** min, 39% *ee*.

**2-((3*S*)-2-Allyl-1-(*tert*-butoxycarbonyl)pyrrolidin-3-yl)acetic acid (224)**

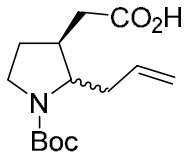

**194** (212 mg, 0.748 mmol, 1 equiv) and allyltrimethylsilane (1.19 mL, 7.48 mmol, 10 equiv) were dissolved in DCM (6 mL anhydrous) and cooled down to 0 °C by the use of a cryostat. Then $BF_3 \cdot OEt_2$ (95 µL, 0.748 mmol, 1 equiv) was added dropwise and the mixture was stirred for 6 d at 0 °C. After 3, 4, 5 d the same volume of $BF_3 \cdot OEt_2$ was added again. When all starting material was consumed, an excess of TFA (4 mL) was added and the mixture was stirred for 24 h at ambient temperature.

The volatiles were removed in vacuo and the crude was dissolved in 0.1 M HCl. The solution was loaded onto a column of DOWEX 50WX8-400 (2x2 cm, 2 times activated with 0.1 M HCl) and the resin was washed with distilled water (500 mL). The product was eluted with

16% $NH_3$ (aq) and the fractions were concentrated and lyophilized. The product (83 mg, 0.49 mmol, 66% over two steps) was obtained as a slight beige-colored amorphous solid and directly used in the next step.

The solid (83 mg, 0.49 mmol, 1 equiv) was dissolved in dioxane/water (1:1, 3 mL each), $NaHCO_3$ (82 mg, 0.981 mmol, 2 equiv) was added and the mixture was cooled down to 0 °C. A solution of $Boc_2O$ (161 mg, 0.735 mmol, 1.5 equiv) in dioxane (4 mL) was added dropwise and the mixture was stirred for 20 h at ambient temperature. Afterwards, EA (10 mL) was added, the phases separated and the aqueous phase was extracted with EA (2x). The combined organic layers were back extracted with sat. $NaHCO_3$ solution (1x) and the combined aqueous phases were acidified to a pH of 2-3 by the addition of 2M HCl. The aqueous phase was extracted with EA (3x) and the combined organic layers were dried over $MgSO_4$, filtered and the solvent was removed under reduced pressure. The crude was purified by column chromatography (DCM/MeOH 19:1) to obtain the product as a colorless oil (66 mg, 0.25 mmol, 50% over 3 steps, inseparable mixture of diastereomers, *dr* 1:1.2).

**$R_f$** = 0.22 (DCM/MeOH 19:1). – **$^1$H NMR** (300 MHz, $CDCl_3$) δ = 5.79 – 5.60 (m, 1H), 5.07 – 4.90 (m, 2H), 3.61 – 3.15 (m, 3H), 2.58 – 2.33 (m, 3H), 2.33 – 2.15 (m, 2H), 2.11 – 1.89 (m, 1H), 1.67 – 1.47 (m, 1H), 1.39 (s, 9H). – **$^{13}$C NMR** (75 MHz, $CDCl_3$) δ = 177.3, 154.7, 154.6, 135.4, 134.5, 134.4, 117.74, 117.65, 117.0, 116.8, 79.8, 79.5, 62.1, 61.9, 45.1, 44.7, 38.9, 38.4, 38.3, 38.0, 37.9, 37.5, 34.2, 28.9, 28.5 (signal doubling due to rotamers and diastereomers). – **IR** (neat): $\tilde{\nu}$ ($cm^{-1}$) = 3078, 2974, 2937, 1729, 1692, 1640, 1479, 1394, 1252, 1162, 1118, 995, 913, 875, 771. – $[\alpha]_D^{20}$ = +17.9 (*c* 1, DCM). – **LRMS** (ESI): *m/z* = 214.1072 $[M+H-C_4H_8]^+$, 270.1704 $[M+H]^+$, 292.1525 $[M+Na]^+$, 561.3140 $[2M+Na]^+$. – **HRMS** (ESI): *m/z* = 270.1702 $[M+H]^+$; calc. for $[C_{14}H_{24}NO_4]^+$ = 270.1700.

**(1*S*,5*S*,6*S*)-2-*tert*-Butyl 6-methyl 2-azabicyclo[3.1.0]hex-3-ene-2,6-dicarboxylate (201)**[196]

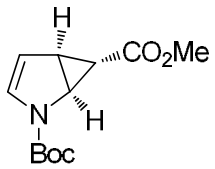


According to literature procedure[196] a freshly prepared solution of NaOMe in MeOH (250 µL anhydrous, 0.49 mmol, 1.2 equiv, 2 M) was added to a solution of **190** (117 mg, 0.42 mmol, 1 equiv) in MeOH (5 mL anhydrous) and the mixture was refluxed under $N_2$-atmosphere for 8

h. The mixture was allowed to cool down to ambient temperature, then sat. $NH_4Cl$ solution (5 mL) was added and the phases were separated. The aqueous phase was extracted with DCM (1x) and the combined organic layers were dried over $MgSO_4$, filtered and evaporated. After purification of the crude by column chromatography (PE/EA 9:1) the product was isolated as a white solid (67 mg, 0.28 mmol, 67%) as well as remaining starting material (22 mg, 0.08 mmol, 19%).

**$R_f$** = 0.33 (PE/EA = 9:1) – **$^1$H NMR** (300 MHz, $CDCl_3$) δ = 6.66 – 6.39 (m, 1H), 5.44 – 5.29 (m, 1H), 4.50 – 4.23 (m, 1H), 3.74 – 3.61 (m, 3H), 2.86 – 2.74 (m, 1H), 1.55 – 1.44 (m, 9H), 1.01 – 0.91 (m, 1H) – **$^{13}$C NMR** (75 MHz, $CDCl_3$) δ = 173.6, 173.3, 151.3, 151.0, 129.9, 129.7, 109.9, 81.7, 51.8, 44.3, 44.2, 32.3, 31.0, 28.2, 22.9, 22.8 (signal doubling due to rotamers) – **HPLC analysis** (Phenomenex Lux Cellulose-1, *n*-heptane/*i*PrOH 99:1, 1 mL/min, 240 nm): $t_r$ = **6.02 min**, 10.12 min; >99% *ee*.

**di-*tert*-Butyl-(*S*)-piperidine-1,3-dicarboxylate (200)**

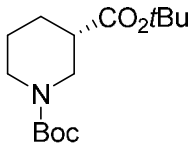


Compound **190** (1.00 g, 3.55 mmol) was dissolved in THF (15 mL anhydrous, 0.2 M) and Pd/C (100 mg, 10 wt% based on starting material, 10% Pd on charcoal, 2.6 mol%) was added. The flask was flushed ten times with hydrogen gas and the mixture was stirred for 3 h at ambient temperature. When all starting material was consumed the mixture was filtered over a plug of celite, washed with DCM and concentrated in vacuo. The crude product was purified by column chromatography (PE/EA 50:1) to obtain the product as a white solid (190 mg, 0.66 mmol, 19%).

**$R_f$** = 0.5 (PE/EA 5:1). – **$^1$H NMR** (300 MHz, $CDCl_3$) δ = 4.16 – 4.00 (m, 1H), 3.94 – 3.82 (m, 1H), 2.89 (dd, *J* = 13.0, 10.6 Hz, 1H), 2.82 – 2.70 (m, 1H), 2.37 – 2.25 (m, 1H), 2.03 – 1.92 (m, 1H), 1.71 – 1.46 (m, 3H), 1.44 (s, 9H), 1.42 (s, 9H). – **$^{13}$C NMR** (75 MHz, $CDCl_3$) δ = 172.8, 154.7, 80.6, 79.6, 45.8, 44.0, 42.3, 28.4, 28.0, 27.3, 24.3. – **IR** (neat): $\tilde{\nu}$ ($cm^{-1}$) = 2978, 2937, 2866, 1684, 1722, 1423, 1367, 1312, 1267, 1220, 1177, 1140, 1036, 1002, 925, 849, 767. – **mp** = 77-79 °C. – **$[\alpha]_D^{20}$** = +45.2 (*c* 1, DCM). – **HPLC analysis** (Phenomenex Lux Cellulose-2, *n*-heptane/*i*PrOH 99:1, 0.5 mL/min, 200 nm): $t_r$ = **15.96** min, 17.97 min, >99%

*ee*. – **LRMS** (ESI): *m/z* = 286.2017 $[M+H]^+$, 308.1836 $[M+Na]^+$, 593.3779 $[2M+Na]^+$. – **HRMS** (ESI): *m/z* = 282.2014 $[M+H]^+$; calc. for $[C_{15}H_{27}NO_4]^+$ = 286.2013.

**(*S*)-Piperidine-3-carboxylic acid (237)**[207]

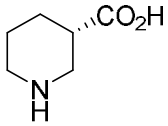

**200** (120 mg, 0.42 mmol) was dissolved in DCM (4 mL) and TFA (2 mL) was added. The mixture was stirred at ambient temperature for 24 h, then the volatiles were removed under reduced pressure. For removal of the counter ion the crude was dissolved in 0.1 M HCl. The solution was loaded onto a column of DOWEX 50WX8-400 (2x2 cm, 2 times activated with 0.1 M HCl) and the resin was washed with distilled water (250 mL). The product was eluted with 16% $NH_3$ (aq.) and the fractions were concentrated and lyophilized. The product **237** (42.6 mg, 0.32 mmol, 78%) was obtained as a white solid.

**$^1$H NMR** (400 MHz, $D_2O$) δ = 3.35 (dd, *J* = 12.6, 3.7 Hz, 1H), 3.29 – 3.21 (m, 1H), 3.16 – 3.00 (m, 2H), 2.66 – 2.57 (m, 1H), 2.07 – 1.98 (m, 1H), 1.96 – 1.84 (m, 1H), 1.81 – 1.64 (m, 2H). – **$^{13}$C NMR** (101 MHz, $D_2O$) δ = 180.2, 45.8, 44.0, 40.9, 25.7, 21.0. – $[\alpha]_D^{20}$ = +4.7 (*c* 1, $H_2O$, Lit[207].: 4.7 *c* 1, $H_2O$). – **LRMS** (ESI): *m/z* = 130.0865 $[M+H]^+$.

**(±)-*tert*-Butyl-6-(hydroxymethyl)-2-azabicyclo[3.1.0]hex-3-ene-2-carboxylate (248)**[225]

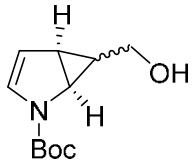

In a flame dried flask under $N_2$-atmosphere $LiAlH_4$ (162 mg, 4.27 mmol, 1.5 equiv) was suspended in THF (30 mL anhydrous) at 0 °C. **190** (800 mg, 2.84 mmol, 1 equiv) in THF (20 mL anhydrous) was added dropwise via an additional funnel and the reaction mixture was stirred at 0 °C for 1 h, then at ambient temperature for 20 h. The mixture was cooled down to 0 °C, EA (10 mL) was added and the reaction was quenched by the dropwise addition of sat. $NH_4Cl$ solution, till no gas evolution was observed anymore. The phases were separated and the aqueous phase was extracted with EA (3x). The combined organic layers were dried over $MgSO_4$, filtered and concentrated under reduced pressure. The crude was purified by column

chromatography (PE/EA 1:1) and the product was obtained as a colorless oil (308 mg, 1.46 mmol, 51%).

**$R_f$** = 0.26 (PE/EA 1:1). – **$^1$H NMR** (300 MHz, $CDCl_3$) δ = 6.40 – 6.19 (m, 1H), 5.29 – 5.17 + 5.11 – 4.99 (m, 1H), 3.79 – 3.25 (m, 4H), 2.18 – 2.01 (m, 1H), 1.42 (s, 9H), 0.60 – 0.49 (m, 1H). – **$^{13}$C NMR** (75 MHz, $CDCl_3$) δ = 152.4, 151.9, 129.6, 128.3, 128.0, 111.3, 106.1, 81.3, 80.9, 62.9, 55.3, 40.1, 40.0, 28.3, 25.2, 24.0, 23.8 (signal doubling due to diastereomers and rotamers).

**(±)-*tert*-Butyl-6-(hydroxymethyl)-2-azabicyclo[3.1.0]hexane-2-carboxylate (249)**

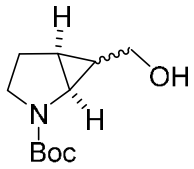


**249** was obtained as a by-product during the hydrogenation of **248**. The crude was purified by column chromatography (PE/EA 1:1) and the product was obtained as a colorless oil (72 mg, 0.37 mmol, 26%).

**$R_f$** = 0.16 (PE/EA 1:1). – **$^1$H NMR** (300 MHz, $CDCl_3$) δ = 3.67 – 3.55 (m, 1H), 3.52 – 3.30 (m, 2H), 3.30 – 3.19 (m, 1H), 3.06 – 2.91 (m, 1H), 2.78 (bs, 1H), 2.18 – 2.02 (m, 1H), 2.01 – 1.88 (m, 1H), 1.53 – 1.46 (m, 1H), 1.45 (s, 9H), 1.26 – 1.17 (m, 1H). – **$^{13}$C NMR** (101 MHz, $CDCl_3$) δ = 155.5, 79.8, 62.8, 45.3, 40.4, 28.6, 26.1, 21.5, 20.1. – **IR** (neat): $\tilde{\nu}$ ($cm^{-1}$) = 3377, 2974, 2933, 2877, 1669, 1390, 1363, 1252, 1170, 1121, 1032, 849, 801, 767. – **LRMS** (ESI): *m/z* = 140.0708 $[M+H-H_2O-C_4H_{10}O]^+$, 214.1439 $[M+H]^+$, 236.1259 $[M+Na]^+$, 427.2809 $[2M+Na]^+$. – **HRMS** (ESI): *m/z* = 214.1439 $[M+H]^+$; calc. for $[C_{11}H_{20}NO_3]^+$ = 214.1438.

**(±)-*tert*-Butyl 3-(hydroxymethyl)piperidine-1-carboxylate (250)**

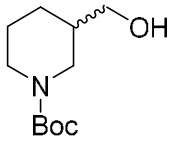


Compound **248** (270 mg, 1.28 mmol) was dissolved in MeOH (5 mL anhydrous, 0.2 M) and Pd/C (30 mg, 10 wt% based on starting material, 10% Pd on charcoal, 2.2 mol%) was added. The flask was flushed ten times with hydrogen gas and the mixture was stirred at ambient temperature for 15 h. When all starting material was consumed the mixture was filtered over a

plug of celite, washed with MeOH and concentrated in vacuo. The crude product was purified by column chromatography (PE/EA 1:1) to obtain the product as a colorless oil (84 mg, 0.39 mmol, 31%).

**$R_f$** = 0.26 (PE/EA 1:1). – **$^1$H NMR** (300 MHz, $(CD_3)_2CO$) δ = 4.11 – 4.00 (m, 1H), 3.93 – 3.82 (m, 1H), 3.72 – 3.60 (m, 1H), 3.53 – 3.28 (m, 3H), 2.85 – 2.48 (m, 1H), 1.82 – 1.70 (m, 1H), 1.67 – 1.51 (m, 3H), 1.42 (s, 9H), 1.24 – 1.10 (m, 1H). – **$^{13}$C NMR** (101 MHz, $(CD_3)_2CO$) δ = 154.3, 78.3, 64.2, 47.3, 46.9, 44.7, 44.0, 38.9, 27.7, 27.1, 24.5 (signal doubling due to rotamers). – **IR** (neat): $\tilde{\nu}$ ($cm^{-1}$) = 3440, 2974, 2929, 2862, 1682, 1669, 1420, 1372, 1263, 1174, 1148, 1077, 1036, 965, 857, 767. – **LRMS** (ESI): *m/z* = 142.0864 $[M+H-H_2O-C_4H_8]_+$, 160.0967 $[M+H-C_4H_8]^+$, 216.1595 $[M+H]^+$, 238.1416 $[M+Na]^+$, 453.2938 $[2M+Na]^+$. – **HRMS** (ESI): *m/z* = 216.1595 $[M+H]^+$; calc. for $[C_{11}H_{22}NO_3]^+$ = 216.1594.

**(±)-Piperidin-3-ylmethanol (251)**[247]

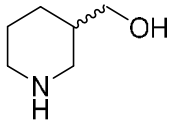


**250** (40 mg, 0.185 mmol) was dissolved in DCM (3 mL), TFA (1 mL) was added and the mixture was stirred at ambient temperature for 24 h. The volatiles were removed under reduced pressure and the resulting brown solid was dissolved in 0.1 M HCl. For removal of the counter ion the crude was loaded onto a column of DOWEX 50WX8-400 (2x2 cm, 2 times activated with 0.1 M HCl) and the resin was washed with distilled water (200 mL). The product was eluted with 16% $NH_3$ (aq.) and the fractions were concentrated and lyophilized. The product was obtained as a colorless liquid (volatile, 11 mg, 0.095 mmol, 51%).

**$^1$H NMR** (300 MHz, $D_2O$) δ = 3.42 – 3.26 (m 2H), 3.21 – 3.06 (m, 2H), 2.63 (td, *J* = 12.7, 3.2 Hz, 1H), 2.45 (t, *J* = 12.0 Hz, 1H), 1.80 – 1.62 (m, 3H), 1.57 – 1.38 (m, 1H), 1.16 – 0.98 (m, 1H).

**(±)-Ethyl-2-tosyl-2-azabicyclo[3.1.0]hexane-6-carboxylate (253)**

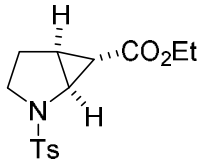


**252** (50 mg, 0.16 mmol) was dissolved in THF (2 mL anhydrous, 0.08 M), Pd/C (5 mg, 10 wt%, 10% Pd on charcoal, 0.029 mol%) was added. The flask was flushed ten times with hydrogen gas and the mixture was stirred at ambient temperature. After 3 h all starting material was consumed and the mixture was filtered over a plug of celite, washed with DCM and concentrated in vacuo. The pure product was obtained as a white solid (49 mg, 0.15 mmol, 97%).

**$R_f$** = 0.18 (PE/EA 5:1). – **$^1$H NMR** (300 MHz, $CDCl_3$) δ = 7.74 – 7.63 (m, 2H), 7.38 – 7.28 (m, 2H), 4.18 – 3.94 (m, 2H), 3.71 (dd, *J* = 6.3, 1.7 Hz, 1H), 3.55 – 3.44 (m, 1H), 2.45 (s, 3H), 2.39 – 2.27 (m, 1H), 2.25 – 2.08 (m, 2H), 1.96 – 1.85 (m, 1H), 1.23 (t, *J* = 7.1 Hz, 3H), 1.07 – 1.02 (m, 1H). – **$^{13}$C NMR** (75 MHz, $CDCl_3$) δ = 170.2, 144.2, 131.7, 129.7, 128.4, 60.6, 45.2, 44.5, 25.6, 24.5, 21.7, 20.7, 14.3. – **IR** (neat): ṽ ($cm^{-1}$) = 2989, 2881, 1714, 1595, 1446, 1414, 1326, 1285, 1237, 1185, 1148, 1088, 984, 924, 902, 849, 805, 749, 708, 663. – **mp** = 118-120 °C. – **LRMS** (ESI): *m/z* = 264.0691$[M+H-EtOH]^+$, 310.1126 $[M+H]^+$, 332.0929 $[M+Na]^+$, 641.1963 $[2M+Na]^+$. – **HRMS** (ESI): *m/z* = 310.1108 $[M+H]^+$; calc. for $[C_{15}H_{20}NO_4S]^+$ = 310.1108.

**(±)-*tert*-butyl-5-(hydroxymethyl)-1,3-dioxo-2-phenyl-1,2,3,3a,4,5,8,8a-octahydro-4,8-epiminocyclohepta[c]pyrrole-9-carboxylate (287)**

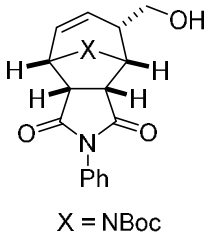


X = NBoc

In a flame dried Schlenk-flask **248** (38 mg, 0.179 mmol, 1 equiv) and *N*-phenylmaleimide (84 mg, 0.485 mmol, 2.7 equiv) in toluene (5 mL anhydrous) were stirred for 17 h at 100 °C. The solvent was removed under reduced pressure and the crude was purified by column

chromatography (PE/EA 2:1) to yield the product as a colorless viscous oil (29 mg, 0.075 mmol, 42%).

**$R_f$** = 0.33 (PE/EA 1:1). – **$^1$H NMR** (400 MHz, $CDCl_3$) δ = 7.50 – 7.35 (m, 3H), 7.19 – 7.13 (m, 2H), 6.06 (dd, *J* = 9.4, 4.8, 1H), 5.73 (ddd, *J* = 9.7, 3.9, 1.1, 1H), 4.94 – 4.85 (m, 2H), 3.87 (t, *J* = 8.9, 1H), 3.75 (dd, *J* = 9.4, 7.0, 1H), 3.69 (dd, *J* = 11.5, 5.1, 1H), 3.55 – 3.43 (m, 1H), 2.79 – 2.70 (m, 1H), 1.51 – 1.44 (m, 9H). – **$^{13}$C NMR** (101 MHz, $CDCl_3$) δ = 174.8, 173.9, 153.0, 131.6, 129.3, 129.00, 126.5, 81.4, 63.4, 54.3, 53.5, 48.9, 41.8, 28.5, 28.3. – **IR** (neat): $\tilde{\nu}$ ($cm^{-1}$) = 3466, 2974, 2933, 1703, 1498, 1423, 1367, 1326, 1244, 1155, 1103, 1054, 1006, 939, 909, 872, 730, 693. – **LRMS** (ESI): *m/z* = 329.1132 $[M+H-C_4H_8]^+$, 407.1573 $[M+Na]^+$, 791.3267 $[2M+Na]^+$. – **HRMS** (ESI): *m/z* = 385.1765 $[M+H]^+$; calc. for $[C_{21}H_{25}N_2O_5]^+$ = 385.1758.

**(±)-8-(*tert*-butyl) 6,7-diethyl-4-(hydroxymethyl)-8-azabicyclo[3.2.1]octa-2,6-diene-6,7,8-tricarboxylate (288)**

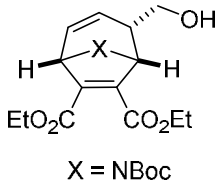


In a flame dried Schlenk-flask **248** (85 mg, 0.402 mmol, 1 equiv) and diethyl acetylendicarboxylate (173 µL mg, 1.09 mmol, 2.7 equiv) in toluene (4 mL anhydrous) were stirred for 14 h at 100 °C. The solvent was removed under reduced pressure and the crude was purified by column chromatography (PE/EA 2:1) to yield the product as a colorless viscous oil (91 mg, 0.238 mmol, 59%).

**$R_f$** = 0.32 (PE/EA 1:1). – **$^1$H NMR** (400 MHz, $CDCl_3$) δ = 6.27 (dd, *J*=8.7, 4.7, 1H), 5.40 (ddd, *J*=9.6, 3.3, 1.7, 1H), 5.07 – 5.03 (m, 1H), 4.89 – 4.76 (m, 1H), 4.20 (qd, *J*=7.1, 2.6, 5H), 3.74 (dd, *J*=11.3, 5.3, 1H), 3.64 – 3.53 (m, *J*=15.4, 1H), 2.42 – 2.35 (m, 1H), 1.40 (s, 11H), 1.25 (td, *J*=7.1, 2.1, 8H). – **$^{13}$C NMR** (101 MHz, $CDCl_3$) δ = 163.0, 162.5, 152.3, 131.5, 131.1, 127.6, 127.4, 81.0, 63.7, 61.6, 61.5, 60.5, 58.4, 40.5, 28.3, 14.4. – **IR** (neat): $\tilde{\nu}$ ($cm^{-1}$) = 3440, 2981, 2937, 2128, 1699, 1416, 1367, 1304, 1256, 1166, 1110, 1077, 1028, 868, 764, 723. – **LRMS** (ESI): *m/z* = 282.1340 $[M+H-C_5H_8O_2]^+$, 404.1686 $[M+Na]^+$, 785.3482 $[2M+Na]^+$. – **HRMS** (ESI): *m/z* = 382.1860 $[M+H]^+$; calc. for $[C_{19}H_{28}NO_7]^+$ = 382.1860.

# F. Appendix

### 1. NMR Spectra

$^{1}$H NMR spectra: upper image

$^{13}$C NMR spectra (DEPT135 integrated): lower image

Solvent and frequency are stated each spectrum.

**di-*tert*-Butyl (3*R*,4*R*)-4-(benzyl((*S*)-1-phenylethyl)amino)pyrrolidine-1,3-dicarboxylate (78)** (300 MHz, $CDCl_3$)

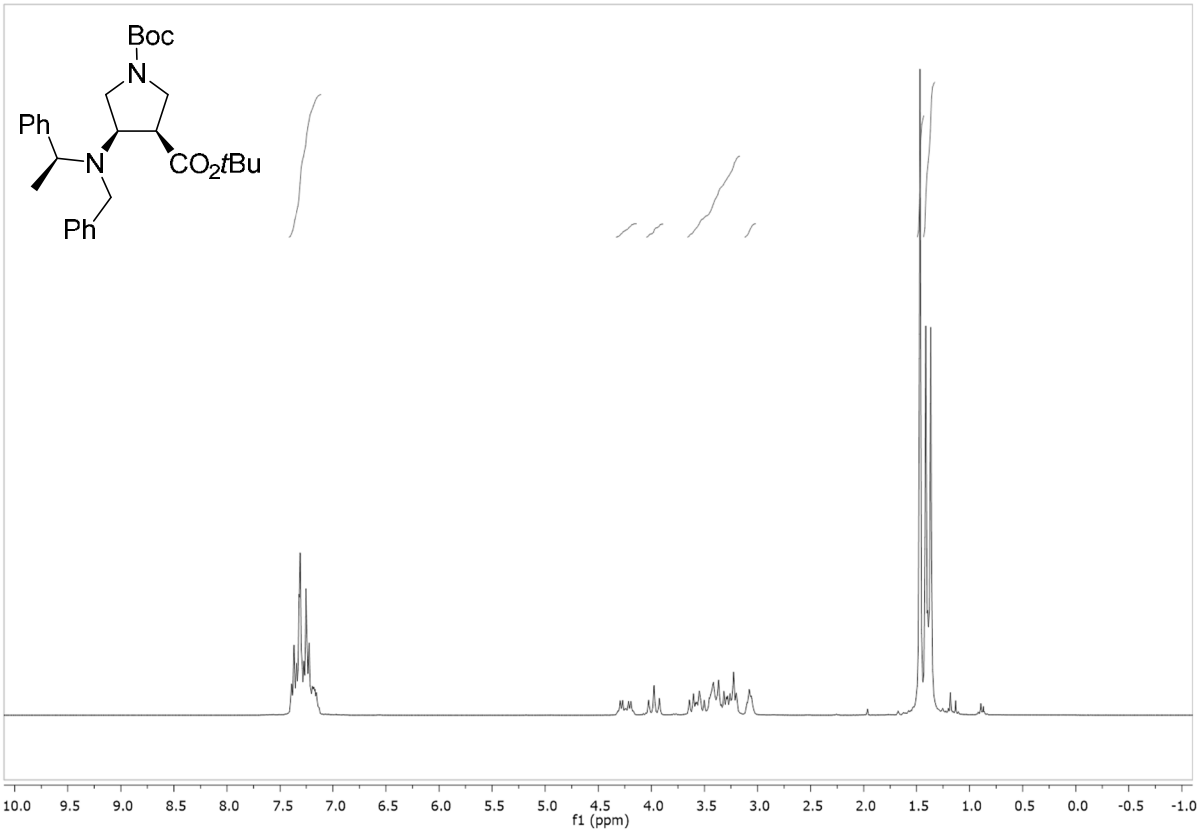


(101 MHz, $CDCl_3$)

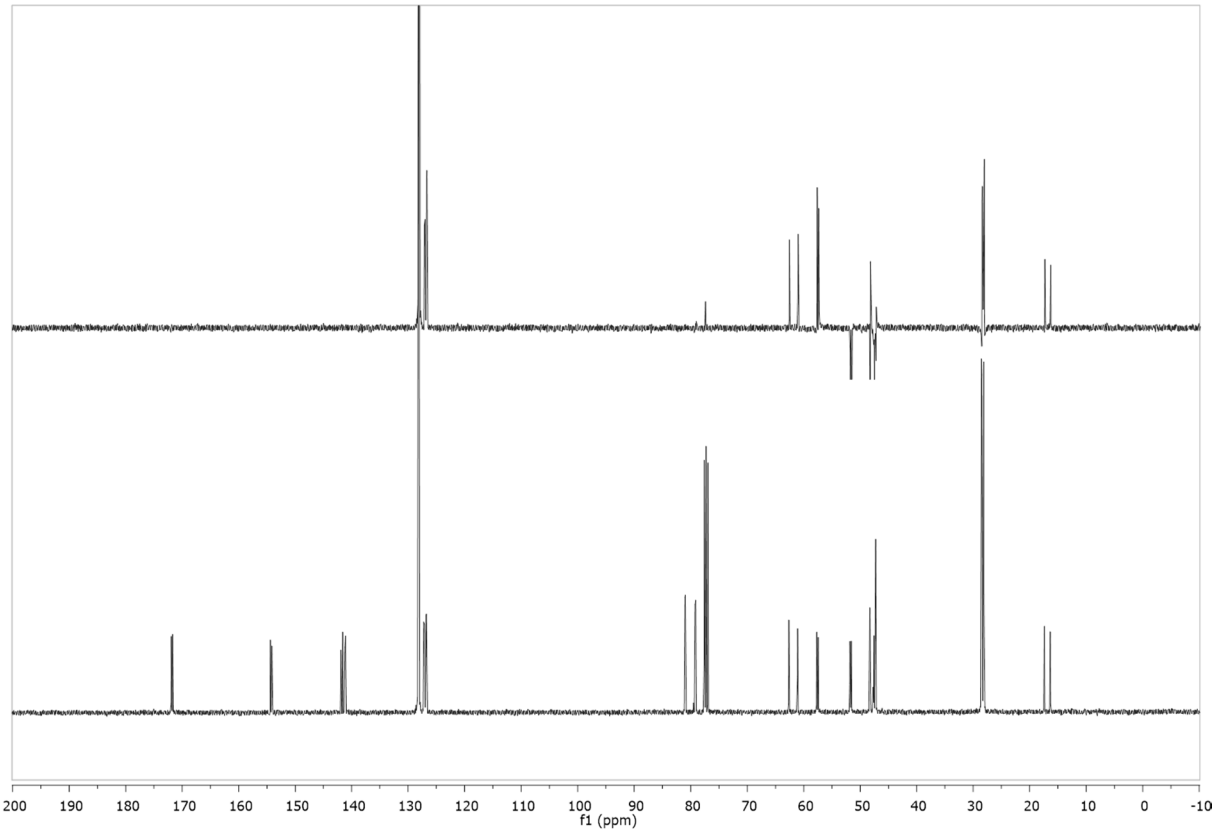

**di-*tert*-Butyl (3*R*,4*R*)-4-((((9H-fluoren-9-yl)methoxy)carbonyl)amino)pyrrolidine-1,3-dicarboxylate (85)** (300 MHz, $CDCl_3$)

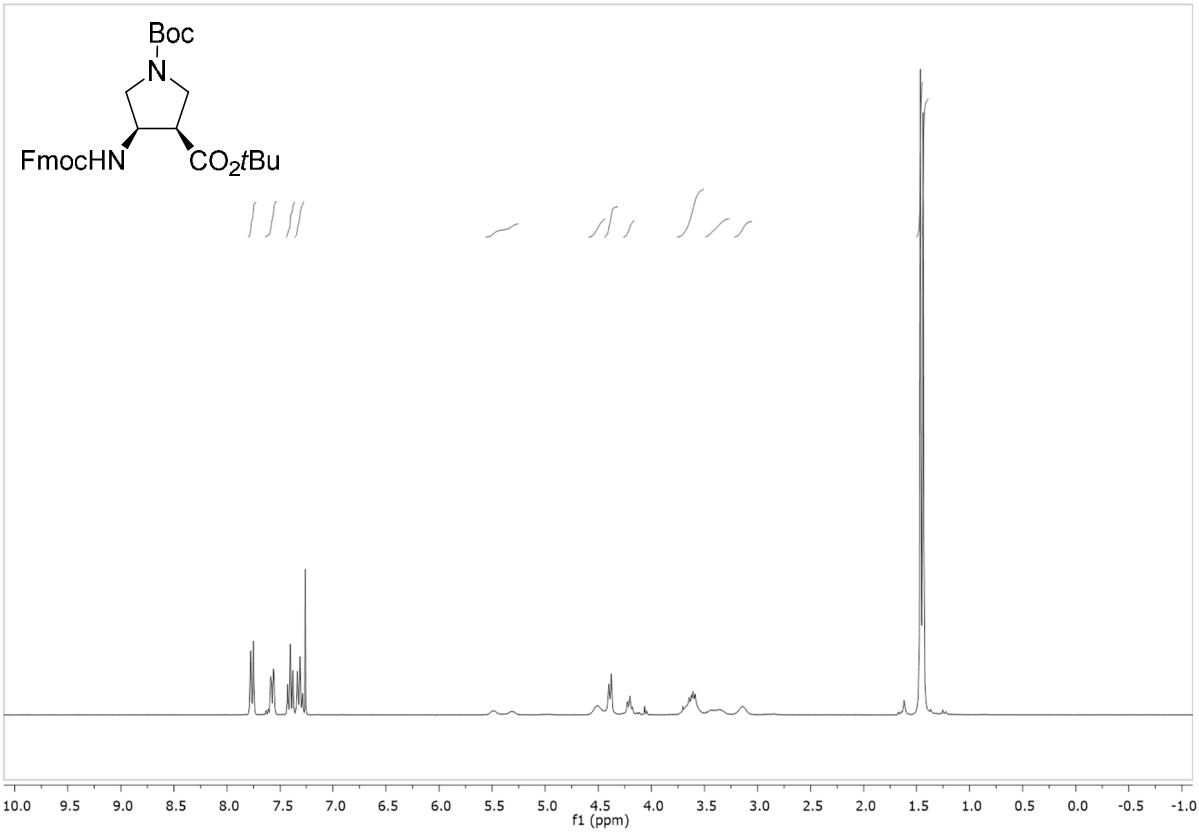


(75 MHz, $CDCl_3$)

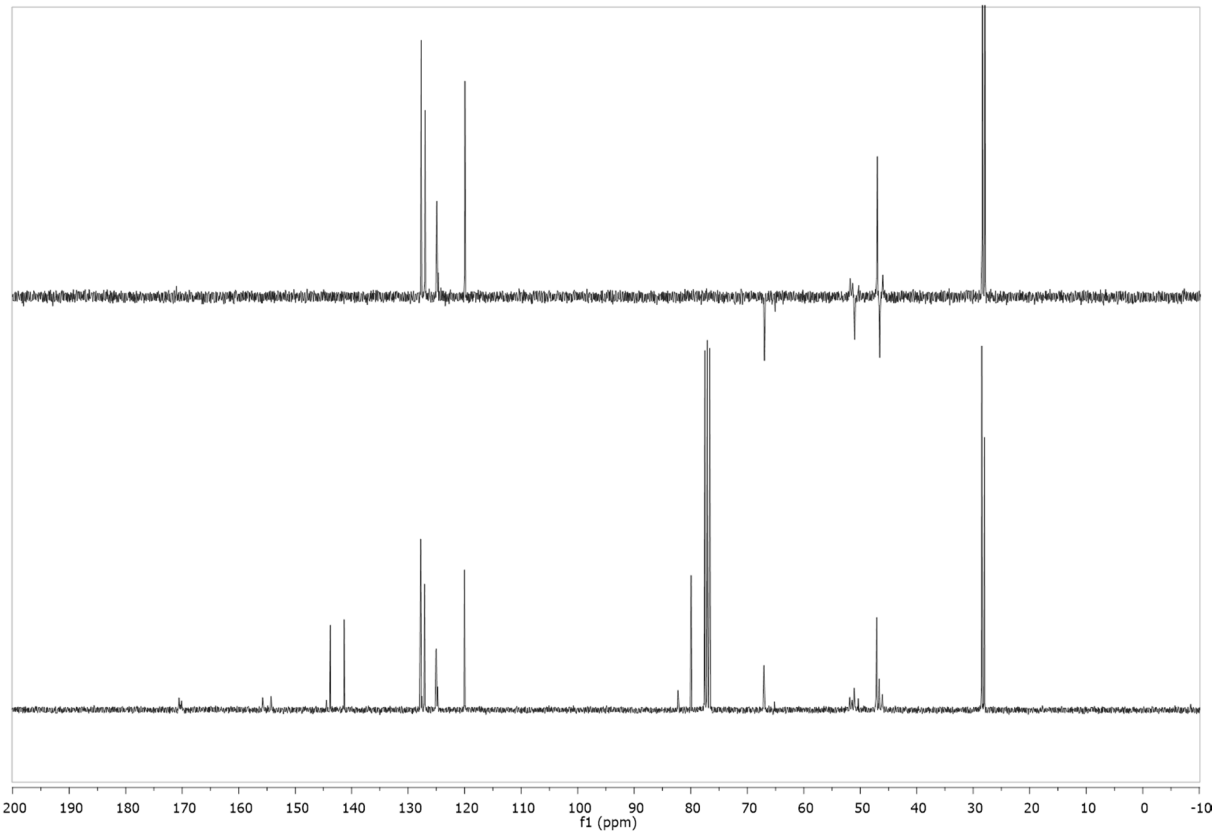

**(3*R*,4*R*)-4-((((9H-fluoren-9-yl)methoxy)carbonyl)amino)-1-(*tert*-butoxycarbonyl)pyrrolidine-3-carboxylic acid (79)** (400 MHz, $CDCl_3$)

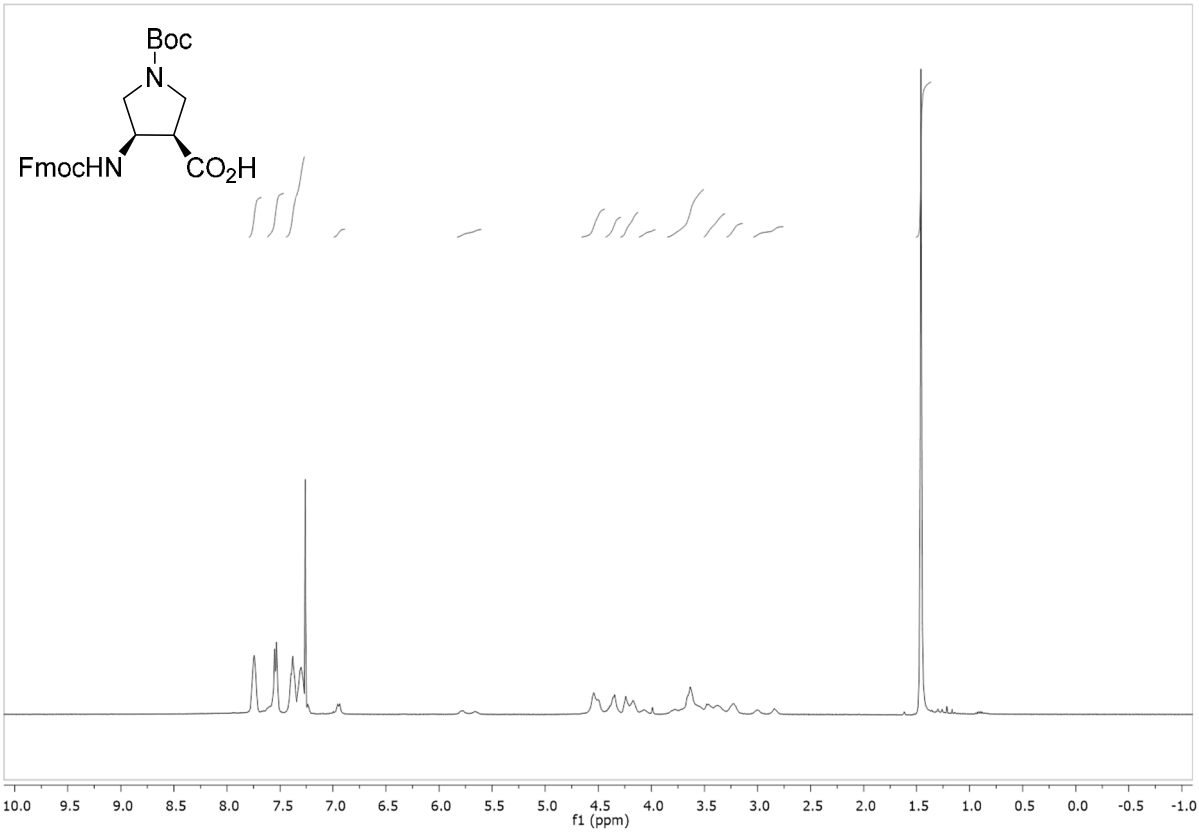


(101 MHz, $CDCl_3$)

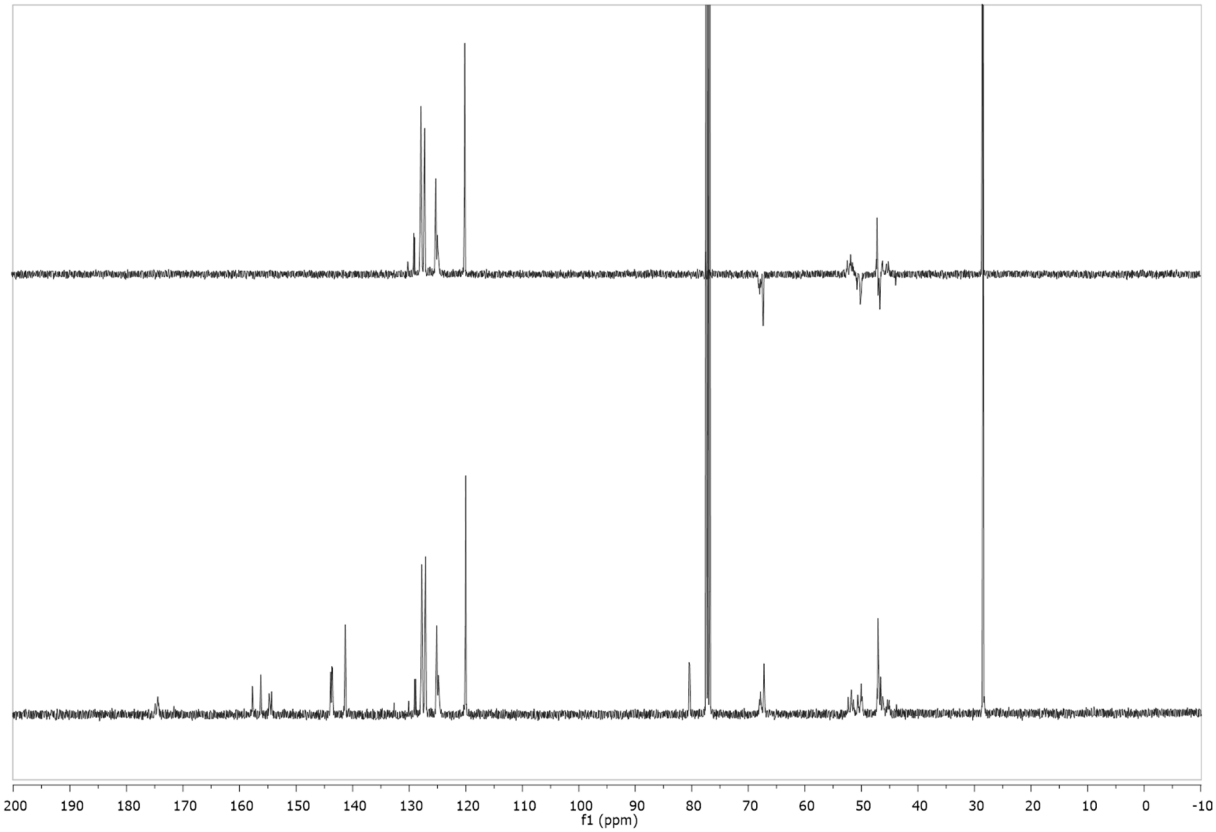

***tert*-Butyl (1*R*,2*S*)-2-(benzyl((*S*)-1-phenylethyl)amino)cyclopentane-1-carboxylate (21)** (300 MHz, $CDCl_3$)

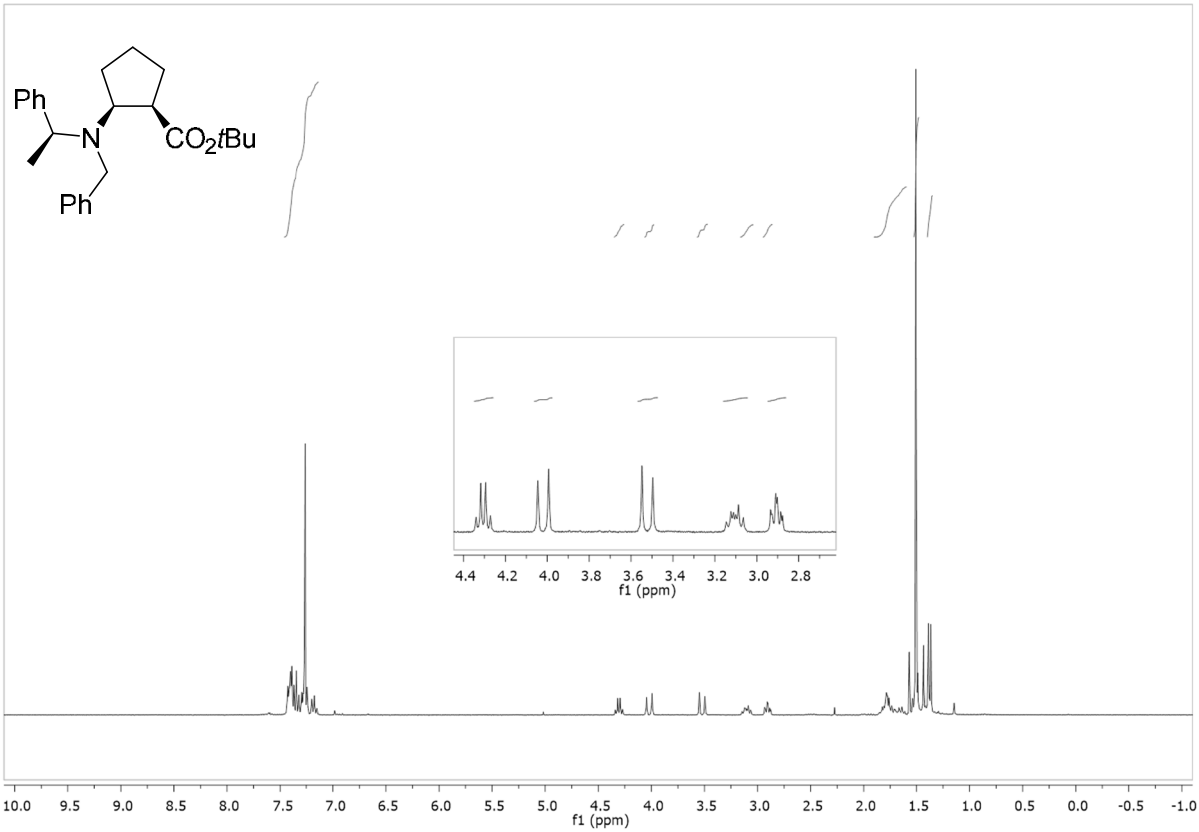


(75 MHz, $CDCl_3$)

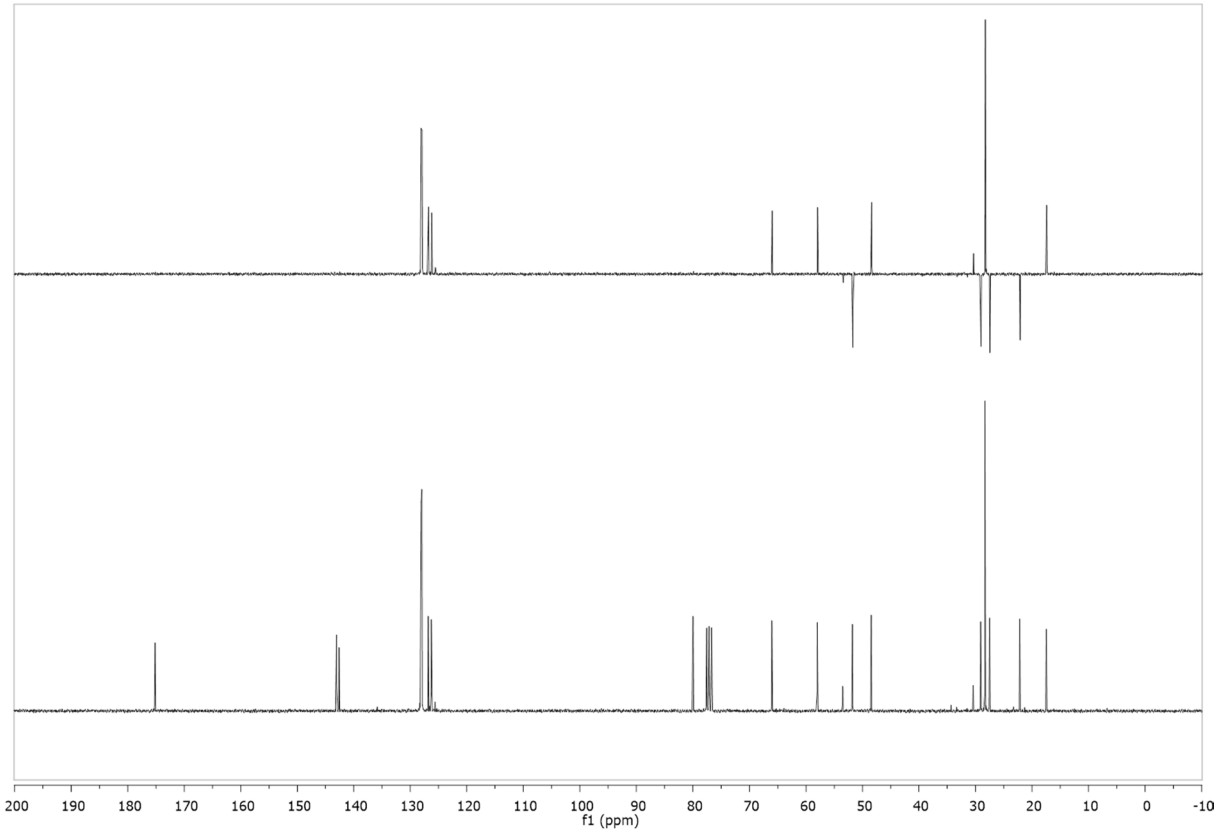

**(1*R*,2*S*)-2-((((9H-fluoren-9-yl)methoxy)carbonyl)amino)cyclopentane-1-carboxylic acid (80)** (300 MHz, $CDCl_3$)

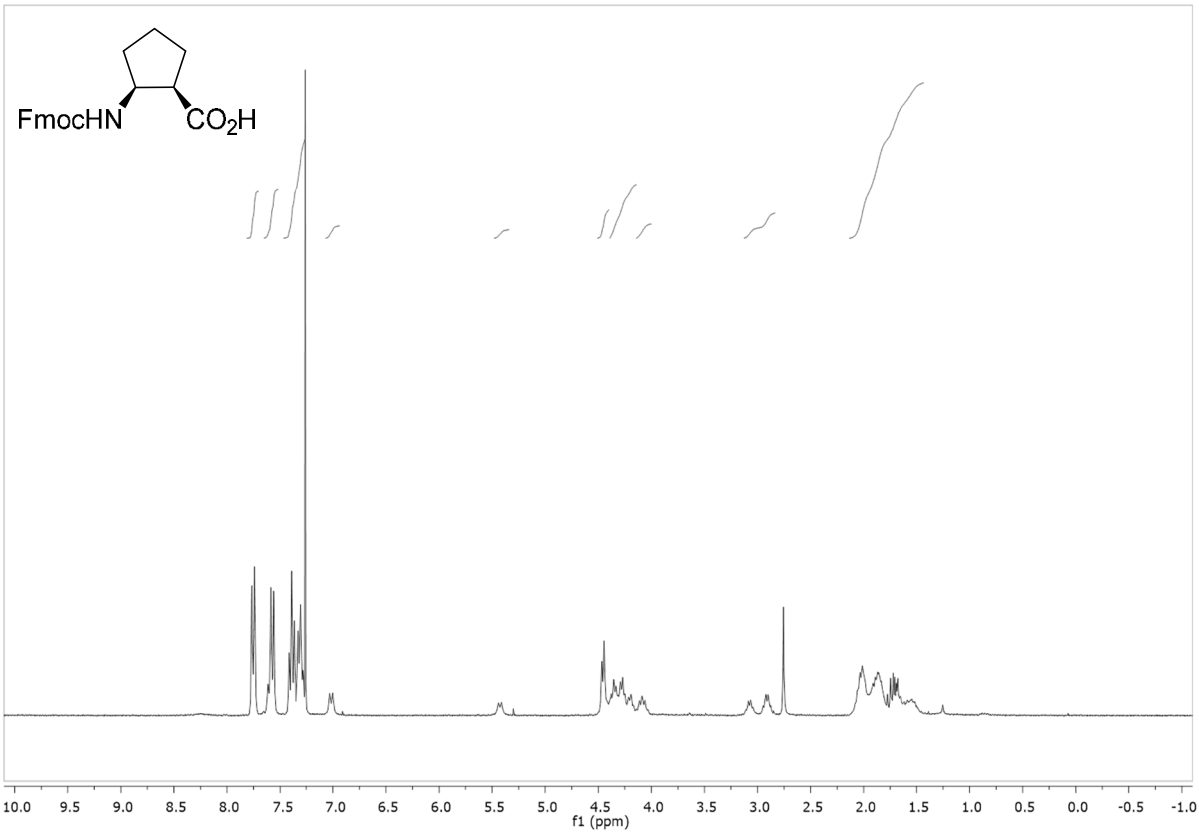


(101 MHz, $CDCl_3$)

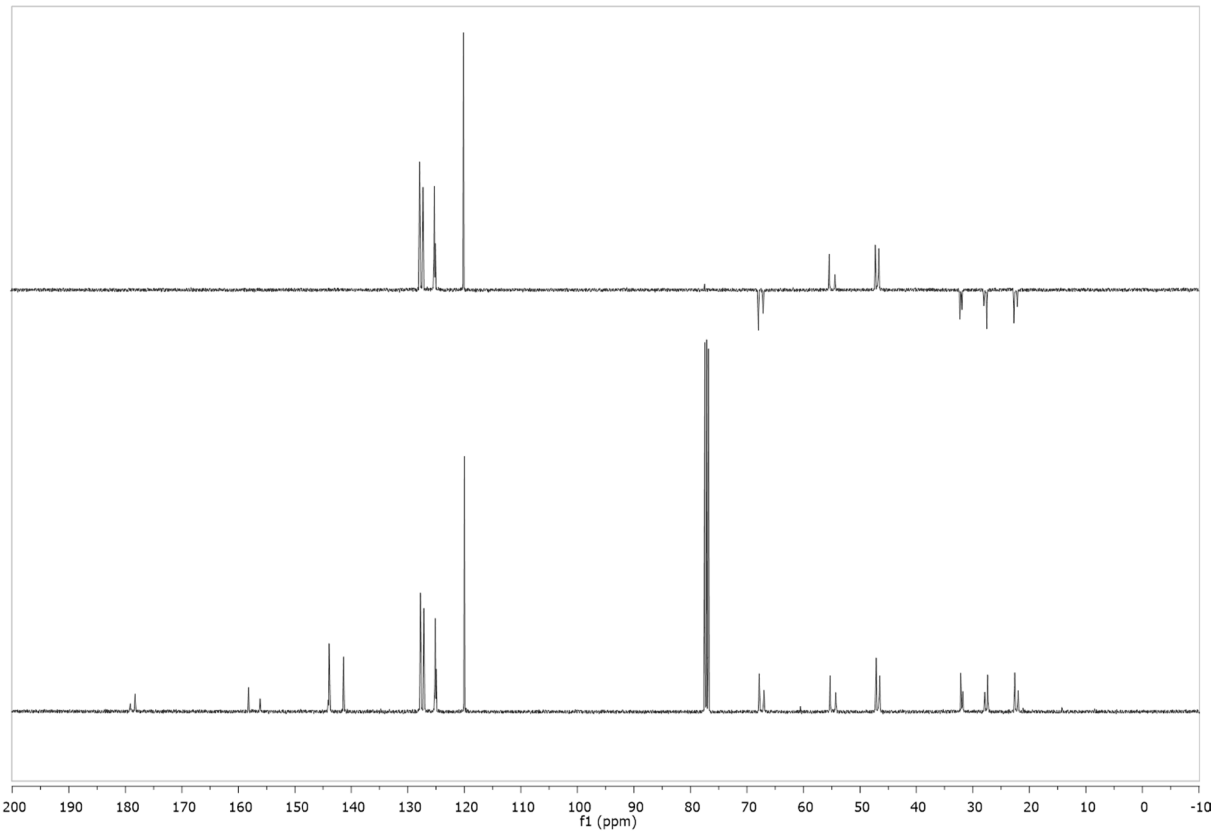

**(3*S*,4*S*)-4-(Benzyl((*R*)-1-phenylethyl)amino)pyrrolidine-3-carboxylic acid ((*ent*)-100)**
(400 MHz, $CDCl_3$)

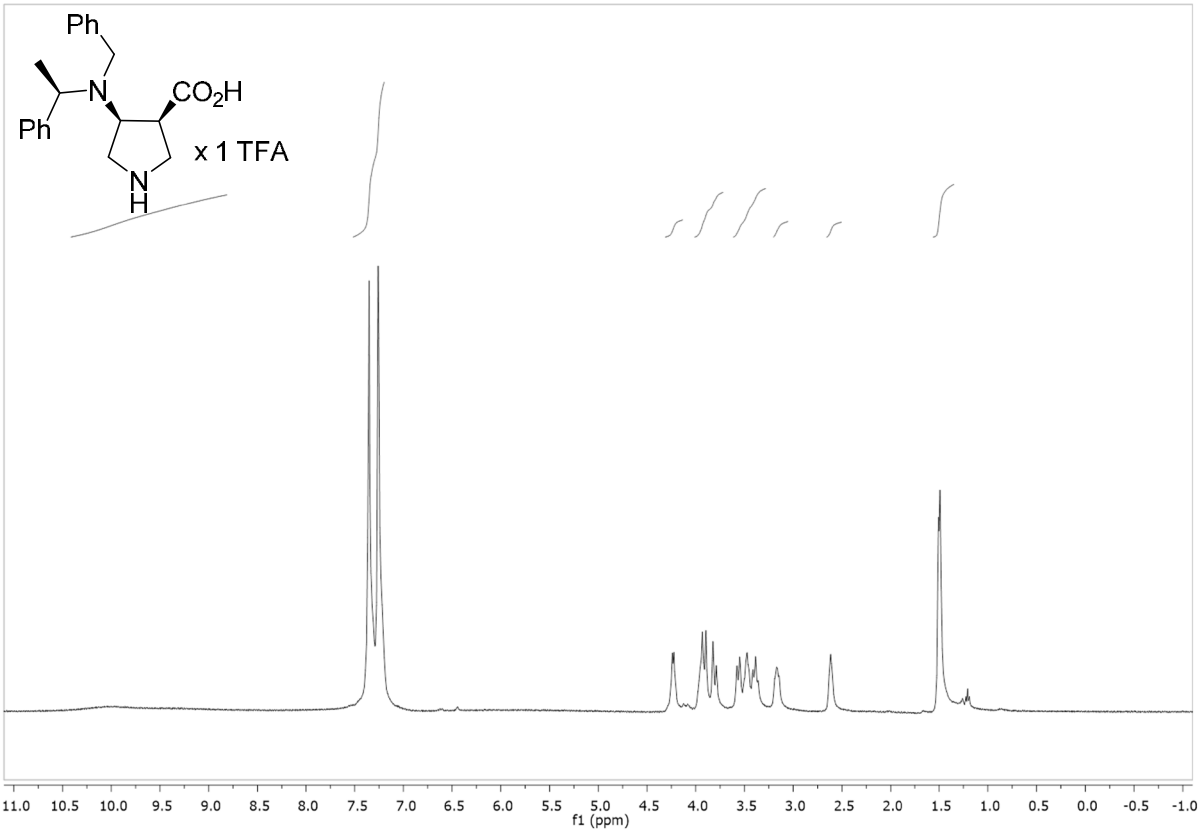


(101 MHz, $CDCl_3$)

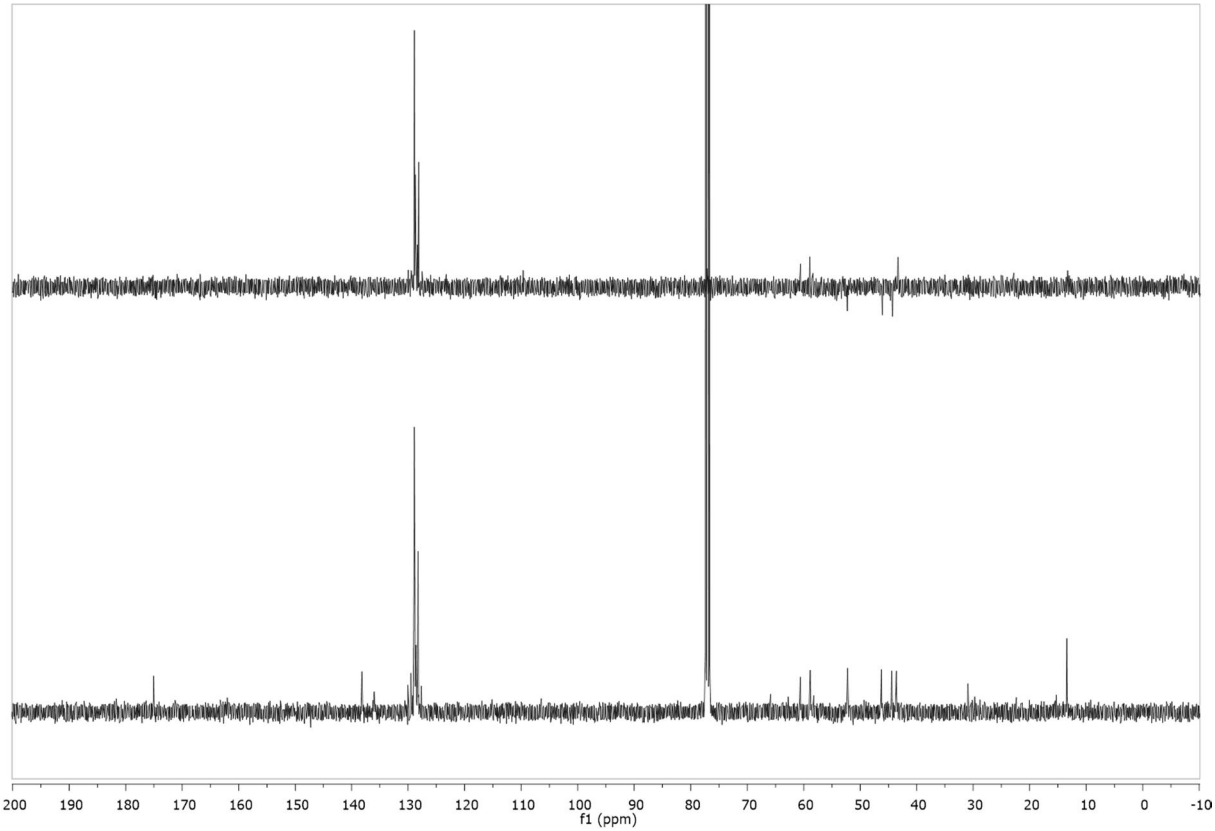

***tert*-Butyl (3*R*,4*R*)-3-((((9H-fluoren-9-yl)methoxy)carbonyl)amino)-4-((*S*)-2-((benzyloxy)carbonyl)pyrrolidine-1-carbonyl)pyrrolidine-1-carboxylate (121)** (300 MHz, $CDCl_3$)

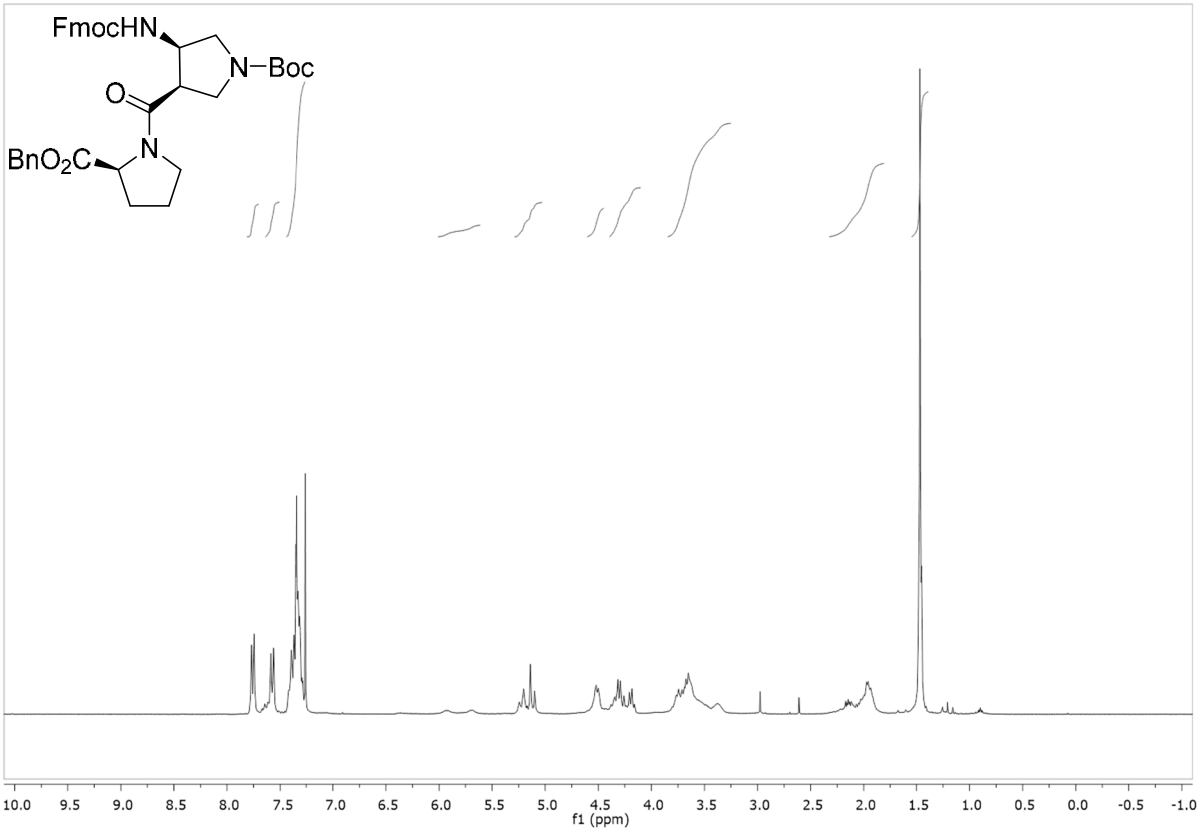


(101 MHz, $CDCl_3$)

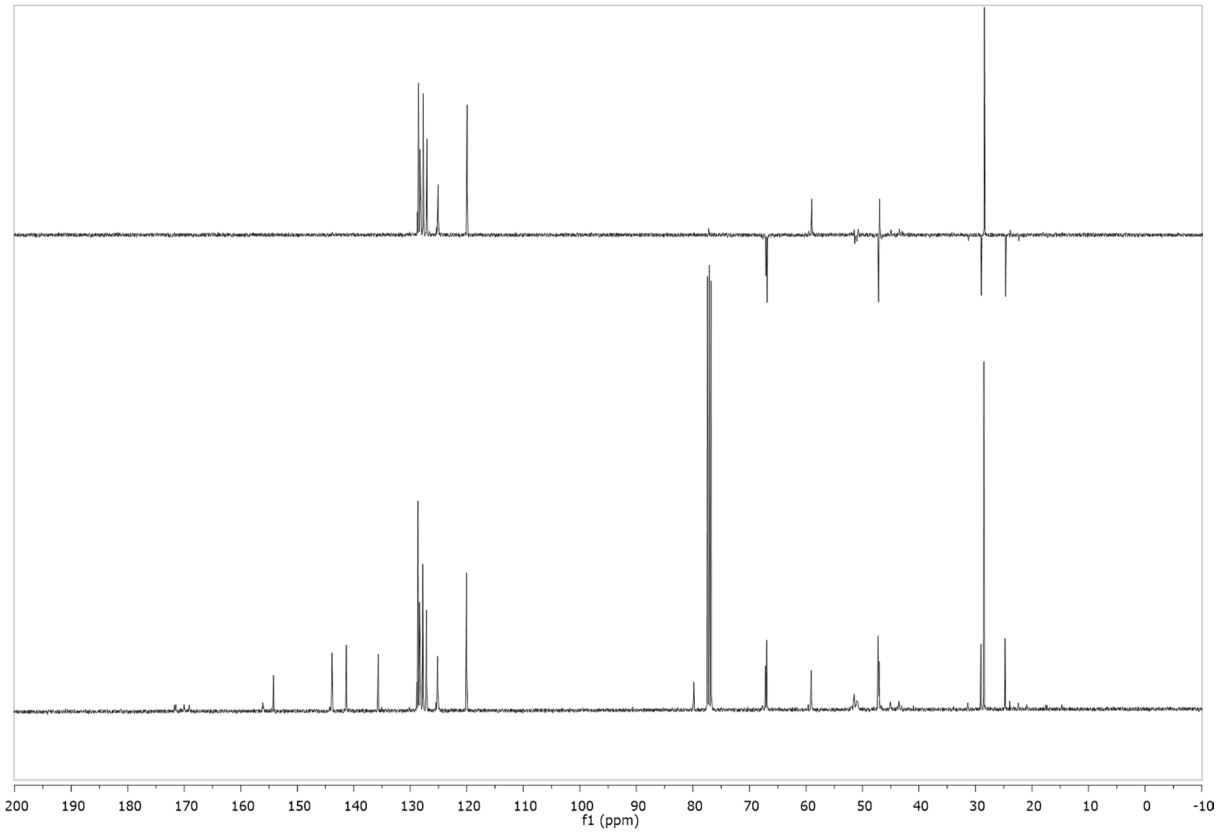

***tert*-Butyl-(3*R*,4*R*)-3-((*S*)-2-((benzyloxy)carbonyl)pyrrolidine-1-carbonyl)-4-((*S*)-1-((benzyloxy)carbonyl)pyrrolidine-2-carboxamido)pyrrolidine-1-carboxylate (122)**
(300 MHz, $CDCl_3$)

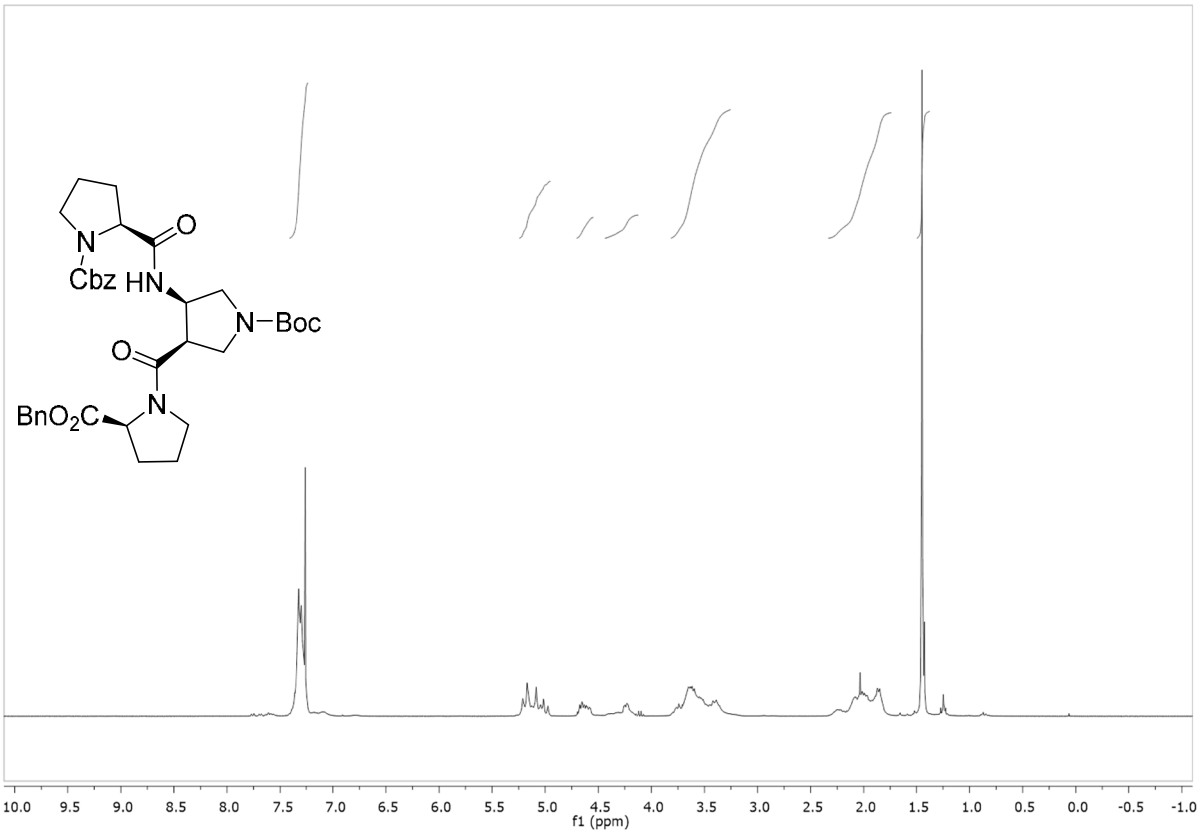


(101 MHz, $CDCl_3$)

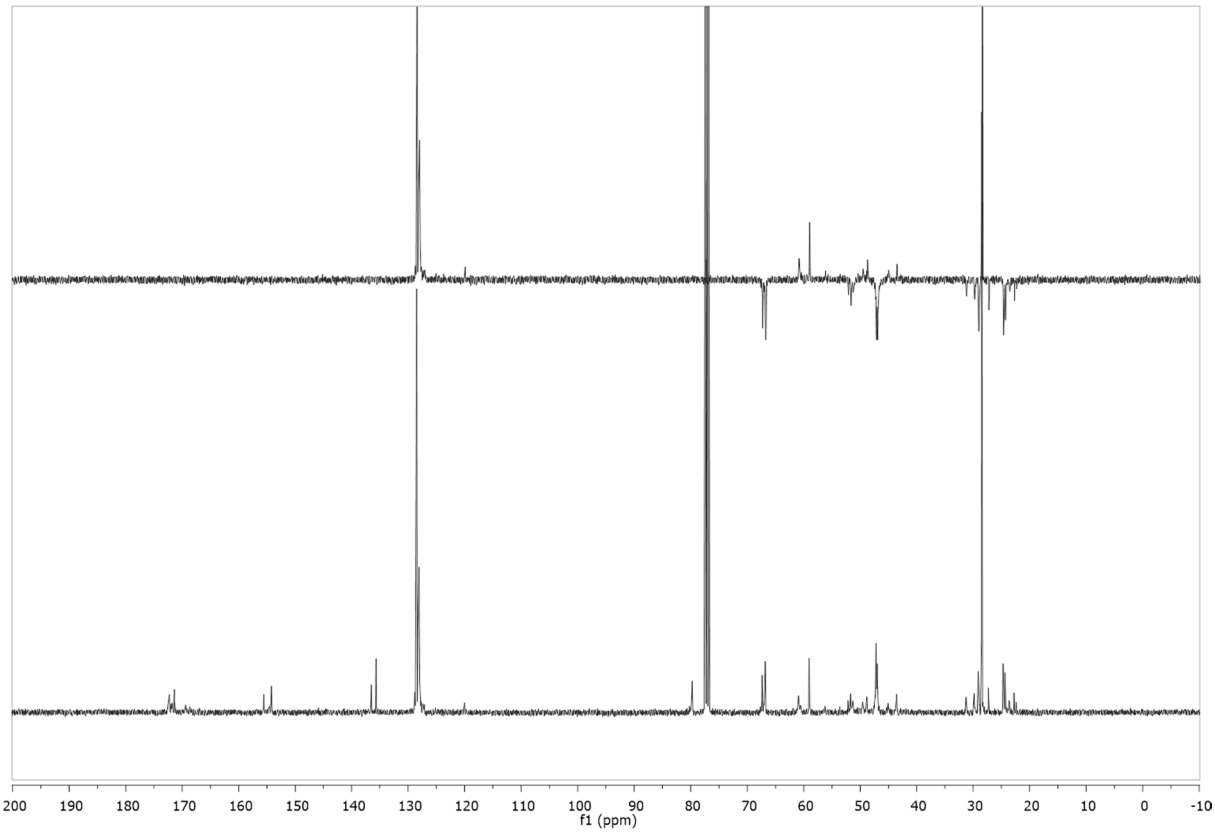

**((3*R*,4*R*)-1-(*tert*-Butoxycarbonyl)-4-((*S*)-pyrrolidine-2-carboxamido)pyrrolidine-3-carbonyl)-*L*-proline (118)** (300 MHz, $CD_3OD$)

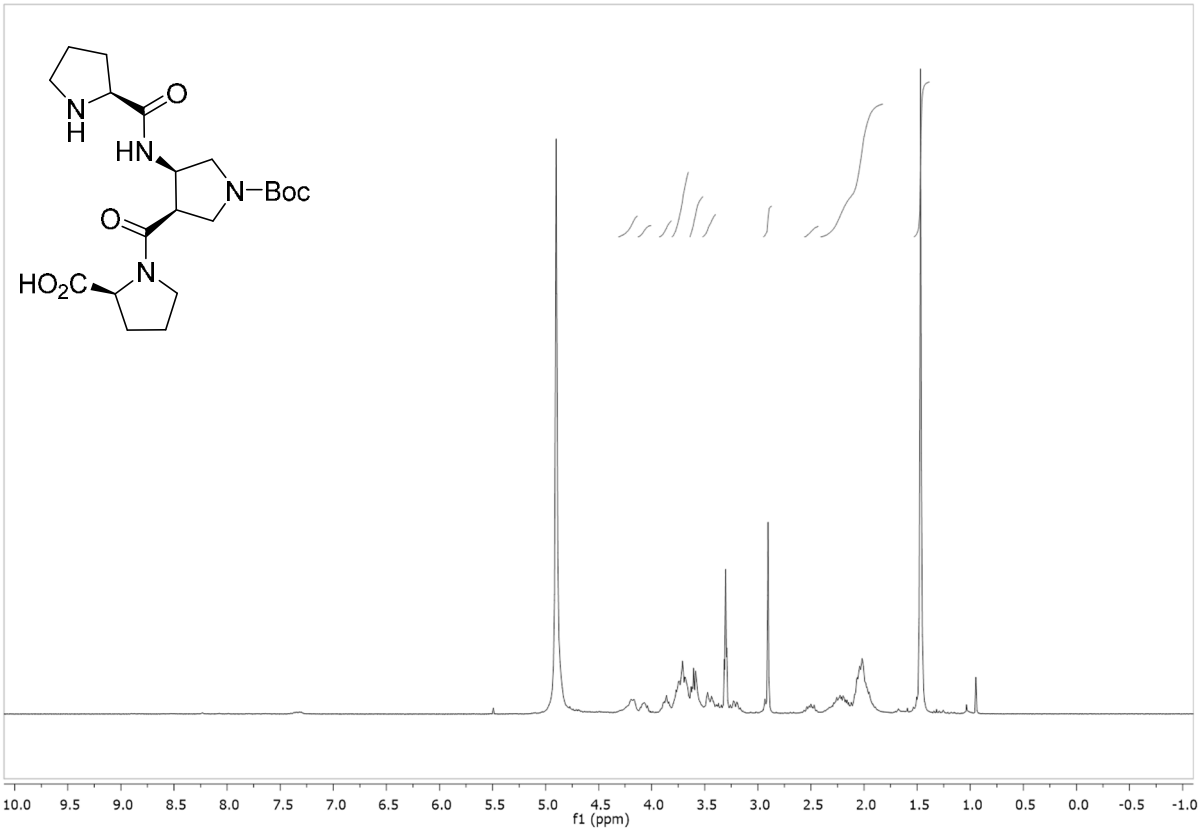


(75 MHz, $CD_3OD$)

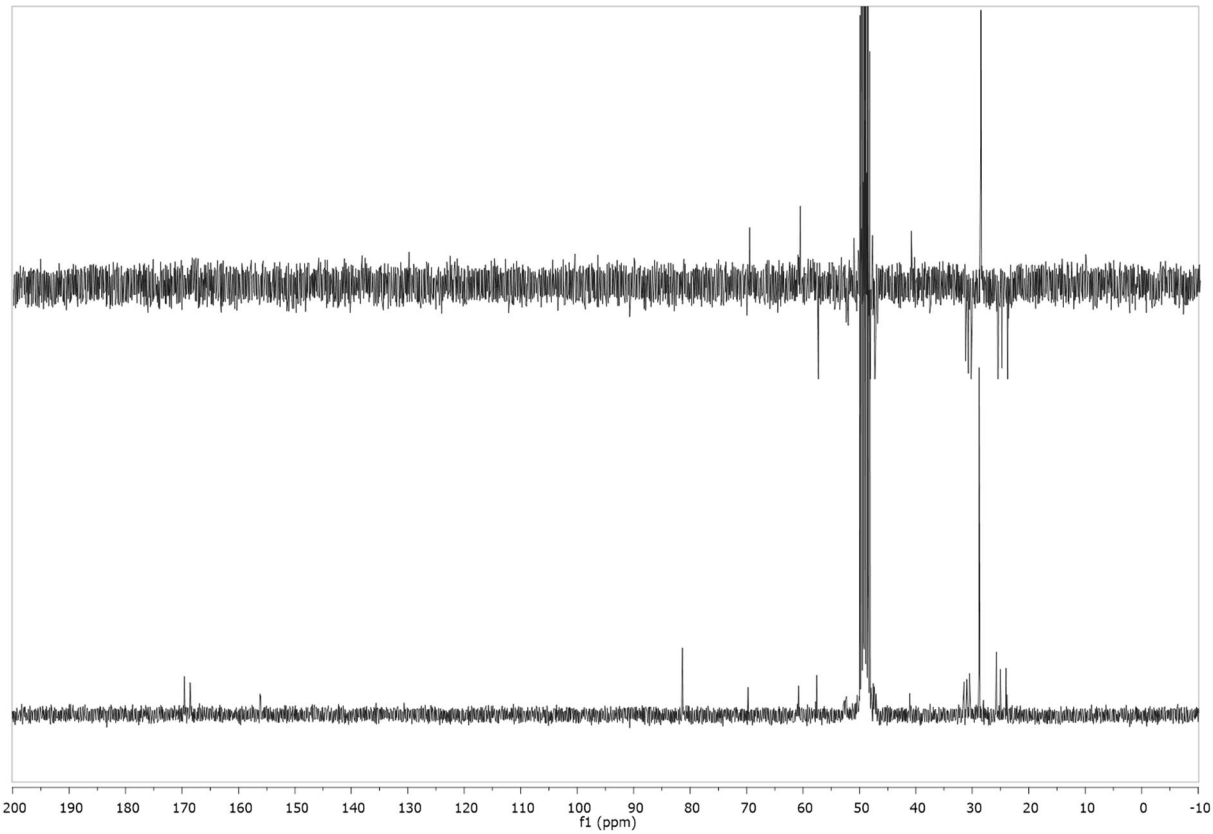

***tert*-Butyl (3*S*,4*S*)-3-((((9H-fluoren-9-yl)methoxy)carbonyl)amino)-4-((*S*)-2-((benzyloxy)carbonyl)pyrrolidine-1-carbonyl)pyrrolidine-1-carboxylate (125)** (300 MHz, $CDCl_3$)

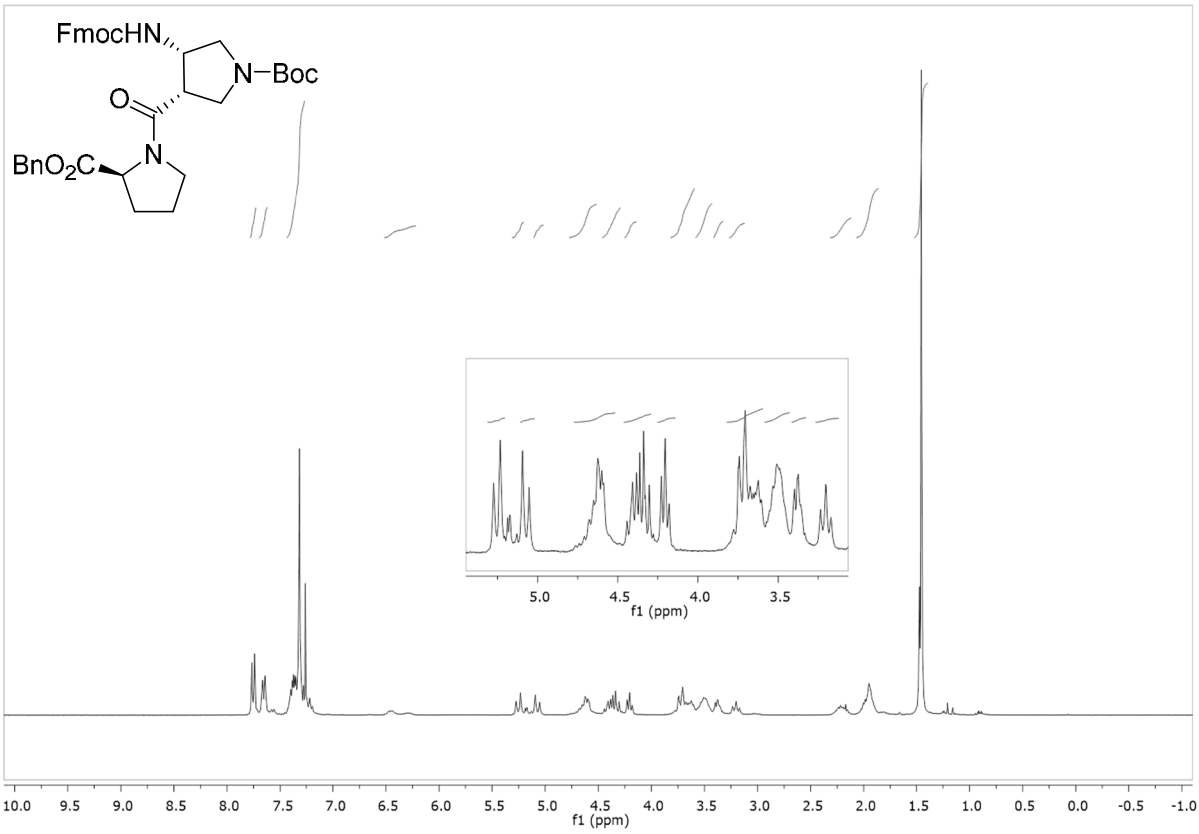


(101 MHz, $CDCl_3$)

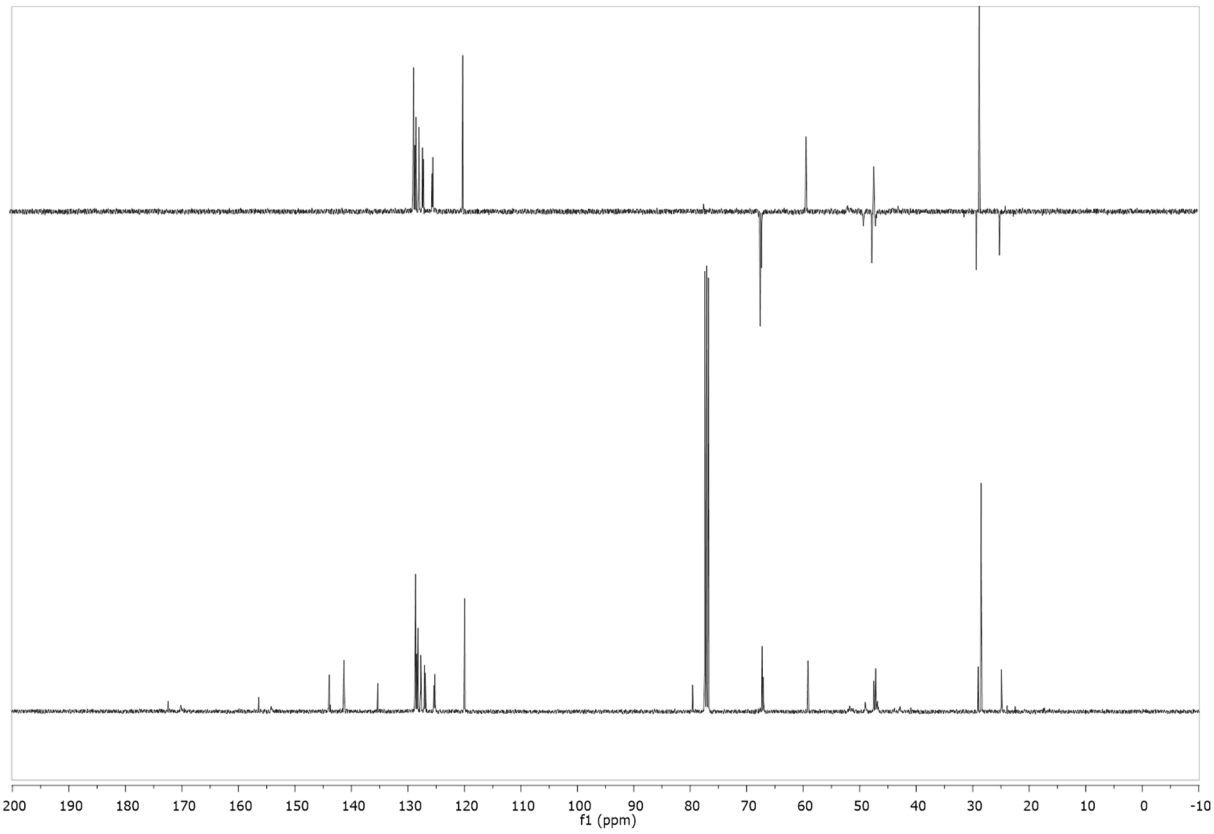

***tert*-Butyl (3*S*,4*S*)-3-((*S*)-2-((benzyloxy)carbonyl)pyrrolidine-1-carbonyl)-4-((*S*)-1-((benzyloxy)carbonyl)pyrrolidine-2-carboxamido)pyrrolidine-1-carboxylate (126)**

(400 MHz, $CDCl_3$)

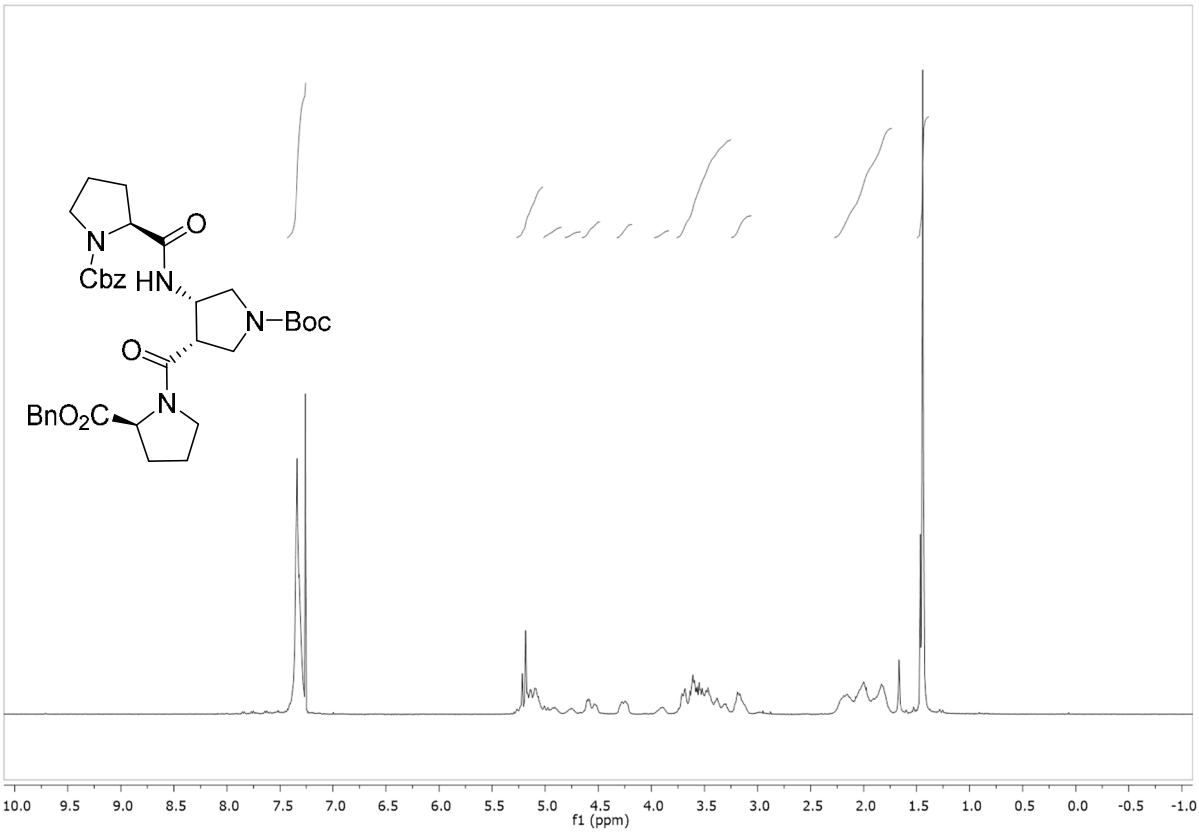


(101 MHz, $CDCl_3$)

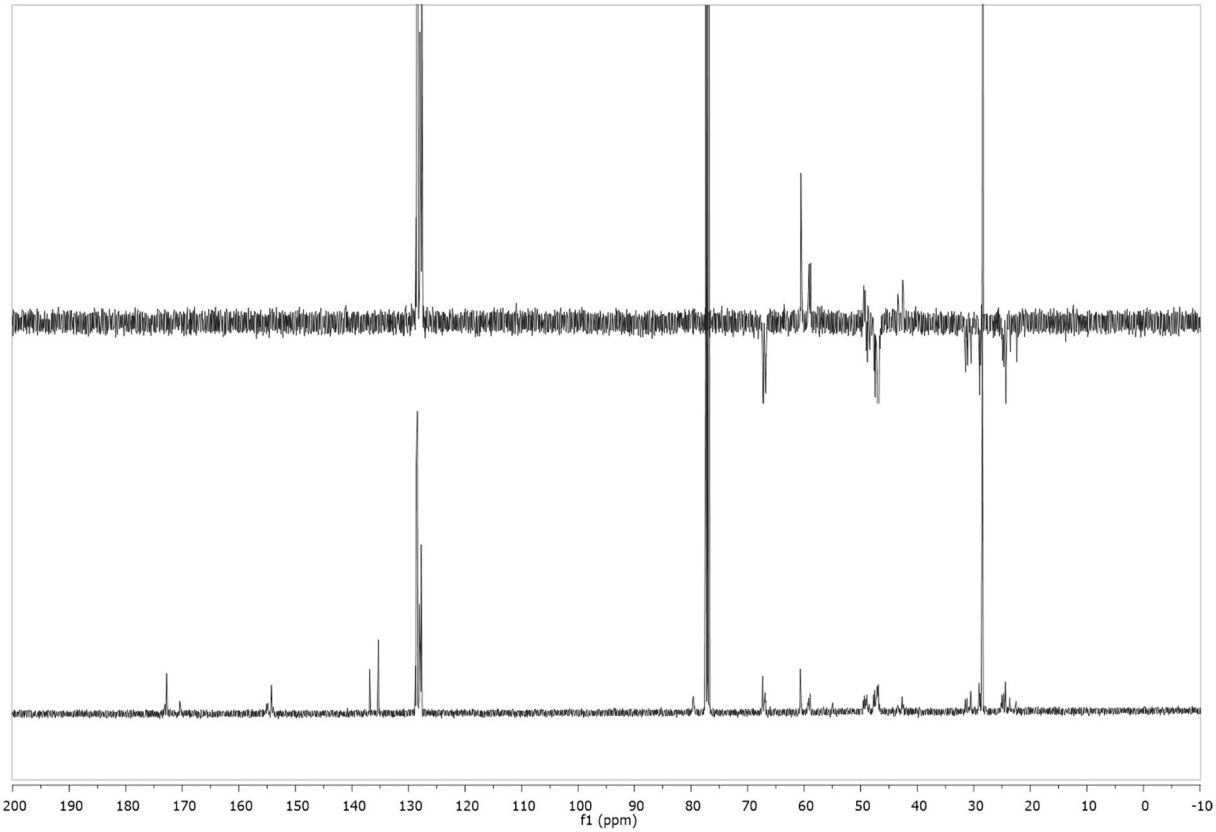

**((3*S*,4*S*)-1-(*tert*-Butoxycarbonyl)-4-((*S*)-pyrrolidine-2-carboxamido)pyrrolidine-3-carbonyl)-*L*-proline (127)** (400 MHz, $(CD_3)_2SO$)

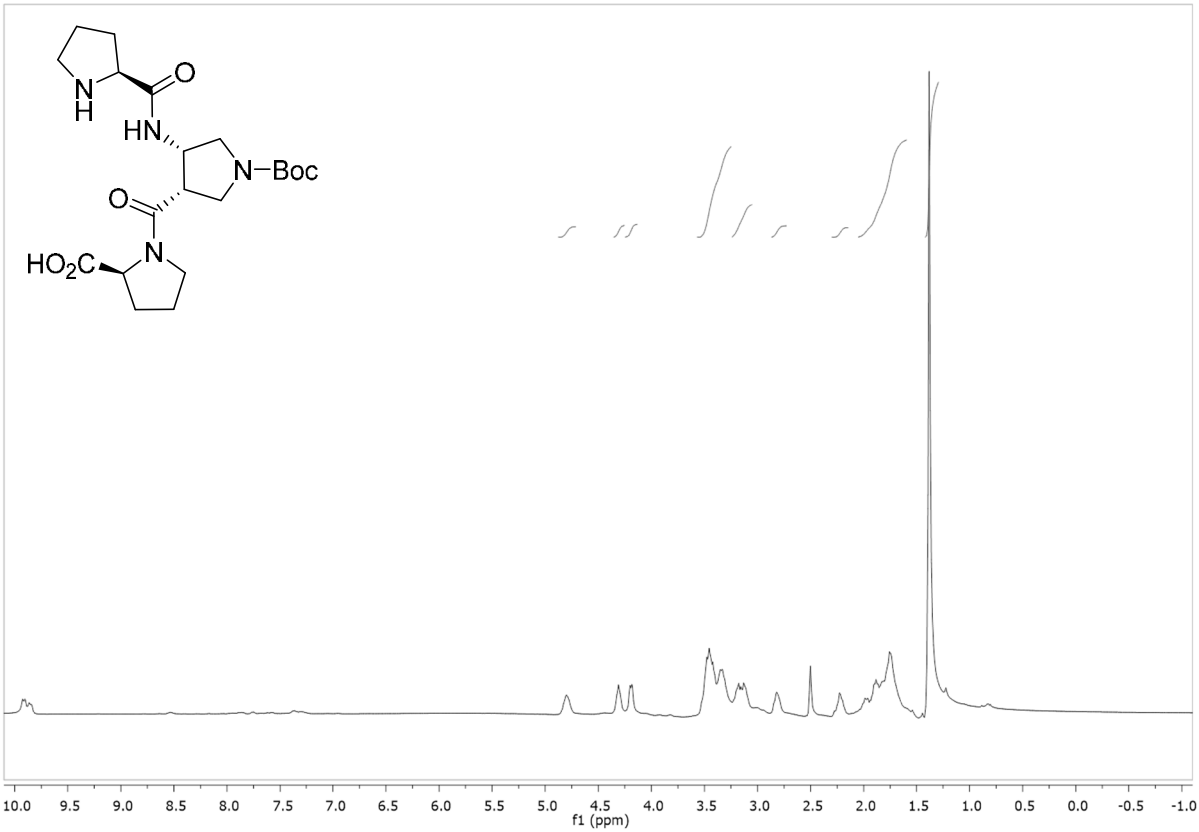


(101 MHz, $(CD_3)_2SO$)

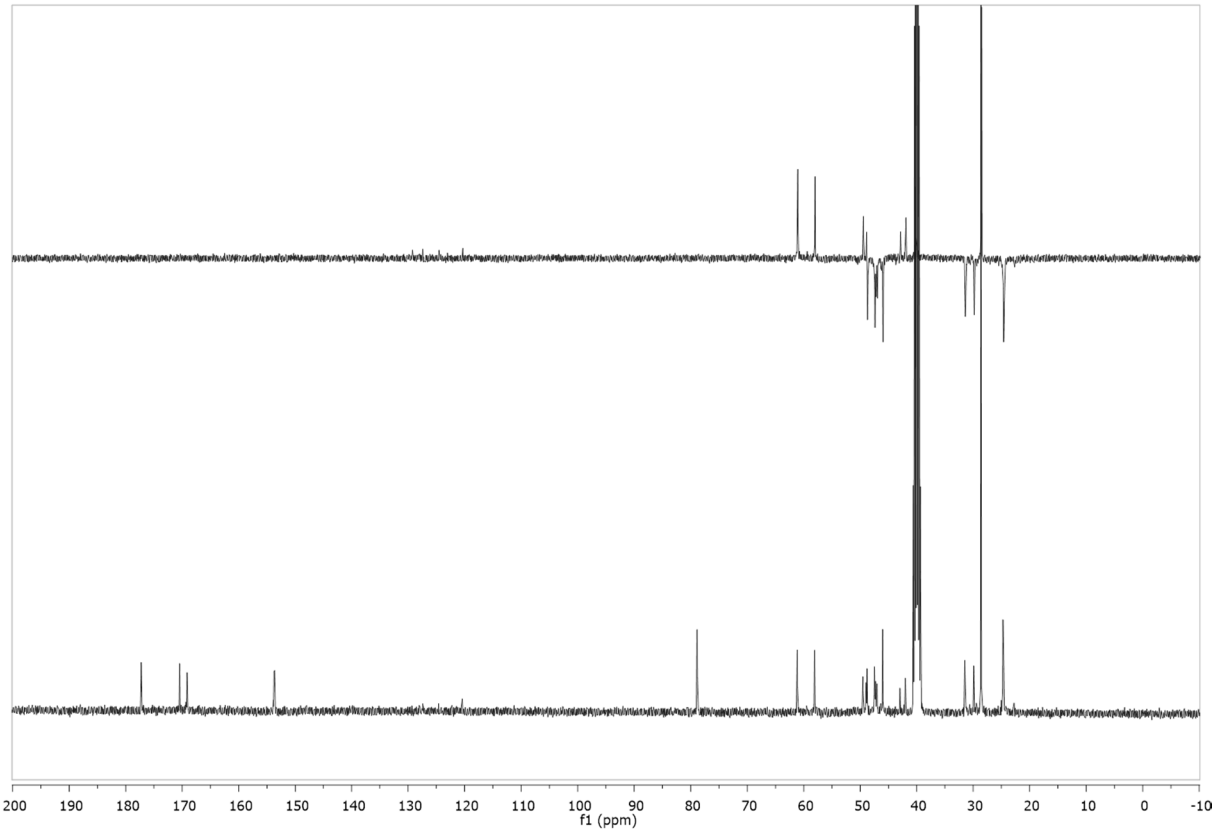

**Benzyl-((1*R*,2*S*)-2-((((9H-fluoren-9-yl)methoxy)carbonyl)amino)cyclopentane-1-carbonyl)-*L*-prolinate (128)** (300 MHz, $CDCl_3$)

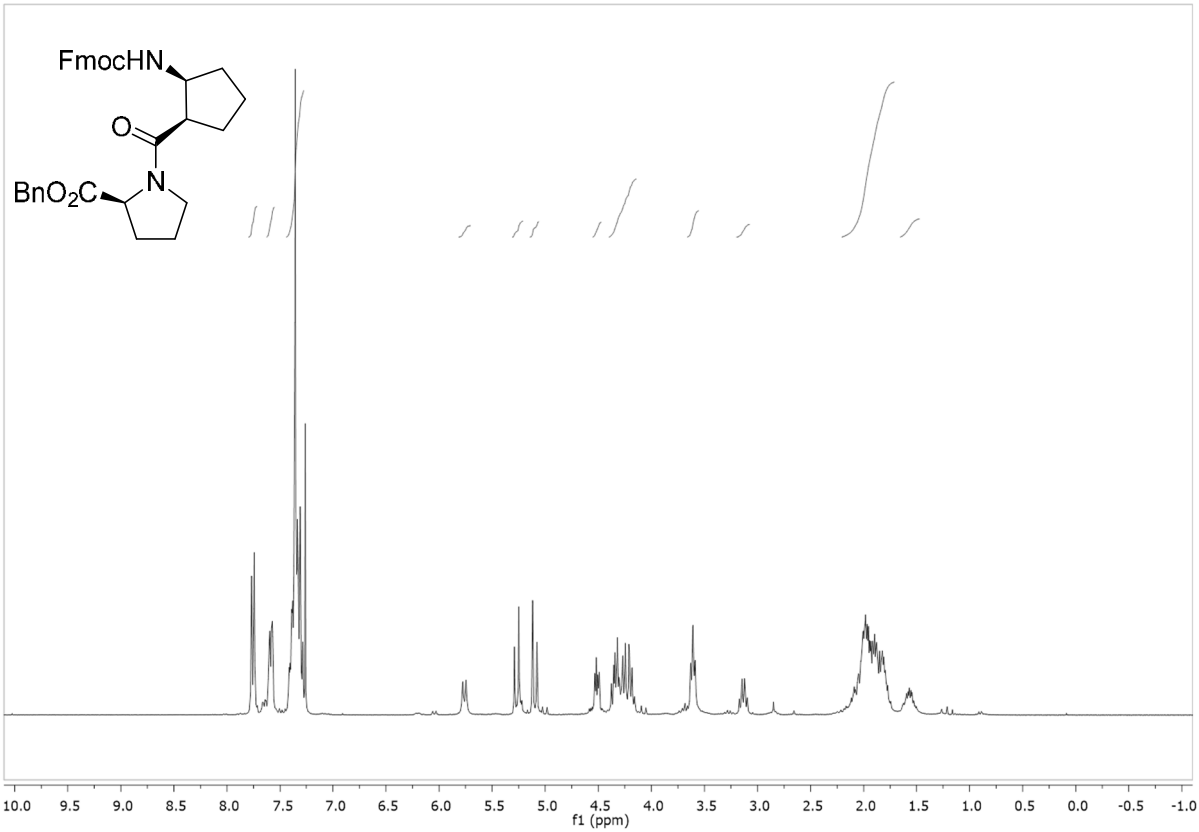


(75 MHz, $CDCl_3$)

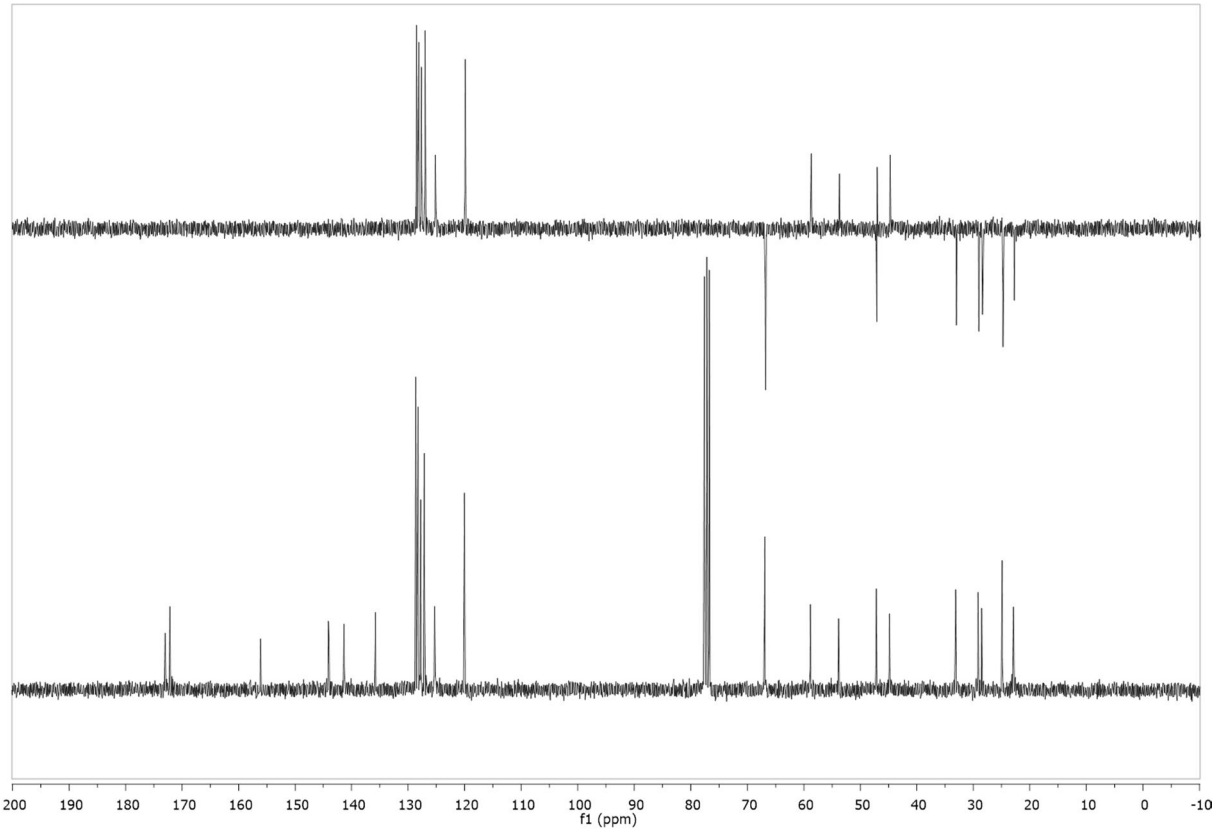

**Benzyl-((1*S*,2*R*)-2-((((9H-fluoren-9-yl)methoxy)carbonyl)amino)cyclopentane-1-carbonyl)-*L*-prolinate (130)** (400 MHz, $CDCl_3$)

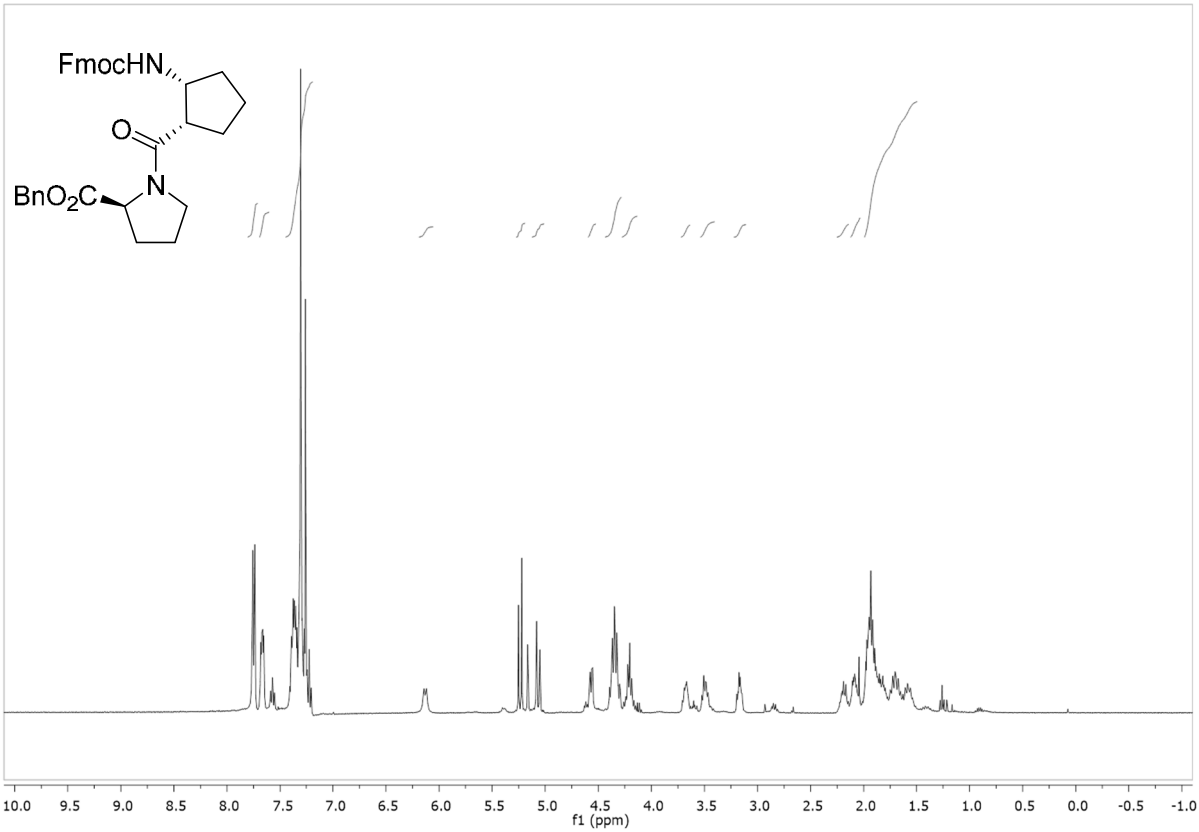


(101 MHz, $CDCl_3$)

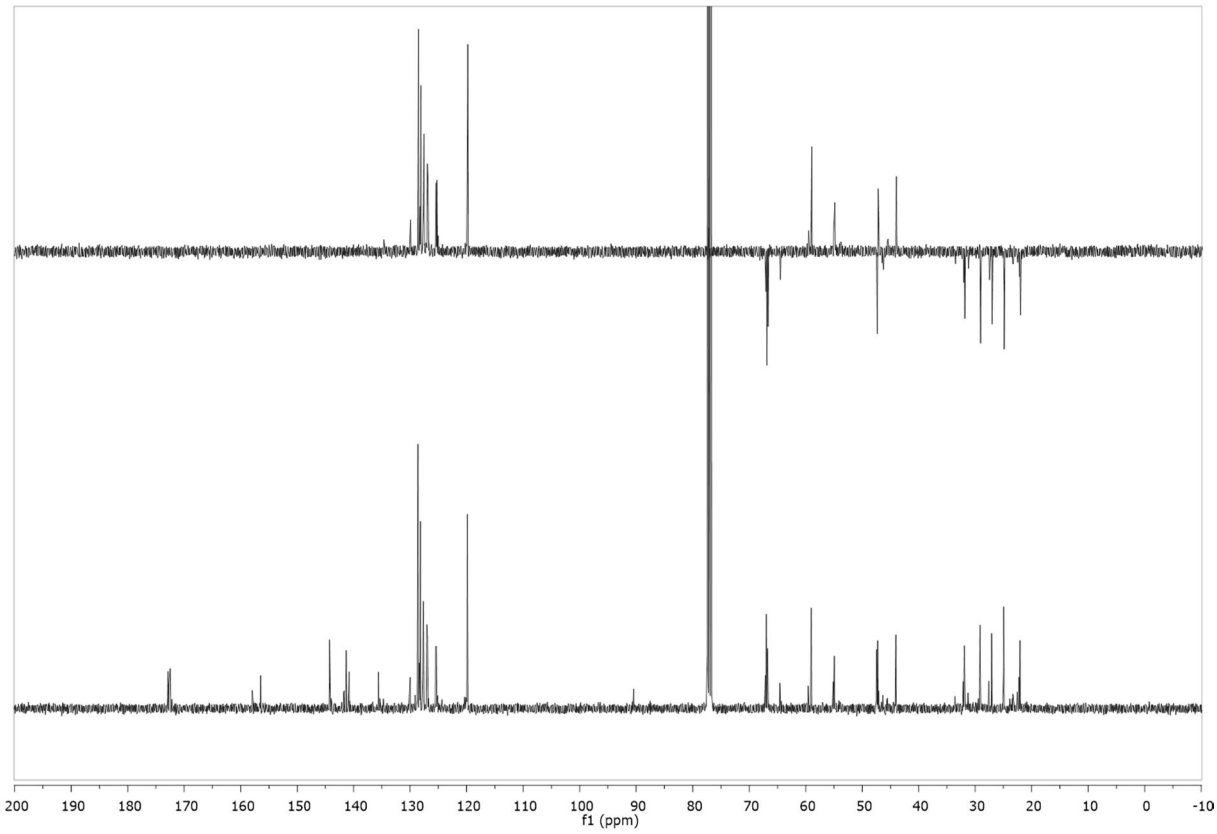

**Methyl (1*S*,2*R*)-2-(benzyl((*R*)-1-phenylethyl)amino)cyclopentane-1-carboxylate ((*ent*)-134)** (300 MHz, $CDCl_3$)

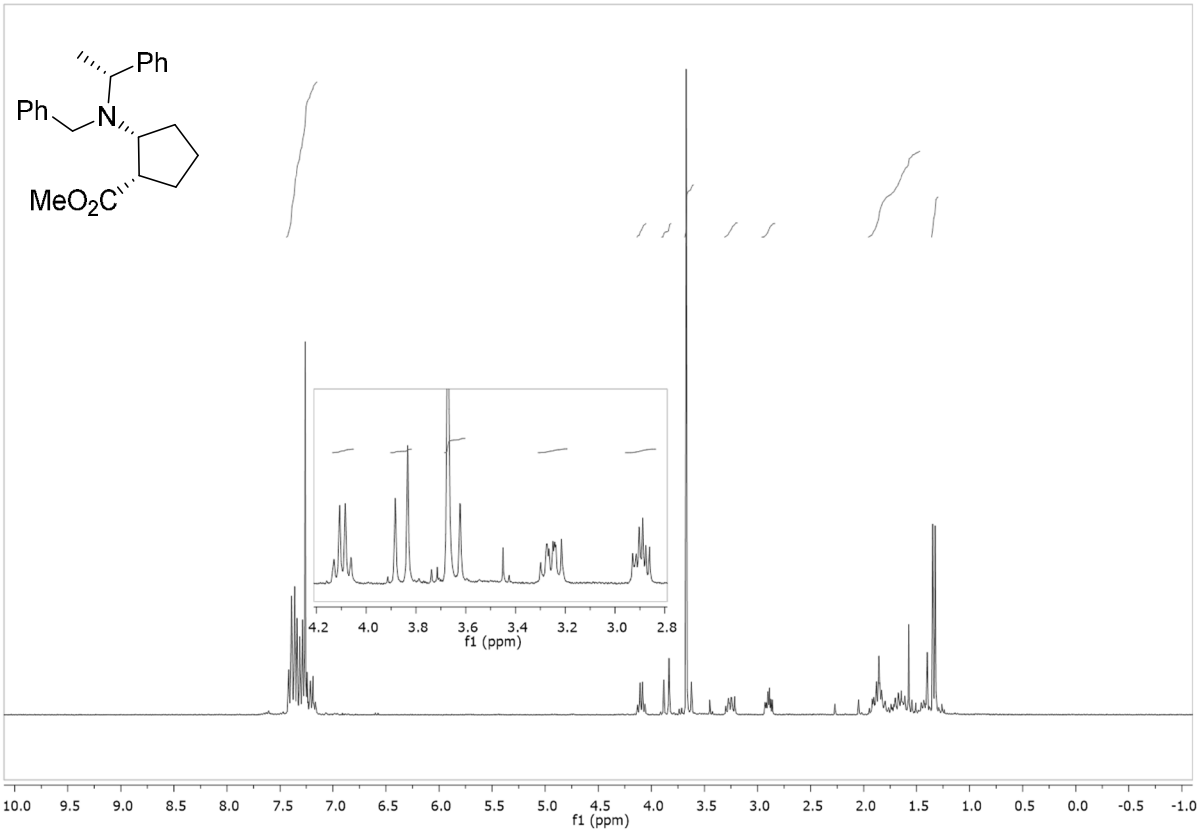


(75 MHz, $CDCl_3$)

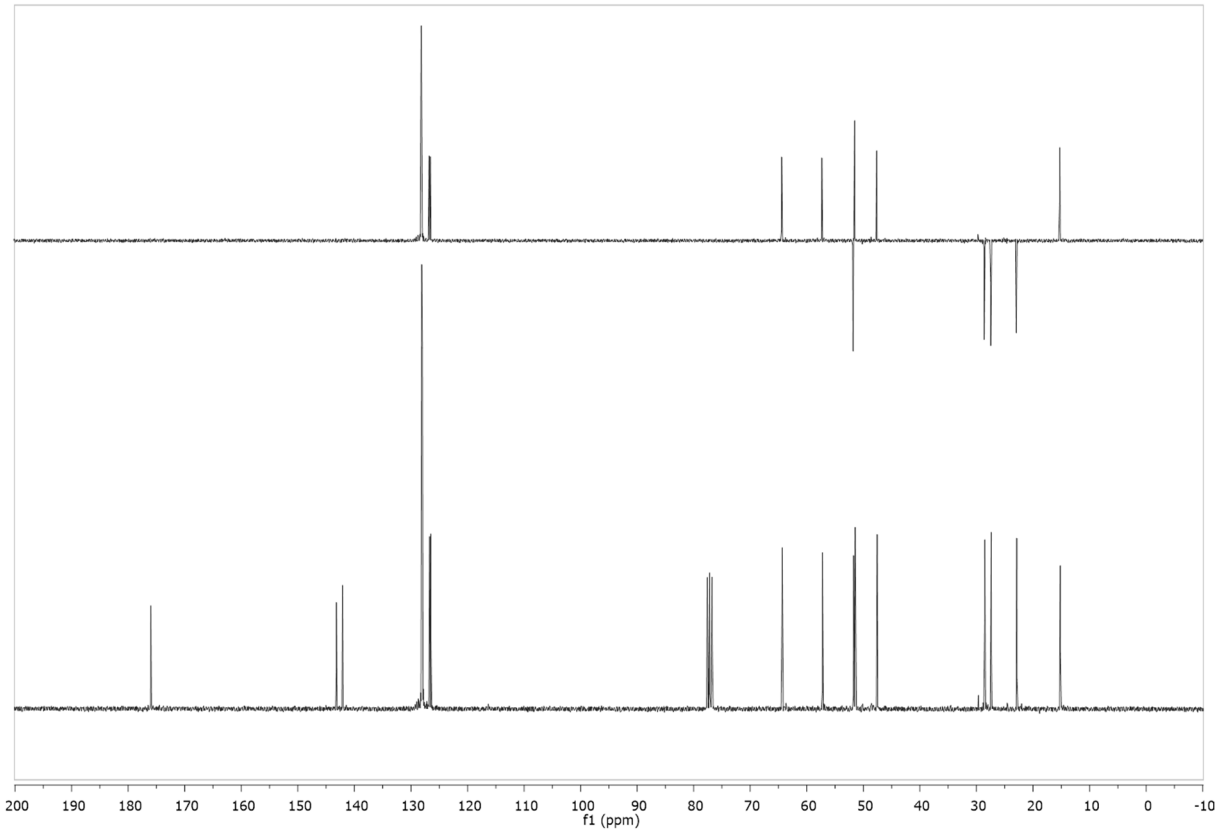

***tert*-Butyl (1*S*,2*R*)-2-(1H-imidazole-1-carboxamido)cyclopentane-1-carboxylate (138)**
(300 MHz, $CDCl_3$)

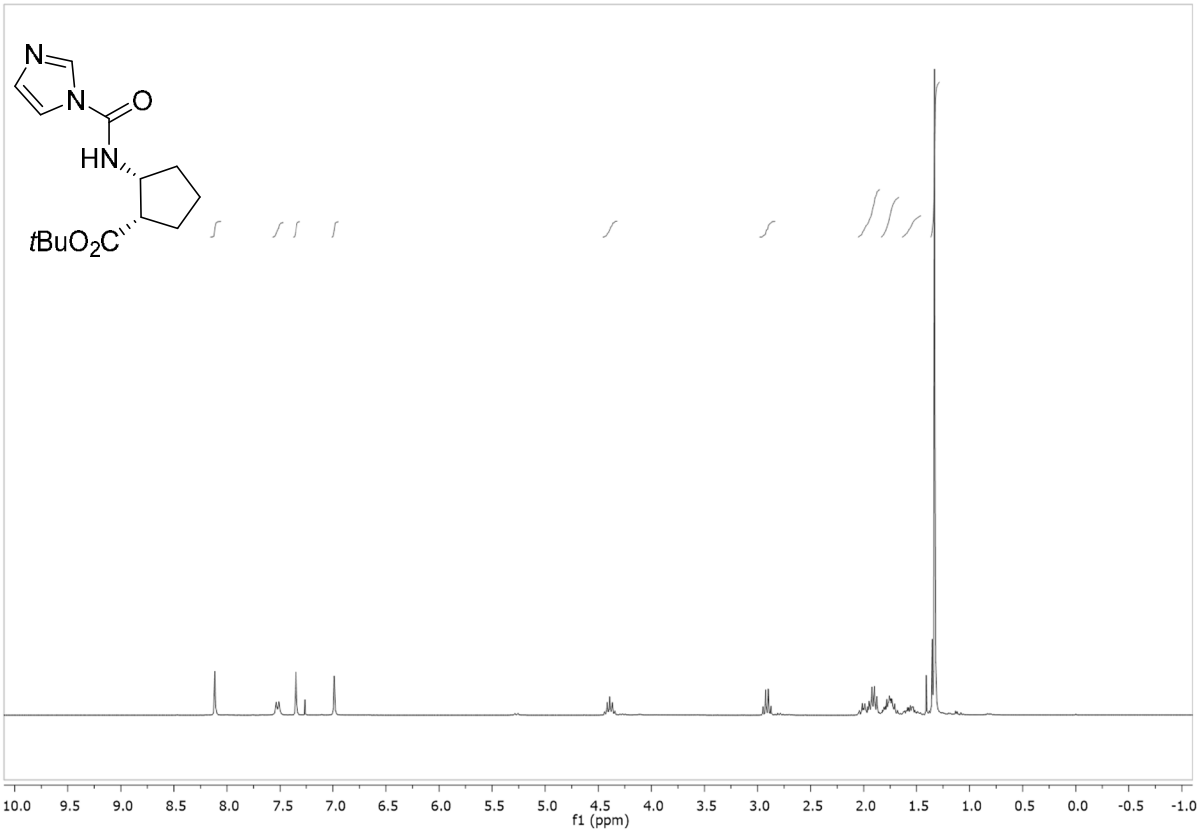


(75 MHz, $CDCl_3$)

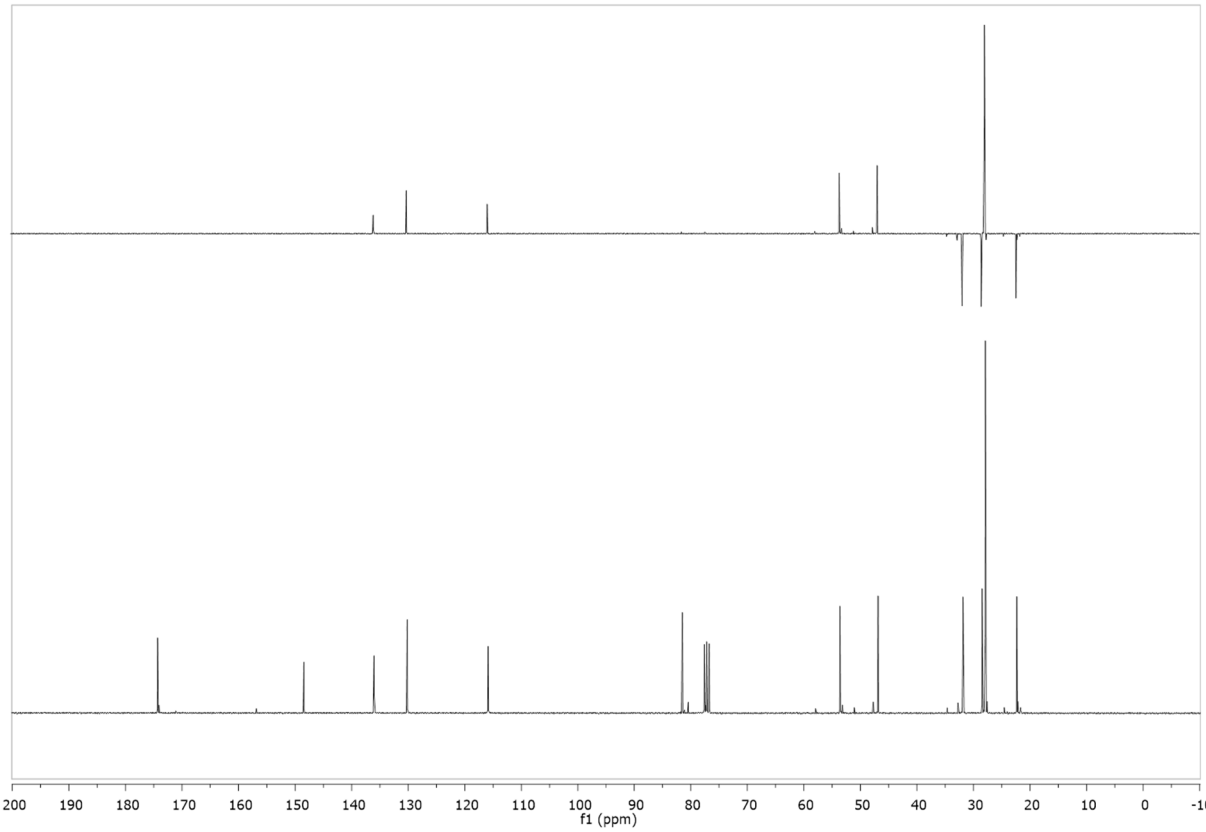

**di-*tert*-Butyl 2,2'-(carbonylbis(azanediyl))(1*S*,1'*S*,2*R*,2'*R*)-bis(cyclopentane-1-carboxylate) (139)** (300 MHz, $CDCl_3$)

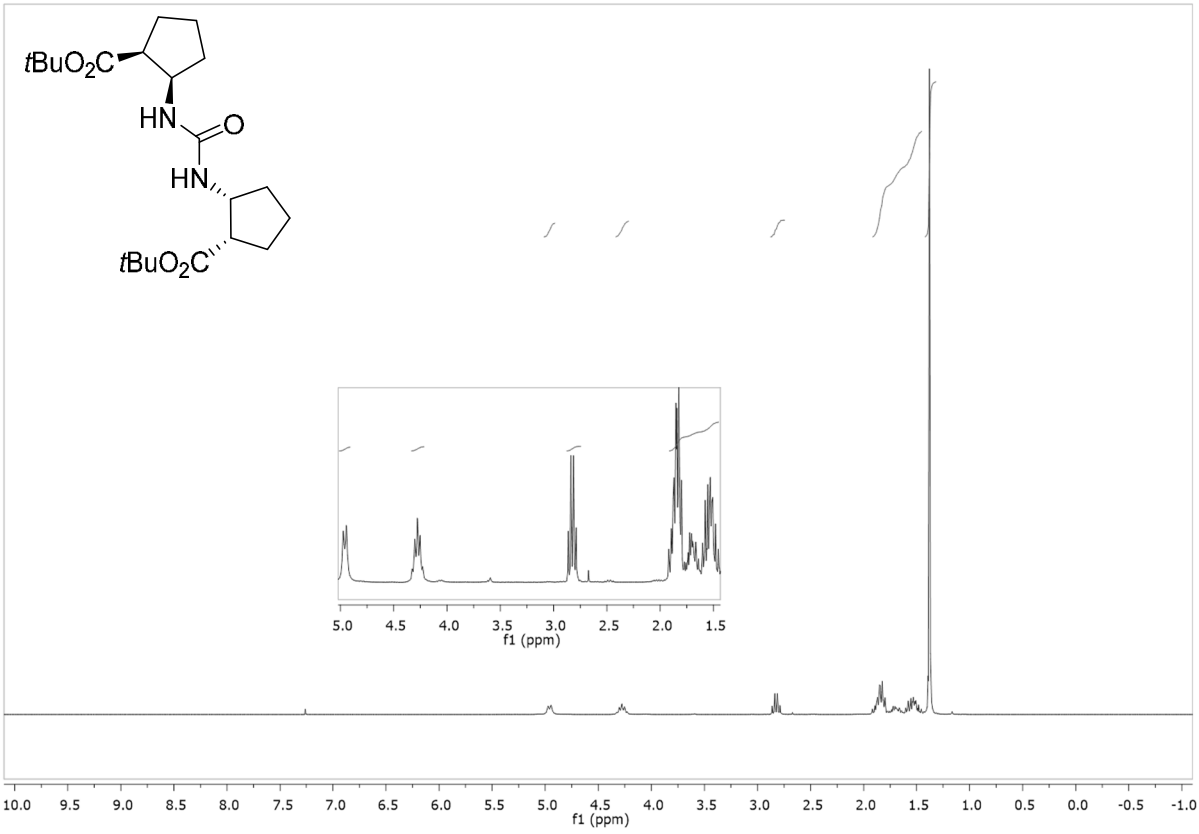


(75 MHz, $CDCl_3$)

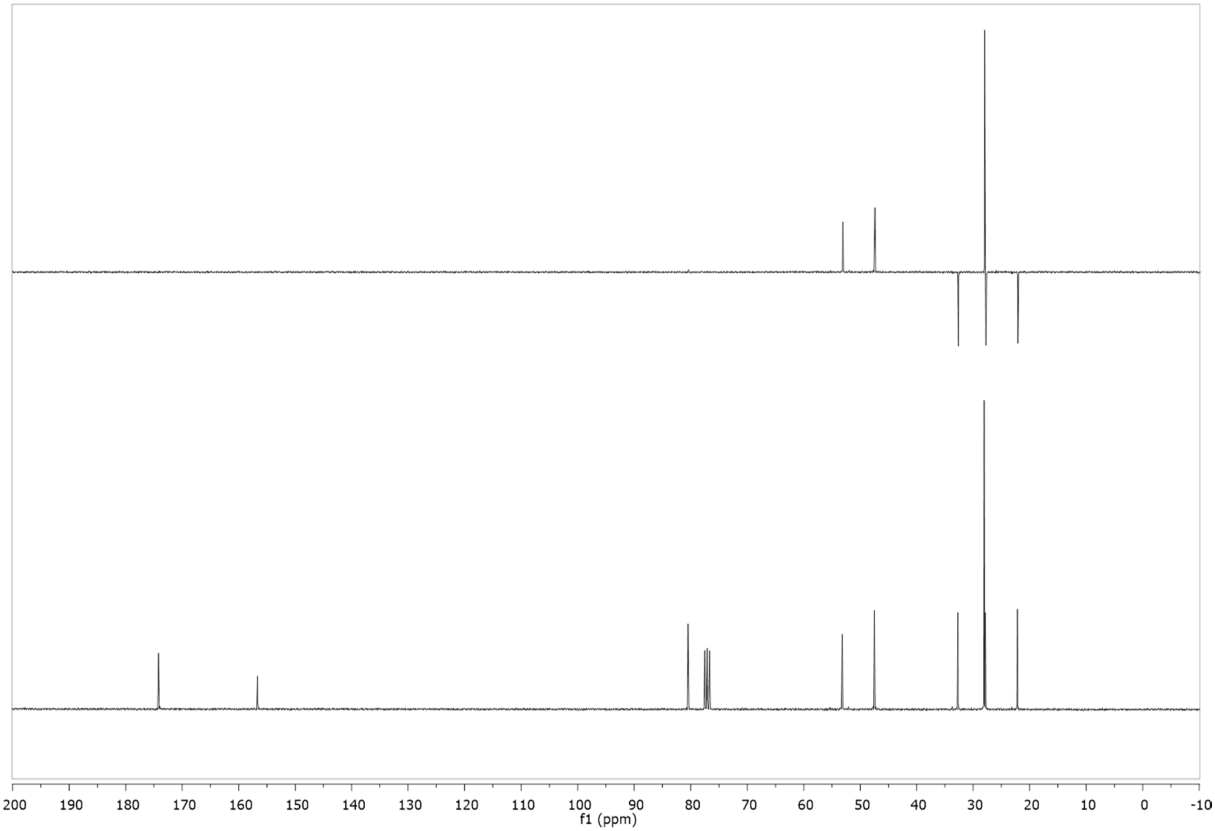

**(1*R*,2*S*)-2-(((Allyloxy)carbonyl)amino)cyclopentane-1-carboxylic acid (144)**
(400 MHz, $CDCl_3$)

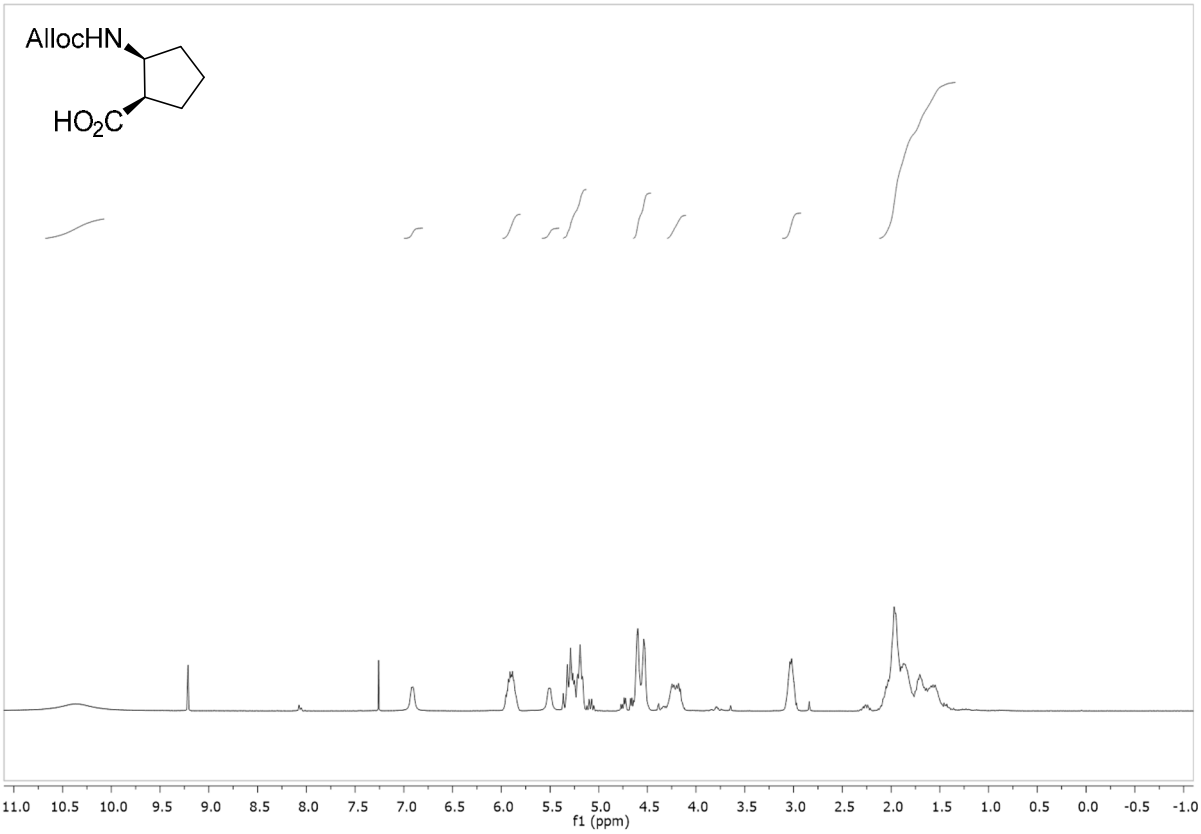


(101 MHz, $CDCl_3$)

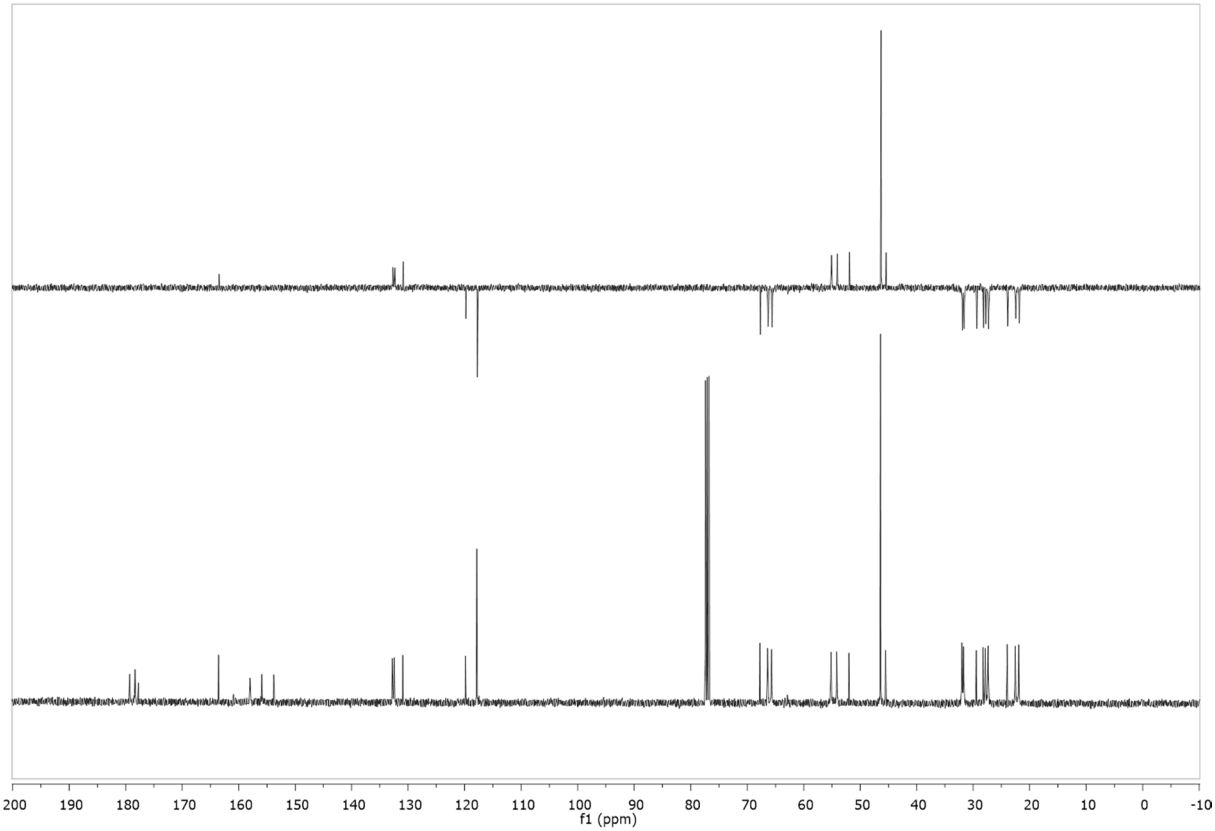

**Benzyl ((1*R*,2*S*)-2-(((allyloxy)carbonyl)amino)cyclopentane-1-carbonyl)-*L*-prolinate (145)** (300 MHz, $CDCl_3$)

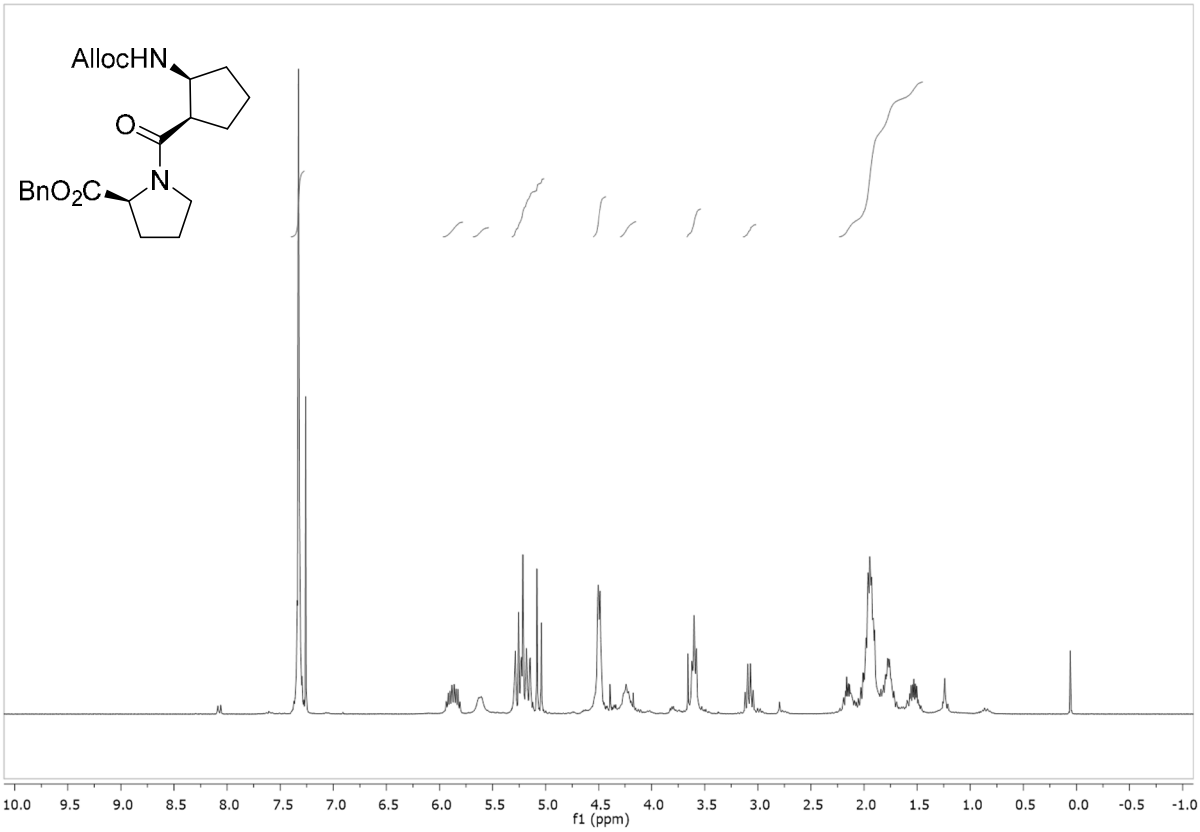


(75 MHz, $CDCl_3$)

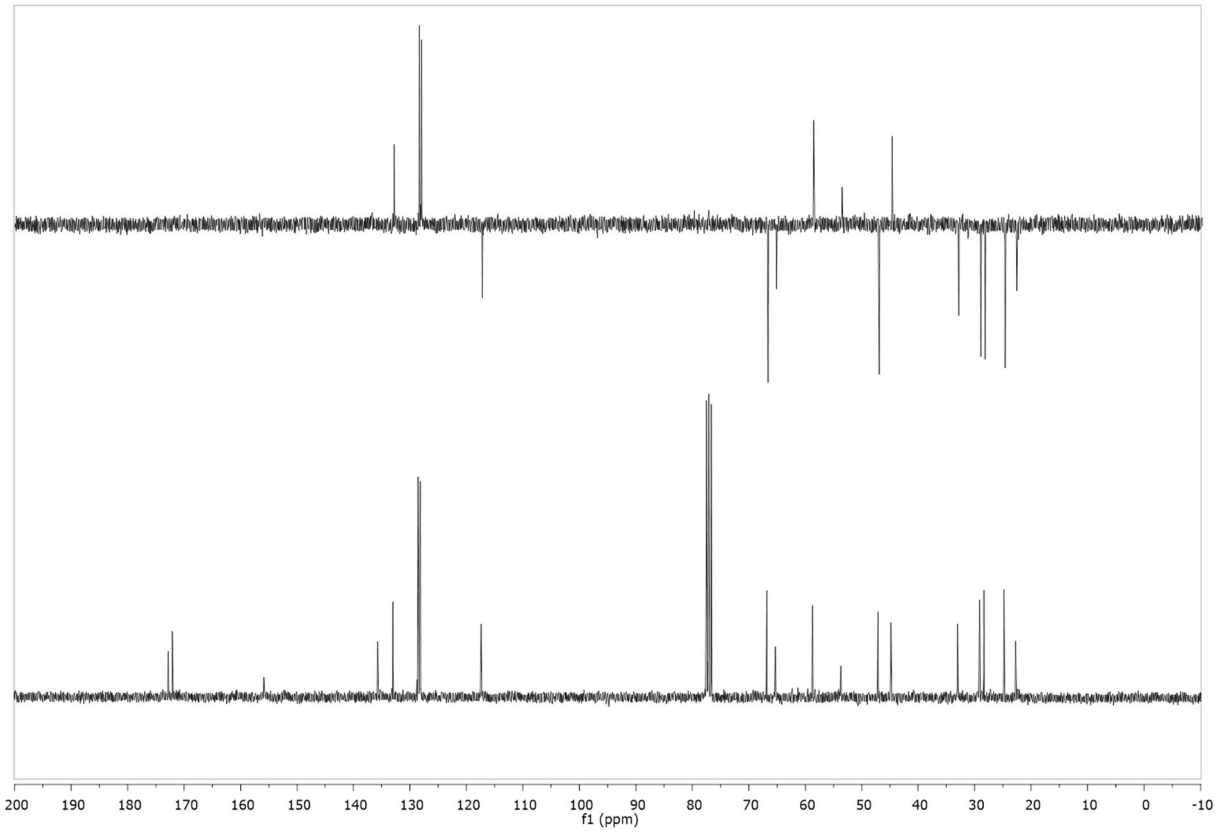

**Benzyl (*S*)-2-(((1*S*,2*R*)-2-((*S*)-2-((benzyloxy)carbonyl)pyrrolidine-1-carbonyl)cyclopentyl)carbamoyl)pyrrolidine-1-carboxylate (129)** (400 MHz, $CDCl_3$)

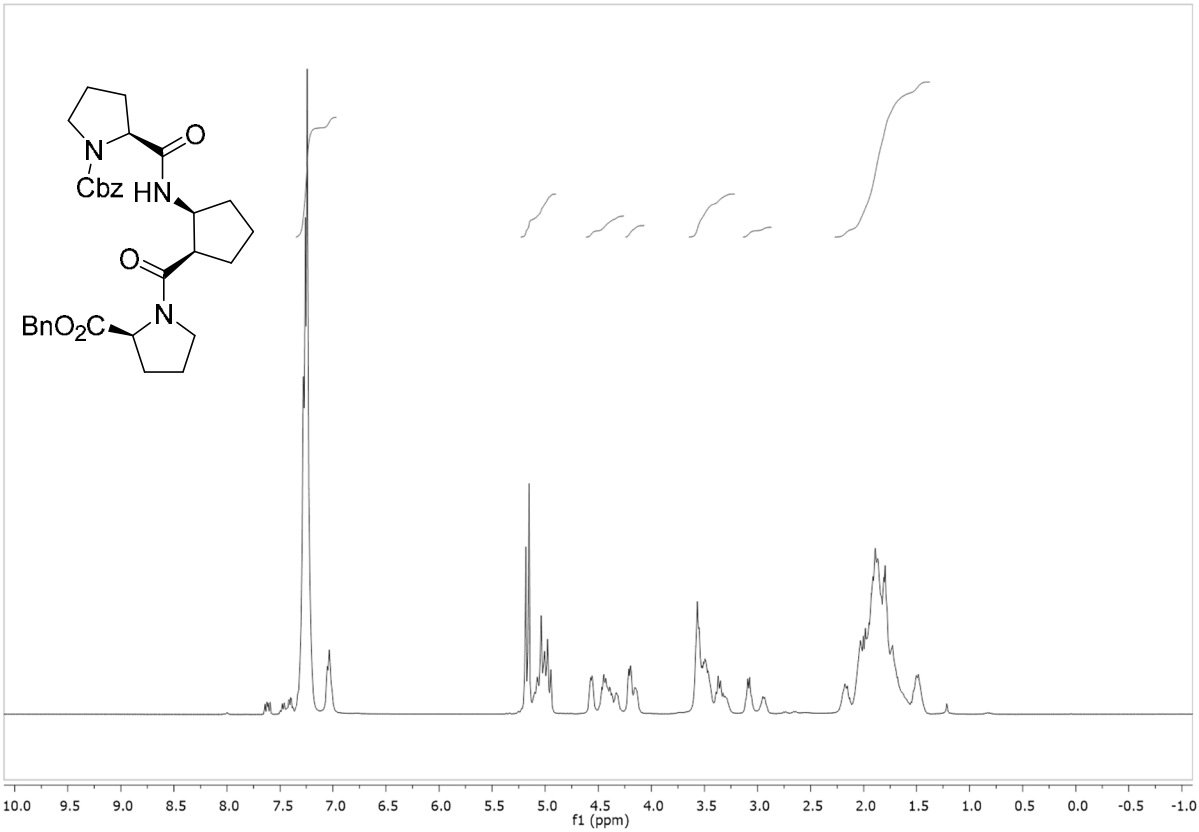


(101 MHz, $CDCl_3$)

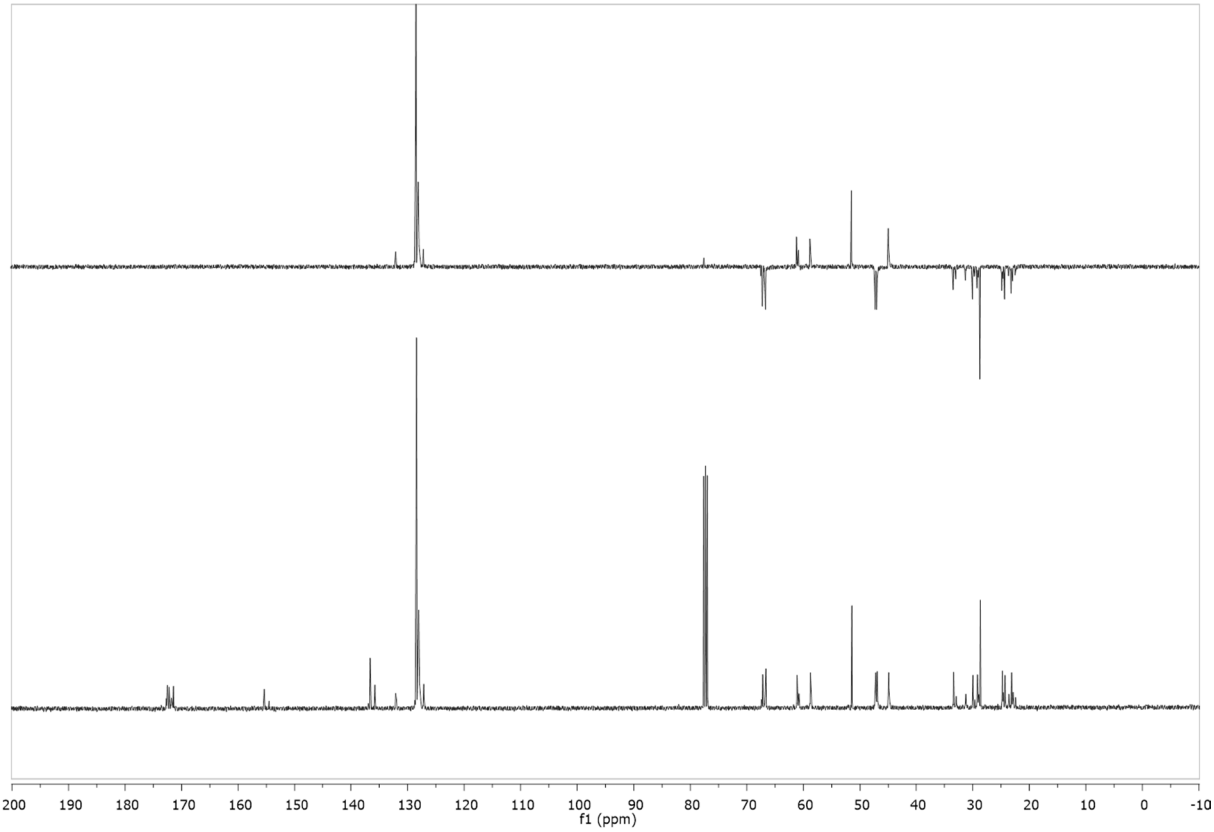

**((1*R*,2*S*)-2-((*S*)-Pyrrolidine-2-carboxamido)cyclopentane-1-carbonyl)-*L*-proline (119)**
(300 MHz, $CDCl_3$)

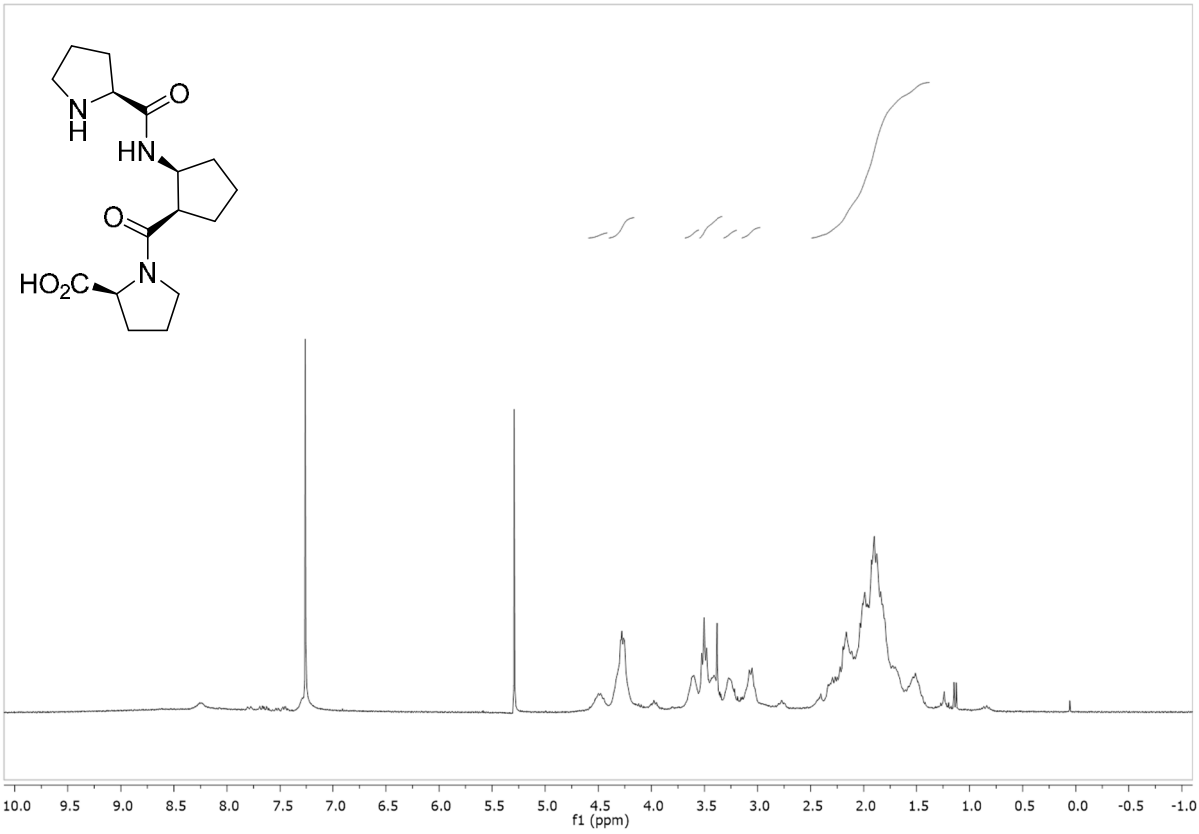


(75 MHz, $CDCl_3$)

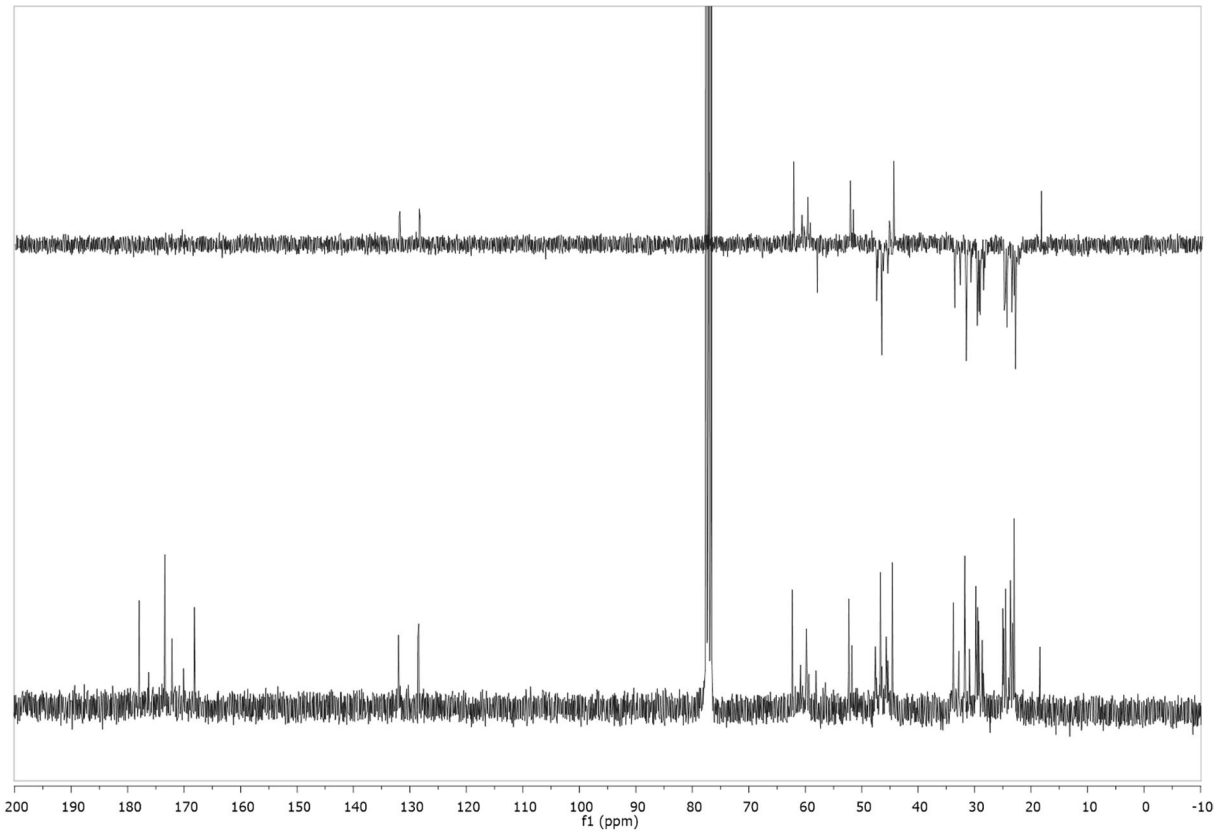

**Benzyl ((1*S*,2*R*)-2-(((allyloxy)carbonyl)amino)cyclopentane-1-carbonyl)-*L*-prolinate (146)** (300 MHz, $CDCl_3$)

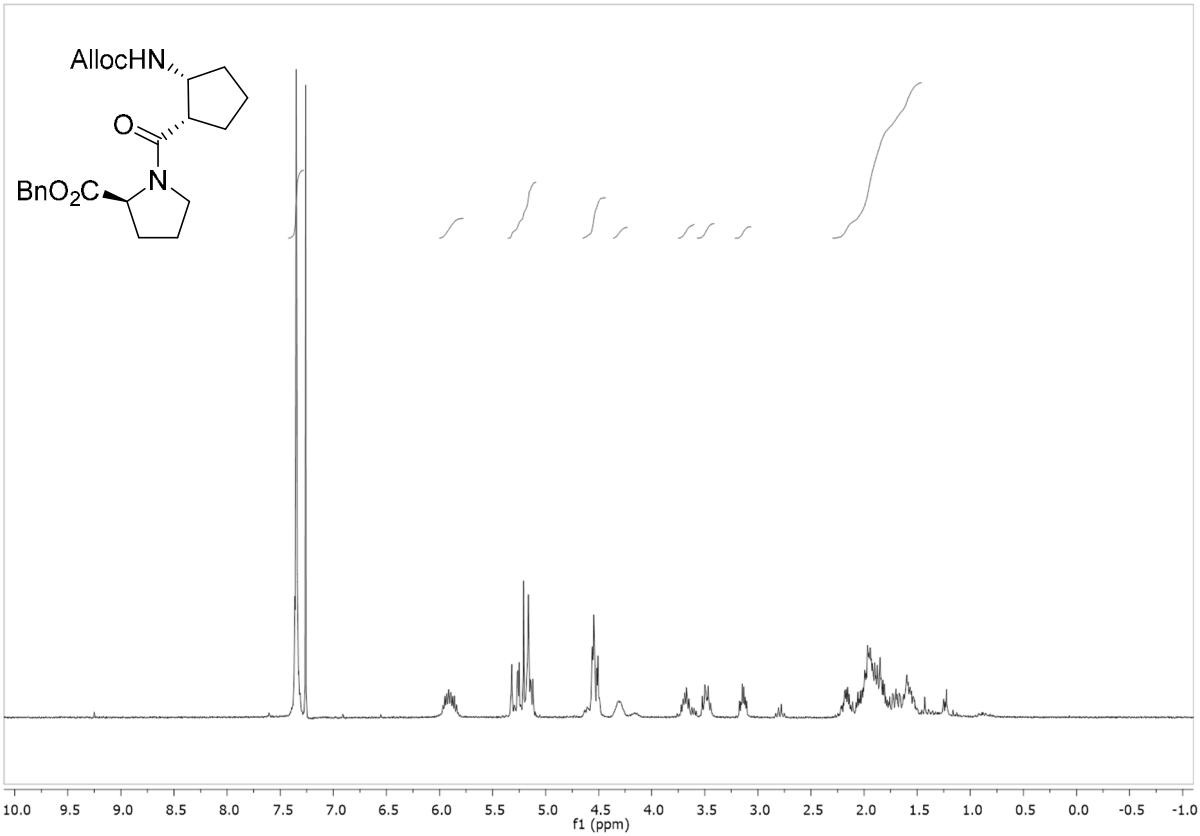


(75 MHz, $CDCl_3$)

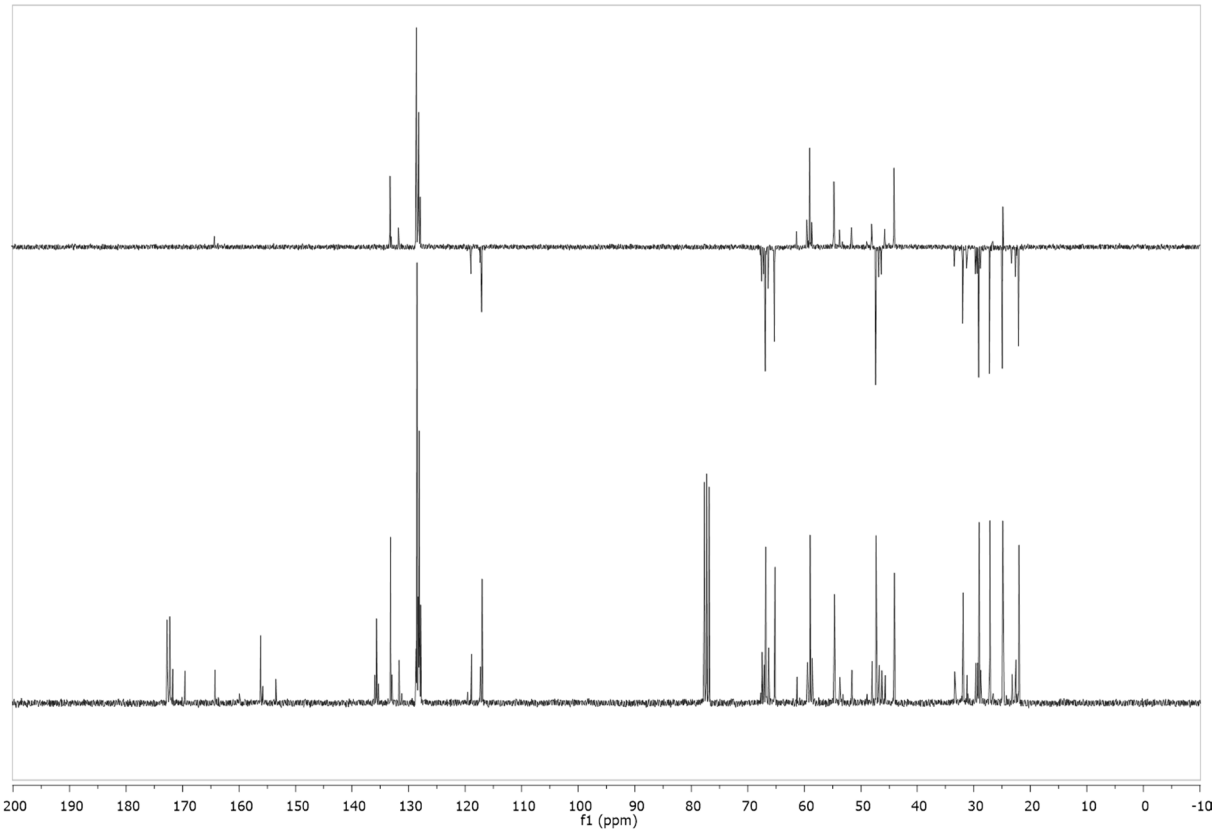

**Benzyl (*S*)-2-(((1*R*,2*S*)-2-((S)-2-((benzyloxy)carbonyl)pyrrolidine-1-carbonyl)cyclopentyl)carbamoyl)pyrrolidine-1-carboxylate (131)** (300 MHz, $CDCl_3$)

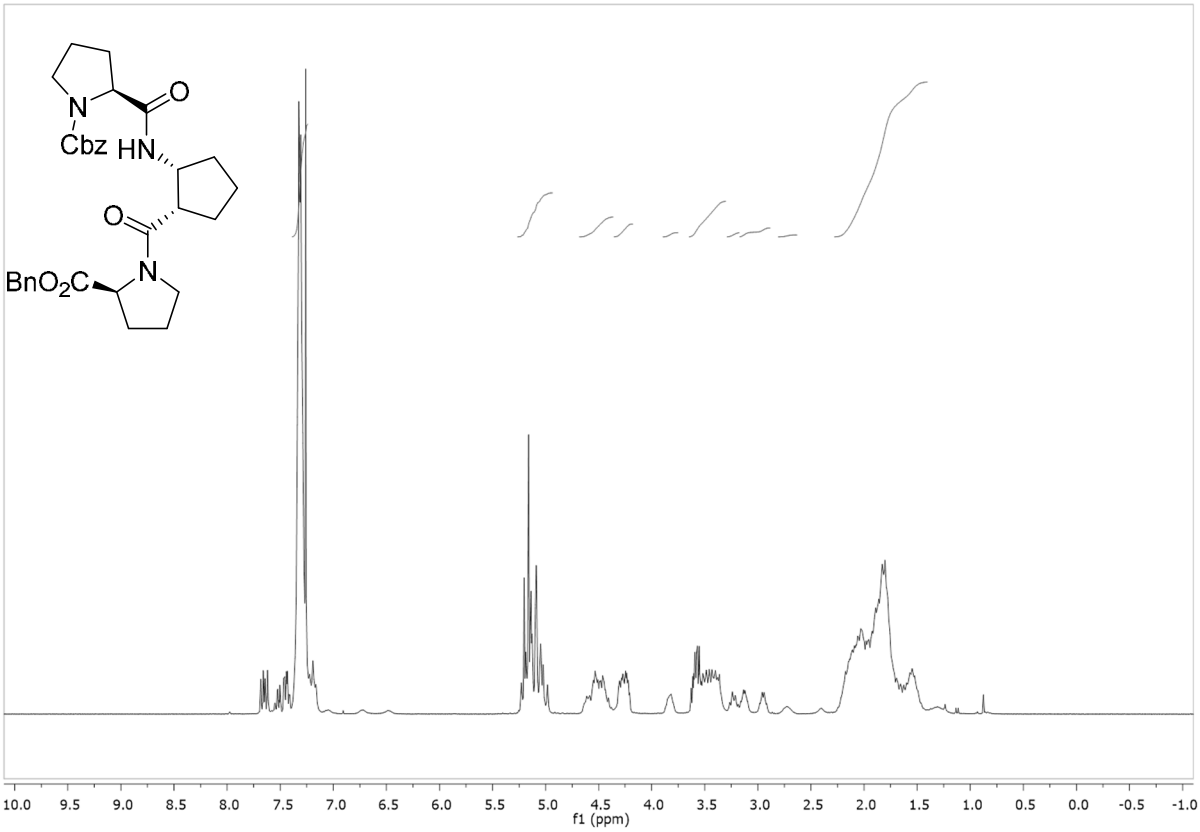


(75 MHz, $CDCl_3$)

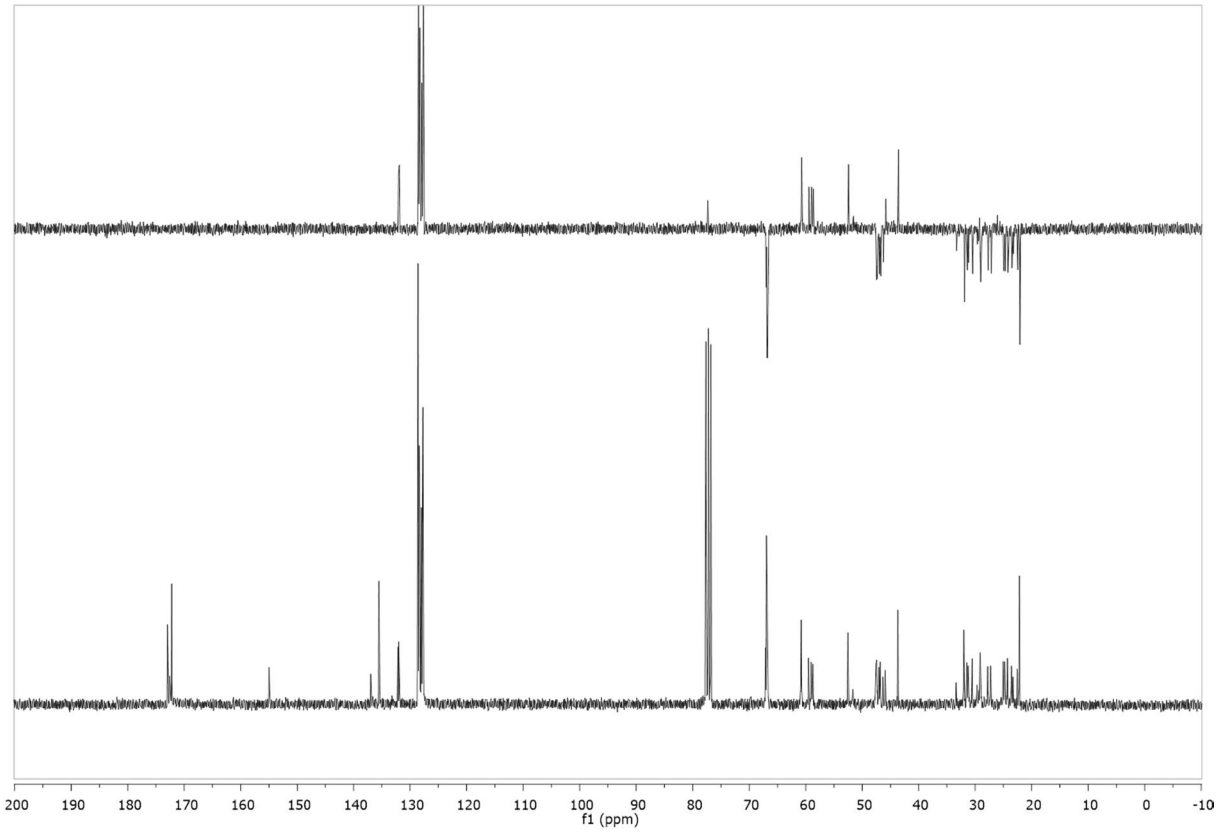

**((1*S*,2*R*)-2-((*S*)-Pyrrolidine-2-carboxamido)cyclopentane-1-carbonyl)-*L*-proline (147)**
(300 MHz, $CDCl_3$)

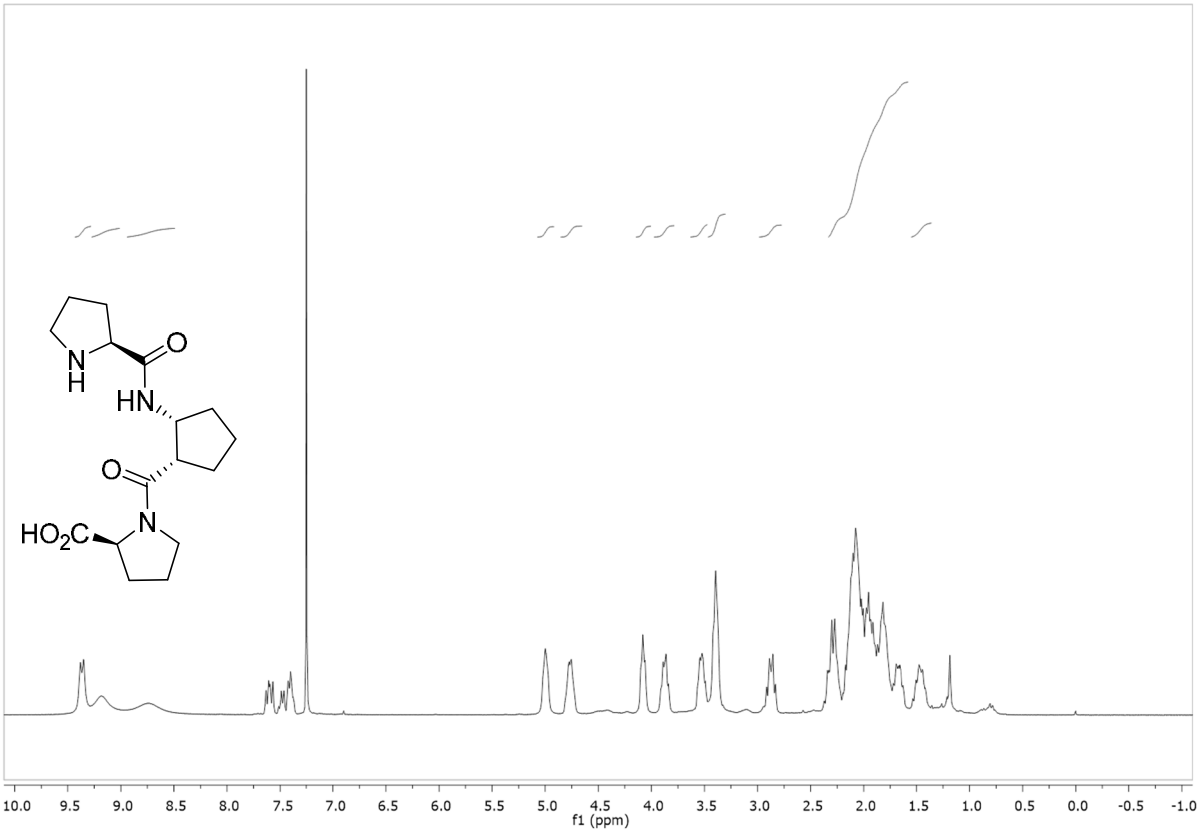


(75 MHz, $CDCl_3$)

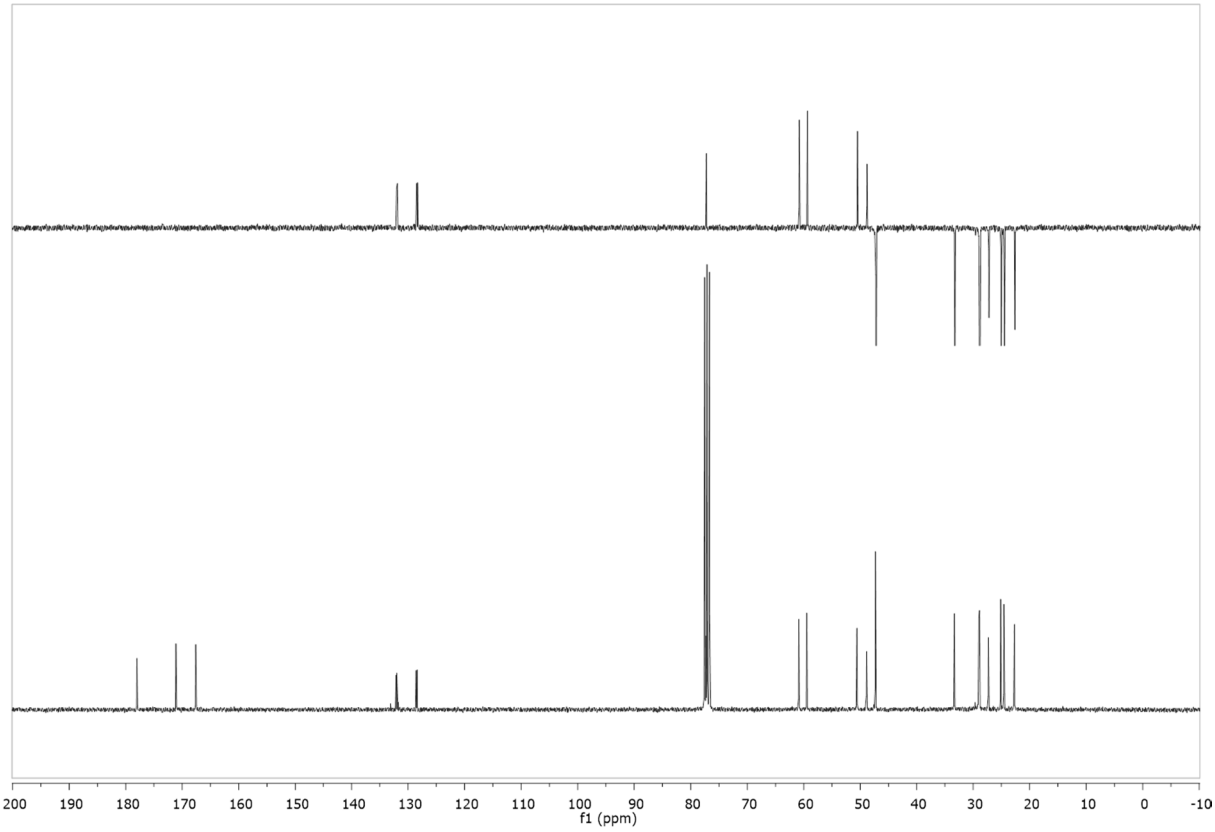

**(2*R*,7*R*)-Diethyl 2,7-bis((*tert*-butoxycarbonyl)amino)oct-4-enedioate (166)**
(300 MHz, $CDCl_3$)

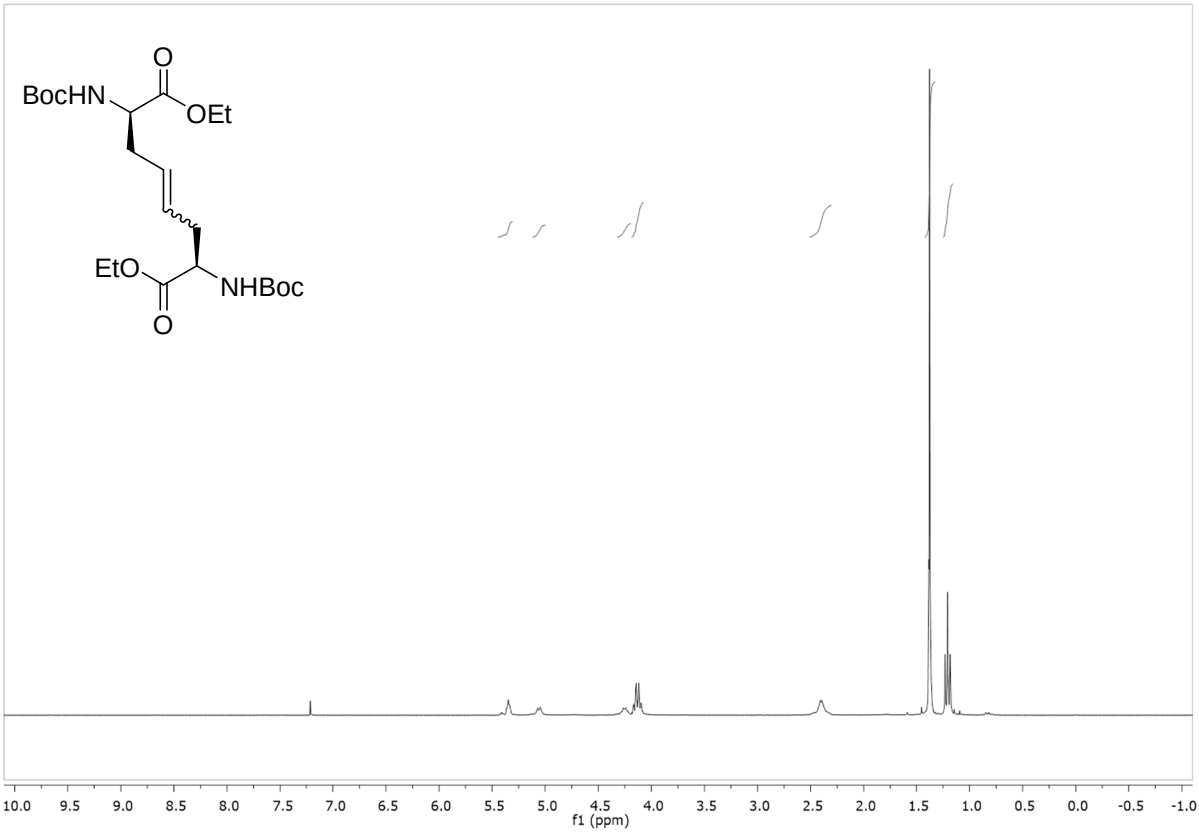


(75 MHz, $CDCl_3$)

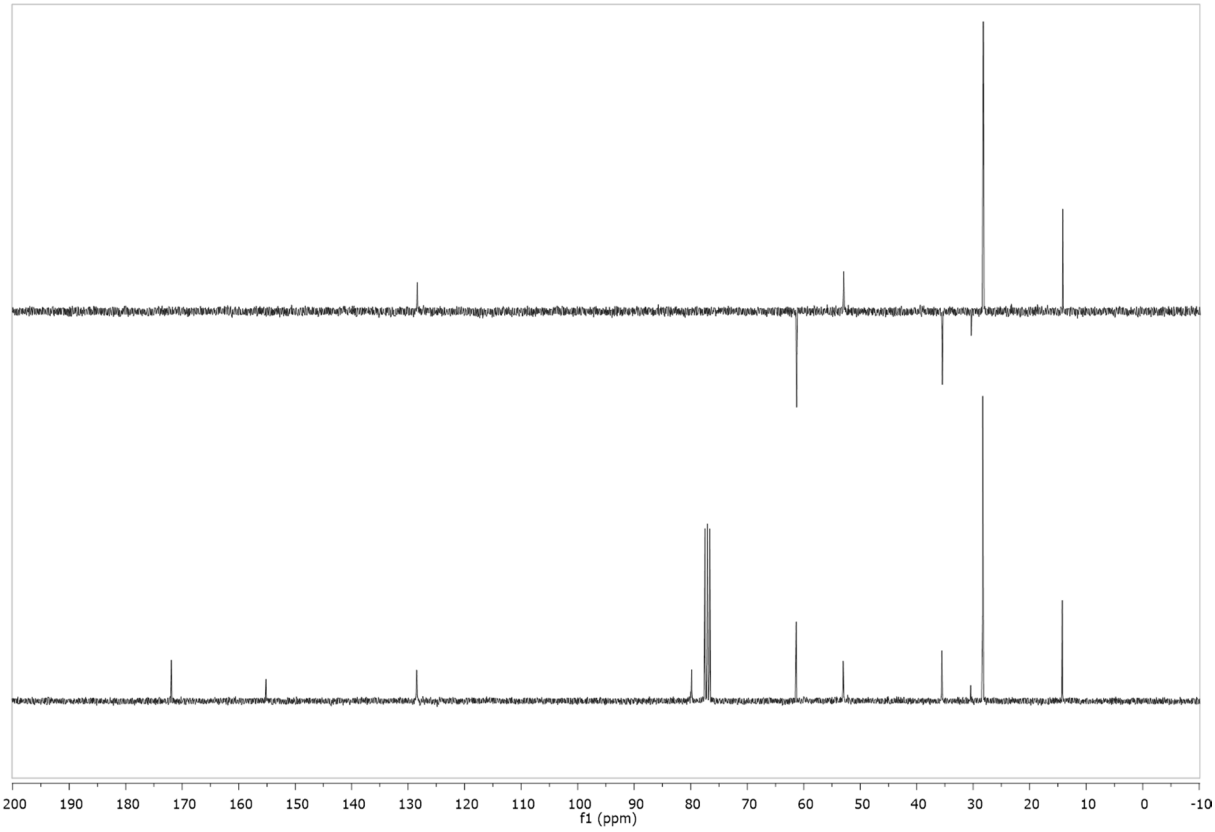

**(2*R*,7*R*)-Diethyl 2,7-bis((*tert*-butoxycarbonyl)amino)octanedioate (167)**

(300 MHz, $CDCl_3$)

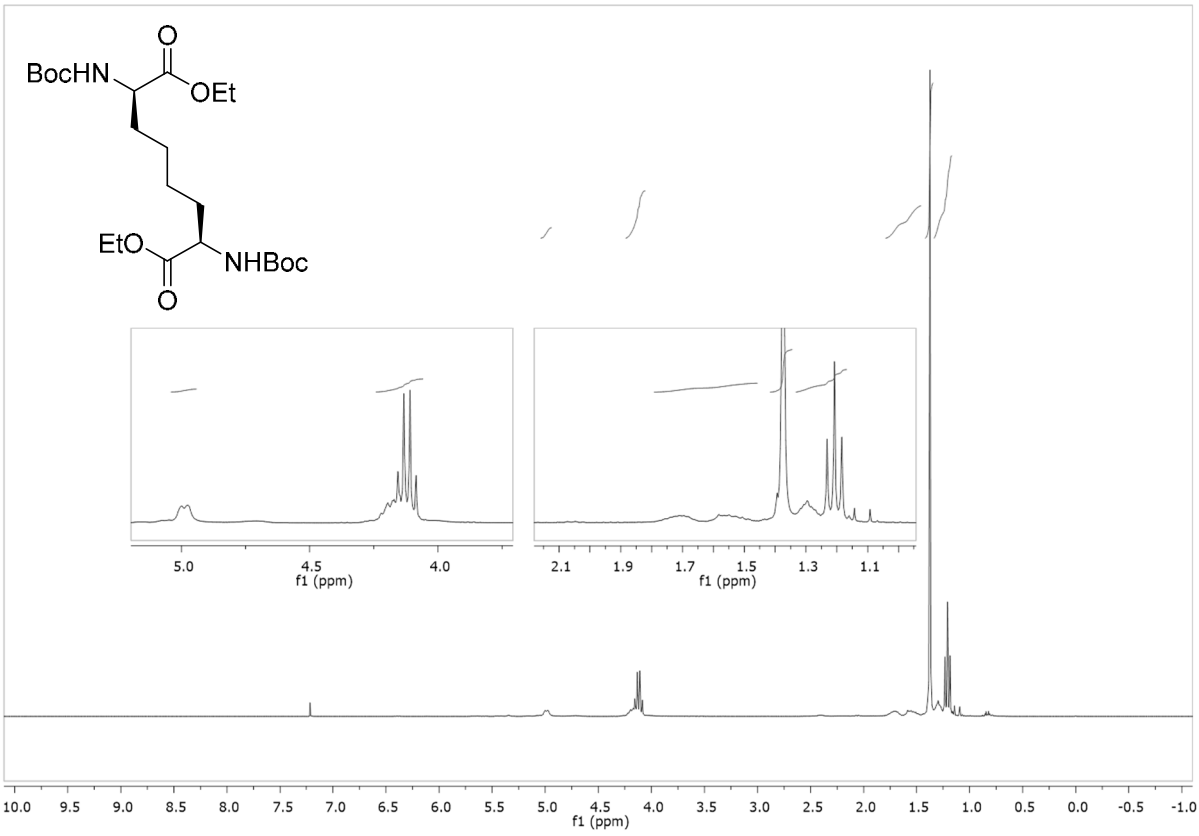


(75 MHz, $CDCl_3$)

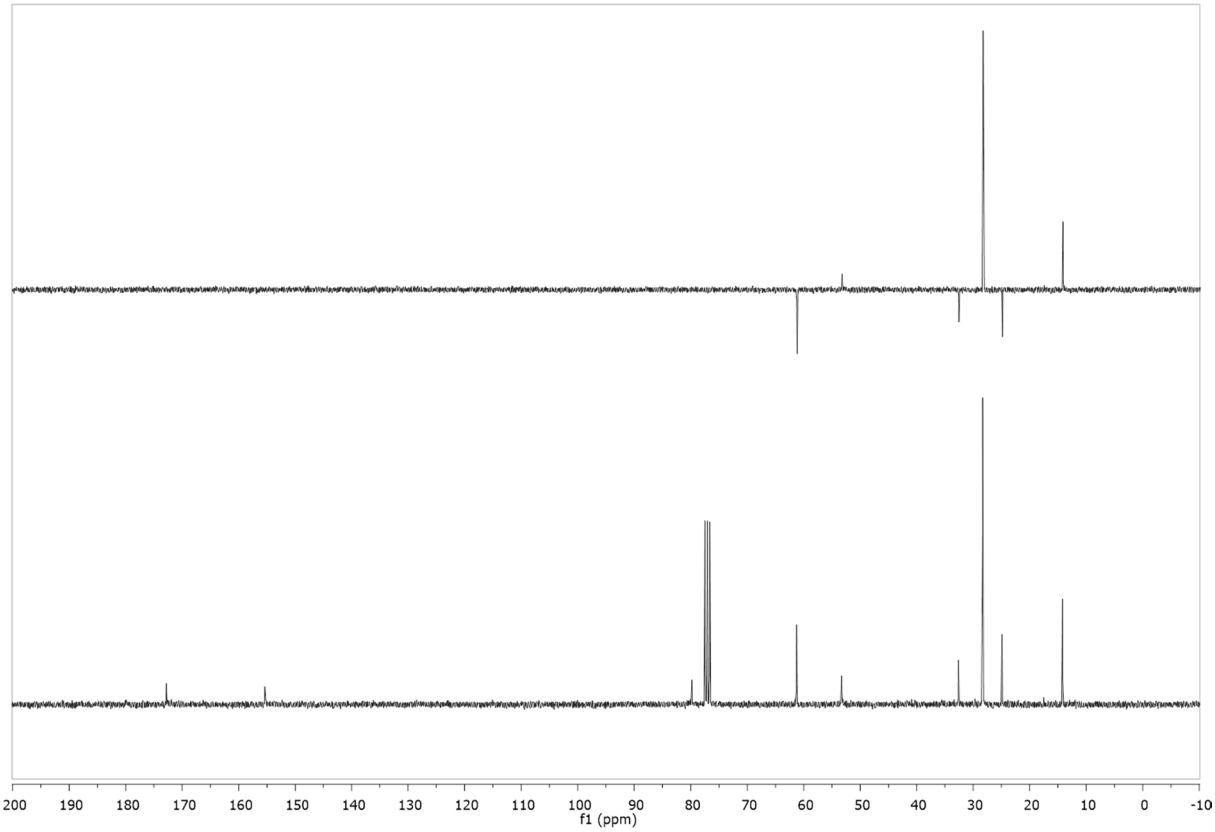

**(2*R*,7*R*)-2,7-Bis((*tert*-Butoxycarbonyl)amino)octanedioic acid (164)** (300 MHz, $CD_3OD$)

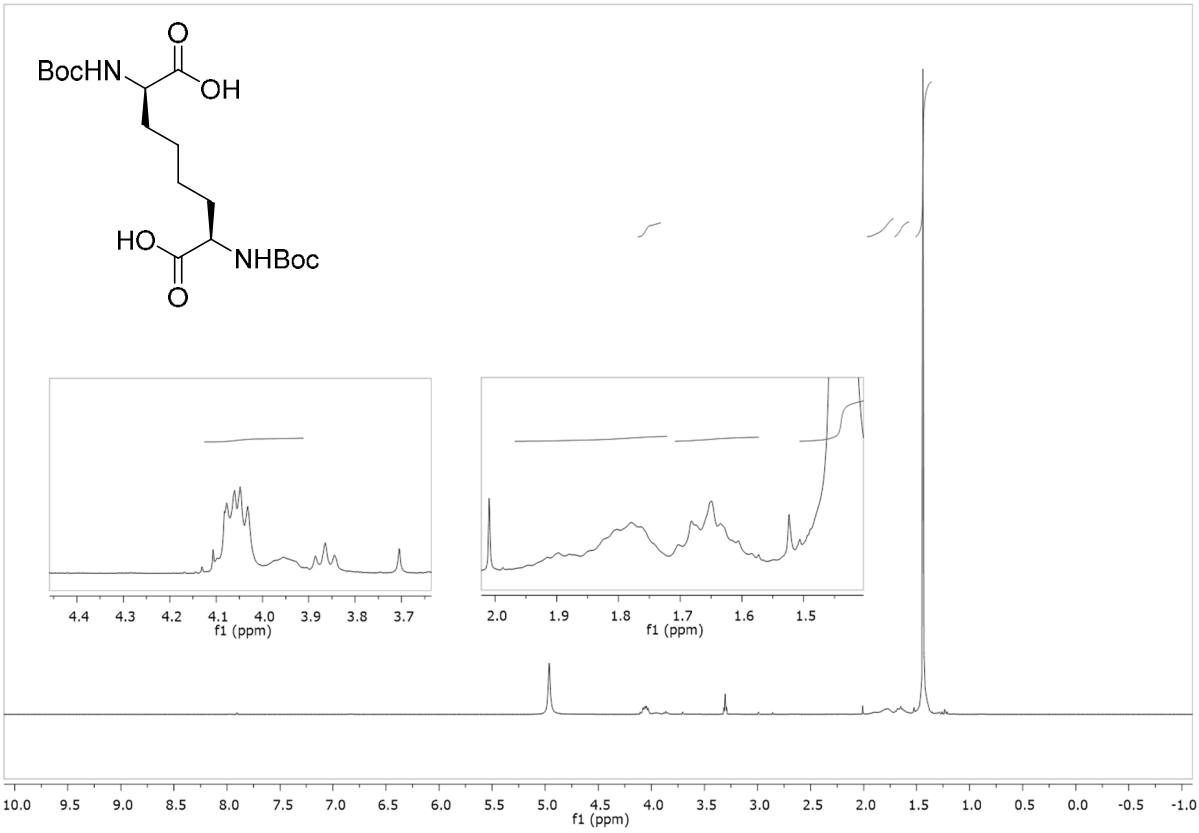


(75 MHz, $CD_3OD$)

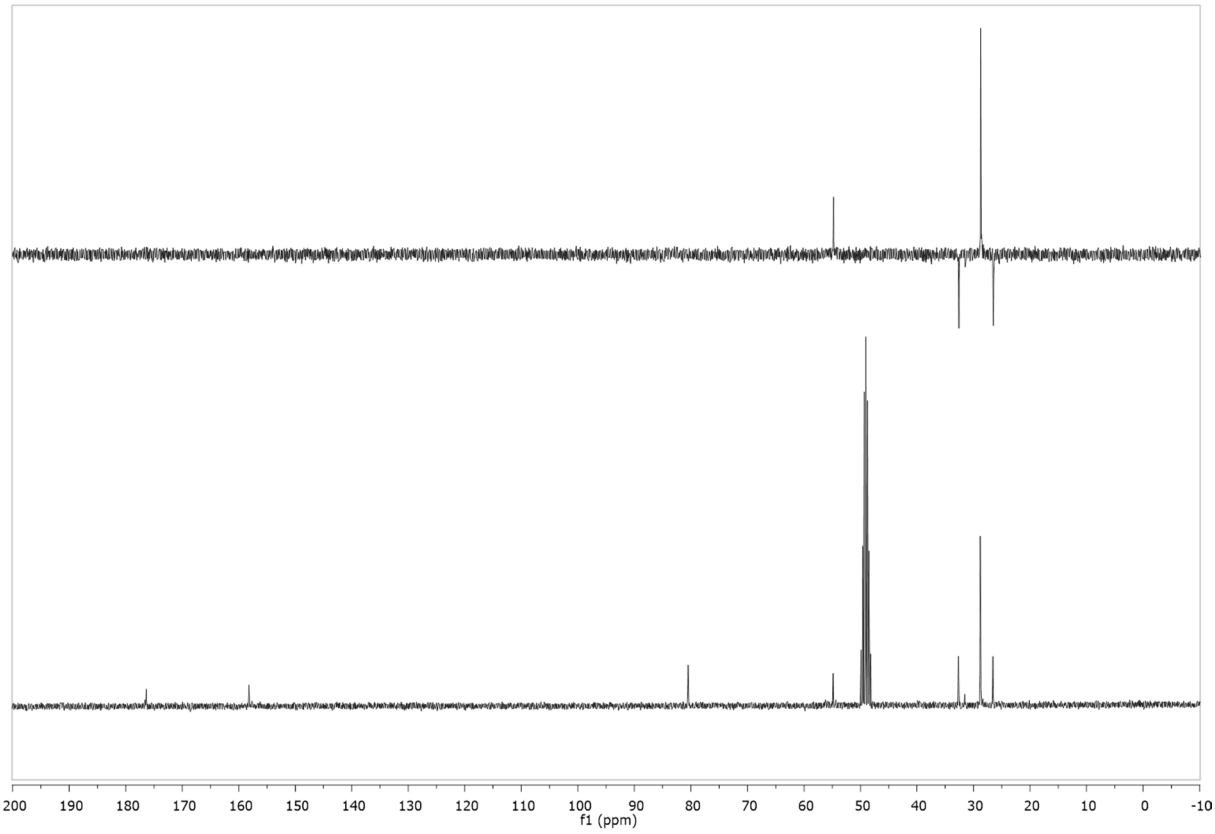

***tert*-Butyl (1*S*,2*S*)-2-(benzyl((*S*)-1-phenylethyl)amino)cyclopentane-1-carboxylate (23)** (300 MHz, $CDCl_3$)

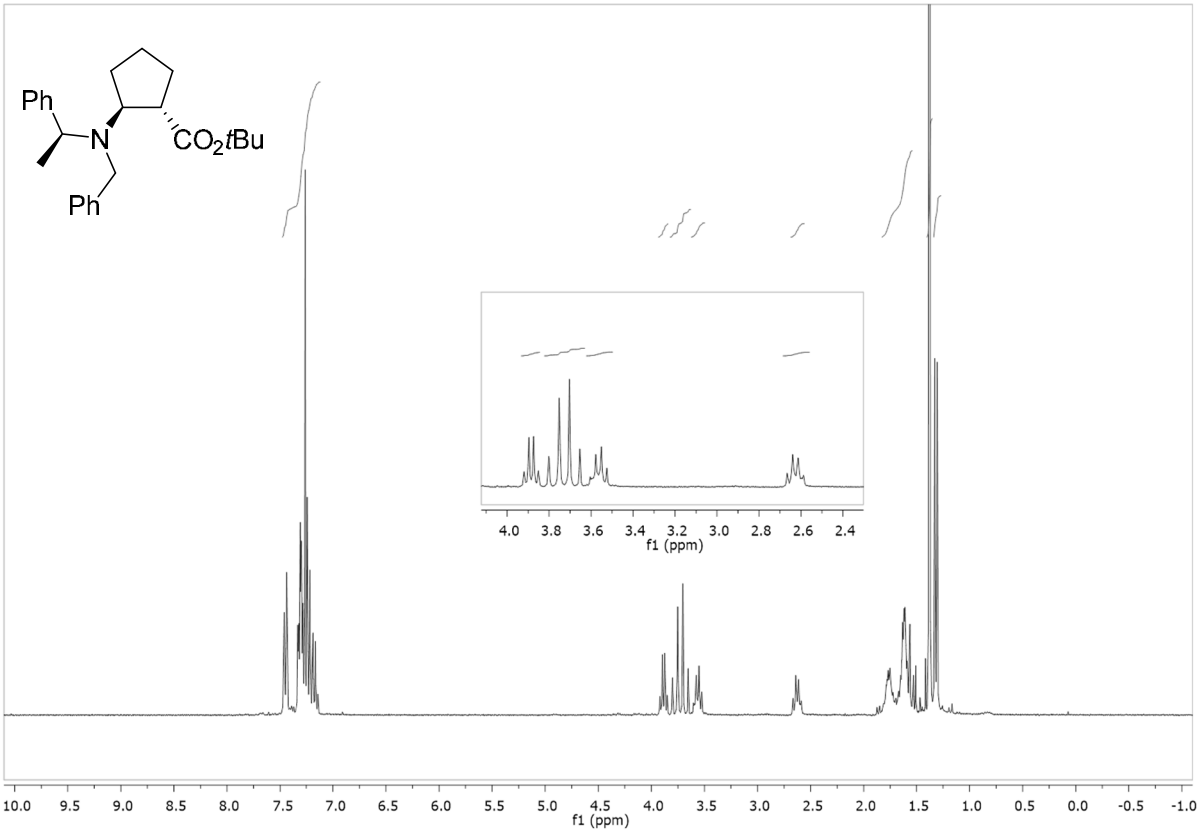


(75 MHz, $CDCl_3$)

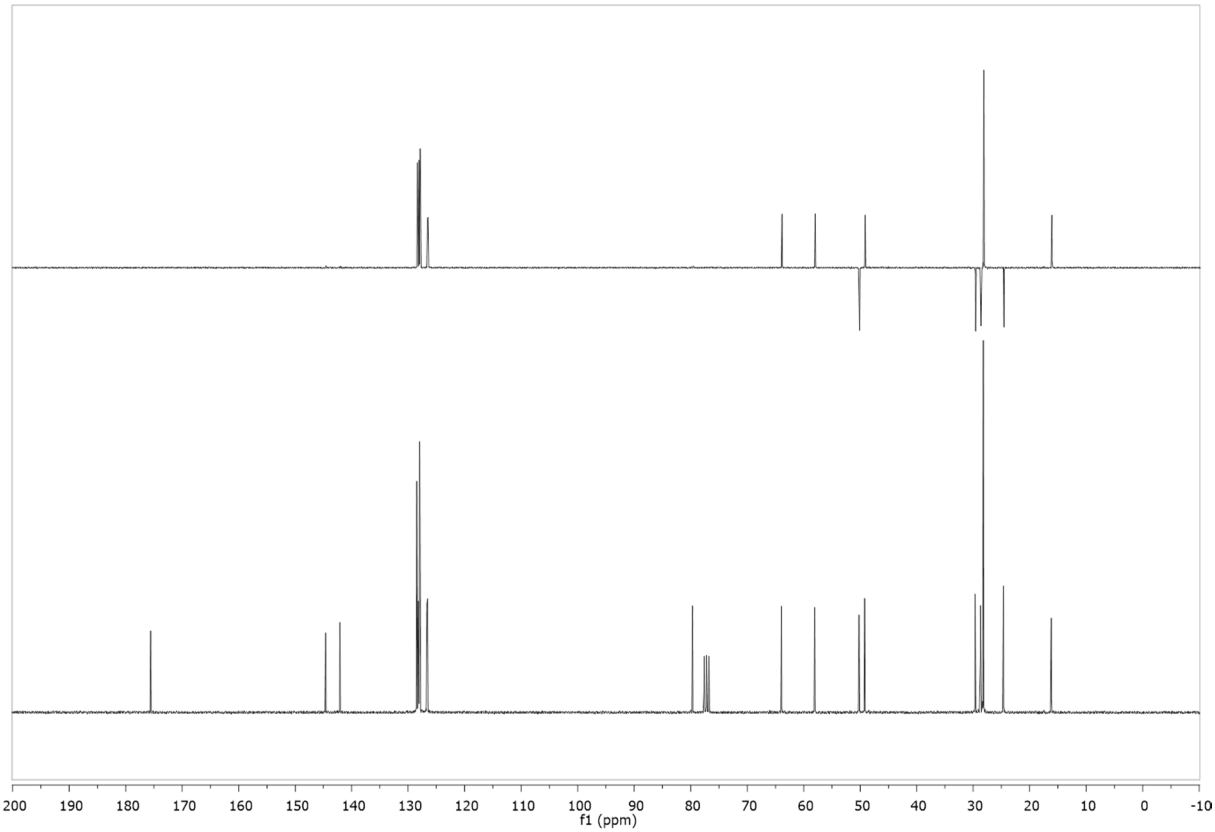

***tert*-Butyl (1*S*,2*S*)-2-((((9H-fluoren-9-yl)methoxy)carbonyl)amino)cyclopentane-1-carboxylate (184)** (300 MHz, $CDCl_3$)

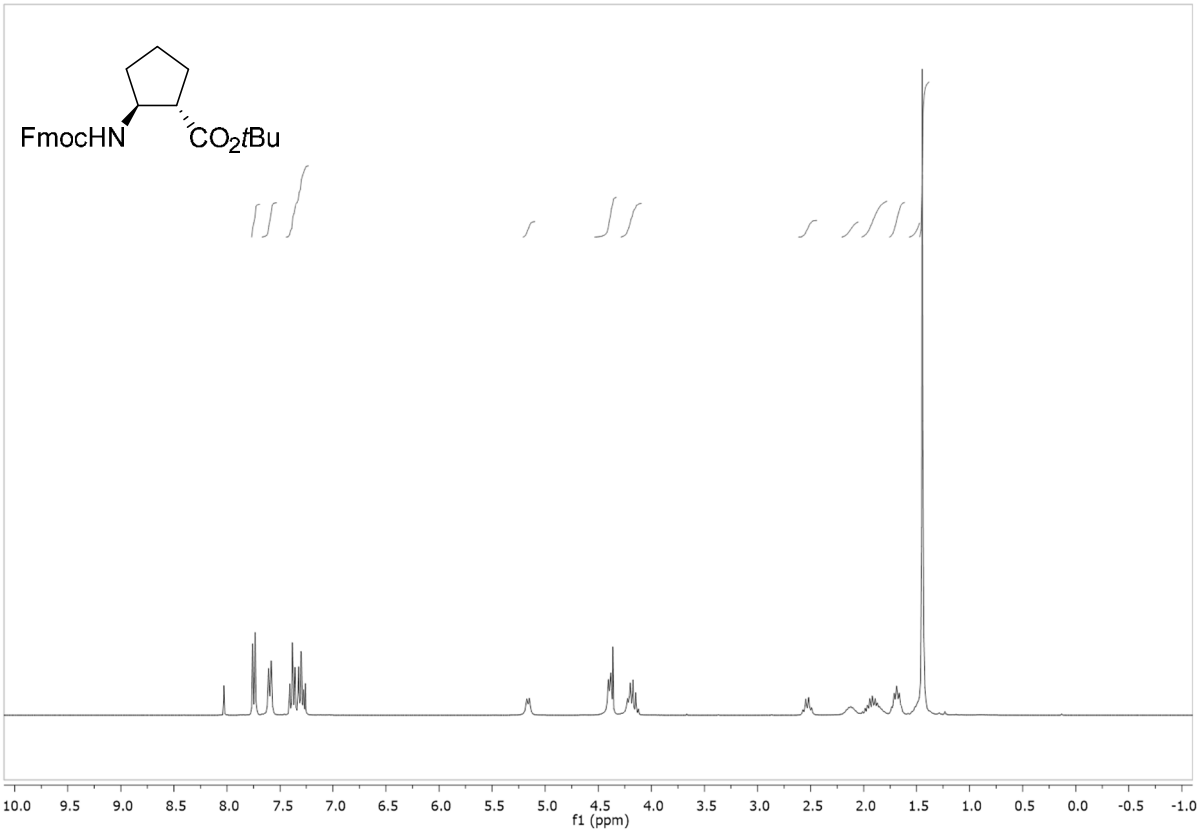


(75 MHz, $CDCl_3$)

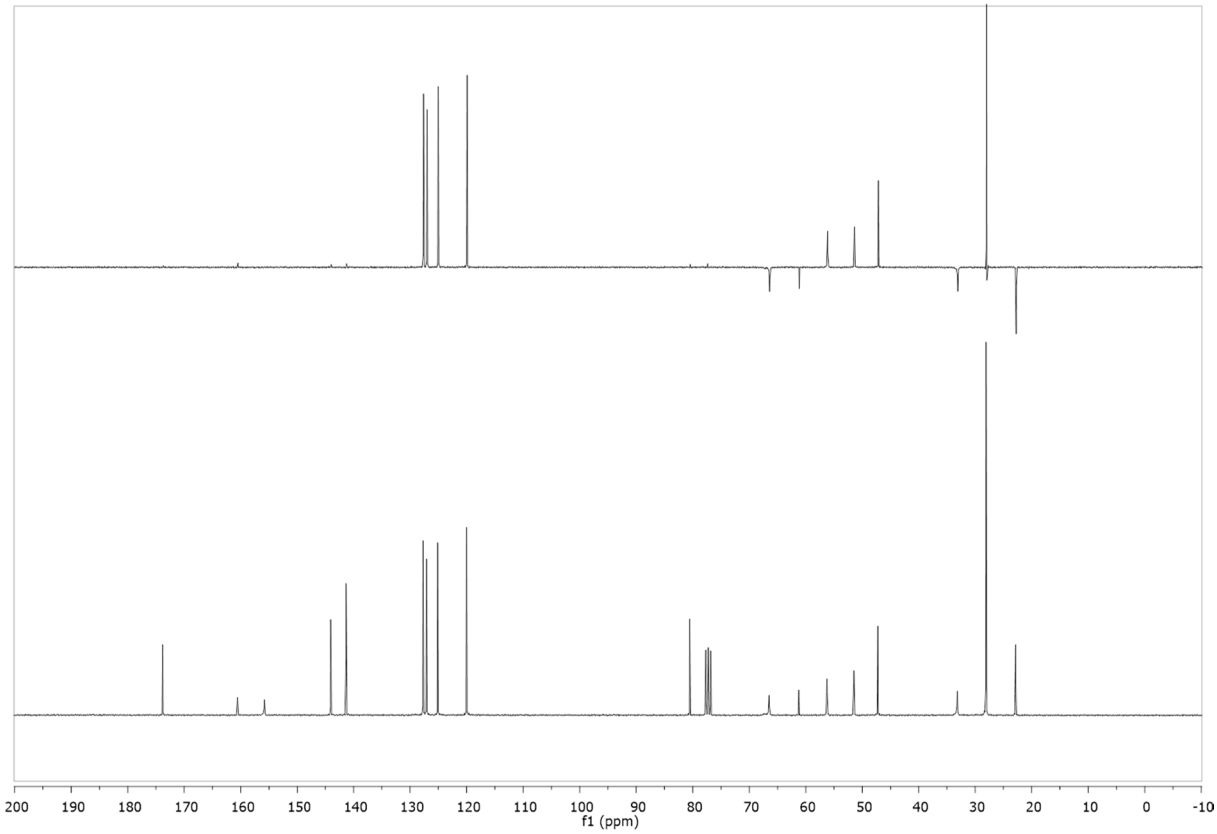

**(1*S*,2*S*)-2-((((9H-fluoren-9-yl)methoxy)carbonyl)amino)cyclopentane-1-carboxylic acid (185)** (300 MHz, $CD_3OD$)

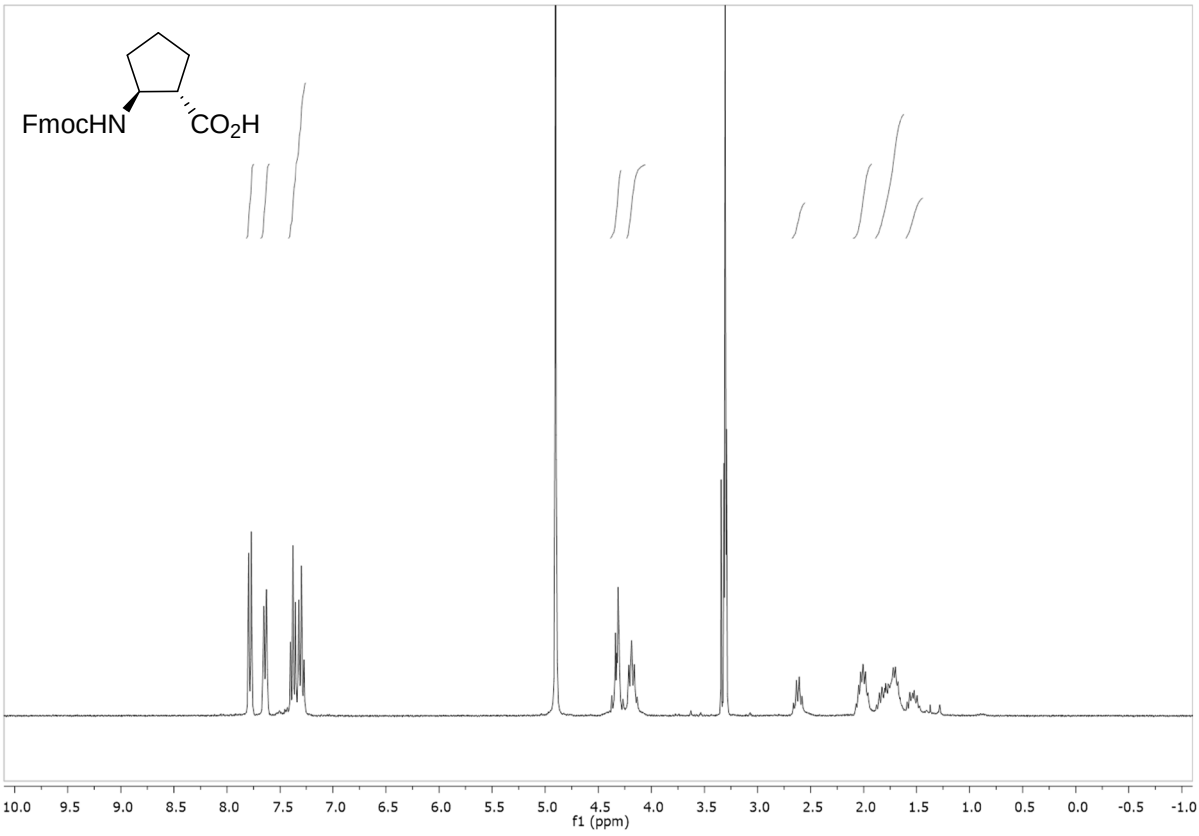


(75 MHz, $CD_3OD$)

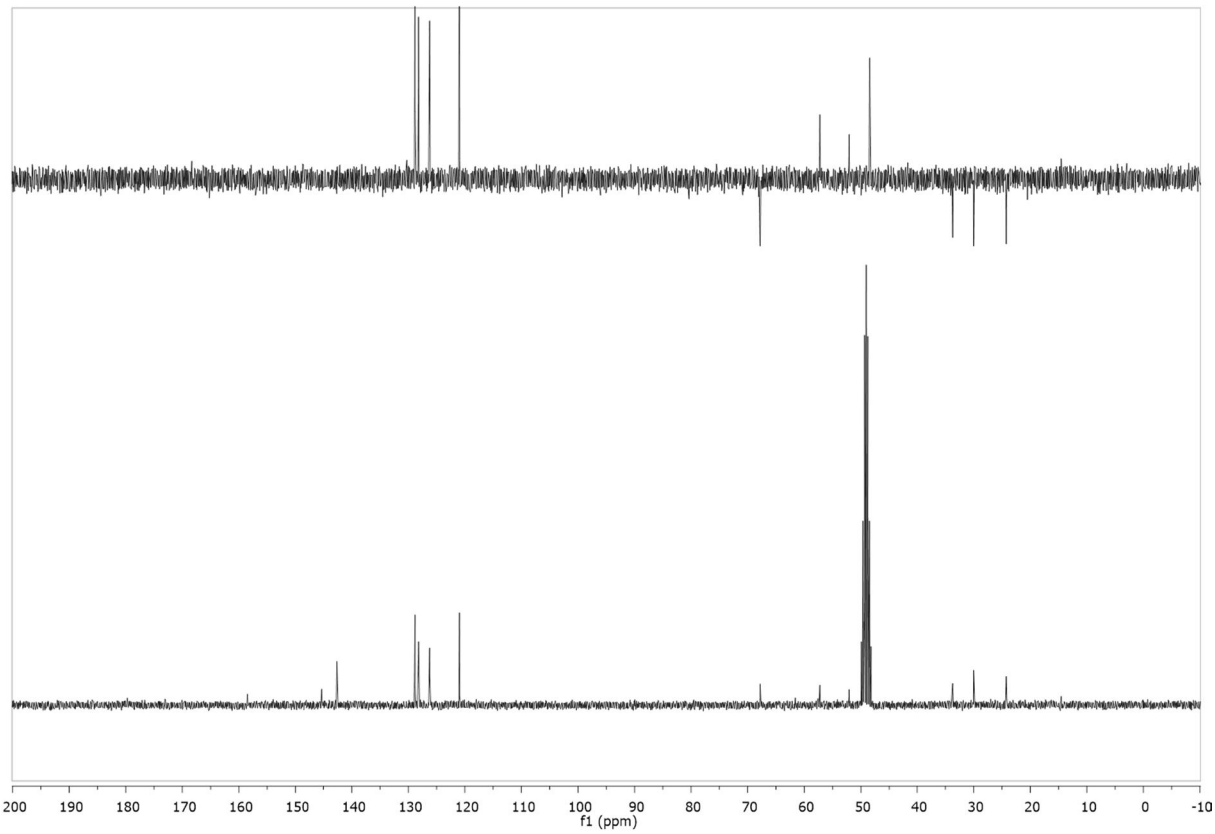

**di-*tert*-Butyl (1*S*,5*S*,6*S*)-2-azabicyclo[3.1.0]hex-3-ene-2,6-dicarboxylate (190)**
(300 MHz, $CDCl_3$)

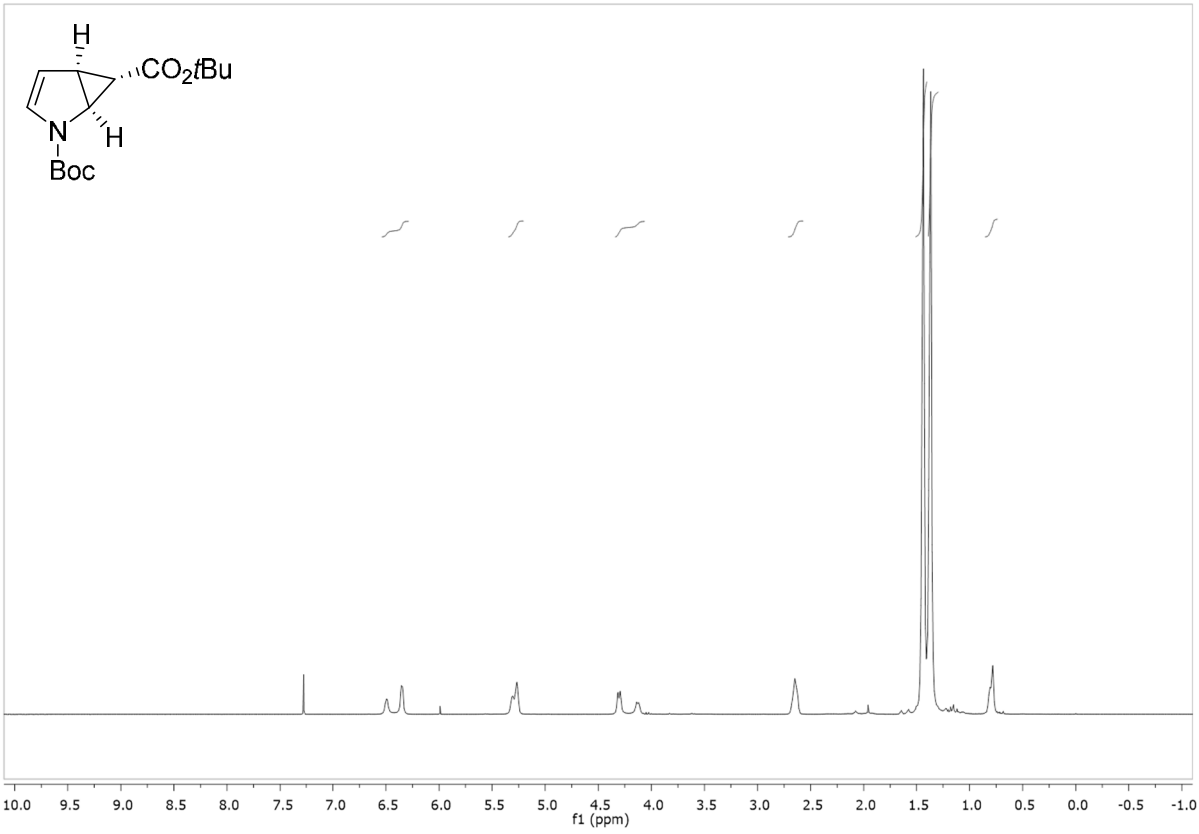


(75 MHz, $CDCl_3$)

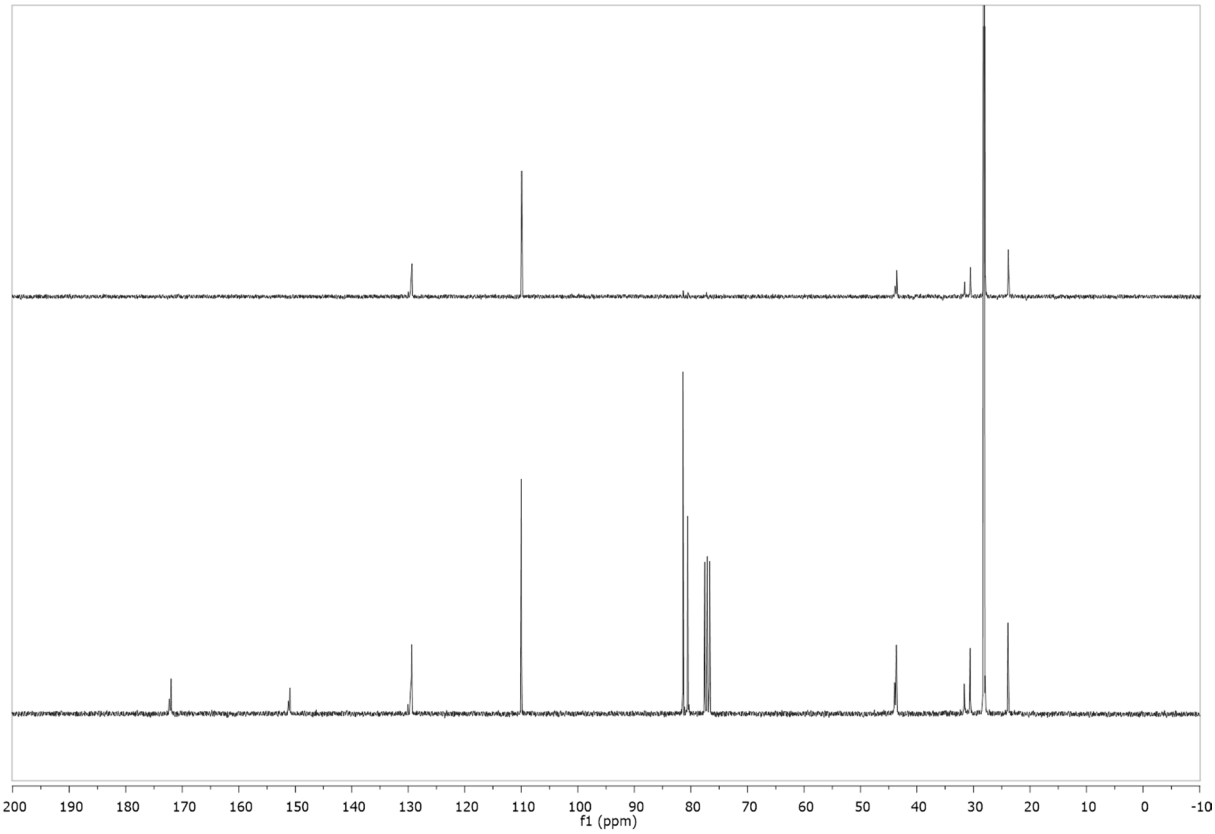

**(1*S*,5*S*,6*S*)-di-*tert*-butyl 2-azabicyclo[3.1.0]hexane-2,6-dicarboxylate (194)**
(300 MHz, $CDCl_3$)

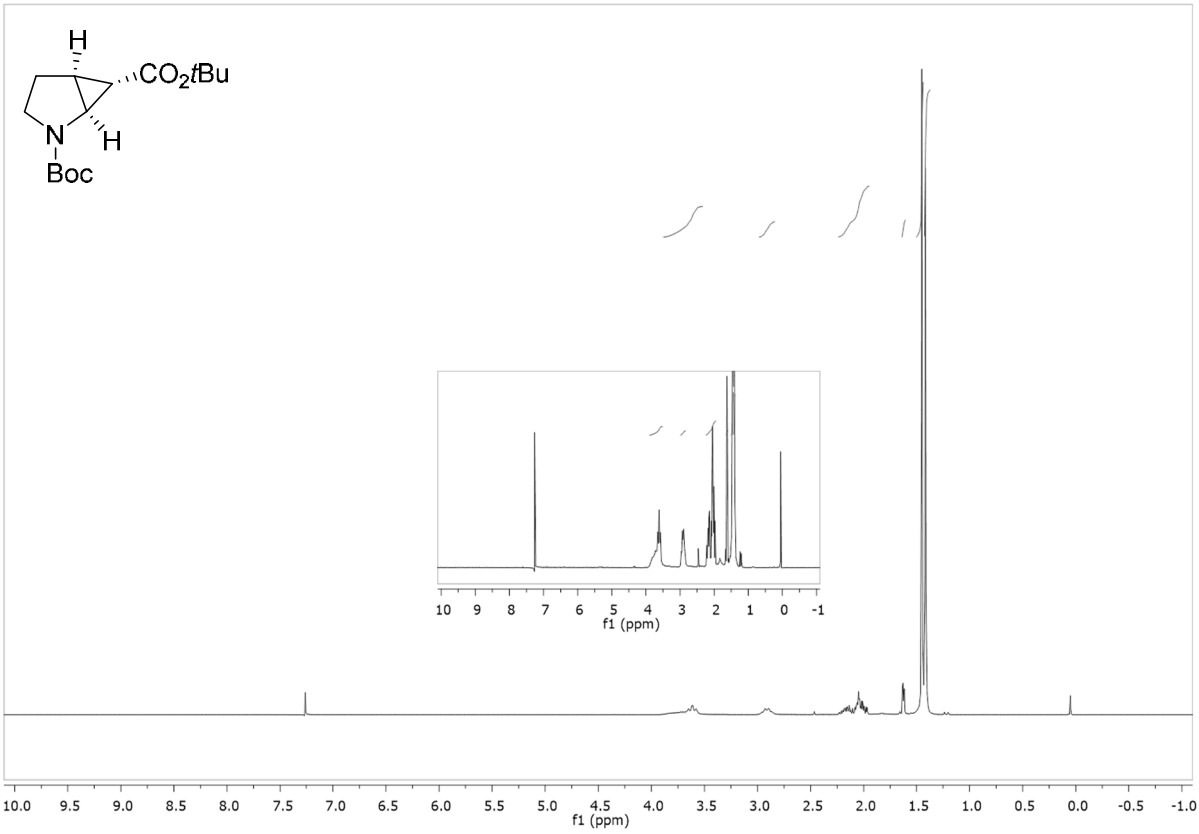


(75 MHz, $CDCl_3$)

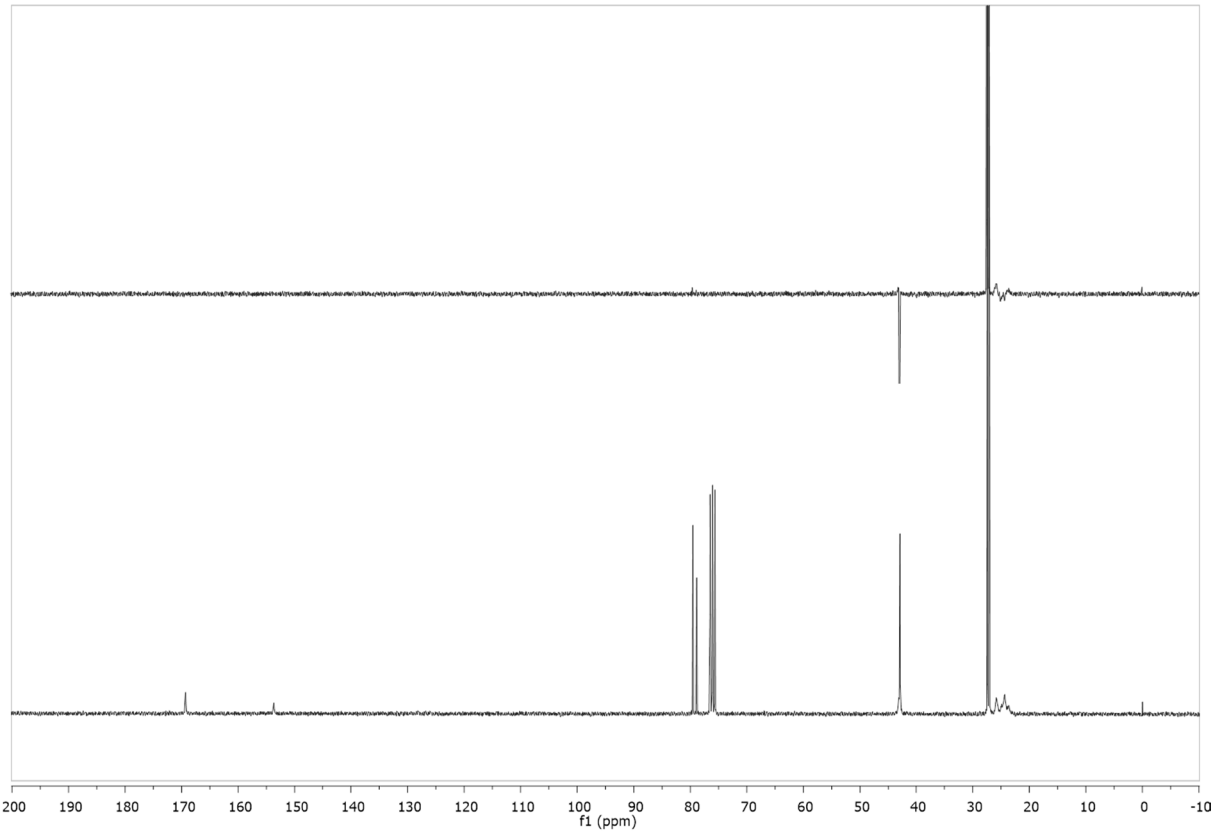

**(*S*)-*tert*-Butyl 3-(2-(*tert*-butoxy)-2-oxoethyl)pyrrolidine-1-carboxylate (189)**
(300 MHz, $CDCl_3$)

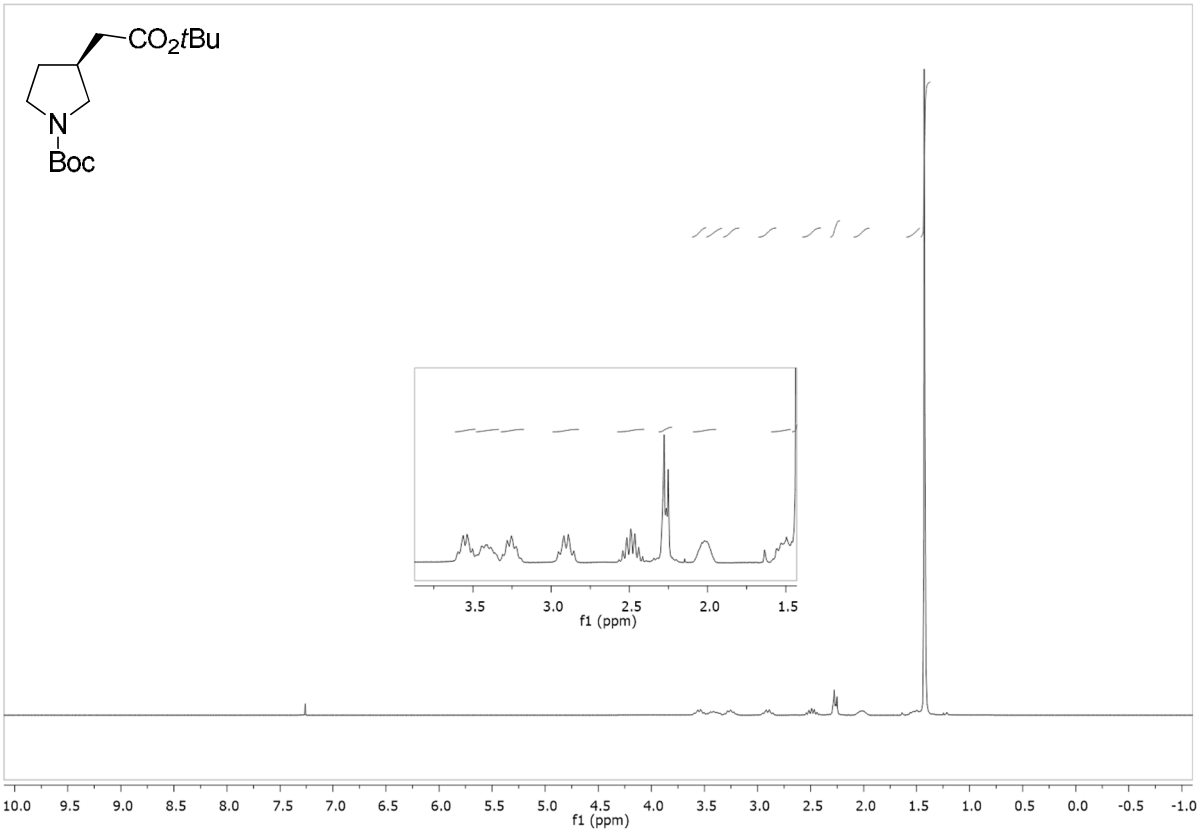


(75 MHz, $CDCl_3$)

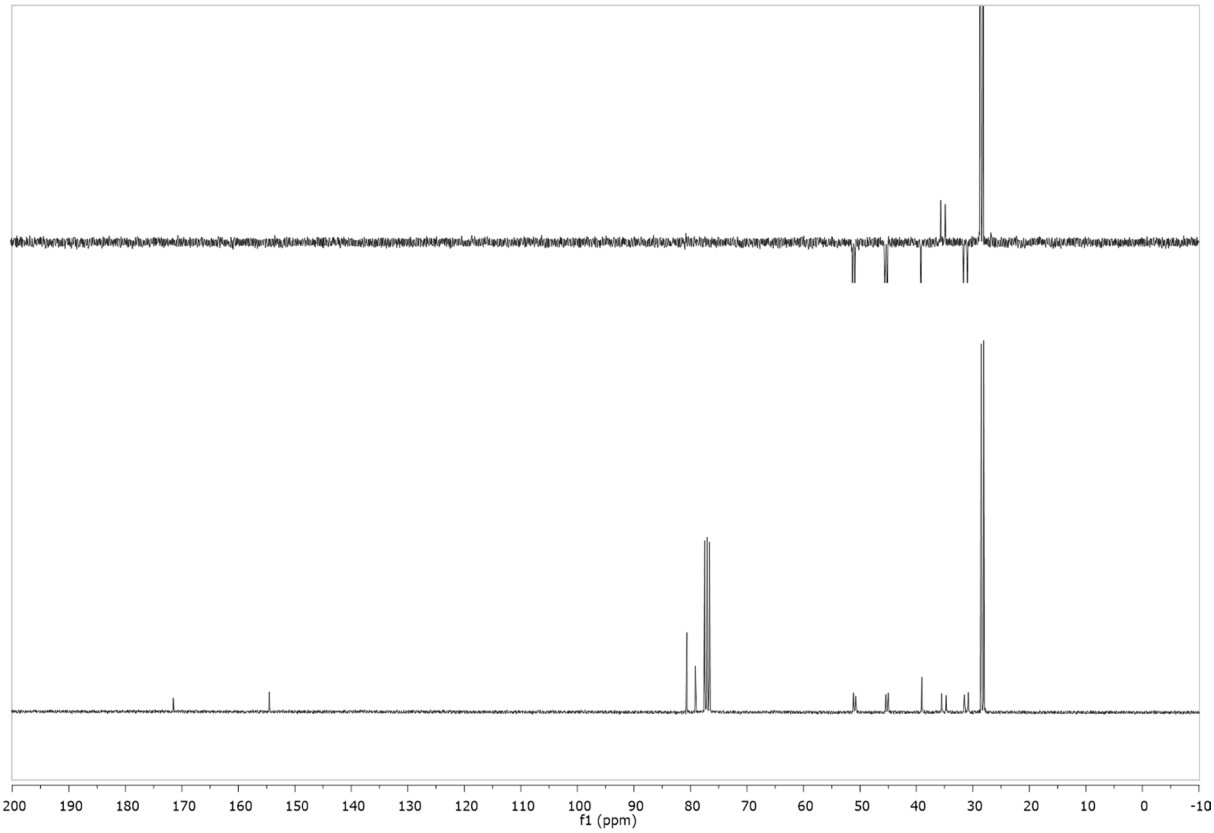

**(*S*)-2-(pyrrolidin-3-yl)acetic acid (188)** (400 MHz, $D_2O$)

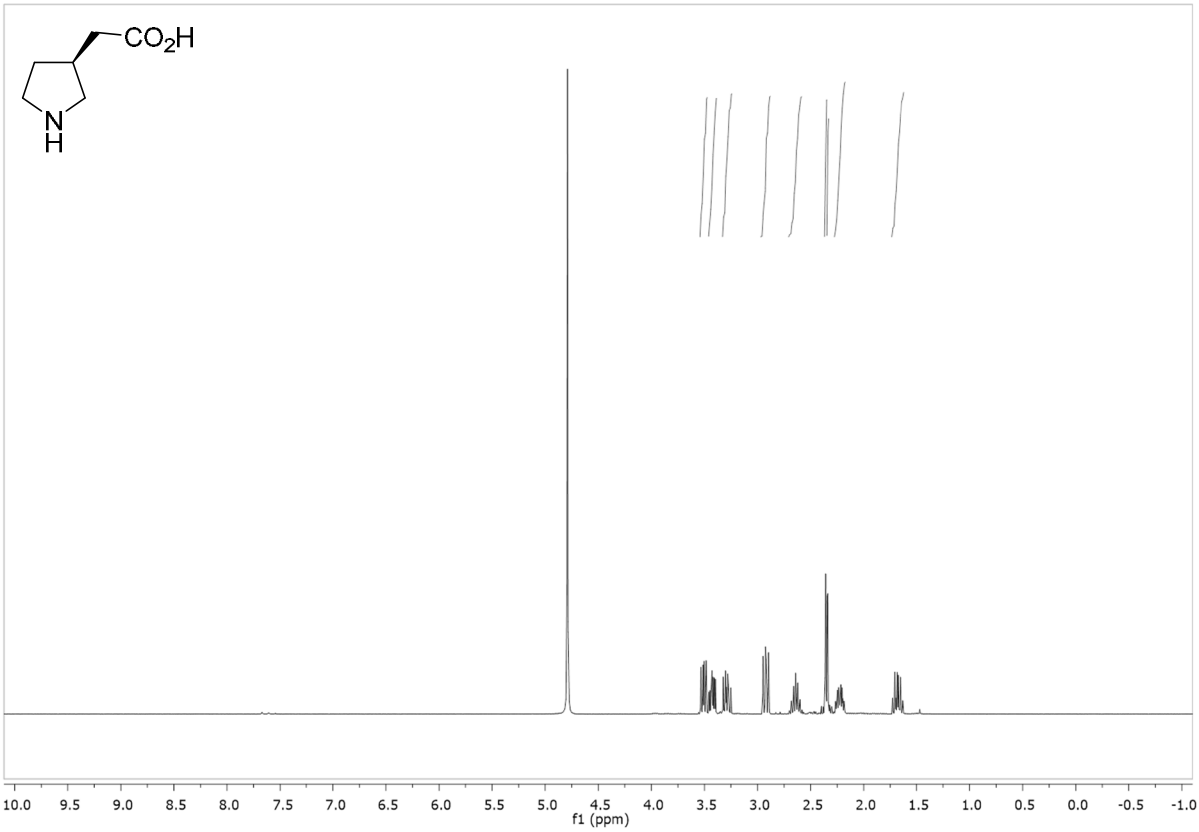


(101 MHz, $D_2O$)

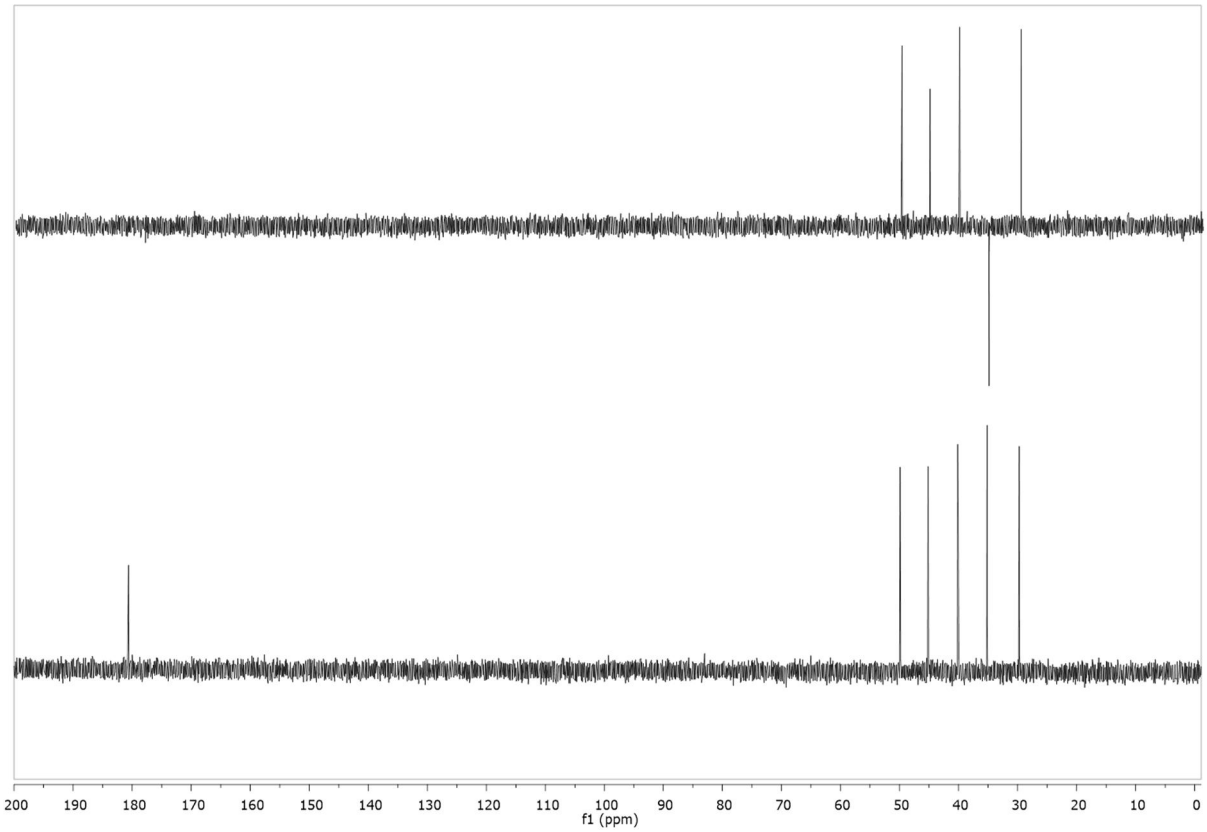

**di-*tert*-Butyl (1*S*,3*S*,4*R*,5*S*,6*S*)-4-azido-3-methoxy-2-azabicyclo[3.1.0]hexane-2,6-dicarboxylate (213)** (400 MHz, $CDCl_3$)

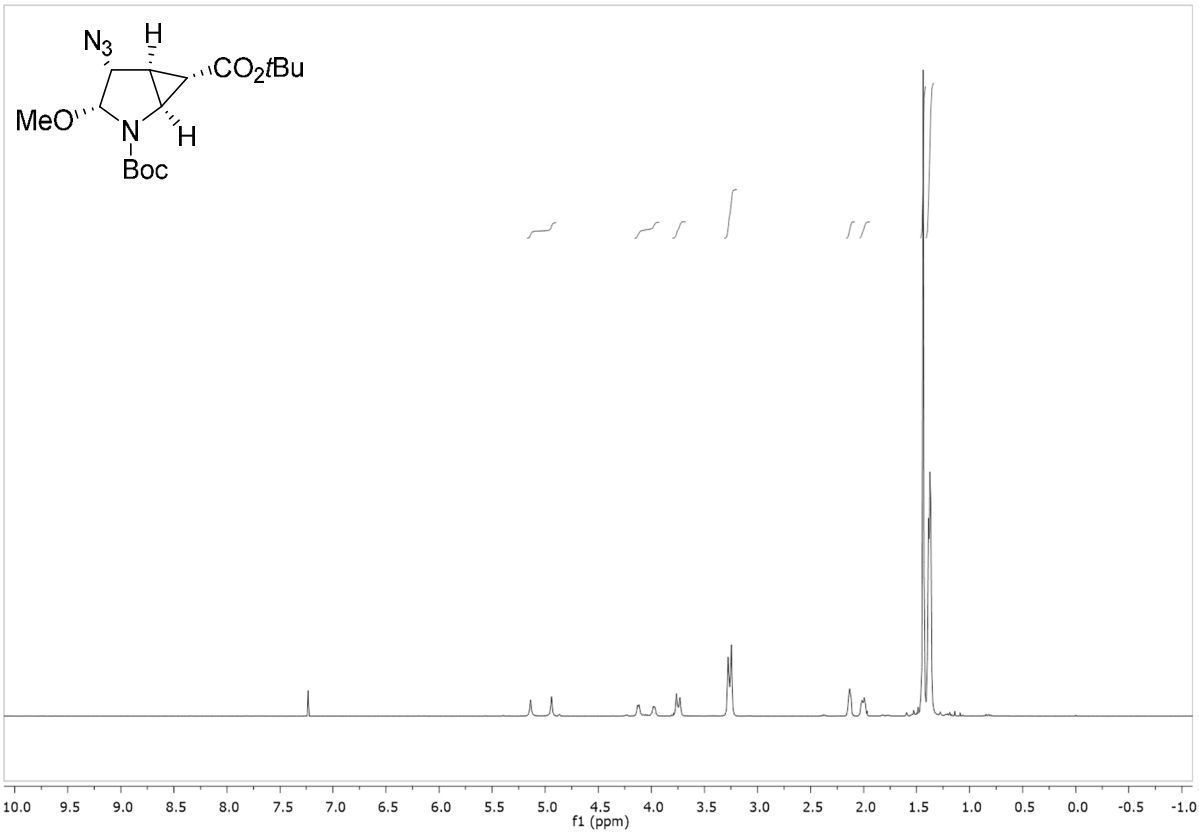


(101 MHz, $CDCl_3$)

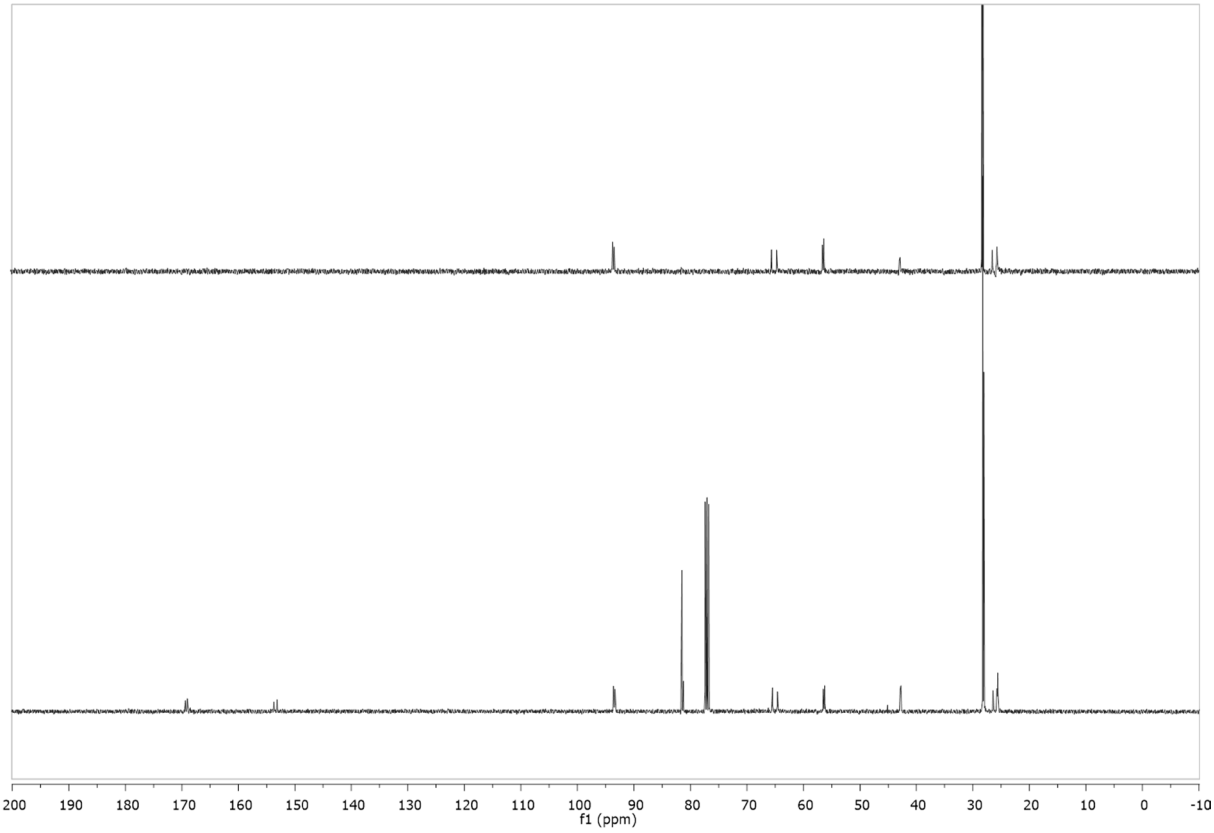

NOESY (400 MHz, $CDCl_3$)

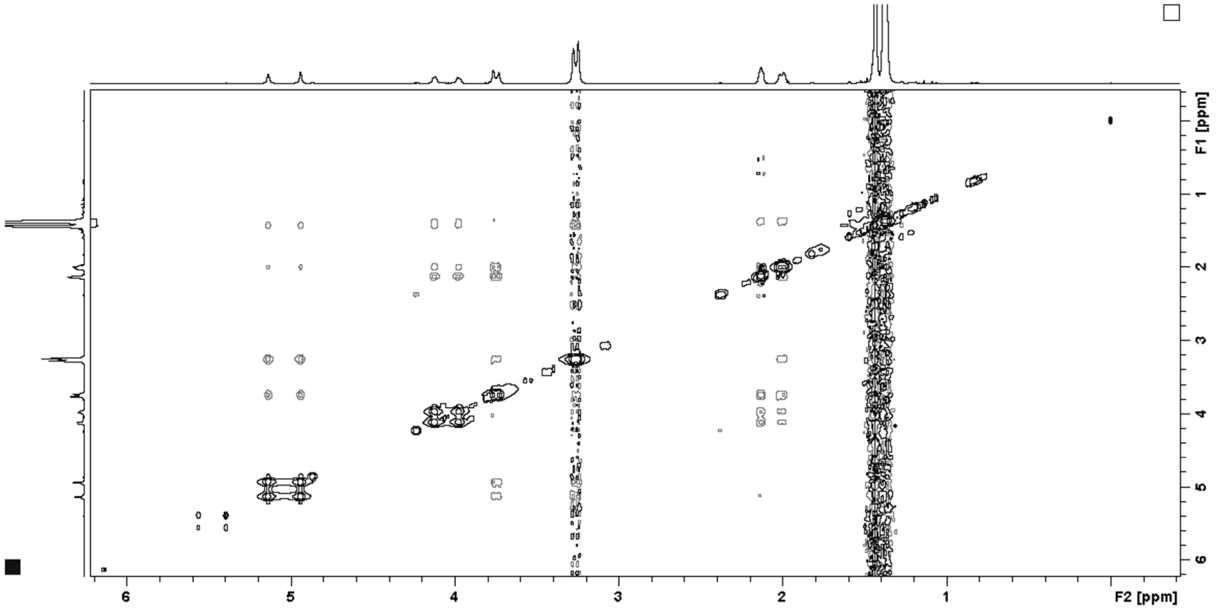

**di-*tert*-Butyl (1*S*,3*S*,4*R*,5*R*,6*S*)-4-amino-3-methoxy-2-azabicyclo[3.1.0]hexane-2,6-dicarboxylate (214)** (300 MHz, $CDCl_3$)

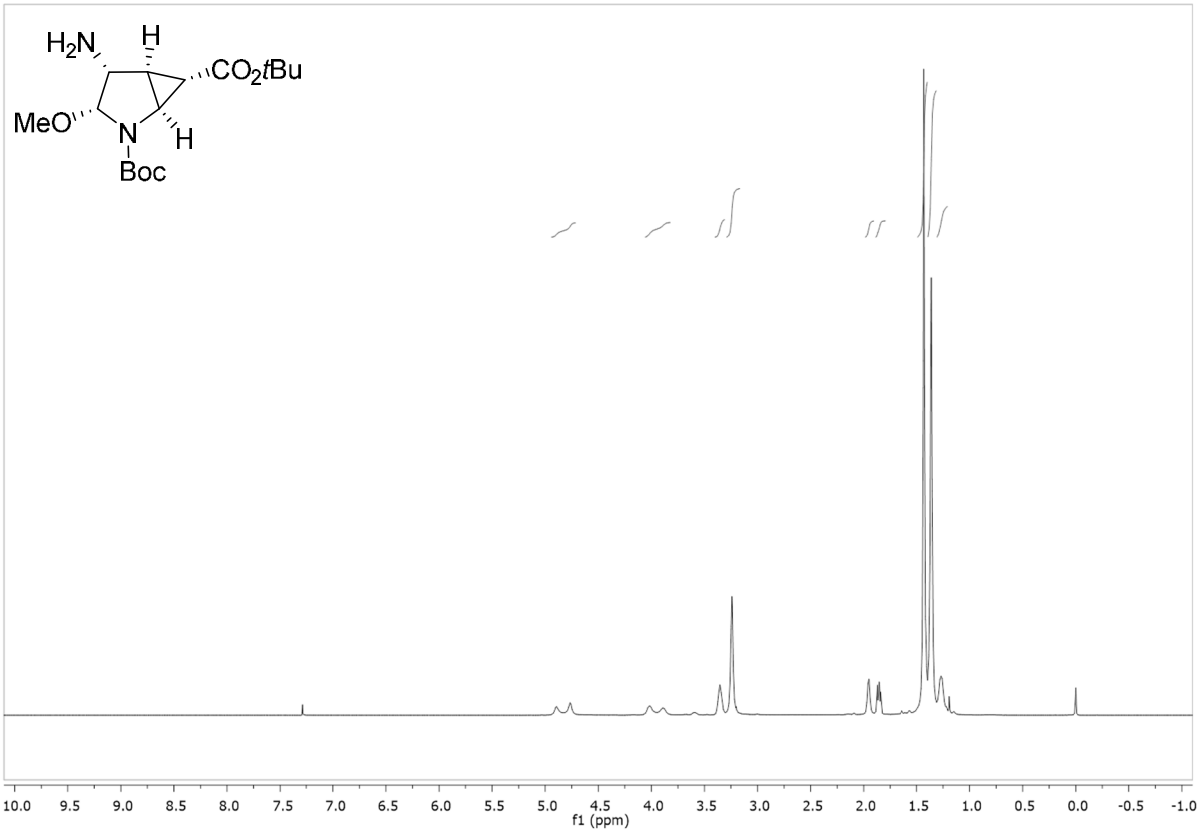


(75 MHz, $CDCl_3$)

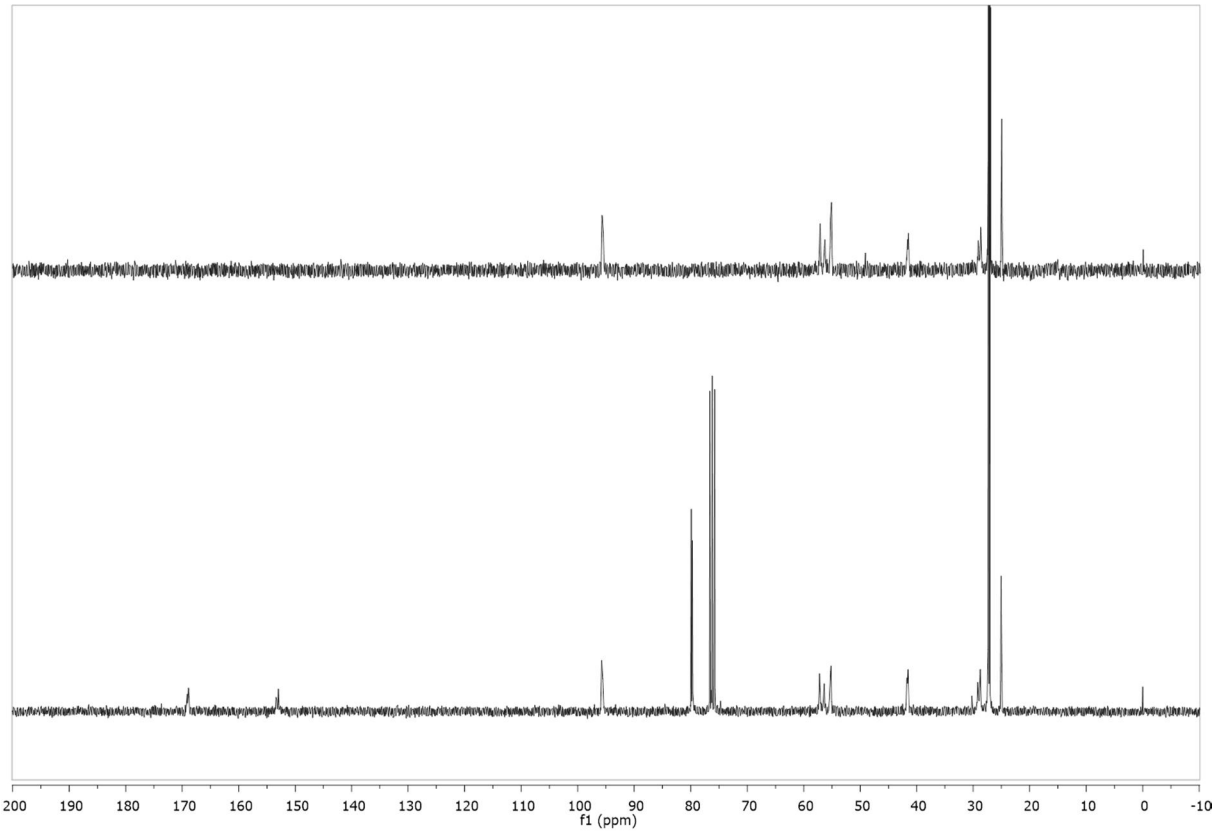

**di-*tert*-Butyl (1*S*,3*S*,4*R*,5*R*,6*S*)-4-((((9H-fluoren-9-yl)methoxy)carbonyl)amino)-3-methoxy-2-azabicyclo[3.1.0]hexane-2,6-dicarboxylate (215)** (300 MHz, $CDCl_3$)

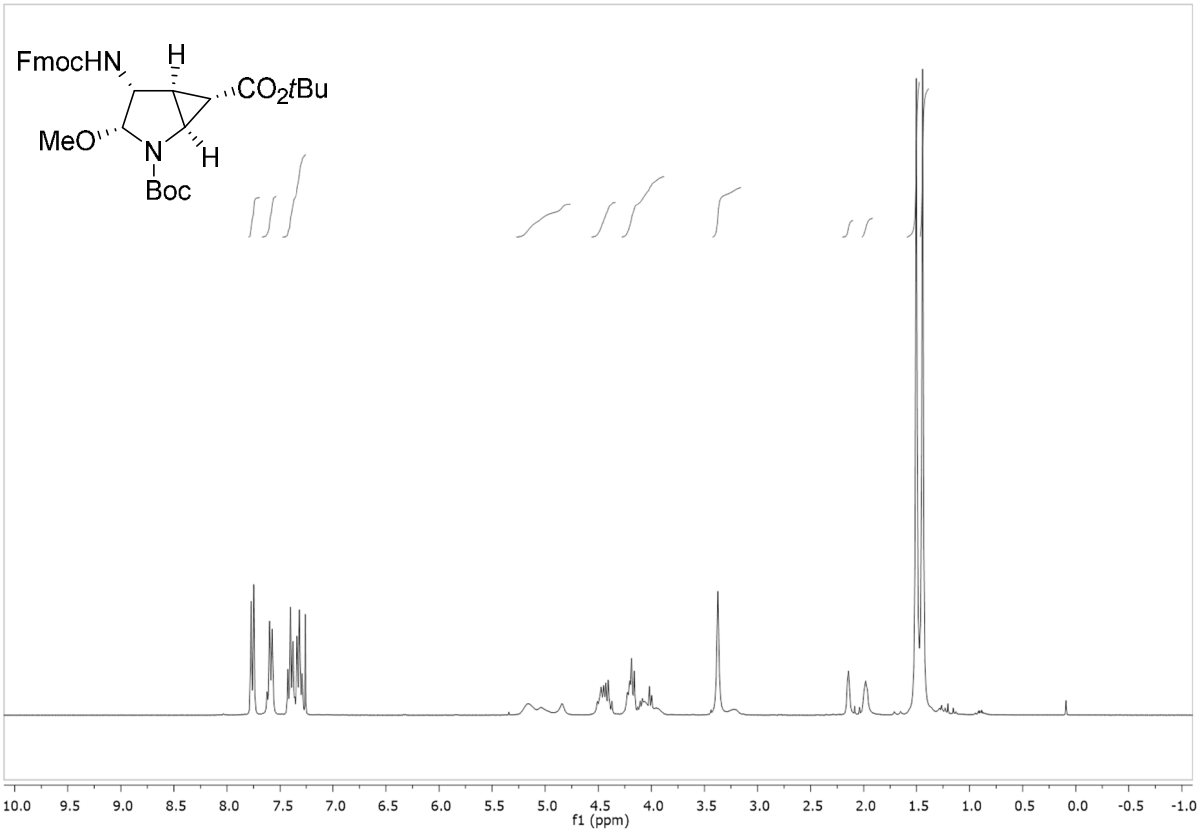


(75 MHz, $CDCl_3$)

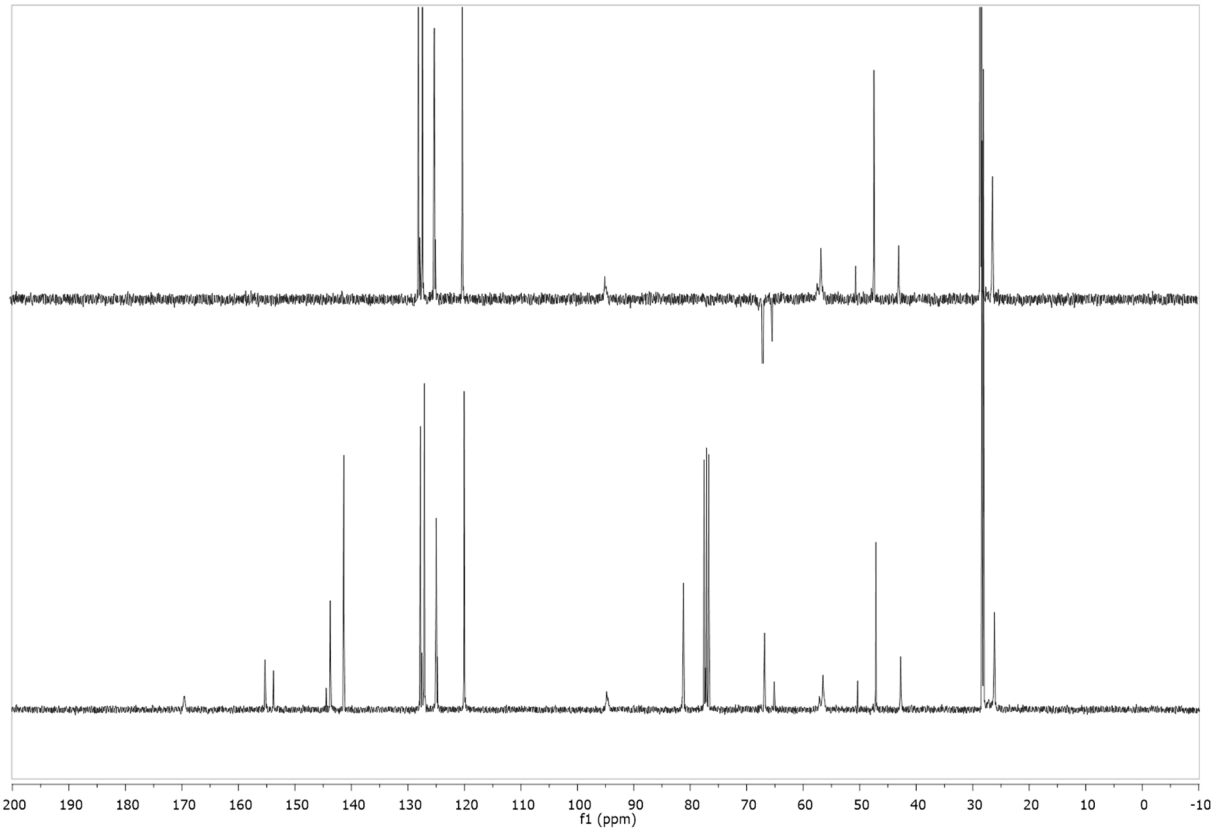

***tert*-Butyl-(3*R*,4*S*)-3-((((9H-fluoren-9-yl)methoxy)carbonyl)amino)-4-(2-(*tert*-butoxy)-2-oxoethyl)pyrrolidine-1-carboxylate (216)** (300 MHz, $CDCl_3$)

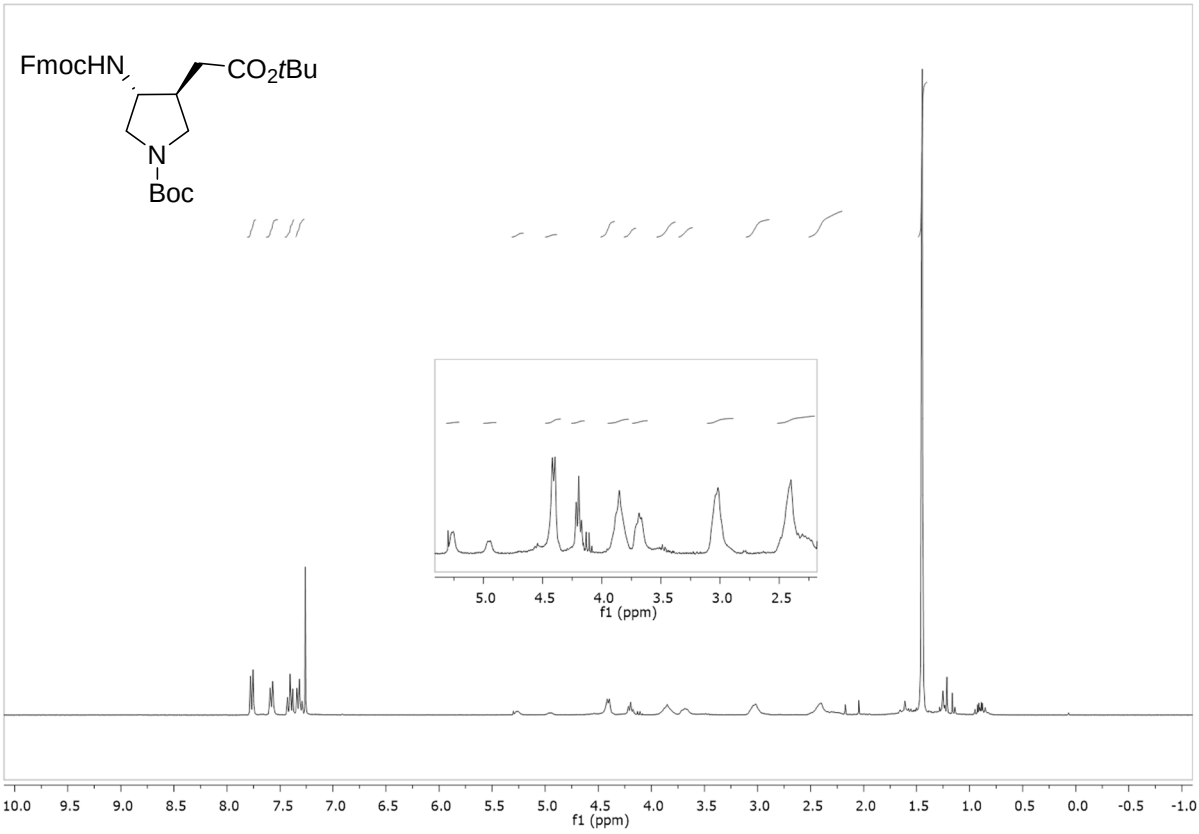


(75 MHz, $CDCl_3$)

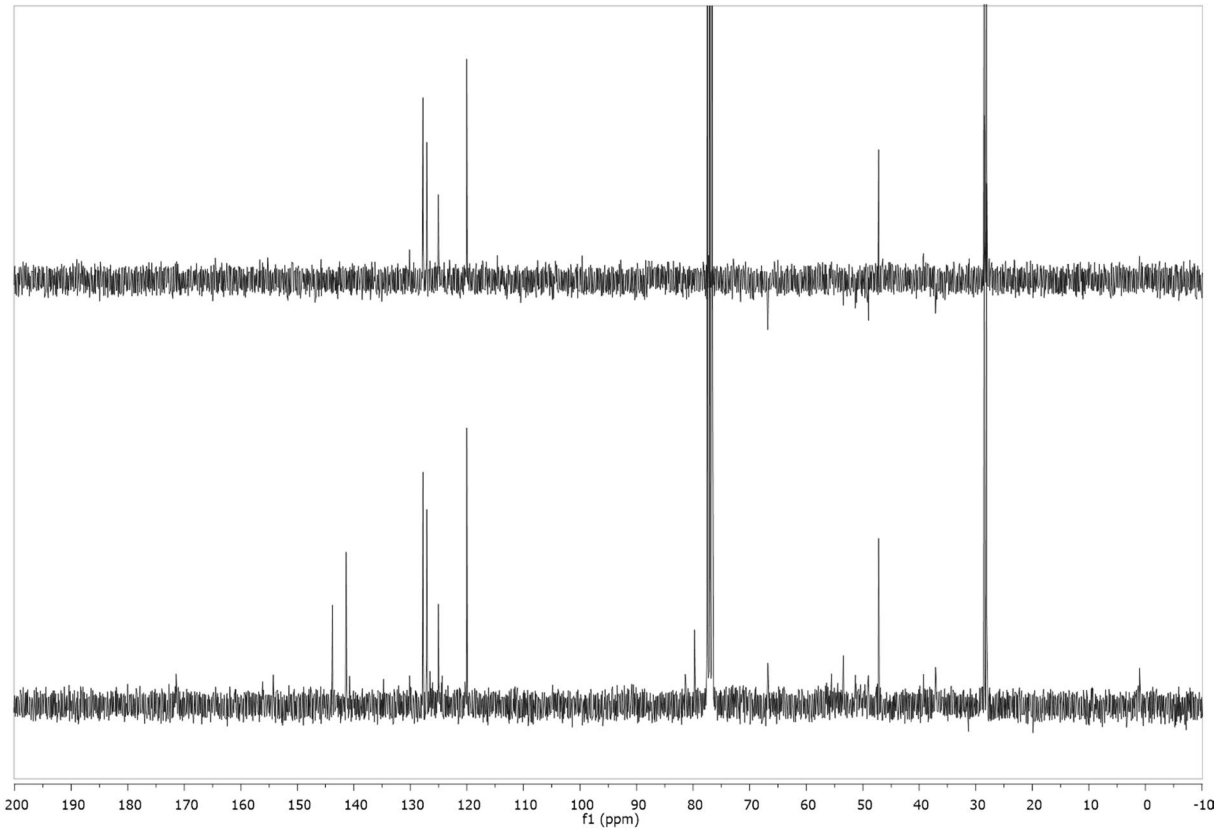

**2-((3*S*,4*R*)-4-((((9H-fluoren-9-yl)methoxy)carbonyl)amino)-1-(*tert*-butoxycarbonyl)pyrrolidin-3-yl)acetic acid (217)** (400 MHz, $CD_3OD$)

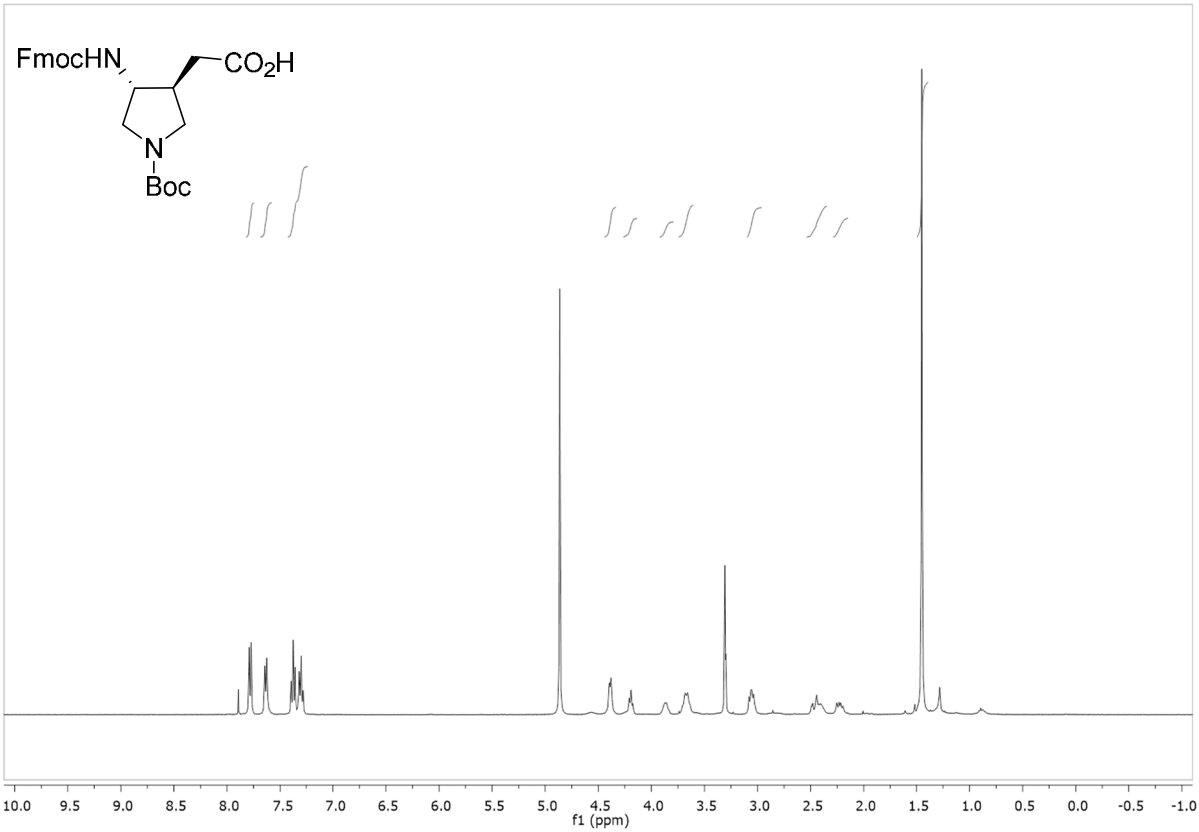


(75 MHz, $CD_3OD$)

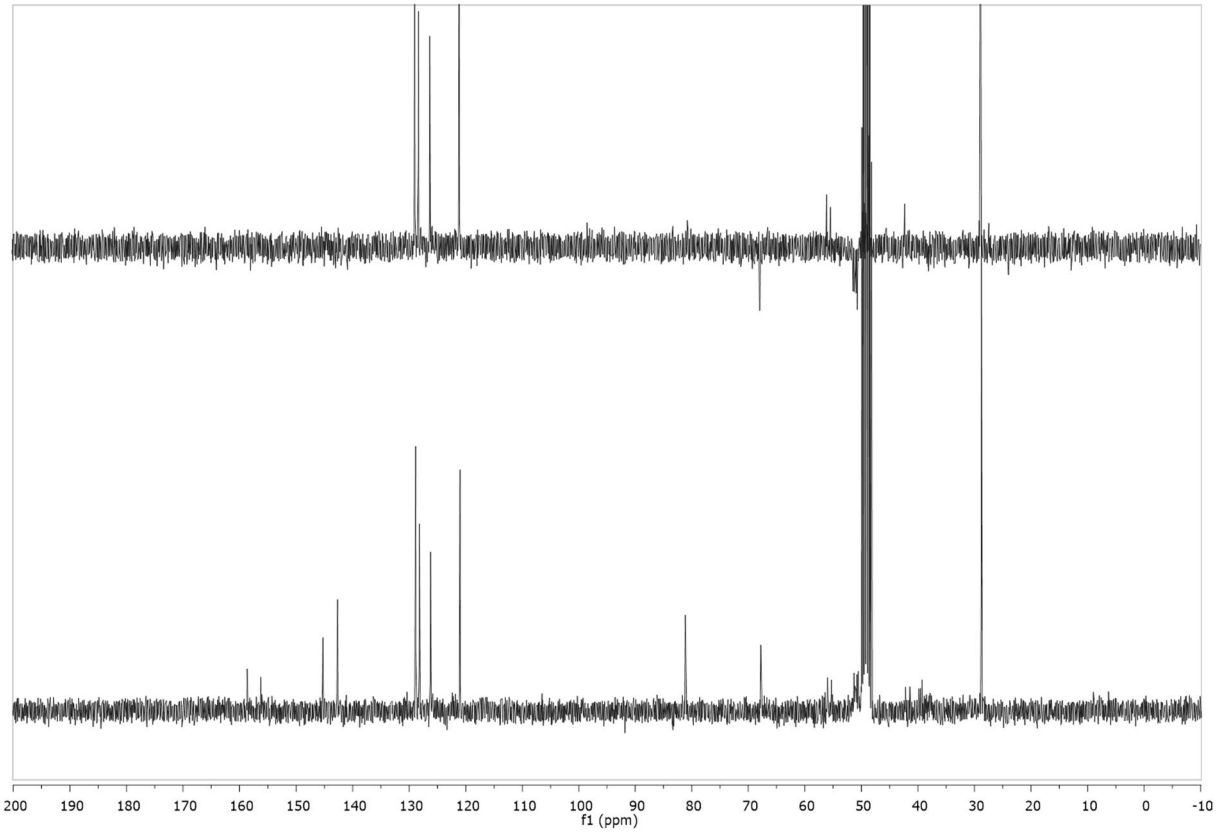

***tert*-Butyl (3a*S*,6a*R*)-2-oxohexahydro-6H-furo[2,3-b]pyrrole-6-carboxylate (222)**
(300 MHz, $CDCl_3$)

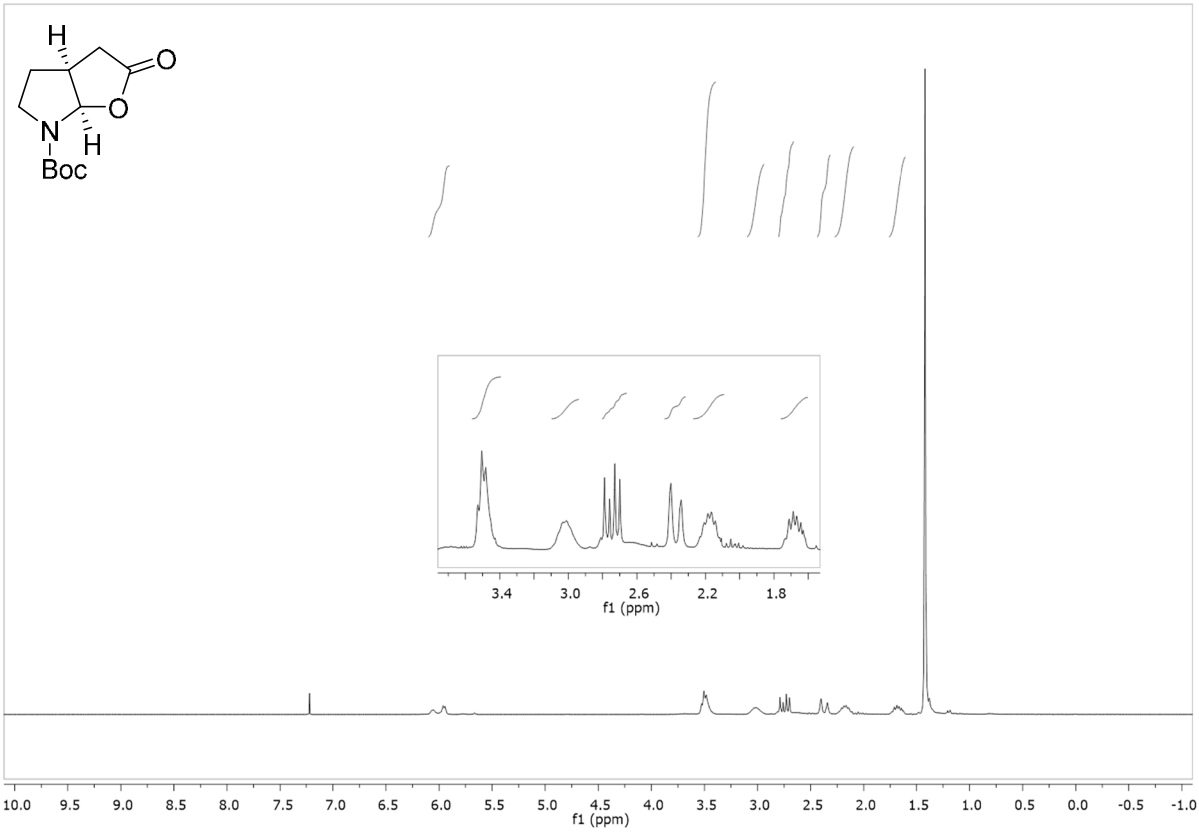


(101 MHz, $CDCl_3$)

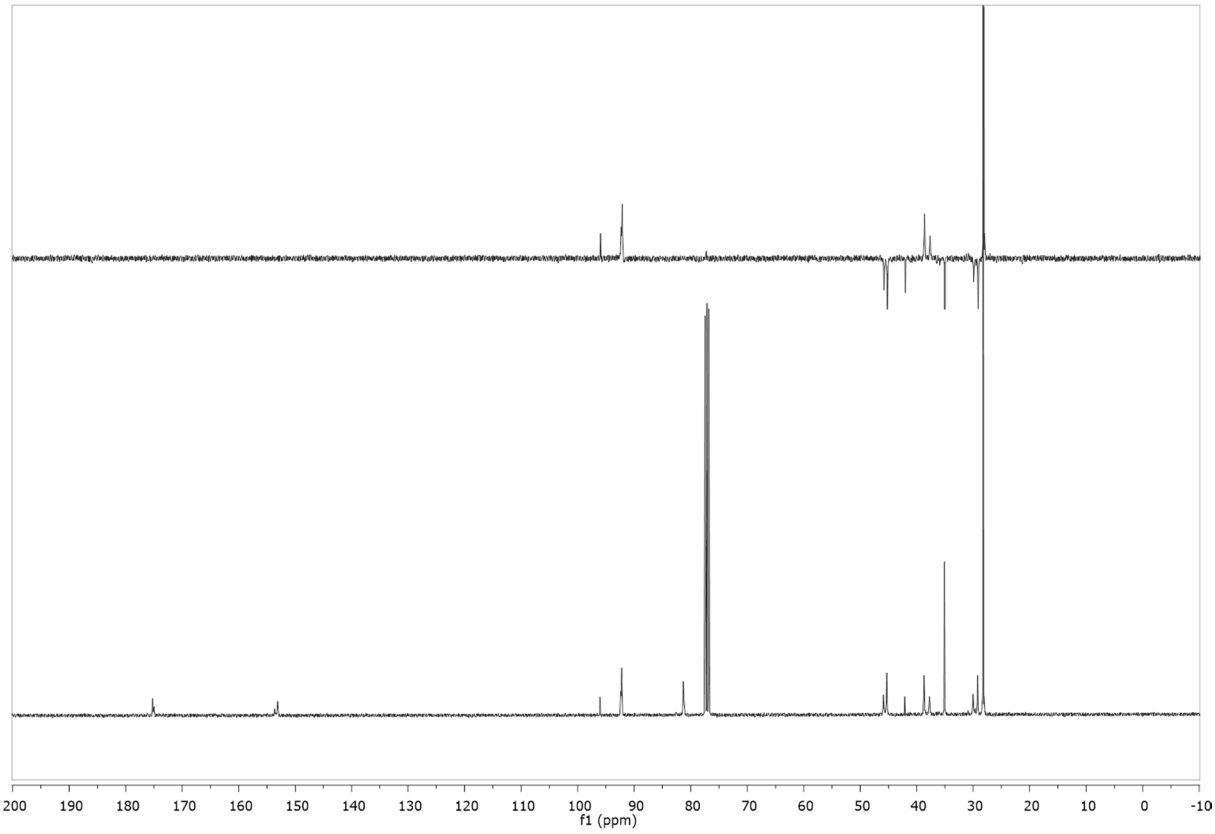

**2-((3*S*)-2-Allyl-1-(*tert*-butoxycarbonyl)pyrrolidin-3-yl)acetic acid (224)** (*dr* = 1:1.2)
(300 MHz, $CDCl_3$)

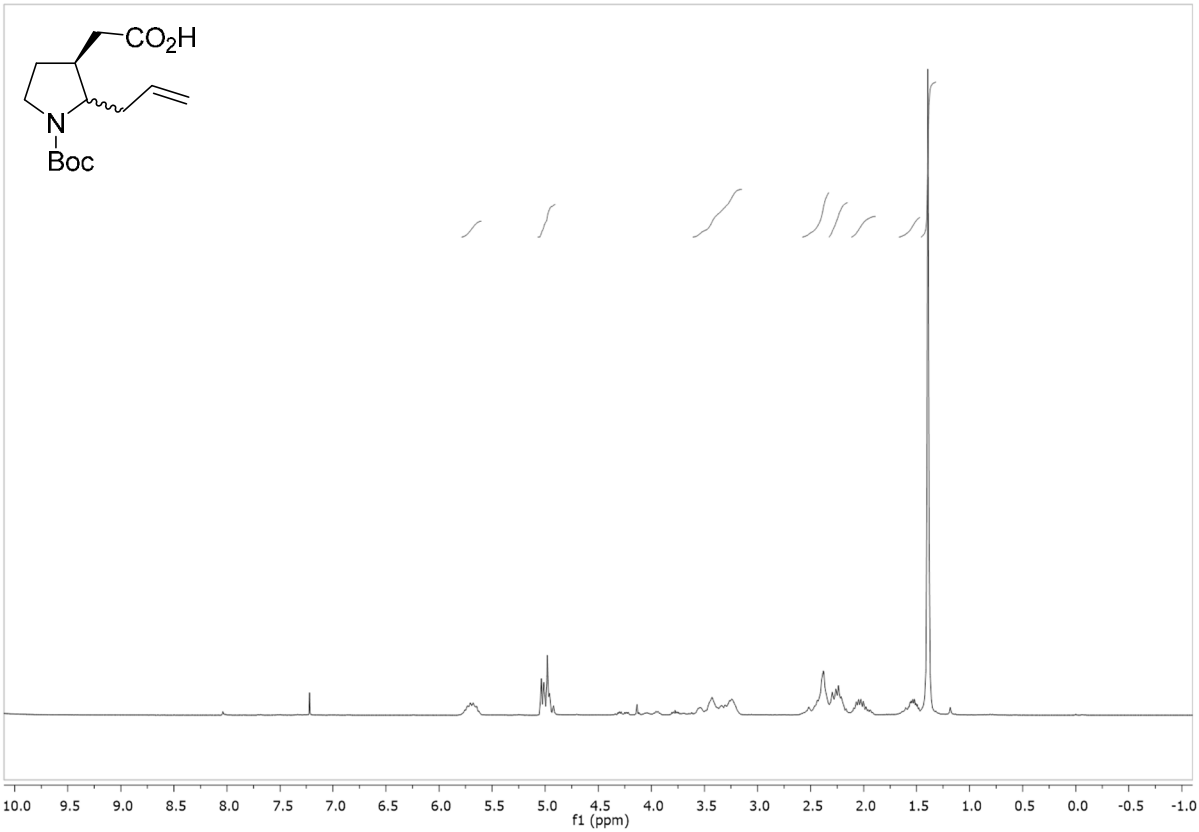


**NMR** (75 MHz, $CDCl_3$)

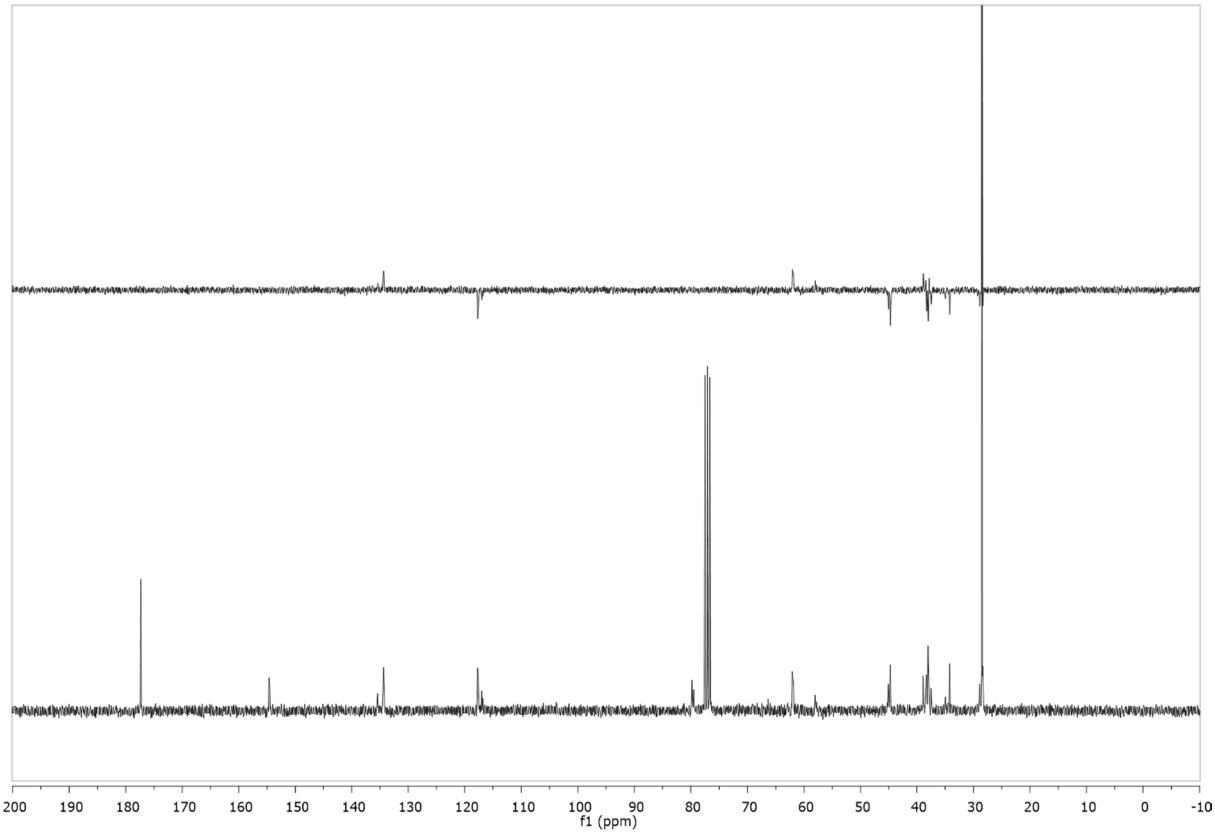

**(1*S*,5*S*,6*S*)-2-*tert*-Butyl 6-methyl 2-azabicyclo[3.1.0]hex-3-ene-2,6-dicarboxylate (201)** (300 MHz, $CDCl_3$)

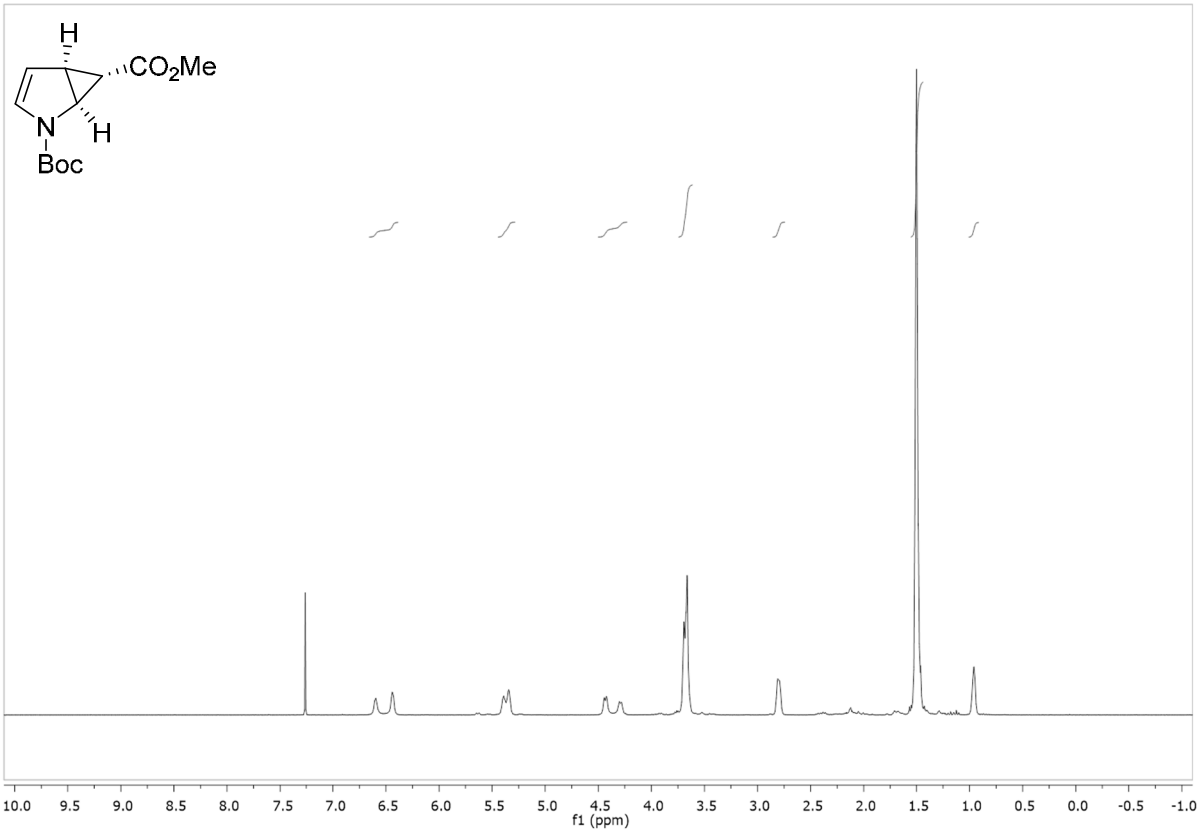


(75 MHz, $CDCl_3$)

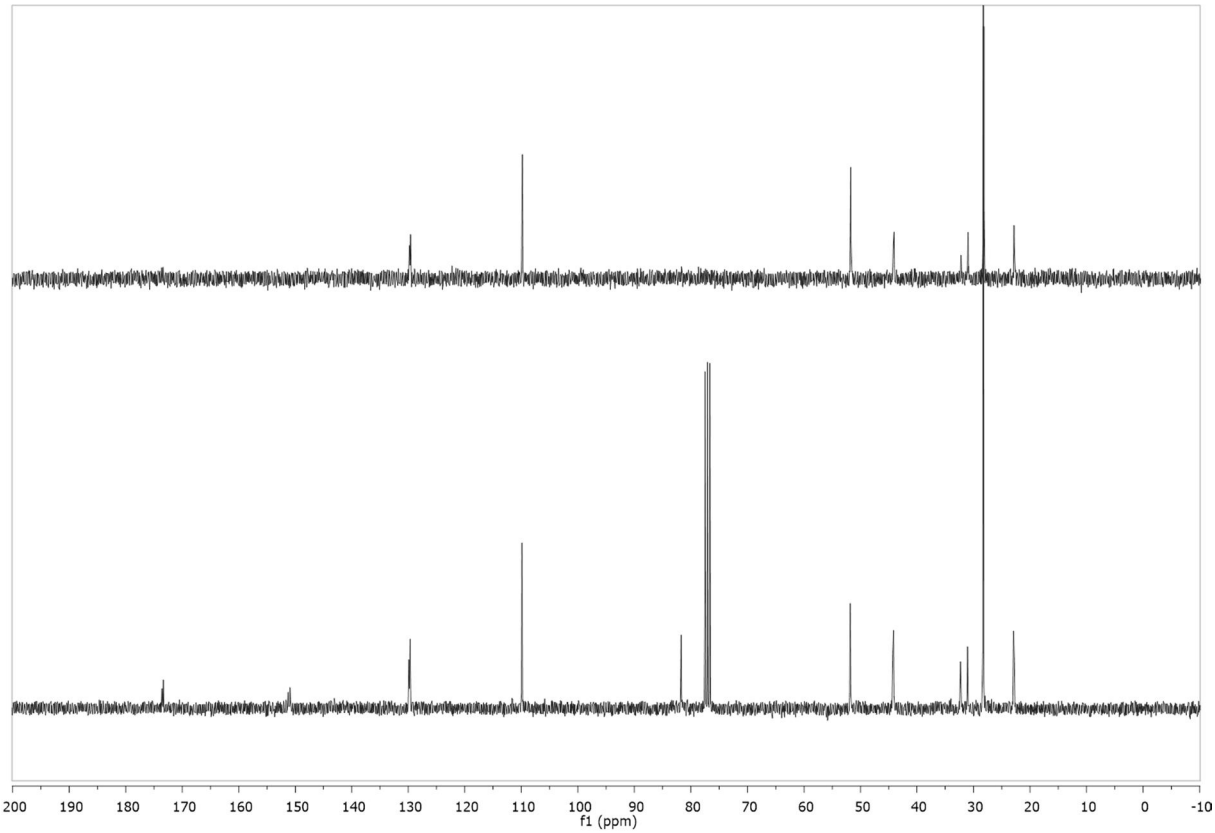

**di-*tert*-Butyl (*S*)-piperidine-1,3-dicarboxylate (200)** (300 MHz, $CDCl_3$)

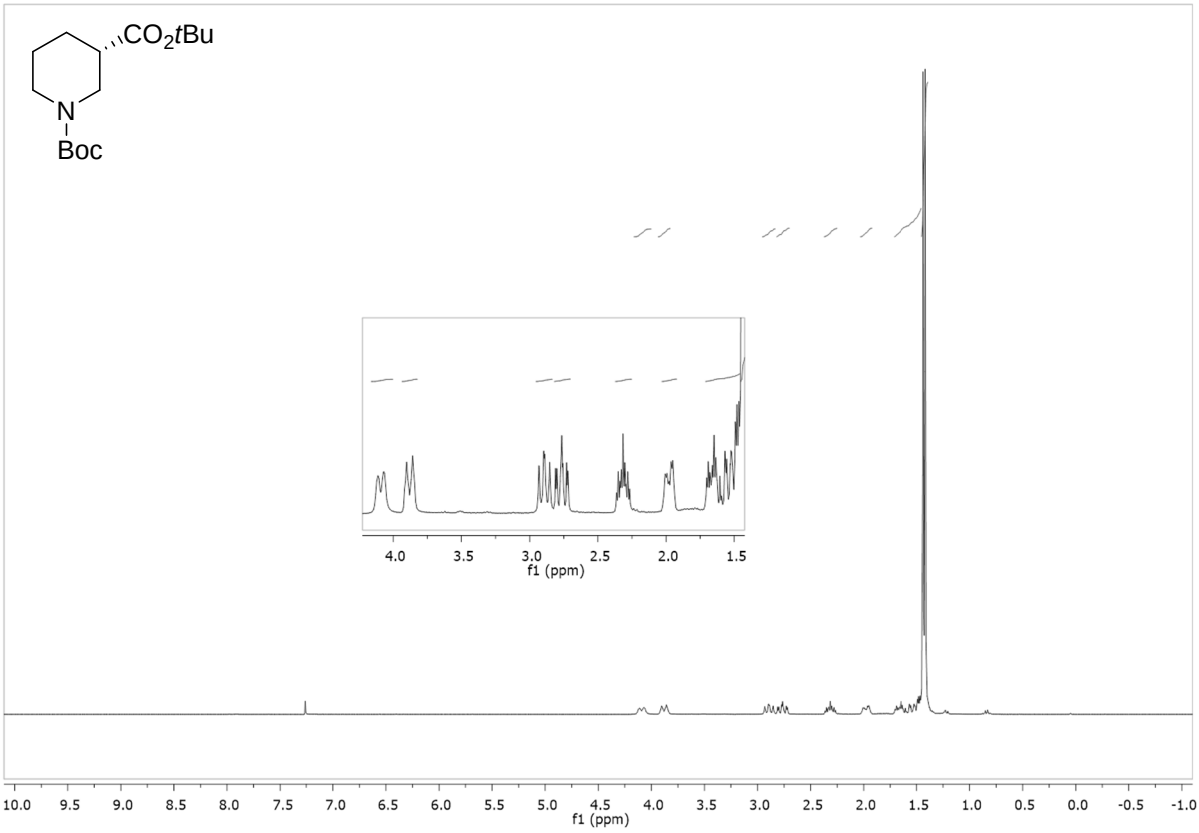


(75 MHz, $CDCl_3$)

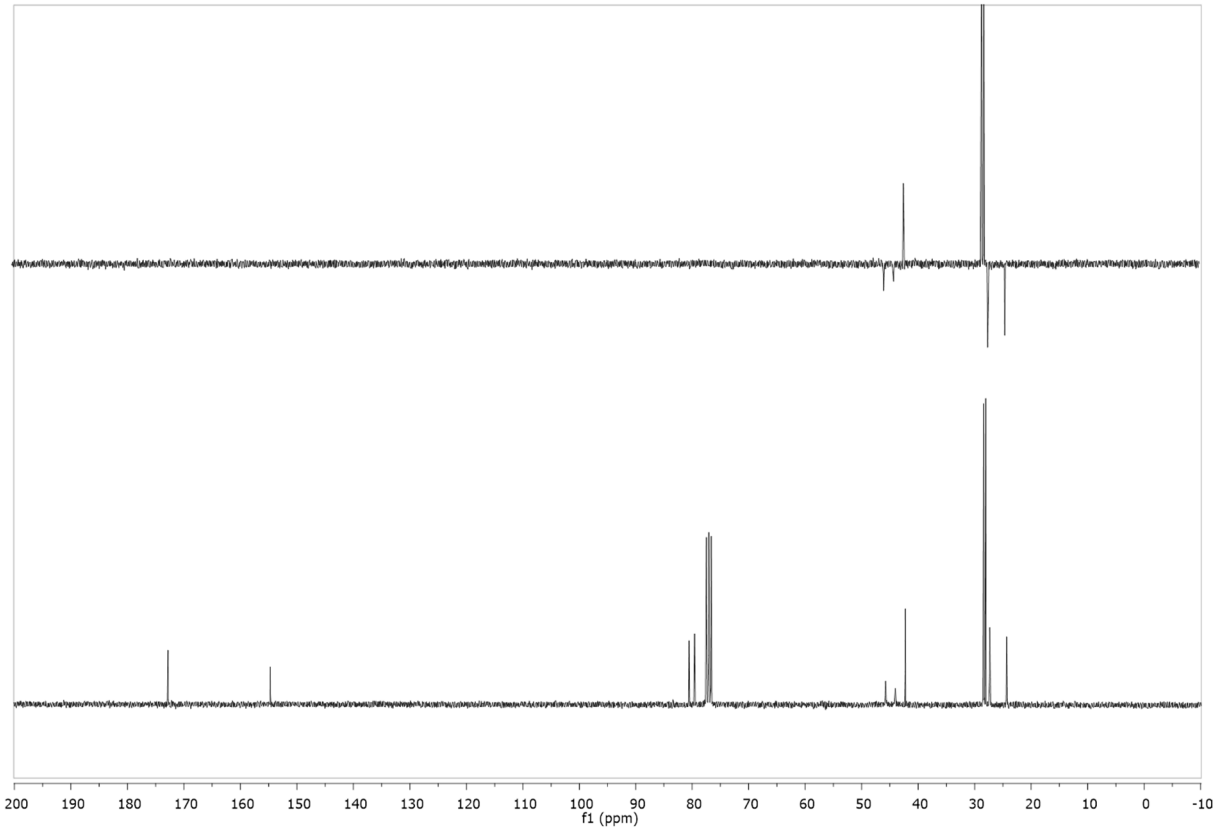

**(*S*)-Piperidine-3-carboxylic acid (237)** (400 MHz, $D_2O$)

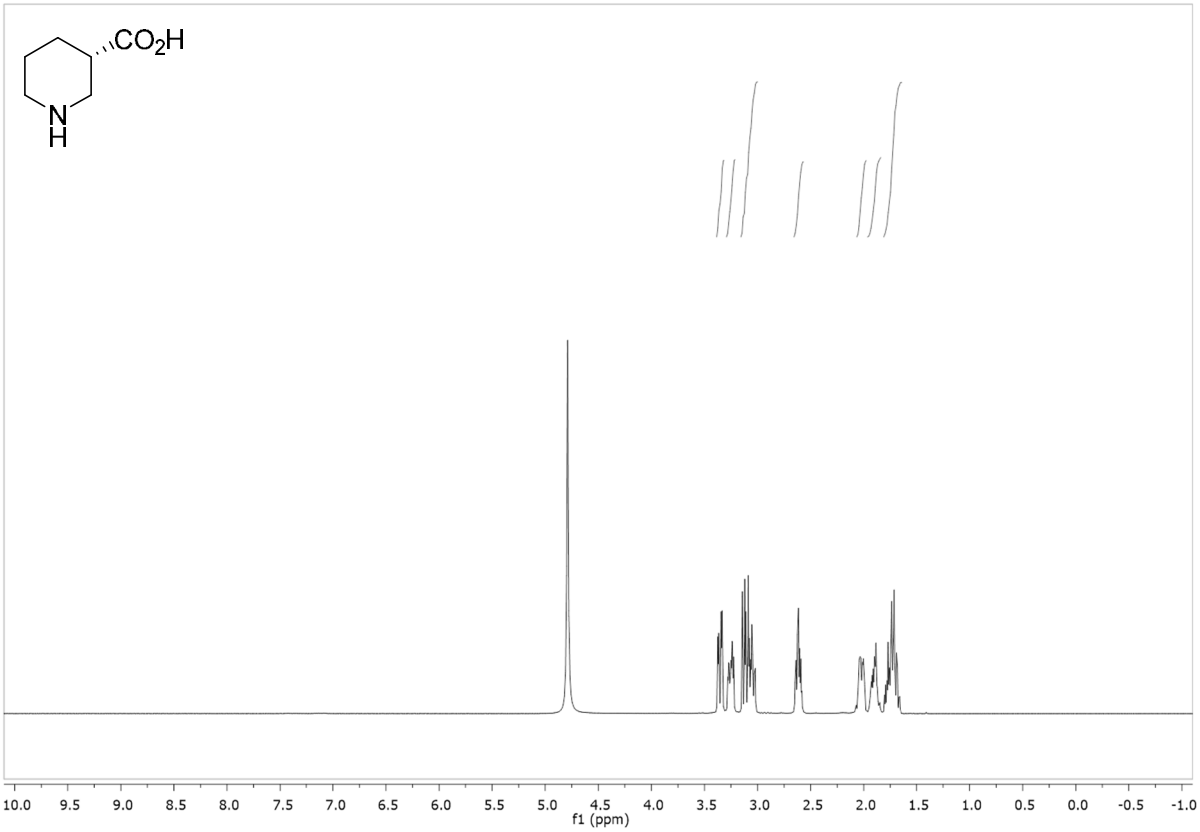


(101 MHz, $D_2O$)

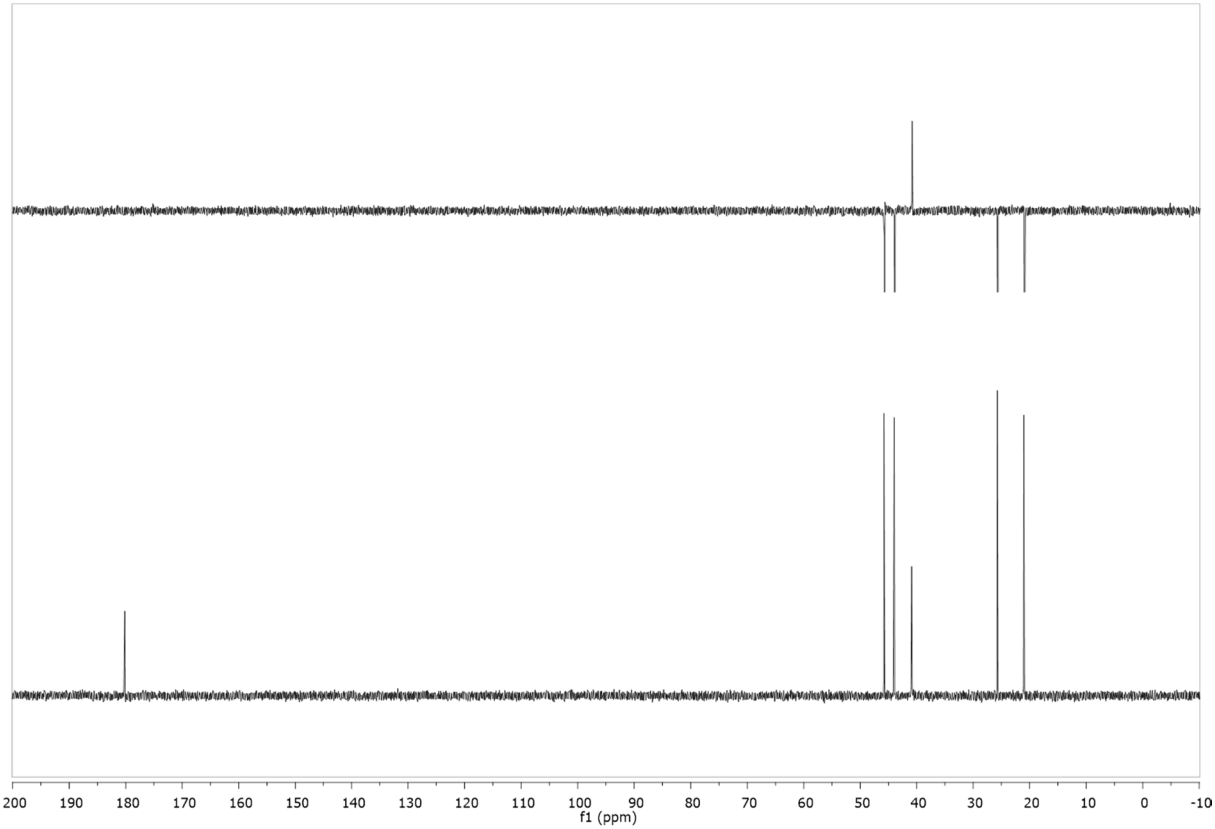

**(±)-*tert*-Butyl-6-(hydroxymethyl)-2-azabicyclo[3.1.0]hex-3-ene-2-carboxylate (248)**

(300 MHz, $CDCl_3$)

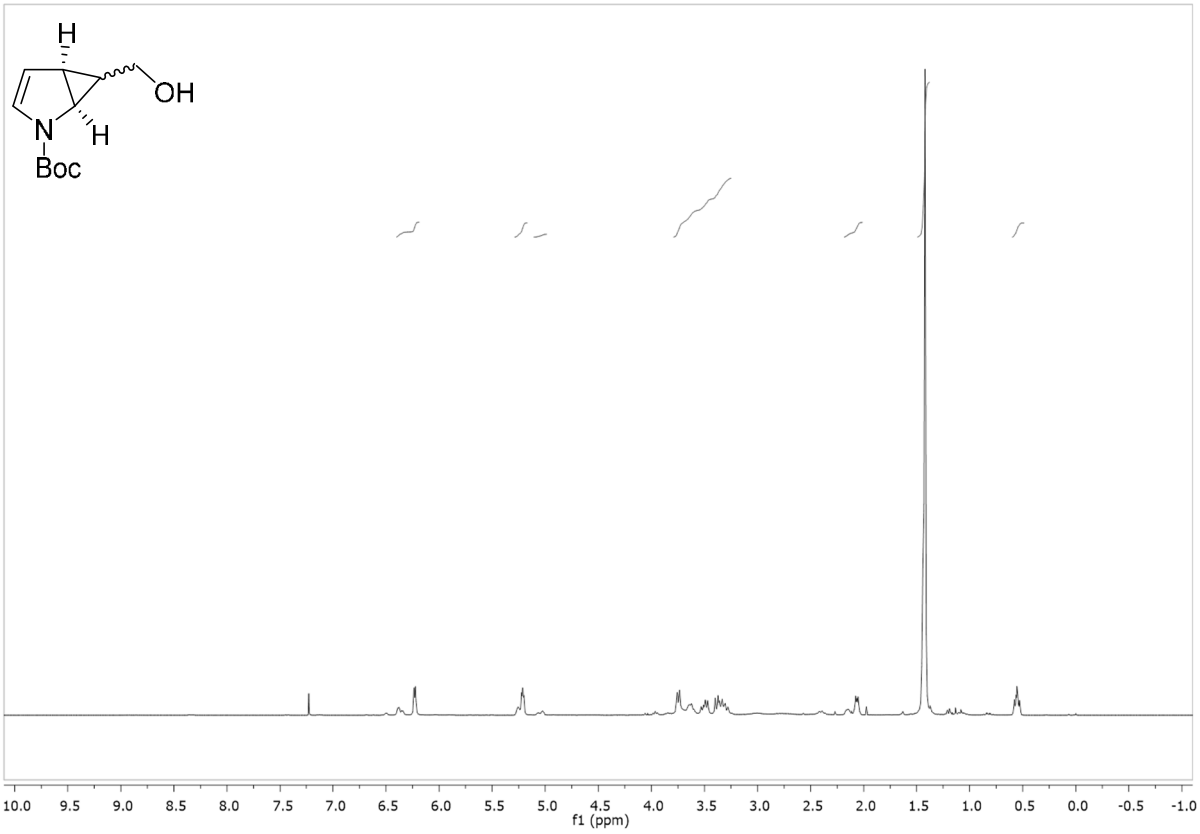


(75 MHz, $CDCl_3$)

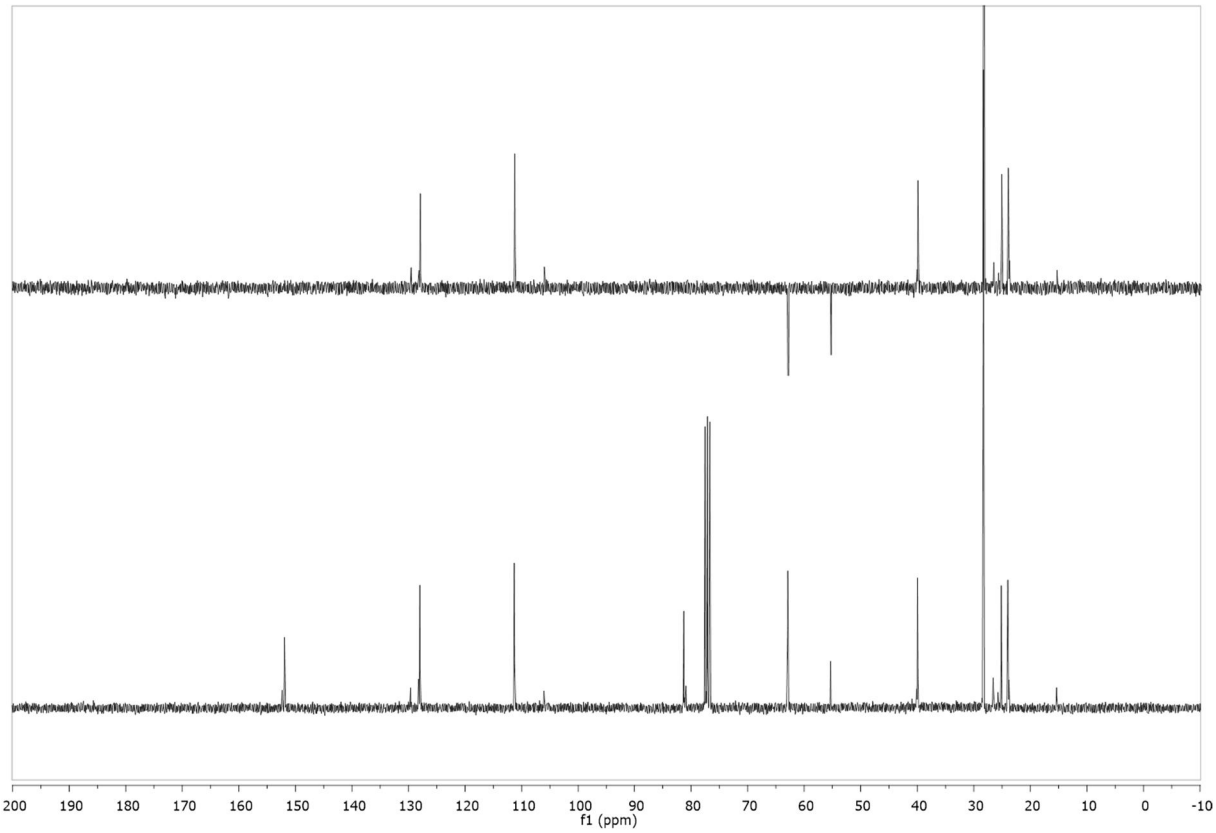

**(±)-*tert*-Butyl-6-(hydroxymethyl)-2-azabicyclo[3.1.0]hexane-2-carboxylate (249)**
(300 MHz, $CDCl_3$)

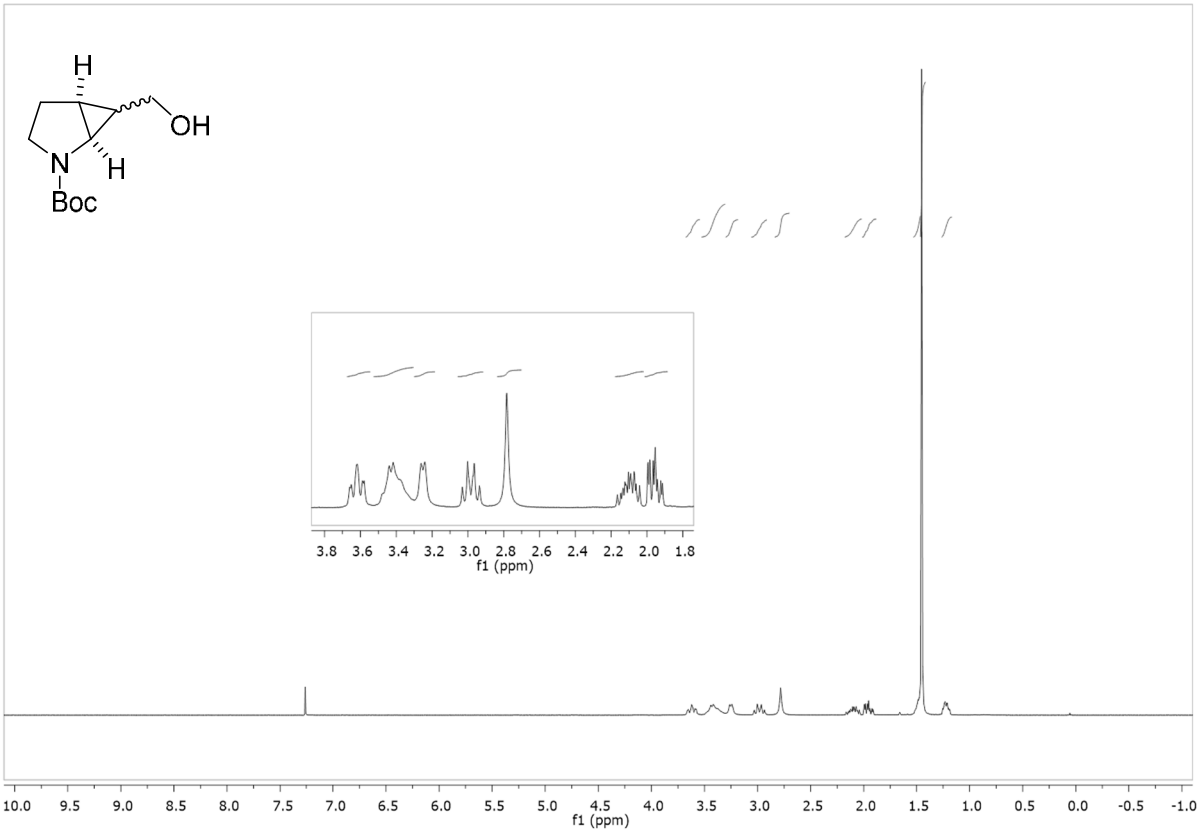


(101 MHz, $CDCl_3$)

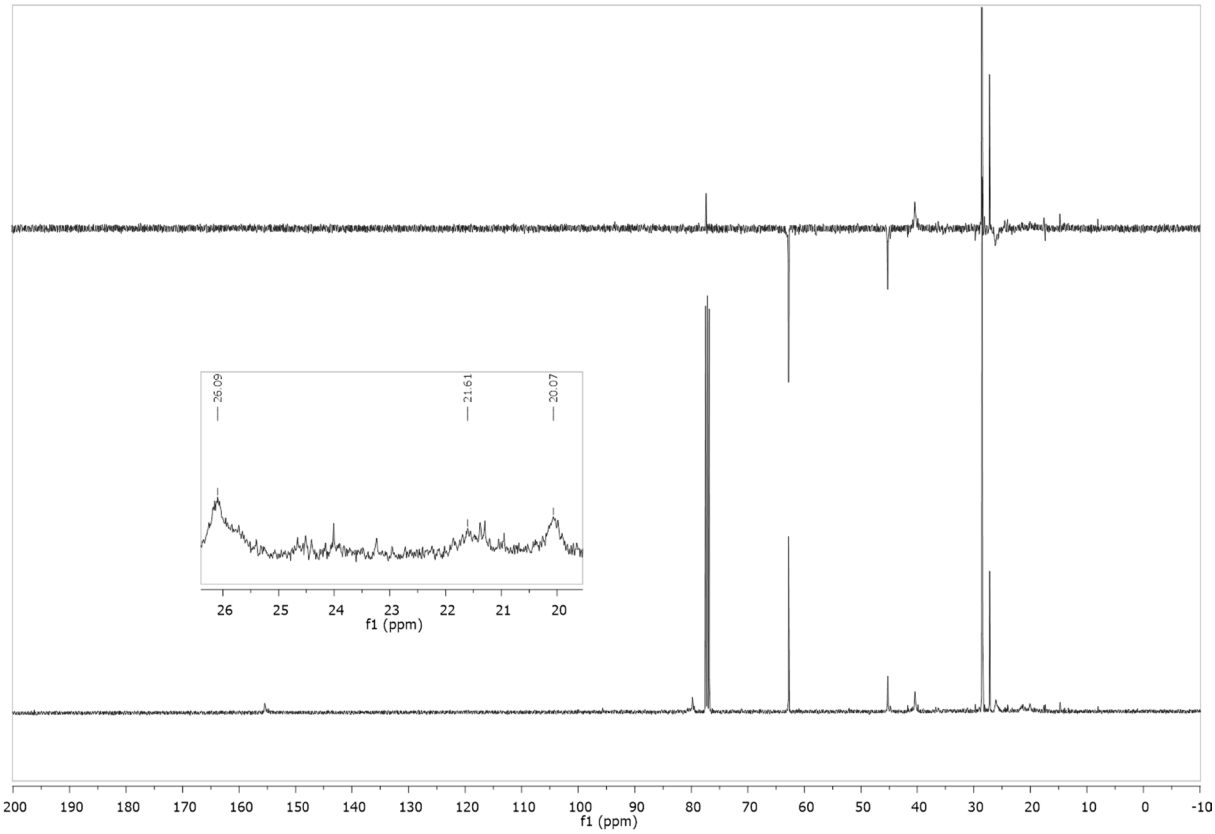

**(±)-*tert*-Butyl-3-(hydroxymethyl)piperidine-1-carboxylate (250)**

(300 MHz, $(CD_3)_2CO$)

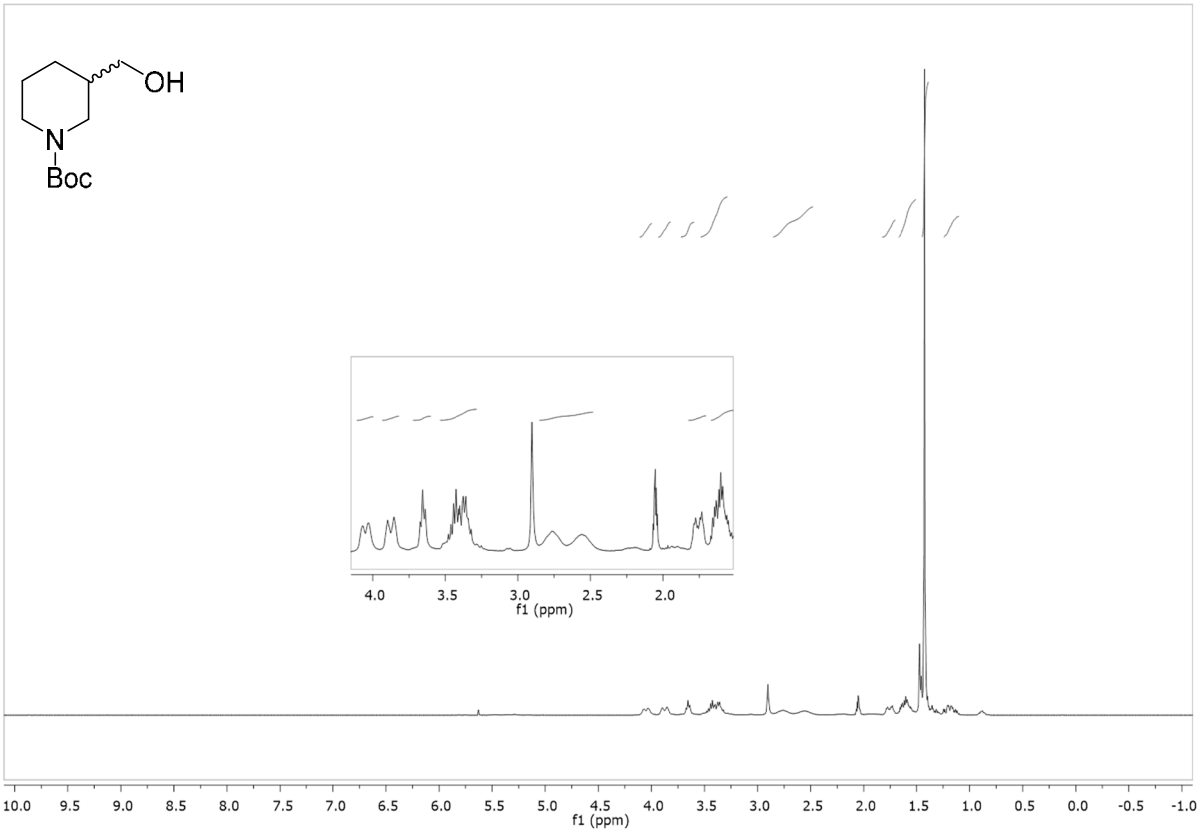


(101 MHz, $(CD_3)_2CO$)

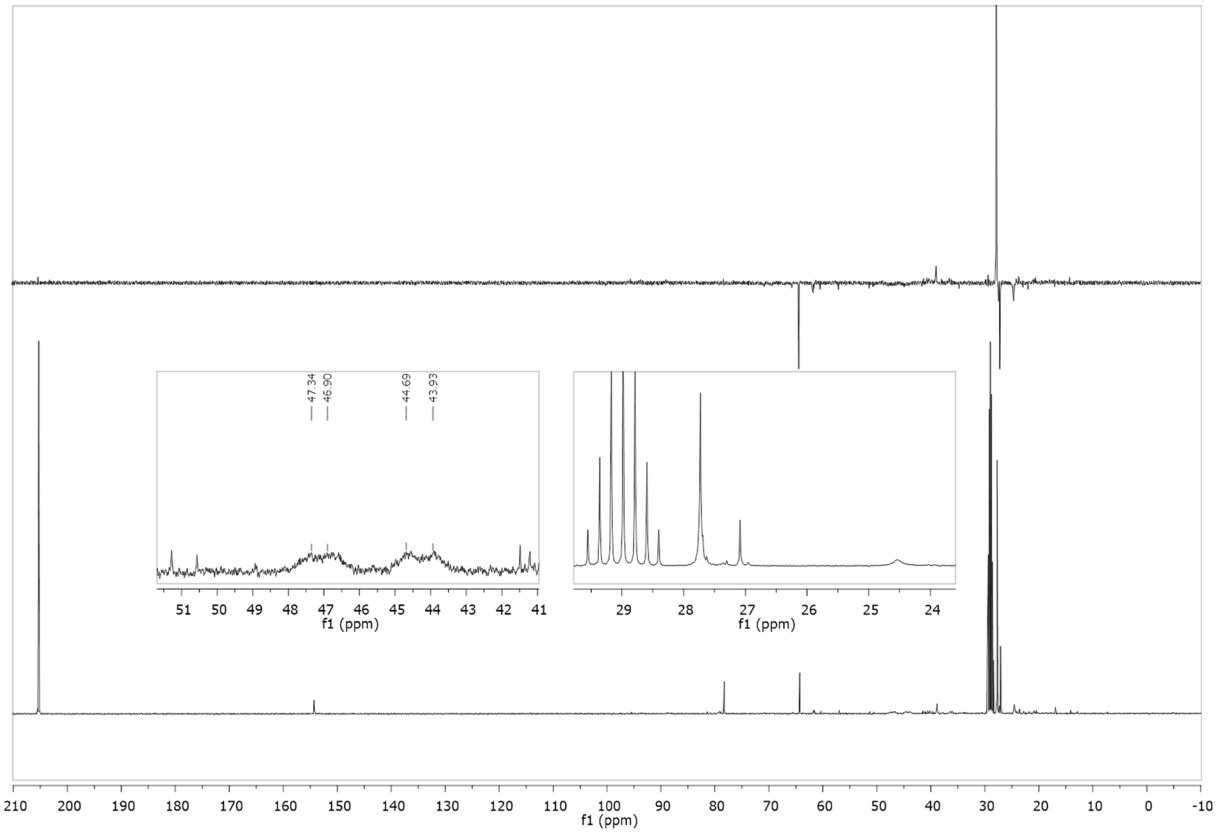

**(±)-Piperidin-3-ylmethanol (251)** (300 MHz, $D_2O$)

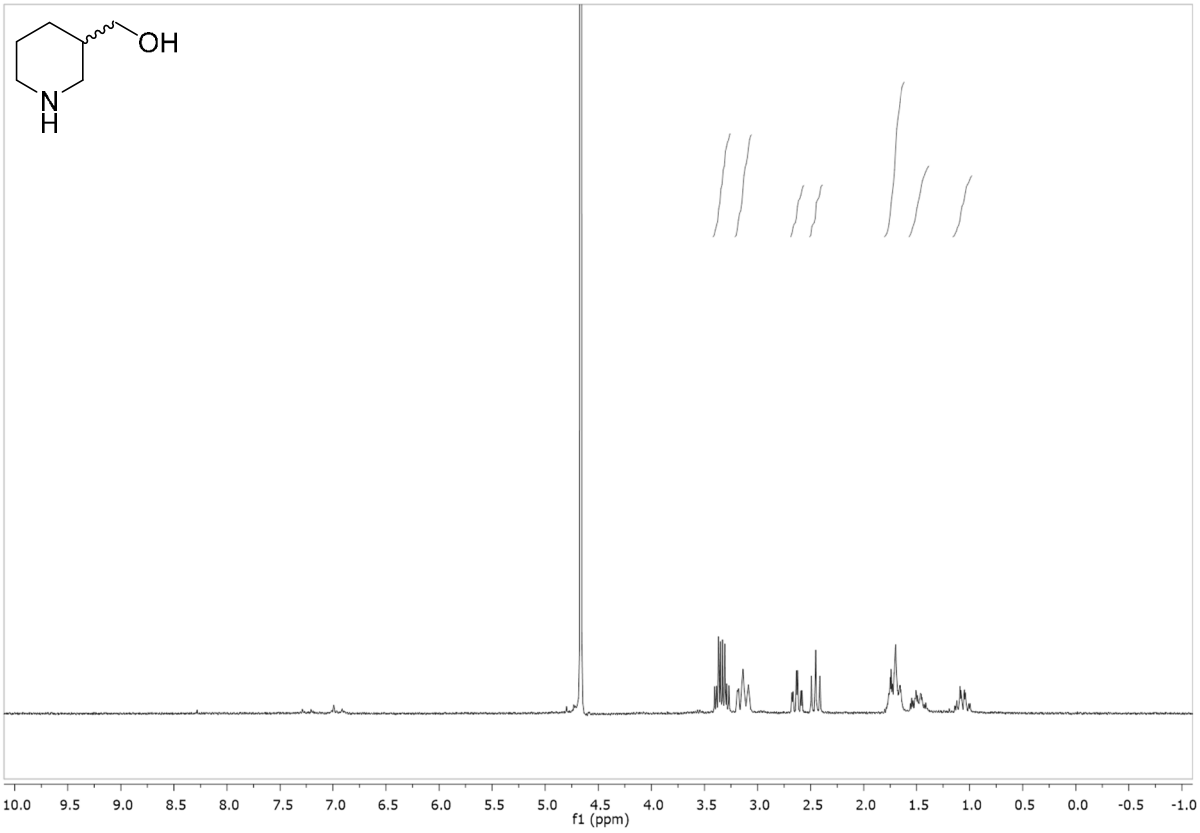

**(±)-Ethyl-2-tosyl-2-azabicyclo[3.1.0]hexane-6-carboxylate (253)** (300 MHz, $CDCl_3$)

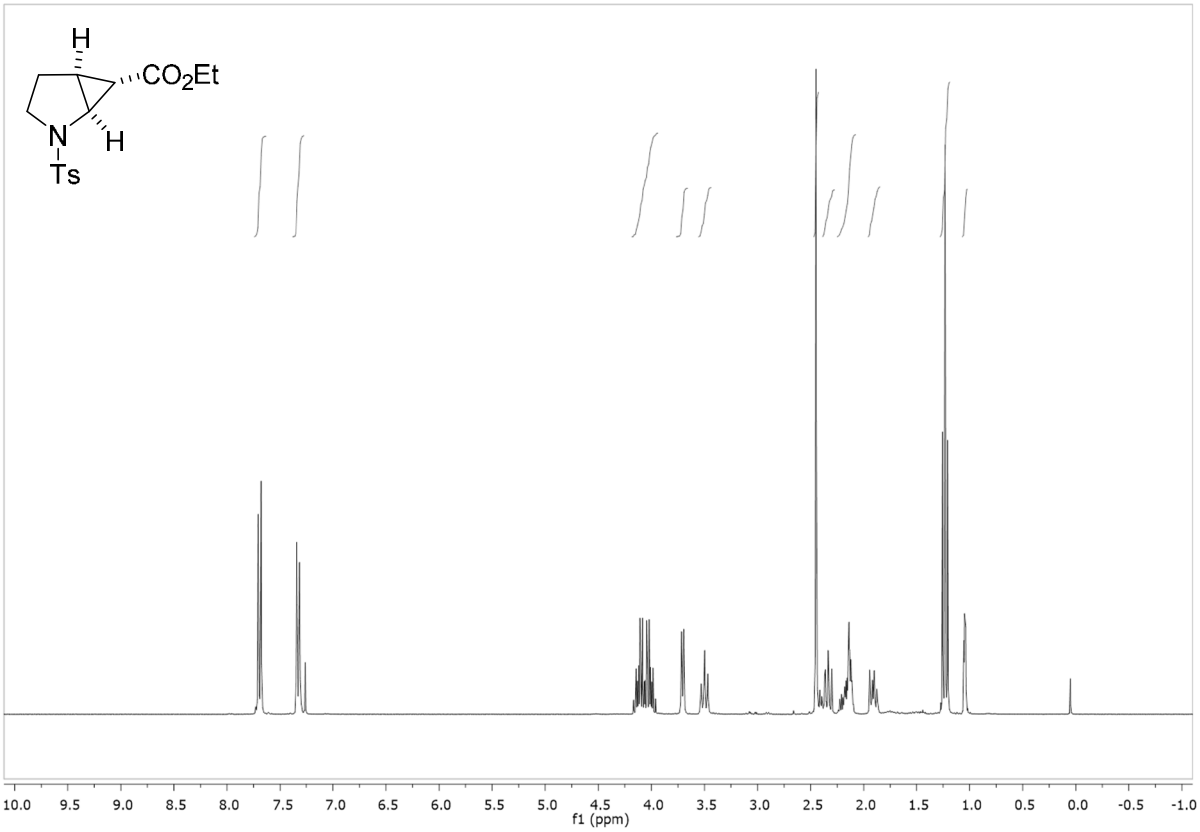


(75 MHz, $CDCl_3$)

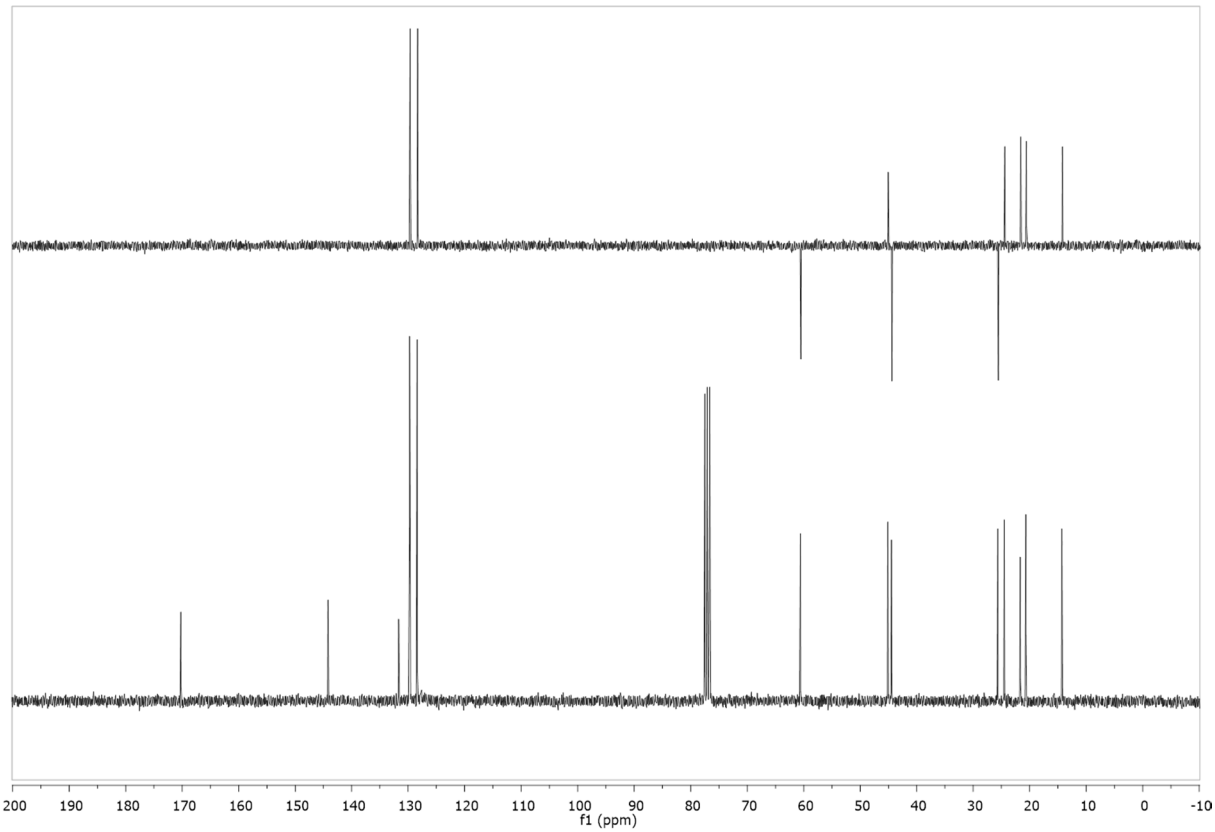

**(±)-*tert*-butyl 5-(hydroxymethyl)-1,3-dioxo-2-phenyl-1,2,3,3a,4,5,8,8a-octahydro-4,8-epiminocyclohepta[c]pyrrole-9-carboxylate (286)** (400 MHz, $CDCl_3$)

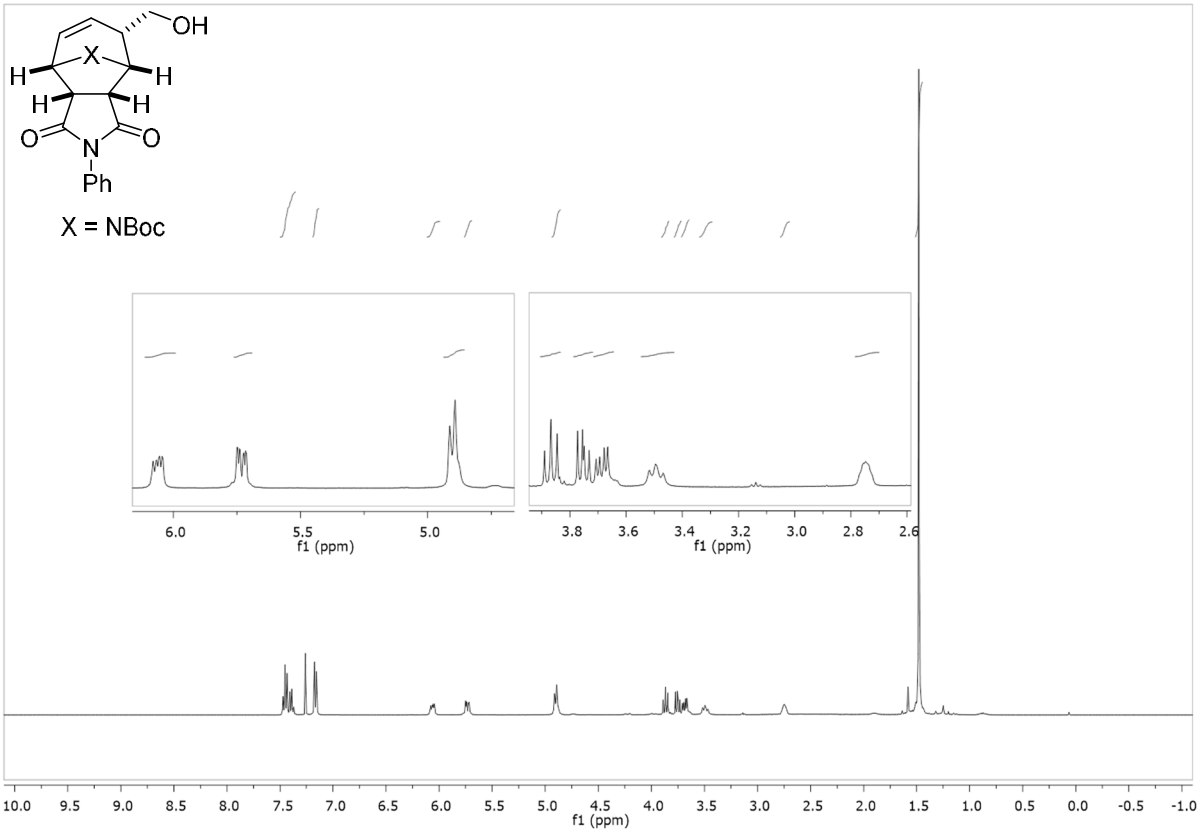


(101 MHz, $CDCl_3$)

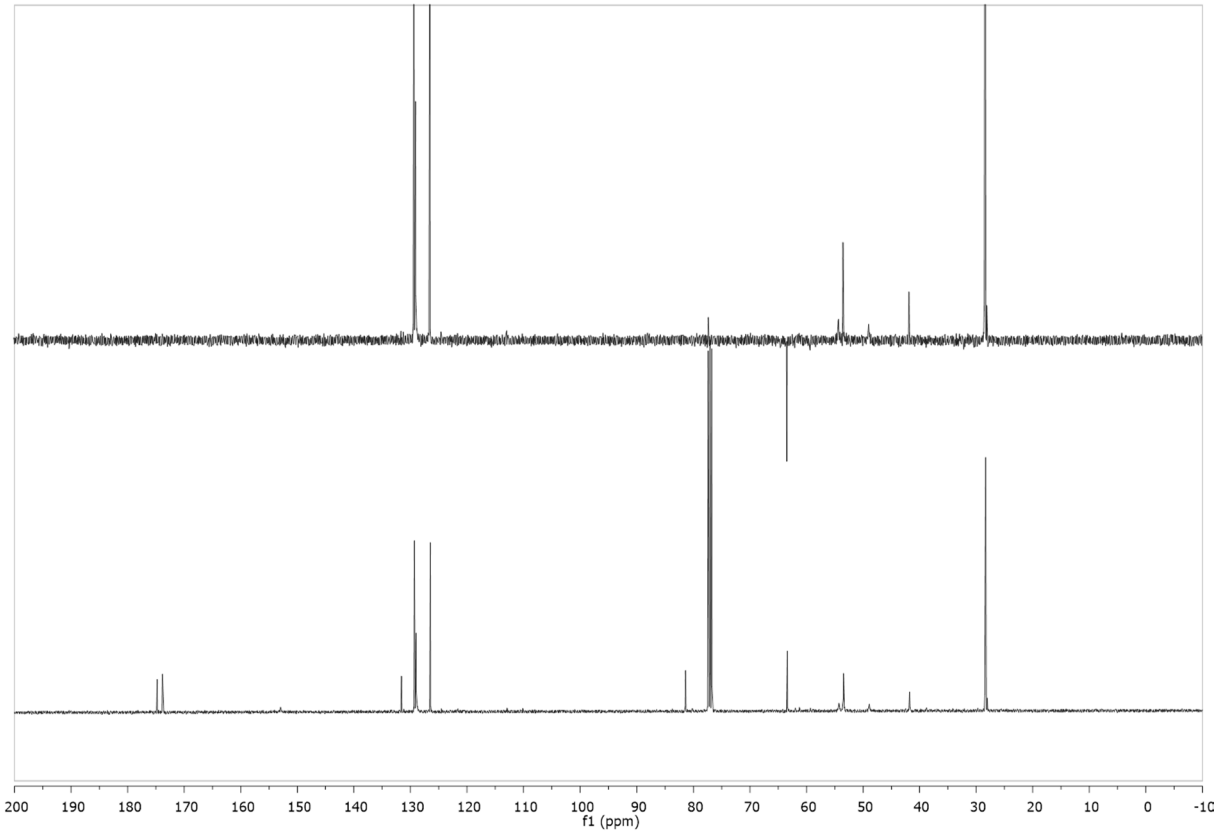

**(±)-8-(*tert*-butyl) 6,7-diethyl-4-(hydroxymethyl)-8-azabicyclo[3.2.1]octa-2,6-diene-6,7,8-tricarboxylate (288)** (400 MHz, $CDCl_3$)

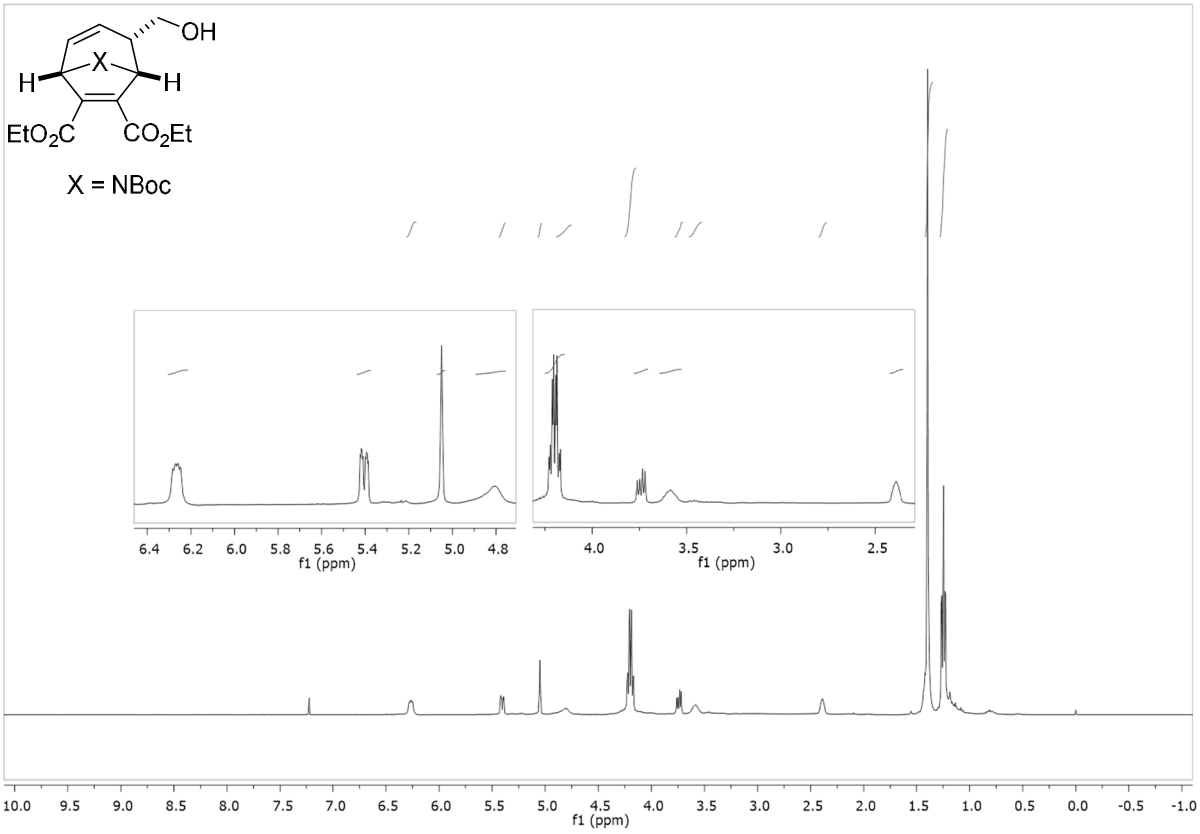


(101 MHz, $CDCl_3$)

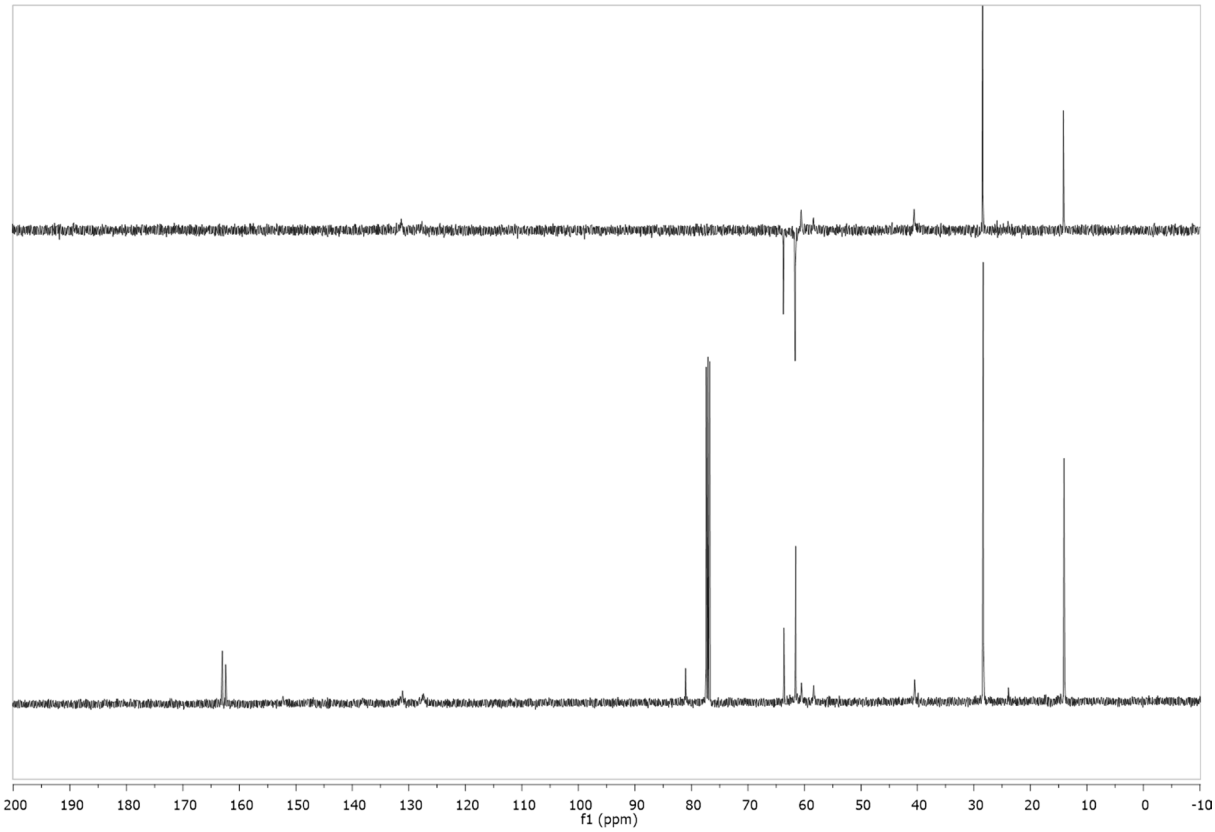

## 2. HPLC Chromatograms

### di-*tert*-Butyl-4-((((9H-fluoren-9-yl)methoxy)carbonyl)amino)pyrrolidine-1,3-dicarboxylate ((rac)-(±)-(85)

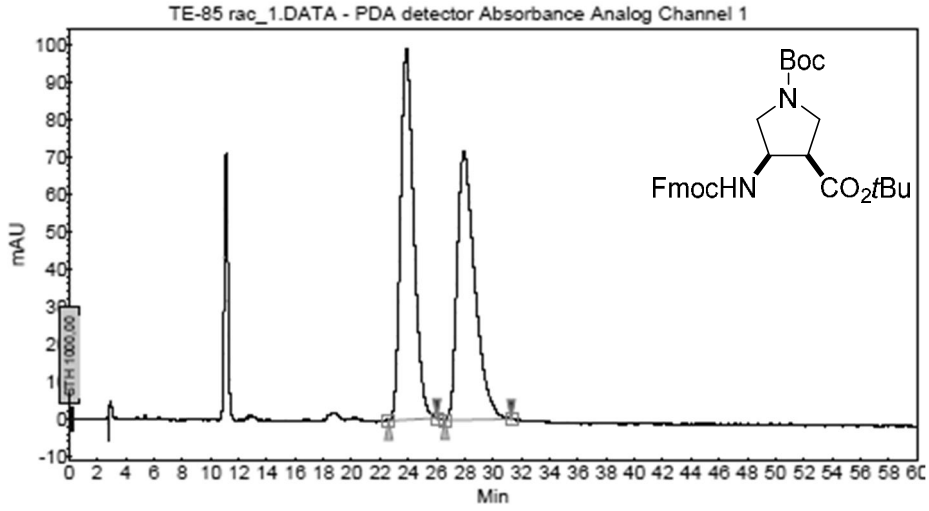


**Peak Results :**

| Index | Name | Time [Min] | Quantity [% Area] | Height [mAU] | Area [mAU.Min] | Area % [%] |
|---|---|---|---|---|---|---|
| 1 | UNKNOWN | 23.87 | 50.96 | 99.2 | 107.7 | 50.956 |
| 2 | UNKNOWN | 27.94 | 49.04 | 71.5 | 103.7 | 49.044 |
| | | | | | | |
| Total | | | 100.00 | 170.7 | 211.4 | 100.000 |

### di-*tert*-Butyl (3*R*,4*R*)-4-((((9H-fluoren-9-yl)methoxy)carbonyl)amino)pyrrolidine-1,3-dicarboxylate (85)

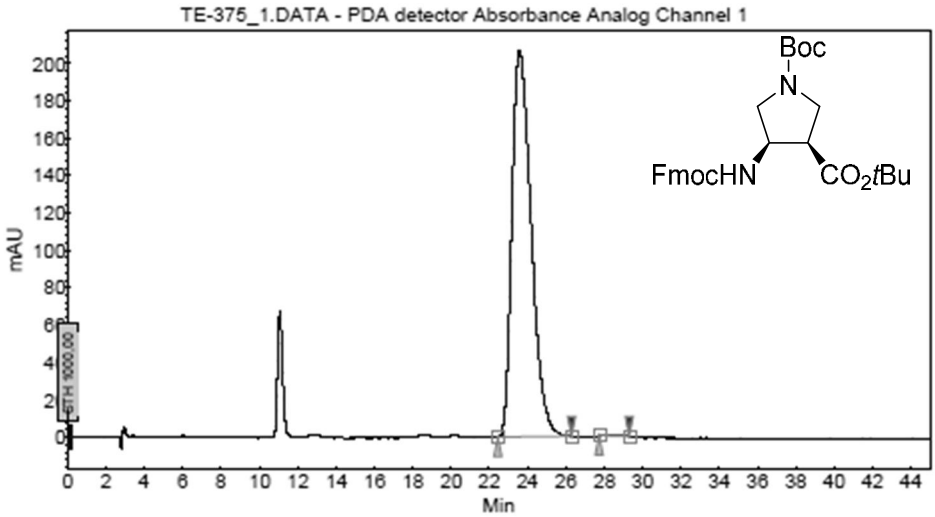


**Peak Results :**

| Index | Name | Time [Min] | Quantity [% Area] | Height [mAU] | Area [mAU.Min] | Area % [%] |
|---|---|---|---|---|---|---|
| 1 | UNKNOWN | 23.57 | 99.67 | 207.1 | 240.9 | 99.669 |
| 2 | UNKNOWN | 26.58 | 0.33 | 0.9 | 0.8 | 0.331 |
| | | | | | | |
| Total | | | 100.00 | 208.0 | 241.7 | 100.000 |

**di-*tert*-Butyl (3*S*,4*S*)-4-((((9H-fluoren-9-yl)methoxy)carbonyl)amino)pyrrolidine-1,3-dicarboxylate ((*ent*)-85)**

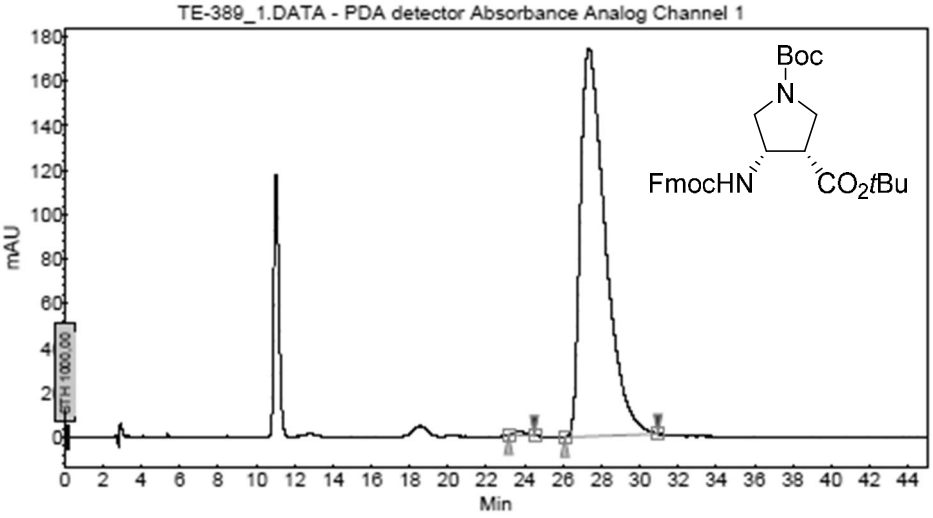


**Peak Results :**

| Index | Name | Time [Min] | Quantity [% Area] | Height [mAU] | Area [mAU.Min] | Area % [%] |
|---|---|---|---|---|---|---|
| 2 | UNKNOWN | 23.69 | 0.43 | 1.5 | 1.1 | 0.429 |
| 1 | UNKNOWN | 27.34 | 99.57 | 174.5 | 261.5 | 99.571 |
| | | | | | | |
| Total | | | 100.00 | 175.0 | 262.7 | 100.000 |

**Ac-Arg-His-Tyr-Ile-Asn-Leu-Ile-Thr-Arg-((3*R*,4*R*)APC)-Arg-Tyr-$NH_2$ (170)**

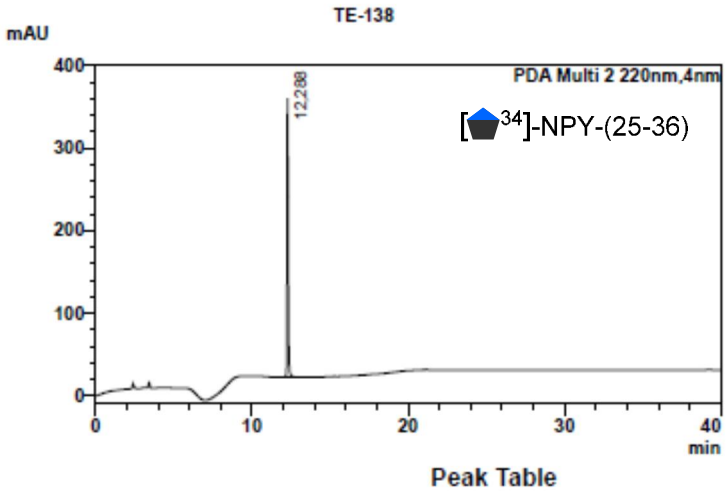


**Peak Table**

PDA Ch2 220nm

| Peak# | Ret. Time | Area% | Height |
|---|---|---|---|
| 1 | 12,288 | 100,000 | 336959 |
| Total | | 100,000 | 336959 |

**Ac-Arg-His-Tyr-Ile-Asn-Leu-Ile-((3*R*,4*R*)APC)-Arg-((3*R*,4*R*)APC)-Arg-Tyr-$NH_2$ (171)**

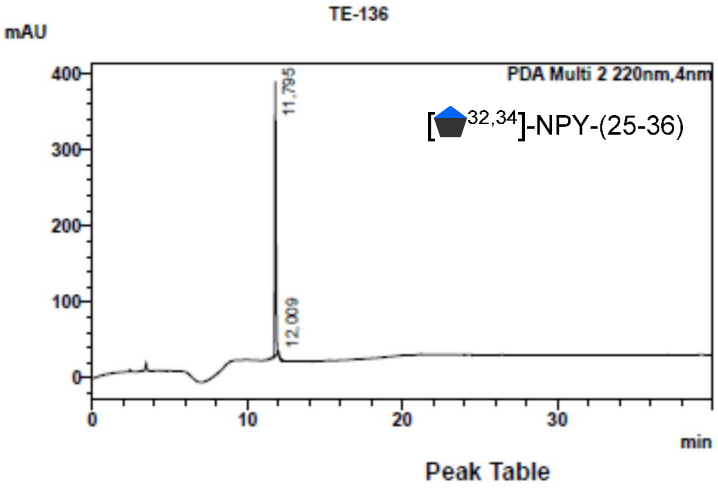


Peak Table

PDA Ch2 220nm

| Peak# | Ret. Time | Area% | Height |
|---|---|---|---|
| 1 | 11,795 | 99,264 | 361604 |
| 2 | 12,009 | 0,736 | 4109 |
| Total | | 100,000 | 365713 |

**Ac-Arg-His-Tyr-Ile-Asn-Leu-Ile-Thr-Arg-((3*S*,4*S*)APC)-Arg-Tyr-$NH_2$ (172)**

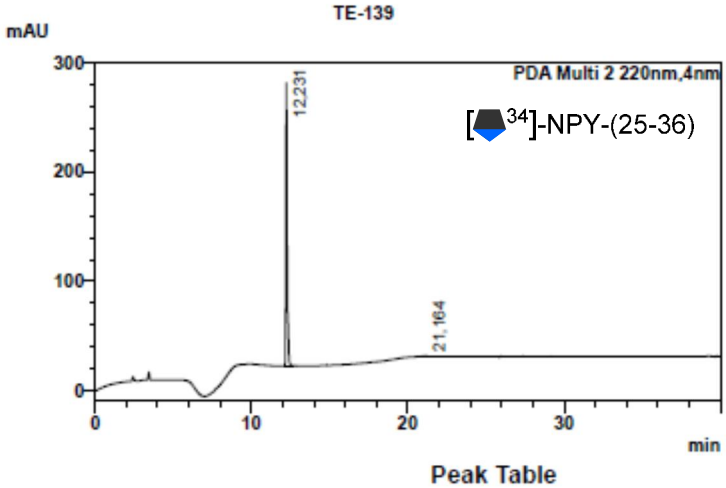


Peak Table

PDA Ch2 220nm

| Peak# | Ret. Time | Area% | Height |
|---|---|---|---|
| 1 | 12,231 | 99,680 | 259767 |
| 2 | 21,164 | 0,320 | 655 |
| Total | | 100,000 | 260422 |

**Ac-Arg-His-Tyr-Ile-Asn-Leu-Ile-((3*S*,4*S*)APC)-Arg-((3*S*,4*S*)APC)-Arg-Tyr-$NH_2$ (173)**

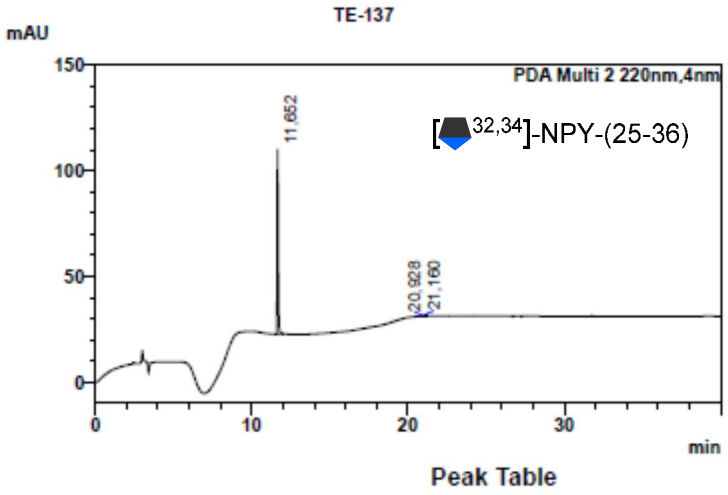


Peak Table

PDA Ch2 220nm

| Peak# | Ret. Time | Area% | Height |
|---|---|---|---|
| 1 | 11,652 | 98,376 | 87661 |
| 2 | 20,928 | 0,265 | 217 |
| 3 | 21,160 | 1,359 | 792 |
| Total | | 100,000 | 88670 |

**Ac-Arg-His-Tyr-Ile-Asn-Leu-Ile-((1*R*,2*S*)ACPC)-Arg-((3*R*,4*R*)APC)-Arg-Tyr-$NH_2$ (174)**

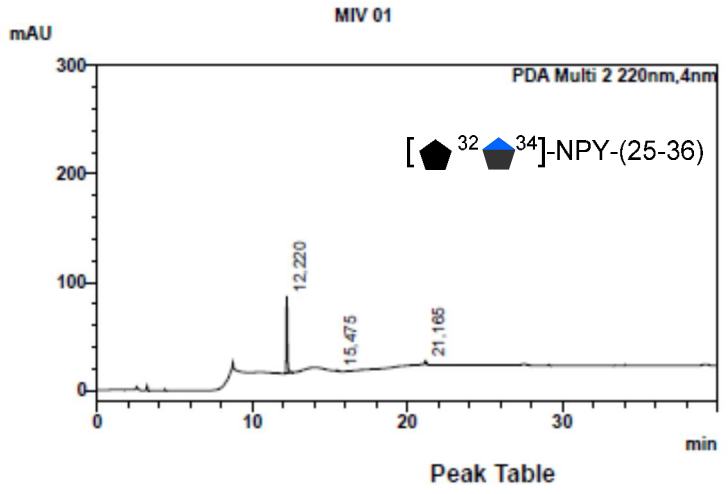


Peak Table

PDA Ch2 220nm

| Peak# | Ret. Time | Area% | Height |
|---|---|---|---|
| 1 | 12,220 | 95,267 | 71252 |
| 2 | 15,475 | 0,647 | 637 |
| 3 | 21,165 | 4,085 | 2595 |
| Total | | 100,000 | 74484 |

**Ac-Arg-His-Tyr-Ile-Asn-Leu-Ile-((1*R*,2*S*)ACPC)-Arg-((3*R*,4*R*)APC)-Arg-Tyr-$NH_2$ (175)**

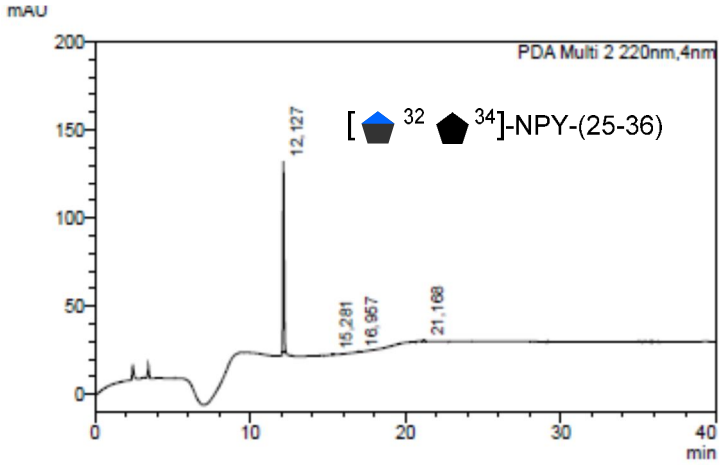


<Peak Table>

PDA Ch2 220nm

| Peak# | Ret. Time | Height | Area% |
|---|---|---|---|
| 1 | 12,127 | 108376 | 98,046 |
| 2 | 15,281 | 520 | 0,478 |
| 3 | 16,957 | 412 | 0,531 |
| 4 | 21,168 | 682 | 0,945 |
| Total | | 109990 | 100,000 |

**di-*tert*-Butyl (1*S*,5*S*,6*S*)-2-azabicyclo[3.1.0]hex-3-ene-2,6-dicarboxylate (190)**

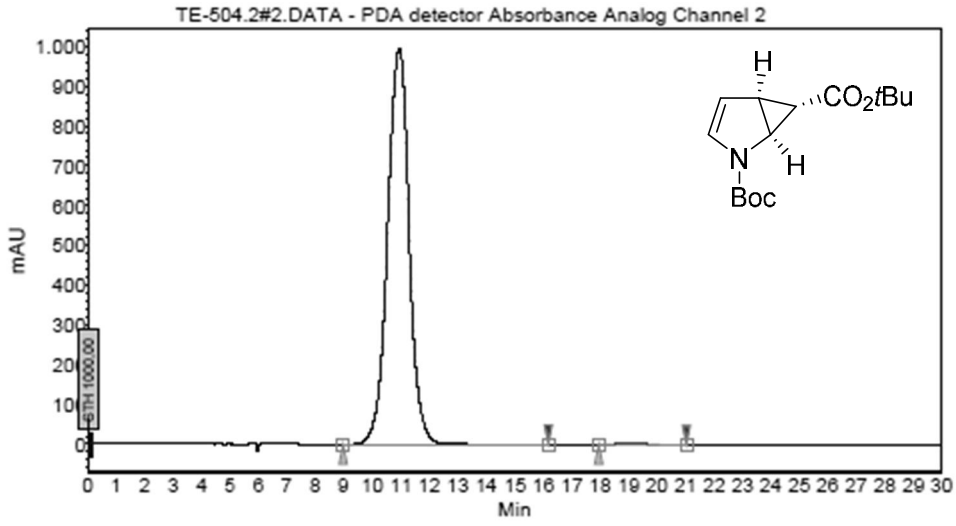


**Peak Results :**

| Index | Name | Time [Min] | Quantity [% Area] | Height [mAU] | Area [mAU.Min] | Area % [%] |
|---|---|---|---|---|---|---|
| 1 | UNKNOWN | 10,95 | 99,58 | 994,5 | 874,7 | 99,584 |
| 2 | UNKNOWN | 19,02 | 0,42 | 3,1 | 3,7 | 0,416 |
| | | | | | | |
| Total | | | 100,00 | 997,6 | 878,4 | 100,000 |

**(1*S*,5*S*,6*S*)-di-*tert*-butyl 2-azabicyclo[3.1.0]hexane-2,6-dicarboxylate (194)**

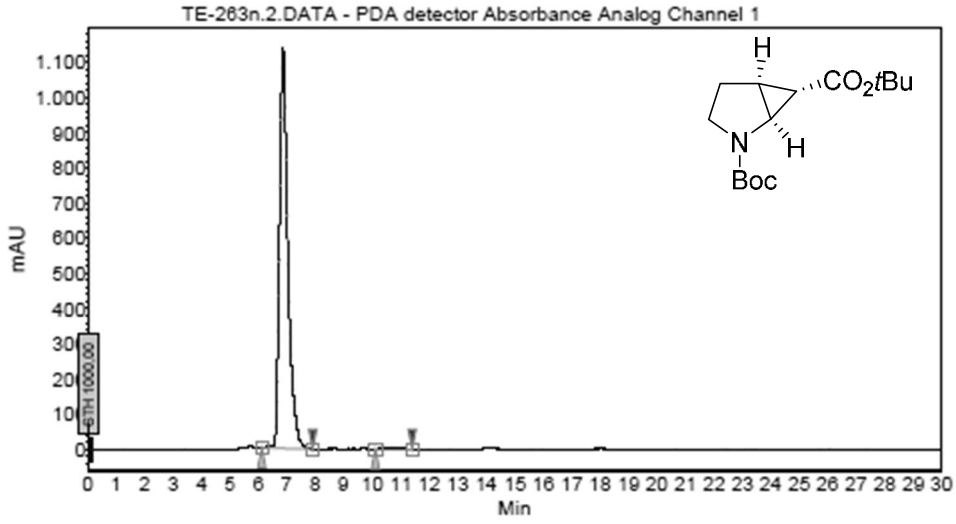


**Peak Results :**

| Index | Name | Time [Min] | Quantity [% Area] | Height [mAU] | Area [mAU.Min] | Area % [%] |
|---|---|---|---|---|---|---|
| 1 | UNKNOWN | 6,87 | 99,06 | 1136,2 | 383,9 | 99,058 |
| 2 | UNKNOWN | 10,54 | 0,94 | 6,0 | 3,7 | 0,942 |
| | | | | | | |
| Total | | | 100,00 | 1142,2 | 387,5 | 100,000 |

***tert*-Butyl 3-(2-(*tert*-butoxy)-2-oxoethyl)pyrrolidine-1-carboxylate ((*rac*)-(±)-189)**

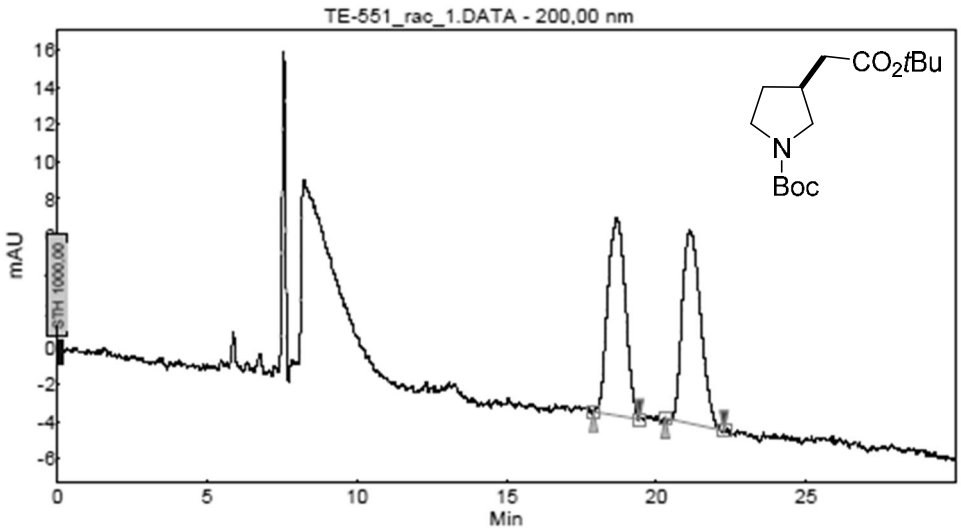


**Peak Results :**

| Index | Name | Time [Min] | Quantity [% Area] | Height [mAU] | Area [mAU.Min] | Area % [%] |
|---|---|---|---|---|---|---|
| 1 | UNKNOWN | 18,66 | 49,50 | 10,6 | 7,2 | 49,502 |
| 2 | UNKNOWN | 21,12 | 50,50 | 10,4 | 7,3 | 50,498 |
| | | | | | | |
| Total | | | 100,00 | 21,0 | 14,5 | 100,000 |

**(*S*)-*tert*-Butyl 3-(2-(*tert*-butoxy)-2-oxoethyl)pyrrolidine-1-carboxylate (189)**

*Ring-opening at 0 °C*

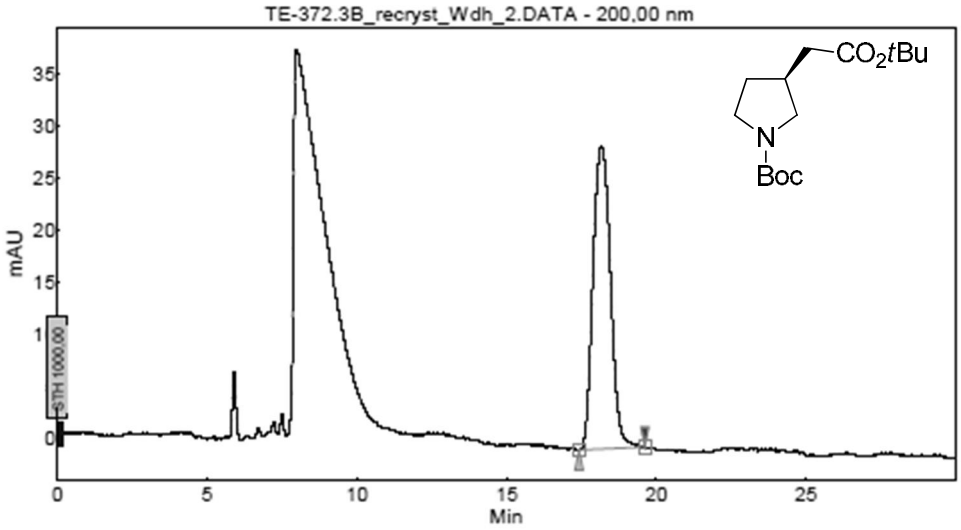


**Peak Results :**

| Index | Name | Time [Min] | Quantity [% Area] | Height [mAU] | Area [mAU.Min] | Area % [%] |
|---|---|---|---|---|---|---|
| 1 | UNKNOWN | 18,16 | 100,00 | 29,0 | 19,5 | 100,000 |
| | | | | | | |
| Total | | | 100,00 | 29,0 | 19,5 | 100,000 |

*Ring-opening at ambient temperature*

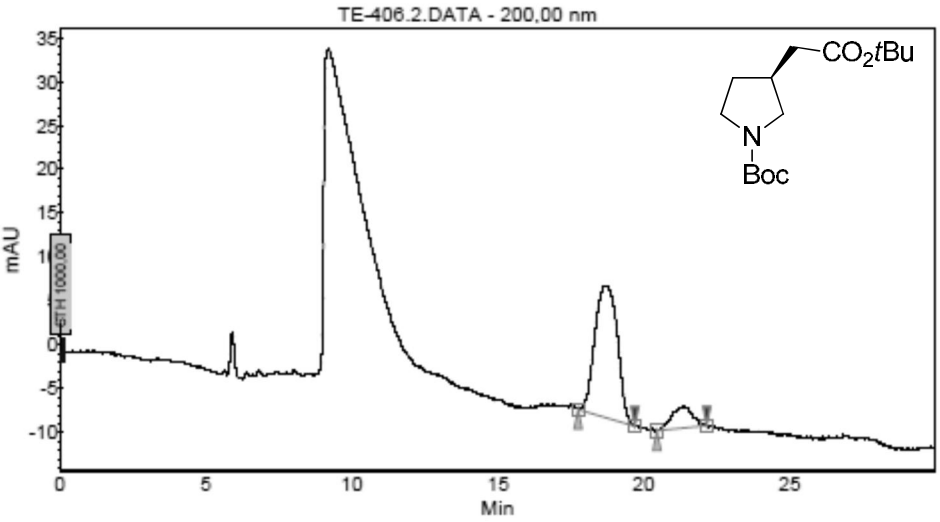


**Peak Results :**

| Index | Name | Time [Min] | Quantity [% Area] | Height [mAU] | Area [mAU.Min] | Area % [%] |
|---|---|---|---|---|---|---|
| 1 | UNKNOWN | 18,75 | 87,06 | 15,1 | 13,5 | 87,056 |
| 2 | UNKNOWN | 21,37 | 12,94 | 2,4 | 2,0 | 12,944 |
| | | | | | | |
| Total | | | 100,00 | 17,5 | 15,5 | 100,000 |

**_tert_-Butyl-2-oxohexahydro-6H-furo[2,3-b]pyrrole-6-carboxylate (rac-(±)-222)**

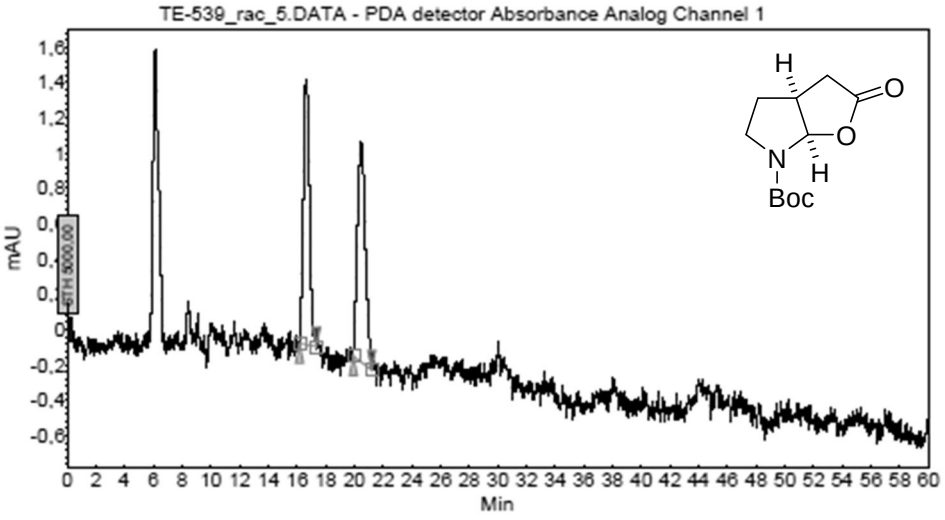


**Peak Results :**

| Index | Name | Time [Min] | Quantity [% Area] | Height [mAU] | Area [mAU.Min] | Area % [%] |
|---|---|---|---|---|---|---|
| 1 | UNKNOWN | 16.63 | 48.19 | 1.5 | 0.8 | 48.185 |
| 2 | UNKNOWN | 20.53 | 51.81 | 1.2 | 0.8 | 51.815 |
| | | | | | | |
| Total | | | 100.00 | 2.7 | 1.6 | 100.000 |

**_tert_-Butyl (3a*S*,6a*R*)-2-oxohexahydro-6H-furo[2,3-b]pyrrole-6-carboxylate (222)**

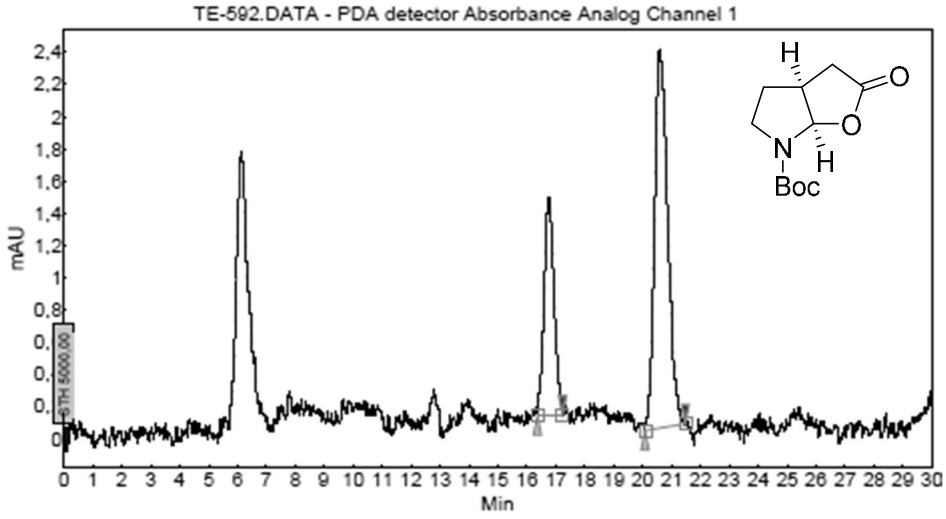


**Peak Results :**

| Index | Name | Time [Min] | Quantity [% Area] | Height [mAU] | Area [mAU.Min] | Area % [%] |
|---|---|---|---|---|---|---|
| 1 | UNKNOWN | 16.77 | 30.28 | 1.4 | 0.5 | 30.277 |
| 2 | UNKNOWN | 20.60 | 69.72 | 2.4 | 1.2 | 69.723 |
| | | | | | | |
| Total | | | 100.00 | 3.7 | 1.8 | 100.000 |

**2-(*tert*-Butyl) 6-methyl-2-azabicyclo[3.1.0]hex-3-ene-2,6-dicarboxylate ((*rac*)-(±)-201)**

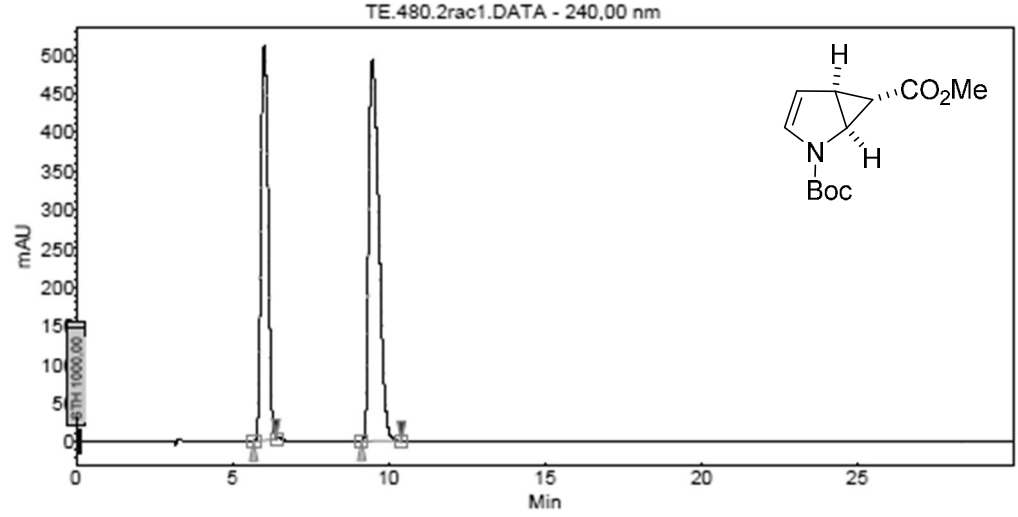


**Peak results :**

| Index | Name | Time [Min] | Quantity [% Area] | Height [mAU] | Area [mAU.Min] | Area % [%] |
|---|---|---|---|---|---|---|
| 1 | UNKNOWN | 6.03 | 42.24 | 508.9 | 135.1 | 42.241 |
| 2 | UNKNOWN | 9.48 | 57.76 | 492.0 | 184.7 | 57.759 |
| | | | | | | |
| Total | | | 100.00 | 1000.9 | 319.7 | 100.000 |

**(1*S*,5*S*,6*S*)-2-*tert*-Butyl 6-methyl 2-azabicyclo[3.1.0]hex-3-ene-2,6-dicarboxylate (201)**

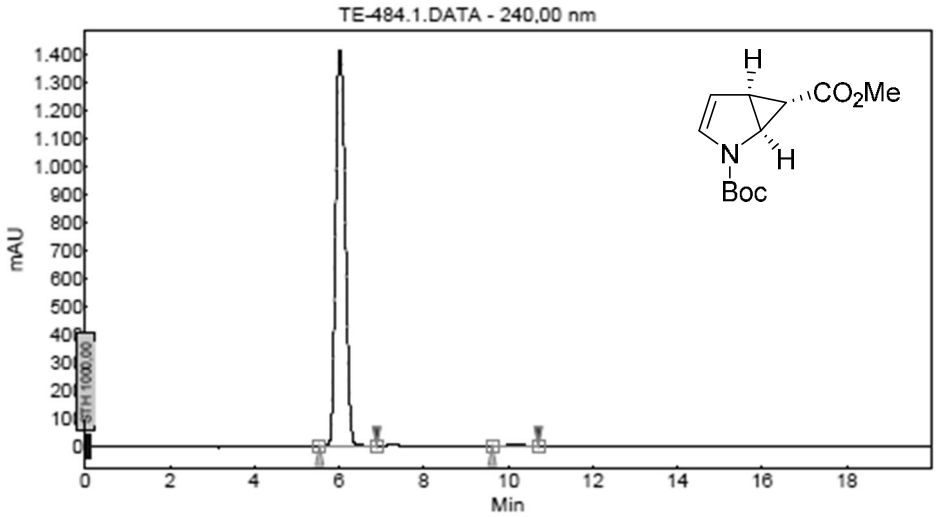


**Peak Results :**

| Index | Name | Time [Min] | Quantity [% Area] | Height [mAU] | Area [mAU.Min] | Area % [%] |
|---|---|---|---|---|---|---|
| 1 | UNKNOWN | 6.02 | 99.51 | 1414.5 | 373.3 | 99.507 |
| 2 | UNKNOWN | 10.12 | 0.49 | 4.1 | 1.9 | 0.493 |
| | | | | | | |
| Total | | | 100.00 | 1418.5 | 375.2 | 100.000 |

**di-*tert*-Butyl-piperidine-1,3-dicarboxylate ((rac)-(±)-(200))**

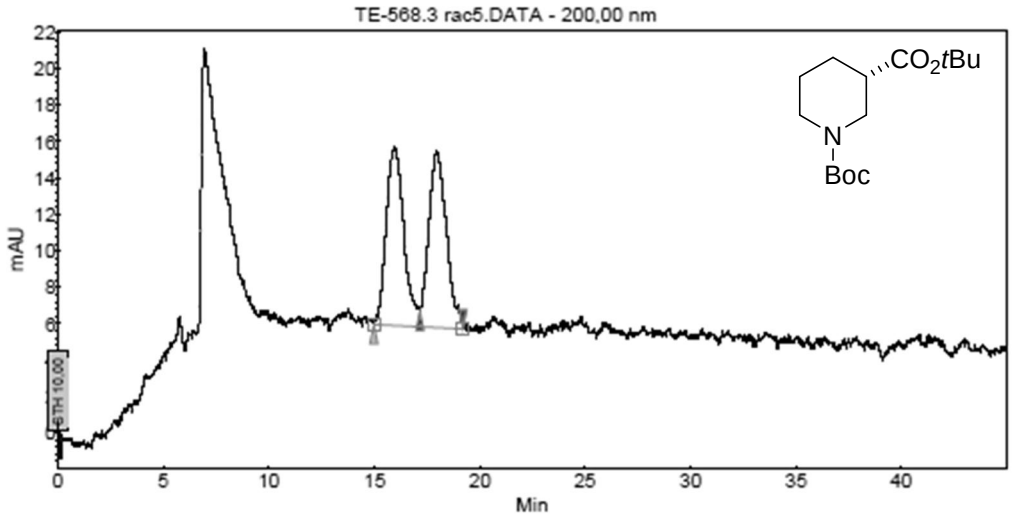


**Peak results :**

| Index | Name | Time [Min] | Quantity [% Area] | Height [mAU] | Area [mAU.Min] | Area % [%] |
|---|---|---|---|---|---|---|
| 1 | UNKNOWN | 15.96 | 50.58 | 9.9 | 9.6 | 50.582 |
| 2 | UNKNOWN | 17.97 | 49.42 | 9.7 | 9.4 | 49.418 |
| | | | | | | |
| Total | | | 100.00 | 19.6 | 18.9 | 100.000 |

**di-*tert*-Butyl (*S*)-piperidine-1,3-dicarboxylate (200)**

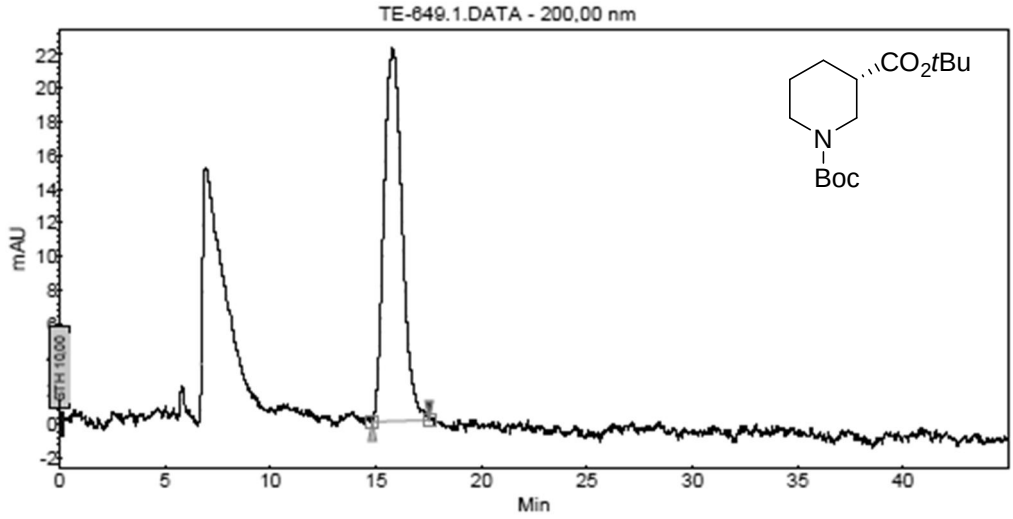


**Peak results :**

| Index | Name | Time [Min] | Quantity [% Area] | Height [mAU] | Area [mAU.Min] | Area % [%] |
|---|---|---|---|---|---|---|
| 1 | UNKNOWN | 15.79 | 100.00 | 22.1 | 22.1 | 100.000 |
| | | | | | | |
| Total | | | 100.00 | 22.1 | 22.1 | 100.000 |

**di-*tert*-Butyl-4-((((9H-fluoren-9-yl)methoxy)carbonyl)amino)-3-methoxy-2-azabicyclo[3.1.0]hexane-2,6-dicarboxylate ((*rac*)-(±)-215)**

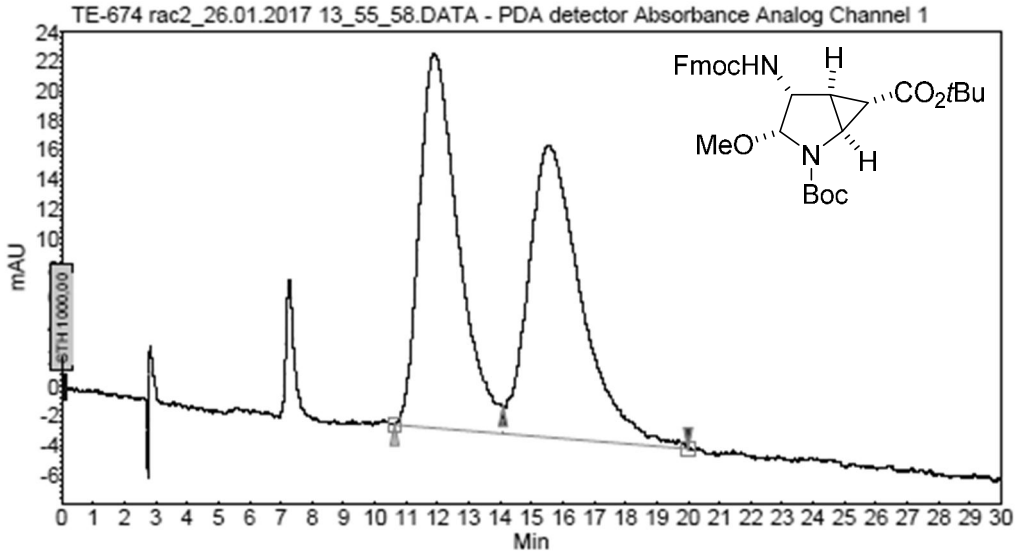


**Peak Results :**

| Index | Name | Time [Min] | Quantity [% Area] | Height [mAU] | Area [mAU.Min] | Area % [%] |
|---|---|---|---|---|---|---|
| 1 | UNKNOWN | 11,88 | 48,74 | 25,4 | 36,8 | 48,737 |
| 2 | UNKNOWN | 15,52 | 51,26 | 19,8 | 38,7 | 51,263 |
| | | | | | | |
| Total | | | 100,00 | 45,2 | 75,5 | 100,000 |

**di-*tert*-Butyl (1*S*,3*S*,4*R*,5*R*,6*S*)-4-((((9H-fluoren-9-yl)methoxy)carbonyl)amino)-3-methoxy-2-azabicyclo[3.1.0]hexane-2,6-dicarboxylate (215)**

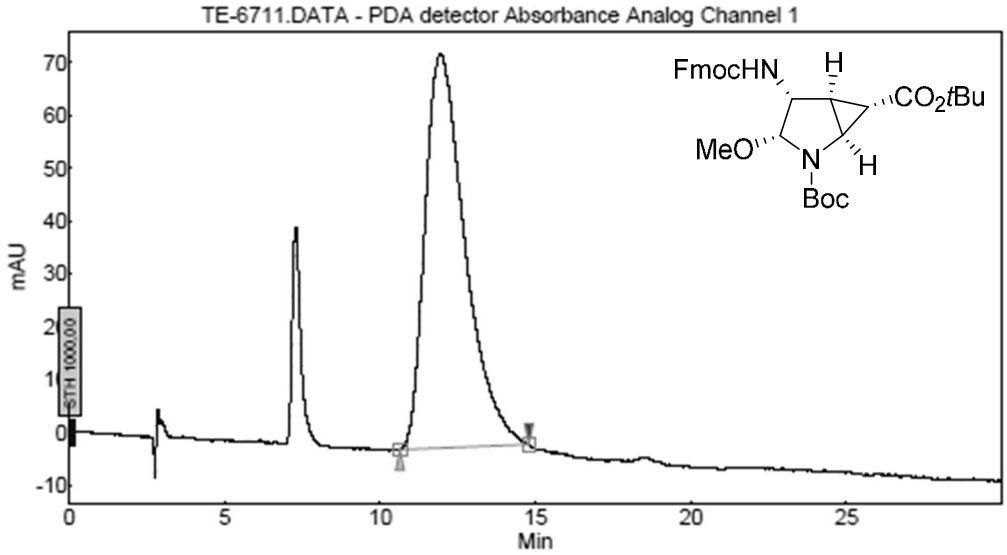


**Peak Results :**

| Index | Name | Time [Min] | Quantity [% Area] | Height [mAU] | Area [mAU.Min] | Area % [%] |
|---|---|---|---|---|---|---|
| 1 | UNKNOWN | 11,94 | 100,00 | 74,8 | 111,8 | 100,000 |
| | | | | | | |
| Total | | | 100,00 | 74,8 | 111,8 | 100,000 |

**_tert_-Butyl-3-((((9H-fluoren-9-yl)methoxy)carbonyl)amino)-4-(2-(_tert_-butoxy)-2-oxoethyl)pyrrolidine-1-carboxylate ((_rac_)-(±)-216)**

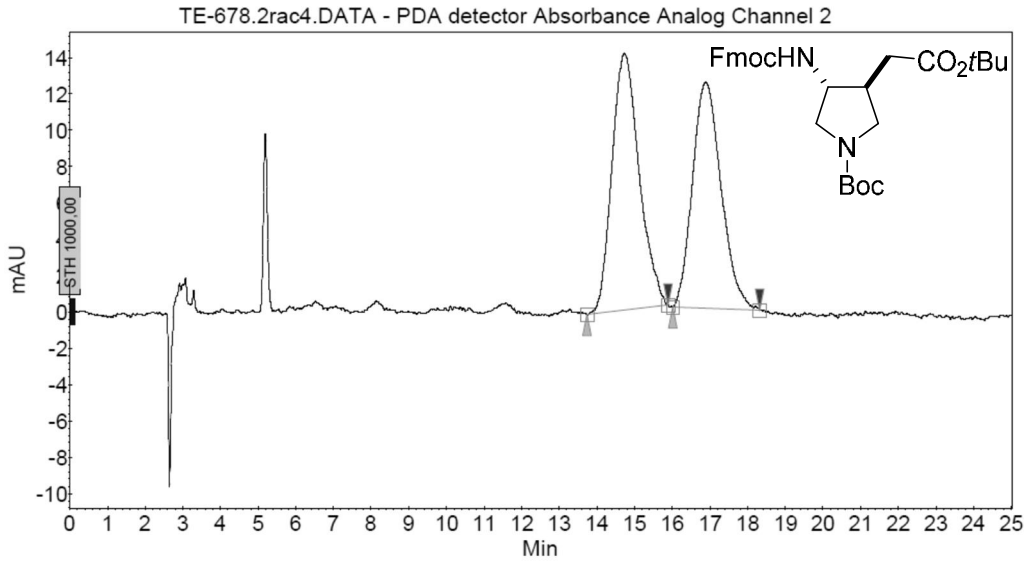


**Peak Results :**

| Index | Name | Time [Min] | Quantity [% Area] | Height [mAU] | Area [mAU.Min] | Area % [%] |
|---|---|---|---|---|---|---|
| 1 | UNKNOWN | 14,72 | 51,82 | 14,2 | 11,8 | 51,819 |
| 2 | UNKNOWN | 16,89 | 48,18 | 12,5 | 11,0 | 48,181 |
| | | | | | | |
| Total | | | 100,00 | 26,7 | 22,8 | 100,000 |

**_tert_-Butyl-(3_R_,4_S_)-3-((((9H-fluoren-9-yl)methoxy)carbonyl)amino)-4-(2-(_tert_-butoxy)-2-oxoethyl)pyrrolidine-1-carboxylate (216)**

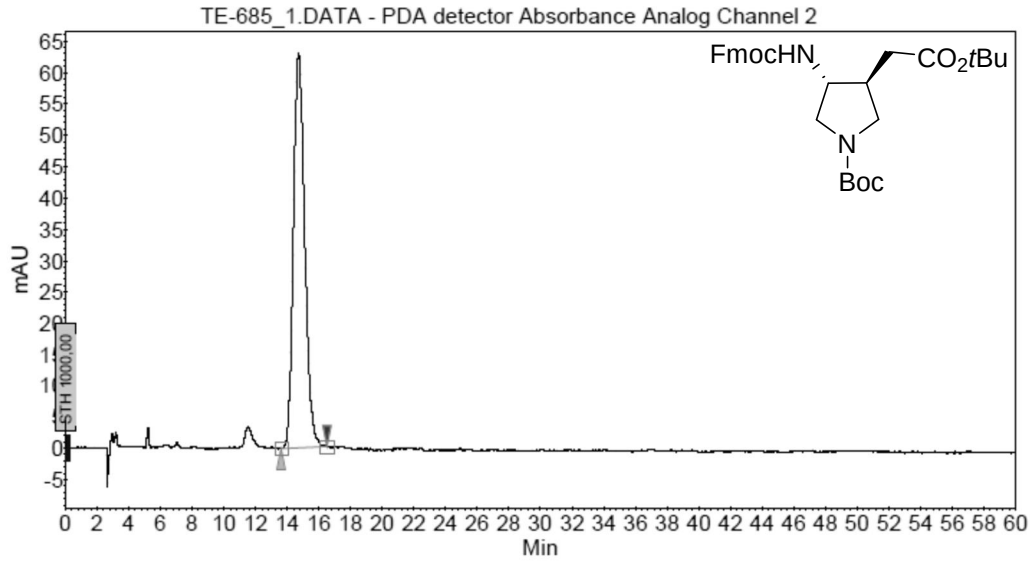


**Peak Results :**

| Index | Name | Time [Min] | Quantity [% Area] | Height [mAU] | Area [mAU.Min] | Area % [%] |
|---|---|---|---|---|---|---|
| 1 | UNKNOWN | 14,72 | 100,00 | 63,0 | 52,0 | 100,000 |
| | | | | | | |
| Total | | | 100,00 | 63,0 | 52,0 | 100,000 |

## 3. X-ray crystallographic data

### (±)-di-*tert*-Butyl-piperidine-1,3-dicarboxylate (200)

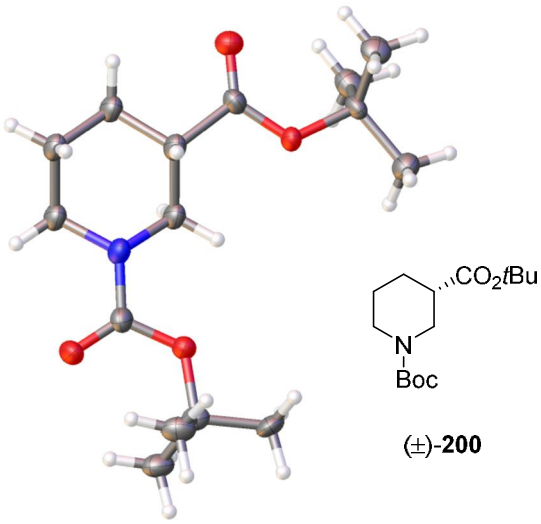


(±)-**200**

**Table 1.** Crystal data and structure refinement for **200**.

| | |
|---|---|
| Identification code | **200** |
| Empirical formula | $C_{15}H_{27}NO_4$ |
| Formula weight | 285.37 |
| Temperature/K | 123.00(10) |
| Crystal system | monoclinic |
| Space group | Ia |
| a/Å | 15.9418(9) |
| b/Å | 8.8090(5) |
| c/Å | 11.6098(7) |
| α/° | 90 |
| β/° | 98.582(6) |
| γ/° | 90 |
| Volume/Å$^3$ | 1612.13(16) |
| Z | 4 |
| $\rho_{calc}$g/cm$^3$ | 1.176 |
| μ/mm$^{-1}$ | 0.684 |
| F(000) | 624.0 |
| Crystal size/mm$^3$ | 0.246 × 0.123 × 0.046 |

| | |
|---|---|
| Radiation | CuKα (λ = 1.54184) |
| 2Θ range for data collection/° | 11.226 to 146.74 |
| Index ranges | -19 ≤ h ≤ 19, -10 ≤ k ≤ 10, -10 ≤ l ≤ 14 |
| Reflections collected | 4547 |
| Independent reflections | 2316 [$R_{int}$ = 0.0173, $R_{sigma}$ = 0.0219] |
| Data/restraints/parameters | 2316/217/242 |
| Goodness-of-fit on $F^2$ | 1.084 |
| Final R indexes [I>=2σ (I)] | $R_1$ = 0.0543, $wR_2$ = 0.1476 |
| Final R indexes [all data] | $R_1$ = 0.0616, $wR_2$ = 0.1571 |
| Largest diff. peak/hole / e $Å^{-3}$ | 0.64/-0.26 |
| Flack parameter | 0.4(5) |

**Table 2.** Fractional Atomic Coordinates (×$10^4$) and Equivalent Isotropic Displacement Parameters ($Å^2$×$10^3$) for **200**. $U_{eq}$ is defined as 1/3 of of the trace of the orthogonalised $U_{IJ}$ tensor.

| **Atom** | ***x*** | ***y*** | ***z*** | **U(eq)** |
|---|---|---|---|---|
| O2 | 4631(3) | 11091(5) | 2838(5) | 32.6(9) |
| O4 | 2721(3) | 11076(5) | 5531(5) | 30.2(9) |
| O3 | 2161(4) | 8857(6) | 6064(5) | 41.0(11) |
| O1 | 5185(4) | 8886(5) | 2295(5) | 40.9(11) |
| C2 | 3944(6) | 8874(9) | 3295(7) | 32.1(6) |
| C9 | 5142(5) | 11820(8) | 1024(6) | 39.4(15) |
| C11 | 2651(4) | 9564(7) | 5601(6) | 32.0(12) |
| C2A | 3400(9) | 8825(11) | 5024(10) | 32.4(6) |
| C12 | 2099(5) | 12058(7) | 6037(6) | 29.2(13) |
| C14 | 1218(4) | 11739(8) | 5443(7) | 39.9(15) |
| C6 | 4664(4) | 9558(7) | 2795(5) | 31.8(12) |
| C7 | 5225(5) | 12043(7) | 2318(6) | 31.5(13) |
| C5 | 3371(7) | 7176(8) | 5198(6) | 32.7(6) |
| C10 | 6135(4) | 11750(8) | 2939(7) | 39.8(15) |
| C13 | 2390(5) | 13657(8) | 5749(7) | 40.5(14) |
| C8 | 4943(5) | 13613(8) | 2578(7) | 39.7(14) |
| C1A | 3442(6) | 9562(14) | 3827(8) | 32.0(6) |
| C15 | 2198(5) | 11817(8) | 7354(6) | 39.4(15) |
| C5A | 3955(10) | 7189(10) | 3243(8) | 32.9(6) |
| C4 | 3377(4) | 6435(11) | 3994(6) | 33.4(6) |
| N1A | 4208(5) | 8796(9) | 3505(8) | 32.6(6) |
| C3A | 3092(5) | 7176(10) | 4789(11) | 33.0(6) |

| | | | | |
|---|---|---|---|---|
| C3 | 4089(5) | 7143(9) | 3402(9) | 32.9(6) |
| C1 | 3910(4) | 9601(10) | 4497(6) | 32.1(6) |
| C4A | 3888(5) | 6430(14) | 4424(8) | 33.2(6) |
| N1 | 3256(5) | 8853(7) | 5097(8) | 32.6(6) |

**Table 3.** Anisotropic Displacement Parameters ($Å^2×10^3$) for **200**. The Anisotropic displacement factor exponent takes the form: $-2\pi^2[h^2a^{*2}U_{11}+2hka^*b^*U_{12}+\ldots]$.

| Atom | $U_{11}$ | $U_{22}$ | $U_{33}$ | $U_{23}$ | $U_{13}$ | $U_{12}$ |
|---|---|---|---|---|---|---|
| O2 | 39(2) | 25(2) | 39(2) | -0.3(19) | 20.2(17) | -0.6(18) |
| O4 | 34.5(18) | 20(2) | 40(2) | -1.5(18) | 17.3(16) | 2.7(17) |
| O3 | 50(2) | 33(3) | 45(3) | 2(2) | 24.0(19) | -2(2) |
| O1 | 50(2) | 28(2) | 52(3) | 1(2) | 33(2) | 4(2) |
| C2 | 34.3(14) | 21.5(10) | 43.0(13) | 0.0(17) | 14.4(10) | 2.3(16) |
| C9 | 47(3) | 39(4) | 36(3) | 6(3) | 15(3) | -8(3) |
| C11 | 34(2) | 29(3) | 37(3) | -4(3) | 17(2) | 1(2) |
| C2A | 34.9(14) | 21.9(10) | 43.3(13) | -0.3(17) | 14.7(10) | 2.7(16) |
| C12 | 34(3) | 28(3) | 30(3) | 0(2) | 17(2) | 8(2) |
| C14 | 43(3) | 45(4) | 33(3) | -1(3) | 10(2) | 8(3) |
| C6 | 44(3) | 24(3) | 30(3) | -3(2) | 13(2) | 0(3) |
| C7 | 35(3) | 30(3) | 31(3) | 4(2) | 9(2) | -2(2) |
| C5 | 35.1(14) | 21.8(10) | 43.8(13) | 0.0(17) | 13.9(10) | 2.4(16) |
| C10 | 33(3) | 47(4) | 42(3) | 7(3) | 11(2) | -6(3) |
| C13 | 52(3) | 29(3) | 43(3) | 4(3) | 17(3) | 2(3) |
| C8 | 55(4) | 22(3) | 46(4) | 6(3) | 22(3) | -8(3) |
| C1A | 34.6(14) | 21.3(10) | 43.0(13) | -0.1(17) | 14.9(10) | 2.7(16) |
| C15 | 52(4) | 41(4) | 27(3) | 2(2) | 8(3) | 2(3) |
| C5A | 35.2(14) | 21.9(10) | 44.0(13) | -0.4(17) | 14.1(11) | 2.7(16) |
| C4 | 35.7(14) | 22(1) | 44.5(13) | 0.0(17) | 13.3(10) | 2.4(16) |
| N1A | 35.3(14) | 21.6(10) | 43.8(13) | -0.1(17) | 15.3(11) | 2.4(16) |
| C3A | 35.7(14) | 21.8(10) | 44.0(13) | 0.2(17) | 14.5(11) | 2.6(16) |
| C3 | 35.5(14) | 21.8(10) | 44.0(13) | -0.5(17) | 14.3(10) | 2.7(16) |
| C1 | 34.7(14) | 21.5(10) | 43.1(13) | -0.3(17) | 14.9(10) | 2.3(16) |
| C4A | 35.6(14) | 21.9(10) | 44.4(13) | -0.1(17) | 13.3(11) | 2.7(16) |
| N1 | 35.2(14) | 21.9(10) | 43.4(13) | -0.2(16) | 15(1) | 2.7(16) |

**Table 4.** Bond Lengths for **200**.

| Atom | Atom | Length/Å | Atom | Atom | Length/Å |
|---|---|---|---|---|---|
| O2 | C6 | 1.352(7) | C12 | C14 | 1.495(8) |

| | | | | | |
|---|---|---|---|---|---|
| O2 | C7 | 1.462(8) | C12 | C13 | 1.535(9) |
| O4 | C11 | 1.340(7) | C12 | C15 | 1.529(8) |
| O4 | C12 | 1.501(7) | C6 | N1A | 1.356(6) |
| O3 | C11 | 1.187(8) | C7 | C10 | 1.541(8) |
| O1 | C6 | 1.233(7) | C7 | C8 | 1.499(9) |
| C2 | C6 | 1.489(12) | C5 | C4 | 1.544(3) |
| C2 | C3 | 1.544(3) | C5 | N1 | 1.491(4) |
| C2 | C1 | 1.544(3) | C1A | N1A | 1.491(4) |
| C9 | C7 | 1.501(9) | C5A | N1A | 1.491(4) |
| C11 | C2A | 1.594(15) | C5A | C4A | 1.544(3) |
| C11 | N1 | 1.355(6) | C4 | C3 | 1.544(3) |
| C2A | C1A | 1.544(3) | C3A | C4A | 1.544(3) |
| C2A | C3A | 1.544(3) | C1 | N1 | 1.490(4) |

**Table 5.** Bond Angles for **200**.

| **Atom** | **Atom** | **Atom** | **Angle/°** | **Atom** | **Atom** | **Atom** | **Angle/°** |
|---|---|---|---|---|---|---|---|
| C6 | O2 | C7 | 121.7(4) | O1 | C6 | C2 | 127.0(5) |
| C11 | O4 | C12 | 118.8(4) | O1 | C6 | N1A | 120.6(6) |
| C6 | C2 | C3 | 108.4(6) | O2 | C7 | C9 | 111.9(5) |
| C6 | C2 | C1 | 108.5(6) | O2 | C7 | C10 | 109.5(5) |
| C1 | C2 | C3 | 111.2(8) | O2 | C7 | C8 | 102.4(5) |
| O4 | C11 | C2A | 107.8(5) | C9 | C7 | C10 | 112.5(6) |
| O4 | C11 | N1 | 111.2(5) | C8 | C7 | C9 | 109.7(5) |
| O3 | C11 | O4 | 128.0(5) | C8 | C7 | C10 | 110.4(5) |
| O3 | C11 | C2A | 124.1(6) | N1 | C5 | C4 | 111.4(7) |
| O3 | C11 | N1 | 120.8(6) | N1A | C1A | C2A | 100.5(8) |
| C1A | C2A | C11 | 110.0(8) | N1A | C5A | C4A | 106.4(8) |
| C1A | C2A | C3A | 107.0(10) | C5 | C4 | C3 | 109.7(8) |
| C3A | C2A | C11 | 102.7(8) | C6 | N1A | C1A | 117.5(7) |
| O4 | C12 | C13 | 101.8(5) | C6 | N1A | C5A | 120.0(8) |
| O4 | C12 | C15 | 109.6(5) | C1A | N1A | C5A | 105.9(10) |
| C14 | C12 | O4 | 110.0(5) | C4A | C3A | C2A | 101.3(9) |
| C14 | C12 | C13 | 111.5(5) | C4 | C3 | C2 | 108.9(8) |
| C14 | C12 | C15 | 112.7(5) | N1 | C1 | C2 | 111.1(7) |
| C15 | C12 | C13 | 110.8(5) | C3A | C4A | C5A | 103.2(10) |
| O2 | C6 | C2 | 110.7(5) | C11 | N1 | C5 | 120.7(6) |
| O2 | C6 | N1A | 116.4(6) | C11 | N1 | C1 | 126.2(6) |
| O1 | C6 | O2 | 122.0(5) | C1 | N1 | C5 | 112.9(7) |

**Table 6.** Torsion Angles for **200**.

| A | B | C | D | Angle/° | A | B | C | D | Angle/° |
|---|---|---|---|---|---|---|---|---|---|
| O2 | C6 | N1A | C1A | 27.4(13) | C12 | O4 | C11 | N1 | 179.5(6) |
| O2 | C6 | N1A | C5A | 158.6(9) | C6 | O2 | C7 | C9 | 62.4(7) |
| O4 | C11 | C2A | C1A | -48.5(11) | C6 | O2 | C7 | C10 | -63.0(7) |
| O4 | C11 | C2A | C3A | -162.1(8) | C6 | O2 | C7 | C8 | 179.9(5) |
| O4 | C11 | N1 | C5 | 172.4(8) | C6 | C2 | C3 | C4 | 176.3(6) |
| O4 | C11 | N1 | C1 | -1.9(13) | C6 | C2 | C1 | N1 | -174.3(6) |
| O3 | C11 | C2A | C1A | 135.5(8) | C7 | O2 | C6 | O1 | -1.6(10) |
| O3 | C11 | C2A | C3A | 21.9(13) | C7 | O2 | C6 | C2 | -175.0(6) |
| O3 | C11 | N1 | C5 | -5.3(14) | C7 | O2 | C6 | N1A | 166.7(6) |
| O3 | C11 | N1 | C1 | -179.6(8) | C5 | C4 | C3 | C2 | -57.8(11) |
| O1 | C6 | N1A | C1A | -164.1(8) | C1A | C2A | C3A | C4A | 73.1(12) |
| O1 | C6 | N1A | C5A | -33.0(14) | C4 | C5 | N1 | C11 | 128.8(9) |
| C2 | C1 | N1 | C11 | -130.9(9) | C4 | C5 | N1 | C1 | -56.2(12) |
| C2 | C1 | N1 | C5 | 54.4(11) | N1A | C5A | C4A | C3A | 70.2(12) |
| C11 | O4 | C12 | C14 | -60.5(7) | C3A | C2A | C1A | N1A | -73.2(12) |
| C11 | O4 | C12 | C13 | -178.8(5) | C3 | C2 | C6 | O2 | -171.3(6) |
| C11 | O4 | C12 | C15 | 63.9(7) | C3 | C2 | C6 | O1 | 15.8(12) |
| C11 | C2A | C1A | N1A | 176.0(8) | C3 | C2 | C1 | N1 | -55.1(11) |
| C11 | C2A | C3A | C4A | -171.1(9) | C1 | C2 | C6 | O2 | -50.4(9) |
| C2A | C1A | N1A | C6 | -152.0(9) | C1 | C2 | C6 | O1 | 136.7(7) |
| C2A | C1A | N1A | C5A | 70.7(11) | C1 | C2 | C3 | C4 | 57.1(11) |
| C2A | C3A | C4A | C5A | -68.0(11) | C4A | C5A | N1A | C6 | 151.1(9) |
| C12 | O4 | C11 | O3 | -3.0(10) | C4A | C5A | N1A | C1A | -72.8(13) |
| C12 | O4 | C11 | C2A | -178.8(7) | N1 | C5 | C4 | C3 | 57.6(11) |

**Table 7.** Hydrogen Atom Coordinates ($Å \times 10^4$) and Isotropic Displacement Parameters ($Å^2 \times 10^3$) for **200**.

| Atom | *x* | *y* | *z* | U(eq) |
|---|---|---|---|---|
| H5 | 3412 | 9077 | 2778 | 38 |
| H9A | 4567 | 12008 | 677 | 59 |
| H9B | 5295 | 10797 | 860 | 59 |
| H9C | 5513 | 12513 | 707 | 59 |
| H2A | 3946 | 8873 | 5539 | 39 |
| H14A | 1050 | 10744 | 5655 | 60 |
| H14B | 1205 | 11788 | 4614 | 60 |
| H14C | 836 | 12480 | 5678 | 60 |
| H13A | 2914 | 6745 | 5558 | 39 |
| H13B | 3901 | 6955 | 5696 | 39 |

| | | | | |
|---|---|---|---|---|
| H10A | 6280 | 10705 | 2845 | 60 |
| H10B | 6166 | 11978 | 3753 | 60 |
| H10C | 6524 | 12387 | 2605 | 60 |
| H13C | 2393 | 13741 | 4926 | 61 |
| H13D | 2951 | 13835 | 6155 | 61 |
| H13E | 2008 | 14396 | 5988 | 61 |
| H8A | 5022 | 13767 | 3405 | 60 |
| H8B | 4354 | 13735 | 2268 | 60 |
| H8C | 5273 | 14344 | 2226 | 60 |
| H1AA | 2939 | 9340 | 3273 | 38 |
| H1AB | 3519 | 10653 | 3891 | 38 |
| H15A | 2786 | 11914 | 7681 | 59 |
| H15B | 2000 | 10821 | 7515 | 59 |
| H15C | 1872 | 12565 | 7694 | 59 |
| H5AA | 4377 | 6677 | 2861 | 39 |
| H5AB | 3413 | 7146 | 2736 | 39 |
| H20A | 2833 | 6593 | 3511 | 40 |
| H20B | 3470 | 5351 | 4087 | 40 |
| H3AA | 2939 | 6707 | 5485 | 40 |
| H3AB | 2612 | 7128 | 4169 | 40 |
| H19C | 4084 | 6702 | 2635 | 39 |
| H19D | 4637 | 6937 | 3862 | 39 |
| H17C | 4461 | 9509 | 4976 | 39 |
| H17D | 3779 | 10672 | 4398 | 39 |
| H4AA | 3817 | 5340 | 4339 | 40 |
| H4AB | 4388 | 6637 | 4989 | 40 |

**Table 8.** Atomic Occupancy for **200**.

| **Atom** | ***Occupancy*** | **Atom** | ***Occupancy*** | **Atom** | ***Occupancy*** |
|---|---|---|---|---|---|
| C2 | 0.570(8) | H5 | 0.570(8) | C2A | 0.430(8) |
| H2A | 0.430(8) | C5 | 0.570(8) | H13A | 0.570(8) |
| H13B | 0.570(8) | C1A | 0.430(8) | H1AA | 0.430(8) |
| H1AB | 0.430(8) | C5A | 0.430(8) | H5AA | 0.430(8) |
| H5AB | 0.430(8) | C4 | 0.570(8) | H20A | 0.570(8) |
| H20B | 0.570(8) | N1A | 0.430(8) | C3A | 0.430(8) |
| H3AA | 0.430(8) | H3AB | 0.430(8) | C3 | 0.570(8) |
| H19C | 0.570(8) | H19D | 0.570(8) | C1 | 0.570(8) |
| H17C | 0.570(8) | H17D | 0.570(8) | C4A | 0.430(8) |
| H4AA | 0.430(8) | H4AB | 0.430(8) | N1 | 0.570(8) |

## 4. Curriculum Vitae

### Personal Data


| | |
|---|---|
| Name | Thomas Johannes Ertl |
| Date of birth | January 25, 1988, Landshut |
| Nationality | German |
| Email | Thomas2.Ertl@chemie.uni-regensburg.de |


### Education

| | |
|---|---|
| 10/2013 – Current | PhD thesis in the group of Prof. Dr. O. Reiser at the University of Regensburg, Germany |
| 12/2013 | Research stay in the group of Prof. Dr. C. Cabrele, University of Salzburg, Austria |
| 09/2013 | Master of Science in chemistry |
| 01/2013-09/2013 | Master thesis in the group of Prof. Dr. O. Reiser at the University of Regensburg, Germany |
| 10/2011 – 09/2013 | Advanced studies in chemistry at the University of Regensburg, Germany |
| 10/2011 | Bachelor of Science in chemistry |
| 03/2011 - 06/2011 | Bachelor thesis in the group of Prof. Dr. O. Reiser at the University of Regensburg, Germany |
| 10/2008 - 09/2011 | Studies in chemistry, University of Regensburg, Germany |
| 09/1998 - 06/2007 | Abitur (A-levels), Burkhart Gymnasium (secondary school) Mallersdorf-Pfaffenberg, Germany (High school Certificate equivalent) |

## Professional References

**Prof. Dr. Oliver Reiser**
Institute für Organische Chemie
Universität Regensburg
Universitätsstr. 31
93053 Regensburg, Germany
Phone: +49-941-9434631
E-mail: oliver.reiser@chemie.uni-regensburg.de

**Prof. Dr. Armin Buschauer**
Institute für Pharmazie
Universität Regensburg
Universitätsstr. 31
93053 Regensburg, Germany
Phone: +49-941-943-4827
E-mail: armin.buschauer@chemie.uni-regensburg.de

**Prof. Dr. Chiara Cabrele**

Institut für Molekulare Biologie
Universität Salzburg
Billrothstraße 11
5020 Salzburg, Austria
Phone: +43-662-8044-7240
E-mail: chiara.cabrele@sbg.ac.at

## List of publications

[1] L. Pilsl,[‡] **T. Ertl**,[‡] O. Reiser *Org. Lett*. **2017**, *19*, 2754–2757.
*Enantioselective Three-Step Synthesis of Homo-β-proline: A Donor–Acceptor Cyclopropane as Key Intermediate.*

[2] K.K. Kuhn, **T. Ertl**, S. Dukorn, M. Keller, G. Bernhardt, O. Reiser, A. Buschauer *J. Med. Chem*. **2016**, *59*, 6049–6058.
*High affinity agonists of the neuropeptide Y (NPY) Y4 receptor derived from the C-terminal pentapeptide of human pancreatic polypeptide (hPP): synthesis, stereochemical discrimination and radiolabeling.*

[3] A. Kreuzer, S. Kerres, **T. Ertl**, H. Rücker, S. Amslinger, O. Reiser *Org. Lett*. **2013**, *15*, 3420–3423.
*Asymmetric Synthesis of Both Enantiomers of Arteludovicinolide A.*

## Conferences

***8th Summer School „Medicinal Chemistry“***, University of Regensburg (Germany)
21.-23.09.2016 *"Synthesis of unnatural cyclic amino acids and their application in NPY-analogues"* (Poster).

***6th EuCheMS Chemistry Congress***, Seville (Spain)
11.-15.09.2016 "*Cyclic β-Amino Acids as Building Blocks for Tripeptide Organocatalysts" (Poster).*

***GDCh Wissenschaftsforum 2015***, Dresden (Germany)
30.08.-02.09.2015 "*Cyclic β-Amino Acids as Switching Tools for Selectivity of NPY-Analogues"* (Poster).

***7th Summer School „Medicinal Chemistry“***, University of Regensburg (Germany),
17.-19.09.2014 *"Synthesis of unnatural cyclic amino acids as building blocks for foldamers – towards NPY analogues"* (Poster).

***Research Day of the Emil Fischer Graduate Programm*** – University of Erlangen (Germany), 09.07.2015 *"New neuropeptide Y ligands"* (oral presentation 15 min).

***Annual GRK 1910 Report Meetings*** (oral presentation, 15 min).

***Regularly Group Seminar Research Report*** (oral presentation, 15 min).

# G. Literature

[1] Purves, W. K.; Sadava, D.; Orians, G. H.; Heller, H.C. *Biologie*, 7th edition, Elsevier Spektrum Akademischer Verlag, 2006, Chapter 3.

[2] Bruice, P. Y. *Organische Chemie*, 5th edition, Pearson Studium 2007, Chapter 21 and 22.

[3] Hoppe, B.; Martens, J. *Chemie in unserer Zeit* **1983**, *17*, 41–53.

[4] Hoppe, B.; Martens, J. *Chemie in unserer Zeit* **1984**, *18*, 73–86.

[5] Izumi, Y.; Chibata, I.; Itoh, T. *Angew. Chem., Int. Ed.* **1978**, *17*, 176–183.

[6] Strecker, A. *Liebigs Ann. Chem.* **1850**, *75*, 27–45.

[7] For recent reviews see: (a) Yet, L. *Angew. Chem., Int. Ed.* **2001**, *40*, 875–877. (b) Gröger, H. *Chem. Rev.* **2003**, *103*, 2795–2828. (c) Najera, C.; Sansano, J. M. *Chem. Rev.* **2007**, *107*, 4584–4671. (d) Wang, J.; Liu, X.; Feng, X. *Chem. Rev.* **2011**, *111*, 6947–6983.

[8] Kingston, D. G. I. *Phytochemistry* **2007**, *68*, 1844–1854.

[9] Stauffer, C. S.; Datta, A. *J. Org. Chem.* **2008**, *73*, 4166–4174.

[10] Ott, G. R.; Asakawa, N.; Lu, Z.; Liu, R.-Q.; Covington, M. B.; Vaddi, K.; Qian, M.; Newton, R. C.; Christ, D. D.; Traskos, J. M.; Decicco, C. P.; Duan, J. J.-W. *Bioorg. Med. Chem. Lett.* **2008**, *18*, 694–699.

[11] Wang, G. T.; Chen, Y.; Wang, S.; Gentles, R.; Sowin, T.; Kati, W.; Muchmore, S.; Giranda, V.; Stewart, K.; Sham, H.; Kempf, D.; Laver, W. G. *J. Med. Chem.* **2001**, *44*, 1192–1201.

[12] Brown, K. M.; Roy, K. K.; Hockerman, G. H.; Doerksen, R. J.; Colby, D. A. *J. Med. Chem.* **2015**, *58*, 6336–6347.

[13] Goto, T.; Toya, Y.; Ohgi, T.; Kondo, T. *Tetrahedron Lett.* **1982**, *23*, 1271–1274.

[14] (a) Ramachandran, G. N.; Ramakrishnan, C.; Sasisekharan, V. *J. Mol. Biol.* **1963**, *7*, 95–99. (b) Banerjee, A.; Balaram, P. *Curr. Sci.* **1997**, *73*, 1067–1077.

[15] (a) Möhle, K.; Günther, R.; Thormann, M.; Sewald, N.; Hofmann, H.-J. *J. Biopolymers* **1999**, *50*, 167–184. (b) Vasudev, P. G.; Chatterjee, S.; Shamala, N.; Balaram, P. *Chem. Rev.* **2011**, *111*, 657–687.

[16] (a) Appella, D. H.; Christianson, L. A.; Karle, I. L.; Powell, D. R.; Gellman, S. H. *J. Am. Chem. Soc.* **1996**, *118*, 13071–13072. (b) Gellman, S. H. *Acc. Chem. Res.* **1998**, *31*, 173–180.

[17] (a) Hook, D. F.; Bindschädler, P.; Mahaja, Y. R.; Sebesta, R.; Kast, P.; Seebach, D. *Chem. Biodiversity* **2005**, *2*, 591–632. (b) Seebach, D.; Ciceri, P. E.; Overhand, M.; Juan, B.; Rigo, D.; Oberer, L.; Hommel, U.; Amstutz, R.; Widmer, H. *Helv. Chim. Acta* **1996**, *79*, 2043–2066. (c) Seebach, D.; Matthews, J. L. *Chem. Commun.* **1997**, 2015–2022. (d) Schmitt, M. A.; Weisblum, B.; Gellman, S. H. *J. Am. Chem. Soc.* **2007**, *129*, 417–428.

[18] Berlicki, L.; Pilsl, L.; Wéber, E.; Mándity, I. M.; Cabrele, C.; Martinek, T. A.; Fülöp, F.; Reiser, O. *Angew. Chem., Int. Ed.* **2012**, *51*, 2208–2212.

[19] Xin, D.; Jeffries, A.; Burgess, K. *ACS Comb. Sci.* **2017**, *19*, 414–421.

[20] Arndt, F.; Eistert, B. *Ber. Dtsch. Chem. Ges.* **1935**, *68*, 200–208.

[21] (a) Pace, V.; Verniest, G.; Sinisterra, J.-V.; Alcántara, A. R.; de Kimpe, N. *J. Org. Chem.* **2010**, *75*, 5760–5763. (b) Pinho, V. D.; Gutmann, B.; Kappe, C. O. *RSC Adv.* **2014**, *4*, 37419–37422.

[22] (a) Kiss, L.; Fülöp, F. *Chem. Rev.* **2014**, *114*, 1116–1169. (b) Risseeuw, M.; Overhand, M.; Fleet, G. W. J.; Simone, M. I. *Amino Acids* **2013**, *45*, 613–689. (c) Ordónez, M.; Cativiela, C.; Romero-Estudillo, I. *Tetrahedron: Asymmetry* **2016**, *27*, 999–1055.

[23] Davies, S. G.; Ichihara, O.; Lenoir, I.; Walters, I. A. S. *J. Chem. Soc., Perkin Trans. 1* **1994**, *2*, 1411–1415.

[24] Abraham, E.; Bailey, C. W.; Claridge, T. D.; Davies, S. G.; Ling, K. B.; Odell, B.; Rees, T. L.; Roberts, P. M.; Russell, A. J.; Smith, A. D.; Smith, L. J.; Storr, H. R.; Sweet, M. J.; Thompson, A. L.; Thomson, J. E.; Tranter, G. E.; Watkin, D. J. *Tetrahedron: Asymmetry* **2010**, *21*, 1797–1815.

[25] Davies, S. G.; Smith, A. D.; Price, P. D. *Tetrahedron: Asymmetry* **2005**, *16*, 2833–2891.

[26] Davies, S. G.; Díez, D.; Dominguez, S. H.; Garrido, N. M.; Kruchinin, D.; Price, P. D.; Smith, A. D. *Org. Biomol. Chem.* **2005**, *3*, 1284–1301.

[27] Forró, E.; Fülöp, F. *Org. Lett.* **2003**, *5*, 1209–1212.

[28] Bolm, C.; Schiffers, I.; Atodiresei, I.; Hackenberger, C. P. *Tetrahedron: Asymmetry* **2003**, *14*, 3455–3467.

[29] Aggerwal, V. K.; Roseblade, S.; Rikki, A. *Org. Biomol. Chem.* **2003**, *1*, 684–691.

[30] Pou, A.; Moyano, A. *Eur. J. Org. Chem.* **2013**, *2013*, 3103–3111.

[31] Gardiner, J.; Anderson, K. H.; Downard, A.; Abell, A. D. *J. Org. Chem.* **2004**, *69*, 3375–3382.

[32] Sadowsky, J. D.; Fairlie, W. D.; Hadley, E. B.; Lee, H.-S.; Umezawa, N.; Nikolovska-Coleska, Z.; Wang, S.; Huang, D. C. S.; Tomita, Y.; Gellman, S. H. *J. Am. Chem. Soc.* **2007**, *129*, 139–154.

[33] Bunnage, M. E.; Davies, S. G.; Roberts, P. M.; Smith, A. D.; Withey, J. M. *Org. Biomol. Chem.* **2004**, *2*, 2763–2776.

[34] Hanselmann, R.; Zhou, J.; Ma, P.; Confalone, P. N. *J. Org. Chem.* **2003**, *68*, 8739–8741.

[35] Selected examples: (a) Guo, L.; Zhang, W.; Reidenbach, A. G.; Giuliano, M. W.; Guzei, I. A.; Spencer, L. C.; Gellman, S. H. *Angew. Chem., Int. Ed.* **2011**, *50*, 5843–5846. (b) Grison, C. M.; Robin, S.; Aitken, D. J. *Chem. Commun.* **2016**, *52*, 7802–7805. (c) Shi, Y.; Teng, P.; Sang, P.; She, F.; Wei, L.; Cai, J. *Acc. Chem. Res.* **2016**, *49*, 428–441. (d) Seebach, D.; Hook, D. F.; Glättli, A. *Biopolymers* **2006**, *84*, 23–37.

[36] Selected examples: (a) Vasudev, P. G.; Chatterjee, S.; Shamala, N.; Balaram, P. *Acc. Chem. Res.* **2009**, *42*, 1628–1639. (b) Bouillère, F.; Thétiot-Laurent, S.; Kouklovsky, C.; Alezra, V. *Amino Acids* **2011**, *41*, 687–707. (c) Basuroy, K.; Dinesh, B.; Reddy, M. B. M.; Chandrappa, S.; Raghothama, S.; Shamala, N.; Balaram, P. *Org. Lett.* **2013**, *15*, 4866–4869. (d) Lengyel, G. A.; Eddinger, G. A.; Horne, W. S. *Org. Lett.* **2013**, *15*, 944–947.

[37] (a) Watterson, M. P.; Edwards, A. A.; Leach, J. A.; Smith, M. D.; Ichihara, O.; Fleet, G. W. *Tetrahedron Lett.* **2003**, *44*, 5853–5857.

[38] (a) Gruner, S. A. W.; Truffault, V.; Voll, G.; Locardi, E.; Stöckle, M.; Kessler, H. *Chem. -Eur. J.* **2002**, *8*, 4365–4376.

[39] (a) Sharma, G. V. M.; Jadhav, V. B.; Ramakrishna, K. V. S.; Jayaprakash, P.; Narsimulu, K.; Subash, V.; Kunwar, A. C. *J. Am. Chem. Soc.* **2006**, *128*, 14657–14668. (b) Sharma, G. V. M.; Chandramouli, N.; Choudhary, M.; Nagendar, P.; Ramakrishna, K. V. S.; Kunwar, A. C.; Schramm, P.; Hofmann, H.-J. *J. Am. Chem. Soc.* **2009**, *131*, 17335–17344.

[40] (a) Giuliano, M. W.; Maynard, S. J.; Almeida, A. M.; Guo, L.; Guzei, I. A.; Spencer, L. C.; Gellman, S. H. *J. Am. Chem. Soc.* **2014**, *136*, 15046–15053. (b) Fisher, B. F.; Gellman, S. H. *J. Am. Chem. Soc.* **2016**, *138*, 10766–10769.

[41] (a) Grison, C. M.; Miles, J. A.; Robin, S.; Wilson, A. J.; Aitken, D. J. *Angew. Chem., Int. Ed.* **2016**, *55*, 11096–11100. (b) Grison, C. M.; Robin, S.; Aitken, D. J. *Chem. Commun.* **2016**, *52*, 7802–7805.

[42] Giuliano, M. W.; Maynard, S. J.; Almeida, A. M.; Reidenbach, A. G.; Guo, L.; Ulrich, E. C.; Guzei, I. A.; Gellman, S. H. *J. Org. Chem.* **2013**, *78*, 12351–12361.

[43] Rodríguez-Vázquez, N.; Salzinger, S.; Silva, L. F.; Amorín, M.; Granja, J. R. *Eur. J. Org. Chem.* **2013**, 3477–3493.

[44] Noole, A.; Pehk, T.; Järving, I.; Lopp, M.; Kanger, T. *Tetrahedron: Asymmetry* **2012**, *23*, 188–198.

[45] Pilsl, L. *Masterthesis* **2010**, Regensburg.

[46] Ertl, T. *Masterthesis* **2013**, Regensburg.

[47] Beak, P.; Lee, W. K. *J. Org. Chem.*, **1993**, *58*, 1109–1117.

[48] Yadav, J. S.; Subba Reddy, B. V.; Sanjeeva Rao, K.; Harikishan, K. *Synlett* **2002**, 826–828.

[49] Yadav, J. S.; Balanarsaiah, E.; Raghavendra, S.; Satyanarayana, M. *Tetrahedron Lett.* **2006**, *47*, 4921–4924.

[50] List, B.; Lerner, R. A.; Barbas, C. F. *J. Am. Chem. Soc.* **2000**, *122*, 2395–2396.

[51] Ahrendt, K. A.; Borths, C. J.; MacMillan, D. W. C. *J. Am. Chem. Soc.* **2000**, *122*, 4243–4244.

[52] Melchiorre, P.; Marigo, M.; Carlone, A.; Bartoli, G. *Angew. Chem.*, Int. Ed. **2008**, *47*, 6138–6171.

[53] MacMillan, D. W. C. *Nature* **2008**, *455*, 304–308.

[54] Mukherjee, S.; Yang, J. W.; Hoffmann, S.; List, B. *Chem. Rev.* **2007**, *107*, 5471–5569.

[55] (a) List, B. *J. Am. Chem. Soc.* **2000**, *122*, 9336–9337. (b) List, B. *Synlett* **2001**, 1675–1686. (c) List, B. *Acc. Chem. Res.* **2004**, *37*, 548–557.

[56] See reference 3 of Zhang, H.; Mitsumori, S.; Utsumi, N.; Imai, M.; Garcia-Delgado, N.; Mifsud, M.; Albertshofer, K.; Cheong, P. H.-Y.; Houk, K. N.; Tanaka, H.; Barbas, C. F. *J. Am. Chem. Soc.* **2008**, *130*, 875–886.

[57] See reference 2 of Zhang, H.; Mitsumori, S.; Utsumi, N.; Imai, M.; Garcia-Delgado, N.; Mifsud, M.; Albertshofer, K.; Cheong, P. H.-Y.; Houk, K. N.; Tanaka, H.; Barbas, C. F. *J. Am. Chem. Soc.* **2008**, *130*, 875–886.

[58] Perera, S.; Sinha, D.; Rana, N. K.; van Trieu-Do; Zhao, J. C.-G. *J. Org. Chem.* **2013**, *78*, 10947–10953.

[59] Zhang, H.; Mifsud, M.; Tanaka, F.; Barbas, C. F. 3. *J. Am. Chem. Soc.* **2006**, *128*, 9630–9631.

[60] Zhang, H.; Mitsumori, S.; Utsumi, N.; Imai, M.; Garcia-Delgado, N.; Mifsud, M.; Albertshofer, K.; Cheong, P. H.-Y.; Houk, K. N.; Tanaka, H.; Barbas, C. F. *J. Am. Chem. Soc.* **2008**, *130*, 875–886.

[61] Nagata, K.; Kuga, Y.; Higashi, A.; Kinoshita, A.; Kanemitsu, T.; Miyazaki, M.; Itoh, T. *J. Org. Chem.* **2013**, *78*, 7131–7136.

[62] Enders, D.; Balensiefer, T. *Acc. Chem. Res.* **2004**, *37*, 534–541.

[63] Enders, D.; Niemeier, O.; Henseler, A. *Chem. Rev.* **2007**, *107*, 5606–5655.

[64] Schreiner, P. R. *Chem. Soc. Rev.* **2003**, *32*, 289-296.

[65] Jenner, G. *Tetrahedron* **2002**, 5185–5202.

[66] Salem, R. B.; Jenner, G. *Rev. High Pressure Sci. Technol.* **1998**, 1268–1270.

[67] Jenner, G. *Angew. Chem., Int. Ed.* **1975**, *14*, 137–143.

[68] Reiser, O. *Top. Catal.* **1998**, *5*, 105–112.

[69] Asano, T.; Le Noble, W. J. *Chem. Rev.* **1978**, *78*, 407–489.

[70] van Eldik, R.; Asano, T.; Le Noble, W. J. *Chem. Rev.* **1989**, *89*, 549–688.

[71] Schettino, V.; Bini, R. *Chem. Soc. Rev.* **2007**, *36*, 869–880.

[72] Hillers, S.; Sartori, S.; Reiser, O. *J. Am. Chem. Soc.* **1996**, *118*, 2087–2088.

[73] (a) Kwiatkowski, P.; Dudzinski, K.; Lyzwa, D. *Org. Lett.* **2011**, *13*, 3624–3627. (b) Lyzwa, D.; Dudzinski, K.; Kwiatkowski, P. *Org. Lett.* **2012**, *14*, 1540–1543. (c) Kwiatkowski, P.; Cholewiak, A.; Kasztelan, A. *Org. Lett.* **2014**, *16*, 5930–5933. (d) Kasztelan, A.; Biedrzycki, M.; Kwiatkowski, P. *Adv. Synth. Catal.* **2016**, *358*, 2962–2969.

[74] Hayashi, Y.; Tsuboi, W.; Shoji, M.; Suzuki, N. *J. Am. Chem. Soc.* **2003**, *125*, 11208–11209.

[75] Pilsl, L. *Dissertation* **2014**, Regensburg.

[76] Hofmann, M. *Masterthesis* **2013**, Regensburg.

[77] Miller, S. J. *Acc. Chem. Res.* **2004**, *37*, 601–610.

[78] Davie, E. A. C.; Mennen, S. M.; Xu, Y.; Miller, S. J. *Chem. Rev.* **2007**, *107*, 5759–5812.

[79] Revell, J. D.; Wennemers, H. *Current Opinion in Chemical Biology* **2007**, *11*, 269–278.

[80] Wennemers, H. *Chem. Commun.* **2011**, *47*, 12036–12041.

[81] Akagawa, K.; Sugiyama, M.; Kudo, K. *Org. Biomol. Chem.* **2012**, *10*, 4839–4843.

[82] Akagawa, K.; Kudo, K. *Angew. Chem., Int. Ed*. **2012**, *51*, 12786-12789.

[83] Chandrasekhar, S.; Kumar, C. P.; Kumar, T. P.; Haribabu, K.; Jagadeesh, B.; Lakshmi, J. K.; Mainkar, P. S. *RSC Adv.* **2014**, *4*, 30325–30331.

[84] Akagawa, K.; Suzuki, R.; Kudo, K. *Adv. Synth. Catal*. **2012**, *354*, 1280-1286.

[85] Samanta, S.; Liu, J.; Dodda, R.; Zhao, C.-G. *Org. Lett.* **2005**, *7*, 5321–5323.

[86] Vishnumaya, M. R.; Singh, V. K. *J. Org. Chem.* **2009**, *74*, 4289–4297.

[87] Zhang, H.; Zhang, S.; Liu, L.; Luo, G.; Duan, W.; Wang, W. *J. Org. Chem.* **2010**, *75*, 368–374.

[88] Raj, M.; Vishnumaya, V.; Ginotra, S. K.; Singh, V. K. *Org. Lett.* **2006**, *8*, 4097–4099.

[89] Grünenfelder, C. E.; Kisunzu, J. K.; Wennemers, H. *Angew. Chem., Int. Ed.* **2016**, *128*, 8713–8716.

[90] Peris, G.; Jakobsche, C. E.; Miller, S. J. *J. Am. Chem. Soc.* **2007**, *129*, 8710–8711.

[91] Davis, R. L.; Stiller, J.; Naicker, T.; Jiang, H.; Jorgensen, K. A. *Angew. Chem., Int. Ed.* **2014**, *53*, 7406–7426.

[92] Akagawa, K..; Kudo, K. *Adv. Synth. Catal*. **2011**, *353*, 843-847.

[93] Akagawa, K.; Nishi, N.; Sen, J.; Kudo, K. *Org. Biomol. Chem*. **2014**, *12*, 3581-3585.

[94] Akagawa, K.; Takigawa, S.; Nagamine, I. S.; Umezawa, R.; Kudo, K. *Org. Lett.* **2013**, *15*, 4964–4967.

[95] Tanaka, T.; Akagawa, K.; Mitsuda, M.; Kudo, K. *Adv. Synth. Catal.* **2013**, *355*, 294-296.

[96] Arakawa, Y.; Wennemers, H. *ChemSusChem* **2013**, *6*, 242-245.

[97] Lewandowski, B.; Wennemers, H. *Current Opinion in Chemical Biology* **2014**, *22*, 40–46.

[98] Krattiger, P.; Kovasy, R.; Revell, J. D.; Ivan, S.; Wennemers, H. *Org. Lett.* **2005**, *7*, 1101–1103.

[99] Cheng, R. P.; Gellman, S. H.; DeGrado, W. F. *Chem. Rev.* **2001**, *101*, 3219–3232.

[100] Hill, D. J.; Mio, M. J.; Prince, R. B.; Hughes, T. S.; Moore, J. S. *Chem. Rev.* **2001**, *101*, 3893–4012.

[101] (a) Voigt, J.; Noltemeyer, M.; Reiser, O. *Synlett* **1997**, 202–204. (b) Bubert, C.; Cabrele, C.; Reiser, O. *Synlett* **1997**, 827–829. (c) Beumer, R.; Bubert, C.; Cabrele, C.; Vielhauer, O.; Pietzsch, M.; Reiser, O. *J. Org. Chem.* **2000**, *65*, 8960–8969. (d) Beumer, R.; Bubert, C; Kreitmeier, P.; Reiser, O.; Meudt, A.; Schulte, M. *Patent DE 199 58 497 A*, Merck KGaA Darmstadt, **1998**.

[102] D'Elia, V.; Zwicknagl, H.; Reiser, O. *Org. Lett.* **2008**, *73*, 3262–3265.

[103] D´Elia, V. *Dissertation* **2009**, Regensburg.

[104] (a) Synthesis of cyclobutyl derivative, see: Robledillo Botines, C. *Masterthesis* **2014**, Barcelona. (b) Catalytic evaluation: Robledillo Botines, C. unpublished results, Universitat Autonoma de Barcelona.

[105] Synthesis and catalytic evaluation, see: Hofmann, M. unpublished results, Universität Regensburg.

[106] Dunetz, J. R.; Xiang, Y.; Baldwin, A.; Ringling, J. *Org. Lett.* **2011**, *13*, 5048–5051.

[107] (a) Gisin, B. F.; Merrifield, R. B. *J. Am. Chem. Soc.* **1972**, *94*, 3102–3106. (b) Alsina, J.; Giralt, E.; Albericio, F. *Tetrahedron Lett.* **1996**, *37*, 4195–4198.

[108] Fischer, G. *Chem. Soc. Rev*. **2000**, *29*, 119–127.

[109] Fox, D. J.; Pedersen, D. S.; Warren, S. *Org. Biomol. Chem.* **2006**, *4*, 3113–3116.

[110] Suppo, J.-S.; de Figueiredo, R. M. ; Campagne, J.-M. *Org. Synth.* **2015**, *92*, 296–308.

[111] Curtius, T. *J. Prakt. Chem.* **1894**, *50*, 275–294.

[112] (a) Zhang, Z.; Schreiner, P. R. *Chem. Soc. Rev.* **2009**, *38*, 1187–1198. (b) Xu, H.; Zuend, S. J.; Woll, M. G.; Tao, Y.; Jacobsen, E. N. *Science* **2010**, *327*, 986–990.

[113] Zorn, C.; Gnad, F.; Salmen, S.; Herpin, T.; Reiser, O. *Tetrahedron Letters* **2001**, *42*, 7049–7053.

[114] Zorn, C. *Dissertation* **2001**, Regensburg.

[115] Guibe, F. *Tetrahedron* **1998**, 2967–3042.

[116] Alsina, J.; Giralt, E.; Albericio, F. *Tetrahedron Lett.* **1996**, *37*, 4195–4198.

[117] Coulson, D. R. *Inorg, Synth*. **1972**, *13*, 121-124.

[118] Dado, G. P.; Gellman, S. H. *J. Am. Chem. Soc.* **1994**, *116*, 1054–1062.

[119] (a) Seebach, D.; Overhand, M.; Kühnle, F. N. M.; Martioni; Oberer, L.; Hommel, U.; Widmer, H. *Helv. Chim. Acta* **1996**, *79*, 913–941. (b) Seebach, D.; Matthews, J. L. *Chem. Commun.* **1997**, 2015–2022.

[120] Selected reviews: (a) Hill, D. J.; Mio, M. J.; Prince, R. B.; Hughes, T. S.; Moore, J. S. *Chem. Rev.* **2001**, *101*, 3893–4012. (b) Pilsl, L. K. A.; Reiser, O. *Amino Acids* **2011**, *41*, 709–718. (c) Avan, I.; Hall, C. D.; Katritzky, A. R. *Chem. Soc. Rev.* **2014**, *43*, 3575–3594. (d) Martinek, T. A.; Fülöp, F. *Chem. Soc. Rev.* **2012**, *41*, 687–702.

[121] Mándity, I. M.; Wéber, E.; Martinek, T. A.; Olajos, G.; Tóth, G. K.; Vass, E.; Fülöp, F. *Angew. Chem.*, **2009**, *121*, 2205–2209.

[122] (a) Greenfield, N. J.; Fasman, G. D. *Biochemistry* **1969**, *8*, 4108–4116. (b) Kelly, S. M.; Jess, T. J.; Price, N. C. *Biochim. Biophys. Acta, Proteins Proteomics* **2005**, *1751*, 119–139. (c) Greenfield, N. J. *Nature Protocols* **2006**, *1*, 2876–2890.

[123] Arvidsson, P. I.; Frackenpohl, J.; Seebach, D. *Helv. Chim. Acta* **2003**, *86*, 1522–1553.

[124] Rajan, R.; Balaram, P. *Int. J. Peptide Protein Res.* **1996**, *48*, 328-336.

[125] Gray, T. S.; Morley, J. E. *Life Sci.* **1986**, *38*, 389–401.

[126] Balasubramaniam, A. A. *Peptides* **1997**, 445–457.

[127] Cabrele, C.; Beck-Sickinger, A. G. *J. Peptide Sci.* **2000**, *6*, 97–122.

[128] Cerda-Reverter, J. M.; Larhammer, D. *Biochem. Cell. Biol*. **2000**, *78*, 371–392.

[129] Tatemoto, K.; Carlquist, M.; Mutt, V. *Nature* **1982**, *296*, 659–660.

[130] Parker, E.; Van Heek, M.; Stamford, A. *Eur. J. Pharmacol*. **2002**, *444*, 173–187.

[131] Kimmel, J. R.; Hayden, L. J.; Pollock, H. G. *J. Biol. Chem*. **1975**, *250*, 9369–9376.

[132] Tatemoto, K.; Mutt. V. *Nature* **1980**, *285*, 417–418.

[133] Blundell, T. L.; Pitts, J. E.; Tickle, I. J.; Wood, S. P.; Wu, C.-W. *Proc. Natl. Acad. Sci. USA* **1981**, *78*, 4175–4175.

[134] Keller, M. *Dissertation* **2008**, Regensburg.

[135] Allen, J.; Novotny, J.; Martin, J.; Heinrich, G. *Proc. Natl. Acad. Sci. USA* **1987**, *84*, 2532–2536.

[136] Beck-Sickinger, A. G.; Weland, H. A.; Wittneben, H.; Willim, K.-D.; Rudolf, K.; Jung, G. *Eur. J. Biochem.* **1994**, *225*, 947–958.

[137] Cabrele, C.; Wieland, H. A.; Langer, M.; Stidsen, C. E.; Beck-Sickinger, A. G. *Peptides* **2001**, 365–378.

[138] Zhang, L.; Bijker, M. S.; Herzog, H. *Pharmacol. Ther.* **2011**, *131*, 91–113.

[139] Berglund, M. M.; Hipskind, P.A.; Gehlert, D. R. *Exp. Biol. Med*. **2003**, *228*, 217–244.

[140] Gehlert, D. R. *Neuropeptides* **2004**, *38*, 135–140.

[141] Lundell, I.; Blomqvist, A. G.; Berglund, M. M.; Schober, D. A.; Johnson, D.; Statnick, M. A.; Gadski, R. A.; Gehlert, D. R.; Larhammar, D. *J. Biol. Chem.* **1995**, *270*, 29123–29128.

[142] Reubi, J. C.; Gugger, M.; Waser, B.; Schaer, J.-C. *Cancer Res.* **2001**, *61*, 4636–4641.

[143] Korner, M.; Waser, B.; Reubi, J. C. *Lab. Invest*. **2004**, *84*, 71–80.

[144] Korner, M.; Reubi, J. C. *Peptides* **2007**, *28*, 419–425.

[145] Werner, H. M.; Horne, W. S. *Current Opinion in Chemical Biology* **2015**, *28*, 75–82.

[146] Kuhn, K. K.; Ertl, T.; Dukorn, S.; Keller, M.; Bernhardt, G.; Reiser, O.; Buschauer, A. *J. Med. Chem.* **2016**, *59*, 6045–6058

[147] Merten, N.; Lindner, D.; Rabe, N.; Rompler, H.; Morl, K.; Schoneberg, T.; Beck-Sickinger, A. G. *J. Biol. Chem.* **2007**, *282*, 7543−7551.

[148] Balasubramaniam, A.; Mullins, D. E.; Lin, S.; Zhai, W.; Tao, Z.; Dhawan, V. C.; Guzzi, M.; Knittel, J. J.; Slack, K.; Herzog, H.; Parker, E. M. *J. Med. Chem.* **2006**, *49*, 2661−2665.

[149] (a) Nutt, R. F.; Strachan, R. G.; Veber, D. F.; Holly, F. W. *J. Org. Chem.* **1980**, *45*, 3078–3080. (b) Hiebl, J.; Blanka, M.; Guttman, A.; Kollmann, H.; Leitner, K.; Mayrhofer, G.; Rovenszky, F.; Winkler, K. *Tetrahedron* **1998**, *54*, 2059–2074.

[150] Mazón, A.; Nájera, C.; Ezquerra, J.; Pedregal, C. *Tetrahedron Lett.* **1995**, *36*, 7697–7700.

[151] Collier, P. N.; Campbell, A. D.; Patel, I.; Raynham, T. M.; Taylor, R. J. K. *J. Org. Chem.* **2002**, *67*, 1802–1815.

[152] Lange, M.; Fischer, P. M. *Helv. Chim. Acta* **1998**, *81*, 2053–2061.

[153] Aguilera, B.; Wolf, L. B.; Nieczypor, P.; Rutjes, F. P. J. T.; Overkleeft, H. S.; van Hest, J. C. M.; Schoemaker, H. E.; Wang, B.; Mol, J. C.; Fürstner, A.; Overhand, M.; van der Marel, G. A.; van Boom, J. H. *J. Org. Chem.* **2001**, *66*, 3584–3589.

[154] (a) Schwab, P.; France, M. B.; Ziller, J. W.; Grubbs, R. H. *Angew. Chem., Int. Ed.* **1995**, *34*, 2039-2041. (b) Schwab, P.; Grubbs, R. H.; Ziller, J. W. *J. Am. Chem. Soc.* **1996**, *118*, 100-110.

[155] O´Leary, D. J.; Miller, S. J.; Grubbs, R. H. *Tetrahedron Letters* **1998**, *39*, 1689–1690.

[156] Biagini, S. C. G.; Gibson, S. E.; Keen, S. P. *J. Chem. Soc., Perkin Trans. 1* **1998**, 2485–2499.

[157] Williams, R. M.; Liu, J. *J. Org. Chem.* **1998**, *63*, 2130–2132.

[158] Gao, Y.; Lane-Bell, P.; Vederas, J. C. *J. Org. Chem.* **1998**, *63*, 2133–2143.

[159] (a) Scholl, M.; Ding, S.; Lee, C. W.; Grubbs, R. H. *Org. Lett.* **1999**, *1*, 953–956. (b) Garber, S. B.; Kingsbury, J. S.; Gray, B. L.; Hoveyda, A. H. *J. Am. Chem. Soc.* **2000**, *122*, 8168–8179.

[160] Passarella, D.; Peretto, B.; Blasco y Yepes, R.; Cappelletti, G.; Cartelli, D.; Ronchi, C.; Snaith, J.; Fontana, G.; Danieli, B.; Borlak, J. *Eur. J. Org. Chem.* **2010**, 219–226.

[161] Moffat, D. F. C.; Patel, S. R.; Davies, S. J.; Baker, K. W. J.; Philps, O. J. WO 2008/050096, 2008; *Chem. Abstr*. *148*:517974.

[162] Hupp, C. D.; Tepe, J. J. *J. Org. Chem.* **2009**, *74*, 3406−3413.

[163] Louie, J.; Bielawski, C. W.; Grubbs, R. H. *J. Am. Chem. Soc.* **2001**, *123*, 11312–11313.

[164] Liu, M.; Mountford, S. J.; Richardson, R. R.; Groenen, M.; Holliday, N. D.; Thompson, P. E. *J. Med. Chem.* **2016**, *59*, 6059–6069.

[165] Gerald, C.; Walker, M. W.; Criscione, L.; Gustafson, E. L.; Batzl-Hartmann, C.; Smith, K. E.; Vayasse, P.; Durkin, M. M.; Laz, T. M.; Linemeyer, D. L.; Schaffhauser, A. O.; Whitbread, S.; Hofbauer, K. G.; Taber, R. I.; Branchek, T. A.; Weinshank, R. L. *Nature* **1996**, *382*, 168–171.

[166] Rist, B.; Zerbe, O.; Ingenhoven, N.; Scapozza, L.; Peers, C.; Vaughan, P. F.; McDonald, R. L.; Wieland, H. A.; Beck-Sickinger, A. G. *FEBS Letters* **1996**, *394*, 169–173.

[167] Koglin, N.; Zorn, C.; Beumer, R.; Cabrele, C.; Bubert, C.; Sewald, N.; Reiser, O.; Beck-Sickinger, A. G. *Angew. Chem., Int. Ed*. **2003**, *42*, 202–205.; *Angew. Chem., Int. Ed.* **2003**, *42*, 202–205.

[168] Zwanziger, D.; Bohme, I.; Lindner, D.; Beck-Sickinger, A. G. *J. Pept. Sci.* **2009**, *15*, 856–866.

[169] Cabrele, C.; Martinek, T. A.; Reiser, O.; Berlicki, L. *J. Med. Chem.* **2014**, *57*, 9718–9739.

[170] (a) Gnad, F.; Reiser, O. *Chem. Rev.* **2003**, *103*, 1603–1623. (b) de Pol, S.; Zorn, C.; Klein, C. D.; Zerbe, O.; Reiser, O. *Angew. Chem., Int. Ed*. **2004**, *43*, 511–514. (c) Urman, S.; Gaus, K.; Yang, Y.; Strijowski, U.; Seewald, N.; Pol, S. de; Reiser, O. *Angew. Chem., Int. Ed.* **2007**, *46*, 3976–3978.

[171] (a) Torres, E.; Gorrea, E.; Da Silva, E.; Nolis, P.; Branchadell, V.; Ortuno, R. M. *Org. Lett.* **2009**, *11*, 2301–2304. (b) Fernandez, D.; Torres, E.; Aviles, F. X.; Ortuno, R. M.; Vendrell, J. *Bioorg. Med. Chem.* **2009**, *17*, 3824–3828. (c) Torres, E.; Gorrea, E.; Burusco, K. K.; Da Silva, E.; Nolis, P.; Rua, F.; Boussert, S.; Diez-Perez, I.; Dannenberg, S.; Izquierdo, S.; Giralt, E.; Jaime, C.; Branchadell, V.; Ortuno, R. M. *Org. Biomol. Chem.* **2010**, *8*, 564–575. (d) Gorrea, E.; Pohl, G.; Nolis, P.; Celis, S.; Burusco, K. K.; Branchadell, V.; Perczel, A.; Ortuno, R. M. *J. Org. Chem.* **2012**, *77*, 9795–9806. (e) Sorrenti, A.; Illa, O.; Ortuno, R. M.; Pons, R. *Langmuir* **2016**, *32*, 6977–6984. (f) Alauddin, M.; Gloaguen, E.; Brenner, V.; Tardivel, B.; Mons, M.; Zehnacker-Rentien, A.; Declerck, V.; Aitken, D. J. *Chem. -Eur. J.* **2015**, *21*, 16479–16493. (g) Grison, C. M.; Miles, J. A.; Robin, S.; Wilson, A. J.; Aitken, D. J. *Angew. Chem., Int. Ed.* **2016**, *55*, 11096–11100.

[172] (a) Martinek, T. A.; Fülöp, F. *Chem. Soc. Rev.* **2012**, *41*, 687–702. (b) Panzeri, S. *Dissertation* **2016**, Universitá Degli Studi Dell´ Insumbria, Varese.

[173] Berlicki, L.; Kaske, M.; Gutierrez-Abad, R.; Bernhardt, G.; Illa, O.; Ortuno, R. M.; Cabrele, C.; Buschauer, A.; Reiser, O. *J. Med. Chem.* **2013**, *56*, 8422–8431.

[174] Dukorn, S.; Littmann, T.; Keller, M.; Kuhn, K.; Cabrele, C.; Baumeister, P.; Bernhardt, G.; Buschauer, A. *Bioconjugate Chem*. **2017**, *28*, 1291–1304.

[175] (a) Tatsuoka, S.; Tanaka, K.; Ueno, Y.; Miyamoto, M. JP 34003967 B4 19590525, 1959. (b) Tatsuoka, S.; Tanaka, K.; Ueno, Y.; Morimoto, H. JP 34004820 B4 19590611, 1959. (c) Miyazaki, M.; Mizuno, C.; Umio, S. JP 34005871 B4 19590704, 1959.

[176] (a) Krogsgaard-Larsen, P.; Labouta, I. M.; Meldrum, B.; Croucher, M.; Schousboe, A. GABA Uptake Inhibitors as Experimental Tools and Potential Drugs in Epilepsy Research. In *Neurotransmitters, Seizures and Epilepsy*; Morselli, P., Lloyd, K. G., Löscher, W., Meldrum, B. S., Reynolds, E. H., Eds.; Raven Press: New York, 1981; pp 23–25. (b) Larsson, O. M.; Thorbek, P.; Krogsgaard-Larsen, P.; Schousboe, A. *J.*

*Neurochem*. **1981**, *37*, 1509–1516. (c) Nielsen, L.; Brehm, L.; Krogsgaard-Larsen, P. *J. Med. Chem.* **1990**, *33*, 71–77. (d) Crites, G. J.; Malizia, L. A.; Tunnicliff, G. *J. Basic Clin. Physiol. Pharmacol*. **2002**, *13*, 179–192.

[177] (a) Yunger, L. M.; Fowler, P. J.; Zarevics, P.; Setler, P. E. *J. Pharmacol. Exp. Ther.* **1984**, *228*, 109–115. (b) Ali, F. E.; Bondinell, W. E.; Dandridge, P. A.; Frazee, J. S.; Garvey, E.; Girard, G. R.; Kaiser, C.; Ku, T. W.; Lafferty, J. J.; Moonsammy, G. I.; Oh, H.-J.; Rush, J. A.; Setler, P. E.; Stringer, O. D.; Venslavsky, J. W.; Volpe, B. W.; Yunger, L. M.; Zirkle C. L. *J. Med. Chem.* **1985**, *28*, 653–660. (c) Falch, E.; Jacobsen, P.; Krogsgaard-Larsen, P.; Curtis, D. R. *J. Neurochem.* **1985**, *44*, 68–75. (d) Bonanno, G.; Raiteri, M. *Br. J. Pharmacol.* **1987**, *91*, 237–243. (e) N'Goka, V.; Schlewer, G.; Linget, J. M.; Chambon, J. P.; Wermuth, C. G. *J. Med. Chem.* **1991**, *34*, 2547–2557. (f) Andersen, K. E.; Sørensen, J. L.; Lau, J. Lundt, B. F.; Petersen, H. Huusfeldt, P. O.; Suzdak, P. D.; Swedberg, M. D. B. *J. Med. Chem.* **2001**, *44*, 2152–2163. (g) Wein, T.; Petrera, M.; Allmendinger, L.; Hoefner, G.; Pabel, J.; Wanner, K. T. *ChemMedChem* **2016**, *11*, 509–518. (h) Computational study: Galvez-Ruano, E.; Iriepa, I.; Morreale, A.; Boyd, D. B. *J. Mol. Graph. Model.* **2001**, *20*, 183–197.

[178] Reviews: (a) Parsons, A. F. *Tetrahedron* **1996**, *52*, 4149–4174. (b) Clayden, J.; Read, B.; Hebditch, K. R. *Tetrahedron* **2005**, *61*, 5713–5724. (c) Stathakis, C. I.; Yioti, E. G.; Gallos, J. K. *Eur. J. Org. Chem.* **2012**, 4661–4673. (d) Majik, M. S.; Mandrekar, V. K. *Curr. Org. Chem.* **2016**, *20*, 939–951.

[179] Journal articles: (a) Coleman, D. R.; Ren, Z.; Mandal, P. K.; Cameron, A. G.; Dyer, G. A.; Muranjan, S.; Campbell, M.; Chen, X.; McMurray, J. S. *J. Med. Chem.* **2005**, *48*, 6661–6670. (b) Labroli, M.; Paruch, K.; Dwyer, M. P.; Alvarez, C.; Keertikar, K.; Poker, C.; Rossman, R.; Duca, J. S.; Fischmann, T. O.; Madison, V.; Parry, D.; Davis, N.; Seghezzi, W.; Wiswell, D.; Guzi, T. J. *Bioorg. Med. Chem. Lett.* **2011**, *21*, 471–474. Patents since 2012 and references cited therein: (c) Liu, J.; Balkovec, J. M.; Krikorian, A. D.; Guiadeen, D.; Yang, G.; Jian, T.; Wu, Z.; Yu, Y.; Nargund, R. P.; Vachal, P.; Devita, R. J.; He, S.; Lai, Z.; Blevis-Bal, R. M.; Cernak, T. A; Sperbeck, D. M.; Hong, Q. WO 2012096813 A1 20120719, 2012. (d) Bylock, L. A. WO 2013131901 A1 20130912, 2013. (e) Brunette, S. R.; Abeywardane, A.; Burke, M. J.; Kapadia, S. R.; Kirrane, T. M., Jr.; Netherton, M. R.; Razavi, H.; Rodriguez, S.; Saha, A.; Sibley, R.; Smith K., Lana L.; Takahashi, H.; Turner, M. R.; Wu, J.-P.; Young, E. R. R.; Zhang, Q.; Zhang, Q.; Zindell, R. M. WO 2013134226 A1, 2013.

[180] (a) Thorbek, P.; Hjeds, H.; Schaumburg, K. *Acta Chem. Scand.* **1981**, *B35*, 473–479. (b) Labouta, I. M.; Jacobsen, P.; Thorbek, P.; Krogsgaard-Larsen, P.; Hjeds, H. *Acta Chem. Scand.* **1982**, *B36*, 669–674. (c) Cardillo, B.; Galeazzi, R.; Mobbili, G.; Orena, M. *Synlett* **1995**, 1159–1160. (d) Coldham, I.; Hufton, R. *Tetrahedron* **1996**, *52*, 12541–12552. (e) Galeazzi, R.; Geremia, S.; Mobbili, G.; Orena, M. *Tetrahedron: Asymmetry* **1996**, *7*, 79–88. (f) Galeazzi, R.; Mobbili, G.; Orena, M. *Tetrahedron* **1996**, *52*, 1069–1084. (g) Eustache, J.; Grob, A.; Lam, C.; Sellier, O.; Schulz, G. *Bioorg. Med. Chem. Lett.* **1998**, *8*, 2961–2966. (h) Thomas, C.; Orecher, F.; Gmeiner, P. *Synthesis* **1998**, 1491–1496.

[181] (a) Ye, W.; Jiang, Z.; Zhao, Y.; Goh, S. L. M.; Leow, D.; Soh, Y.-T.; Tan, C.-H. *Adv. Synth. Catal.* **2007**, *349*, 2454–2458. For the key step, an organocatalyzed Michael addition, no yield is reported by the authors. (b) Felluga, F.; Gombac, V.; Pitacco, G.; Valentin, E. *Tetrahedron: Asymmetry* **2004**, *15*, 3323–3327. As key step, the enzymatic desymmetrization of diethyl 3-(nitromethyl)pentanedioate was developed.

[182] Leading reviews: (a) Reissig, H. U.; Zimmer, R. *Chem. Rev.* **2003**, *103*, 1151−1196. (b) Schneider, T. F.; Kaschel, J.; Werz, D. B. *Angew. Chem., Int. Ed.* **2014**, *53*, 5504−5523.

[183] Studies on the cyclopropanation of furans and pyrroles with ethyl diazoacetate: (a) Wenkert, E.; Khatuya, H.; Klein, P. S. *Tetrahedron Lett.* **1999**, *40*, 5171−5174. (b) Wenkert, E.; Khatuya, H. *Tetrahedron Lett.* **1999**, *40*, 5439−5442. (c) Wenkert, E.; Guo, M.; Lavilla, R.; Porter, B.; Ramachandran, K.; Sheu, J.-H. *J. Org. Chem.* **1990**, *55*, 6203−6214. (d) Tanny, S. R.; Grossman, J.; Fowler, F. W. *J. Am. Chem. Soc.* **1972**, *94*, 6495−6501.

[184] (a) Böhm, C.; Reiser, O. *Org. Lett.* **2001**, *3*, 1315−1318. (b) Kalidindi, S.; Jeong, W. B.; Schall, A.; Bandichhor, R.; Nosse, B.; Reiser, O. *Angew. Chem., Int. Ed.* **2007**, *46*, 6361−6363. (c) Harrar, K.; Reiser, O. *Chem. Commun.* **2012**, *48*, 3457−3459. (d) Kreuzer, A.; Kerres, S.; Ertl, T.; Ruecker, H.; Amslinger, S.; Reiser, O. *Org. Lett.* **2013**, *15*, 3420−3423. (e) Bergmann, A.; Reiser, O. *Chem. -Eur. J.* **2014**, *20*, 7613–7615.

[185] Böhm, C.; Schinnerl, M.; Bubert, C.; Zabel, M.; Labahn, T.; Parisini, E.; Reiser, O. *Eur. J. Org. Chem.* **2000**, 2955−2965. (b) Schinnerl, M.; Böhm, C.; Seitz, M.; Reiser, O. *Tetrahedron: Asymmetry* **2003**, *14*, 765−771. (c) Glos, M. *Dissertation* **2000**, Regensburg. (d) Poleschak, M. *Dissertation* **2002**, Regensburg.

[186] Hedley, S. J.; Ventura, D. L.; Dominiak, P. M.; Nygren, C. L.; Davies, H. M. L. *J. Org. Chem.* **2006**, *71*, 5349−5356.

[187] Davies, H. M. L.; Hedley, S. J. *Chem. Soc. Rev.* **2007**, *36*, 1109–1119.

[188] Glos, M.; Reiser, O. *Org. Lett.* **2000**, *2*, 2045–2048.

[189] Werner, H.; Vicha, R.; Gissibl, A.; Reiser, O. *J. Org. Chem.* **2003**, *68*, 10166–10168.

[190] Evans, D. A.; Woerpel, K. A.; Hinman, M. M.; Faul, M. M. *J. Am. Chem. Soc*. **1991**, *113*, 726−728. (b) Lowenthal, R. E.; Abiko, A.; Masamune, S. *Tetrahedron Lett.* **1990**, *31*, 6005−6008.

[191] (a) Gissibl, A.; Finn, M. G.; Reiser, O. *Org. Lett.* **2005**, *7*, 2325–2328. (b) Geiger, C.; Kreitmeier, P.; Reiser, O. *Adv. Synth. Catal.* **2005**, *347*, 249–254. (c) Rasappan, R.; Hager, M.; Gissibl, A.; Reiser, O. *Org. Lett.* **2006**, *8*, 6099–6102. (d) Rasappan, R.; Olbrich, T.; Reiser, O. *Adv. Synth. Catal.* **2009**, *351*, 1961–1967. (e) Hager, M. *Dissertation* **2010**, Regensburg.

[192] (a) Fraile, J. M.; Garcia, J. I.; Herrerias, C. I.; Mayoral, J. A.; Reiser, O.; Socuellamos, A.; Werner, H. *Chem. -Eur. J.* **2004**, *10*, 2997–3005. (b) Werner, H.; Herrerías, C. I.; Glos, M.; Gissibl, A.; Fraile, J. M.; Pérez, I.; Mayoral, J. A.; Reiser, O. *Adv. Synth. Catal.* **2006**, *348*, 125–132. (c) Fraile, J. M.; Pérez, I.; Mayoral, J. A.; Reiser, O. *Adv. Synth. Catal.* **2006**, *348*, 1680–1688. (d) Schätz, A.; Hager, M.; Reiser, O. *Adv. Funct. Mater.* **2009**, *19*, 2109–2115. (e) Schätz, A.; Grass, R. N.; Kainz, Q.; Stark, W. J.; Reiser, O. *Chem. Mater.* **2010**, *22*, 305–310. (f) García, J. I.; Herrerías, C. I.; López-Sánchez, B.; Mayoral, J. A.; Reiser, O. *Adv. Synth. Catal.* **2011**, *353*, 2691–2700.

[193] McKennon, M. J.; Meyers, A. I.; Drauz, K.; Schwarm, M. *J. Org. Chem.* **1993**, *58*, 3568–3571.

[194] Roy, S.; Reiser, O. *Angew. Chem., Int. Ed.* **2012**, *51*, 4722–4725.

[195] Reference values for (*S*)-(+)-**188** reported in the literature: +9.6 (*c* 1, $H_2O$), ref [176c] (Nielsen 1990); +8.6 (*c* 1, $H_2O$), ref [180h] (Thomas 1998); +9.2 (*c* 1, $H_2O$), ref [180e] (Galeazzi 1996); +9.3 (*c* 2, $H_2O$), ref [181b] (Felluga 2004); +8.3 (*c* 0.4, $H_2O$), ref [181a] (Ye 2007; 92% ee).

[196] Pilsl, L. K. A.; Ertl, T.; Reiser, O. *Org. Lett.* **2017**, *19*, 2754–2757.

[197] (a) Norton Matos, M. R. P.; Afonso, C. A. M.; Batey, R. A. *Tetrahedron Lett.* **2001**, *42*, 7007–7010. (b) Norton Matos, M.; Afonso, C. A. M.; Batey, R. A. *Tetrahedron* **2005**, *61*, 1221–1244.

[198] Cardona, W.; Quiñones, W.; Robledo, S.; Vélez, I. D.; Murga, J.; García-Fortanet, J.; Carda, M.; Cardona, D.; Echeverri, F. *Tetrahedron* **2006**, *62*, 4086–4092.

[199] Le Corre, L.; Kizirian, J.-C.; Levraud, C.; Boucher, J.-L.; Bonnet, V.; Dhimane, H. *Org. Biomol. Chem.* **2008**, *6*, 3388.

[200] For related rearrangements see: (a) Wenkert, E.; Hudlicky, T. *J. Org. Chem.* **1988**, *53*, 1953–1957. (b) Harrar, K.; Reiser, O. *Chem. Commun.* **2012**, *48*, 3457–3459.

[201] Parsons, A. F. *Tetrahedron* **1996**, *52*, 4149–4174.

[202] (a) Stathakis, C. I.; Yioti, E. G.; Gallos, J. K. *Eur. J. Org. Chem.* **2012**, 4661–4673. (b) Shi, H.; Li, J.; Liu, Y.; Du, Z.; Huang, Z.; Zhao, N.; Li, N.; Yang, J. *Tetrahedron* **2016**, *72*, 5502–5506.

[203] Gheorghe, A.; Schulte, M.; Reiser, O. *J. Org. Chem*. **2006**, *71*, 2173−2176.

[204] Reiser, O. *Isr. J. Chem.* **2016**, *56*, 531–539.

[205] (a) Otera, J.; Danoh, N.; Nozaki, H. *J. Org. Chem.* **1991**, *56*, 5307–5311. (b) Orita, A.; Sakamoto, K.; Hamada, Y.; Mitsutome, A.; Otera, J. *Tetrahedron* **1999**, *55*, 2899–2910.

[206] Kreuzer, A. *Dissertation* **2015**, Regensburg.

[207] Gugger, P. A.; Hockless, D. C.; Kilah, N. L.; Mayadunne, R. C.; Wild, S. B. *Tetrahedron: Asymmetry* **2008**, *19*, 1810–1812.

[208] Andersen, K. E.; Braestrup, C.; Groenwald, F. C.; Joergensen, A. S.; Nielsen, E. B.; Sonnewald, U.; Soerensen, P. O.; Suzdak, P. D.; Knutsen, L. J. S. *J. Med. Chem.* **1993**, *36*, 1716–1725.

[209] Hellenbrand, T.; Hofner, G.; Wein, T.; Wanner, K. T. *Bioorg. Med. Chem.* **2016**, *24*, 2072–2096.

[210] Freifelder, M. *J. Org. Chem.* **1963**, *28*, 1135.

[211] Muldakhmetov, M. Z.; Gazaliev, A. M.; Kirilyus, I. V.; Fazylov, S. D. *Russ. J. Appl. Chem.* **2007**, *80*, 1087–1089.

[212] Naoki, T. JP 2009263341 A Nov 12, 2009.

[213] Ismail, K. A.; Bergmeier, S. C. *Eur. J. Med. Chem*. **2002**, *37*, 469–474.

[214] (a) Schleich, S.; Helmchen, G. *Eur. J. Org. Chem.* **1999**, 2515–2521. (b) Song, S.; Zhu, S.-F.; Pu, L.-Y.; Zhou, Q.-L. *Angew. Chem., Int. Ed.* **2013**, *52*, 6072–6075.

[215] Lei, A.; Chen, M.; He, M.; Zhang, X. *Eur. J. Org. Chem.* **2006**, 4343–4347.

[216] Willstätter, R.; Bruce, J. *Chem. Ber.* **1907**, *40*, 3979–3999.

[217] Danishefsky, S.; Singh, R. K. *J. Am. Chem. Soc.* **1975**, *97*, 3239–3241.

[218] De Meijere, A.; Seebach, M.; Zöllner, S.; Kozhushkov, S.; Belov, V. N.; Boese, R.; Haumann, T.; Benet-Bichholz, J.; Yufit, D. S.; Howard, J. A. K. *Chem. -Eur. J.* **2001**, *7*, 4021–4034.

[219] Sone, Y.; Kimura, Y.; Ota, R.; Mochizuki, T.; Ito, J.; Nishii, Y. *Eur. J. Org. Chem.* **2017**, 2842–2847.

[220] For example see: (a) Schultz, A. L. *J. Org. Chem.* **1971**, *36*, 383–386. (b) Roje, M.; Vinković, V.; Šunjić, V. *Tetrahedron* **1998**, *54*, 9123–9128. (c) Kiwus, R.; Schwarz, W.; Roßnagel, I.; Musso, H. *Chem. Ber.* **1987**, *120*, 435–438. (d) Royer, F.; Felpin, F.-X.; Doris, E. *J. Org. Chem.* **2001**, *66*, 6487–6489. (e) Stahl, K.-J.; Hertzsch, W.; Musso, H. *Liebigs Ann. Chem.* **1985**, 1474–1484. (f) González-Juárez, D. E.; García-Vázquez, J. B.; Zúñiga-García, V.; Trujillo-Serrato, J. J.; Suárez-Castillo, O. R.; Joseph-Nathan, P.; Morales-Ríos, M. S. *Tetrahedron* **2012**, *68*, 7187–7195.

[221] Sone, Y.; Kimura, Y.; Ota, R.; Mochizuki, T.; Ito, J.; Nishii, Y. *Eur. J. Org. Chem.* **2017**, 2842–2847.

[222] Gröger, C.; Musso, H. *Chem. Ber.* **1980**, *113*, 3621–3628.

[223] (a) Hoffmann, R. *Tetrahedron Lett.* **1970**, 2907–2909. (b) Hoffmann, R.; Stohrer W.-D. *J. Am. Chem. Soc.* **1971**, *93*, 6941–6948.

[224] Günther, H. *Tetrahedron Lett*. **1970**, 5173–5176.

[225] Beumer, R. *Dissertation* **2000**, Regensburg.

[226] Toya, H.; Okano, K.; Takasu, K.; Ihara, M.; Takahashi, A.; Tanaka, H.; Tokuyama, H. *Org. Lett.* **2010**, *12*, 5196–5199.

[227] Frost, C. G.; Howarth, J.; Williams, J. M. J. *Tetrahedron: Asymmetry* **1992**, *3*, 1089–1122.

[228] Tsuji, J.; Takahasi, H.; Morikawa, M. *Tetrahedron Lett.* **1965**, *49*, 4387–4388.

[229] Weaver, J. D.; Recioll, A.; Grenning, A. J.; Tunge, J. A. *Chem. Rev*. **2011**, *111*, 1846–1913.

[230] Trost, B. M. *Chem. Rev*. **1996**, *96*, 396–422.

[231] Trost, B. M.; Zhang, T.; Sieber, J. D. *Chem. Sci.* **2010**, *1*, 427–440.

[232] See selected examples: (a) Storsberg, J.; Yao, M.-L.; Ocal, N.; Meijere, A. de; Adam, A. E. W.; Kaufmann, D. E. *Chem. Commun.* **2005**, 5665–5666. (b) Meazza, M.; Guo, H.; Rios, R. *Org. Biomol. Chem.* **2017**, *15*, 2479–2490. (c) Baeckvall, J. E.; Bjoerkman, E. E.; Pettersson, L.; Siegbahn, P.; Strich, A. *J. Am. Chem. Soc.* **1985**, *107*, 7408–7412.

[233] Wilhelm, D.; Bäckvall, J.-E.; Nordberg, R. E.; Norin, T. *Organometallics* **1985**, *4*, 1296–1302.

[234] Ylijoki, K. E. O.; Stryker, J. M. *Chem. Rev*. **2013**, *113*, 2244–2266.

[235] (a) Fowler, F. W. *Angew. Chem., Int. Ed*. **1971**, *10*, 135–136. (b) Tanny, S. R.; Fowler, F. W. *J. Org. Chem.* **1974**, *39*, 2715–2718.

[236] Cai, P.-J.; Shi, F.-Q.; Wang, Y.; Li, X.; Yu, Z.-X. *Tetrahedron* **2013**, *69*, 7854–7860.

[237] IUPAC. Compendium of Chemical Terminology, 2nd ed. (the "Gold Book"). Compiled by A. D. McNaught and A. Wilkinson. Blackwell Scientific Publications, Oxford (1997). XML on-line corrected version: http://goldbook.iupac.org (2006-) created by M. Nic, J. Jirat, B. Kosata; updates compiled by A. Jenkins. ISBN 0-9678550-9-8. DOI of this term: https://doi.org/10.1351/goldbook.C01496.

[238] Cheng, Y.; Prussoff, W. H. *Biochem. Pharmacol*. **1973**, *22*, 3099-3108.

[239] Fuson, R. C.; Walker, J. T. *Org. Synth*. **1933**, *13*, 32.

[240] Lengyel, G. A.; Frank, R. C.; Horne, W. S. *J. Am. Chem. Soc*. **2011**, *133*, 4246-4249.

[241] Ward, M. D.; Zhu, Z. U.S. Pat. Appl. Publ., 20120316236, **13 Dec 2012**.

[242] Aguilera, B.; Wolf, L. B.; Nieczypor, P.; Ritjes, F. P. J. T.; Overkleeft, H. S.; van Hest, J. C. M. Schoemaker, H. E.; Wang B.; Mol, J. C.; Fürstner, A.; Overhand, M.; van der Marel, G. A.; van Boom, J. H. *J. Org. Chem*. **2001**, *66*, 3584-3589.

[243] Hiebl, J.; Blanka, M.; Guttmann, A.; Kollmann, H.; Leitner, K.; Mayrhofer, G.; Rovenszky, F.; Winkler, K. *Tetrahedron* **1998**, *54*, 2059-2074.

[244] LePlae, P, R.; Umezawa, N.; Lee, H.-S.; Gellman, S. H. *J. Org. Chem*. **2001**, *66*, 5629-5632.

[245] Jaschinski, T.; Hiersemann, M. *Org. Lett*. **2012**, *14*, 4114-4117.

[246] Nicewicz, D. A.; Breteche, G.; Johnson, J. S. *Org. Synth*. **2008**, *85*, 278-286.

[247] Magnus, P.; Turston, L. S. *J. Org. Chem*. **1991**, *56*, 1166-1170.

# H. Acknowledgment

Ich bedanke mich bei Prof. Dr. Oliver Reiser für die Überlassung des äußerst interessanten Themas und seine beständige Unterstützung während der gesamten Arbeit.

Vielen Dank an Prof. Dr. Chiara Cabrele und Saskia Neukirchen für die Betreuung während meines Aufenthaltes in Salzburg und für die Synthesen der NPY-Analoga.

Für Finanzielle Unterstützung während meiner Promotion bedanke ich mich bei der DFG Research Training Group GRK 1910.

Ich danke Herrn Prof. Dr. Armin Buschauer für die Co-Betreuung des NPY Projektes im Rahmen des GRK.

Herzlichen Dank an Dr. Kilian Kuhn und Dr. Stefanie Dukorn vom AK Buschauer für die Durchführung der biologischen Tests und Hilfe bei fachlichen Fragenstellungen.

Den Mitarbeitern der zentralen Analytik danke ich für die Hilfe bei der Aufnahme von NMR Spektren und für die Durchführung der Massenspektroskopien. Ebenso danke ich Herrn Dr. Axel Dürkop für die Hilfe bei den CD-Messungen.

Herzlichen Dank an Dr. Peter Kreitmeier für seine Hilfe bei technischen und chemischen Problemen sowie für die unzähligen fachlichen, aber besonders für die nicht fachlichen Diskussionen. Ebenso bedanke ich mich Klaus Döring, Roxane Harteis, Helena Konkel und Brigitte Eichenseher für synthetische Unterstützung. Besonders herzlicher Dank gilt unserer Sekretärin Antje Weigert für Hilfe jeglicher Art!

Ich bedanke mich bei meinen Laborkollegen Dr. Dattatraya Bagal, Dr. Corina Eichenseer, Robert Eckl, Michael Leitner, Sabine Kerres und Dr. Andreas Kreuzer für die stets freundschaftliche Atmosphäre und gute Zusammenarbeit im Labor.

Den Kollegen des *Wahren Powerlabors* danke ich ganz besonders für die super Zeit, die wir zusammen hatten! Danke für eure Freundschaft!

Mein ganz besonderer Dank gilt Dr. Ludwig Pilsl für seine Freundschaft, Unterstützung und Hilfe jeglicher Art während der letzten Jahre.

Ebenso möchte ich mich herzlich bei meinem *Tripeptid-Leidensgenossen* Martin Hofmann für seine Freundschaft und Unterstützung bedanken.

Bei meiner Büro- und Leidensgenossin Verena bedanke ich mich für die gute Atmosphäre während des Schreibens dieser Arbeit.

Ich danke allen aktuellen und ehemaligen Mitarbeitern am Lehrstuhl für die gute und kollegiale Atmosphäre, im Besonderen Bergmann., Dobi, Corina, der Mutti, Christian, Easy, Jimmy, Michi, Benni, Goofy, Matze, Sabine, dem General, Paul, Petermeister, Kreuzer, Roberto, Verena, Lu und Berni, Karin, Sharon, Nanaji, Carina und Lisa.

Danke an meine Bachelor- und Masterstudenten Sebastian Krickl, Matthias Schmalzbauer, Christoph Müller, Nele Berg, Martina Tremmel, Katrin Gradl, Alexander Roether, Lukas Wunderlich, Tobias Götz und Sascha Grotjahn für synthetische Unterstützung.

Für das Korrekturlesen dieser Arbeit bedanke ich mich herzlich bei Dr. Corina Eichenseer, Martin Hofmann, Michael Leitner, Sabine Kerres, Saerom Park und Dr. Ludwig Pilsl.

Mein ganz großer Dank gilt meinen Freunden und Studienkollegen außerhalb des Lehrstuhls Matthias, Markus, Angie, Ferdi, Pius, Nine, Felix, Vera, Ramona, Hans und Kathi für eure Freundschaft, eure unermüdliche Unterstützung und sämtliche Aktivitäten außerhalb der Uni.

Saerom, my acknowledgment here can not verbalize how I feel thankful to you. I thank you so much for your help, support, discussions and your trust, that I can manage this all. Thanks, thanks, thanks!

Zu guter Letzt gilt mein aller größter Dank meinen Eltern, Geschwistern und Großeltern. Nicht nur für eure finanzielle, sondern auch für die moralische Unterstützung über all die Jahre hin möchte ich mich bei euch herzlich bedanken. Ihr habt immer an mich geglaubt und mich ermutigt. Ohne euch wäre dieses Studium und diese Arbeit so niemals möglich gewesen!

# I. Declaration

Herewith I declare that this present thesis is a presentation of my original work prepared single-handed. Wherever contributions from others are involved, all of them are marked clearly, with reference to the literature, license, and acknowledgment of collaborative research.

Regensburg, July 31, 2017

Thomas Ertl